Fakultät Wissenschaftszentrum Weihenstephan für Ernährung, Landnutzung und Umwelt

Technische Universität München

Generation and analysis of a systematic map of the *Arabidopsis thaliana* phytohormone signaling interactome

Melina Altmann

Vollständiger Abdruck der von der Fakultät Wissenschaftszentrum Weihenstephan für Ernährung, Landnutzung und Umwelt der Technischen Universität München zur Erlangung des akademischen Grades eines

Doktor der Naturwissenschaften (Dr. rer. nat.)

genehmigten Dissertation.

Vorsitzende:

Prof. Dr. Caroline Gutjahr

Prüfende der Dissertation:

1. Prof. Dr. Claus Schwechheimer
2. Prof. Dr. Pascal Falter-Braun,
   Ludwig-Maximilian Universität
3. Prof. Dr. Geert De Jaeger,
   Universität Gent

Die Dissertation wurde am 27.06.2019 bei der Technischen Universität München eingereicht und durch die Fakultät Wissenschaftszentrum Weihenstephan für Ernährung, Landnutzung und Umwelt am 29.11.2019 angenommen.

Abstract

Plants need to adapt their life cycle and development to biotic and abiotic environmental influences. For this adaptation, phytohormone signaling pathways play an essential role to convey environmental signals and initiate or inhibit specific developmental processes and stress responses. The precise control of these processes by synergistic as well as antagonistic interactions of different phytohormone signaling pathways has long been known. Recent studies now suggest that these interactions are at least partially regulated by reciprocal transcriptional regulation and some direct protein-protein interactions. However, the extent of signal integration across individual phytohormone signaling pathways is not yet well understood.

The central aim of this work was to elucidate how phytohormone signaling pathways interact with each other, particularly at the molecular level, and to what extent signal integration takes place via protein-protein interactions. To address this question, I have generated a phytohormone ORFeome collection consisting of approximately 1,200 open reading frames as an experimental resource for the protein interaction map. For this collection, all ORFs were selected whose corresponding mutant plant lines showed genetic evidence of involvement in phytohormone signal transduction. With appropriate enrichment, complete gene families were additionally included. With this ORF collection, a systematic protein interaction network map was generated using an established high throughput mapping pipeline based on the yeast-two-hybrid system. The resulting interaction network map contains 475 interactions between 251 proteins and showed hundreds of direct interactions between all phytohormone signaling pathways. To identify hormone-dependent protein interactions, phytohormone receptors were screened in presence and absence of the respective hormone against the phytohormone ORFeome collection and a published *Arabidopsis* ORF collection. These screens resulted in 241 interactions between 138 proteins of which 99 were hormone-dependent. In particular, a high number of new hormone-dependent interactions could be identified for the karrikin signaling pathway, of which only few direct interactions were known so far. Additionally, various non-core pathway interactions of phytohormone receptors could be detected, which have only been described very rarely in the literature. These interactions suggest new pathway-independent functions of phytohormone receptors that may be induce a fast and short term reactions to bridge suddenly occurring environmental influences. To validate the newly identified points of signal integration, a set of 19 interactions between 27 proteins was tested in planta. The corresponding 27 *Arabidopsis thaliana* mutant lines were analyzed in hormone-treated seedling assays to identify unknown functions in the phytohormone signaling pathways of their respective interaction partner. For 24 mutant lines (89 %) new phenotypes could be detected, which suggest new functions in additional phytohormone pathways for these proteins. Furthermore, these results indicate that protein functions for multiple hormone pathways are more common than previously known.

In summary, the results of this thesis indicate that the different phytohormone signaling pathways are strongly interconnected through direct protein-protein interactions

that form a dense signaling network. This suggests that incoming environmental signals are transmitted through this network to regulate various developmental processes and stress responses. The identification of different core pathway-independent interactions of receptors indicates involvement in different developmental processes and stress responses and possibly a rapid molecular mechanism to overcome spontaneous biotic or abiotic hazards. The high rate of newly identified hormone-induced phenotypes confirm signal integration points between all phytohormone signaling pathways.

Zusammenfassung

Pflanzen müssen ihren Lebenszyklus und ihre Entwicklung an biotische und abiotische Umwelteinflüsse anpassen. Für diese Anpassungen spielen Phytohormon-Signalwege eine wesentliche Rolle, um Umweltsignale zu übermitteln und spezifische Entwicklungsprozesse und Stressreaktionen einzuleiten oder zu hemmen. Die genaue Steuerung dieser Prozesse durch synergistische und antagonistische Wechselwirkungen verschiedener Phytohormon-Signalwege ist seit langem bekannt. Neuere Studien deuten nun darauf hin, dass diese Wechselwirkungen zumindest teilweise durch die wechselseitige transkriptionelle Regulierung und einige direkte Protein-Protein-Interaktionen reguliert werden. Das Ausmaß der Signalintegration über einzelne Phytohormon-Signalwege hinweg ist jedoch noch nicht gut verstanden.

Zentrales Ziel dieser Arbeit ist es, aufzuklären, wie Phytohormon-Signalwege miteinander interagieren, insbesondere auf molekularer Ebene, und inwieweit die Signalintegration über Protein-Protein-Interaktionen erfolgt. Um diese Frage zu beantworten, habe ich eine Phytohormon ORFeom-Sammlung mit ca. 1.200 offenen Leserahmen als experimentelle Ressource für die Protein-Interaktionskarte generiert. Für diese Sammlung wurden alle ORFs ausgewählt, deren entsprechende mutierte Pflanzenlinien genetische Hinweise auf eine Beteiligung an der Phytohormon-Signaltransduktion zeigten. Bei entsprechender Anreicherung wurden zusätzlich komplette Genfamilien aufgenommen. Mit dieser ORF-Sammlung wurde eine systematische Protein-Interaktions-Netzwerkkarte mit einer etablierten Hochdurchsatz-Mapping-Pipeline auf Basis des Hefe-Zwei-Hybridsystems erstellt. Die resultierende Interaktions-Netzwerkkarte enthält 475 Interaktionen zwischen 251 Proteinen und zeigt Hunderte von direkten Interaktionen zwischen allen Phytohormon-Signalwegen. Um hormonabhängige Proteininteraktionen zu identifizieren, wurden Phytohormonrezeptoren in An- und Abwesenheit des jeweiligen Hormons gegen die Phytohormon ORFeom-Sammlung und eine veröffentlichte *Arabidopsis* ORF-Sammlung getestet. Diese Screens führten zu 241 Interaktionen zwischen 138 Proteinen, von denen 99 hormonabhängig waren. Insbesondere für den Karrikin-Signalweg, von dem bisher nur wenige direkte Interaktionen bekannt waren, konnte eine hohe Anzahl neuer hormonabhängiger Interaktionen identifiziert werden. Darüber hinaus konnte eine Vielzahl von Nicht-Hauptsignalweg Interaktionen von Phytohormonrezeptoren, die in der Literatur nur sehr selten beschrieben wurden, nachgewiesen werden. Diese Interaktionen deuten auf neue Hauptsignalweg-unabhängige Funktionen von Phytohormonrezeptoren hin, die möglicherweise eine schnelle und kurzfristige Reaktion induzieren können, um plötzlich auftretende Umwelteinflüsse zu überbrücken. Um die neu identifizierten Punkte der Signalintegration zu validieren, wurde ein Set von 19 Interaktionen mit 27 Proteinen *in planta* getestet. Die entsprechenden 27 *Arabidopsis thaliana*-Mutantenlinien wurden auf neue Phänotypen in hormonbehandelten Keimling-Assays analysiert, um unbekannte Funktionen in den Phytohormon-Signalwegen ihres jeweiligen Interaktionspartners zu identifizieren. Für 24 Mutantenlinien (89 %) konnte ein neuer Phänotyp nachgewiesen werden, der neue Funktionen in zusätzlichen Phytohormonwe-

gen für diese Proteine nahelegt. Darüber hinaus deuten diese Ergebnisse darauf hin, dass Proteinfunktion in mehreren Hormonsignalwegen häufiger sind als bisher bekannt.

Zusammenfassend zeigen die Ergebnisse dieser Arbeit, dass die unterschiedlichen Phytohormon-Signalwege durch direkte Protein-Protein-Interaktionen stark miteinander verbunden sind, welche ein dichtes Signal-Netzwerk bilden. Dies deutet darauf hin, dass eingehende Umweltsignale über dieses Netzwerk übertragen werden, um verschiedene Entwicklungsprozesse und Stressreaktionen zu regulieren. Die Identifizierung verschiedener Hauptsignalweg unabhängige Interaktionen von Rezeptoren weisen auf die Beteiligung an unterschiedlichen Entwicklungsprozessen und Stressreaktionen hin und möglicherweise dadurch eventuell einen schnellen molekulare Mechanismus zur Überwindung spontan eintretender biotischer oder abiotischer Gefahren. Die hohe Rate neu identifizierter hormoninduzierter Phänotypen bestätigt Signalintegrationspunkte zwischen allen Phyto-Hormon-Signalwegen.

Contents

List of Figures

List of Tables

Acronyms

ABA	Abscisic acid
ABCB	ATP-BINDING CASSETTE subfamily B
ABI	ABSCISIC ACID-INSENSITIVE
ABRE	ABSCISIC ACID RESPONSE ELEMENT
ACC	1-Aminocyclopropane-1-carboxylic acid
AD	activation domain
AFB	AUXIN SIGNALING F-BOX
AFP	ABI FIVE BINDING PROTEIN
AHK	ARABIDOPSIS HISTIDIN KINASEs
AHP	ARABIDOPSIS HISTIDINE PHOSPHOTRANSFER
AHP2	ARABIDOPSIS HISTIDIN CONTAINING PHOSPHOTRANSMITTER2
AI1	Arabidopsis Interactome 1
amiR	artificial micro RNA
AMPK	ADENOSIN MONOPHOSPHAT-ACTIVATED PROTEIN KINASE
AP2/EREBP	APETALA 2/ETHYLENE RESPONSIVE ELEMENT BINDING PROTEIN
ARF	AUXIN RESPONSE REGULATOR
ARR	ARABIDOPSIS RESPONSE REGULATOR
AS1	ASYMMETRIC LEAVES1
ATJ3	DNAJ HOMOLOG 3
AUX1	AUXIN RESISTANCE 1
AUXIAA	AUXININDOL-3-ACETIC ACID
AuxRE	Auxin Response Element
BA	6-Benzylamino purine
BAK1	BRI1-ASSOCIATED-RECEPTOR KINASE 1
BEE	BR-ENHANCED EXPRESSION
BiFC	bimolecular fluorescence complementation
BIM1	BES1-INTERACTING MYC-LIKE1
BIN2	BRASSINOSTEROID INSENSITIVE 2
BKI1	BRI1 KINASE INHIBITOR1
BKS1	BRASSINOSTEROID SIGNALLING KINASE 1
BL	Brassinolide
BPM3	BTB-POZ AND MATH DOMAIN3
BR	Brassinosteroids
BRI1	BRASSINOSTEROID INSENSITIVE 1
BSU1	BRI1-SUPPRESSOR1
BZR	BRASSINAZOLE RESISTANT

CBL9	CALCINEURIN B-LIKE PROTEIN 9
CDG1	CONSTITUTIVE DIFFERENTIA GROWTH 1
cDNA	complementary DNA
CHASE	Cyclases/Histidine kinases Associated Sensory Extracellular
CHX	cyclo-heximide
CIPK	CBL-INTERACTING PROTEIN KINASE
CK	Cytokinins
CLSM	confocal laser scanning microscope
CO	CONSTANS
COI1	CORONATIVE INSENSITIVE 1
Col	Columbia
COS1	COI1 SUPPRESSOR1
CTR1	CONSTITUTUVE TRIPLE RESPONSE1
D14	DWARF14
D14L	DWARF14 LIKE
D6PK	D6 PROTEIN KINASE
DAD2	DECREASED APICAL DOMINANCE 2
DB	DNA binding domain
DDL	DAWDLE
EBF	EIN3 BINDING F-BOX
EDS1	ENHANCED DISEASE SUSCEPTIBILITY
EIN	ETHYLENE INSENSITIVE
ERS1	ETHYLENE RESPONSE SENSOR
ET	Ethylene
ETR	ETHYLENE RESPONSE
FDR	False discovery rate
FP6	FARENSYLATED PROTEIN 6
FQR1	FLAVODOXIN-LIKE QUINONE REDUCTASE 1
FT	FLOWERING LOCUS T
GA	Gibberellins
GAI	GIBBERELLIC ACID-INSENSITIVE
GI	GIGANTEA
GID1	GA-INSENSITIVE DWARF1
GL3	GLABRA3
GO	Gene Ontology
HB21	HOMEOBOX 21
HHO	HYPERSENSITIVITY TO LOW PI-ELICITED PRIMARY ROOT SHORTENING HOMOLOGOLOGY
HPK	HISTIDINE PROTEIN KINASE

HSI2	HIGH LEVEL EXPRESSION OF SUGAR-INDUCIBLE GENE2
HSP	HEAT SHOCK PROTEIN
HUB1	HISTONE MONO-UBIQUITINATION 1
IAA	Auxins
IBR5	INDOL-3-BUTYRIC ACID RESPONSE 5
IDD	INTERMEDIATE DOMAIN
IMPA	IMPORTIN ALPHA ISOFORM
JA	Jasmonic acid
JAM2	JASMONATE ASSOCIATED MYC2 LIKE 2
JAZ	JASMONATE ZIM DOMAIN
KAI2	KARRIKIN INSENSITIVE 2
KAR	Karrikins
LBD	LATERAL ORGAN BOUNDARIES DOMAIN
LCI	literature curated interactions
Ler	Landsberg erecta
LRR	Leucin Rich Repeat
MAPKKK	MAPKK-KINASES
MAX2	MORE AXILLARY BRANCHES 2
MEE44	MATERAL EFFECT EMBRYO ARRESTED 44
MeIAA	methyl IAA
MHC	multiple hypothesis correction
MKK	MAPK-KINASES
MPK	MITOGEN ACTIVATED PROTEIN KINASE
NAP1;1	NUCLEOSOME ASSEMBLY PROTEIN1;1
NF-YA	Nuclear factor YA
NIA2	NITRATE REDUCTASE2
NIMIN	NIM1 INTERACTING
NINJA	NOVEL INTERACTOR OF JAZ
nM	nanomolar
NPR	NONEXPRESSER OF PATHOGENESIS-RELATED GENES
OPDA	12-oxophytodienoic acid
ORF	open reading frame
PAC	Paclobutrazol
PAMP	Pathogen-Associated Molecular Pattern
PAT	Polar Auxin Transport
PCD	programmed cell death
PGP1	PHOSPHATIDYLGLYCEROLPHOSPHATE SYNTHASE

PhI	Phytohormone Interactome
PhO	Phytohormone ORFeome
PID	PINOID
PIN	PIN FORMED
PKS	PROTEIN KINASE S
pM	picomolar
PP2A	PROTEIN PHOSPHATASE 2A
PP2AA2	PROTEIN PHOSPHATASE 2A SUBUNIT A2
PP2CA	PROTEIN PHOSPHATASE 2CA
PP2Cs	PROTEIN PHOSPHATASE 2C
PPI	protein-protein interactions
PTI	PAMP-triggered immunity
PUB39	PROTEIN UBIQUITINATION 39
PYL	PYR1-LIKE
PYR1	PYRABACTIN RESISTANCE1
QR	QUINONE REDUCTASE
RCAR	REGULATORY COMPONENT OF ABA RECEPTOR
RCN1	ROOTS CURL IN NPA
Rep-TF	repressor transcription factor screen
RGA	REPRESSOR of GAI
ROS	reactive oxygen species
SA	Salicylic acid
SAR	Systemic Acquired Resistance
SCF	SKP1-CULLIN-F-BOX
SCR	SCARECROW
SHR	SHORT ROOT
SIP	SOS-INTERACTING PROTEIN
SKP1	ARABIDOPSIS SERIN/THREONIN KINASE ASK1
SL	Strigolactones
SLY1	SLEEPY1
SMAX	SUPRESSOR OF MAX2
SMXL	SMAX-LIKE
SNF1	SUCROSE NON FERMENTING 1
SNRKs	SNF1-Related protein Kinase
SOC1	SUPPRESSOR OF OVEREXPRESSION OF CO 1
SOS	SALT OVERLY SENSITIVE
SPY	SPINDLY
TCP	TEOSINTE BRANCHED, CYCLOIDEA AND PCF
TF	transcription factor
TGA	TGACG SEQUENCE-SPECIFIC BINDING
TIR1	TRANSPORT INHBITOR RESPONSE 1
TPL	TOPLESS

TT4	TRANSPARENT TESTA 4
TTL	TRANSTHYRETIN-LIKE
WRKY	WRKY
Y2H	yeast-two-hybrid

1 Introduction

1.1 Phytohormone function in regulation of developmental processes and stress responses

Plants are forced to adapt to all environmental changes, due to their immobility, in order to complete their life cycle efficiently. They are able to adapt to the changing seasons by recognizing the light intensity and day length. However, they are also able to detect temperature, humidity, drought and mineral occurrence and optimize the plant development accordingly. Plants have developed different strategies to survive environmental changes successfully. However, due to climate change, the seasons change and long periods of drought, heavy rainfall and floods, storms and cold snaps occur. These strongly fluctuating abiotic factors are a challenge for all plants, and can cause extreme problems in agriculture. The agriculture today is based on monoculture to gain high yield with minimal input of workload and money. This kind of agriculture focus on less variation in crops with a small range for biodiversity inside the crop-species (genetic erosion) [1]. Due to the low biodiversity and monoculture of modern cultivars, environmental changes, biotic and abiotic stresses often claim complete loss of yield [2]. Additionally, the shift in seasons and temperatures, as well as changes in humidity lead to the immigration of new pathogens.

The strategies for adaptation influence both the morphology of the plant and their decisions to induce or inhibit different developmental stages by altering biochemical and physiological processes [3, 4]. The adaptation to drought stress, for example, has the consequence that plants modify their growth and root architecture, but can also lead to the acceleration of reproductive processes in order to ensure the survival of the plant [5, 6]. By adapting to drought stress, the plants can become more susceptible to pathogens [7, 8]. Through the temperature changes the appearance of additional pathogens from other climatic regions makes plant defense even more difficult. In order to compensate abiotic and biotic stress factors, the plant must detect, transmit, combine and integrate different environmental signals to ensure survival. In these signal pathways, phytohormones play a very important role. In the last decades, research has intensely investigated the different phytohormone signaling pathways and discovered the influence of different signaling pathways on individual development processes and response to biotic and abiotic stresses.

In order to understand exactly how these different phytohormone signaling pathways influence or interact with each other, it was necessary to analyze the core signaling pathways of all phytohormones and to understand the individual steps in each signaling pathway. Therefore all phytohormone signaling pathways are explained in more detail in the following sections.

1.2 Overview of phytohormone signaling pathways

Phytohormones are structurally unrelated small molecules, which occur in picomolar (pM) or nanomolar (nM) concentrations in the cells [9, 10, 11], and represent the starting point in signaling cascades. These hormones are known to be necessary for regulating plant growth, development and defense. According to the current state of research, there are ten different classes of phytohormones known: auxins , abscisic acid, brassinosteroids, cytokinins, gibberellins, ethylene, karrikins, jasmonic acid, salicylic acid and strigolactones.

1.2.1 Auxins

Auxins were discovered in 1935 by Thiemann and Koepfli as a growth inducing substance in shoot and root [12]. Since then, various studies have discovered a multitude of auxin regulated developmental processes. Auxins are essential for embryonic and postembryonic development [13, 14], in the organization and development of the root [15, 16, 17, 18] and shoot [19, 20] and for almost every growth and development step through the regulation of cell division, cell elongation [21, 22] and cell differentiation in the plant [23, 24, 25]. The indol-3-acetic acid molecule is a weak organic acid consisting of a planar indole ring structure carrying a side chain with a terminal carboxyl group. This carboxyl group is protonated at low pH and can diffuse across the membranes. Additionally, auxins can be actively transported into cells by the AUXIN1/LIKE-AUX1 (AUX/LAX) auxin influx transporters. Since a higher pH value exists within the cytosol, the auxin molecules are deprotonated and thus negatively charged. With this negative charge auxins have to be transported across the membrane by PIN FORMED (PIN) efflux transporters or PHOSPHATIDYLGLYCEROLPHOSPHATE SYNTHASE 1 (PGP1), also an efflux transporter. Through this plasma membrane localized influx and efflux transporters, auxins are actively transported across cells and tissues in the plant. With these transporters the plant is able to establish auxin gradients as well as auxin maxima and minima, which play an essential role in auxin controlled development processes [26]. The regulation of these transporters is controlled by the D6 PROTEIN KINASE (D6PK) [27, 28] and the kinase PINOID (PID) [29, 26], which both belong to the AGCVIII kinase family [30]. PID encodes a protein serine/threonine kinase and is known for its role as a regulator of polar auxin transport (PAT) [31, 30]. A series of studies have shown that PID phosphorylates auxin efflux carrier PIN proteins and auxin efflux transporter ATP-BINDING CASSETTE subfamily B (ABCB) [32, 33]. But the complex mechanism how PID leads to altered PIN1 polarity, shown by a PID overexpressor line [34], is not fully understood. Overall, PID specifically regulates the auxin transport by the subcellular localization of the PIN proteins [29] and the ABCB transport [32, 33]. Studies have shown that the PAT is additionally controlled by the activity of MITOGEN ACTIVATED PROTEIN KINASEs (MAPK). The MAP-kinase cascades were first investigated in humans and yeast [35, 36, 37] and later discovered in plants. In plants, the MAP-kinase cascade is not only known to be involved in plant defense (biotic) or stress responses (abiotic) [38, 39, 40, 41], but also in different steps in plant development and hormone signaling [42, 43]. In 2006, a regulatory function of the MAP-kinase cascade on the PAT was demonstrated for the first time [44]. Ten years later Jia et al., 2016 [45] reported that MKK7-MPK6 cascade is able influence PAT by PIN1 phosphorylation through MPK6. PAT is necessary to regulate the differential distribution of auxins in the

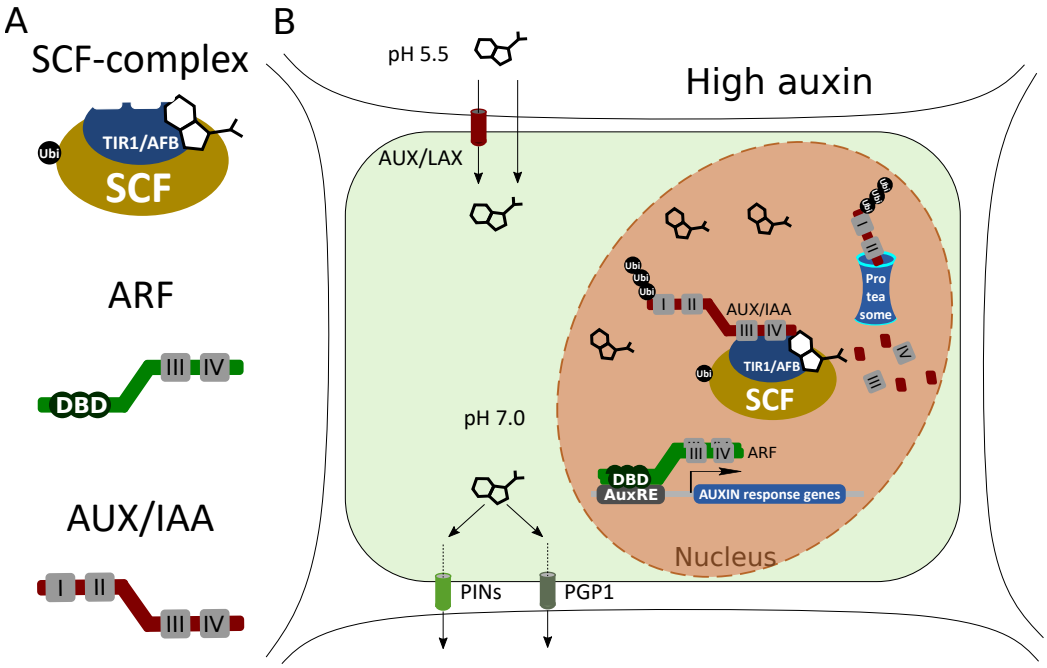

Figure 1.1: Auxin signaling pathway. (A) Exemplary representation of the three core components, SKP1-CULLIN-F-Box (SCF) TIR/AFB complex, the AUXIN RESPONSE FACTOR (ARF) and the AUX/IAA proteins. (B) Exemplary representation of the auxin signaling pathway in the presence of high auxin concentration. Auxin import by AUX/LAX influx carrier and PINs as well as PGP1 auxin efflux transporter. In the presence of auxin the SCF-TIR/AFB complex binds AUX/IAA and promotes their degradation via the proteasome. Thereby the ARF protein is able to induce expression of the auxin response genes.

plant tissues and cells to generate auxin gradients, which are essential for several auxin regulated developmental processes [46, 47].

The auxin core pathway contains three substantials, the SFC complex in combination with different co-receptors (SKP1-CULLIN-F-BOX (SCF), TRANSPORT INHIBITOR RESPONSE1 (TIR1) and AUXIN SIGNALING F-BOX (AFB)1-5), the AUXIN RESPONSE FACTOR (ARF) proteins and all members of the AUXIN/INDOL-3-ACETIC ACID (AUX/IAA) protein family. The SCF complex is an E3 ubiquitin ligase complex that is responsible for the ubiquitination and transduction to degradation of proteins in the different signaling pathways. The F-box protein is the variable component that enables the SCF complex to bind specifically to different proteins. TIR1 and AFB1-5 are the co-receptors and F-box proteins that are necessary components of the SCF-E3 ubiquitin ligase complex in the auxin signaling pathway. The ARF are transcription factors (TF) and the protein family contains of 23 members [48]. These TF are responsible for the induction and repression [49] of the target genes in the auxin signaling pathway /see figure 1.1 and A.1). ARF bind to the auxin response element (AuxRE) in the promoter of the target genes and induce or repress transcription. The AUX/IAA protein family contains 29 members and act as transcriptional repressors in the auxin signaling pathway [50, 51].

At low auxin levels, AUX/IAA proteins directly dimerize with ARF proteins to prevent their physical interaction with transcription initiation complexes in the promoter region of target genes[52] (see figure A.1 in the appendix). At high auxin concentrations, auxins

bind to the receptors, e.g. TIR1, in the SFC complex, which enables the complex to bind to the AUX/IAA, followed by their ubiquitination and transduction to the the 26S proteasome for degradation. The ARF are then able to initiate the transcription of the target genes through recruitment of chromatin remodeling enzymes (see figure 1.1). In the following text auxins were abbreviated with IAA and auxin signaling pathway with IAA signaling pathway.

Although Auxins (IAA) play a very important role in plant development, other hormones are necessary to regulate developmental processes. CK is known to act as antagonist to IAA in the development of the root, but both hormones are necessary to establish the correct combination of cell division zone, cell elongation zone and cell differentiation zone in the root [53, 54, 55]. In addition, ET plays an important role in lateral root formation, whereby IAA and ET act antagonistically [56, 57, 17]. IAA stimulates and ET inhibits lateral root formation and both together regulate the elongation of the primary root. The SA signaling pathway is involved in root development with regard to non necrotrophic pathogen defense responses and inhibits the IAA signaling pathways [58], whereas IAA and JA signaling pathways are required to mediate resistance to necrotrophic pathogens [59, 60].

1.2.2 Abscisic acid

Abscisic acid (ABA) is a classical plant hormone and was discovered by various research groups in the early 1950s as acidic compound. ABA was found to accelerate abscission via stabilization of an ethylene biosynthesis enzyme, which leads to a higher ET production [61, 62]. In the last three decades different studies could demonstrate that ABA has a function as a central regulator to abiotic stress like drought and as key regulator for seed maturation, seed dormancy, germination and early seedling development [63, 64, 65].

During seed development, endogenous ABA is upregulated and influences seed development, e.g in starch accumulation. [66, 67, 68]. In the later stages of seed maturation, ABA accumulates in the seeds and induce and maintain seed dormancy [69]. The ABA concentration decreases after seed imbibition by upregulation of ABA catabolism. The decrease in ABA in turn leads to GA accumulation, which then induces seed germination [70, 71].

The ABA signaling pathway consists of three core components: the ABA receptors, called REGULATORY COMPONENT OF ABA RECEPTORS (RCARs), also called PYRABACTIN RESISTANCE 1 (PYR1) and PYR1-LIKE (PYL) proteins, the negative regulators or repressors of ABA signaling, the PROTEIN PHOSPHATASE 2C (PP2Cs) from clade A, and the SNF1-related protein kinases (SNRK2s) (see figure 1.3).

The RCAR protein family consists of 14 members, and all have been suggested to function as ABA receptors [73, 74]. In the following text the ABA receptors are referred to RCAR1 – RCAR14. These receptors can be divided in three subclasses. Subclass I includes RCAR1-4, subclass II includes RCAR5-10 and subclass III includes RCAR11-14. The receptors from subgroup I and II (RCAR1-10) exists as monomers and dimers and are able to interact with the PP2Cs in the presence and in the absence of ABA. RCAR11-14 are present as inactive homodimers and need to be activated by ABA to inhibit PP2Cs function [75].

The PP2C super-family contains 80 members in *Arabidopsis thaliana*, however, only 9 members, called clade A, are involved in ABA signaling [76]. In the absence of ABA, the PP2Cs inactivate the SnRK2s by dephosphorylating their serine and thre-

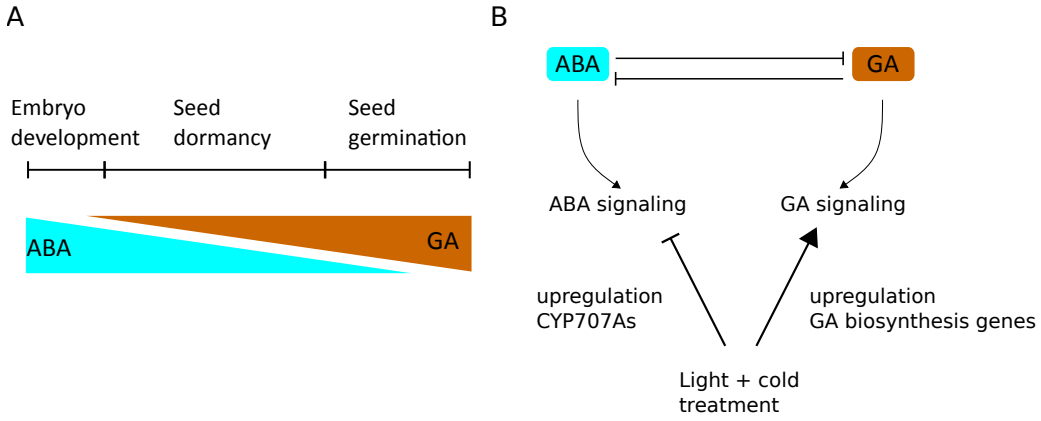

Figure 1.2: ABA function in dormancy. (A) Simplified presentation of the reciprocal influence of abscisic acid (ABA) and gibberellins (GA) during embryo development and seed germination. (B) a simplified regulatory mechanism of the ABA and GA interaction in seed germination. Light and cold treatment leads to upregulation of GA biosynthesis genes and upregulation of *CYC707A*s, ABA catabolism genes [72].

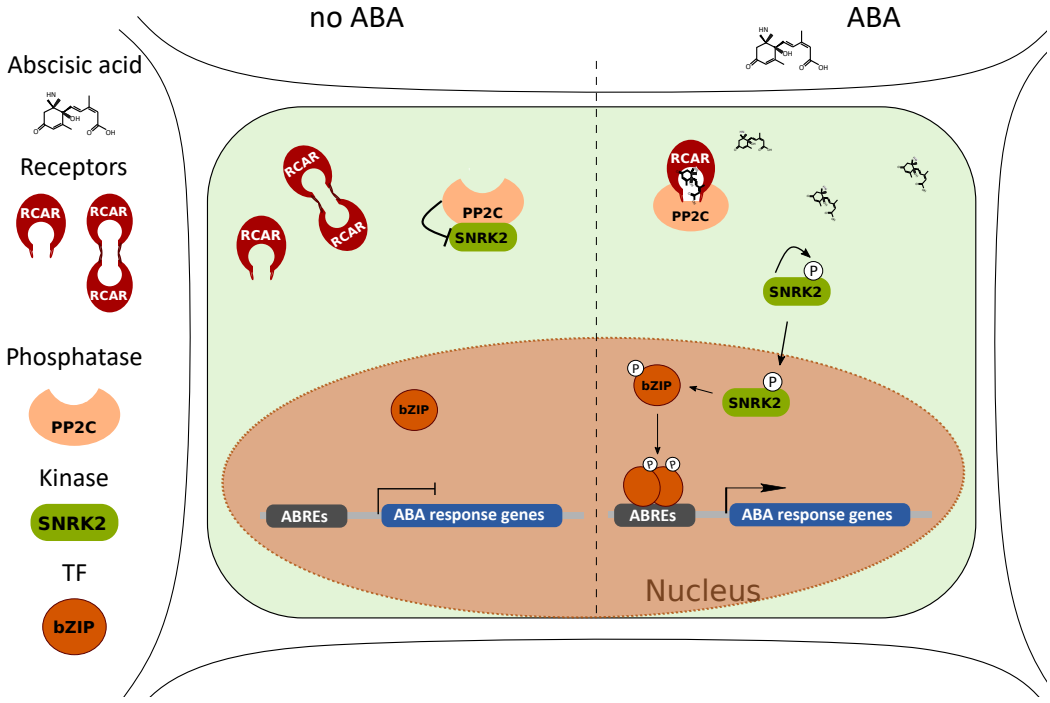

Figure 1.3: ABA signaling pathway. In the absence of ABA, RCARs are present as single molecules (RCAR1-10) or exists in homo or hetero-dimers (RCAR11-14). The PP2Cs bind and dephosphorylate SNRK2s to keep them in their inactive form to prevent expression of ABA response genes. In the presence of ABA, a single RCAR with bound ABA interacts with PP2Cs and interrupts their interaction with the SNRK2s. The released SNRK2s become active through autophosphorylation and induce downstream expression of ABA response genes by activating transcription factors through phosphorylation.

onine residues in their activation loop [77, 78]. The SNRK super-family contains 38 family members and form three clades based on sequence similarity and domain structure SnRK1, SnRK2 and SnRK3. The SNRK1-clade is the smallest of the three clades, but most closely related to yeast SUCROSE NON FERMENTING 1 (SNF1) in yeast and to ADENOSIN MONOPHOSPHAT-ACTIVATED PROTEIN KINASE (AMPK) from animals [79]. These SNF1/AMPK family protein kinases are highly conserved and known to its function in energy homeostasis in mammals, plants and fungi [80]. The SNRK2-clade contains 10 family members (SNRK2.1 – SNRK2.10) which can be divided in three subgroups. Subgroup 1 (SNRK2.1, 2.10, 2.4, 2.5, 2.6), contains kinases that are not activated by ABA. Subgroup 2 (SNRK2.7, 2.8) are not or only very weakly activated by ABA (depending on plant species) and subgroup 3 (SNRK2.2, 2.3, 2.6) are strongly activated by ABA [81]. The SNRK3-clade is the largest group with 25 members, and consists of the CBL-INTERACTING PROTEIN KINASE (CIPK) proteins, SALT OVERLY SENSITIVE 2 (SOS2), SOS3-INTERACTING PROTEINs (SIP) and PROTEIN KINASE S (PKS) [79]. In low ABA concentration, for RCAR1-RCAR10, or in high concentration of ABA, for RCAR11-RCAR14, the RCARs bind to the PP2Cs. This results in the release of the SnRK2s. The SnRK2s are now able to auto-phosphorylate and additionally phosphorylate downstream bZIP proteins, which then bind as dimers to the ABSCISIC ACID RESPONSE ELEMENTs (ABRE) in the promoter of the target gene e.g. *ABI5*, and thereby induce transcription (see figure 1.3).

ABA is not alone responsible for drought stress responses, these abiotic stress responses are complex interactions of different phytohormones. During drought stress, the JA pathway [82, 83], the SA pathway [84, 85, 86], the GA pathway [87, 88] and the BR pathway [89, 90, 91] are known to interact with the ABA pathway to regulate the drought stress responses. For the CK [92] and IAA [93] signaling pathways, this has not yet been demonstrated, but first research results indicate that these might also be involved. Concerning the regulation of developmental processes in relation to abiotic stress, MYB TF family, with 133 members[94, 95], and the WRKY TF family with 72 members [96], become more important to play a roles in possible signal integration.

1.2.3 Brassinosteroids

In the 1930s to 1940s, the United States Department of Agriculture discovered that pollen extract promotes growth. After the investigation of numerous pollen from different plant species, Mitchell and his colleagues discovered in 1970 a new type of plant hormone, the Brassins [97, 98]. Of these brassinolides, or brassinosteroids today, 70 different compounds are known to date. Loss of function mutants with defects in BR biosynthesis or signal transduction show a dwarfed phenotype with reduced cell elongation, cell division, dark green color, reduced apical dominance, increased senescence and delayed flower induction [99, 100, 101, 102, 103]. This strong mutant phenotype already suggests that BR is involved in many developmental processes. Through further studies it was possible to determine the BR signal pathway [104, 105].

The BR core pathway consists of several important components, the receptor for BR and its co-receptor, two kinases with distinct repressive or inhibitory functions and two phosphatases, which are involved in activating the downstream signaling. The BR receptor BRASSINOSTEROID INSENSITIVE 1 (BRI1) is a transmembrane protein. BRI1 encodes a leucine-rich-repeat (LRR) receptor like kinase, which receives the extracellular BR signal and leads to intracellular phosphorylation events [106, 107, 99]. In the absence

or low BR concentrations BRI1 KINASE INHIBITOR1 (BKI1) binds intracellular to BRI1 c-terminal part [108]. This impedes BRI1 from transmitting a signal via auto and trans-phosphorylation to the co-receptor BRI1-ASSOCIATED-RECEPTOR-KINASE 1 (BAK1) to the downstream signaling components of the signaling pathway. BAK1, also a transmembrane protein, encodes a serin/threonine kinase with five LRR structures [109, 110].

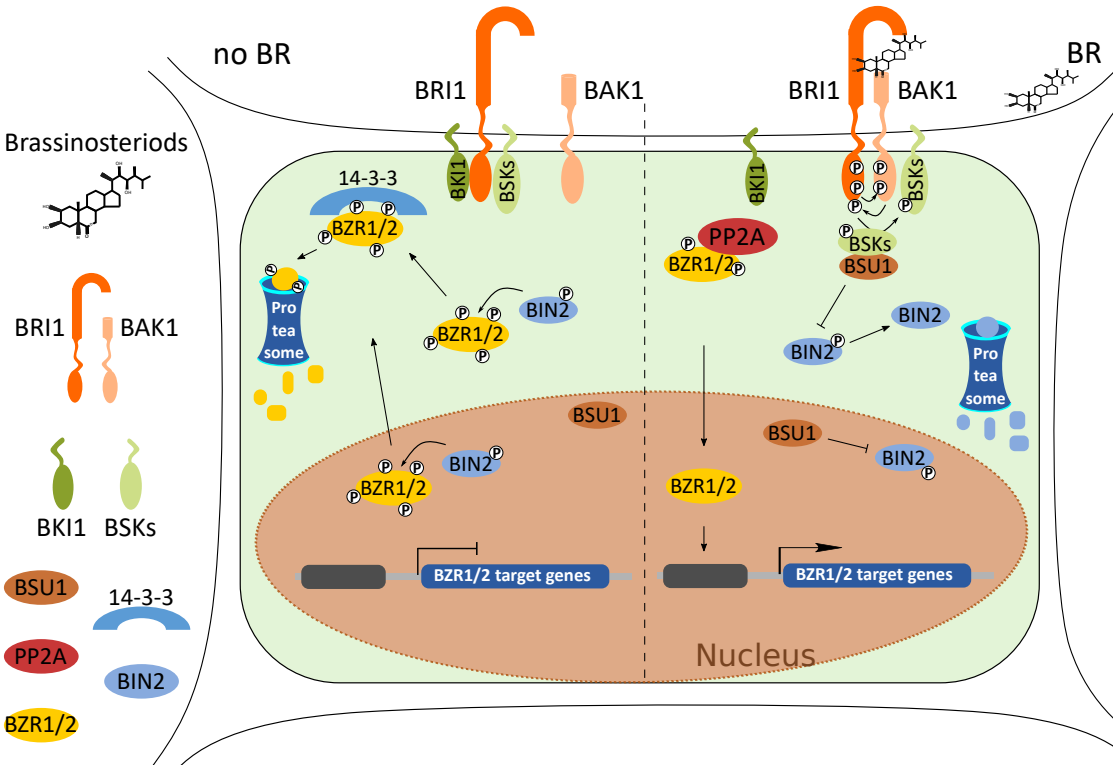

Figure 1.4: Brassinosteroid signaling pathway. In the absence of BR (left half of the cell), the receptor BRI1 is inhibited by BKI1 and BIN2 phosphorylates the transcription factors BZR1 and BZR2 in the cytosol as well as in the cell nucleus and mark them for degradation. Phosphorylated BZR1/2 are guided via 14-3-3 proteins to the 26S proteasome for degradation. In the active BR signaling pathway (right half of the cell) BR binding to BRI1 results in BRI1 BKI1 separation, which leads to auto and trans-phosphorylation between BRI1 and BAK1 and the phosphorylation of BSK proteins. The activated BSK proteins bind to BRI1-SUPPRESSOR1 (BSU1) and activate the phosphatase, which then dephosphorylates BIN2, which leads to the degradation via the 26S proteasome. The transcription factors (BZR1/2) are dephosphorylated in the cytosol by the PP2A and migrate into the cell nucleus to control the transcription of the target gene.

Intracellularly, in the absence of BR, the transcription factors BRASSINAZOLE RESISTANT 1(BZR1) and BZR2 (also known as BRI1-EMS-SUPPRESSOR 1 (BES1)) are phosphorylated by the kinase BRASSINOSTEROID INSENSITIVE 2 (BIN2) and guided to the 26S proteasome by 14-3-3 proteins for degradation. BIN2 phosphorylates BZR1/2 in the cytosol but also in the nucleus, which prevents further induction of targets via BZR1/2 (see figure 1.4 left part) [111, 112, 113]. If BR is bound by BRI1, BKI1 and BRI1 become separated (see figure 1.4). In addition, BRI1 auto-phosphorylates itself and transphosphorylates BAK1, which in turn phosphorylates BRI1 at an additional site (see figure 1.4). BRI1 then activates two membrane-anchored cytoplasmic kinases, BRASSINOSTEROID-SIGNALLING KINASE1 (BSK1) and CONSTITUTIVE

DIFFERENTIAL GROWTH1 (CDG1) (CDG1 is not in figure 1.4) through their phosphorylation [114, 115]. BSK proteins and CDG1 now bind to the phosphatase BRI1-SUPPRESSOR1 (BSU1) and activate it by phosphorylation [114, 116, 117]. BSU1 now dephosphorylates BIN2, which leads to its degradation via the 26S proteasome [118]. The two transcription factors BZR1 and BZR2 are now dephosphorylated by the PROTEIN PHOSPHATASE 2A (PP2A) [119] and migrate into the cell nucleus, where they bind to the promoter of their target genes and activate or repress target genes [120, 121, 122, 123] (see figure 1.4 part right).

Most of these developmental processes are known to be regulated by different phytohormone signaling pathways. This has been confirmed for ABA and BR in seed germination [70, 124, 125], for IAA and BR in hypocotyl elongation and root development [126, 127], and GA and BR in promoting stem elongation and plant growth [128, 129]. This indicates the important role of the BR signaling pathway and at the same time it confirms the regulation of developmental processes by several phytohormone signaling pathways.

1.2.4 Cytokinins

Cytokinin (CK) was first identified as a cell division promoting substance extracted from herring sperm and was called kinetin [130]. A few years later a kinetin-like compound, isolated from maize and later called zeatin, could be isolated [131]. Further studies described the stimulating or inhibiting functions of CK in different development processes such as seed germination, leaf initiation, onset of flowering and root growth as well as root branching [131, 54, 132]. The cytokinin signaling pathway has similarities to bacterial and yeast two-component signal transduction pathways.

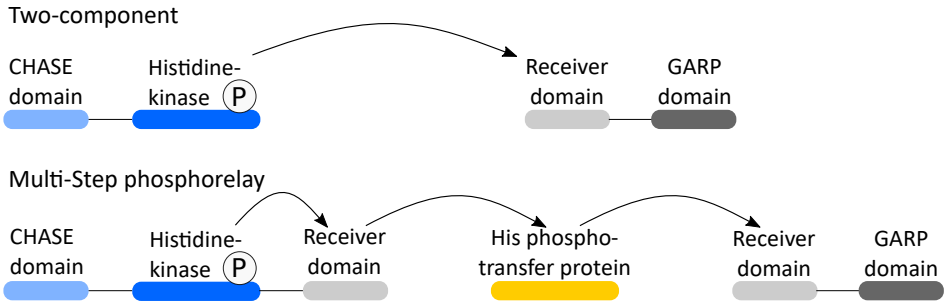

Figure 1.5: Two component vs multi-step phosphorelay system. The two component system consists of a kinase (blue) and a response regulator (gray). Upon environmental stimulus the kinase autophosphorylates and trans-phosphorylates the receiver domain of the response regulators. A multi-step phosphorelay system consist of a kinase with receiver domain, a histidine phosphotransfer protein (yellow) and a response regulator. In this system an environmental stimulus leads to autophosphorylation. This phosphoryl group is transferred from His to Asp in the receiver domain of the kinase. Then the phosphoryl group is transferred to the His phosphotransfer protein and subsequently to the receiver domain of the response regulator. Modified from [133]

Those two-component systems consist of a membrane localized HISTIDINE PROTEIN KINASE (HPK) that sense environmental stimuli, and a second component, the response regulator, that transmits the output signal [134, 135]. HPK are present in bacteria, archaea and eukaryotes (not in animals) and serve together with a response regulator as signal-transduction enzymes [136]. The two component system in bacteria is known to be required for immediate responses to external stimuli [137]. The more complex multistep

His-to-Asp phosphorelay system (see figure 1.5), which forms the bases of the core CK pathway, was found to be more sensitive to external stimuli and responses more robustly to noises [137].

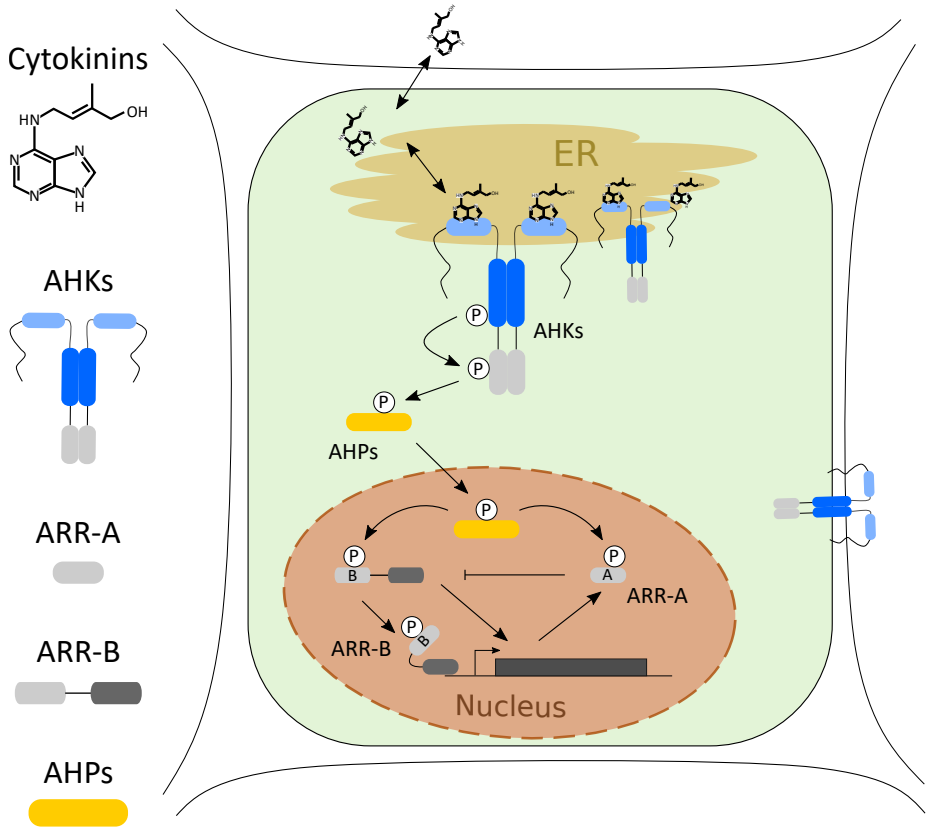

Figure 1.6: Cytokinin signaling pathway. When cytokinin is bound to the CHASE (Cyclases/Histidine kinases Associated Sensory Extracellular) domain of the cytokinin receptors (AHK), the histidine kinase domain autophosphorylates their receiver domain. The receiver domain phosphorylates the AHP which then migrates into the nucleus to phosphorylate type-A (ARR-A) and type-B ARR (ARR-B). Once activated by phosphorylation the ARR type A and Type B regulates transcription. AHK1 is localized at the plasma membrane which is involved in perceiving changes in osmolarity and regulation of further physiological mechanisms. Other AHK (AHK2-4) are integrated by an unknown mechanism into the ER to induce CK regulated transcription. Modified from [133]

The CK signaling pathway in *Arabidopsis thaliana* consists of three core components, the ARABIDOPSIS HISTIDIN KINASEs (AHK), the ARABIDOPSIS HISTIDINE PHOSPHOTRANSFER proteins (AHP) and the ARABIDOPSIS RESPONSE REGULATOR (ARR) proteins. The *Arabidopsis thaliana* genome encodes 10 putative histidine kinases, five are ethylene receptor histidine kinases and five non-ethylene receptor histidine kinases AHK2, AHK3, AHK4, AHK5 and CKI1 [138]. For AHK2, AHK3 and AHK4 it could be confirmed that these are CK receptors [139, 140]. The AHP are a small family of six related proteins (AHP1-AHP6) [141]. The AHP mediate a phosphotransfer between the CK receptors to type A and type B ARR [142, 143, 141]. The ARR family consists of 17 members which can be categorized into type A and type B. There are 10 type A ARR and 7 type B ARR [144]. The type B ARR are transcription factors with a GARP-like DNA binding domain (C-terminal) [145] and an N-terminal receiver

domain, which are known as transcriptional activators. Type A ARR do not have a DNA binding domain but only a receiver domain and are known as transcriptional repressors in CK signaling pathway [146] (see figure 1.6 part A). At high CK concentrations, the transmembrane receptors (AHK) are able to bind CK via the extracellular CHASE domain (Cyclases/Histidine kinases Associated Sensory Extracellular) and send a signal as phosphotransfer from the histidine kinase domain to their receiver domain. The CHASE domain is a predicted ligand-binding domain that mediates signal transduction in the CK receptors [147]. The receiver domain then phosphorylates the AHP as mediator between receptor and response regulators. The AHP phosphorylate type A ARR, to prevent their repressive function. At the same time, type B ARR are also phosphorylated, which bind to the DNA and initiate the transcription of CK responsive genes (see figure 1.6).

The CK signaling pathway is known to be involved in root development together with IAA but is also involved in adaptation to drought through CK and ABA signaling pathway interactions. Under drought stress, ABA induced MYB2 expression results in downregulation of *ISOPENTENYLTRANSFERASEs* (*IPTs*), resulting in reduction of endogenous CK levels. This ABA-CK interplay results in reduced shoot growth and enhanced root growth under drought stress [148, 149, 92].

1.2.5 Ethylene

Unlike other phytohormones, ethylene (ET) is a simple hydrocarbon gas (C_2H_4) produced in most plant tissues and cell types. Already around 1920 this gas was discovered to trigger plant growth, fruit ripening and senescence [150]. Additionally, ET is involved in leaf growth and development, as well as leaf senescence [151]. The function of ET in fruit ripening is well known and ET is used by industry for post ripening of unripe harvested fruits. ET gas is detected in plants via five receptors.

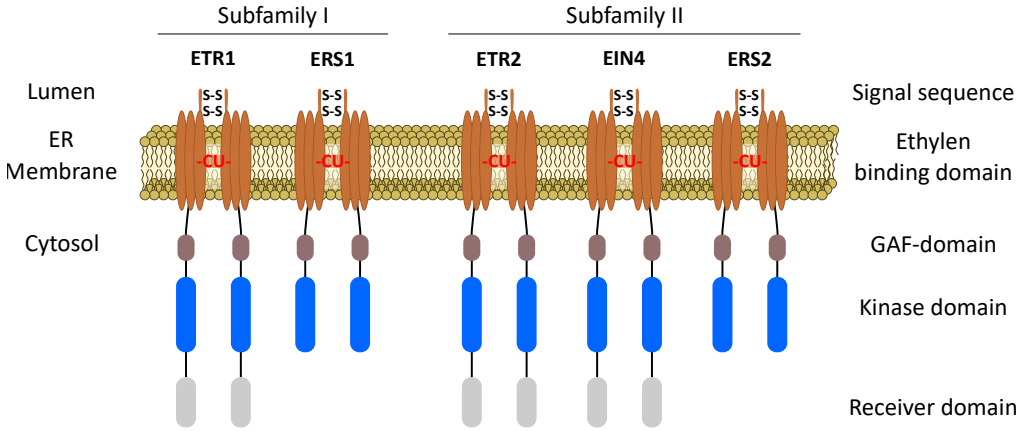

Figure 1.7: Ethylene receptors. The ET receptors are divided into two subfamilies due to the presence of the receiver domain. The receptors form homodimers at the membrane of endoplasmic reticulum (ER). The homodimer is stabilized by two disulfide bonds. The N-terminal transmembrane domain is, through a copper co-factor, more sensitive to ET binding and serves as ET binding domain. After the ET binding domain follows the GAF domain and the kinase domain, which groups the receptors into the subfamilies. This figure was modified form [152].

The first of five ethylene receptors ETHYLENE RESPONSE 1 (ETR1) [153, 154, 155] was discovered around 1988. The other four receptors ETR2, ETHYLENE RESPONSE SENSOR 1 (ERS1) and ERS2, as well as ETHYLENE INSENSITIVE 4 (EIN4) were

discovered between 1995-1998 [156, 157, 158]. These five receptors are transmembrane receptors, mostly located in the endoplasmic reticulum [159, 160], and are homologous to the bacterial two-component histidine kinases see figure 1.5. An N-terminal transmembrane domain consisting of three alpha helices was predicted for all five receptors. This is followed by the GAF (cGMP-specific phosphodiesterase, adenylyl cyclase, and FhlA) domain. The GAF domain was analyzed in yeast and it could be shown that this domain represents a new class of cyclic nucleotide receptors [161], but the function in the ET receptors could not yet be determined [162]. The GAF domain is followed by a kinase domain, that divides the five receptors into two subfamilies. The subfamily I (ETR1 and ERS1), contains all important amino acid residues required for the function of a histidine kinase [154, 156]. Subgroup II members (ETR2, ERS2 and EIN4) have a degraded histidine kinase but functions in vitro as a viable serine/threonine kinase [157, 158, 163, 164].

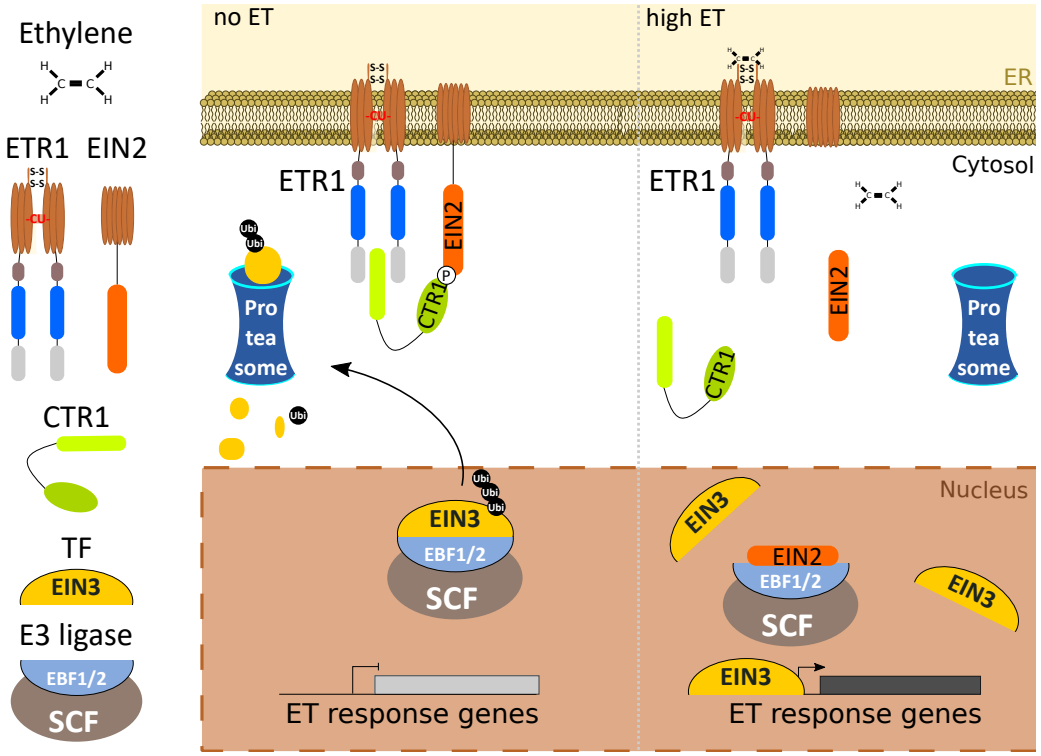

Figure 1.8: Ethylene signaling pathway. ETR1 interacts with CTR1 in the absence of ET, which leads to phosphorylation of EIN2 by CTR1. By inhibiting EIN2, the SCF EBF1/2 complex is active and ubiquitinates EIN3 for degraded via the 26S proteasome. At high ET concentration ET binds to the receptor, which leads to its inactivation and release of CTR1. Thus EIN2 cannot be further phosphorylated by CTR1 and subsequently cleaves off its C-terminal part, which migrates into the cell nucleus and inhibits the E3 ubiquitin ligase complex. EIN3 is no longer degraded, accumulates in the nucleus and starts the transcription of the target genes. The outgoing ethylene response is proportional to the amount of accumulating EIN3 protein.

The receptors ETR1, ETR2 and EIN4 also contain a receiver domain. However, studies in ETR1 have shown that the receiver domain is not necessary for growth regulation (or inhibition) triggered by ethylene [165, 166] (see receptor overview in figure 1.7). In contrast to other phytohormone signaling pathways, ET receptors actively transmit signals in the absence of phytohormone. This signal is transmitted to the negative regulator

CONSTITUTUVE TRIPLE RESPONSE1 (CTR1) bound at the C-terminus of the receptors in the absence of ET. CTR1 belongs to the family of RAF-like MKK kinases, and inhibit the transmembrane protein EIN2 by direct interacting and phosphorylation [167]. By rising ET concentrations, ET binds to the receptor. This leads to inactivation of the receptor and also to release of CTR1. Without the negative regulation of CTR1, EIN2 C-terminus is cleaved off and moves into the nucleus. In the nucleus EIN2 inhibits the $SCF_{EBF1/2}$ (EIN3 BINDING F-BOX protein 1/2) E3 ubiquitin ligase complex and thus prevent the degradation of EIN3 [168]. EIN3 is known for its function as ethylene positive regulator and for the activation of all known ethylene responses. Additionally, the protein level of EIN3 directly reflects the strength of the resulting ethylene signal [168]. This accumulation of EIN3 in the nucleus finally leads to binding to the promoters of the target gene, i.e. the ethylene response factors (ERF) and their transcriptional regulation. The ERF belong to one of the major transcription factor families in *Arabidopsis thaliana*, the APETALA 2/ETHYLENE RESPONSIVE ELEMENT BINDING PROTEIN (AP2/EREBP). The AP2/EREBP transcription factors have been implicated in hormone, sugar and redox signaling in context of abiotic stresses such as cold and drought [169, 170]. Although the ET pathway is involved in several developmental processes, none of these are regulated by ET alone. For example, the ET pathway interacts with the IAA signaling pathway to promote root hair elongation [15, 16] or for fruit ripening [171] and it interacts with the GA signaling pathway to regulate leaf growth under water-limiting conditions [151]. ET is also known to play a important role in pathogen defense, either together with SA signaling pathway against biotrophic pathogens or with JA signaling pathway against necrotrophic pathogens [172, 173]. ET is also known to negatively regulate seed dormancy by inhibiting ABA signaling, whereas ABA and ET inhibit root growth synergistically [174].

1.2.6 Gibberellins

Gibberellins (GA) were discovered in 1917 as secondary metabolites of the rice pathogenic fungus *Fusarium fujikuroi* (*teleomorph Gibberella fujikuroi*) [175]. The disease, caused by the fungus, leads to abnormal plant growth, yellowish-green leaves and root lesions, as well as defects in grain production, resulting in dramatically reduced grain yields. Over the next few years, intensive research was carried out on these substances, which triggered these effects in the plant. In 1955 it was possible to separate the abnormal growth of young tissue causing substances into three components of Gibberellin A [176]. The GA can be divided into two groups, those with 19 or 20 carbon units, which form either four or five ring systems. Studies with plants, fungi and bacteria resulted in the identification of 136 different GA [177]. However, all bioactive GA are the C19-GA and their most important ones are GA1, GA3, GA4 and GA7. The GA signaling pathway plays a role in the regulation of seed germination [178], stem elongation and growth [179] as well as transition from vegetative into reproductive phase. The *Arabidopsis thaliana* GA core pathway consists of three components: the three GA-INSENSITIVE DWARF1 (GID1) receptors, the five DELLA repressors and the $SCF_{SLEEPY1\ (SLY1)}$ E3-ubiquitin ligase complex. Ueguchi-Takana identified the receptor GID1 in rice in 2005 and showed its high affinity for GA4 and its binding to the repressor SLENDER1, the only DELLA protein in rice [180]. Further studies then identified the three currently known GA receptors GID1A, GID1B and GID1C in *Arabidopsis*, which are orthologues to rice GID1 [181]. Also these GID1 receptors from *Arabidopsis* had a high affinity for GA and bound

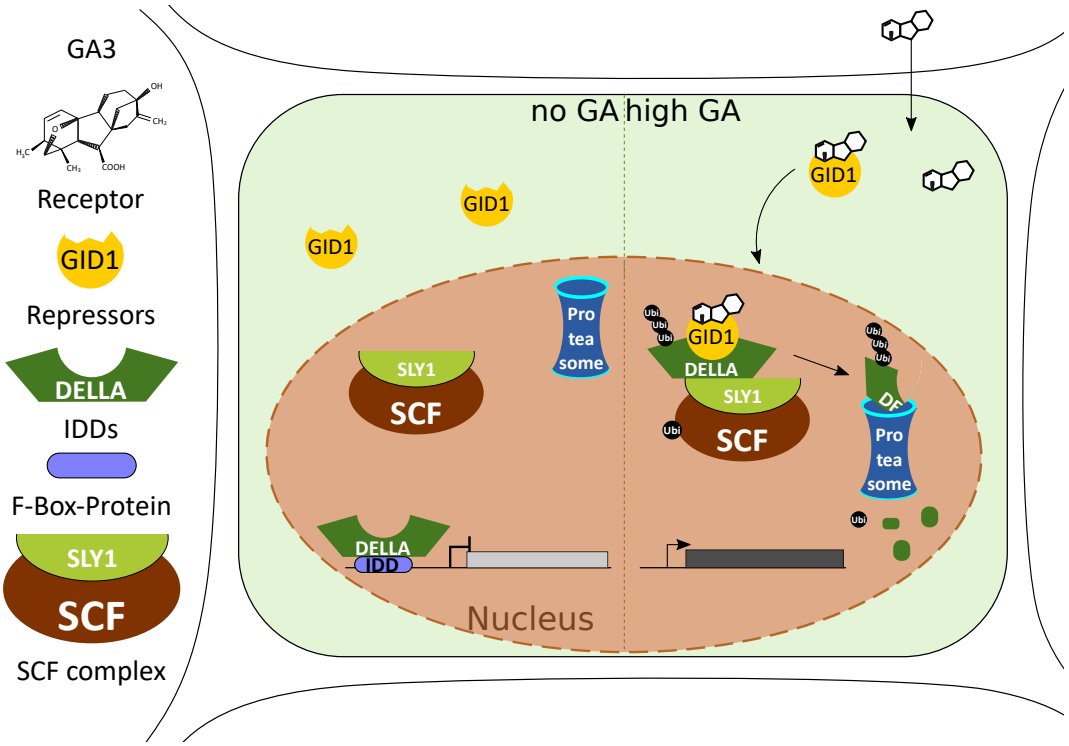

Figure 1.9: Gibberellin signaling pathway. In the absence of GA, the transcription of GA responsive genes are suppressed by the GA repressors, DELLA proteins. These bind to so called INTERMEDIATE DOMAIN family proteins (IDD) bound to the promoters of GA responsive genes and block transcription. In the presence of GA, GA binds to the receptors GA INSENSITIVE DWARF1 (GID1) (A,B,C). Through a conformational change, the GID1 receptor can now bind to the repressors (DELLA proteins) and recruit them to the SCF_{SLY1} E3 ubiquitin ligase complex. This complex ubiquitinates DELLA proteins, which lead to their degradation by the 26S proteasome. This results in transcriptional initiation of GA responsive genes.

to DELLA proteins. In contrast to SL1 in rice, *Arabidopsis* contains five homologous DELLA proteins. These DELLA proteins, founding members of the GRAS protein family, are known for their function as repressors in the GA signaling pathway. GRAS proteins are an important family of transcriptional regulators in plants, named after the first three members: GIBBERELLIC ACID-INSENSITIVE (GAI), REPRESSOR of GAI (RGA), and SCARECROW (SCR). Various studies identified the five DELLA proteins RGA, GAI, RGA-Like1 (RGL1), RGL2 and RGL3 and investigated their role in the GA signaling pathway [182, 183, 184, 185, 186]. The last core component in the GA signaling pathway is the SCF_{SLY1} E3-ubiquitin ligase complex. The binding specificity regarding to the GA signaling pathway of the SCF complexes is mainly due to the F-box protein SLY1. SLY1, which is the orthologues F-box protein to rice GID2 F-box protein, can bind to DELLA proteins and the SCF complex targets them for degradation [187, 188]. This core pathway is involved in multiple developmental steps, which can be specifically regulated due to the different GID1-DELLA combinations.

In the absence of bio-active GA, the DELLA proteins inhibit various GA target genes. For a long time it was unclear how exactly DELLA proteins repress the expression of GA response genes, since they lack a DNA binding domain. Recent studies showed that DELLA proteins bind to the IDD proteins to repress gene regulation [189]. In high GA

concentrations GA bind to the GID1 receptors. This leads to a conformational change of the receptor and enables interaction with the DELLA proteins and binding to the SCF E3-ubiquitin ligase complex and subsequent degradation by the 26S proteasome (see figure 1.9).

The GA signaling pathway is involved in many developmental processes and GA is assumed as positive regulator, whereas ABA negatively regulates these processes and can therefore be considered a GA antagonist in some processes [190]. Besides the seed germination inducing effect of GA, the DELLA proteins together with the ABA specific transcription factors ABI3 and ABI5 have an inhibitory effect on seed germination [191]. This example shows the complexity of the GA signaling pathway in growth promoting processes. DELLA proteins also play a major role in cell elongation by preventing transcription factors from the BR and IAA pathways from forming a complex that can induce cell elongation [192, 193, 194, 195]. DELLA proteins also have an important role with regard to the fine tuning mechanism defense over growth, where DELLA proteins interact directly with JAZ1 and thereby initiate JA-specific defense reactions [196, 197].

1.2.7 Salicylic acid

In addition to abiotic environmental influences, plants are also constantly exposed to biotic stresses. Plants have developed a complex protection system to minimize pathogen infections. After pathogen attack, plants recognize so-called conserved pathogen-associated molecular pattern (PAMP) on the cell surface through their pattern recognition receptors [198]. The PAMP then induces PAMP-triggered immunity (PTI) as an active defense system [199]. The PTI induces a wave of immune response in the more distant (distal) tissue of the plant, known as Systemic Acquired Resistance (SAR) [198]. SAR is a defense mechanism that primes the plant after primary pathogen infection to produce a more rapid and strong cellular defense response after the secondary pathogen infection [200, 201]. In order to counteract this PTI defense mechanism, various pathogens can inject so-called effectors into the infected plant cell, which can interrupt the PTI signaling pathway. These effectors can be recognized by intracellular receptors, which trigger the effector triggered immunity (ETI) in the plant, often associated with the programmed cell death (PCD) of the infected cells. Both PTI and ETI also trigger SAR, which starts the production of the immune signal salicylic acid (SA) in chloroplasts and initiates the salicylic acid (SA) signaling pathway. The SA pathway and the resulting immune responses such as PTI, ETI and PCD are specifically regulated by the amount of SA in the cell. The immune signal and plant hormone SA is recognized by the SA receptor NONEXPRESSER OF PATHOGENESIS-RELATED GENES (NPR) 1, and its homologous NPR3 and NPR4 (NPR1, NPR3, NPR4).

The SA core signaling pathway contains three components, the receptor and simultaneously co-activator NPR1, and its homologous NPR3, NPR4, the repressors the NIM1 INTERACTING (NIMIN) proteins (NIMIN1-3) and the TGACG SEQUENCE-SPECIFIC BINDING proteins (TGA), which are transcription factors that bind to the promoter regions of the SA target genes.

The SA receptor NPR1, was identified by Cao et al. in 1994 and was intensively investigated [204, 205, 206]. NPR1 exists in two forms in the cell. At low SA concentrations (no pathogen attack), NPR1 is partially present as an oligomer in the cytoplasm. Monomeric NPR1 proteins interact with NPR4. This interaction leads to interaction with an cullin-RING E3 ubiquitin ligase complex and the immediate degradation of NPR1, thus pre-

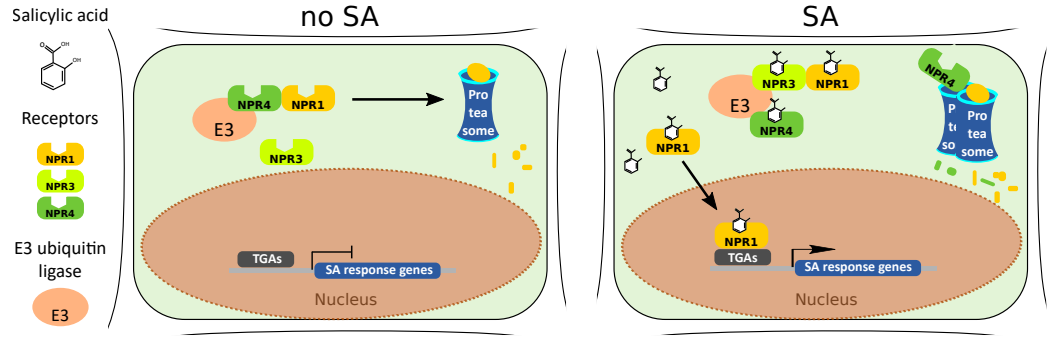

Figure 1.10: Salicylic acid signaling pathway. In the absence or at very low SA concentrations, NPR1 is bound by NPR4 and degraded by the cullin RING E3 ubiquitin-ligase complex [202] to prevent a permanent plant immune response. After infection with a pathogen and increasing SA concentration, NPR1 enters the cell nucleus and acts as a co-activator by binding to the TGA transcription factors. This induces transcription of the PR genes and thus immune response to the pathogen infection. Additionally, SA binds to NPR3 and NPR4, which leads to NPR3-NPR1 binding and results in NPR1, NPR3 and NPR4 degradation via the 26S proteasome. Modified from Fu et al., 2012 [203].

venting a permanent defense response of the plant. After infection with a pathogen, i.e. at medium SA concentrations, the NPR1 oligomers dissolve and monomeric NPR1 enters the cell nucleus and acts as a transcriptional co-activator at the target gene promoter [207, 208]. NPR1 is known as a co-activator and bind to TGA proteins, which are bound to the promoter of the *PATHOGENESIS-RELATED* genes (*PR*) and activates their expression, leading to the induction of SAR. At the same time, NPR3 and NPR4, which have a lower affinity to SA, bind to the cullin RING E3 ubiquitin ligase complex [202] and undergo degradation. At a very high SA concentration, SA also binds to NPR3 and NPR4, interacting with the NPR1-SA complex and degrading it by the E3 ubiquitin ligase complex (see figure 1.10). This step stops PR gene induction and usually leads to PCD. The TGA family consists of 10 members, which can be divided into three classes: category 1 with TGA1 and TGA4, category 2 with TGA2, TGA5 and TGA6, and category 3 with TGA3 and TGA7. The members TGA9, TGA10 and PERIANTHIA are separated. For category 2 and 3 it is known that they bind to the promoter of PR1 and interact with NPR1 [209, 210, 211]. Class 1 TGA interaction with NPR1 has not yet been demonstrated in yeast and in vitro, but is possible in vivo in SA treated leaves [212]. In addition to the TGA proteins, NPR1 also interacts with a second group of proteins, the NIMIN proteins. In *Arabidopsis* there are four NIMIN genes NIMIN1, NIMIN1b, NIMIN2 and NIMIN3 [213]. Many studies have focused on NIMIN proteins and their direct interaction with NPR1 has been discovered, as well as their function in the repression and regulation of SAR response [214, 215]. NIMIN1, -2 and -3 are expressed differently in *Arabidopsis*. While NIMIN3 is constantly expressed at a low level, NIMIN1 and NIMIN2 are responsive to SA. NIMIN1 and NIMIN3 suppress SA induced PR1 expression, while NIMIN2 does not negatively affect SA induced PR1 gene expression [215].

SA and JA are both phytohormone signaling pathways that control plant defense against pathogens. These two pathways are antagonistic to each other and are known for their direct interaction [216]. Through this interaction they control the type of defense

strategy related to the type of pathogen [217]. SA signaling pathway is not only involved in the defense against pathogens but also plays a big role in the plant response to abiotic stresses like drought in combination with the ABA signaling pathway, as mentioned before, but is additionally known to play a role in response to salinity and cold stress (ABA pathway) [84, 85, 86, 218].

1.2.8 Jasmonic acid

Additionally, to the biotic stress response through the SA signaling pathway, jasmonic acid (JA) has been identified to play a key role in the survival of plants regarding to response to necrotrophic pathogens and herbivores. On one hand, JA support the adaptation of the plant to biotic and abiotic stresses, as well as the fine-tuning between growth and defense to ensure the plant's optimal fitness [219]. On the other hand, they coordinate different developmental processes such as root growth and fertility [220, 221]. JA were first isolated as jasmonic acid methyl ester in 1962 from the oil of the *Jasminum grandiflorum* plant [222]. Later on jasmonate isoleucine was discovered as a bioactive hormone which binds to the JA receptor to start the signaling pathway [223].

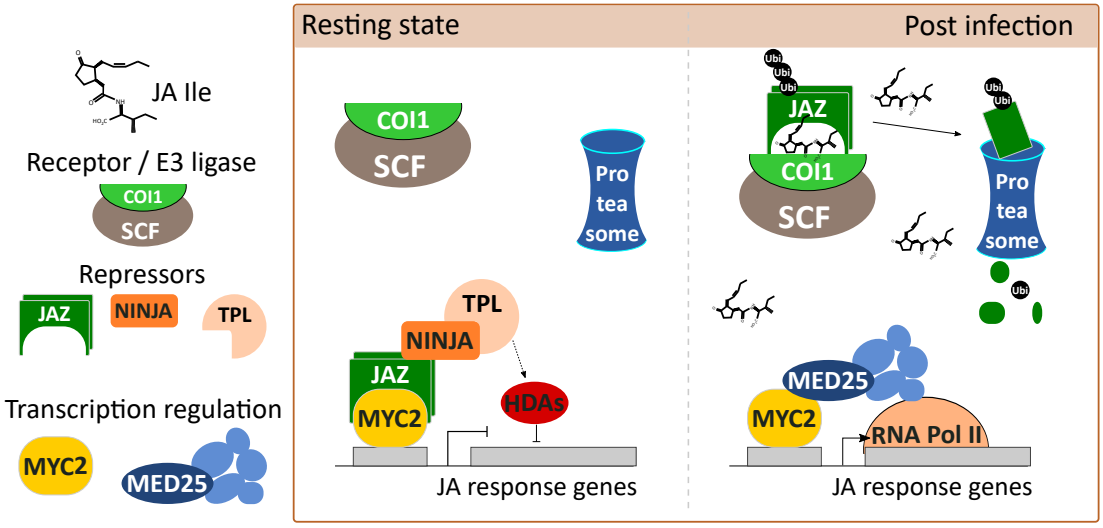

Figure 1.11: Jasmonic acid signaling pathway. In the absence of JA, in the resting state, a transcription factor e.g. MYC2 is bound to the promoter of JA responsive genes, but transcription is inhibited by a repressor complex. This complex consists of the homo or heterodimers of the direct repressors, the JAZ proteins, the adapter protein NINJA and the co-repressor TPL. TPL recruits different histone deacetylases (HDA), which additionally prevent transcription. In the presence of JA, after infection or wounding, JA binds to the receptor COI1, an F-box protein that is a component of the SCF complex. This leads to the degradation of JAZ repressors via ubiquitination by the SCF E3-ubiquitin ligase complex. Thus, the transcription factors, such as MYC2 here, together with the mediator complex (MED25) can recruit RNA Pol II and initiate the transcription of the target genes.

In the 1980s the growth-inhibiting effect of JA was detected by different groups [224, 225]. The discovery of the *coronatine insensitive* mutant (*coi1*) [226] in 1994 brought a major breakthrough in JA research. Further investigations have shown that COI1 encodes an F-box protein, which acts in combination with the SCF complex as E3 ubiquitin ligase [220]. In the following years, the importance of the SCF_{COI1} complex for the JA responses was determined [227], but the receptor was not yet identified. When

it was discovered in 2005 that TIR1, an F-box protein, is an IAA receptor [228, 229], COI1 was analyzed as possible JA receptor, which was confirmed in 2008 [230, 231]. After the discovery of the JA receptor, the entire JA core pathway was identified. This core pathway consisted of the SCF_{COI1} E3 ubiquitin ligase complex including the receptor, the repressors, JASMONATE ZIM DOMAIN (JAZ) proteins [232, 233, 234], a general co-repressor TOPLESS (TPL) and its TPL-related proteins, an adapter protein, linking repressors and co-repressors, called NOVEL INTERACTOR OF JAZ (NINJA) [235, 236], and several important transcription factors, for example MYC2. The JAZ proteins belong to the TIFY gene family, which in total consists of 18 members that share the specific ZIM domain. The JAZ proteins (JAZ1-12) are known to negatively regulate the JA signaling pathway [236]. They have a weakly conserved N-terminal domain, a strongly conserved ZIM domain, which is required for JAZ dimerisation and interaction with the adapter protein NINJA, and a C-terminal JAZ domain, which mediates interaction with the transcription factors [237, 236, 238]. The adapter protein NINJA binds with its C-terminal domain to the ZIM domain of the JAZ proteins and with the their N-terminal EAR domain to the co-repressor TPL. This special EAR domain is not specific for one protein family, but is found in differently categorized families [239]. All these proteins containing an EAR domain, were grouped as EAR repressome family with 398 members by Kagale et al. in 2010. Many of these EAR domain containing proteins are known for their function as repressors, some of these also form a repressor complex with the co-repressor TPL [240]. In the absence of JA, homo- and heteromeric JAZ proteins [241, 237, 242] form a repressor-complex with NINJA and TPL that binds to transcription factors to repress induction of JA responsive genes. Additionally, TPL recruits HISTONE DEACETYLASES (HDA) that prevent the binding of transcription factors to the DNA through histone modifications [243] (see figure 1.11). This complex can be found in plants that are not exposed to stress, i.e. at rest state (see figure 1.11 part left). If stimulation occurs, e.g. by a necrotrophic pathogen, JA-Ile is produced. JA-Ile binds to COI1 in the SCF-E3 ubiquitin ligase complex. This binding leads to JAZ protein ubiquitination and subsequent degradation via the 26S proteasome. Since the repressor complex of JAZ-NINJA and TPL is dissolved, the transcription factor bound to the promoter, can initiate the transcription of the JA responsive genes. The recruitment of the mediator (MED) complex leads to the binding of the RNA Pol II polymerase. The MED complex is known for its fine tuning function in the gene specific and pathway specific plant immunity response [234, 244, 245, 246] (see figure 1.11 part right).

The JA signaling pathway is important and necessary for the defense responses against biotic stress factors such as herbivorous insects or necrotrophic pathogens. These defense responses have to be fine-tuned and require additional regulation via the ET and the ABA signaling pathways [247]. Next to the defense responses the JA signaling pathway is also involved in stamen development, which is regulated together with the GA signaling pathway [248]. The JA pathway, like all other pathways is interconnected to regulated the different developmental processes.

1.2.9 Strigolactones and karrikins

Strigolactones (SL) and karrikins (KAR) differ in their structure, however, they both function in a signaling pathway with the same or homologous proteins of the same protein families (see figure 1.12), whereas the resulting signal and the targets are different. While the SL pathway is known for its regulatory function in shoot branches, root growth and

arbuscular mycorrhiza formation, KAR is known for its stimulating effect on germination of smoke-responsive species and hypocotyl elongation. Particularly in root development, the SL and the IAA signal pathway work closely together [249, 250, 251].

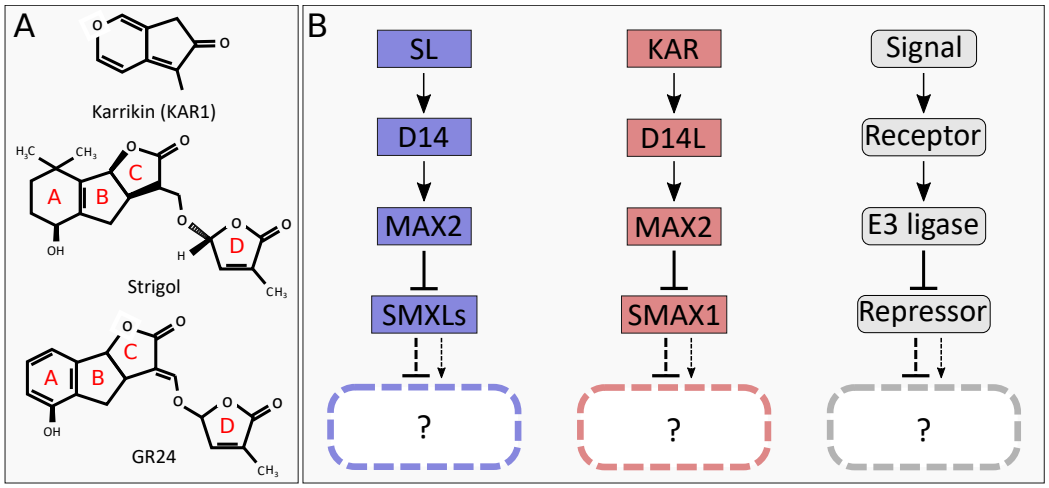

Figure 1.12: Strigolactone and Karrikin pathway overview. (A) shows the structural formula of karrikin (top), strigolactone (middle) and the synthetically produced strigolactone analog GR24 (bottom). (B) shows a simplified representation of SL and KAR signal transduction from hormone to unknown downstream targets.

In 1972 the structure of strigol was discovered [252]. SL are terpenoid lactones consisting of a central tricyclic lactone (ABC rings) connected to the butenolide group (D ring) via an enol ether bridge. The D-ring and the enol ether bridge are essential features of the known natural and active SL [253, 254, 255]. Since then, several studies have shown that SL are secondary metabolites produced in the roots which serve as stimulators for seed germination for parasitic plants [256, 257]. In addition to this function, SL also have properties to support hyphal branching in symbiotic arbuscular mycorrhizal fungi [258, 257] and promote symbiotic interaction between plants and rhizobia [259, 260]. These symbiotic interactions occur in about 80 % of land plants [261]. In recent years, SL and their functions have been intensely studied and SL were confirmed to play a role in the regulation of root growth, lateral root formation [262, 250], and shoot branching via crosstalk with the auxin signaling pathway, showed by genetic and physiological assays [263, 264, 265, 266, 267]. Additionally, SL is known to function as a positive regulator in response to drought and salt stress together with the ABA signaling pathway [268]. SL are mainly expressed in the root and, similar to cytokinin, should be transported acropetal from the root to the shoot [269]. The molecular mechanism, how SL is transported, is not yet exactly determined. Studies investigated the transport via xylem, but came up with to contradictory results [270, 271]. However, SL have an influence on the auxin efflux transporters PIN1 and PIN2 and it is possible that SL could be transported via cell to cell transport through these PIN efflux carriers [271, 272, 273].

Karrikin (KAR): Around the 1980's, the attention was directed to substances contained in smoke and burned plant material that stimulate seed germination. The active substances were extracted with water and further experiments with various plants showed an increased germination effect [274, 275]. In 2004, this most important bioactive compound was then isolated from the smoke [276]. This was a butenolide with a similarity to the butenolide (lactone) unit and the unsaturated ester functionality known

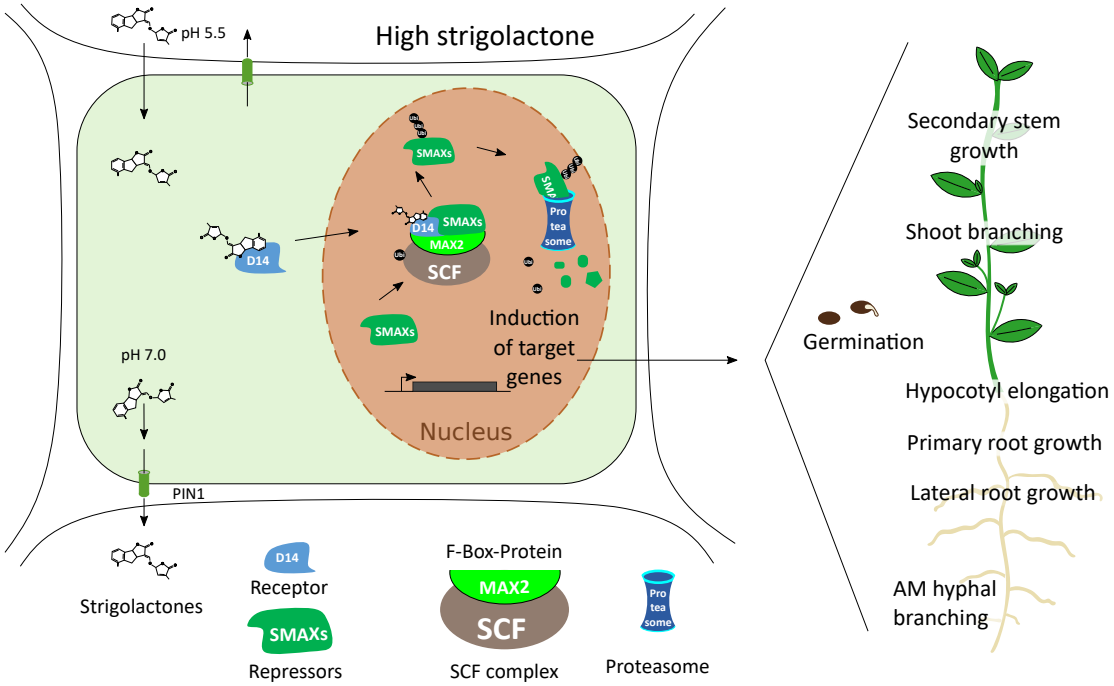

Figure 1.13: Strigolactone signaling pathway. SL can diffuse into the cells but can possibly also be transported out via PIN1. D14 binds SL and in the nucleus, the activated D14/D14L-MAX2-SCF complex binds to the SMXLs repressor. After ubiquitination the repressors are degraded via the proteasome and thus enables the expression of the target genes. This gene expression then leads to different developmental processes in the plant (see figure on the right).

from strigolactones. To distinguish these compounds from other butenolids, the family was given the collective term karrikins [277, 278]. Unlike SL, KAR are not synthesized in plants, but are produced as a by-product of the combustion of plant material [279]. Since both SL and KAR were known to increase the germination rate and contained a similar functional group, it was likely that a common mechanism of action was involved. To determine whether SL can stimulate the germination of smoke-sensitive species and whether KAR stimulate the germination of parasitic weed species, numerous studies were carried out. These showed that KAR can stimulate the germination of many parasitic weeds [280], but not all species that responded to SL [281]. In addition, much higher amounts of GR24, a synthetic SL, was required to achieve an increased germination rate in smoke-responsive species, compared to KAR.

After several studies, the current model of three core components has been established. The SL/KAR signal pathway starts with the receptors DWARF14 (D14) for SL and DWARF14-like/KARRIKIN INSENSITIVE 2 (D14L/KAI2) for KAR, both alpha beta hydrolase superfamily proteins, followed by the SCF complex with the F-Box protein MORE AXILLARY BRANCHES 2 (MAX2), and the repressors, SUPRESSOR OF MAX2 (SMAX) and SMAX-Like (SMXL) proteins see figure 1.13. Like all F-box proteins in the SCF E3-ubiquitin ligase complex, MAX2 works as the substrate selection subunit. The selected substrated become ubiquitinated via the SCF complex and subsequently degraded via the 26S proteasome. MAX2 is primarily nuclear localized [264] and D14 is both nuclear and cytoplasmic localized in *Arabidopsis*, therefore it is likely that these two can interact *in planta* [282, 283]. This has already been shown for orthologues in

rice [283]. Wang et al, 2013 reported, however, that MAX2 and D14 would not interact in vitro in *Arabidopsis* [284]. However, the signaling pathway from rice predicted a D14/D14L interaction with MAX2 in the presence of SL or KAR respectively, which leads to ubiquitination and degradation of the repressor SMAX1 or SMXL proteins (see figure 1.13). The important differences between SL and KAR signaling pathways are the specific repressors SMAX (KAR) and SMXL proteins (SL). Studies have shown that the functions of SL for shoot branching, leaf morphology and support of hyphal branching are due to the degradation of SMXL7, SMXL8 and SMXL6 [285]. However, the role of KAR in germination and hypocotyl elongation is related to the degradation of SMAX1 [286]. For both SL and the KAR signaling pathway, it is assumed that the hormones can be transported into the cell or diffuse across membranes if the hormones are present in high concentrations. In the cytosol as well as in the nucleus the hormones can bind to their receptors, respectively, which leads to an interaction of the receptors with MAX2 and the SCF complex. This complex formation enables MAX2 to ubiquitinate specifically SMAX1 or another SMXL protein and subsequently release it for degradation via the 26S proteasome. By degrading the repressors, SL or KAR specific target genes can be expressed, which then causes the respective physical effect in plant development (see figure 1.13).

1.3 Signal integration between the phytohormone signaling pathways

Considering the individual phytohormone signaling pathways and their functions in plant development as well as strategies to cope with abiotic and biotic stress, it becomes obvious that the signaling pathways regulate and influence these processes synergistically or antagonistically. To investigate how different hormones influence a common set of transcriptional targets, Nemhauser et al., 2006 [287] used microarray approaches. For this purpose, seedlings were treated with six different hormones (GA, IAA, ET, CK, BR, JA) in individual approaches and timepoints. They assumed that if there was a highly interconnected system of all hormones, that a treatment with one particular hormone cause changes in the metabolism of other hormones. However, this could not be confirmed. They found that different hormone treatments had an effect on individual members of a gene family, but that only a very small number of genes were co-regulated by several hormone treatments. These results led to the question how exactly the underlying mechanism works, by which different signaling pathways influence synergistically and antagonistically developmental processes. And it was concluded that detailed knowledge of cellular conditions and biochemical functions is needed, along with transcription data, to answer this question and that the signal network that controls growth processes is much more complex than previously thought.

Ten years later, Ristova et al, [288] investigated the question of how signal integration of nutrients and hormones influences root growth and development. They combined nitrate and ammonium treatments with IAA, CK and ABA hormones and specifically investigated transcriptional regulation in the root (in *Arabidopsis thaliana*). They discovered nearly 10,000 different regulated genes in the root, of which 4,200 genes showed transcriptional changes at different treatments. This discovery confirmed their hypothesis that nutrient and hormones influence root development. Unfortunately, the underlying mechanism of how these signals are integrated is still unknown.

However, transcriptome analysis is limited to certain time points and tissues and can only show influence of phytohormones on developmental processes or responses to biotic and abiotic stresses, but cannot explain how signal integration takes place physically or biochemically. In order to understand how the individual signaling pathways interact with each other, it is necessary to analyze the functions of individual components of the signaling pathways in more detail. These were done for single proteins in different studies.

Physiological investigations of mutants revealed that both the GA pathway and the BR pathway have a regulatory role in cell elongation in photomorphogenesis [104, 289]. However, the molecular mechanism behind it was not known. To elucidate this mechanism, Gallego-Bartolome and colleagues [290] used the specific GA and BR mutants for transcriptome analysis and then further focused on two proteins, the GA repressor GAI and BZR1, a transcription factor that regulates the expression of the BR target genes. This interaction was confirmed with different binary interaction detection methods (binary methods). Thus, the molecular mechanism of signal integration between two signaling pathways could be uncovered. Another examples for interactions between JA and GA signaling pathway are MYC2 and RGA interaction [291] and JAZ1 and RGA [197]. These interactions or crosstalks between these two phytohormone signaling pathways were confirmed by various *in planta* assays and by binary interaction detection assays, in these cases a yeast-two-hybrid (Y2H) assay and a bimolecular fluorescence complementation (BiFC) assay. As illustrated by these examples, binary-interaction-detection methods were used to identify a physical interaction that explains the molecular biology of the known genetic interaction. These results suggest that the direct physical interaction plays an important role as a linkage between the individual phytohormone signaling pathways. To understand to what extent the hormone signaling pathways are linked by protein-protein interactions (PPI) and how strong these links are between the pathways, all proteins involved in the phytohormone signaling pathways would have to be investigated. Therefore one of the most commonly used binary methods, the Y2H system, is most suitable. The Y2H system is a cell based, *in vivo* system used to detect PPI in *Saccharomyces cerevisiae* [292]. The system used in this thesis is based on the yeast transcription factor GAL4, which has a domain for binding to DNA (DNA-Binding / DB) and a domain that activates transcription in the cell (activation domain/AD). These two GAL4 domains have been separated into DB domain and AD domain and are used to produce hybrid proteins. The hybrid proteins consist of the DB domain plus ORF of a specific protein (DB-X, bait), as well as the AD domain plus a second ORF (AD-Y, prey). The AD and DB hybrid proteins are transformed into yeast. If an interaction takes place, the yeast cells are able to grow on selective media. The AD domain can recruit the RNA polymerase and the reporter gene, in most cases *HIS3*, which enables the cells to produce histidine, is transcribed. In order to exclude those DB-hybrid proteins that are able to start the transcription of the reporter gene independently (autoactivator), a control step using cyclo-heximide (CHX) is performed [293]. The AD plasmid contains a *CHY2* gene encoding a yeast L29 ribosomal protein (see figure A.26, A.27), which is involved in polypeptide elongation. This function is blocked by CHX treatment, which results in inhibited yeast growth [294, 295]. With this system PPI can be detected, whereby it is not restricted to expression at certain developmental time points or in different tissues. More important is that the Y2H assay can be used in a high throughput system, allowing to build large PPI network maps. This has already been shown for *Arabidopsis thaliana* for the Arabidopsis Interactome 1 (AI1) [296], with about 8,000 proteins.

1.4 Objective

Plants need to adapt their life cycle and development to biotic and abiotic environmental influences. For this adaptation, the phytohormone signaling pathways play an essential role in convey environmental signals and initiate or inhibit specific developmental processes. In order to decide whether to initiate or inhibit development processes, synergistic and antagonistic interactions of the different phytohormone signaling pathways are necessary. These interactions were observed for various phytohormone pathways and developmental processes over the last decades. Recent studies showed that these interactions of phytohormone pathways could occur partially through reciprocal transcriptional regulation, and direct protein-protein interaction. Some of these direct interactions could be identified as points for signal integration between different phytohormone signaling pathways and facilitate new crosstalk hypothesis. Based on these data the importance of protein-protein interactions as points of signal integration between phytohormone signaling became obvious. The aim of my work was to identify new points of signal integration between the individual phytohormone signaling pathways using an established Y2H mapping pipeline. Therefore a new phytohormone ORFeome collection will be generated and used for systematic Y2H assays. Through the resulting systematic-interaction network map the connection between the different phytohormone signaling pathways, found in genetic studies, should be detectable on a molecular level. To identify hormone-dependent protein interactions, phytohormone receptors will be screened in presence and absence of the respective hormone against the phytohormone ORFeome collection and a published *Arabidopsis* ORF collection.

The generation of a systematic network map, binary interaction detection methods and the data analysis are described in the following chapter. The complete project was separated in a bioinformatic part, performed by Stefan Altmann and a biological part, performed by myself. Due to the extensive collaboration, some calculations and lists compiled by Stefan Altmann are mentioned in the results section, as they are necessary to clarify the results. First, the Y2H system is briefly explained and how the phytohormone ORFeome (PhO) collection was prepared (2.2). Followed by the process of the phytohormone interactome (PhI) mapping (2.3) and the analysis of the PhI (2.4). Additional network mapping, based on a repressor transcription factor screen (2.7) and PhO tested against the 12,000 ORF *Arabidopsis* collection (AtORFeome) (2.6), we were able to connect the interactions of the PhI with processes outside the phytohormone network. In section 2.5 an example is given to explain how a systematic network map can be used to investigate new insights in signaling pathways. Since PhI mapping was performed without addition of hormones and most phytohormone signaling pathways are only initiated by the recognition of the specific hormone, individual screens with the respective hormone were performed (2.8). In section 2.9 individual interactions, as points of signal integration, were validated in different seedling assays.

2 Results

2.1 Extensive literature analysis of phytohormone pathway interactions

In the previous descriptions of the individual signaling pathways it became obvious that many developmental processes are influenced by several phytohormone signaling pathways. In order to get an overview of how many processes and stress responses are regulated by different phytohormone signaling pathways, an extensive literature search was conducted involving all plant species. Therefore different processes stress responses in combination with all phytohormones were used as basic search terms (arbuscular mycorrhiza, embryo development, flower development, germination, leaf development, root development, and shoot development). This analysis showed that most signaling pathways have been implicated in all analyzed processes and in the response to biotic and abiotic stresses (see figure 2.1). In order to provide a general overview, connections of individual signaling pathways to developmental processes or the responses to abiotic and biotic stresses, which have only been investigated in one species, were added to this analysis (see figure 2.1). Most of these studies were based on genetic studies with different mutants as well as expression data of certain marker genes under a certain treatment. Less than 10 % of the studies are based on direct physical interactions between proteins. It was noticeable that SA appears to be involved in only four developmental processes or stress responses. Similar findings were made for KAR, which appears to have an effect on root elongation, germination and abiotic stress. The question remains whether these two signaling pathways were never analyzed for their involvement in other processes or responses or whether these results were not published.

However, this overview supports the notion that most developmental processes and stress responses are positively or negatively influenced or regulated by at least 6 different phytohormone signaling pathways.

2.2 Generation of the Phytohormone ORFeome collection

For the PhO-collection, 1216 genes were selected as target ORFs. These genes either have genetic evidence for involvement in phytohormone signaling or belong to gene families enriched with hormone annotations in the Arabidopsis Hormone Database 2.0 (AHD2.0) [417]. Of this target collection, 529 ORFs were cloned and 688 ORFs were available as Gateway clones [296]. From the 529 ORFs, 276 ORFs were available by ABRC as Gateway or template clones. The remaining 253 ORFs had to be amplified from tissue-specific cDNAs, due to their very low expression levels limited to specific tissues in a certain time of development. Therefore all plant organs or tissues from different developmental stages were separated to produce these cDNAs. It was expected that most ORFs could be isolated from the tissue with the highest expression value. To ensure a high ORF amplification rate, three tissues with highest expression levels (1°, 2°, 3°) were selected

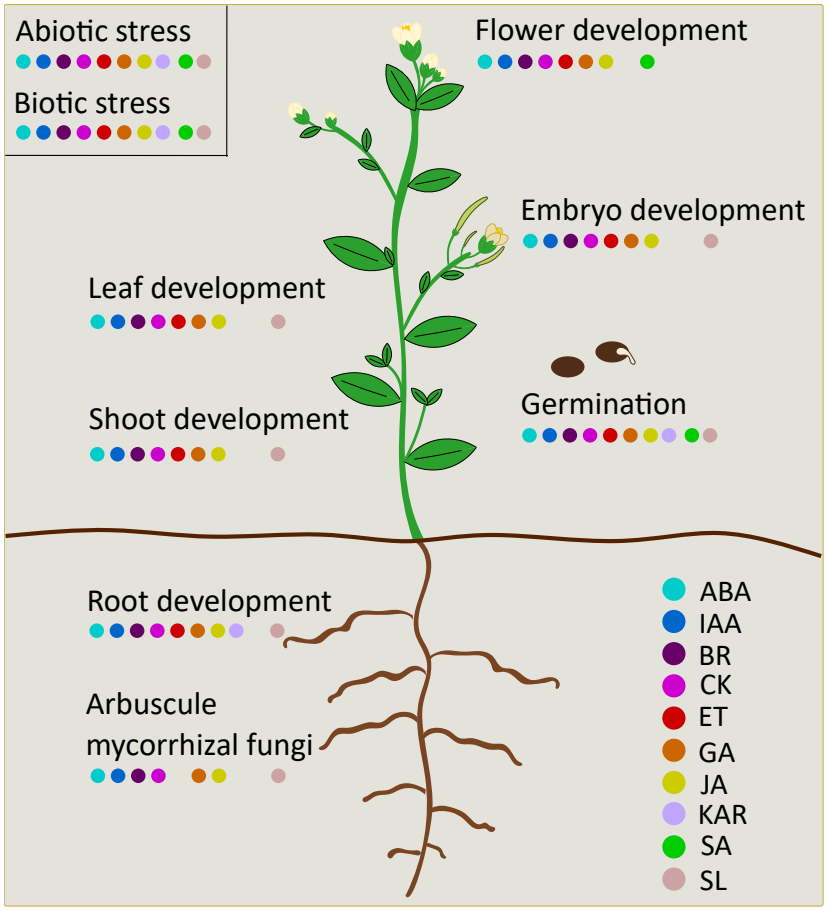

Figure 2.1: Overview phytohormones in plant development. IAA: embryo development [13, 14], root development [15, 17, 16, 18], shoot development [19, 20], flower development [297, 298], leaf development [21, 22, 23, 24, 25], Arbuscular Mycorrhiza (AM) [299, 300, 301, 302], germination [303, 304], abiotic stress [93, 305, 306], biotic stress [307, 308, 302]. ABA: embryo development [66, 67, 68, 71], root development [309, 62, 310], shoot development [311, 312], flower development [313, 314, 315], leaf development [316], AM [317], germination [69, 70, 71], abiotic stress [63, 64, 65], biotic stress [318, 319, 320, 321]. BR: embryo development [322, 323, 324], root development [325, 326, 126, 127], shoot development [327, 128, 129], flower development [328] leaf development [329], AM [325], germination [124, 125], abiotic stress [330, 331, 332], biotic stress [333, 334, 335, 336]. CK: embryo development [337], root development [54, 131, 132, 338], shoot development [339], flower development [340, 341, 342], leaf development [343, 344], AM [345], germination [92], abiotic stress [346, 347], biotic stress [348, 349, 350]. ET: embryo development [351], root development [352, 353, 354, 355], shoot development [356, 357], flower development [358], leaf development [151], germination [359, 360], abiotic stress [361, 362], biotic stress [363, 364, 365, 366]. GA: embryo development [367, 368, 369], root development [370, 371], shoot development [179], flower development [372, 373, 374], leaf development [375, 376], AM [377], germination [178, 378], abiotic stress [379, 380], biotic stress [196]. JA: embryo development [381, 382], root development [188, 219, 383], shoot development [221, 384], flower development [385, 386], leaf development [387, 388], AM [389], germination [390], abiotic stress [361, 391], biotic stress [247, 392, 393]. KAR: root development [394, 395], germination [396, 281], abiotic stress [397, 398, 399]. SA: flower development [400], germination [401], abiotic stress [84, 85, 86, 402], biotic stress [403]. SL: embryo development [404], root development [249, 250, 251, 405], shoot development [406, 272], leaf development [407], AM [408, 409, 410, 411], germination [412], abiotic stress [413, 414, 415], biotic stress [416].

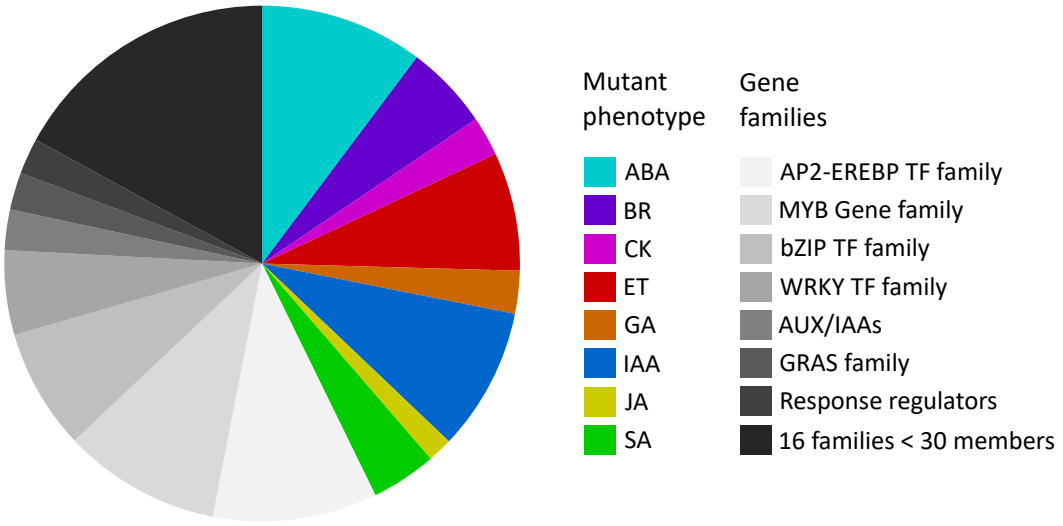

Figure 2.2: Target genes separated in gene families and genetic evidence. Colored right side showed ORFs with specific genetic evidence, left side colored in gray to black are the added gene families.

for each ORF of interest (list was compiled by S. Altmann). Surprisingly, 33 % of the ORFs in PhO could be extracted from the primary cDNA with the highest expression values. Another 18 % could be amplified from the secondary cDNA and further 9 % were extracted from the tertiary cDNA (see figure 2.3 part A). However, for almost 39 % it was not possible to extract the ORFs from the primary to tertiary cDNAs and it was necessary to test 4 to 6 different cDNAs (see figure 2.3) to obtain them. Eventually, 91 % of the desired ORFs could be amplified using a mixture of all cDNAs in equal proportions. The ORFs were amplified in the first PCR followed by a second PCR (nested-PCR), to attach the full Gateway cloning sites (attB1, attB2). All ORFs were sequence verified after the first cloning step (entry plasmids). After ORFeome cloning into destination vectors, the PhO-collection was transformed into the two haploid yeast strains used of the Y2H system.

The overall cloning success was about 97.8 % (1190/1216 ORFs) and for some ORFs various splicing variants could be amplified, which were added to the PhO. In addition 24 ORFs were cloned in a second set after PhI screening, which were identified as important and 11 ORFs were provided by experts, therefore these 35 ORFs were also included. The final PhO contains 1227 loci covered by 1254 ORFs (see table A.1 in appendix) which was used for all screens except from the PhI screen which was performed with 1201 unique ORFs.

2.3 Phytohormone interactome mapping

To generate the PhI I used an established Y2H mapping pipeline, already used for AI1 [296], plant pathogen interactome 1 (PPIN1) and PPIN2 [418, 419]. This Y2H pipeline consists of four stages. The first stage is the screening, individual DB-X hybrid proteins were screened against AD-Y hybrid protein pools of 188 ORFs, followed by a retest of the primary positives to identify and remove spontaneous autoactivators (phenotyping). The resulting (secondary) positives yeast colonies were lysed and the lysis mixtures were

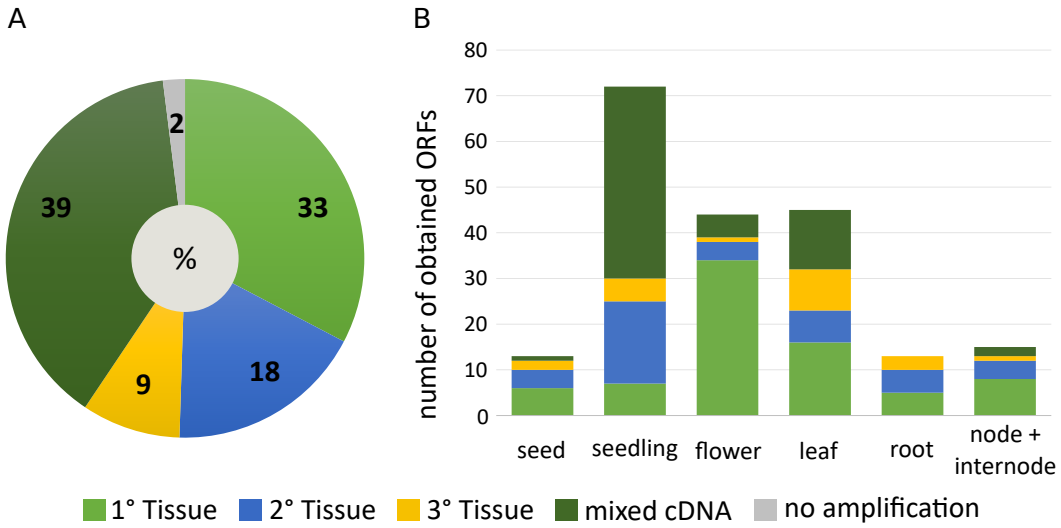

Figure 2.3: PCR success rate separated by different tissues. (A) shows the obtained ORFs per tissue in percent. The description primary (1°), secondary (2°) and tertiary (3°) tissue identifies the highest expression levels of each ORF in three different tissues. (B) shows the number of ORFs obtained from different tissues

used for multiplex PCRs with barcode tagged primers, followed by Next-Generation Sequencing (NGS). In the final step (verification) the candidate interactions were verified by four independent assays. The yeast spots were manually scored according to growth and interactions detected in at least three out of four repeats were considered as confirmed interactions (see figure 2.4) [293]. For the PhI, screening and phenotyping steps were repeated three times and all pairs were tested in the two different fusion-protein combinations (AD-Y – DB-X and DB-Y – AD-X).

The resulting PhI contains 475 interactions between 251 proteins, of which 322 are new interactions. The network has been visualized using the program Cytoscape [420]. The hormone annotations of the individual nodes have been additionally imported as node attribute file into the Cytoscape program. The list of hormone annotations is based on the genetic evidence information from the database of AHD2.0 and the Gene Ontology information from TAIR10 (compiled by Stefan Altmann). This list of hormone annotations was imported as node attributes into every Cytoscape file used to visualize my experimental data in my work (see network map in figure 2.5). Identical data set are visualized almost identically by the deterministic layout algorithm used in Cytoscape.

2.4 Quality assessment

The first step in the analysis of a PPI-network like the PhI is to answer the questions, to what extent the used system can detect interactions, and how much interactions are missed or false positives. This kind of analysis is known from other PPI networks like AI1, PPIN1, and PPIN2, whereas those networks were based on the AtORFeome collection. However, the PhI is based on the PhO collection, which contains a precise selection of ORFs to analyze specifically the phytohormone signaling pathways in *Arabidopsis thaliana*. This selection could influence the number of interactions to be detected via the Y2H system due to the specific biological function of the proteins, e.g. receptors and repressors of individual signaling pathways.

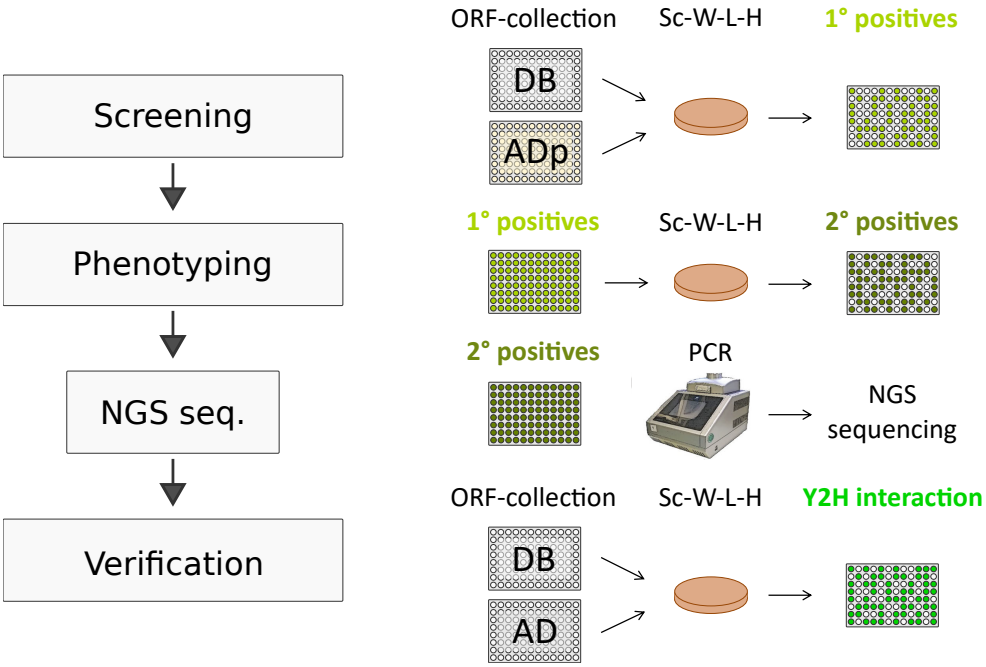

Figure 2.4: High-throughput Y2H screening pipeline. The pipeline consists of four steps: screening, phenotyping, sequence identification, and verification (left side). For screening, 96 different DB-X constructs are mated against an AD-Y pools. The positive colonies (1° positives) are picked from selective plates and retested on selective plates in the phenotyping step to identify spontaneous autoactivators. Candidate interaction pairs (2° positives) are amplified by PCR and sequence identified by Sanger or NGS sequencing. The resulting candidate interactors are confirmed by a fourfold independent verification. For verification, all candidates will be tested pairwise and in both directions (AD-Y – DB-X and DB-Y – AD-X). All pairs that score positive at least three times are considered bona fide Y2H interactions.

To evaluate the quality of the Y2H mapping system in combination with this new ORFeome collection, the quality parameters completeness, sampling sensitivity and assay sensitivity, described in recent publications, were used [296, 421, 418, 419]. Completeness is a percentage value that indicates the extent to which the search space in a screen has been covered. The PhI was screened with 1201 unique ORFs of which 1185 ORFs were cloned in AD and DB fusion constructs, 12 ORFs only in AD and 4 ORFs only in DB fusion constructs. Consequently from the 1,505,529 possible interaction pairs that would result from the complete search space 1,423,233 interaction pairs were tested. For the PhI a high completeness of 94.6 % was obtained (see figure A.3 part A in appendix). The sampling sensitivity describes the degree of saturation of a screen. After three screening repeats a sampling sensitivity for the PhI of approx. 77.6 % ±4.7 % was achieved (calculated by Stefan Altmann) (see figure A.3 part B in appendix). The assay sensitivity indicates the percentage of interactions that can be detected with a particular assay. In order to calculate the assay sensitivity, a Positive Reference Set (PRS) and a Random Reference Set (RRS) were prepared, as already described in Yu et al., 2008, [422] and tested in this Y2H system. The PRS consists of interaction pairs described in recent published studies. The PRS candidates were assembled by Stefan Altmann and all underlying publications were manually curated by our working group. The resulting 92 PRS pairs and 96 RRS pairs were tested in a four fold independent assays in AD-Y DB-X and AD-X DB-Y orientation. The resulting 25 interactions, of which 19 were unique,

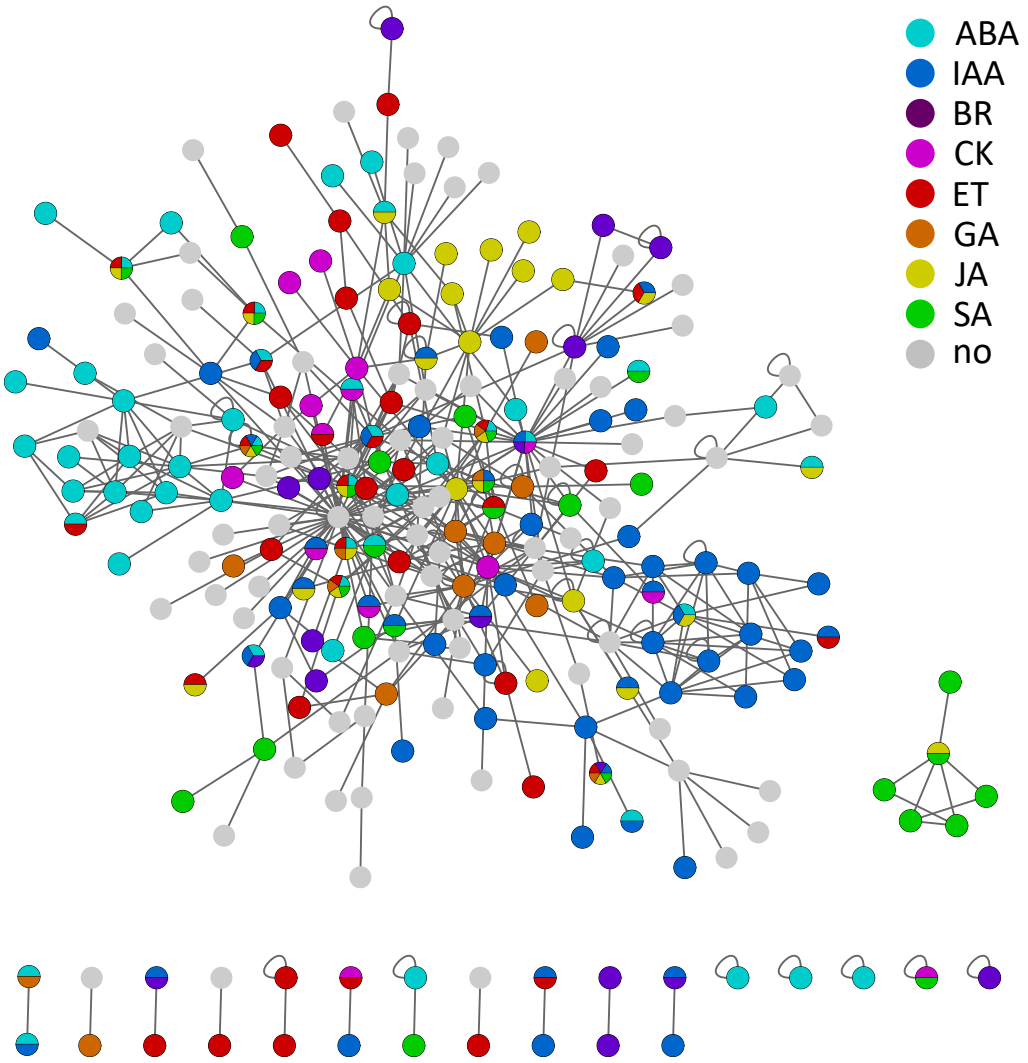

Figure 2.5: Phytohormone Interactome consists of 475 interactions between 251 proteins. Colored nodes represent proteins with annotations for different phytohormone signaling pathways. These are based either on proteins inferred by mutated phenotypes (AHD2.0) or GO annotations (TAIR 10). Gray nodes have no annotations for phytohormone signaling. Interactions detected in at least three out of four repeats were considered as confirmed interactions. Edges between the nodes show physical interactions.

originate from PRS, whereas no interaction was observed for the RRS. From these interactions an assay sensitivity of 20.7 % ±4.2 % and a calculated false positive rate of ≤ 1 per 100 interactions, were calculated (see figure A.3 part C in appendix). Some of the interactions, used in the PRS set, only take place with ORF fragments or with the addition of phytohormones. In this experiment, however, only full-length proteins were used and no hormone of any kind was added. Thus, the comparability between the assay sensitivity between PRS and PhI could be ensured.

The values of the sampling sensitivity and the assay sensitivity were used to calculate the overall sensitivity of 16 % ± 2.0 % for the PhI [423]. By multiplying the overall sensitivity with the completeness of the PhI, the overall completion with 15.1 % ± 2.0 % was calculated [423], which indicates the percentage of detected interaction over the search

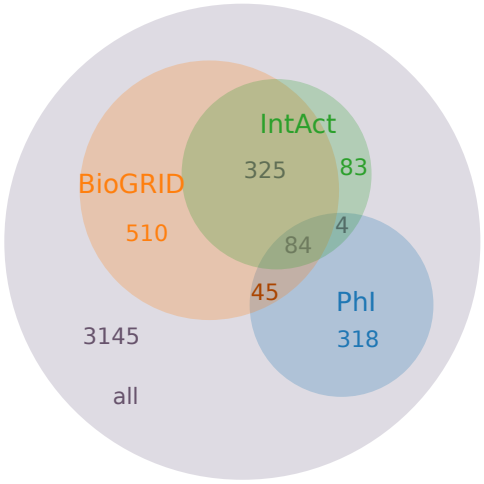

Figure 2.6: Overall completion PhI and literature overlap. (all) indicates 3145 estimated interactions, BioGRID has about 964 interactions, IntAct has about 492 interaction (all interactions used for this analysis from BioGRID and IntAct are binary multiple (BM) or binary single (BS) interactions), PhI indicated 15.1 % (475) of all estimated interaction. Overlap between PhI and BioGRID is about 13,4 % (129 interactions), overlap between PhI and IntAct is about 17,9 % (88 interactions), overlap between BioGRID and IntAct is about 409 interactions.

space of PhO. The number of possible interactions over the search space of PhO could be calculated from the overall completion, which is 3145 interactions. When combining the PhI with the interactions from the BioGRID [424] and IntAct [425] databases using the search space of PhO, the overlap between the PhI and the literature interactions can be illustrated (see figure 2.6). For unbiased data sets it can be assumed that an overlap with PhI of 15.1 % would also be achieved for BioGRID and IntAct, but the overlap from PhI to BioGRID is 13.4 % and from PhI to IntAct is 17.9 %. The data from BioGRID and IntAct databases are biased, due to using interaction data from various studies, which were directed towards specific topics, but also due to using different curation tools. However, the overall completion from PhI and the overlap of both databases correspond to the exception derived from the quality assessment.

The quality assessment of the network map showed that 95 % of the possible binary interactions, in the selected search space, were tested, and 78 % of the interactions, detectable with our system, were found. In addition, it could be shown that almost exclusively true positives were found and that the probability for false negatives is about ≤ 1 per 100 interactions.

2.5 New insights in individual phytohormone signaling pathways

The fundamental questions of this work were how the phytohormone signaling pathways interact with each other on a molecular level, and to which extent signal integration takes place via protein-protein interactions. With the results of the PhI it could be shown that the phytohormone signaling pathways are highly connected on PPI level. In order to analyze this network at the molecular level and to identify the hypothetical function of these interactions, one signaling pathways were investigated in more detail. Signaling pathways begin with an upstream signal and process this signal further via a signaling

cascade and lead finally to a change in enzyme activity, gene expression or ion channel activity. With a systematic network map it is theoretically possible to detect this kind of signaling cascades. However, in order to identify a signaling cascade in a network with 475 interactions, the network must be filtered for signal cascade starting points. Thus a sub-network can be generated by filtering for the direct interaction partners of these proteins in the PhI.

2.5.1 MAP-kinase interactions

Some of the already well studied MAP kinases have found to be involved in several different phytohormone signaling pathways. Therefore, the family of MAP-kinases seemed to be very useful to investigate their signaling pathway in more detail. The MAP-kinase family can be divided into three large groups the MAP-KINASES (MPK), the MAPK-KINASES (MAPKK/MKK) and the MAPKK-KINASES (MAPKKK/MEKK). In *Arabidopsis* 20 MPK proteins are known, they form the lower part of the MAP-kinase cascade. MPK substrates are often, but not always, transcription factors that regulate immune response [426, 427], and growth or differentiation signals via hormone pathways, e.g. auxin [45]. The MKK form the smallest group in *Arabidopsis thaliana* that contains 10 members. The MKK form the middle part of the core MAP-kinase cascade and phosphorylate various MPK to activate them. The MKKK form the third and largest group, with 60 members, which most often induce the MAP-kinase cascades. This group responds to multiple external stimuli and transmits them via the MAP-kinase cascade to regulate cell responses ([428] in *Arabidopsis thaliana*, [429] in human). The PhI was filtered for MKK and MKKK proteins and their direct interaction partners to generate a sub-network. The final sub-network consists of one MAPKKK, six MKK and eight MPK proteins and combines already known interactions (16 interactions) with new interactions (35 interactions) (see figure 2.7). In addition to the interactions of MPK with other proteins, 11 interactions between MKK and non-MAP-kinase cascade proteins were observed, which are hardly described in literature. Of particular interest was the new interaction between MKK7 and PINOID (see figure 2.7).

[430, 431] Recent studies demonstrated that MKK7 has a function in positive regulation of basal and systemic acquired resistance [432]. and plays an important role in PAT and auxin-regulated development in leaf morphology and shoot branching with MPK3 and MPK6.

To investigate whether a *pid mkk7* double mutant alters the *pid* typical mutant phenotype or even showed a more severe phenotype, an artificial micro RNA (amiR) was generated using the WMD3-Web MicroRNA Designer. The amiR MKK7 construct was generated according to the WMD3 online protocol and inserted into pALIGATOR3 plasmid. The pALIGATOR3 vector contains a C-terminal At2S3::GFP construct, that results in a fluorescent seed coat after successful transformation which allows immediate selection of the transformed seeds in the F1 generation (kindly provided by Dr. Francois Parcy [433]). The amiR MKK7 construct was transformed into Col-0 and *pid* mutant by floral dipping method. After transformation, 21 fluorescent seeds could be selected from the amiR MKK7-Col-0 and 27 fluorescent seeds from the amiR MKK7-*pid* (see figure 2.8 (B)). The plants of the F1 generation of amiR MKK7-Col-0 and amiRMKK7-*pid* plants showed almost all a dwarfed phenotype with dark green cotyledons and leaves compared to Col-0 control (mock transformed). The plants remained dwarf with 6-8 leaves even after four weeks, but were able to induce flowering (see figure 2.9). Most plants produced

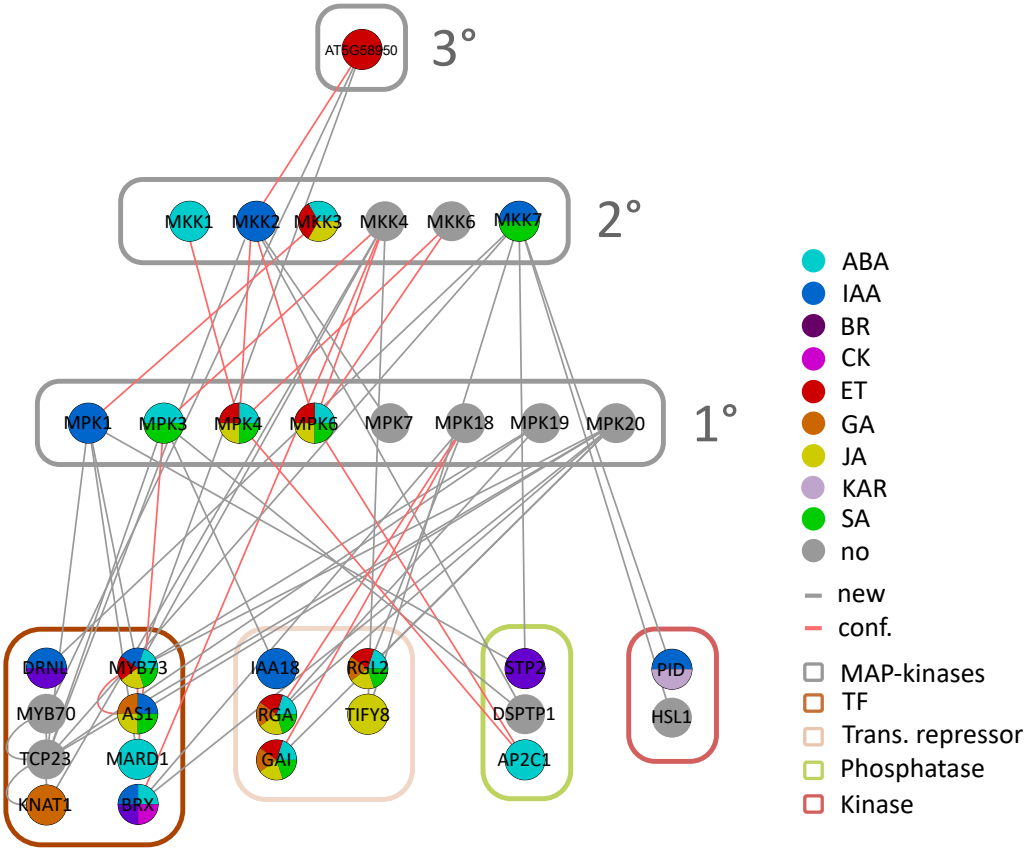

Figure 2.7: MAP-kinases interactions extracted from PHI. The MAP-kinases are separated into three subgroups. 1° indicates MPK protein kinases, 2° indicates MAPKK protein kinases, 3° indicates MAPKKK protein kinases. The target proteins are grouped according to their protein properties as transcription factors (TF), transcriptional repressors (Trans. repressor), protein phosphatases (Phosphatase) and kinases (Kinase). Edges in gray indicate new interactions, edges in red indicate confirmed interactions.

no or less than five seeds, but 5 lines of amiR MKK7-Col-0 and 6 lines of amiR MKK7 *pid* could be successfully propagated further. Additionally to the low seed number, the remaining seeds had defects in germination, which were not further analyzed. Therefore more than 5 seeds per line were necessary to obtain one seedling that could be used for further propagation.

For the amiR MKK7 -Col-0 lines, 11 plants showed the phenotype of the amiR #4 line shown in the figure 2.9 part A, which produced almost no seeds, and 10 showed the phenotype of amiR #11, of which only five plants produced enough seeds for propagation (like plant #5). For amiR MKK7 in *pid* background, the distribution was much more dramatic. Here 16 plants showed a phenotype as shown for amiR#14 line in figure 2.9 part A and only 6 plants had a more wild type phenotype as shown in amiR#5. However, since the phenotype of high accumulation of anthocyanin in dwarfish plants appear in both backgrounds, it can be assumed that this is a *MKK7* knockout phenotype. The *pid* single mutants has a pin-shaped flower phenotype similar to the *pin1* mutants and alterations in cotyledon and leaf number, shape and size [434, 435, 31]. The flower phenotype as well as the cotyledon and leaf alterations could be detected in the amiR MKK7 *pid* double mutant. To determine whether the observed phenotype is MKK7

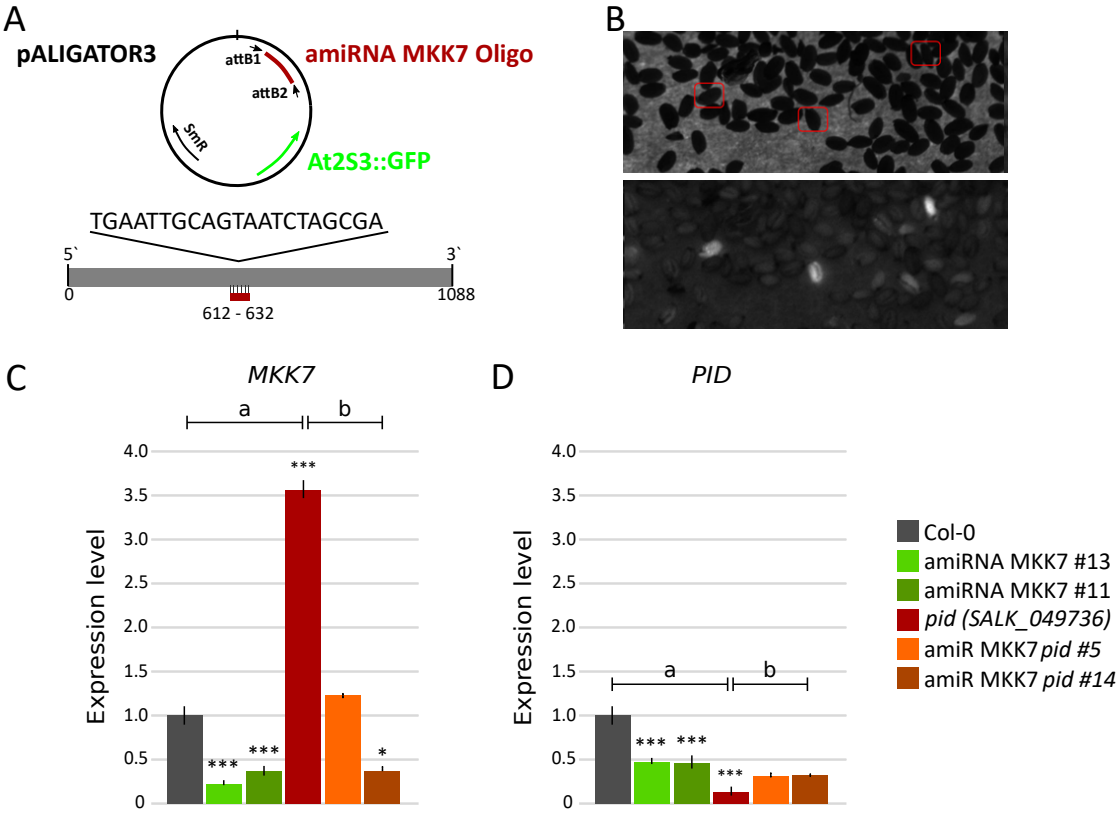

Figure 2.8: amiR MKK7 plant lines. (A) simplified representation of the pALIGATOR3 vector with sequence information and position of the binding site for the amiR MKK7 construct. (B) seeds of the transformed F1 amiR line are shown. The upper part shows the bright field image and markings of individual seeds. In the lower part the three fluorescent seeds that carrier the amiR construct are shown. In (C) and (D) exemplary expression level of *MKK7* (C) and *PID* (D) of Col-0, *pid*, amiR MKK7-Col-0 #13, amiR MKK7-Col-0 #11, amiR MKK7-*pid* #5, amiR MKK7-*pid* #14 are shown. The expression data are based on four technical and four biological replicates. Error bars indicate standard deviation of four biological replicates. two-sided t-test calculation marked with (a) are calculated to Col-0 background, marked with (b) are calculated to *pid* mutant background. *** p-value <0.001, * p-value <0.05

specific, the amiR-MKK7 sequence was tested for unspecific binding using blast search against TAIR10 gene models (see blast result A.4.1 in appendix). The blast search showed potential binding of the amiR MKK7 sequence to six additional genes (AT3G18350, AT3G22010, NEK1, LBD37, MYB102, and GSNAP). For all six genes the expression levels were analyzed in amiR MKK7 Col-0 line #11 and #13, but none of the genes showed altered expression levels compared to Col-0 (see A.4 in appendix).

Additionally, the gene expression levels of *PID* as well as *MKK7* were investigated (in the F2 generation) for amiR MKK7-Col-0 lines, *pid* and amiR MKK7 *pid* lines. As shown in figure 2.8 part C and D, the amiR MKK7-Col-0 and *pid* lines are knock down mutants. However, it was noticeable that in the amiR MKK7-Col-0 mutants *PID* expression is reduced by half (see figure 2.8 part (D)). This suggests that MKK7 is somehow involved in the regulation of *PID*. For the *pid* mutant one fifth of the *PID* expression compared to Col-0 could be detected, as it was expected, but surprisingly, the expression level of *MKK7* in the *pid* mutant line was increased to 3.5 fold compared to Col-0 (see figure 2.8 part (C)). These results indicate that the transcriptional regulation of *PID* and *MKK7*

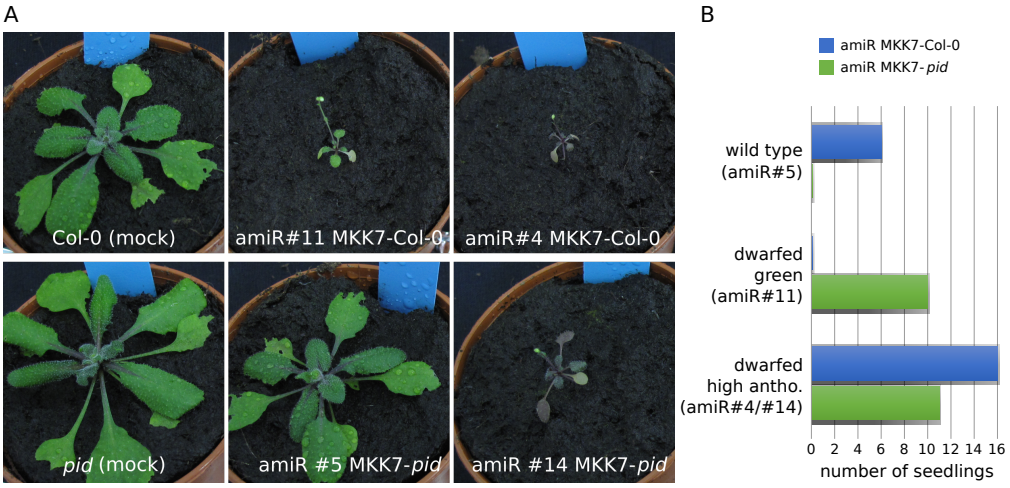

Figure 2.9: First generation (F1) of amiR MKK7 lines. (A) four weeks old Col-0 mock line and a *pid* mock line for control are shown, both mock lines are based on seeds from plants resulting from floral dipping method without amiR MKK7 construct (mock transformed). Two representative amiR MKK7 lines in Col-0 or *pid* background are shown. (B) Number of seedlings for both amiR-MKK7 lines sorted by mutant phenotype. Blue bar graphs indicate amiR-MKK7-Col-0, green bar graphs indicate amiR-MKK7 *pid* lines.

must be connected. The expression level of *MKK7* is similar in the amiR MKK7-*pid* #5 double mutant compared to Col-0, which supports the suggestion that the dwarfish phenotype is based on the amiR MKK7-Col-0 mutant, whereas amiR MKK7-*pid* #14, which showed the dwarfish phenotype shows also a reduced *MKK7* expression level. The *PID* expression in both double mutants (#5, #14) is higher than in *pid* single mutant but not significantly different. Compared to Col-0 the *PID* expression in the double mutants still indicate a *pid* knock down mutant.

To validate the Y2H interaction of PID and MKK7 a bimolecular fluorescence complementation (BiFC) assay was performed. For the assay, MKK7 and $PID_{K\text{-}E}$, a kinase dead version (Dr. Zourelidou, Plant Systems Biology, TUM) were cloned in pDEST-GW-VYNE and pDEST-GW-VYCE [436], transformed into *Agrobacterium tumefaciens*, and infiltrated into *Nicotiana benthamiana* leaves. As shown in figure 2.10 top row, a YFP signal could be detected at the plasma membrane of the cells when both proteins are expressed, regardless of whether they are cloned with C-terminal or N-terminal YFP fragments. However, the YFP signal could also be observed at the plasma membrane and partly in the nucleus (see arrow heads figure 2.10 middle row) when MKK7 was expressed with an empty vector alone. It is known that a combination of a protein-fusion with an empty vector can exhibit in some cases significant non-specific background fluorescence. Therefore a close homologue of *PID*, *PID2* (AT2G6700) [437], was planned to be used as negative control in this assay. After cloning, the sequence analysis showed an additional base exchange, which leads to an amino acid exchange. Therefore the assay was performed with empty vector controls. The expression of $PID_{K\text{-}E}$ with an empty vector does not produce a YFP signal (see figure 2.10 bottom row). Since MKK7 can only be found in connection with the empty vector in the cell nucleus, it could be assumed that the interaction with PID inhibits transport into the cell nucleus, either due to the size of MKK7-YFP-PID, or through a function of both proteins at the plasma membrane.

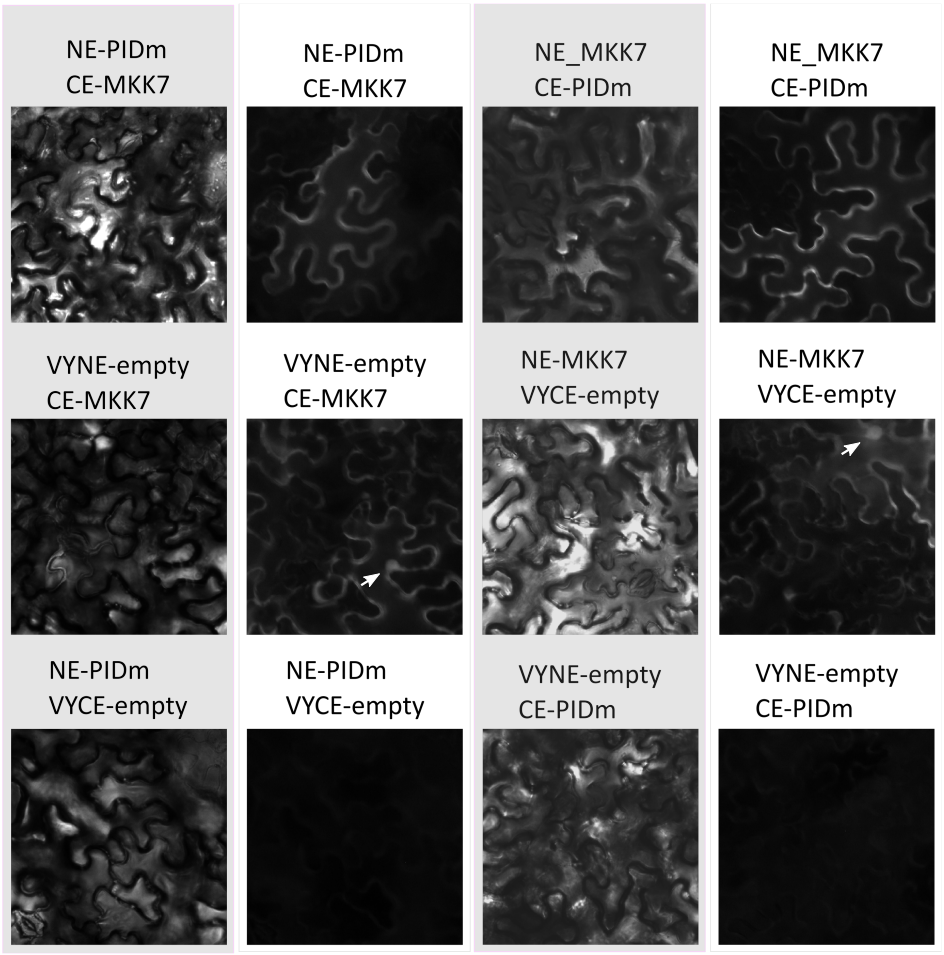

Figure 2.10: BiFC MKK7-PID validation. MKK7 and PIDm (kinase dead version (K-E)) were cloned into pDEST-GW-VYNE and pDEST-GW-VYCE [436], transformed into *Agrobacterium tumefaciens* and subsequent infiltrated in single leaves. The gray boxes show the bright field pictures, the white boxes show the YFP pictures. The white arrows marks the nucleus. The assay was performed with four independent repeats.

To prove these hypothesis, co-localization and BiFC experiments with the confocal laser scanning microscope (CLSM) and a corrected *PID2* mutant are necessary.

The expression data of the amiR MKK7-Col-0 and *pid* lines indicate that both proteins influence the transcriptional regulation of each other. The double mutant amiR MKK7 *pid* showed an additive mutant phenotype similar to the single mutant amiR MKK7 Col-0 with pin-formed structures instead of flowers. Additionally, the expression levels of *MKK7* in the the double mutant line #5 suggests that the dwarfish phenotype is a *mkk7* mutant phenotype. In order to investigate the function of MKK7-PID interaction, further experiments for localization of both proteins in *Arabidopsis thaliana*, interaction *in planta*, and kinase assays, to determine the function of the interaction, have to be performed. In general, it could be shown that a systematically generated PhI is very well suited to frame new hypotheses about the interactors and their possible role in a signaling pathway and to observe new components in signaling cascades.

2.6 Phytohormone ORFeome vs AtORFeome screen

In order to identify a broader signal transmission beyond the phytohormones, PhO was screened against the 12k *Arabidopsis* collection. The resulting network map, called PhI_{out}, contains 698 interactions with 581 proteins. Since 688 ORF from AtORFeome were also used to prepare the PhO collection, a subset of PhO (688 ORFS) was screened against each other. Of the total of 698 interactions in PhI_{out}, 103 interactions from the PhO subset were found and 595 interactions between the proteins from the PhO and proteins from the AtORFeome, which are not in the search space of PhO.

In order to identify the function of the proteins originating from the AtORFeome in PhI_{out}, a GO enrichment analysis [439, 440] was performed. Therefore the nodes from PhI_{out} were separated into a group originating from the AtORFeome (At-nodes) and a second group originating from the PhO (PhO-nodes). Both groups were analyzed using Panther [438] for GO enrichment and Revigo [441] for converting these data into a GO tree map (see TreeMap A.5 part A and B in appendix). As reference lists the AtORFeome and PhO were used, respectively. By including a multiple hypothesis correction (MHC), only the GO terms RNA-processing and cellular localization remained significantly enriched for the At-nodes, whereas using only the Fisher exact test, several significant enriched GO terms could be detected (see figure 2.11). The lack of significantly enriched GO terms after MHC, combined with a high number of interactions, may indicate involvement in many different processes. For the PhO nodes, most of the significantly enriched GO terms with MHC remained significant, suggesting that a very specific set of proteins with function in defense and stress response regulation interact with various proteins from the AtORFeome.

For the At-nodes, 21 GO terms could be identified (see figure 2.11 part A), which majority can be categorized in RNA processing, cellular localization and plasma membrane fusion (see TreeMap A.5 part A in appendix). The majority of the 15 GO terms identified for the PhO-nodes (see figure 2.11 part B) can be categorized in cellular response to chemical stimulus and regulation of cell communication (see TreeMap A.5 part B in appendix). The GO terms of both groups suggest that cell development and regulation of mRNA as well as transport in the cell play a very important role, particularly in defense against pathogens or herbivores, but also in other types of stress responses.

2.7 Convergence of signal integration on transcription factor level

Transcription factors play a very important role in each signaling pathway. In order to address the question of signal integration between the different hormone signaling pathways, repressors and non-DNA binding regulators of each phytohormone signaling pathway were selected and screened against a 90 % complete collection of transcription factors published in 2014 by Pruneda-Paz and colleges [442]. The repressors used differ in particular in their ability to bind to DNA in order to repress transcription or to inhibit transcription through physical interaction with transcription factors. It is known from studies that transcriptional repressors with a DNA binding domain can interact directly with a transcription factor and thus downregulate gene expression [443, 444]. In order to detect these rarely described direct interactions of repressors containing a DNA binding domain with transcription factors [445, 446], these transcriptional repressors

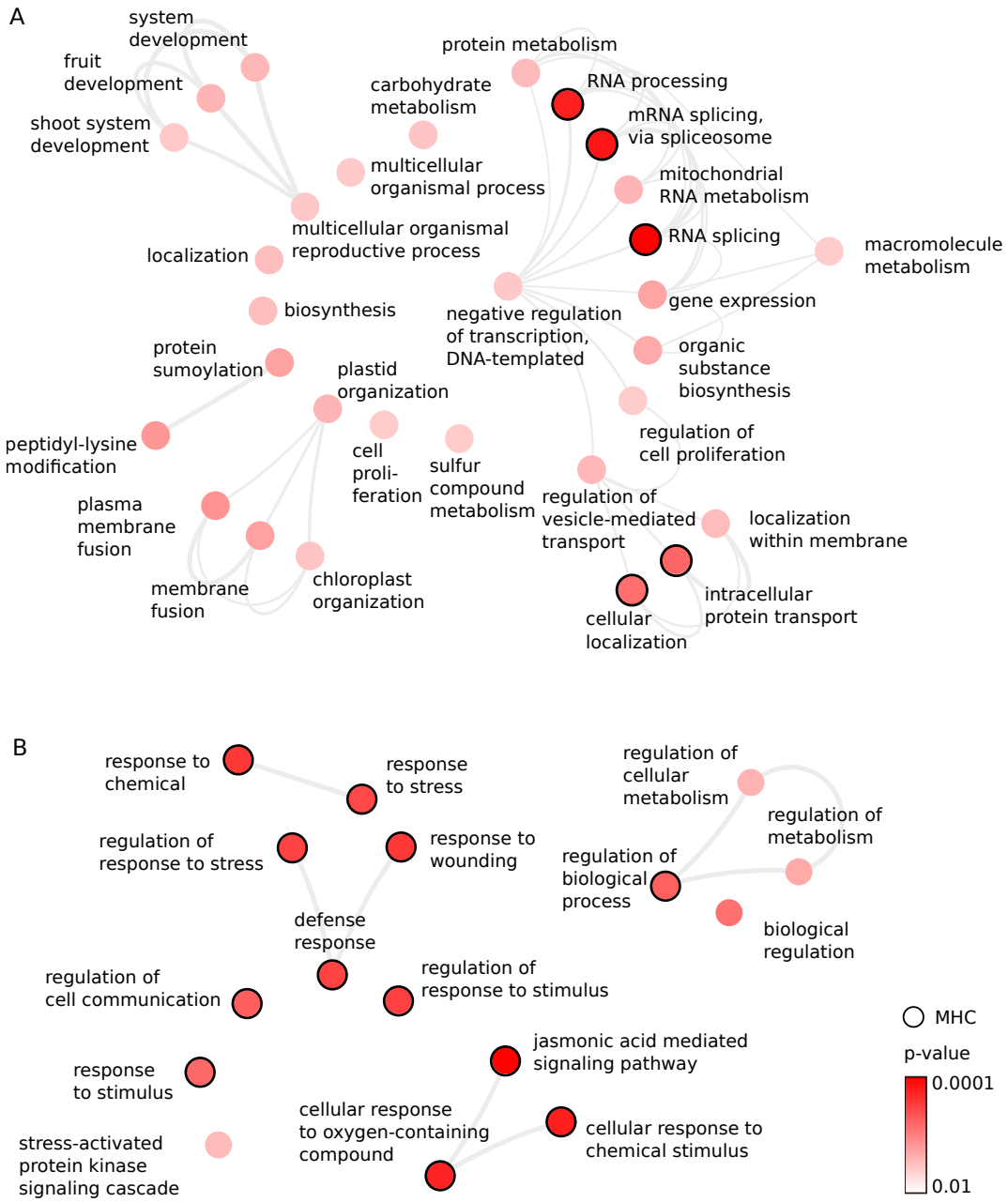

Figure 2.11: PhI_{out} GO enrichment analysis. The interactions in PhI_{out} were sorted by At-nodes (A) and PhO-nodes (B). Both groups of nodes were analyzed using the GO enrichment tool Panther [438]. For the analysis the Fisher exact test was used (red dots). Additionally, these GO enrichment's were multiple hypothesis corrected (MHC) using false discovery rate. All GO terms, which stay enriched after MHC, are marked with a black circle. The p-value is indicated by the strength of the GO-node color.

were included in the screen. Six groups of repressors/regulators were selected for this screen. For the IAA pathway, 29 AUX/IAA proteins were selected (IAA1-IAA20, IAA26-IAA34), which have the ability to block transcription due to their ability to bind directly to the DNA at the AuxRE domain [447, 448, 449, 450] and their ability to bind directly to ARF and inhibit transcription of target genes [451]. For the JA pathway, 12 JAZ proteins were selected (JAZ1-JAZ12), which bind to transcription factors that are already bound to DNA. With the co-repressor NINJA and co-repressor TPL (see introduction figure 1.11) the expression of the JA signaling gene is suppressed. In this screen only the JAZ proteins were used due to their direct binding to transcription factors [233, 452]. For the BR pathway, two repressors were selected, BZR1 and BES1 (or BZR2) that are both transcriptional repressors which bind to the DNA [120]. Additionally, BIN2, a kinase responsible for the degradation of BZR1 and BES1, but also a known repressor [453] was included. For the ET pathway, eight ERF proteins (ERF3-ERF4, ERF7-12) were chosen, which are transcriptional repressors that bind to DNA [454, 455]. For the cytokinin pathway, 9 type A ARR (ARR3, ARR4, ARR6-9, ARR15-17) were selected as repressors that are transcriptional repressors, which bind to DNA and can be inactivated by phosphorylation via AHP proteins [456, 457, 458, 459, 460, 461, 462]. For the SA pathway, three NIMIN proteins were selected as repressors. NIMIN proteins do not have a DNA binding domain, but interact with transcription factors that are already bound to the DNA and thus inhibit the expression of target genes of the SA signaling pathway [213, 463, 215, 464]. The PP2Cs of Clade A would be suitable repressors for the ABA signaling pathway. However, these were tested in separate Y2H assays and were therefore not included in this assay. The interactions of the PP2Cs with transcription factors are shown in figure 2.12 part B and were included in the analysis. The repressors for SL and KAR, SMAX1 (KAR) and SMXL6,7,8 (SL), were first identified at the end of 2015 [285]. By this time, the Y2H experiment was already ongoing. Therefore the repressors for SL and KAR were not tested in this assay. For the GA pathway, the DELLA proteins are known for their repressive function, but they show autoactivation as DB-fusion proteins in the Y2H system. In order to avoid this, the N-terminal part of the DELLA proteins would need to be removed. Since only full length ORFs were tested, the DELLA repressors were excluded from this experiment.

All possible interaction candidates discovered during the screen were systematically tested against all repressors/regulators in the verification process. The resulting network showed 628 interactions with 121 proteins (see figure 2.12 part A) of which 283 interactions are derived from interactions between the 27 AUX/IAA proteins. Specific for the PP2Cs (ABA pathway), 12 interactions with 15 proteins were found (as shown in figure 2.12 part B)that are included in the following analysis.

The repressors/regulators are separated according to their affiliation to phytohormone signaling pathways (see figure 2.13 part A). These assays observe at least one up to 15 specific transcription factor-repressor interaction specific for the individual phytohormone signaling pathways (see figure 2.13.

The interactions of two LATERAL ORGAN BOUNDARIES DOMAIN (LBD) proteins LBD4 and LBD42 with two repressors from the ethylene pathway (LBD4-ERF12, LBD42-ERF8) (see figure 2.13 part B) were highly interesting. These LBD proteins belong to a plant specific gene family with 42 members and play an essential role in the regulation of lateral organ development and metabolic processes [465, 466, 467]. Recent studies have revealed interactions of LBD proteins with basic helix-loop-helix proteins [468], which seem to regulate LBD function in lateral organ development. As well as the function

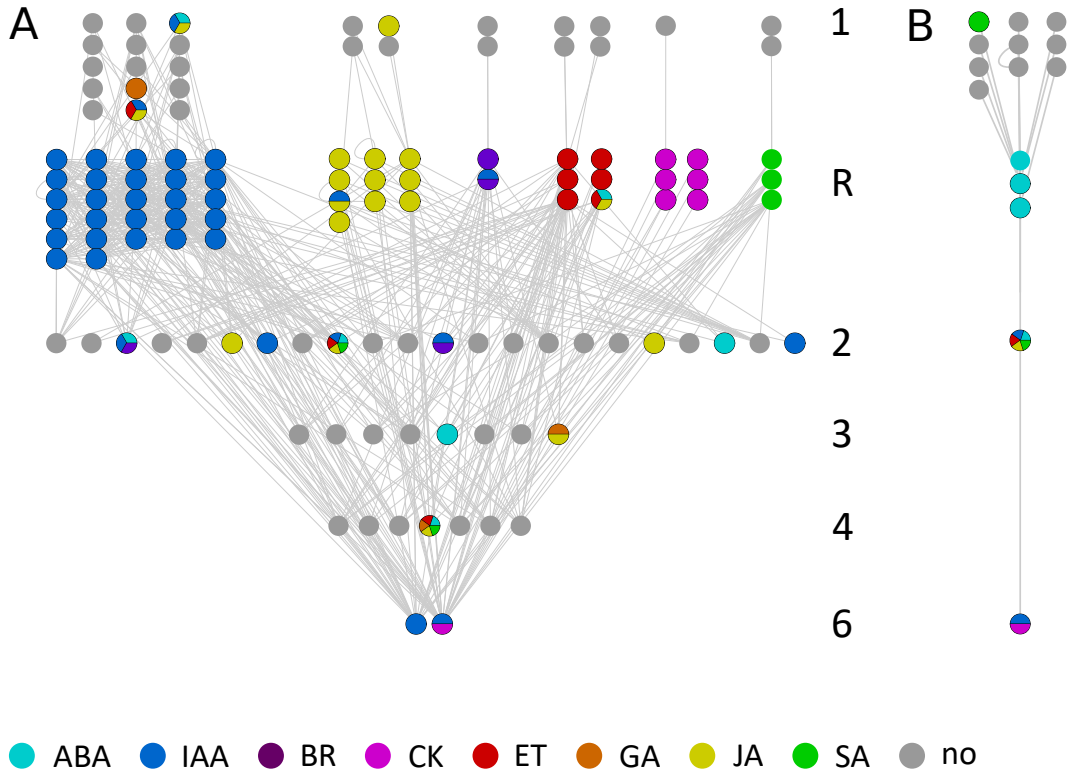

Figure 2.12: Network map of the repressor vs transcription factor screen. (A) shows the interaction network. The numbers 1-6 indicate the number of repressor groups with which the individual transcription factors interact. R indicates the group of repressors of the phytohormone signaling pathways. In (B) the PP2C interactions with transcription factors from a separate Y2H assay are shown. The transcription factors are sorted according to the numbers of interacting repressor groups in (A). All interactions are verified by four independent Y2H assays.

of different LBD proteins that play an important role in the auxin signaling pathway [468, 469]. The ET pathway is known to inhibit lateral root formation by altering IAA transport [56]. These direct interactions with two repressors of the ethylene pathway with LBD proteins allow new hypotheses about the regulation of lateral root formation except from altering IAA transport.

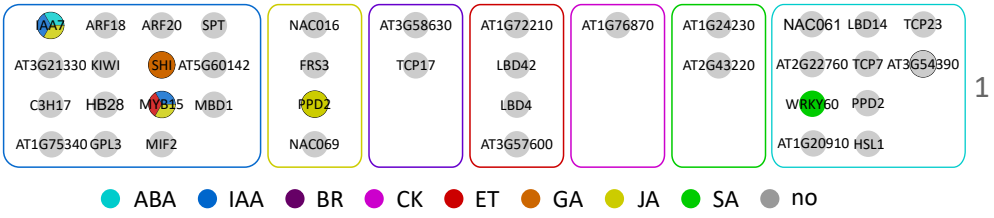

Figure 2.13: Rep-TF part 1: Interactions specific for one repressor group. The transcription factors are grouped per repressors of individual phytohormone signaling pathways. The groups are identified by colored boxes corresponding to the phytohormone pathway to which the repressors belong.

One specific LBD interactions was observed between the ABA repressor HAI3 and LBD14 (see figure 2.13). LBD14 is known to play a role in ABA mediated control in lateral root growth and root system architecture specific under salt and drought stress.

However, the molecular mechanisms how LBD14 is directly regulated could not be shown [470, 471]. This direct interaction leads to the hypothesis that LBD14 function in lateral root formation that can be inhibited by HAI3 in an ABA-dependent manner.

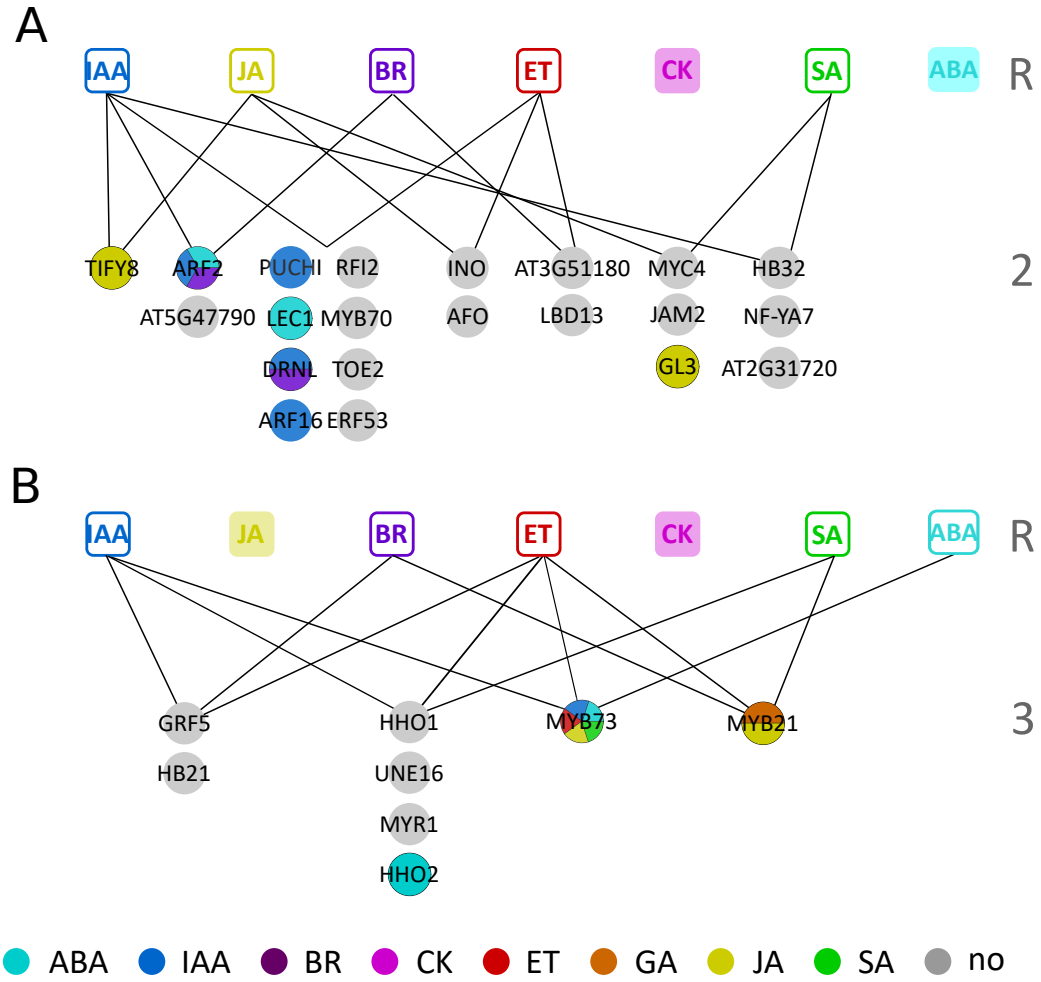

Figure 2.14: Rep-TF part 2: Interactions with two and three repressor groups. In (A) interactions of transcription factors with two repressor groups are shown. In (B) Interactions of transcription factors with three repressor groups are shown. Repressor groups are indicated as boxes and labeled with color and abbreviation of the respective phytohormone signaling pathway. R indicates repressor group, numbers 2 and 3 indicate the number of repressor groups, which are interacting with single transcription factor.

Figure 2.14 part A illustrates interactions of transcription factors with two different groups of repressors/regulators. Most common interactors have been found between IAA and ET repressor groups, reflecting the known co-regulation of lateral root elongation [56, 57, 17], or for fruit ripening [171] via IAA and ET pathways. The other repressor groups share less interactors, like three transcription factors that interact with JA and SA repressors. The interactors MYC4 and JASMONATE ASSOCIATED MYC2 LIKE 2 (JAM2), which both play a role in fine tuning JA response, also interact with NIMIN2. The transcription factor GLABRA3 (GL3) with known function in trichome development and in JA responses [472, 473, 474], interacted here with NIMIN1. This suggests that the known defense induced trichome development is not only controlled by JA but also by SA [475]. Also in this subgroup an interaction of an LBD protein with the ET

signaling pathway is shown, which also interact with BIN2 from BR signaling (LBD13-BIN2). It is possible that the family of LBD proteins plays a role in signal integration across several phytohormone signaling pathways. The number of interactions with three repressor groups (see figure 2.14 part B) becomes much smaller. The transcription factor MYB21, which is annotated with JA and GA [248, 476, 477], interacts with BZR1 (BR), ERF12 (ET) and NIMIN2 (SA). Some of the MYB transcription factors are multiple annotated with different phytohormone signaling pathways, like MYB73 (see figure 2.14 part B), which play an important role in ABA mediated salt stress response [431], and different defense responses in SA [478] and JA [478, 479] signaling pathways. The fact that more than 50 % of the hormone annotated MYB transcription factors are multiple annotated (see figure A.6) and the common network connectivity suggests that MYB21 is also a transcription factor that is controlled by several signaling pathways.

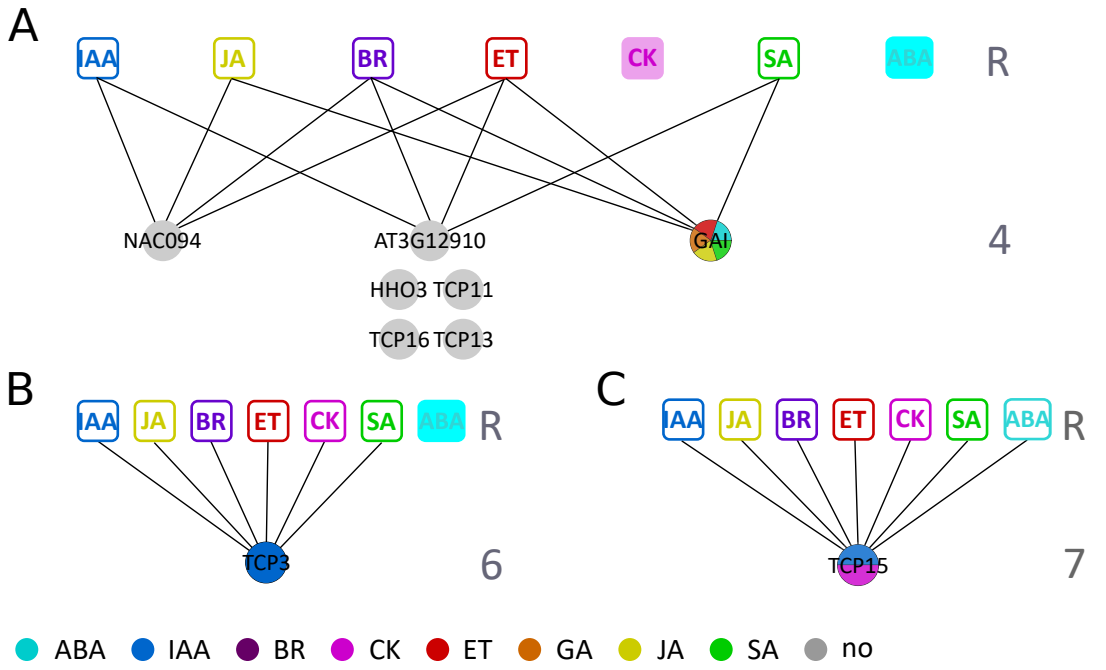

Figure 2.15: Rep-TF part 3: Interactions with four, six and seven repressor groups. In (A) interactions of transcription factors with four repressor groups are shown. In (B) interaction of one transcription factor with six repressor groups and in (C) an interaction with on transcription factor with seven repressor groups are shown. Repressor groups are indicated as boxes and labeled with color and abbreviation of the respective phytohormone signaling pathway. R indicates repressor group, numbers 4, 6 and 7 indicate the number of repressor groups, which are interacting with single transcription factor.

The number of transcription factors which interact with four (see figure 2.15 part A) or more groups as six or seven (see figure 2.15 part B and C) was decreasing. Of these 9 transcription factors, five belong to the TEOSINTE BRANCHED, CYCLOIDEA AND PCF (TCP) family. TCP proteins are known for their role in leaf development and defense mechanisms [418, 419]. For TCP4, for example, it has already been demonstrated that it interacts with the IAA, GA and ABA signaling pathways [480]. Also other TCP proteins are involved in different developmental steps in different phytohormone signaling pathways [481, 482, 483, 484].

The TCP proteins have shown a prominent role, due to their strong interconnection with different repressor groups and therefore with different phytohormone signaling pathways. Recent studies showed high number of interactions with TCP13, TCP14 and TCP15 with different pathogen effectors, linking their function with plant defense (JA or SA) [418, 419]. This strongly indicates that TCP proteins, like the MYB transcription factors, can be important points of signal integration over all signal pathways.

In summary, the Rep-TF screen could identify a high number of interactions with an unexpectedly low number of 67 transcription factors. At the same time, the large number of interactions were considered as possible points for signal integration and thus confirm our expectations to identify points of signal integration on the level of transcription factors. Additionally, 266 interactions of transcriptional repressors (with DNA binding domain), like BZR1/2, ERF proteins, ARR proteins and AUX/IAA proteins with transcription factors could be detected. These high number of interactions indicate that transcriptional repressors, with DNA binding domain, inhibit several signals not only via binding to DNA but also via direct interactions.

2.8 New insights in hormone-dependent receptor interactions

In order to understand how the phytohormone signaling pathways interact with each other, it is important not to disregard the function of the phytohormones in the signaling pathways. It is known that some PPI can only take place in the presence of a specific phytohormone, such as the GA-dependent interaction of the DELLA proteins with the GA receptors [485]. Three of these GA receptor DELLA interactions are contained in the PRS set and could not be detected without the addition of GA, but could be confirmed in a hormone-dependent assay (see section 2.8.3). To cover also those interactions, which are dependent or even inhibited by a specific hormone, the receptors from the different phytohormone signaling pathways were screened against PhO and AtORFeome collections in the presence and absence of the respective hormone. These assays were performed for receptors from ABA, IAA, GA, JA, SA and SL pathways. However, no screens were performed for BR, CK and ET because their membrane bound receptors. The activated membrane bound receptors phosphorylate cytosolic proteins that starts the downstream signaling cascades. These signaling processes, consist of more than two proteins for the signal transduction, which can not be supported by a Y2H assay. For all tested phytohormone screens the respective hormone were added in 100 μM final concentration to the selective Y2H plates, for ABA screens only 30 μM abscisic acid were used (personal communication, Prof. Grill lab members, [486]).

2.8.1 ABA screens

All RCARs were screened against the PhO and the AtORFeome with and without ABA. The resulting network consists of 68 proteins with 142 interaction, of those 104 were new and 38 were confirmed interactions between RCARs and PP2Cs (shown in figure A.7). In total 48 interactions were ABA-dependent, of those, 10 belong to the confirmed interactions. RCAR1, which has more specific interactions compared to all the other RCARs, is known to promote drought resistance and is involved in leaf senescence [487]. The 17 RCAR1 specific interaction partners were almost all transcription factors. Some of those interactors have a function in response to salt stress (MYB73 [431], LSU1 [488]), or

drought stress, like the protein AT5G51440, which belongs to the HEAT SHOCK PROTEIN (HSP)20-like chaperones super-family, is known for involvement in response to heat (annotation based on Pfam:PF00011). The gene Fes1C encodes one of the *Arabidopsis* orthologues of the human Hsp70-binding protein 1 and has so far no GO annotation, but the gene Fes1A, a close family member, is already known for its important role in heat response signaling pathways [489]. The other interaction partners, mostly transcription factors, are known for different function throughout plant development like positive regulation of seed germination (HSI2) [490], which is known for function in ABA signaling. All interactions of RCAR1 are ABA-independent, as expected from literature data. RCAR3 is known for its role in lateral root growth and the regulation of the ABA signaling pathway in the root, as well as the antagonistic role of ABA to IAA through the different regulation and interactions of RCAR3 with MYB77 or MYBR1 [430, 491, 492]. Of the four interacting proteins, three have an annotation for auxin, which make these interactions very likely. Also RCAR3 showed only ABA-independent interactions. Another interesting candidate is RCAR9, which is known for its role in crosstalk between ABA and JA with ABA-dependent interaction via MYC2 [493]. Also in this screen RCAR9 showed almost exclusively ABA-dependent interactions, but most of the specific interactors are proteins with unknown function. The third group of RCARs (RCAR11-14) showed no specific interaction in this screen. Additionally, a group of 19 transcription factors (marked in figure 2.16 as multiple) showed interaction with two or more receptors which result in 61 interactions, including 25 ABA interactions. Six of these transcription factors were TCP proteins which showed already high numbers of interactions in the PhI and Rep-TF network map.

ABA is known for its function in leaf development as well as leaf senescence [316], which matches the functions of the TCP interactors. TCP3, TCP10, TCP13, TCP9 [495, 496] and TIFY8 [497] have a GO annotation in leaf development and or leaf senescence, whereby TCP19 [418] and TIFY 8 [235, 498] are associated with functions in pathogen defense, which has also been documented for RCAR3 in recent studies [499]. The ABA signaling pathway is known for its negative regulatory role during germination. Here we found a direct interaction of RCAR1, RCAR3, and RCAR9 with TCP15, whereby the interaction with RCAR9 was hormone-dependent. TCP15 is known for its interaction with GAI and RGL2 and its role in seed germination via regulation of GA [483], which indicates a new point of signal integration between GA and ABA to regulate germination. ABA is also known for its negative regulation of flowering through the inhibition of the floral transition. This is regulated by the upregulation of FLC via ABSCISIC ACID-INSENSITIVE 4 (ABI4) [500]. Additionally, ABA is involved in the regulation of flowering time with regard to drought escape response via SUPPRESSOR OF OVEREXPRESSION OF CO 1 (SOC1), FLOWERING LOCUS T (FT) and CONSTANS (CO) [501]. In this screen, interactions from RCAR1, RCAR2 and RCAR10 to NAC089 and RCAR1, RCAR6 (+ABA) and RCAR9 (+ABA) to DRN could be detected, which have functions in floral organ development or floral initiation [502, 503].

An important role of the ABA signaling pathway has been previously demonstrated in lateral root growth [491, 430] via an ABA-dependent RCAR3-MYB77 interaction. In this screen I could additionally show interactions between RCAR1, RCAR4 (+ABA), RCAR5 (+ABA), RCAR8 and RCAR9 (+ABA) with MYB77, which could indicate a more specific ABA-dose-dependent interaction patter with MYB77. The RCARs are known to have different ABA affinities [504], possibly the interaction of the RCARs with MYB77 is necessary for lateral root elongation and has to take place during different developmental

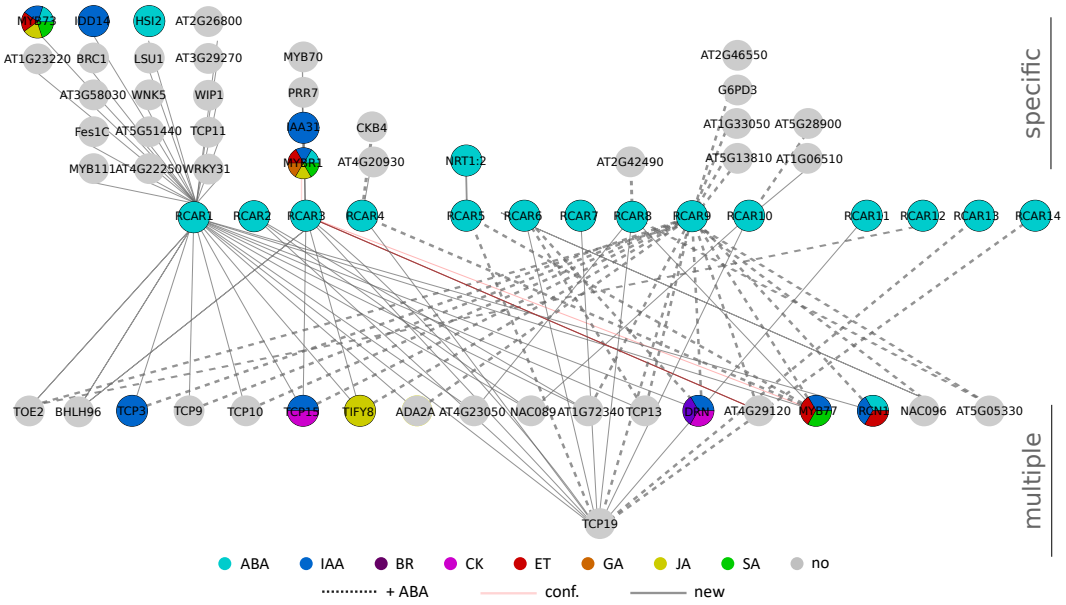

Figure 2.16: ABA Y2H network map. The RCAR receptors are centered in the network and represented in the three subgroups (RCAR1-4, RCAR5-10, RCAR11-14) [494]. The remaining nodes represent the interaction partners of the receptors. Interactors specific for single RCARs are shown above the RCARs and marked as specific. The interactors shown below the receptors interact with two or more receptor, and are marked as multiple. The nodes are colored according to their hormone annotations based on AHD2.0 and TAIR10. Dashed lines represent ABA-dependent interactions. Solid lines represent ABA-independent interactions. Light red lines indicate confirmed interactions, gray lines indicate new interactions. These interactions are independently tested four times and could be confirmed at least 3 times. The verification was systematically performed with and without ABA (30 μM).

steps, regulated by different ABA hormone levels in the plant. In line with this hypothesis, interactions between RCAR1, RCAR9 and ROOTS CURL IN NPA (RCN1) could be detected. RCN1 is known to control root growth via the auxin signaling pathway as well as via BR and glucose [505, 506]. Here RCAR1 interacts hormone-independently with RCN1 (-ABA), whereas RCAR9 interacts with RCN1 only in presence of ABA.

With this ABA receptor screen, a large number of new direct interactions could be shown. These direct interactions, especially the interactions of several RCARs with an interactor, which partly only occur in dependence on ABA, allow hypotheses about an ABA specific regulation of different processes or stress responses. Possibly those direct interactions induce fast and short-term reactions to bridge suddenly occurring environmental influences, e.g defense responses through RCAR9 with MYB77 and TCP13. Additionally, the specific interactions of the RCARs, especially for RCAR1, indicates that the RCARs might have a separate function besides the receptor function in the ABA signaling pathway. The known RCAR-PP2C interactions, of which several were confirmed both as ABA-dependent and independently, reflect the known core ABA pathway, in which phosphatases negatively regulate the ABA pathway. With regard to the function of PP2Cs in the ABA pathway, the question arises whether PP2Cs have an effect on other interactions of RCARs, or whether RCARs and PP2Cs together as complex enable further interactions that could not be shown so far. To address these questions, a Y3H screen was performed in which the PP2Cs were cloned into an adapter plasmid

to detect also their inhibitory functions. All possible RCAR-PP2C combinations were screened against PhO and AtORFeome and candidate interactions were verified in four independent Y3H assays.

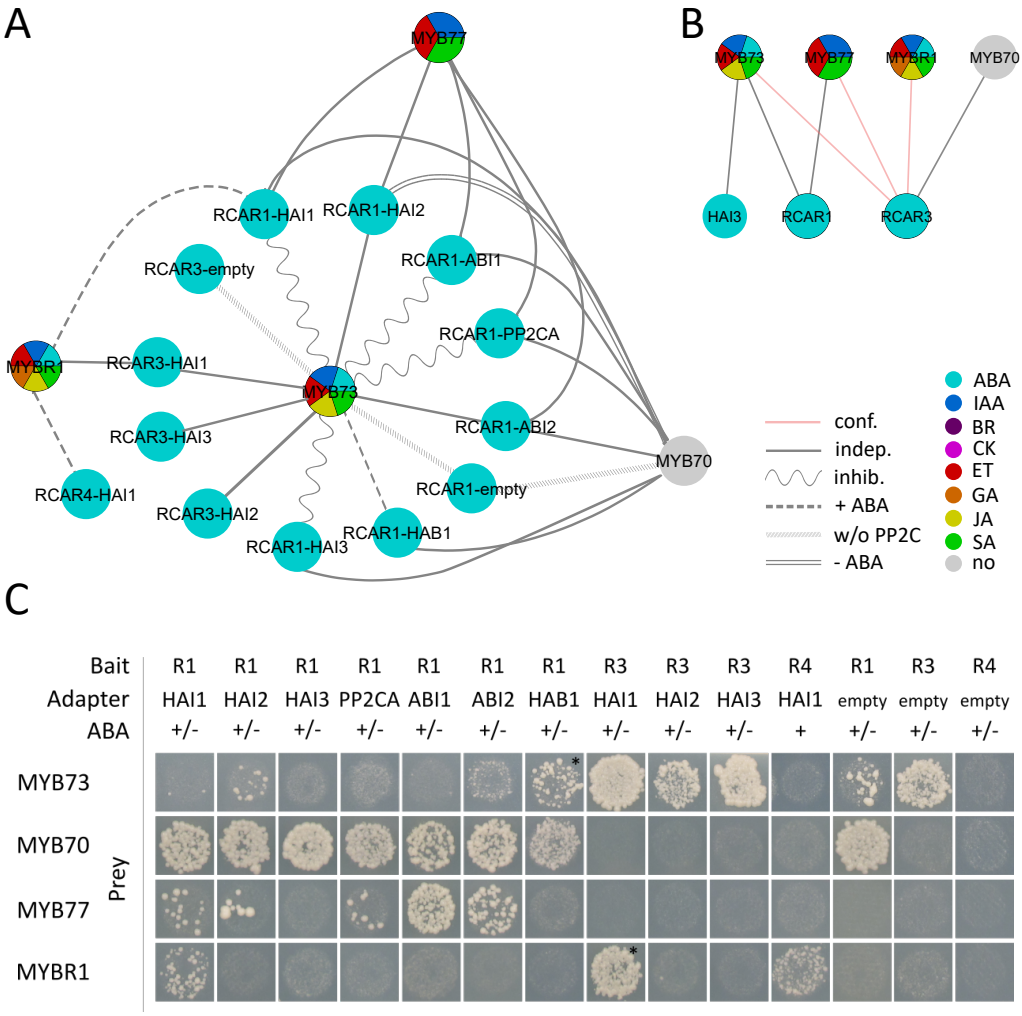

Figure 2.17: MYB subgroup 22 interactions. (A) Y3H interaction map. Sine-wave lines indicate inhibited interactions, dashed lies indicate ABA-dependent interactions and solid lines indicate ABA-independent interactions, structure line indicates empty control interactions, double line indicates interactions only without ABA. Light red line indicate confirmed interactions. (B) Y2H interactions with the MYB subgroup 22 found in my Y2H screens, partially confirmed interactions. (C) Y3H interaction pictures from one representative repeat out of four repeats. R1 indicates RCAR1, R3 indicates RCAR3, R4 indicates RCAR4. ± indicates ABA-independent interaction, + indicates ABA-dependent interaction, stars in the pictures marks only ABA-dependent interactions.

The ABA Y3H experiment resulted in a very complex network with 204 interactions. These interactions can be divided into 90 ABA-dependent interactions, 89 ABA-independent interactions, 16 RCAR-empty control interactions (DB-RCAR + adapter-empty + AD-interactor) and 9 blocked interactions by certain PP2C combinations (see tables A.7,A.8 and figure A.9, A.10, A.11). The MYB transcription factor family subgroup 22 (MYB 44/MYBR1, MYB70, MYB73, MYB77) [94] showed interactions in the Y2H screen with RCAR1 (RCAR1-MYB73, RCAR1-MYB77) and RCAR3 (RCAR3-

MYBR1, RCAR3-MYB70), which were reidentified in the Y3H. MYB73 and MYBR1 are known to be involved in different phytohormone signaling pathways, including ABA pathway, whereas MYB77 and MYB70 were so far not known to be involved in ABA signaling. Through the Y3H screen it was possible to discover a potential inhibitory function of some PP2Cs on the interaction of MYB73 with RCAR1, detected in the Y2H assay (see figure 2.16).

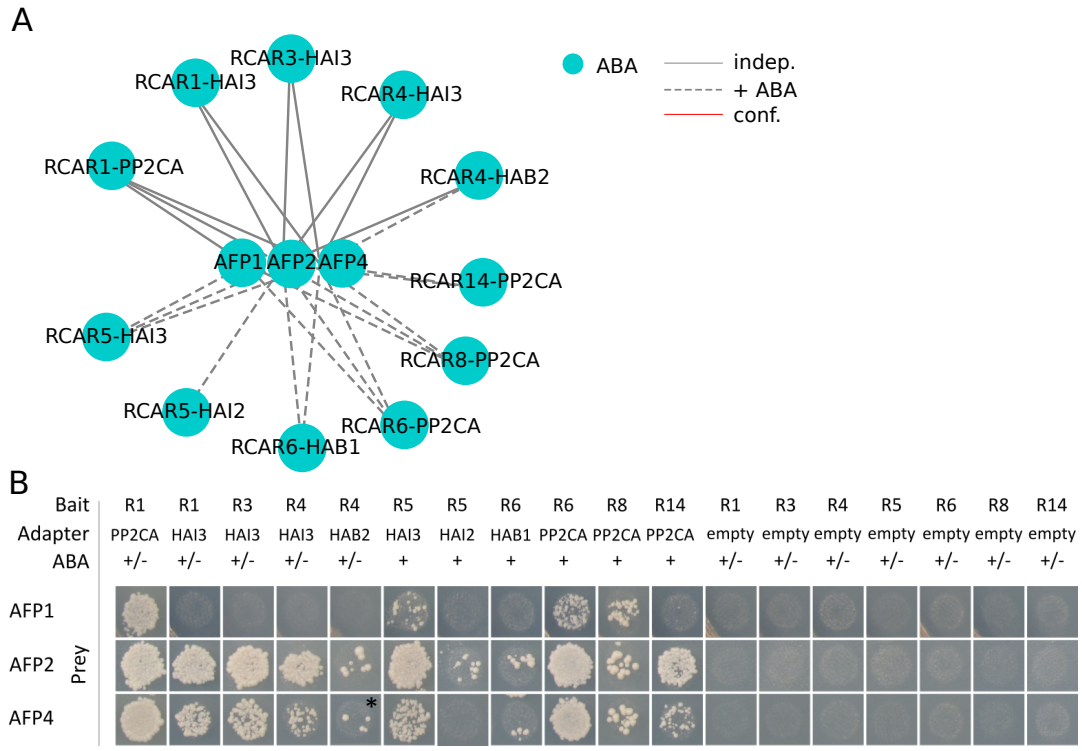

Figure 2.18: ABA Y3H AFP interactions. (A) AFP1, AFP2, AFP4 interactions with different PP2C combinations. (B) Y3H interaction pictures from one representative repeat out of four repeats. ± indicates ABA-independent interactions. + indicates ABA-dependent (30 μM ABA). Dashed lies indicate ABA-dependent interactions and solid lines indicate ABA-independent interactions. Star marks ABA-dependent interaction.

This interaction could not be detected, when ABI1, PP2CA, HAI1 and HAI3 were tested as RCAR1-PP2C combinations, whereas the interaction was not disturbed by HAI2, HAB1 and ABI2 in combination with RCAR1. In the Y2H assay, however, RCAR1 interacts with HAI1, HAI2, HAI3 and ABI1. Thus, one could assume that the binding affinity of RCAR1 to HAI1, HAI3 and ABI1 is stronger than that of RCAR1 to HAI2. In the analysis of all PP2Cs of *Arabidopsis* by Xue et al., 2008 [507] the three HAI phosphatases cluster together with other ABA related phosphatases (clade A). But an protein alignment of all nine ABA related phosphatases alone display differences in the N-terminal part of the proteins (see A.7.2), which might explain the different binding affinity of RCAR1 with MYB73 in combination with the HAI phosphatases. Considering the confirmed interaction of RCAR3 with MYB73 (see figure 2.17 and 2.16) [430] it seems that this interaction was not inhibited by HAI1, HAI2 and HAI3. On the contrary it seems that HAI1 and HAI3 even enhance the interaction, indicated by a stronger yeast growth (see figure 2.17 part C).

In summary, it can be concluded that the PP2C clade A phosphatases in this Y3H assay, depending on the interaction partner, produce a stronger interaction with the receptor and thereby inhibit interactions between bait and prey fusion proteins. To get an overview of the binding affinity or inhibitory effects of all PP2Cs on RCAR interactions, all combinations have to be tested side-by-side with and without ABA treatment in different concentrations.

In addition to these interactions with MYB TFs of subgroup 22 and their different regulation, interactions with the ABI FIVE BINDING PROTEIN (AFP) were observed. The AFP proteins form a small family of four highly conserved, plant-specific proteins that have been known for several years for their function in negative regulation of ABA response genes [508, 509] and their function in ABA and salt stress responses [510]. AFP proteins are negative regulators in the ABA pathway by promoting the degradation of ABSCISIC ACID INSENSITIVE5 (ABI5) [508]. It is assumed that the AFP proteins are responsible for the fine tuning of germination, seedling growth and the stress response of seedlings, via ABI5 degradation [509]. AFP2 and AFP4 interactions with PP2Cs such as HAI1, PP2CA and ABI1 are already known from the publication Lumba et al., 2014 [511]. In addition, the PhI_{out} screen has shown an interaction of AFP2 with AHG1 and AFP4 with HAI3 (see figure A.8). In this Y3H assay AFP1, AFP2 and AFP4 interact with RCARs in combination with PP2CA, HAI3, HAI2, HAB1 and HAB2 (see figure 2.18 A and B). Since all RCARs without PP2Cs do not show any interactions, it can be assumed that the interactions are mainly caused by the PP2C-AFP interaction. In interactions with AFP1 it is striking that three RCAR-PP2CA combinations allow an interaction, but only one RCAR-HAI3 combination was detected, which was also weaker than the three other interactions. Unlike AFP1, AFP2 and AFP4 show strong interactions with RCAR-PP2CA and RCAR-HAI3 combinations. Interestingly, interactions with RCAR1, RCAR3, and RCAR4 in PP2C combinations occur independently of ABA, whereas all interactions with RCAR5, RCAR6, RCAR8, and RCAR14 occur ABA-dependent only. These results indicate that the RCARs have an effect on the PP2C-AFP interactions.

In summary, the ABA receptor screen (Y2H and Y3H) identified a high number of ABA-dependent interactions (48 in Y2H, 90 in Y3H), as well as possible new functions for single RCARs, like RCAR1 and RCAR9. To validate different ABA-dependent and independent interactions in the Y2H and Y3H systems in plants, 58 polymorphism lines of interactors were ordered and currently analyzed to obtain homozygous mutant lines. Additionally, collaborations with Prof. Grill (Botany, TUM) are ongoing to validate several interactions.

2.8.2 IAA screen

The auxin signaling pathway contains 6 auxin receptors: TIR1 [512] and AFB1-5 [513, 514], which bind to the SCF complex to form a functional E3 ubiquitin ligase complex. For the Y2H screen, all six receptors were tested in the presence and absence of 100μM IAA or 100μM 2,4D against the PhO and the AtORFeome. The screens resulted in 10 interactions among 9 proteins as shown in figure 2.19. This low number was surprising, due to the known TIR1/AFB interactions with several AUX/IAA proteins from recent publications [515, 516]. One possible explanation why this Y2H screen did not detect more of the known interactions is the use of another Y2H system and other plasmids. For the interactions published by Villalobos et al, 2012 both a LexA Y2H system and other plasmids with a 2μ plasmid-origin-of-replication [515], were used. Possibly these

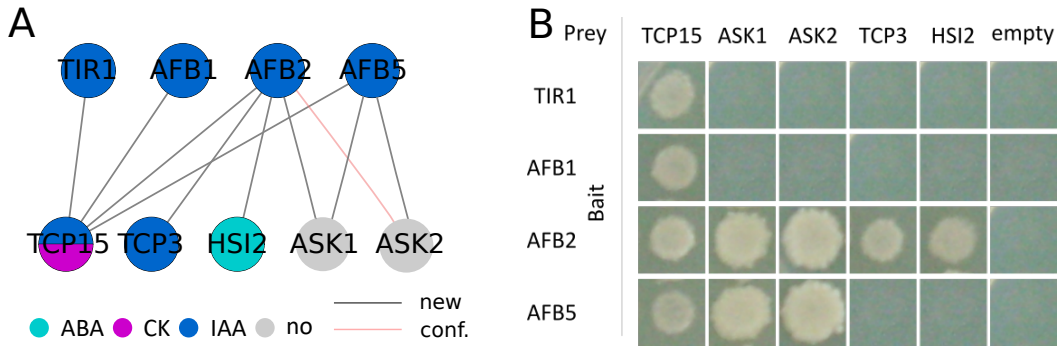

Figure 2.19: IAA Y2H interactions. (A) IAA Y2H interaction network. (B) Y2H interaction pictures from one representative repeat out of two repeats. Nodes are colored according to their hormone annotation. Gray edges indicate new interactions. Light red edges indicate confirmed interactions. empty indicates DB fusion mated with AD empty vector as control for DB autoactivators.

interactions are only detectable with the use of 2μ plasmids, since a large amount of both interaction partners is required to detect these interactions.

AFB2 and AFB5 showed interactions with ASK1 and ASK2 which are SCF complex subunits. The interaction between AFB2 and ASK2 was already published by Kuroda in 2012 [517]. Therefore additional interactions with the ASK proteins were not surprising. Interestingly TIR1, AFB1, AFB2 and AFB5 interacted with TCP15, which is known for its function in regulating IAA biosynthesis. TCP15 overexpression plants have reduced YUCCA1 and YUCCA4 mRNA levels compared to wild type [484], which are both part of the IAA biosynthetic pathway and the downregulation of both genes leads to lower IAA production. This result could indicate that IAA biosynthesis may be controlled by TCP15 using a feedback loop. For AFB2 two specific interactions with TCP3 and HIGH LEVEL EXPRESSION OF SUGAR-INDUCIBLE GENE2 (HSI2) were found. TCP3 is known for its function in IAA signaling, by regulating the promoter activity of IAA3 [495]. TCP3 is also known to regulate the gene expression of ASYMMETRIC LEAVES1 (AS1) and a miR164A, which are responsible for leaf differentiation. The interactions shown here could indicate a new direct regulation of TCP3 via the IAA receptors. This could provide an additional, possible fast inducible regulatory mechanism for certain IAA regulated developmental processes. HSI2 is known to suppress sugar-induced expression of the seed maturation program in seedlings and play a major role in regulating the transition from seed maturation to seedling growth [490]. However, no link between HSI2 and the IAA signaling pathway is known yet. IAA may also play a role in the regulation of seed maturation through regulating HSI2. Although the number of interactions resulting from the screen was relatively small, the interactions found fit very well to the development processes regulated by IAA and indicate new possible regulatory mechanisms within the IAA signaling pathways.

2.8.3 Gibberellin screen

The three GA receptors GID1A, GID1B and GID1C were tested against the PhO and the AtORFeome in presence and absence of 100μM GA3. The screen results in 19 interactions among 11 proteins. The known GA-dependent interactions of the three receptors with all five DELLA proteins could be confirmed (see figure 2.20 part A) [485]. However, there

seems to be a difference in the strength of the interaction between GID1 and the DELLA proteins. Perhaps the interaction between GID1A and the DELLA proteins is stronger than the interaction of the other two receptors to the DELLA proteins (see figure 2.20 part B). In order to elucidate different strength of GID1-DELLA interactions, the GID1-DELLA interactions have to be tested with different GA3 concentrations. In addition four GA3-independent interactions could be detected between GID1A and GID1B with METHYL ESTERASE 17 (MES17). Studies have shown that methyl esterases are able to convert IAA to methyl IAA (MeIAA) [518, 519, 520] and that MES17 is able to convert IAA to MeIAA, which is an inactive form of IAA. This could indicate that MeIAA functions as a quickly available storage form of IAA, compared to active IAA [521]. With this interaction a new hypothesis about a direct crosstalk between IAA and GA can be formulated, whereby it is possible that the homeostasis of IAA is regulated by the GA signal pathway. Specific for GID1C, interactions with AT2G20950, a protein

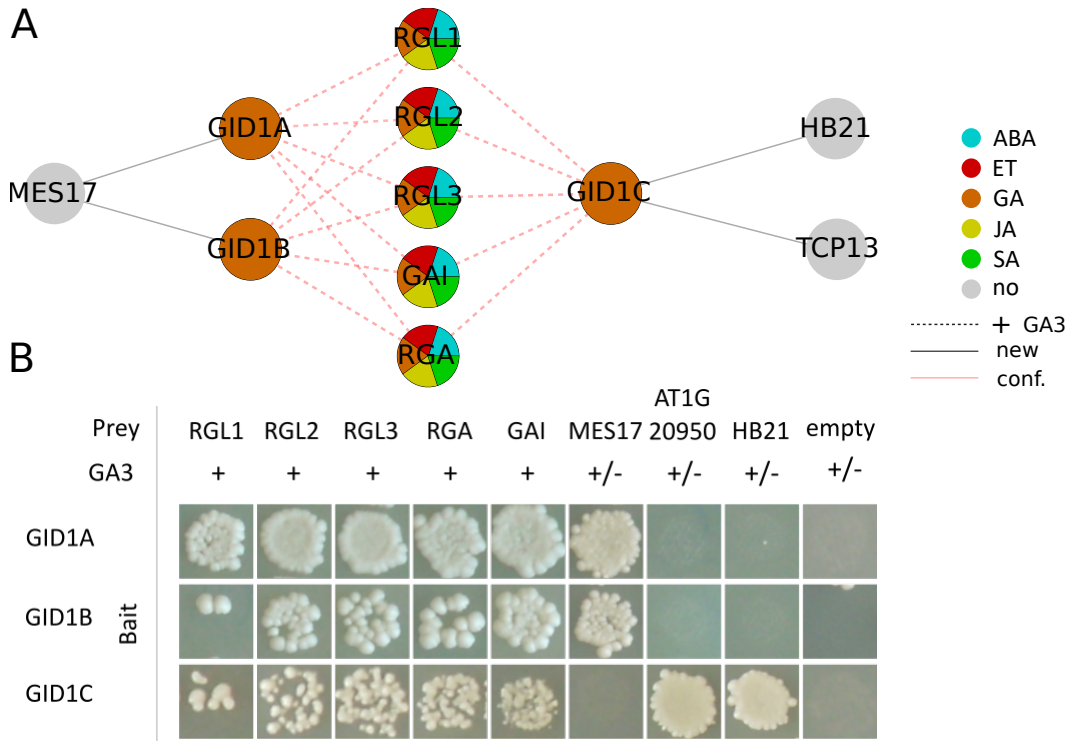

Figure 2.20: GA Y2H interactions. (A) GA Y2H interaction network. Edges in gray indicate new interactions, edges in light red indicate confirmed interactions and dashed edges indicate ABA-dependent interactions. (B) Y2H interaction pictures from one representative repeat out of four repeats. empty indicates DB fusion mated with AD empty vector as control for DB autoactivators.

from the phosphofructokinase family, could additionally be found, and an interaction with the protein HOMEOBOX 21 (HB21). Both proteins do not yet have a known function, but they can now be linked to the GA signaling, which can serve as a basis for further hypotheses.

2.8.4 Salicylic acid screen

The salicylic acid pathway contains three receptors, of those NPR1 and NPR3 could be cloned and were used for the hormone-dependent interaction screen against PhO and AtORFeome collection in the presence and absence of 100μM SA.

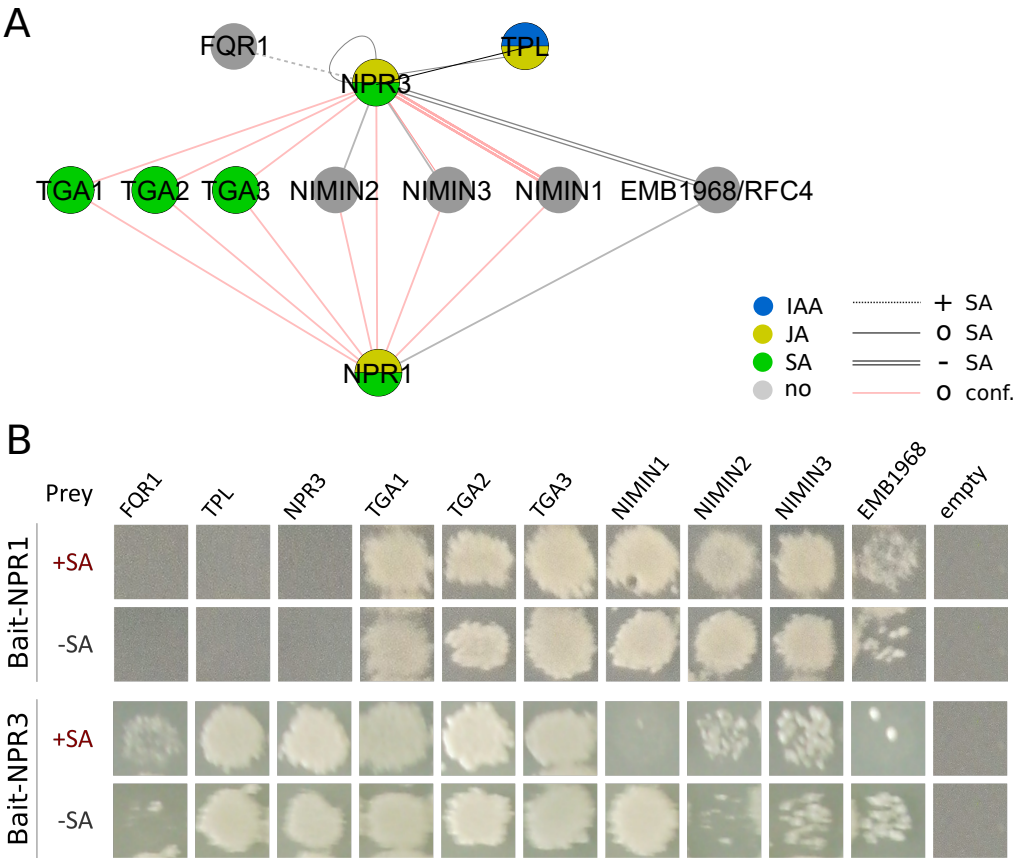

Figure 2.21: SA Y2H interactions. (A) SA Y2H interaction network. Edges in gray indicate new interactions, edges in light red indicate confirmed interactions, dashed lines indicate SA-dependent interactions, double lines indicate interactions, inhibited by SA. (B) Y2H interaction pictures from one representative repeat out of three repeats. empty indicates DB fusion mated with AD empty vector as control for DB autoactivators.

The screen results in 18 interactions with 11 proteins (see figure 2.21), in which NPR1 and NPR3 showed SA-independent interactions with TGA1, TGA2, TGA3, and with NIMIN1, NIMIN2 and NIMIN3. While NPR1 interacts SA-independently with the three NIMIN proteins, NPR3 shows only an interaction with NIMIN1, in the absence of SA, an increased interaction of NPR3 with NIMIM2 in the presence of SA and just the NPR3-NIMIN3 interaction is SA-independent. Interactions of NPR1 and NPR3 with TGA or NIMIN proteins are already known from recent studies, but not this specific SA regulated NPR3-NIMIN interactions. Interesting is the interaction of NPR3 with a FLAVODOXIN-LIKE QUINONE REDUCTASE 1 (FQR1) (AT5G58800), which was SA-dependent. QRs have been little studied in plants but have a demonstrated role in the regulation of protosomal degradation in humans and yeast [522, 523]. A recent study focused on the five QRs found in *Arabidopsis*, in which the QRs showed a higher susceptibility to a necrotrophic fungal infection as over-overexpressor, while the knock

out mutants were much more resistant due to a higher reactive oxygen species (ROS) level. An interaction of NPR3 with FQR1 in the presence of SA could initiate a defense response by ROS accumulation and thus induce a further defense mechanism with no PR gene activation [524]. The interaction of NPR3 with TPL, which was SA-independent, also seems to be quite interesting. TPL is known as co-repressor in JA and IAA signaling pathways [235, 525]. TPL interacts with other proteins through their EAR domain. It is known that TPL also interacts with NIMIN2 and NIMIN3 [296], which have an EAR domain and also have a repressive effect on the SA signaling pathway. Possibly TPL-NIMIN and NPR3 interact in a complex way. This screen shows a possible new defense regulation via an interaction with a QR, which could be independent of the transcription of PR genes, as well as a differentiated SA regulated NPR3-NIMIN interaction, which is currently further analyzed by colleagues.

2.8.5 Strigolactone screen

The SL and the KAR signaling pathway have only recently been intensively investigated compared to the other hormone signaling pathways. The previous studies, however, have identified a very important role of both signaling pathways in different development processes and stress management strategies. The exact molecular biological basics are not well understood, therefore these two Y2H assays were very important. The SL and KAR screens were performed in cooperation with Prof. Caroline Gutjahr. For this purpose, D14 as SL receptor and D14L/KAI2 as KAR receptor with and without the specific hormone were screened against the AtORFeome (KAR2 (10μM final conc.) and *rac*-GR24 (5μM final conc.)). As the option was available, the screens for both receptors and MAX2 were tested with and without the presence of *rac*-GR24 as well as with KAR. The verification was also performed systematically, with and without *rac*-GR24 or KAR. The resulting network contains of 28 interactions with 23 proteins, and 20 of these interactions were *rac*-GR24-dependent (see figure 2.22). Contrary to expectations no interactions of KAI2 in presence of KAR2 were found, but an interaction of D14 with protein FARENSYLATED PROTEIN 6 (FP6) in presence of *rac*-GR24 could be detected. MAX2-D14 and MAX2-D14L in both versions (AD-X DB-Y, AD-Y DB-X) were tested as positive controls. Only the interaction of AD-MAX2 with DB-KAI2 was confirmed. The interaction of MAX2 and D14 shown by Hamiaux et al 2012 as well as by orthologues in rice by Zhou et al 2013 [283] should be possible in *Arabidopsis*. However, this interaction could not be detected in my screen or by the previous study from Wang et al., 2013 [284]. It is possible that the molecular biological functions of DECREASED APICAL DOMINANCE 2 (DAD2) (petunia) [526] and D14 (rice) [283] are more different from those of D14 of *Arabidopsis thaliana* than previously assumed.

Of great interest, however, were the interactions found with KAI2. KAI2 interacts independently of *rac*-GR24 or KAR2 with PROTEIN UBIQUITINATION 39 (PUB39) (see figure 2.22 part B group I),TCP14 and TIFY8, which are known for their involvement in defense response [418, 527] (see figure 2.22 part B group II). Furthermore, an interaction with *Arabidopsis thaliana* DNAJ HOMOLOG 3 (ATJ3) was found (see figure 2.22 part B group V). This protein is known as a homologous to the co-chaperon DNAJ protein of *E.coli* and for its involvement in the response to different types of stress [528] and in flowering time regulation [529, 530]. An interaction with FP6, but also independent of *rac*-GR24, could also be observed for KAI2. This is the only interaction KAI2 and D14 have in common. FP6 is known for its role in heat acclimation as it is upregu-

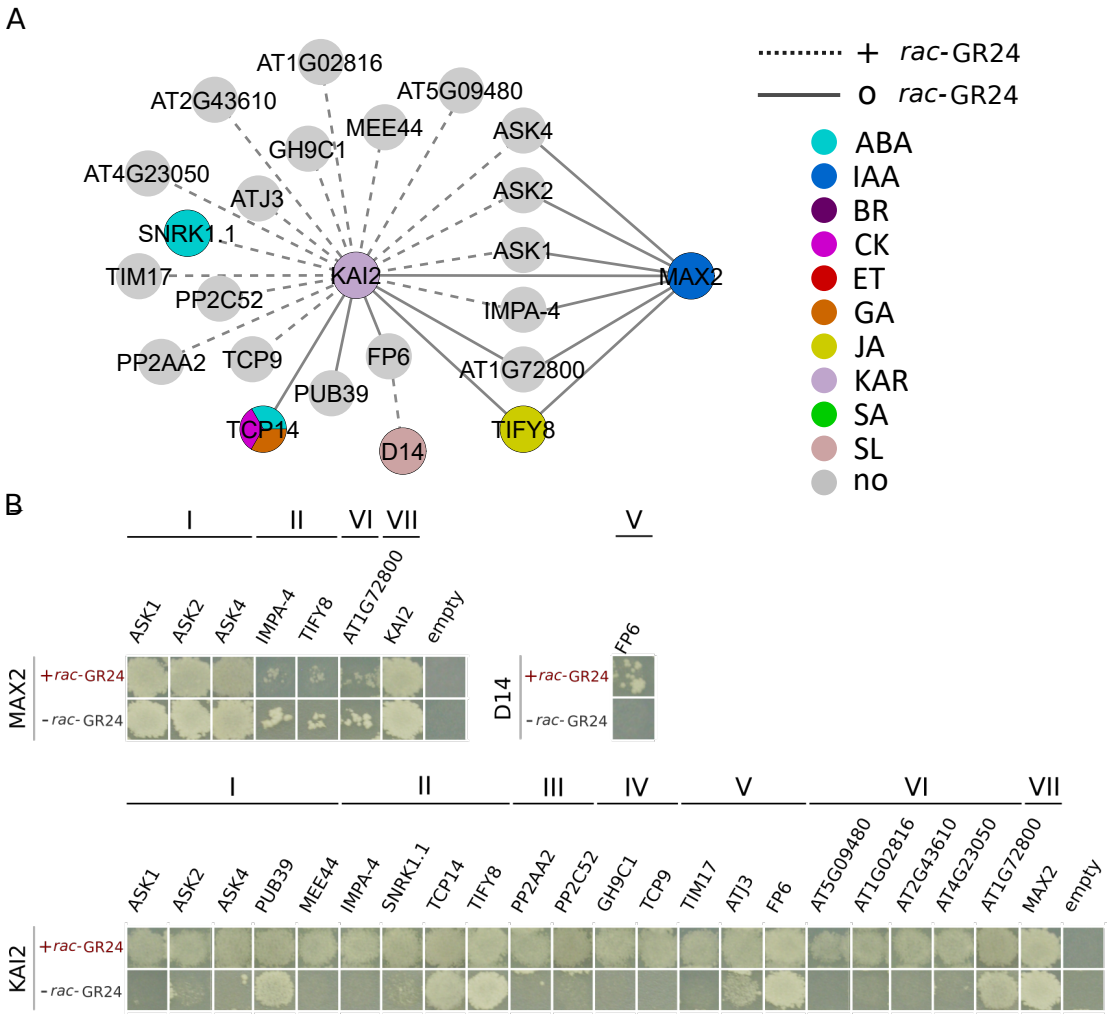

Figure 2.22: SL Y2H interactions. (A) SL Y2H interaction network. (B) Y2H interaction pictures from one representative repeat out of four repeats. Group I contains interaction partners with function in ubiquitination as well es embryo development. Group II contains interaction partners with function in defense and viral protein interaction. Group III contains phosphatases as interaction partners. Group IV proteins are involved in root and root hair development. Group V and VI proteins have different or unknown functions. Group VII contains the positive and negative control. The negative control (empty) were DB fusion proteins mated with AD empty vector as control for DB autoactivators. The positive control was the interaction between MAX2 and KAI2. Star indicates interaction was SL (*rac*-GR24)-dependent with a final concentration of 5μM.

lated after heat stress [531]. Interestingly were interactions of KAI2 that occurred only in presence of *rac*-GR24. The synthetic *rac*-GR24 is a racemic mixture of four stereoisomers of which two (butenolide D ring 2'R and 2'S configuration) are able to bind to KAI2 and D14 [532], therefore interactions of KAI2 in a *rac*-GR24-dependent manner were not unlikely. KAI2 interacts with ARABIDOPSIS SERIN/THREONIN KINASE ASK1 (SKP1), ASK2 (SKP1B) and ASK4 (SPK1like 4), which can act as subunit of the SCF complex. The interaction with MATERAL EFFECT EMBRYO ARRESTED 44 (MEE44) also shows a possible function in embryo development for KAI2, which is expressed in developing embryos [533] (see figure 2.22 part B group I). KAI2 also shows

rac-GR24-dependent interactions with SUCROSE NON FERMENTING 1 (SNRK1.1), which plays a role in delay of flowering [534]. Additionally SNRK1.1 is involved in salt stress via an interaction with MYC2 [535] and is known to interact with viral proteins [536]. Therefore the interaction of KAI2 with SNRK1.1 could indicated a possible new regulation of flower induction as stress response. Another interaction partner of KAI2 is IMPORTIN ALPHA ISOFORM 4 (IMPA-4), which has a function in NLS-bearing protein import into the nucleus and plays a role in *Arabidopsis* during *Agrobacterium* transformation. IMPA-4 is known to interact with VIRD2 and VIRE2, two virulence proteins from *A. tumefaciens* [537] (see figure 2.22 part B group II). KAI also showed a *rac*-GR24-dependent interaction with two phosphatases (see figure 2.22part B group III). For the PROTEIN PHOSPHATASE 2A SUBUNIT A2 (PP2AA2) it is known that it has a role in the regulation of the PIN phosphorylation. Together with RCN1 they are mediating the stress response in the root [505, 538, 539]. This interaction is currently being investigated in collaboration with Prof. Dr. Gutjahr's research group. Six interactions were observed for MAX2. Three of them, *rac*-GR24-independent, with ASK1, ASK2 and ASK4 (see figure 2.22 part B group I), which was expected since MAX2 is an F-box protein. However, the three *rac*-GR24-dependent interactions with TIFY8 and IMPA-4 (see figure 2.22 part B group II) indicate MAX2 involvement in defense mechanisms. This interaction could be an indication that MAX2, as F-box protein of the SCF complex, is either involved in other signaling pathways, or that SL is also involved in defense mechanisms through TIFY8. A large number of interactions were detected for the KAR signaling pathway, many of which were *rac*-GR24-dependent. These interactions indicate that the KAR pathway is involved in several other processes, which could be shown by direct PPI. The interactions in this KAR screen also showed interactions with proteins for defense and root development, allowing new hypotheses for the function of the KAR signaling pathway.

In summary, the Y2H system has proven to be very successful for most receptor screens. Especially for ABA, SA and KAR many highly interesting interactions could be discovered. Many new interactions with receptors were detected, which do not seem to match the core pathways and possibly represent new functions of the receptors.

2.9 Genetic validation *in planta*

The central hypothesis, that signal integration between signaling pathways is based on PPI could be supported by hundreds of direct interactions. The question arises whether these direct interactions are signal integrations and whether they have a biological function in the plant that is specific for certain phytohormone signaling pathways.

For the new detected interactions between the signaling pathways, the first criterion is met, to check the second criterion different experiments were performed in the plant. For the experiments in plants special assays were selected, which can be performed with seedlings or seeds. Therefore, a selection of interactions from the PhI was chosen, whose interaction partners are expressed in the respective seedling stage and additional T-DNA lines were available. After the selection 34 interactions remained (see figure A.13). These 34 interactions were divided into two categories, category 1 are interactions between different hormone-annotated proteins, and category 2 defines interactions between a multiple annotated protein, which among others also has the hormone-annotation of its interaction partner. For the responding 45 interaction partners T-DNA lines were ordered, which have the insertion in the first exon to increase the probability for a knock-out

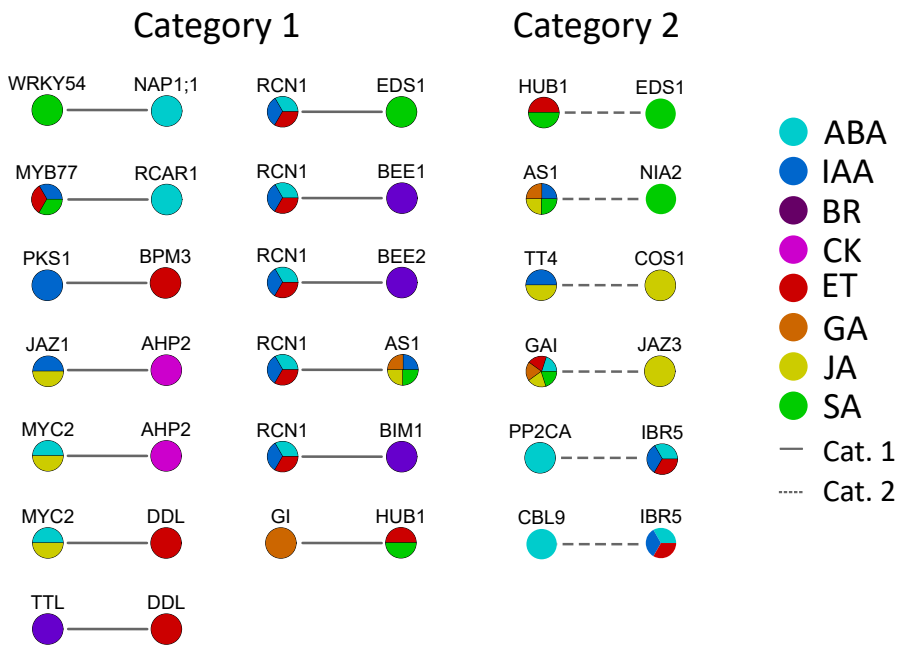

Figure 2.23: Selected Y2H interaction pairs for seedling assays. Interactions that take place between two differently annotated proteins were assigned to category 1. Interactions between proteins, one of which is annotated multiple times and among those carries the hormone annotation of the interaction partner, are assigned to category 2.

mutant (overview of ordered polymorphism lines see table 4.1). In addition, for all phytohormone treated assays a well documented positive controls were added to the test sets. All lines were genotyped by PCR and then propagated for 2 generations to get enough seed material. Furthermore, the lines selected for the experiments were tested in parallel by qRT-PCR to determine whether the T-DNA lines were knock out or knock down mutants. Of the 45 T-DNA lines 27 lines, corresponding to 19 interaction pairs, remained as homologous lines and were tested in different assays (see figure 2.23). These pairs can be separated by our definition in 13 interaction pairs from category 1 and 6 from category 2. Each T-DNA line was tested in the assay corresponding to its involvement in a phytohormone signaling pathway and additionally in the assay corresponding to the involvement in a phytohormone signaling pathway of the interaction partner (see figure 2.1). For some mutant lines it was not possible to test all hormone annotations, as e.g. in the case of the *gai* mutant, which is known to play a role in five phytohormone signaling pathways. In order to perform the assays in an unbiased and objective manner, the assays were performed separately and as blind experiments (only numbers) (see table 2.1). The assays for BR, CK, ET, GA and ABA were performed by myself. Especially for ABA, the ABA titration pre-experiments were performed by a member of Prof. Grill's lab (Botany, TUM). The assays for IAA and JA were planned by me and all required materials were provided, but the experiments were carried out by colleagues, which showed no significant results. The assay for SA was performed in cooperation with Dr. Vlot-Schuster (BIOP, HMGU) and results are attached in the appendix.

Table 2.1: Matrix of T-DNA lines tested for points of signal integration. Black dots stands for the known annotation for each protein; red dots mark the hormones in which this line has to be tested. All lines marked with a cross are used in a particular assay as positive control. The plus indicated the corresponding wild type line for the tested T-DNA lines in each assay.

Locus ID	Symbol	Annotation	ABA	BR	IAA	GA	JA	SA	ET	CK
AT3G29350	AHP2	CK	●		●		●			●
AT2G37630	AS1	GA,IAA,JA,SA	●		●	●	●	●	●	
AT1G18400	BEE1	BR	●	●	●				●	
AT4G36540	BEE2	BR	●	●	●				●	
AT5G08130	BIM1	BR	●	●	●				●	
AT2G39760	BPM3	ET			●				●	
AT5G47100	CBL9	ABA	●		●				●	
AT2G44050	COS1	JA			●		●			
AT3G20550	DDL	ET	●	●			●		●	
AT3G48090	EDS1	SA	●		●			●	●	
AT1G14920	GAI	ABA,ET,GA,JA,SA	●			●	●	●	●	
AT1G22770	GI	GA				●		●	●	
AT2G44950	HUB1	SA,ET				●		●	●	
AT2G04550	IBR5	ABA,IAA, ET	●		●				●	
AT1G19180	JAZ1	IAA, JA			●		● x			●
AT3G17860	JAZ3	JA	●			●	● x	●		
AT3G50060	MYB77	ET, IAA, SA	●		●			●	●	
AT1G32640	MYC2	ABA, JA	●				●		●	●
AT4G26110	NAP1;1	ABA	●					●		
AT1G37130	NIA2	SA			●	●	●	●		
AT2G02950	PKS1	IAA			●				●	
AT3G11410	PP2CA	ABA			●			●	●	
AT1G01360	RCAR1	ABA	●		●			●		
AT1G25490	RCN1	ABA, ET, IAA	●	●	●	●	●	●	●	
AT5G13930	TT4	IAA,JA			●		●			
AT5G58220	TTL	BR		●					●	
AT2G40750	WRKY54	SA	●					●		
AT4G26080	ABI1	ABA	x							
AT3G24650	ABI3	ABA	x							
AT3G20770	EIN3	ET							x	
AT2G01570	RGA	GA				x				
	RGA/GAI	GA				x				
AT3G11540	SPY	CK								x
Ecotype	Col-0		+	+	+	+	+	+	+	+
Ecotype	Ler-0		+			+				

2.9.1 Brassinosteroid assay

Brassinosteroids are known for there involvement in differentiation and development like stem elongation. Former studies identified BR function in hypocotyl elongation [103] and root growth [540]. These studies showed severe phenotypes by applying exogenous brassinolide (BL). To identify a function of different candidate lines in BR signaling, a hypocotyl measurement in light conditions were performed. The hypocotyl measurement showed no difference between background control (Col-0), positive controls *BR-enhanced expression 1* (*bee1*), *bee2* [541], *BES1 interacting MYC-like 1* (*bim1*)[122] and tested mutant lines *dawdle* (*ddl*) and *root-curl-in-NPA* (*rcn1*) on control plates (see figure A.16). Also the log2 fold change values were all close to zero as expected for mock treatment. However, there was a wide variation in the values per line. The values for the treated lines showed less variation per line and the log2 fold change values were larger, however,

for significant p-values additional repeats are needed (see figure A.16 in appendix). The hypocotyl measurement were also performed in the dark, which showed similar results (data not shown). Hypocotyl measurements using dark grown seedlings were not continued because the positive controls had extreme germination problems in the presence of 1μM BL. The control Col-0 and the candidate lines were able to germinate well (data not shown).

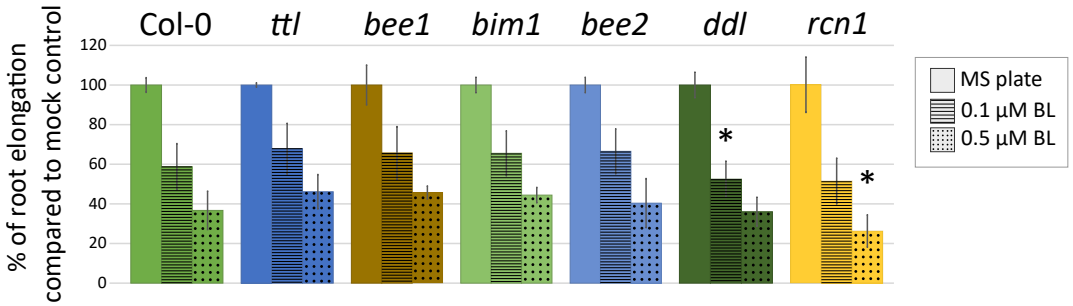

Figure 2.24: Brassinosteroid treated root elongation assay .The assay were performed in three independent replicates with a minimal number of 25 seedlings per line. The bar graphs show percentage of root elongation compared to mock control. The dashed bars indicate root elongation on 0.1 μM BL plates, the dotted bars indicate root elongation on 0.5 μM BL. Error bars indicate standard deviation of four biological replicates. * indicates a p-value of < 0.05.

In addition to the hypocotyl measurements, root elongation assays were performed in parallel. The seedlings were transferred 5 DAG from MS plates to plates with 0.1 μM and 0.5 μM BL, as well as mock, and the root elongation was determined after 9 days. The values from the root elongation showed a significant difference for *ddl* and *rcn1* compared to *Col-0*. Surprisingly, none of the known BR mutants like *bee1*, *bee2* and *bim1* showed a significant difference in root length compared to Col-0 (see figure 2.24). The analysis of the expression values of these three mutant lines showed that *bee1* and *bim1* are knock down mutants, but *bee2* is a knock-out mutant (see figure A.14 in appendix). Thus a significant difference was expected at least for *bee2*. The significant difference of *ddl* and *rcn1* compared to Col-0 and the verified Y2H interaction (see figure 2.23) indicate that an additional annotation for the brassinosteroid might be added to DDL and RCN1 proteins. The interaction between RCN1 with BEE1, BEE2 and BIM1 is very interesting (interaction pair overview see figure 2.23), because RCN1 is known to be involved in the control of root growth, not only via the IAA signaling pathway [505] but also via the BR signaling pathway [506]. The molecular mechanism, how RCN1 alters root growth via BR signaling, was not completely understood. These interactions of RCN1 with BEE1, BEE2 and BIM1 could link IAA and BR signaling pathway to control root growth. In this assay the *ddl* mutant was shown to have an effect in BR signaling. DDL is known to be involved in plant growth and pathogen defense and was linked to the ET pathway. The interaction of DDL and TRANSTHYRETIN-LIKE protein (TTL) (interaction pair overview see figure 2.23) indicate a point for signal integration between BR and ET signaling pathway to regulate plant growth, because TTL is known for its negative role in BR mediated plant growth[542]. Additionally, TTL was also tested in the ET assay (see section 2.9.3 figure 2.27) and showed an effect in ET treatment, which supports the described point of signal integration between BR and ET signaling pathway.

2.9.2 Cytokinin assay

Cytokinin plays an important role in meristem activity and also in shoot and root growth [54] As a pre-experiment for a cytokinin assay, a root elongation assay was performed to determine whether the analysis of root elongations suitable for this purpose. In this assay, seedlings at 5 DAG were transferred from MS medium plates to MS plates containing either 0 μM, 1 μM or 10 μM 6-benzylamino purine (BA) and 1 % or 3 % sucrose. It is known that not only CK but also glucose have an important function in root growth. Therefore the addition of glucose or sucrose to the plant medium can stimulate root growth [543]. Especially in studies on CK regulated root growth, the addition of glucose/sucrose should be tested, as this can lead to different growth of mutant lines [544]. In this assay, the T-DNA lines of *myc2*, *jasmonate-zim-domain protein 1* (*jaz1*) as candidates, *arabidopsis histidine-containing phosphotransmitter 2* (*ahp2*) and *spindly* (*spy*), as positive control, and Col-0 as background control, were used. The root elongation values showed more variations between the individual lines in 1 % sucrose compared to 3 % sucrose regardless of BA treatment. Strongest effects could be detected in 10 μM BA with 1 % sucrose compared to 1 μM BA with 1 % sucrose. The mutant line *myc2* and *ahp2* have already 25 - 30 mm longer roots on MS plates with 1 % sucrose compared to Col-0 (see figure A.17). To elucidate the difference in root length between mock and BA treatment the log2 fold change of root length in Col-0 vs mutants per experimental setting, were calculated. These values show differences in the log2 fold change of *myc2*, *spy* and slightly for *ahp2* between MS with 1 % sucrose compared to 10 μM BA with 1 % sucrose. The results from this pre-experiment showed that the use of 3 % sucrose minimize the root length differences between the tested lines. The use of 10 μM seem to be too high, due to the smaller root in *spy* mutant compared to Col-0, whereas 1 μM showed longer root for *spy*, as expected, but similar root length for *ahp2* compared to Col-0.

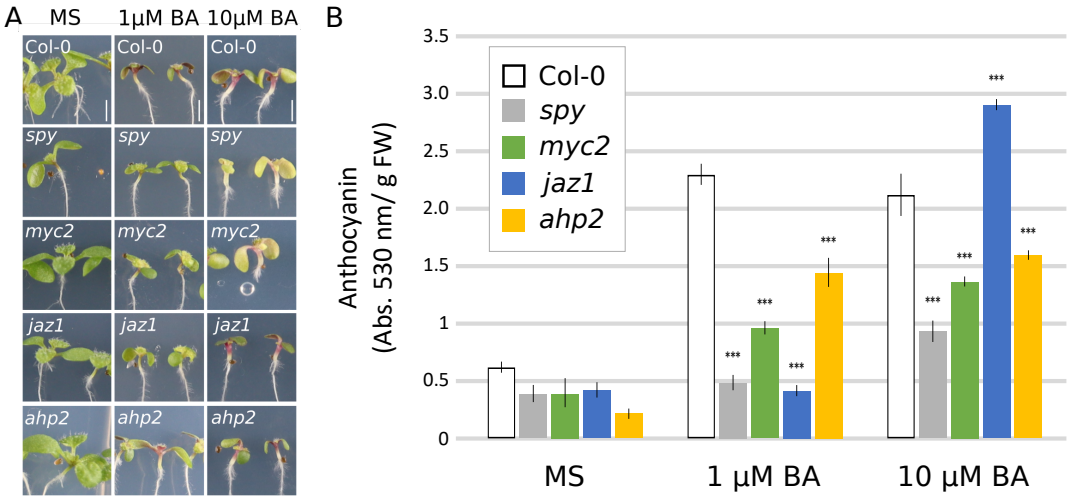

Figure 2.25: Cytokinin assay: Anthocyanin content measurement. Anthocyanin content measured in 10 day old seedlings grown on MS plates with 1 % sucrose and with and without 1 or 10 μM BA. (A) showed seedling at time point of harvest, (B) show anthocyanin calculations. Significance were calculated by using two-sided t-test. *** indicate a p value of < 0.001.

Additionally, CK are known to be involved in the induction of anthocyanin accumulation in *Arabidopsis thaliana* [545], and for *spy* mutant is has been shown that BA treatment results in lower anthocyanin content compared to Col-0 [546]. Therefore in

parallel to the root elongation assay for cytokinin, an additional anthocyanin content measurement was performed. The anthocyanin content were similar on the control plate and showed less variation in the four repeats. However, *myc2*, *jaz1* and *spy* were all significantly different from Col-0 in both tested BA concentrations (1 or 10 μM BA). The difference between *ahp2* and *Col-0* is also highly significant, but weaker compared to the other three lines. The expression values of the *AHP2* in the *ahp2* candidate line showed almost three fold upregulation. To determine, if this gene upregulation was caused by a contamination in the qRT-PCR or primers, new primers were designed and new cDNA samples were prepared, additionally to the initially used cDNA, but showed the same results (see figure A.14 and A.15). Despite the overexpression of *AHP2*, the anthocyanin values were still significantly different to Col-0. MYC2 is involved in JA [547, 548] and ABA [549, 550] signaling pathways and JAZ1 is known to be involved in JA [233] and IAA [551] signaling pathways, for both a direct interaction link to CK and a mutant phenotype was hitherto unknown. With this result, a link could be established between JAZ1 and MYC2 to the cytokinin pathway that indicate new points of signal integration.

2.9.3 Ethylene assay

To test the different mutant lines for involvement in ethylene signaling, the mutants were tested for the ethylene triple response [552]. The triple response was first identified in sweet pea by Knight L.I. in 1910 [553]. The triple response reactions like apical hook elevation, radial hypocotyl swelling, shorter hypocotyl length and root elongation enable the plant to overcome small stones in the soil to reach sunlight. The shorter and more compact hypocotyl gives more stability to penetrate through dense soil, while the apical hook performs loops to reach another area through which one can grow. In the different studies, that determine a phenotype for ET by using ET treatment, mostly hypocotyl and or root length were used [554, 555, 57]. For this analysis apical hook exaggeration, hypocotyl length and root elongation were measured and a mutant phenotype was considered a confirmation if one of the measured values were significant. For this assay the protocol from An et al., 2010 [554] were used, with an adaptation of a 1-hour light step. This step was necessary because most lines do not germinate when the light step was missing. Only the mutant lines of *dawdle* (*ddl*), *gigantea* (*gi*) and *roots curl in npa* (*rcn1*) were not affected in the dark and germinated as well as in light. The seedlings were treated with 10 μM 1-aminocyclopropane-1-carboxylic acid (ACC). The ET assay were performed with 4 repeats but only two could be analyzed.

Figure 2.26 shows the comparison between Col-0 and the positive controls *ethylene insensitive 3* (*ein3-1*) [552], *histone mono-ubiquitination 1* (*hub1*) and *rcn1* [556, 557]. For *ein3* a significant difference to Col-0 could be observed with all three measurements, whereas for *hub1* and *rcn1* only a significant difference could be observed with the apical hook vs apical loop.

Figure 2.27 shows the comparison between Col-0 and *gi*, *br enhanced expression 1* (*bee1*) and *ttl*. A significant difference in apical hook vs apical loop formation could be observed for *gi* compared to Col-0. *bee1* showed no significant difference in all three measurements. However, *bee1* mutant showed almost 80 % normal apical hook formation on ACC treatment, but the value was not significant due to the high biological variations. The mutant line *ttl*, known for regulatory function in plant growth in a BR-dependent manner [542, 117] and endosperm development [558] showed a significant difference to Col-0 in apical hook vs loop formation and hypocotyl length.

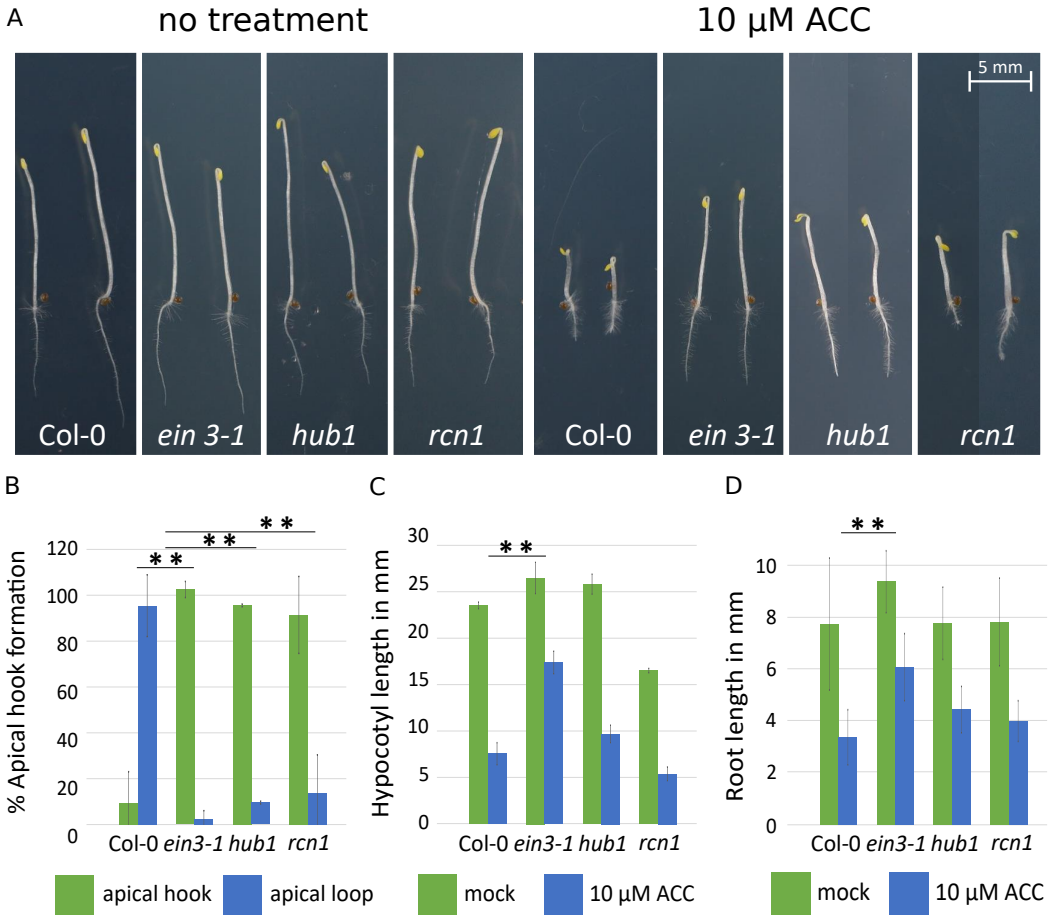

Figure 2.26: Ethylene triple response of *ein3*, *hub1*, and *rcn1*. (A) shows two representative seedlings with and without treatment. (B-D) To determine the triple response, (B) the apical hook formation vs apical loop formation, (C) hypocotyl length and root length were evaluated. Values are based on two repeats with 30-40 seedlings per line. Error bars indicate standard deviation of two biological replicates. Significance was calculated using two-sided t-test. * indicates a p-value of < 0.05, ** < 0.005, *** < 0.001.

CALCINEURIN B-LIKE PROTEIN 9 (CBL9) is known for its function in ABA signaling and stress induced ABA biosynthesis induction [559]. In this assay, *cbl9* showed significant difference to Col-0 in apical hook vs loop formation, but no differences in hypocotyl length and root length (see figure 2.28). The mutant (*bim1*) displayed no significant difference compared to Col-0. However, nearly 80 % of the seedlings showed an normal apical hook under ACC treatment, but due to the high biological variation there was no significant difference to Col-0. The *ddl* mutant line displayed wild type phenotype in apical hook formation and hypocotyl length, but showed significant shorter root length compared to Col-0. This indicates an enhanced sensitivity to ACC [560] and confirm this by a new mutant phenotype. The results for the mutant lines of *ttl* and *ddl* in this ET assay and the BR assay support the hypothesis that the DDL-TTL interaction could be a new point for signal integration between the BR and ET signaling pathway.

The comparison between Col-0 with *indol-3-butyric acid response 5 (ibr5)*, *protein phosphatase 2 ca (pp2ca)* and *myc2* is shown in figure 2.29. IBR5 is annotated with ET base on information from the Arabidopsis Hormone Database 2.0 (AHD2.0). In the

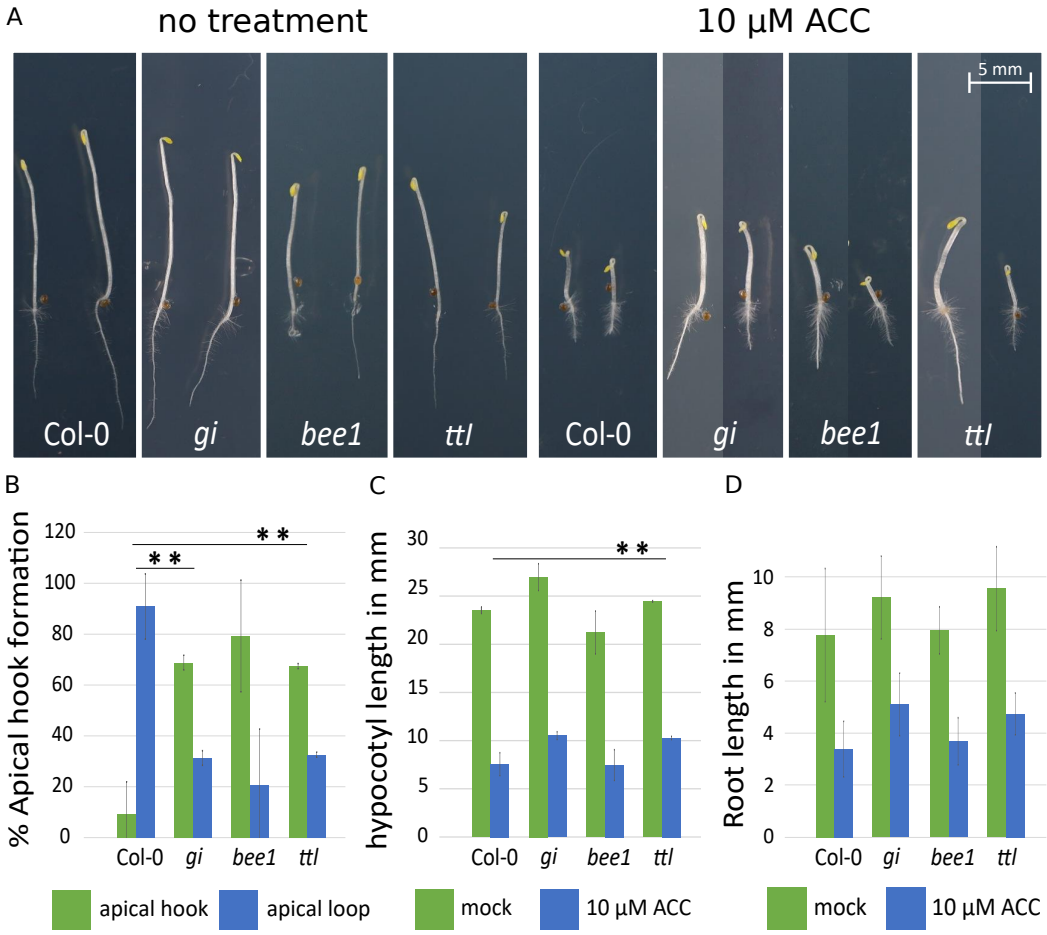

Figure 2.27: Ethylene triple response of *gi*, *bee1*, and *ttl*. (A) shows two representative seedlings with and without treatment. (B-D) To determine the triple response, (B) the apical hook formation vs apical loop formation, (C) hypocotyl length and root length were evaluated. Values are based on two repeats with 30-40 seedlings per line. Error bars indicate standard deviation of two biological replicates. Significance was calculated using two-sided t-test. * indicates a p-value of < 0.05, ** < 0.005, *** < 0.001.

respective publication no information about IBR5 or ethylene signaling was given [561]. In this ET assay the formation of an apical hook vs apical loop in the *ibr5* mutant was significantly different compared to Col-0 (see figure 2.29), which indicates that IBR5 could have a function also in ET. For *pp2ca* mutant a significant difference in root length was observed compared to Col-0. The 50 % apical hook vs apical loop formation in the presence of ACC was not significantly different from Col-0, because of the high standard deviation.

In figure 2.30 *enhanced disease susceptibility 1* (*eds1*), *phytochrome kinase substrate 1* (*pks1*) and *bee2* were compared to Col-0. The only significant difference to Col-0 was observed for *pks1* mutant, which shows longer roots under treatment of ACC, whereas *bee2* and *eds1* showed no significant differences. In the last comparison *asymmetric leaves 1* (*as1*) mutant, which is known to be involved in GA signaling, was compared to Col-0 (see figure 2.31). AS1 has an annotation for GA [562] and additional annotation for SA, JA and IAA [478]. In this assay *as1* mutant showed no significant difference to Col-0.

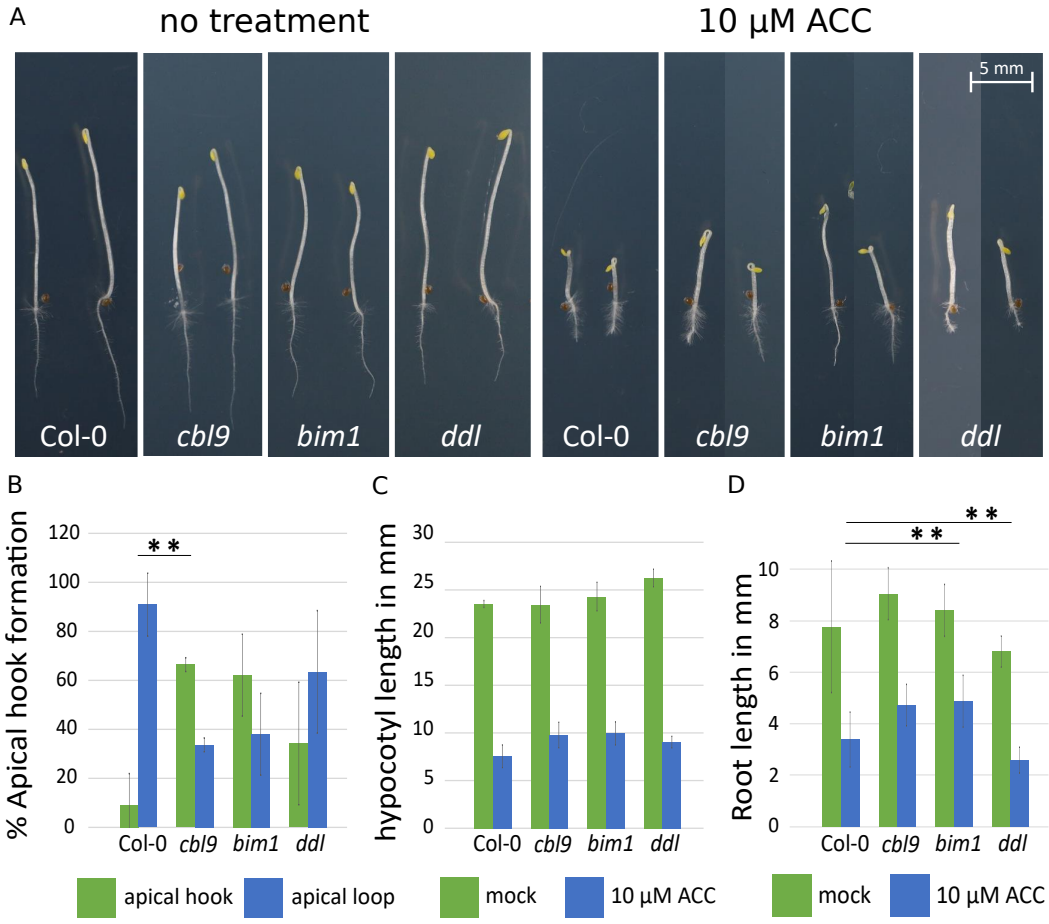

Figure 2.28: Ethylene triple response of *cbl9*, *bim1*, and *ddl*. (A) shows two representative seedlings with and without treatment. (B-D) To determine the triple response, (B) the apical hook formation vs apical loop formation, (C) hypocotyl length and root length were evaluated. Values are based on two repeats with 30-40 seedlings per line. Error bars indicate standard deviation of two biological replicates. Significance was calculated using two-sided t-test. * indicates a p-value of < 0.05, ** < 0.005, *** < 0.001.

Overall, the ET assay indicate for 7 out of 11 candidate lines an effect in the ET signaling pathway, which is about 63 %. Often only one of the three tested markers was significantly different, because some mutant lines already have a phenotype in the other markers, e.g. *gi*, which shows significant differences in hypocotyl and root length to Col-0 without treatment. For those lines it would be necessary test higher ACC concentrations to overcome this effect. Some of the mutants examined here could not be tested as positive due to the high biological variability, which is based on only two repetitions. The individual lines are currently being propagated and will be tested again in the near future.

2.9.4 Gibberellin assay

GA are involved in seed germination [563, 564], cell elongation and meristem size [179, 565] and also flowering [566, 567]. To interrogate different aspects of GA biology I used a germination assay. All lines were tested for GA3 (0.1 μM, 1 μM, 10 μM) and Paclobutrazol (PAC) (0.5 μM, 1.0 μM) treatments. For GA the following candidate lines

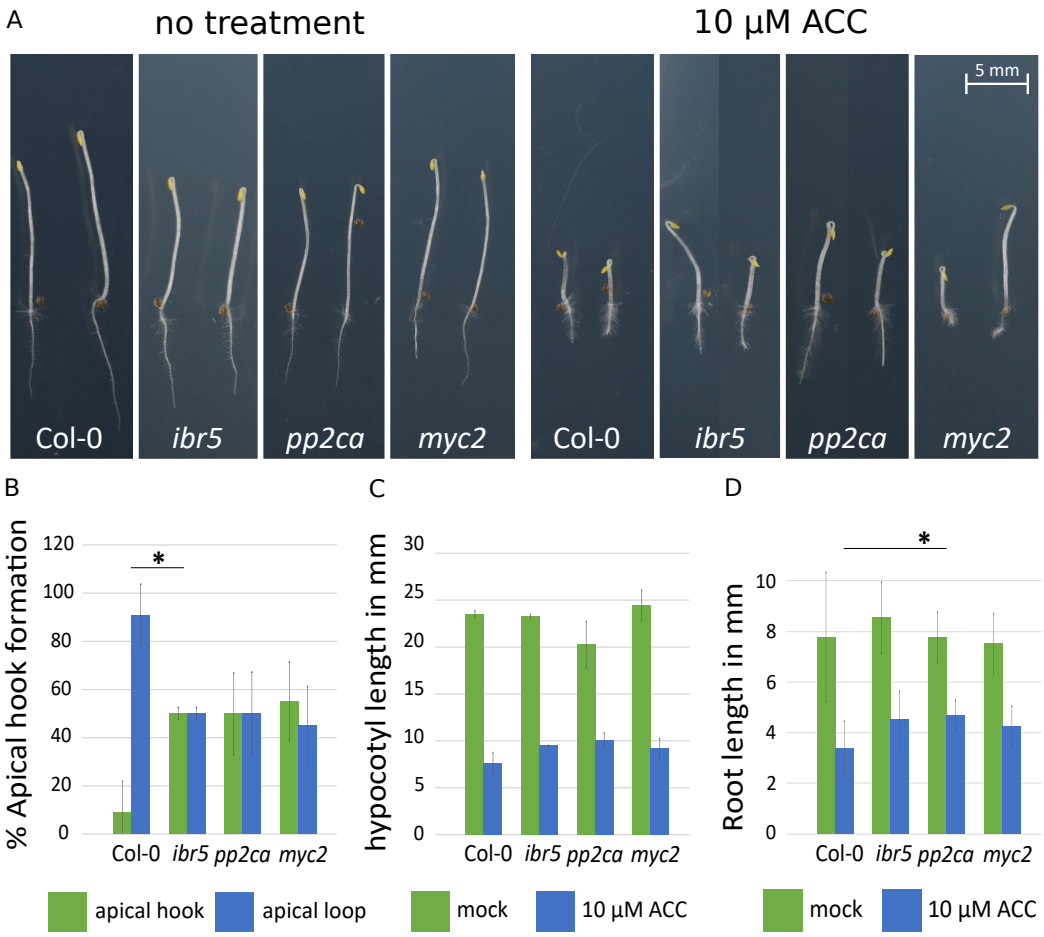

Figure 2.29: Ethylene triple response of *ibr5*, *pp2ca*, and *myc2*. (A) shows two representative seedlings with and without treatment. (B-D) To determine the triple response, (B) the apical hook formation vs apical loop formation, (C) hypocotyl length and root length were evaluated. Values are based on two repeats with 30-40 seedlings per line. Error bars indicate standard deviation of two biological replicates. Significance was calculated using two-sided t-test. * indicates a p-value of < 0.05, ** < 0.005, *** < 0.001.

were tested: *gi*, *as1*, *hub1*, *nia2*, *rcn1*, *jaz3*, *gibberellic acid insensitive* (*gai*). As control two *repressor of ga* (*rga*) lines in Col-0 background and one double mutant *rgagai* [568] in a Ler background were used (Prof. Schwechheimer, (Plant Systems Biology,TUM). All lines showed germination on both GA3 and mock plates, and no germination on the PAC plates, except five seedling from *rgagai* mutant line (five out of > 100 seeds) (data not shown). Due to GA involvement in cell elongation [179], hypocotyl length were analyzed under Pac treatment (see figure A.18 in appendix). From this assay only data from one repeat are shown. The only lines which showed slide differences to control were *gi*, which is known to have a longer hypocotyl, and the positive control *rga-gai*.

Finally, root elongation assay showed differences under PAC treatment (see figure 2.32). The positive controls and mutant lines, which are known to be involved in GA signaling, are shown in the upper part of figure 2.32, except from *as1*, which is shown with the four candidate lines in the lower part of figure 2.32. All control lines and mutant lines with a GA annotation showed a phenotype and a significant difference to their wild type control. The candidate lines *hub1* and *nia2* showed also significant differences in root elongation

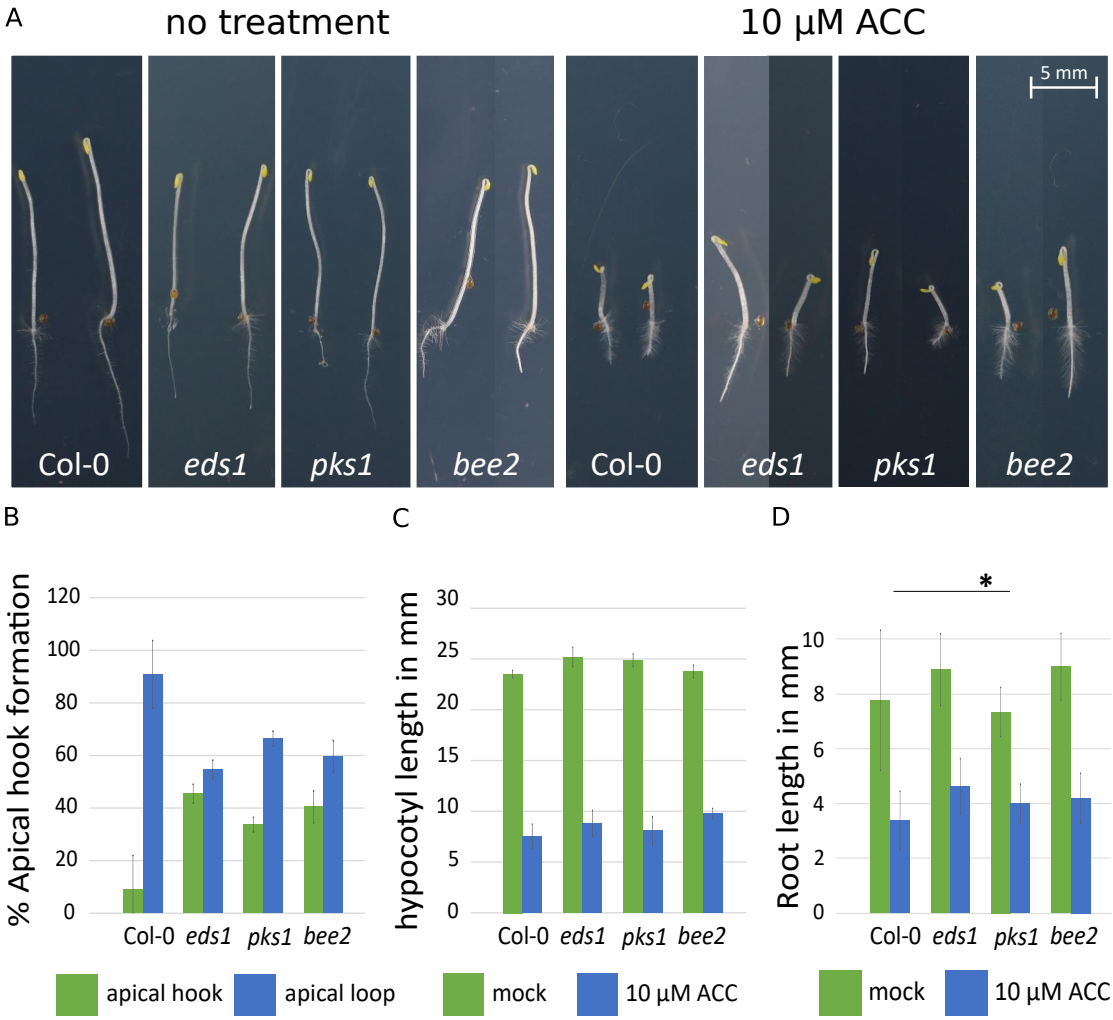

Figure 2.30: Ethylene triple response of *eds1*, *pks1*, and *bee2*. (A) shows two representative seedlings with and without treatment. (B-D) To determine the triple response, (B) the apical hook formation vs apical loop formation, (C) hypocotyl length and root length were evaluated. Values are based on two repeats with 30-40 seedlings per line. Error bars indicate standard deviation of two biological replicates. Significance was calculated using two-sided t-test. * indicates a p-value of < 0.05, ** < 0.005, *** < 0.001.

compared to Col-0. The candidate lines *rcn1* and *jaz3* were not significantly different to Col-0, although the root was longer in *jaz3* compared to wild type, no significance could be calculated due to the high biological variability. For HUB1 and NIA2, these results could indicate a new point of signal integration between GA with ET (via *hub1*) as well as GA with SA (via *hub1* and *nia2*).

2.9.5 Abscisic acid assay

The ABA signaling pathway is a key regulator in seed germination. Therefore, a germination assay is used to determine whether a gene is involved in the ABA pathway. The germination assays were performed using 30 μM ABA, which showed the biggest germination differences in the titration pre-experiments (see figure A.21). The high amount of ABA, used in this assay, caused no significant difference of the positive controls *abscisic*

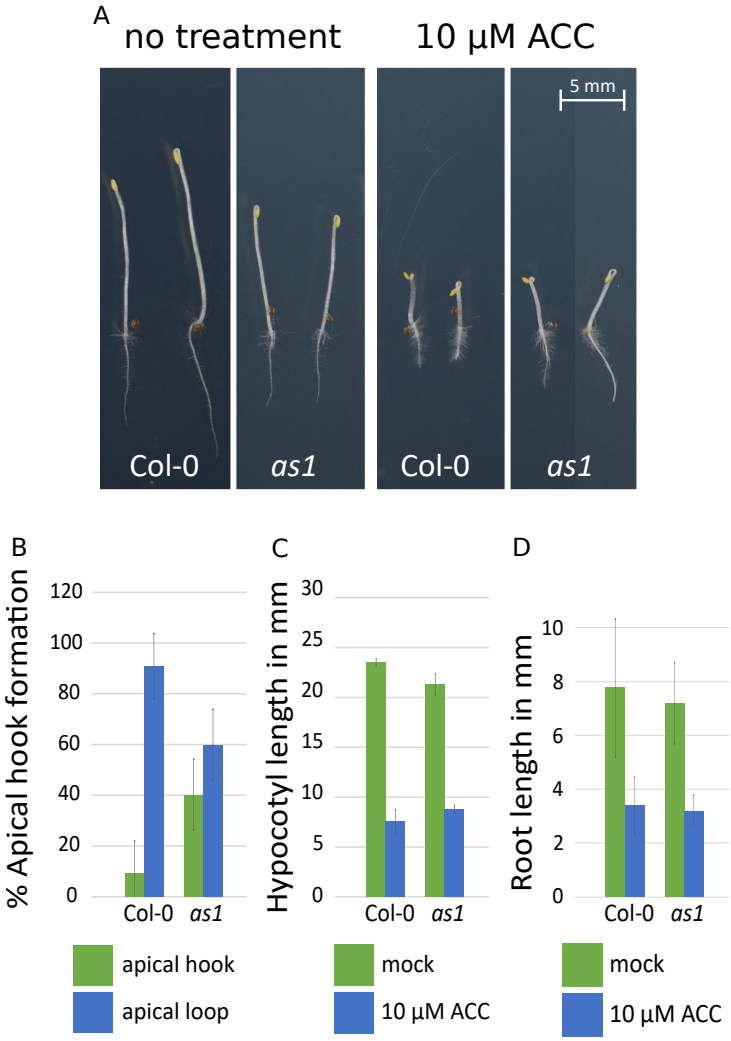

Figure 2.31: Ethylene triple response of *as1*.(A) shows two representative seedlings with and without treatment. (B-D)To determine the triple response, (B) the apical hook formation vs apical loop formation, (C) hypocotyl length and root length were evaluated. Values are based on two repeats with 30-40 seedlings per line. Error bars indicate standard deviation of two biological replicates. Significance was calculated using two-sided t-test. * indicates a p-value of < 0.05, ** < 0.005, *** < 0.001.

acid insensitive 1 (*abi1*) and *abi3* compared to control *Arabidopsis thaliana* Landsberg (Ler) (see figure A.20). However, among all tested mutant lines were nine candidate-lines (see figure 2.33 group II) and seven mutant lines, which are already known for their function in ABA signaling, and therefore could be used as positive controls (see figure 2.33 group I). Testa rupture and radical emerge were counted as germination. Of the positive controls, five of the seven lines showed a significantly higher germination rate than the background control Col-0.

From the candidate lines, seven showed a significantly higher germination rate than Col-0 while one candidate line showed a significantly lower germination rate compared to background control. The detected higher germination rate of *ahp2* was very unexpected, since a recent study showed that double and triple mutants of *ahp2*, *ahp3* and *ahp5* in the presence of 1-2 mM ABA have a lower germination rate compared to control [569].

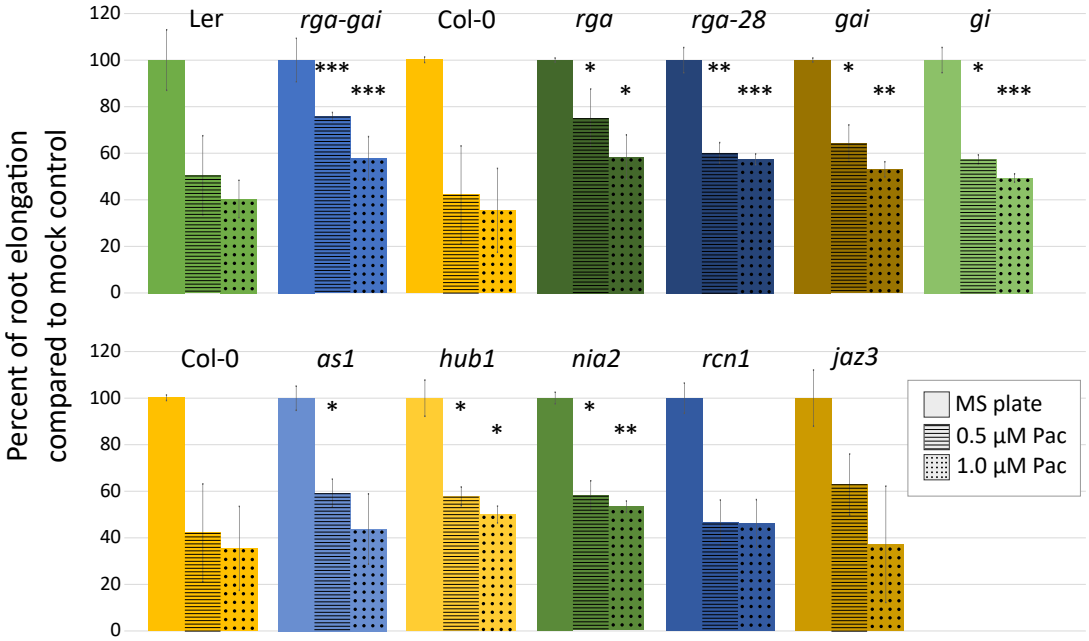

Figure 2.32: Gibberellin assay: root elongation. Root elongation was calculated from seedlings grown on MS medium (bar graph without any markings), MS plus 0.5 μM Pac (bar graph with lines) and MS plus 1 μM Pac (bar graph with dots). The values of the root elongation of the seedlings under treatment were compared with the mock treatment (MS only). This assay was performed with four repeats and 30-40 seedlings per line. Error bars indicate standard deviation of four biological replicates. Significance were calculated by two-sided t-test. * indicates a p-value of < 0.05, ** < 0.005, *** < 0.001.

Therefore, it was expected that the single mutant would also show a lower germination rate. As the gene expression analysis of *ahp2* showed, this candidate line is an *AHP2* overexpressor. Therefore, the higher germination rate is appropriate and suggests a new function of AHP2 in ABA signaling. Of great interest were the results from the three BR signaling pathway related candidate lines, which showed a higher germination rate under ABA treatment compared to Col-0 (see figure 2.33). ABA and BR signaling are known to regulate plant growth antagonistically and a recent study showed that antagonistic regulation takes place between the phosphatases ABI1, ABi3 and the BR kinase BIN2 [570]. The results from this assay indicate, that the BR and ABA signaling pathways interact with each other also on transcription factor level, due to the significant higher germination rate of *bee1*, *bee2* and *bim1* under ABA treatment.

The mutant phenotype of *myb77* under ABA treatment supports the hypothesis, that the interaction of RCAR1 with MYB77 shows a point of signal integration between ABA and SA signaling pathway according to the direct interaction of MYB77 and RCAR1. A second validation for signal integration between ABA and SA could be given by the mutant phenotype of *wrky54* in the ABA germination assay. WRKY54 is known for its role in defense response [571, 572] and showed an interaction with NAP1;1, which is known for its function in abiotic stress response related chromatin remodeling [573].

In this ABA germination assay a high number of candidate lines showed a higher germination rate under ABA treatment compared to control. Of major interest is the connection between the BR signaling pathway (BEE1, BEE2, BIM1) and the ABA signaling pathway (RCN1) and several connections between the SA signaling pathway (WRKY54,

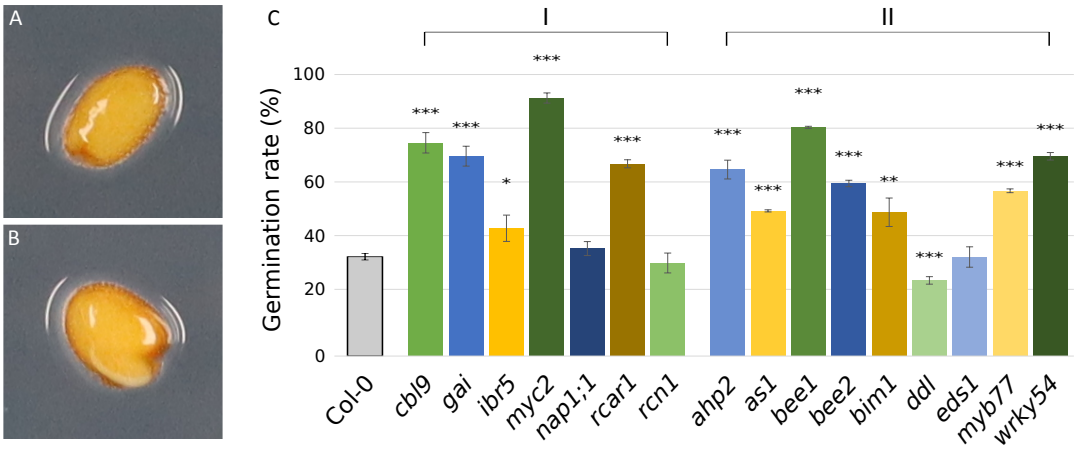

Figure 2.33: ABA germination assay. Seeds were stratified for three days at 4°C in the dark followed by two days LD light conditions. Seeds are directly plated on MS plates containing 30 μM ABA (treatment) and MS plates (control). After two days pictures were taken and analyzed by counting of testa rupture and radical emergence. Col-0 is used as control line. Group I indicated plant lines, which are known to be involved in ABA signaling, based on TAIR GO annotation or based on mutant phenotype, data extracted from AHD2.0. Group II indicates the candidate plant lines. This assay was performed with four repeats with 90-120 seed per candidate line. Error bars indicate standard deviation of four biological replicates. * indicates a p-value of < 0.05, ** < 0.005, *** < 0.001.

MYB77) and the ABA signaling pathway. This assay also elucidated the strong connection of the phytohormone signaling pathways.

In this last section, all 27 candidate mutant lines were tested in at least one plant assays with different hormone treatment for ABA, BR, CK, ET, and GA. Of these, for 21 candidate lines at least one phenotype could be detected under a certain hormone treatment (see overview A.22 in appendix), which suggest at least one new function in a phytohormone signaling pathway. In total, a phenotype could be detected in each assay for at least 50 % of the candidate lines (see figure 2.34 part A). Considering the relation of the single hormone annotation to multiple hormone annotations of the proteins, a shift of the relation can be observed (see figure 2.34 part B). In order to demonstrate this shift more accurately, a Hormone Pleiotropy Index (HPI) was calculated before and after my plant assays (see figure 2.34 part C), which showed a 10-fold increase of pleiotropy according to the tested proteins. These results support the observation that the connectivity of the individual hormone signaling pathways is much stronger than previously assumed. Consequently, the hypothesis can be formulated that a large number of proteins which have a confirmed function for one hormone signaling pathway probably could trigger downstream signals influenced by multiple phytohormone pathways. and therefore have a functions in different hormone signaling pathways.

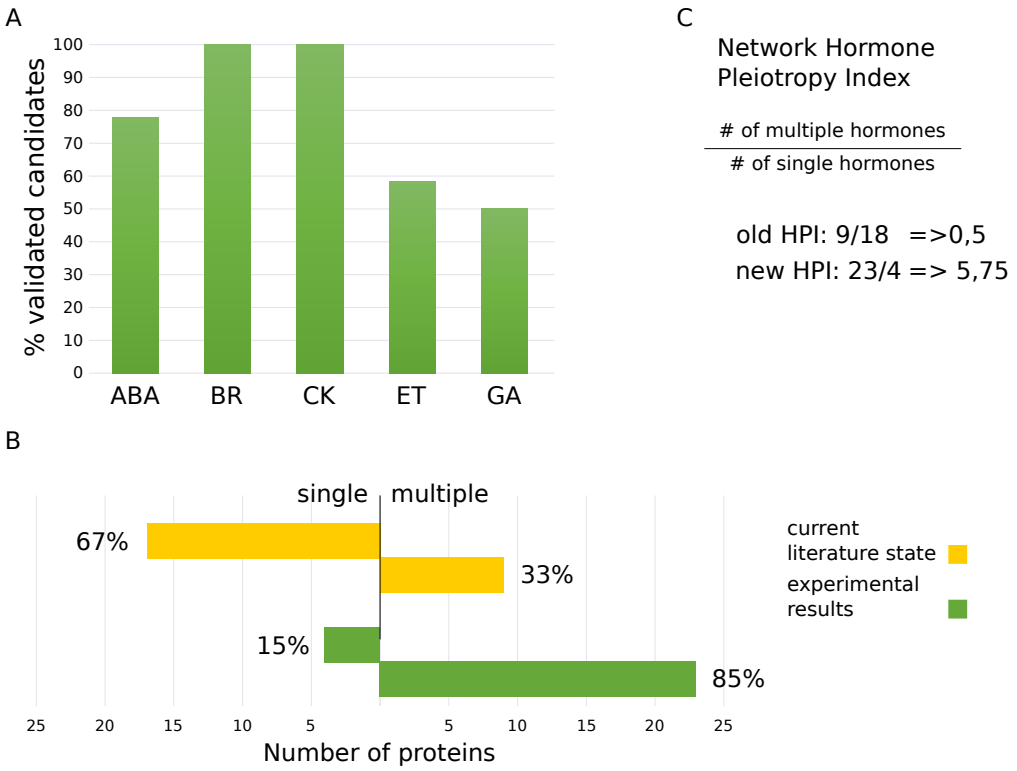

Figure 2.34: Hormone Pleiotropy Index. (A) show percentage values for validated candidates separated into ABA, BR, CK, ET and GA bargraphs. In (B) comparison of single or multiple annotations based on current literature state of new experimental results. In (C) the calculation of the hormones Pleiotropy indexes is shown.

3 Discussion

Plants are able to detect signals from the environment and adapt their life cycle optimal to environmental conditions. Most of these biotic and abiotic signals are detected and transmitted by the phytohormone signaling pathways. Studies have shown that the individual phytohormone signaling pathways are interconnected (genetic studies), partially through transcriptional regulation (microarray and RNA seq analysis [287, 288]). In a few studies could be demonstrated that protein-protein interactions play an important role in the connection of different phytohormone signals [290, 191, 291]. In this work I could demonstrate that the phytohormone signaling pathways are strongly connected by direct PPI, which takes place at different levels in the signaling pathways. The systematic approach of the PhI (475 interactions between 251 proteins) resulted in a strongly connected network map, whereas the Rep-TF screen (628 interactions between 121 proteins) allows to focus on TF targets which showed interactions with repressors or non-DNA-binding regulators from single or multiple phytohormone signaling pathways. Additionally, the hormone-dependent interactions of phytohormone receptor (indicated new non-core pathway function, which supports the strong connection of the phytohormone signaling pathways to regulate different developmental processes and stress responses. The result of the PhI_{out} (698 interactions between 581 proteins) combines phytohormone signaling pathways with a broader *Arabidopsis* network and allow insight in hormone pathway influenced regulation of RNA processing and splicing as well as protein localization and transport. With these new results, the comprehension for signal transduction and signal integration within the phytohormone signaling pathways change. The signal transmission in the individual core signal pathways do not lose validity. However, none of the development processes or stress responses are regulated by a single phytohormone signaling pathway.

3.1 Extensive phytohormone signaling pathway connections by direct PPI

The main network (PhI)(figure 2.5) and displays a strong interconnection between the single phytohormone signaling pathways (figure 3.1). To prove this, the mean distance between the proteins of a hormone signaling pathway and between the hormone signaling pathways were calculated. The hormone distance matrix clearly demonstrates the strong interconnection in PhI (see figure 3.1 left matrix) in contrast to the literature curated interactions (LCI) (see figure 3.1 right matrix). This high interconnectedness was validated using different bioinformatic approaches by Stefan Altmann. Additionally, small clusters of proteins which share the same hormone annotation, can be detected in PhI (Figure 2.5). This observation was confirmed by a community analysis, which indicate that the PhI contains a significantly higher number of communities showing an accumulation of proteins annotated for a single hormone compared to a random rewired network (see community figure A.2 in appendix). The quality of the PhI network map was determined and resulted an assay sensitivity of 20.7 % $\pm$4.2 % and a calculated false positive

rate of ≤ 1 per 100 interactions. In Braun et al., 2009, different experimental methods were compared with regard to their assay sensitivity. It could be shown that the use of low copy plasmids in a Y2H system leads to an assay sensitivity between 16 % and 25 % and a false positive rate of ≤ 1 per 100 reactions, whereas the use of high copy plasmids leads to rise of the assay sensitivity up to 40 % with simultaneous increase a false positive rate of ≥ 4 per 100 reactions [574]. This indicated that the assay sensitivity of the PhI is in the expected range. The overall sensitivity was calculated by multiplying the sampling sensitivity with the assay sensitivity and resulted in 16.2 % ±4.2 % by low likelihood of false positives (figure A.3). The comparison with the overall sensitivity of $AI1_{MAIN}$ [296] about 13.3 % ±3.2 %, showed a similar sensitivity to PhI, indicating a robust mapping system, while at the same time detection of less false positive interactions.

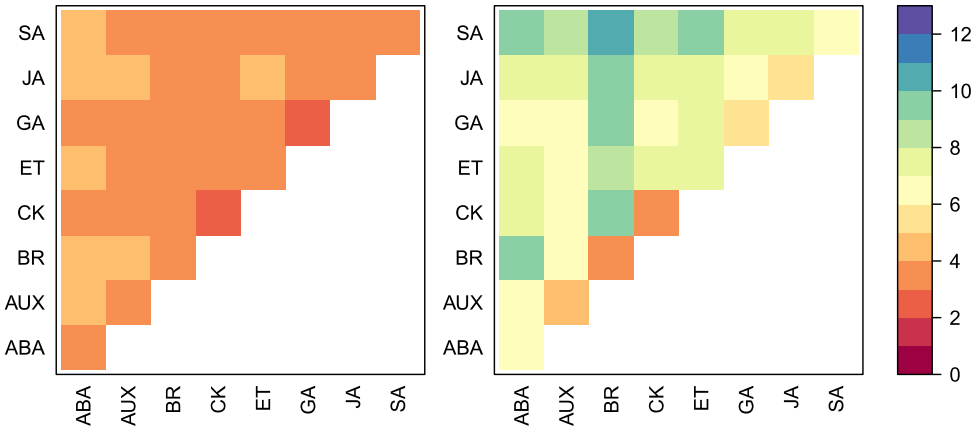

Figure 3.1: Hormone distance matrix PhI vs LCI. The hormone distance matrix is calculated by counting the shortest path between two hormone-announced proteins in the PhI. It has been calculated for proteins with the same as well as different hormone annotation. The left matrix is based on PhI, the right matrix is based on binary single and binary multiple interactions from the literature. Only interactions between proteins in the PhO search space were included.

The PhI_{out} is based on 698 interactions with 581 proteins, with only 103 from PhO and 595 from the AtORFeome. For these two groups a GO enrichment analysis were performed, which indicate an GO enrichment in RNA processing, cellular transport and intracellular localization for the proteins originated from AtORFeome. For the PhO based proteins, GO was term enriched for defense responses and the JA signaling pathway, suggesting that specifically plant defense responses have major influence in RNA metabolism, mRNA splicing events and cellular transport to adjust plant growth and induce different defense systems (see figure 2.11). In a defense situation against necrothrophic pathogens or herbivores, the synthesis of JA, in particular MeJa and the preliminary 12-oxophytodienoic acid (OPDA), starts in cell, which is the systemic induction of the defense response of the plant. These substances must be transported within the cell during and after production, although it is not yet fully understood how this transport to the plasma membrane takes place [575, 576, 577], but possibly by vesicle transport. Furthermore, the production of volatiles and defense substances, e.g. the production of galacturonic acid (OGA), is used in the defense situation, which plays an important role for the rapid induction of oxidative burst through the release of ROS [578, 579, 580, 581].

The combination of all interaction network maps show a highly complex network that transmit signals from the environment which then influences developmental processes

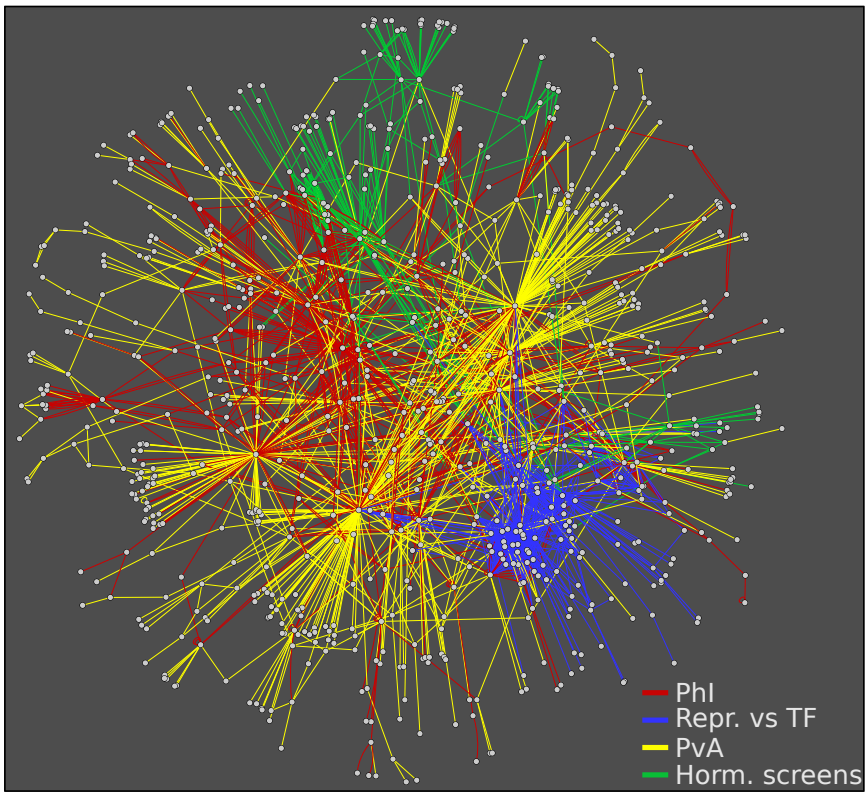

Figure 3.2: Combined network map $PhI_{combined}$ (PhI_{comb}). Summary of all interactions based on PhI (edges in red),Rep-TF (edges in blue), PhI_{out} (edges in yellow), and hormone dependent receptor screens (Horm.screens) (edges in green). All interactions shown were independently confirmed at least three times in the verification.

and stress responses through various hormone-dependent and independent PPI. This combined network, called PhI_{comb}, contains 2215 interactions among 983 proteins (see figure 3.2), of which 479 are confirmed interactions (not marked in the figure). By reducing the PhI_{comb} on the PhO search space 1922 interactions between 962 proteins remains, of which 382 are confirmed interactions. In total the interactions from all screens reach a coverage of 61 % of the estimated interaction number of 3145 within the PhO search space. The PhI interactions seem to spread across the entire network, whereas large hubs can be observed in the PhI_{out} interactions, whose interaction partners have less connection. The interactions of the receptor screens still seem to be connected with the others, while the Rep-TF interactions are very separate and strongly interconnected. This overall network can be used for the development of hypotheses about the interconnection of individual signaling pathways, which can then be investigated in small scale assays and particularly in plants.

3.1.1 New insights in individual phytohormone signaling pathway and signal integration

Many MAP kinases have multiple hormone annotations and recently it has been found that PAT is also regulated via MKK7-MPK6/ MKK7-MPK3 cascade [44, 45]. In PhI an interaction between MKK7 and PID was discovered. This leads to the hypothesis that the PAT is not only regulated by both kinases individually, but is also influenced by

their direct interaction. The BiFC experiment in *N. benthamiana* was not clear enough to confirm this interaction *in planta* doubtless, due to fluorescence from MKK7-fusion protein with empty vector control, but expression of both proteins showed altered fluorescence in the nucleus (see figure 2.10). The interaction data can be supported by the kinase-substrate analysis from Stefan Altmann, to estimate the potential of kinases to phosphorylate an interaction partner. The predicted position of PID to be phosphorylated by any MKK is T294 as shown in figure 3.3. The low number of known MKK substrates, which were use in this algorithm, might lower the reliability of this result, but the additionally detected known MKK substrates like EIN3, a substrate of MKK4 and MYBR1, a substrate of MKK9 [582, 583, 584], that have a lower product of frequency compared to the prediction for PID, could support the PID phosphorylation via MKK.

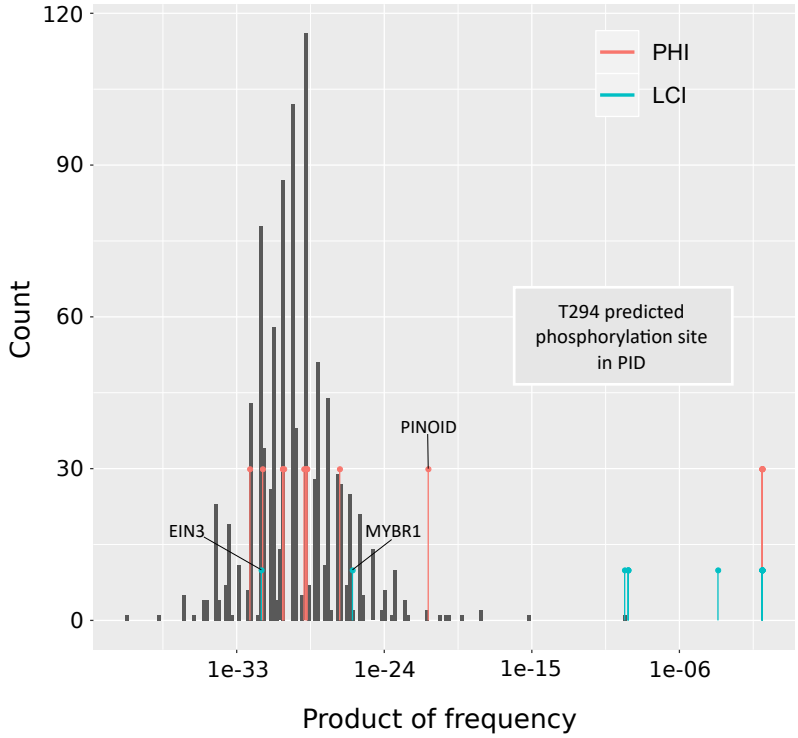

Figure 3.3: Phosphorylation predictions of MKK interaction partners. The x-axis shows how well the position weight matrix (PWM) of this cluster matches the interaction partners in PhI (red), literature interactors (blue) or other *Arabidopsis thaliana* proteins (gray background distribution). For this purpose, frequency of matching amino acids are determined from the PWM around the phosphorylatable residue. The product of all frequencies determines the accuracy of fit of the PWM. A higher value means the protein is more likely to be a substrate of the MKK family. On the y-axis the number of proteins corresponding to the respective value on the x-axis is shown.

To investigate the interaction *in planta* a *pid* amiR MKK7 double mutant was generated, that showed an additive severe mutant phenotype of the *pid* mutant and the single amiR MKK7-Col-0 phenotype (shown in figure 2.9), which suggested that both proteins might be in the same linear pathway but being involved at two separate levels. Additionally, the single mutants were analyzed for *PID* and *MKK7* gene expression. The data showed, that downregulation of *MKK7* (amiR MKK7-Col-0 line) influence *PID* expression, which was reduced by half compared to control, whereas *MKK7* expression was 3.5

fold upregulated in the *pid* mutant (see figure 2.8). However, the regulatory mechanism for these transcriptional regulation have to be elucidated by further experiments with a Y1H assay. PID is known to play a major role in PAT and is known to phosphorylate PIN1. A recent studies indicates that the phosphorylation of PIN1 by PID does not serve as signal for PIN1 intracellular transport and change PIN1 polarity and that possibly an PID interactor together with PID control PIN1 polarity [34]. With regard to the function of PID, the hypothesis can be raised as to whether PID changes trans-phosphorylation activity to PIN1 through phosphorylation of MKK7, and thus changes PIN1 polarity. PID is activated by PDK1 phosphorylation in the activation loop, which leads to strong auto-phosphorylation and also trans-phosphorylation. The estimated position T294 in PID to be phosphorylated by MKK is close to the PDK1 phosphorylated serine in the activation loop [585] and may change PID function. If the direct interaction between KK7-PID leads to polarity change in PIN1 has to be analyzed in further studies.

3.1.2 Signal integration via non-core pathway interactions

Besides the known phytohormone receptor interactions, many interactions have been found, which are different from the core signaling pathways. These often indicate a different function of the receptors, which has not been demonstrated so far. In the ABA network, the interactions of RCAR1, which all take place independently of ABA, and the interactions of RCAR9, which are mostly ABA-dependent, show many of those none-core pathway interactions (see figure 3.4), which indicate new functions of these receptors. Recently, the ABA-dependent interaction between RCAR9 and MYC2 was published in Aleman et al., [493], that showed a transcriptional modulation of the JA key regulator by an ABA receptor. RCAR1 and RCAR9 have 14 none-core pathway interactions in common, also with other RCARs (see figure 2.16) which have known functions in leaf and flower development, defense, and more ABA related functions. Additionally both receptors have a high number of specific interactors which might be related to the RCAR specific spatio-temporal expression differences [504]. All RCARs are expressed at a low level almost everywhere, but differ in the strength of their expression as well as in the tissue or the time of their expression, e.g. RCAR1 which is three fold higher expressed than RCAR9. In addition, RCAR1 is specifically expressed in cauline leaves and senescent leaves, while RCAR9 is most strongly expressed in developing embryos and in the stamen [586]. The RCAR1-MYB77 interaction was analyzed *in planta* and it could be shown, that *rcar1* mutant is more resistant to *Pst* DC3000 infection compared to wild type (see figure A.23), and that *myb77* mutant shown by significant higher germination rate under ABA treatment compared to wild type, indicating a function of MYB77 in ABA signaling (see figure 2.33). These results support the biological viability of the Y2H interactions and the hypothesis that can be driven from these data.

3.1.3 Convergence of signal integration on transcription factor level

The analysis of interactions from the Rep-TF screen showed new downstream targets of different repressors. Some interactions were specific for single repressor groups, others showed interactions with multiple repressor groups (see figure 2.13, 2.14, 2.15). In the Rep-TF screen a high number of interactions with LBD proteins were identified. The LBD proteins belong to a plant specific gene family with 42 members, which play an essential role in the regulation of lateral organ development and metabolic processes [465, 466, 467]. Recent studies have revealed interactions of LBD proteins with basic

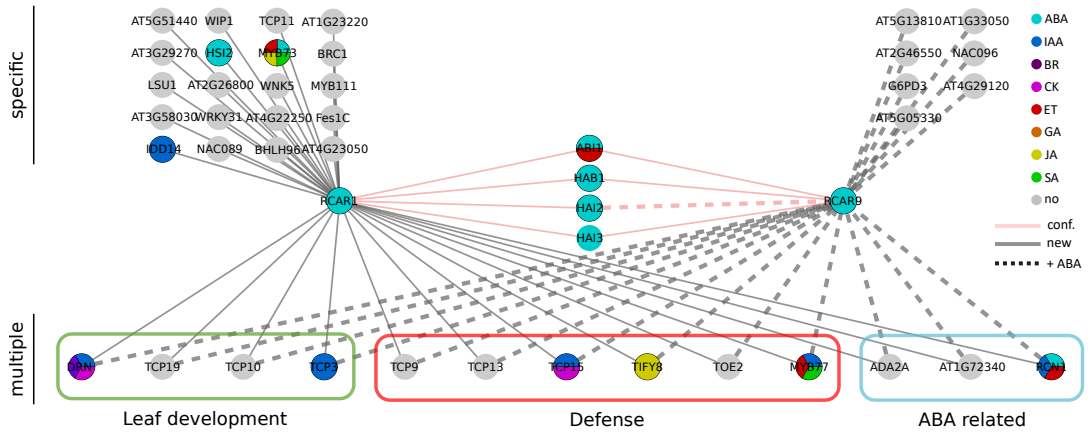

Figure 3.4: RCAR1/RCAR9 non-core pathway interactions. RCAR1 and RCAR9 interactions are extracted from the Y2H ABA receptor screen. Nodes are colored according to their hormone annotation based on AHD2.0 (genetic evidence) or TAIR10 (GO annotations). Edges in gray indicate new interactions, edges in light red indicate confirmed interactions and edges in dashed lines indicate ABA-dependent interactions. Green box indicates involvement in leaf development, red box indicates involvement in defense response and blue box indicates involvement in ABA-related developmental processes. All interactions are at least three times confirmed in independent Y2H assays.

helix-loop-helix proteins [468], which seem to regulate LBD function in lateral organ development. Different LBD proteins are also know to play an important role in the auxin signaling pathway [468, 469]. Publications from Negi, 2008 and Lewis, 2011 had confirmed that ET has an influence on lateral root development, by regulating IAA accumulation [56, 355]. However, no direct influence of ET on lateral root formation could be shown. The new direct interaction of ERF12 with different LBD proteins (LBD4, LBD42, LBD13 [587]) (see figure 2.13 part B) suggests that the ET signaling pathway could regulate lateral root formation independently. Another LBD interaction was identified between BIN2 and LBD13. A recent publication showed that BIN2 phosphorylates ARF7 and ARF19 to suppress their function with some AUX/IAA proteins, which leads to an upregulation of LBD16 and LBD29 and subsequently to regulation of lateral root formation [588]. The interaction of BIN2-LBD13 leads to the hypothesis that the BR signaling pathway influences directly the regulation of lateral root formation. These interactions of ERF12 to several LBD proteins and of BIN2 to LBD13 present the LBD proteins as new components in signal transduction for BR and ET and indicate that lateral root formation could be regulated IAA-independent. The HAI3 interaction with LBD14 (see figure 2.13)raised the hypothesis that LBD14 function in lateral root formation that can be inhibited by HAI3 in an ABA-dependent manner. The main function of the PP2Cs in the ABA core signaling pathway is to repress ABA downstream signaling,whereby in presence of ABA, the PP2C phosphatases are inhibited (see figure 1.3). However, for the HAI phosphatases (HAI1-HAI3) a recent study showed that their expressions are induced in presence of ABA and stay active to act in feedback regulation of the ABA signaling [589]. This specific regulation of HAI phosphatases could enable an interaction of HAI3 with LBD14 in the presence of ABA to prevent lateral root growth during salt or drought stress.

Additional points for signal integration between the BR, ET and IAA signaling pathways, with regard to different developmental processes, could be validated in different

seedling assays. RCN1 interacted in PhI with BEE1, BEE2 and BIM1 and could now be validated for its function in BR signaling through protein-protein interactions as well as through the genetic validation. *BEE1* and *BEE2* belong to the early response genes that are upregulated under BR treatment. However, only the triple mutant *bee1*, *bee2*, *bee3* is less responsive to BR and shows changes in flowering and seedlings that are characteristic of BR mutants. Single mutants show no difference to wild type *Arabidopsis thaliana*. It has been hypothesized that BEE1, BEE2 and BEE3 not only play a role in the BR pathway, but also function as a link to other hormone signaling pathways, e.g. it could be shown that IAA induces the expression of *BEE1* and *BEE3* [541]. In general BR signaling is known to be involved in different root developmental steps, but so far there were no link between BEE1, BEE2, BIM1 and RCN1 [590, 325]. RCN1 plays a role in ABA and ET as well as in IAA signaling and is known for its function in meristem organization [538]. It is possible that RCN1 works as a linker between IAA and BR signaling via interaction with BEE1, BEE2 or BIM1 to regulate specific functions in the root meristem. Additionally to the validation of RCN1 function in BR signaling (see figure 2.24), a function of BIM1 in ET signaling could be observed in the ET triple response assay (see figure 2.28). This further function additionally demonstrates the interaction of RCN1 to the BR signal pathway, but also allows further impact from the ET signal pathway via BIM1 specifically for root development.

3.1.3.1 Signal integration between JA and CK via MYC2

For the CK seedling assay a mutant phenotype of *myc2* and *jaz1* could be confirmed by anthocyanin content measurements. Both mutants, similar to the positive control *spy*, produced less anthocyanin under BA treatment than the control Col-0 (see figure 2.25). Also for *ahp2* a significant difference to Col-0 could be shown, which was expected due to the CK annotation. AHP2 is the second core element in the CK signaling pathway and was recently discovered in a study as a negative regulator in the drought stress response [569]. Also for the JA pathway there were connections to drought stress, as exogenous JA leads to an increased drought stress tolerance [591]. In 2017 it could be shown in rice that OsJAZ1 negatively regulates the drought stress response [592]. With this CK assay the interactions of AHP2 with MYC2 and JAZ1 could be validated, through the mutant phenotype in anthocyanin content under BA treatment and an additional annotation for CK could now be added to both. Additionally to this validation *in planta*, my student J. Palme identified a positive regulation of MYC2 function via CK repressors in his Y1H based functional assay, mentioned before. This suggested that MYC2 is functionally regulated by CK repressors the ARR and interacts additionally with AHP2, a core component in the CK signaling pathway, which in turn activated CK regulated transcription and inactivates CK signaling pathway repression but also MYC2 repression through de-dephosphorylating the type A ARR.

3.1.3.2 SA signaling pathway in response to nitrogen or phosphate deprivation

The maintenance of homeostasis of inorganic phosphate (Pi) and nitrogen is essential for plant growth. Therefore the interactions of transcriptional regulators with four transcription factors, which have a function in phosphate or nitrogen starvation, were of great interest. The interaction of NIMINS with the transcription factors HYPERSENSITIVITY TO LOW PI-ELICITED PRIMARY ROOT SHORTENING HOMOLOGOLOGY 1-3 (HHO1-3) and Nuclear factor YA7 (NF-YA7) may indicate a new function of the SA

signal pathway in phosphate and nitrogen homeostasis regulation. HHO1 and HHO2 have functions in nitrates [593] and phosphate regulation [594]. The NF-YA7 transcription factor is a subunit of a heterotrimeric complex and is involved in different developmental processes or responses to environment. NF-YA proteins subunits are highly regulated in nitrate and phosphate deprivation environment [595]. Possibly the NIMIN proteins repressors have an inhibitory function in the regulation of the response to nitrate and phosphate deficiency in connection with plant defense. This assumption could be supported by the interaction of NF-YA7 with TCP13 and TCP14 [587]. These two TCP proteins in turn play an important role in the plant defense response [419]. Additionally, NF-YA7 is known to interact also with TPL as well as TPL-RELATED2(TPR2) and TRP3 [525], which could indicate a regulation of NF-YA7 trough NIMIN-TPL-NF-YA7 complex interaction. To confirm this hypothesis, further analysis and experiments are needed to explain the function of the NIMINS and SA signaling pathway in the plant response to nitrogen or phosphate deprivation. Through this screen it was possible to develop a new hypothesis regarding new insights into the signaling pathway of the SA signaling pathway. The four transcription factors HHO1-HHO3 and NF-YA7 also interact with four repressors of the IAA repressor group (see figure 2.13, 2.14, 2.15). IAA involvement in the response to phosphate or nitrate starvation could be demonstrated by the mutant phenotype of *hho2* in Nagarajan et al., 2016 [594]. The *hho2* mutant has both a reduced number and length of lateral roots. This is regulated in wild type by the interaction of SCARECROW (SCR) and SHORT ROOT (SHR) with HHO2, both SCR and SHR are linked to the IAA signaling pathway [596]. Thus, these four transcription factors would be possible points for signal integration between IAA and SA.

NIMIN proteins are known for their repressive function in the SA signaling pathway by binding to the receptors NPR1 and NPR3. In AI1 it could be demonstrated that NIMIN2 and NIMIN3 also interact with the co-repressor TPL [296]. We assumed that a TPL-NIMIN-NPR1/3 complex would be used for direct regulation of the PR gene. How this regulation takes place is currently analyzed by Dr. P. Rodrigues (INET, HMGU). In general only 12 direct interactions have been shown for the NIMIN proteins whereas only 6 are with NPR1, NPR3 and TPL (see table A.10). In this Rep-TF screen 28 interactions of the three NIMINS could be shown (see figure A.24 in appendix). Five of the interactors had an annotation for JA. Since both signaling pathways are mainly involved in defense against pathogens, it is possible that the same transcription factors can be considered as common targets [597, 598].

3.1.3.3 TCPs as co-regulators in phytohormone signaling

The TCP transcription factors are a plant specific [599] and in *Arabidopsis thaliana* the TCP family contains 24 members. TCPs are associated with different growth processes like axillary meristem outgrowth [600], floral symmetry [601], and leaf growth [602] due to their regulation of cell cycle genes and cell division [603, 604].

Additionally, for some TCPs functions in phytohormone signaling pathways could be demonstrated like TCP20 and TCP9 are involved in JA signaling [496], TCP9 is involved in BR signaling [606, 607] or TCP3 is involved in IAA signaling [495]. Recently, TCP14 and TCP15 were found to act as hubs in PPIN1 and PPIN2 [418, 419] and were identified as effector target from different pathogens and both TCPs are also linked to the CK signaling pathway [608]. In my screens I could detect an enrichment in TCP interactions 4.2.16.2 in the PhI and several hormone-receptor screens. In total 207 TCP

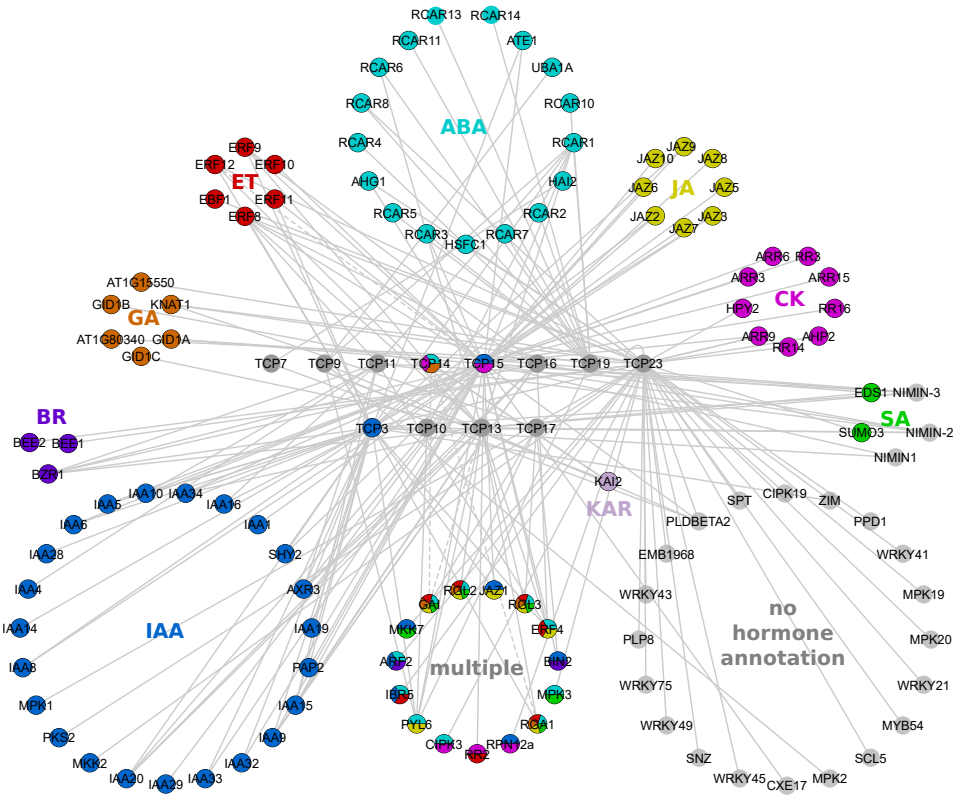

Figure 3.5: Overview TCP interactions. Interactions are extracted from PhI_{comb} and were verified at least three times. TCPs are separated in class I (upper row) and class II (lower row) according to Li et al., 2015 [605]. TCP interactors are sorted according to hormone annotations based on genetic evidence (AHD2.0) or GO annotations (TAIR10), except from NIMIN proteins, which were sorted to the SA group. Solid lines indicate new interactions, dashed lines indicate confirmed interactions.

interactions with mainly hormone annotated proteins could be detected (see figure 3.5, which dramatically expand the number of TCPs that indicate involvement in different phytohormone signaling pathways. Some of the interactor groups, according to their hormone annotation, interact only with specific TCPs, like all JA and CK annotated protein are interacting only with TCP15 and TCP3. Even more specific are the interactions of TCP19, which was so far known for regulation of defense response [418], but showed 13 interactions with ABA annotated proteins. On one hand some TCPs act more pathway specific like TCP19, on the other hand TCP15, which is known for function in CK and IAA, could be shown to interact with 52 different proteins from almost all phytohormone signaling pathways. To analyze the function of this high number of interactions with TCP15, a Y1H based assay was performed by J. Palme (master student) to identify the regulatory function of those interactors on TCP15. He could show that TCP15 is repressed by SA, CK, and IAA and additionally induced and repressed by BR and ET linked proteins (see figure A.25). These data support the functionality of these interactions and indicated TCPs as co-regulators in hormone regulated growth processes.

Additionally, in the ABA, IAA and KAR hormone-dependent Y2H screens (see sections 2.8.1, 2.8.2, 2.8.5) I observed an enrichment in TCP interactions .

3.1.4 Phytohormone pleiotropy

In the PhO collection 55 % of the ORFs have a hormone annotation, of those 26 % were multiple annotated. In my work several of those multiple annotated proteins like MYB73, MYB77, MYB21, DELLAs, and TCP15 have a high number of interactions and seemed to have functions in additional phytohormone pathways. The validation assays *in planta* indicate that most of these proteins have additional functions in other pathways, which could be shown for 23 out of 27 candidate lines (see figure 2.34 and A.22). These results indicate that phytohormone pleiotropy is more in common than expected. Additionally the new observed mutant phenotypes in these assays strengthen the biological relevance of the new detected interactions. An interesting interaction pair which could be validated *in planta* in all tested hormone assay is HUB1-GI. HUB1 is known for its regulatory function in biotic and abiotic stresses through histone H2B monoubiquitination [609, 610] as well as involvement in photomorphogenesis [611] and transcript level regulation in circadian clock regulations[612]. GI is known for its function in regulation of the circadian clock and flowering via CONSTANCE [613, 614], but recently also to be involved in abiotic stress like salt stress and cold stress [615, 616, 617]. The *gi* mutant was tested in the ET assay (see figure 2.27) as well as in the SA infection assay (see figure A.23) and showed a phenotype in both assays, in addition *hub1* mutant showed a phenotype the GA plant assay. These validation results lead to the hypothesis that GI and HUB1 play an essential role as signal integration points between SA, ET and GA signaling pathways, but furthermore link pathogen defense response initiation via HUB1 [556] with induction of flowering [618, 619] via GI as direct stress response mechanism. This example elucidates the necessity of a high interconnection between the phytohormone signaling pathways to regulate the developmental processes and stress responses in response to environmental influences, which could be demonstrated in this thesis by hundreds of direct PPI.

3.2 Conclusion

In this thesis it could be shown that hundreds of points of signal integration connects the phytohormone signaling pathways and that these interactions can take place on all steps in a signaling pathway. However, the large number of connection points showed that the known core signaling pathways are all part of a large highly connected network that controls the different developmental processes and stress responses. Additionally, the experiments revealed a high number on non-core pathway interactions of phytohormone receptors, which supports the hypothesis of a highly complex network. The validation assays *in planta* confirmed the the biological relevance of those direct interaction due to new functions in phytohormone signaling pathways and indicate that multiple hormone annotated proteins might be more common than an exception.

4 Material and methods

4.1 Materials

4.1.1 Polymorphism/plant lines

Table 4.1: The table includes all plant lines ordered for the 34 crosstalk pairs, positive control lines and background/ecotype lines. Abbreviation hom. indicates homozygous plant line; low seed number comments indicate plant line exclusion from the experiments , due to low seed numbers; partner line mis. indicates that the partner plant line is missing and therefore this plant line was not used for experiments. LS CS indicated that the line was provided from the Chair of Systems Biology from Claus Schwechheimer (WZW TUM). Abbreviation for polymorphism specificity: fn- fast neutron, nmu- nitrosomethyl urea. positive control indicates assay specific mutant plant lines.

Locus ID	Symbol	Polymorphism	NASC	hom.	used	comment
AT1G01360	RCAR1	SALK_083621	N583621	yes	yes	
AT1G04250	AXR3	*axr3-1*	N57504	yes	-	low seed number
AT1G06400	ARA-2	SALK_013803	N513803	yes	-	low seed number
AT1G14920	GAI	*gai* (Ler)	NW63	yes	-	low seed number
AT1G14920	GAI	SAIL_587_C02	N862987	yes	yes	
AT1G15550	GA3OX1	*ga3ox1* (SALK_004521)	N6943	yes	-	low seed number
AT1G15550	GA3OX1	SALK_098513	N598513	-	-	heterozygous
AT1G19180	JAZ1	SALK_011957	N511957	yes	yes	
AT1G22770	GI	SAIL_813_F04	N863022	yes	yes	
AT1G23860	RSZ21	SAIL_910D06	N841015	yes	-	partner line mis.
AT1G23860	RSZ21	SALK_100950c	N659506	yes	-	partner line mis.
AT1G25490	RCN1	*resistant to NPA* (WS-2)	N3875	yes	-	low seed number
AT1G25490	RCN1	SAIL_1231_C01	N862894	yes	yes	
AT1G37130	NIA2	SALK_138297c	N686876	yes	yes	
AT1G66350	RGL1	*rgl1-2* (ema)	N16353	yes	-	partner line mis.
AT1G66350	RGL1	SALK_136162c	N654916	yes	-	partner line mis.
AT2G02950	PKS1	*pks1-1*	N9508	yes	yes	
AT2G04550	IBR5	SAIL_1239_G03	N878790	yes	yes	
AT2G04550	IBR5	SALK_113554	N613554	-	-	heterozygous
AT2G25490	EBF1	SAIL_1230_E10	N863574	yes	-	heterozygous
AT2G25490	EBF1	SALK_020997	N520977	-	-	heterozygous
AT2G34650	PID	SALK_049736	N549736	yes	yes	
AT2G37630	AS1	*as1-1* (x-ray)	N3374	yes	-	low seed number
AT2G37630	AS1	SALK_023987	N523987	yes	yes	
AT2G39760	BPM3	SAIL_275_F09	N812781	-	-	heterozygous
AT2G40750	WRKY54	SAIL_319_E03	N873142	yes	-	low seed number
AT2G40750	WRKY54	SALK_017254c	N655310	yes	yes	
AT2G44050	COS1	SAIL_1272_D01	N847196	yes	-	low seed number
AT2G44950	HUB1	*hub1-4* (SALK_122512)	N9777	yes	-	low seed number
AT2G44950	HUB1	WiscDsLox433B10	N855571	yes	yes	
AT3G05120	GID1A	SAIL_536_G10 (gid1a-2)	N822797	yes	-	low seed number
AT3G11410	PP2CA	SAIL_452_F12	N874331	yes	yes	
AT3G11410	PP2CA	WiscDsLox341D03	N851888	-	-	heterozygous
AT3G17860	JAZ3	SAIL_81D12	N803842	yes	yes	
AT3G17860	JAZ3	SALK_152372	N652372	-	-	heterozygous
AT3G20550	DDL	*ddl-1* (Ws)	N6932	yes	-	low seed number
AT3G20550	DDL	SAIL_1281_F08	N879196	yes	yes	
AT3G23050	IAA7	*axr2* (ems)	N3077	yes	-	low seed number
AT3G23050	IAA7	WiscDsLox332C10	N851504	-	-	heterozygous
AT3G29350	AHP2	SAIL_1291_C12	N879311	yes	yes	
AT3G45640	MAPK3	SAIL_2G04	N800169	yes	-	Col-3
AT3G48090	EDS1	SALK_057149	N057149	-	-	heterozygous
AT3G50060	MYB77	*myb77-2* (SALK_055373)	N555373	-	-	het.
AT3G50060	MYB77	SAIL_251_C07	N874032	yes	yes	
AT4G08150	KNAT1	*bp-1* (Ler) (ems)	NW30	yes	-	low seed number
AT4G08150	KNAT1	*bp-11* (Col-0) (x-ray)	N3161	yes	-	partner line mis.
AT4G17720		SAIL_32_A12	N801543	yes	-	partner line mis.
AT4G17720		SAIL_365_B01	N816993	yes	-	partner line mis.
AT4G26110	NAP1;1	SALK_013610c	N68613	yes	-	low seed number
AT4G26110	NAP1;1	SALK_144711c	N68614	yes	yes	
AT4G36540	BEE2	SALK_305833c	N695160	yes	yes	
AT5G04870	CPK1	SALK_080155	N580155	-	-	heterozygous
AT5G05440	PYL5	SAIL_318_D12	N814762	yes	-	low seed number
AT5G05730	ASA1	*tpr5-1* (nmu)	N8558	yes	-	low seed number

Table 4.1 continued from previous page

Locus ID	Symbol	Polymorphism	NASC	hom.	used	comment
AT5G08130	BIM1	SALK_012835	N512835	-	-	heterozygous
AT5G08130	BIM1	SALK_044682	N544682	yes	yes	
AT5G13930	TT4	*tt4-11* (Col-0)	N2105573	yes	yes	
AT5G17690	TFL2	*tfl2-1* (fn)	N3796	yes	-	low seed number
AT5G17690	TFL2	*tfl2-2* (ems)	N3797	yes	-	low seed number
AT5G25890	IAA28	SALK_129988c	N669043	yes	-	low seed number
AT5G58220	TTL	SAIL_431_D05	N819899	yes	yes	
AT2G39760	BPM3	GK-436E12.11	N441820	yes	yes	
AT2G44050	COS1	GK-828H05.17	N479481	yes	yes	
AT3G48090	EDS1	GK-232H08.18	N422268	yes	yes	
AT5G04870	CPK1	GK-101D07	N409643	yes	-	partner line mis.
AT4G28910	NINJA	GK-237F06	N422722	yes	-	partner line mis.
AT5G47100	CBL9	GK-292G03	N428011	yes	yes	
AT2G38120	AUX1	*aux1-112* (Ws) (ems)	N9592	yes	-	positive control
AT2G01570	RGA	SALK_137951c	N657029	yes	yes	positive control
AT3G11540	SPY	*spy* (ems)	N6266	yes	yes	positive control
AT2G38120	AUX1	*aux1-7* (ems)	N3074	yes	yes	positive control
AT3G20770	EIN3	*ein3* (ems)	N8052	yes	yes	positive control
AT4G26080	ABI1	*abi1-1*(Ler)(ems)	N22	yes	yes	positive control
AT3G24650	ABI3	*abi3-1* (Ler) (ems)	N24	yes	yes	positive control
AT4G39400	BRI1	*bri1-4* (Ws-2)(ema)	N3953	yes	yes	positive control
AT4G33430	BAK1	*bak1-1* (Ws-2)	N6125	yes	yes	positive control
	RGA/GAI	*rga, gai*	LS CS	yes	yes	positive control
Ecotype	Ler-0	Landsberg erecta	NW20	yes	yes	background control
Ecotype	Ws-2	Wassilewskija	N6891	yes	yes	background control

4.1.2 Bacterial strains

Dh5α *E. coli* cells were used for common cloning. DB3.1 *E. coli* cells were used to propagate empty Gateway plasmids. GV3101 and GV3101 (pMP90RK) *Agrobacterium tumefaciens* strains were used for floral dipping assays with *Arbaidopsis thaliana* and infiltration assays with *Nicotiana benthamiana*.

4.1.3 Yeast strains

Y8800 and Y8930 The *S. cerevisiae* strains Y8800 (MATa), for AD-Y constructs, and Y8930 ($MAT\alpha$), for DB-X constructs, contain deletions of the GAL4 and GAL80 genes encoding Gal4p and its repressor Gal80p, respectively. The reporter genes are HIS3, providing for growth on Sc-H plates, and ADE2, providing growth on Sc-A plates, additionally the strength of the Gal4p expression changes the color from white to red colonies. Both strains are resistant to cycloheximide (CHX), therefore it can be used to identify autoactivators. The strains Y8800 and Y8930 were generated by X. Xin in C. Boone's laboratory by adding CHX resistance to the PJ69-4 Y2H strains. PJ69-4 is described in [620].

4.1.4 Plasmids

Following Gateway DONR plasmids were used for common cloning, pDONR223, pDONRZeo, pDONR221, and pDONR207. Additionally, the following Gateway destination plasmids were used for Y2H assays pPC86GW (pDEST-AD) and pPC97 (pDEST-DB), for floral dipping in *Arabidopsis thaliana* pALIGATOR3 was used (provided from Dr. Francois Parcy [433]), and for *Agrobacterium tumefaciens* infiltration assays in *Nicotiana benthamiana* pDEST–VYNE, pDEST-VYCE plasmids were used [436, 621].

4.1.5 Antibiotics and soluble molecules

Table 4.2: Antibiotics

Antibiotica	Company	Cat. no.
Ampicillin sodium salt	Roth	K029
Carbenicillin disodium	Roth	6344
Gentamycin sulphate	Duchefa	G0124
Rifampicin	Duchefa	R0146
Spectinomycin HCL penthahydrate	Duchefa	S0188
Zeocin	Thermo Fisher Scientific	R25001

Table 4.3: Soluble molecules / phytohormones

Soluble molecules/ phytohormones	Company	Cat. no.
1-aminocyclopropane-carboxylic acid	Sigma-Aldrich	A-3903
6-benzylamino purine	Sigma-Aldrich	B3408
Abscisic acid	Sigma-Aldrich	A1049
Brassinolide	Sigma-Aldrich	B1439
Gibberellic acid 3	Duchefa	G0907
Indol-3-acetic acid	Sigma-Aldrich	I2886
Karrikin2	Toronto Research Chemicals	F864800
Paclobutrazol	Duchefa	P0922
rac-GR24	Chiralix	CX23880
Salicylic acid	Sigma-Aldrich	S5922

4.1.6 Oligonucleotides

Table 4.4: List of oligo nucleotides

Locus ID	Name	Sequence	Use
AT1G14920	GAI for	GCAGGCTCAGGAATGAAGAGAGATCATCAT	cloning
AT1G14920	GAI DELLA for	GCAGGCTCAGGAGGCATGGATGAGCTTCTA	cloning
AT1G14920	GAI TV motif for	GCAGGCTCAGGAACTGAGACTGTTCACTAT	cloning
AT1G14920	GAI o. N-term for	GCAGGCTCAGGAATGCTCACCGACCTTAAT	cloning
AT1G14920	GAI 'GRAS'domain for	GCAGGCTCAGGAGTGCGTCTCGTTCACGCG	cloning
AT1G14920	GAI rev	GAAAGCTGGGTCTCAATTGGTGGAGAGTTTCCA	cloning
AT1G14920	GAI only N-term rev	GAAAGCTGGGTCTCACGCGTGAACGAGACGCAC	cloning
AT1G18350	MKK7_amiRNA_Oligo1 #I	GATGAATTGCAGTAATCTAGCGATCTCTCTTTTGTATTCC	cloning
AT1G18350	MKK7_amiRNA_Oligo1#II	GATCGCTAGATTACTGCAATTCATCAAAGAGAATCAATGA	cloning
AT1G18350	MKK7_amiRNA_Oligo1#III	GATCACTAGATTACTCCAATTCTTCACAGGTCGTGATATG	cloning
AT1G18350	MKK7_amiRNA_Oligo1#IV	GAAGAATTGGAGTAATCTAGTGATCTACATATATATTCCT	cloning
AT1G18350	MKK7_amiRNA_Oligo2#I	GATATAATTGCGATTTGGGTCAGTCTCTCTTTTGTATTCC	cloning
AT1G18350	MKK7_amiRNA_Oligo2#II	GACTGACCCAAATCGCAATTATATCAAAGAGAATCAATGA	cloning
AT1G18350	MKK7_amiRNA_Oligo2#III	GACTAACCCAAATCGGAATTATTTCACAGGTCGTGATATG	cloning
AT1G18350	MKK7_amiRNA_Oligo2#IV	GAAATAATTCCGATTTGGGTTAGTCTACATATATATTCCT	cloning
AT1G18350	MKK7_amiRNA_Oligo3#I	GATACGACGCACATTAACGGCGCTCTCTCTTTTGTATTCC	cloning
AT1G18350	MKK7_amiRNA_Oligo3#II	GAGCGCCGTTAATGTGCGTCGTATCAAAGAGAATCAATGA	cloning
AT1G18350	MKK7_amiRNA_Oligo3#III	GAGCACCGTTAATGTCCGTCGTTTCACAGGTCGTGATATG	cloning
AT1G18350	MKK7_amiRNA_Oligo3#IV	GAAACGACGGACATTAACGGTGCTCTACATATATATTCCT	cloning
AT1G18350	MKK7 for1	GCAGGCTCAGGAATGGCTCTTGTTCGTAAA	cloning
AT1G18350	MKK7 for2	GCAGGCTCAGGAGTCGAGAAACTCCACGTT	cloning
AT1G18350	MKK7 for3	GCAGGCTCAGGACTCCACTCACTCAAGATC	cloning
AT1G18350	MKK7 for4	GCAGGCTCAGGAAACGAAGTTAAAATCGCT	cloning
AT1G18350	MKK7 for5	GCAGGCTCAGGAGATATCTGGAGTTTCGGA	cloning
AT1G18350	MKK7 rev1	GAAAGCTGGGTCAAGACTTTCACGGAGAAA	cloning
AT1G18350	MKK7 rev2	GAAAGCTGGGTCTCCGAAACTCCAGATATC	cloning
AT1G18350	MKK7 rev3	GAAAGCTGGGTCAGCGATTTTAACTTCGTT	cloning
AT1G18350	MKK7 rev4	GAAAGCTGGGTCGATCTTGAGTGAGTGGAG	cloning
AT1G18350	MKK7 rev5	GAAAGCTGGGTCAACGTGGAGTTTCTCGAC	cloning
AT1G18350	MKK7 for S193->A	TCATTACCCGAGCTTTAGATTACTG	cloning
AT1G18350	MKK7 rev S193->A	CAGTAATCTAAAGCTCGGGTAATGA	cloning
AT1G18350	MKK7 for S199->A	AGATTACTGCAATGCTTACGTCGGC	cloning
AT1G18350	MKK7 rev S199->A	GCCGACGTAAGCATTGCAGTAATCT	cloning
AT1G18350	MKK7 for T203->A	TACGTCGGCGCTTGCGCTTACATGA	cloning

Table 4.4 continued from previous page

Locus ID	Name	Sequence	Use
AT1G18350	MKK7 rev T203->A	TCATGTAAGCGCAAGCGCCGACGTA	cloning
AT1G18350	MKK7 for S193->D	TCATTACCCGAGATTTAGATTACTG	cloning
AT1G18350	MKK7 rev S193->D	CAGTAATCTAAATCTCGGGTAATGA	cloning
AT1G18350	MKK7 for S199->D	AGATTACTGCAATGATTACGTCGGC	cloning
AT1G18350	MKK7 rev S199->D	GCCGACGTAATCATTGCAGTAATCT	cloning
AT1G18350	MKK7 for T203->E	TACGTCGGCGAATGCGCTTACATGA	cloning
AT1G18350	MKK7 rev T203->E	TCATGTAAGCGCATTCGCCGACGTA	cloning
AT1G51600	GATA28_1for	GCAGGCTCAGGAATGGATGACCTACATGGA	cloning
AT1G51600	GATA28_2for	GCAGGCTCAGGAGGTGTGGAAACAGACATT	cloning
AT1G51600	GATA28_3for	GCAGGCTCAGGATCACCTCATCAGAACAAC	cloning
AT1G51600	GATA28_4for	GCAGGCTCAGGAGAAGCTGCATCTGCTGGA	cloning
AT1G51600	GATA28_1rev	GAAAGCTGGGTCTGTTTCCACACCCTCACT	cloning
AT1G51600	GATA28_2rev	GAAAGCTGGGTCATGAGGTGATCCTAGGCC	cloning
AT1G51600	GATA28_3rev	GAAAGCTGGGTCCCAGCTAGATCCAGCAGA	cloning
AT1G51600	GATA28_4rev	GAAAGCTGGGTCTCACTGTGAGTTGCTTAT	cloning
AT1G64280	NPR1 for 1	GCAGGCTCAGGATTGCTCTCCAACAGCTTC	cloning
AT1G64280	NPR1 for 2	GCAGGCTCAGGAAAGCTATTGGATAGATGT	cloning
AT1G64280	NPR1 for 3	GCAGGCTCAGGACTTCATTTCGCTGTTGCA	cloning
AT1G64280	NPR1 for 4	GCAGGCTCAGGAAGTGCATCAGAAGCAACT	cloning
AT1G64280	NPR1 for 5	GCAGGCTCAGGAACTGGTACGAAGAGAACA	cloning
AT1G64280	NPR1 rev 1	GAAAGCTGGGTCTCAATTAGCAAGCTTGAGTAT	cloning
AT1G64280	NPR1 rev 2	GAAAGCTGGGTCTCATGCAACAGCGAAATGAAG	cloning
AT1G64280	NPR1 rev 3	GAAAGCTGGGTCTCAGCATTGCTCCGGGATATT	cloning
AT1G64280	NPR1 rev 4	GAAAGCTGGGTCTCATGTTCTCTTCGTACCAGT	cloning
AT1G64280	NPR1 rev 5	GAAAGCTGGGTCTCAACGATGAGAGAGTTTACG	cloning
AT1G66350	RGL1 for	GCAGGCTCAGGAATGAAGAGAGAGCACAAC	cloning
AT1G66350	RGL1 DELLA for	GCAGGCTCAGGAGGAGTTGACGAGCTTTTG	cloning
AT1G66350	RGL1 TV motif for	GCAGGCTCAGGAGATGAAACTGTTCATTAC	cloning
AT1G66350	RGL1 o. N-term for	GCAGGCTCAGGAATGCTCTCGGATCTTGAC	cloning
AT1G66350	RGL1 'GRAS'domain for	GCAGGCTCAGGAGTGCGTTTAGTCCACGCG	cloning
AT1G66350	RGL1 rev	GAAAGCTGGGTCTCAAAGGTGTGCTAACTAAGC	cloning
AT1G66350	RGL1 only N-term. Rev	GAAAGCTGGGTCTCAGCGCACCTGATTTGCGTG	cloning
AT2G01570	RGA for	GCAGGCTCAGGAATGAAGAGAGATCATCAC	cloning
AT2G01570	RGA DELLA for	GCAGGCTCAGGAATGGACGACGAGCTTCTC	cloning
AT2G01570	RGA TV motif for	GCAGGCTCAGGAACGGATACTGTTCATTAT	cloning
AT2G01570	RGA o. N-term. for	GCAGGCTCAGGAATGCTCTCTGAGCTTAAT	cloning
AT2G01570	RGA 'GRAS'domain for	GCAGGCTCAGGAAACGGTGTTCGTTTAGTC	cloning
AT2G01570	RGA rev	GAAAGCTGGGTCTCACATGCGGCGGCAGCTCTC	cloning
AT2G01570	RGA only N-term. Rev	GAAAGCTGGGTCTCACTGATTTGCTTGTGGCAA	cloning
AT2G34650	PID for1	GCAGGCTCAGGAATGTTACGAGAATCAGAC	cloning
AT2G34650	PID for2	GCAGGCTCAGGACGAAGACGAAAAAAACAA	cloning
AT2G34650	PID for3	GCAGGCTCAGGAGGTCACATTATGCTCTCT	cloning
AT2G34650	PID rev1	GAAAGCTGGGTCGATACGACGCATGAGGCG	cloning
AT2G34650	PID rev2	GAAAGCTGGGTCCGAAGACGAGGAAGATTC	cloning
AT2G34650	PID rev3	GAAAGCTGGGTCGAACGAACCGGACCGGGC	cloning
AT2G34650	PID rev4	GAAAGCTGGGTCAAAGTAATCGAACGCCGC	cloning
AT3G03450	RGL2 for	GCAGGCTCAGGAATGAAGAGAGGATACGGA	cloning
AT3G03450	RGL2 DELLA for	GCAGGCTCAGGAATGGATGATGAGCTTCTT	cloning
AT3G03450	RGL2 TV motif for	GCAGGCTCAGGAAACGACTCTGTTCATTAT	cloning
AT3G03450	RGL2 o. N-term for	GCAGGCTCAGGAATGCTTTCTGAGCTGAAC	cloning
AT3G03450	RGL2 'GRAS'domain for	GCAGGCTCAGGAGGAGTTAGACTTGTCCAC	cloning
AT3G03450	RGL2 rev	GAAAGCTGGGTCTCAGGCGAGTTTCCACGCCGA	cloning
AT3G03450	RGL2 only N-term rev	GAAAGCTGGGTCTCAGTGGACAAGTCTAACTCC	cloning
AT3G21175	GATA24_1for	GCAGGCTCAGGAATGGATGATCTTCATGGA	cloning
AT3G21175	GATA24_2for	GCAGGCTCAGGATCTCACCCTGGAAACTCA	cloning
AT3G21175	GATA24_3for	GCAGGCTCAGGAGAACAATAGGGTACTG	cloning
AT3G21175	GATA24_4for	GCAGGCTCAGGAGATTCTGGATCCACTGGA	cloning
AT3G21175	GATA24_1rev	GAAAGCTGGGTCGTTTCCAGGGTGAGAAGG	cloning
AT3G21175	GATA24_2rev	GAAAGCTGGGTCCTATTGTTCTGATGAGGT	cloning
AT3G21175	GATA24_3rev	GAAAGCTGGGTCTCCAGAATCATCATTGCT	cloning
AT3G21175	GATA24_4rev	GAAAGCTGGGTCTCACTGTGTGTTGCTAAT	cloning
AT4G24470	GATA25_1for	GCAGGCTCAGGAATGTTTGGTCGCCATTCG	cloning
AT4G24470	GATA25_2for	GCAGGCTCAGGAGATTTGATTCCCGATGGC	cloning
AT4G24470	GATA25_3for	GCAGGCTCAGGAGAACTAGCTCAACAGCAG	cloning
AT4G24470	GATA25_4for	GCAGGCTCAGGAACAGATGGGGCTTATAAC	cloning
AT4G24470	GATA25_1rev	GAAAGCTGGGTCAATCAAATCGGAGGCAGC	cloning
AT4G24470	GATA25_2rev	GAAAGCTGGGTCAGCTAGTTCCATCACCTG	cloning
AT4G24470	GATA25_3rev	GAAAGCTGGGTCTGTGCCAGAGTTATAAGC	cloning
AT4G24470	GATA25_4rev	GAAAGCTGGGTCTTAGTGATCACCTAACAG	cloning
AT4G29810	MKK2 for T229->A	GTTATGACAAACGCTGCAGGTTTAG	cloning
AT4G29810	MKK2 rev T229->A	CTAAACCTGCAGCGTTTGTCATAAC	cloning
AT4G29810	MKK2 for T235->A	CAGGTTTAGCAAACGCTTTTGTGGG	cloning
AT4G29810	MKK2 rev T235->A	CCCACAAAAGCGTTTGCTAAACCTG	cloning
AT4G29810	MKK2 for T239->A	TTTGTGGGGGCTTACAATTATATGT	cloning
AT4G29810	MKK2 rev T239->A	ACATATAATTGTAAGCCCCCACAAA	cloning
AT4G29810	MKK2 for T229->D	GTTATGACAAACGATGCAGGTTTAG	cloning
AT4G29810	MKK2 rev T229->D	CTAAACCTGCATCGTTTGTCATAAC	cloning
AT4G29810	MKK2 for T235->E	CAGGTTTAGCAAACGAATTTGTGGG	cloning
AT4G29810	MKK2 rev T235->E	CCCACAAATTCGTTTGCTAAACCTG	cloning
AT4G29810	MKK2 for T239->D	TTTGTGGGGGATTACAATTATATGT	cloning
AT4G29810	MKK2 rev T239->D	ACATATAATTGTAATCCCCCACAAA	cloning
AT5G17490	RGL3 for	GCAGGCTCAGGAATGAAACGAAGCCATCAA	cloning
AT5G17490	RGL3 DELLA for	GCAGGCTCAGGAAACATGGACGAGTTTCTT	cloning
AT5G17490	RGL3 TV motif for	GCAGGCTCAGGAAATGACACCGTTCATTAC	cloning
AT5G17490	RGL3 o. N-term for	GCAGGCTCAGGAATGCTCTCGGATCTTAAT	cloning
AT5G17490	RGL3 'GRAS'domain for	GCAGGCTCAGGAGTTAGACTCGTTCAGGCG	cloning
AT5G17490	RGL3 rev	GAAAGCTGGGTCTCACCGCCGCAACTCCGCCGC	cloning
AT5G17490	RGL3 only N-term rev	GAAAGCTGGGTCTCACTAGCGCCTGAACGAGTC	cloning
AT5G45110	NPR3 for 1	GCAGGCTCAGGAATGCTAACCAAACTCAGC	cloning
AT5G45110	NPR3 for 2	GCAGGCTCAGGAAATGTTCTTCCCATTCTT	cloning

Table 4.4 continued from previous page

Locus ID	Name	Sequence	Use
AT5G45110	NPR3 for 3	GCAGGCTCAGGAGAAACCAGTCCCAAGATT	cloning
AT5G45110	NPR3 for 4	GCAGGCTCAGGACGTAGCGCAGTTAATATA	cloning
AT5G45110	NPR3 for 5	GCAGGCTCAGGATTCTTTCCAACGGAAGCT	cloning
AT5G45110	NPR3 rev 1	GAAAGCTGGGTCTCAGAAAGCAACCATAAGAAT	cloning
AT5G45110	NPR3 rev 2	GAAAGCTGGGTCTCAAAGCAATTTCTCCGAAATCTT	cloning
AT5G45110	NPR3 rev 3	GAAAGCTGGGTCTCATCTTCTTAATATATTAAC	cloning
AT5G45110	NPR3 rev 4	GAAAGCTGGGTCTCAAGCAACTTTAGCTTCCGT	cloning
AT5G45110	NPR3 rev 5	GAAAGCTGGGTCTCATGTTGTCTTGTGCAG	cloning
AT1G01360	RCAR1_gen_for	ATGGTGTTAGACATTTAGCTT	genotyping
AT1G01360	RCAR1_gen_rev	CGTCAAAATCGACGAGTAATT	genotyping
AT1G06400	ARA2 gen rev 2	AGTTACAACCTCGATAAGATT	genotyping
AT1G06400	ARA2 gen for 3	CAGCCGACTCTCCTCCTCCAT	genotyping
AT1G06400	ARA-2_gen_for_1	TATTAAACCATGTCATGTCCA	genotyping
AT1G06400	ARA-2_gen_for_2	GTAGACCCATATATGAGGGAT	genotyping
AT1G06400	ARA-2_gen_rev	GGTGTATACTGTTTATTGTTA	genotyping
AT1G14920	GAI gen for 2	TTATTTAATAAGACTATACTAAATA	genotyping
AT1G14920	GAI_gen_for	ATTAGTTTATTAATTTCAATA	genotyping
AT1G14920	GAI_gen_rev	TGGTGGAGAGTTTCCAAGCCG	genotyping
AT1G15550	GA3OX1 gen for 2	TAGCAACCAAACAAGATGAAT	genotyping
AT1G15550	GA3OX1_gen_for	ACGTTAACCACGAGCGAGCCA	genotyping
AT1G15550	GA3OX1_gen_rev	TATTAATCCAATAAACAAGTA	genotyping
AT1G18350	MKK7 for	ATGGCTCTTGTTCGTAAACGCCGT	genotyping
AT1G18350	MKK7 for2	TTTAAATGCATATAAATCTAATCA	genotyping
AT1G18400	BEE1_gen_for	ATGGCAAATTTCGAGAATCTT	genotyping
AT1G18400	BEE1_gen_rev	AGTGAGTTTCATCGAGAGGAA	genotyping
AT1G19180	JAZ1 gen for 2	TTAGGCTCGTGAAGGAGGGCA	genotyping
AT1G19180	JAZ1 gen rev 2	TACATACAAATATATGAAGTTTCC	genotyping
AT1G19180	JAZ1_gen_for	ATCTTGATCTTGAAAACTTTT	genotyping
AT1G19180	JAZ1_gen_rev	GGTTTAGATGTCACGTTGTTC	genotyping
AT1G22770	GI_gen_for	AGATAACCAACCAACAAACTC	genotyping
AT1G22770	GI_gen_rev	GTTTACCAGATCCTCGAGAAG	genotyping
AT1G23860	RSZ21_genfor	GCGCCACAGAGTAGATATAGC	genotyping
AT1G23860	RSZ21_gen_rev	ATACAAGTACTGATGCAAAAG	genotyping
AT1G25490	RCN1_gen_ for1	TCACATAAGATGGCTATGGTA	genotyping
AT1G25490	RCN1_gen_ for2	CGAAGAGCTGCTGCATCTAAC	genotyping
AT1G25490	RCN1_gen_rev1	CCGTAAAAGATAATTCAGTCA	genotyping
AT1G25490	RCN1_gen_rev2	TGCTAAAAGCGGGCTAACCCT	genotyping
AT1G32640	MYC2 for	TCTACAAGGTCATCCTAGTCACTTA	genotyping
AT1G32640	Myc2 gen rev 2	AACGTTGTTAGCATGTGTTTA	genotyping
AT1G37130	NIA2_gen_ for	ATACGGCTTTGTGTCACGAAT	genotyping
AT1G37130	NIA2_gen_rev	CTCTTGATGGATCCATGGCAT	genotyping
AT1G51600	GATA28 for	GTAGATTGATGAAAAGCAACCATG	genotyping
AT1G51600	GATA28rev	TCACTGTGAGTTGCTTATGTCATTGGC	genotyping
AT1G66350	RGL1_gen_ for	AGTACGATCTTAGAGCTATTC	genotyping
AT1G66350	RGL1_gen_rev	AACCTTCATTCTCTTCCACAT	genotyping
AT1G67090	RBCS1A for	ATGGCTTCCTCTATGCTCTCTTCC	genotyping
AT1G67090	RBCS1A rev	TTAACCGGTGAAGCTTGGTGGCTT	genotyping
AT1G67090	RBCS1A for	ATGGCTTCCTCTATGCTCTCTTCC	genotyping
AT2G01570	RGA_gen_ for	AATCTCAAATTCACTCGACTC	genotyping
AT2G01570	RGA_gen_rev	TTTGACTCTAGCGGAAGCTCT	genotyping
AT2G01570	RGA_gen_ for2	GAGAGACGGTAGATCCGCCGC	genotyping
AT2G01570	RGA_gen_rev2	ATAGAGAAGTCACATGTTCCT	genotyping
AT2G02950	PKS1_gen_ for	GAATCTTGATCAGTTCTGTGT	genotyping
AT2G02950	PKS1_gen_rev	TTCGATTATTCTCCATTGATT	genotyping
AT2G04550	IBR5_gen_ for	GTTTTTCAGTAGAAGATTCAG	genotyping
AT2G04550	IBR5_gen_rev	GGATACTTGAAGCAGGAGATG	genotyping
AT2G25490	EBF1 gen for 2	GTAATATACAACGAAATGAGA	genotyping
AT2G25490	EBF1 gen rev 2	TATCTCCTCGATCTTCATGTG	genotyping
AT2G25490	EBF1_gen_ for	CCTTGAGCCCACACAGATCAA	genotyping
AT2G25490	EBF1_gen_rev	GAGATTGTGGTCGACCCGGTG	genotyping
AT2G37630	AS1_gen_ for	CACTGTGGAAGGCGATAATGT	genotyping
AT2G37630	AS1_gen_rev	AGGAGGAGTAGGAGATGAAAG	genotyping
AT2G38120	AUX1 for	CCACTCTTGGGTCTTTCTTGC	genotyping
AT2G38120	AUX1 rev	CAAGAAGAGCACCGACAGCGG	genotyping
AT2G39760	BPM3 gen for 3	TTGAAAGTGAGGTTTCCTTCTG	genotyping
AT2G39760	BPM3_gen_ for	GGAAGAACCCGGAGGACCAGT	genotyping
AT2G39760	BPM3_gen_rev	GTAAGAATTGGTGCTGTTCAG	genotyping
AT2G39760	BPM3_gen_ for2	AACAATGGCAATAGTAACAGA	genotyping
AT2G39760	BPM3_gen_rev2	TTGACAAATACACGCCACCAT	genotyping
AT2G40750	WRKY54 gen for 2	AAGTCTCTTTACACTCTTTAG	genotyping
AT2G40750	WRKY54 gen rev 2	TATGAATACGATTGATTGGAT	genotyping
AT2G40750	WRKY54 gen rev 3	ATATTCATTAGGATCCTTCTGCTT	genotyping
AT2G40750	WRKY54_gen_ for	ATCATTCCAGATTTGGATGTT	genotyping
AT2G40750	WRKY54_gen_for	TATATCTTGTCAACATTTATC	genotyping
AT2G43790	MPK6 for	ATGGACGGTGGTTCAGGTCAACCG	genotyping
AT2G44050	COS1_gen_ for	GACGACGCCATTAACCTGTGA	genotyping
AT2G44050	COS1_gen_rev	CGTAATCTTCGCTCGCCGACA	genotyping
AT2G44950	HUB1 gen rev2	ACCAAGCCGCAAAACTGCCAG	genotyping
AT2G44950	HUB1 gen for 2	CTCACACGAACAGAGCATGA	genotyping
AT2G44950	HUB1_gen_ for	TATTTCCAAGACTCAACACTG	genotyping
AT2G44950	HUB1_gen_for	TTATAAGACTACTTAATTTGC	genotyping
AT2G45680	TCP9 gen for 2	TAAACTGGTGGTGCTGACCCA	genotyping
AT2G45680	TCP9 gen rev 2	GTTACATCTAGTTACCGTCGA	genotyping
AT3G02150	TCP13 for	CTTTGGAACTCATGTAAGAAA	genotyping
AT3G05120	GID1A_gen_ for	CAATTTCACACTTAACTTCAA	genotyping
AT3G05120	GID1A_gen_rev	ACAACTGCAGAGTGCAGACCC	genotyping
AT3G11410	PP2CA_gen_ for	TCGAAGGCACATGCGAGCCAC	genotyping
AT3G11410	PP2CA_gen_rev	TTGGGCCACGTTAACGGCGTA	genotyping
AT3G11540	SPY_gen for	TTTCGGAGGAGCGAGGCGGAG	genotyping
AT3G11540	SPY_gen rev	TGTATTGAGGGTGTAATCTTG	genotyping

Table 4.4 continued from previous page

Locus ID	Name	Sequence	Use
AT3G17860	JAZ3 gen rev 2	CTTTCGAAAACCGTGTCTAA	genotyping
AT3G17860	JAZ3 gen rev 3	AGCAATATGGGGATACGCTCG	genotyping
AT3G17860	JAZ3 gen for 2	GTTATAGTTATAAATTAATGGTACG	genotyping
AT3G17860	JAZ3_gen_ for	ATGCAACGTGCAAATGTTTAT	genotyping
AT3G17860	JAZ3_gen_rev	ATTAGGGAACATCCTCACTCC	genotyping
AT3G20550	DDL_gen_ for	ACAGGTGATATTCTTAAATGA	genotyping
AT3G20550	DDL_gen_rev	AGGGTACGACGTTACAAGCGG	genotyping
AT3G21175	GATA24 for	ATTGGGGGTCAAACCAGAGCTGGG	genotyping
AT3G21175	GATA24 rev	GTCTTAAATATTTAACTAATT	genotyping
AT3G23050	IAA7 gen rev 2	ACAAACATCCGAATATTAAAACT	genotyping
AT3G23050	IAA7 gen for 2	TGTTGGAACTTCAATTTTACA	genotyping
AT3G23050	IAA7_gen_ for	CTCAATATTCTCATAGATCAT	genotyping
AT3G23050	IAA7_gen_rev	TTGTGCTCCATAGTTTCCTTG	genotyping
AT3G25800	PP2AA2 for	AATGTGTTGGACACAATCCTG	genotyping
AT3G25800	PP2AA2 fl for	ATAAGCAGAGAGACAAGATCT	genotyping
AT3G25800	PP2AA2 rev	ATTCTATCATTTGTATCGGTAATG	genotyping
AT3G29350	AHP2_gen_ for	GGGTTTACGATATTCATATTC	genotyping
AT3G29350	AHP2_gen_rev	TAAAATGTGGGCGGCGTAATT	genotyping
AT3G45640	MPK3 for	ATGAACACCGGCGGTGGCCAATAC	genotyping
AT3G45640	MPK3 for	TGGACCATGTCCGAACACAAC	genotyping
AT3G45640	MPK3 for2	TGACCCCAACAGAAGAATCAC	genotyping
AT3G45640	MAPK3 gen rev 2	TCTAGCTCTATAATGTCTCCC	genotyping
AT3G48090	EDS1_gen_ for	TTCTATCCATGCTAGTTTCTT	genotyping
AT3G48090	EDS1_gen_rev	AGCGAACAAATCTCCTCATTC	genotyping
AT3G50060	MYB77_gen_ for	GGTTACTGTATAGCTCTATGA	genotyping
AT3G50060	MYB77_gen_rev	TGTGCGAATAATATCAGAGCT	genotyping
AT3G53480	ABCG37 for	TGTTCAGGTGAAATATCTTAC	genotyping
AT3G53480	ABCG37_2 for	CTGGTGCTTCTTAAAAGAGGT	genotyping
AT3G53480	ABCG37 rev	GTGATGAATGCGGCCATAACA	genotyping
AT3G53480	ABCG37_2 rev	ATGTCTAAAAATAGATGTCTA	genotyping
AT4G17720	AT4G17720_gen_ for	AACCCACGTGGCACCTGTGAG	genotyping
AT4G17720	AT4G17720_gen_rev	TTCACATCAAATCCGCGACCA	genotyping
AT4G17720	AT4G17720_gen_ for2	AGATCTCTATCGGTTGCTCCT	genotyping
AT4G17720	AT4G17720_gen_rev2	AAACCCCGCCACTAAATTATC	genotyping
AT4G24470	ZIM	CGGCATTAGTTCCAAATG	genotyping
AT4G24470	ZIM	TTAATGAAACCGGATGAT	genotyping
AT4G24470	ZIM	AGGGTGATATTTATAAGA	genotyping
AT4G24470	GATA25 for	CAGTTTCCGATGTTTGGTCGCCAT	genotyping
AT4G24470	GATA25 rev	CAACAGCGACAACACAGCATCCAC	genotyping
AT4G26110	NAP1,1_gen_ for	GGCACAGCGTTATGAGATTGT	genotyping
AT4G26110	NAP1,1_gen_rev	CTTCATCCTCATCATCATCGT	genotyping
AT4G28910	Ninja gen for 2	GTAAGAGTTTGACATTATTCT	genotyping
AT4G28910	NINJA_gen_ for	GTTATGGTTATATATAATTTC	genotyping
AT4G28910	NINJA_gen_rev	GCATCCCATGTTTCAACTGCG	genotyping
AT4G29810	MKK2 for	ATGAAGAAAGGTGGATTCAGCAAT	genotyping
AT4G29810	MKK2 for	ACTGTTTGTTATATGTGTTTATTG	genotyping
AT4G36540	BEE2_gen_ for	TATATGATAATACCCTCATGA	genotyping
AT4G36540	BEE2_gen_rev	ATAAGATACATTATTAGGCTG	genotyping
AT5G04870	CPK1_gen_ for	CATTATCAACATTCAACCAAT	genotyping
AT5G04870	CPK1_gen_rev	AGAAGTTCTTCGAAAGCGTTA	genotyping
AT5G04870	CPK1_gen_ for2	CTCTTCTCACATCCTCAACGT	genotyping
AT5G04870	CPK1_gen_rev2	ACGCGTTTTTCAAACTGGTTC	genotyping
AT5G08070	TCP17 rev	TGCTCGCATCAGATTTGGCGT	genotyping
AT5G08130	BIM1_gen_ for	ACCGTCTCTCCGCCACTGGCC	genotyping
AT5G08130	BIM1_gen_rev	TTGCATTTACTTCGACGCATG	genotyping
AT5G13930	TT4_gen_ for	GATTAGTAGGAGCTAATGATG	genotyping
AT5G13930	TT4_gen_rev	AGATTTGATGTCATTCAAGAC	genotyping
AT5G18930	BUD2 for	GACGGTTCCGGAGCCTGGAAA	genotyping
AT5G18930	BUD2 rev	TCAAAGGAGTTAAACCATGTT	genotyping
AT5G23280	TCP7 for	GAGTTTGGTCCCCACGCGACC	genotyping
AT5G25890	IAA28_gen_ for	ATCCGCATCACATTCGTAGAA	genotyping
AT5G25890	IAA28_gen_rev	ACCTCTCTCTATTCCTTGCCA	genotyping
AT5G47100	CBL9_gen_ for	CTTGTTTATCAAGCCATCGTC	genotyping
AT5G47100	CBL9_gen_rev	GTCAAACAACAATAATGGCTT	genotyping
AT5G51910	TCP19 rev	CAGATAACATTTTTCGTCAAA	genotyping
AT5G58220	TTL_gen_ for	CTACTCACAATGAGTCTAGAT	genotyping
AT5G58220	TTL_gen_rev	GGAGATCGGAGAAGATGAATG	genotyping
	Gabi kat lines O8409	ATATTGACCATCATACTCATTGC	genotyping
	SALK lines pROK2 LB 1.3	ATTTTGCCGATTTCGGAAC	genotyping
	SAIL lines pCSA110 LB3	TAGCATCTGAATTTCATAACCAATCTCGATACAC	genotyping
	WiscDsLox lines p745	AACGTCCGCAATGTGTTATTAAGTTGTC	genotyping
AT1G18350	MKK7 rev	AAGACTTTCACGGAGAAAAGGGTG	genotyping
AT1G32640	MYC2 rev	GTAGAACTTGACGTCGAAAAA	genotyping
AT1G67090	RBCS1A rev	TTAACCGGTGAAGCTTGGTGGCTT	genotyping
AT2G43790	MPK6 rev	TTGCTGATATTCTGGATTGAAAGC	genotyping
AT3G45640	MPK3 rev	ACCGTATGTTGGATTGAGTGCTAT	genotyping
AT3G45640	MPK3 rev	TCAACAGAAGCTCAGGTGCTC	genotyping
AT3G45640	MPK3 rev2	AAAAGAGAATGGCTTTTGACAGA	genotyping
AT4G29810	MKK2 rev	CACGGAGAACGTACCAGACAGGTT	genotyping
AT4G29810	MKK2 rev	TTCTTACTTGTCTAAAGATGGCAG	genotyping
AT1G01030	for	GCAGGCTCAGGAATGGATCTATCCCTGGCTCCG	ORFeom
AT1G01030	rev	GAAAGCTGGGTCTCATGGATTGAAATTGAGAGAAAGTGA	ORFeom
At1g01250	for	GCAGGCTCAGGAATGTCACCACAGAGAATGAAGCT	ORFeom
At1g01250	rev	GAAAGCTGGGTCTCACAGACACGCCATGAACT	ORFeom
AT1G02190	for	GCAGGCTCAGGAATGGCGTCGAGGCCCGGAG	ORFeom
AT1G02190	rev	GAAAGCTGGGTCTCATAGAGGAGATGGTGGGAGA	ORFeom
AT1G02205	for	GCAGGCTCAGGAATGGCCACAAAACCAGGAGT	ORFeom
AT1G02205	rev	GAAAGCTGGGTCTTAATGATGTGGAAGGAGGAGAGG	ORFeom
At1g02400	for	GCAGGCTCAGGAATGGTTTTGCCATCTTCAACACC	ORFeom
At1g02400	rev	GAAAGCTGGGTCCTATAAAGTCTTGAAAAACTCGAGACG	ORFeom

Table 4.4 continued from previous page

Locus ID	Name	Sequence	Use
AT1G02630	for	GCAGGCTCAGGAATGGTTGATGAGAAAGTGATTGTTGA	ORFeom
AT1G02630	rev	GAAAGCTGGGTCTCAGATGAGCCAGAGCCAAC	ORFeom
AT1G03445	BSU1 for	GCAGGCTCAGGAATGGCTCCTGATCAATCTTATCA	ORFeom
AT1G03445	BSU1 rev	GAAAGCTGGGTCTTATTCACTTGACTCCCCTCGA	ORFeom
AT1G04100	for	GCAGGCTCAGGAATGAATGGTTTGCAAGAA	ORFeom
AT1G04100	IAA10 for	GCAGGCTCAGGAATGAATGGTTTGCAAGAA	ORFeom
AT1G04100	rev	GAAAGCTGGGTCCTACTTACCTACTCCAGC	ORFeom
AT1G04100	IAA10 rev	GAAAGCTGGGTCCTACTTACCTACTCCAGC	ORFeom
AT1G04120	ABCC5 for	GCAGGCTCAGGAATGGATTTTATTGAGATCTCGTTGA	ORFeom
AT1G04120	ABCC5 rev	GAAAGCTGGGTCTCATAATTCAGGGATTCCAGT	ORFeom
AT1G04240	IAA3 for	GCAGGCTCAGGAATGGATGAGTTTGTTAAC	ORFeom
AT1G04240	IAA3 rev	GAAAGCTGGGTCTCATCATACACCACAGCCTAA	ORFeom
AT1G04550	for	GCAGGCTCAGGAATGCGTGGTGTGTCAGAA	ORFeom
AT1G04550	IAA12 for	GCAGGCTCAGGAATGCGTGGTGTGTCAGAA	ORFeom
AT1G04550	rev	GAAAGCTGGGTCCTAAACAGGGTTGTTTCT	ORFeom
AT1G04550	IAA12 rev	GAAAGCTGGGTCCTAAACAGGGTTGTTTCT	ORFeom
At1g06160	for	GCAGGCTCAGGAATGGAATATCAAACTAACTTCT	ORFeom
At1g06160	rev	GAAAGCTGGGTCTCAAGAACATGATCTCATAAGCTCT	ORFeom
AT1G07340	STP2 for	GCAGGCTCAGGAATGGCTGTTGGTTCGATGAA	ORFeom
AT1G07340	STP2 rev	GAAAGCTGGGTCCTAGTCTTTGAAATATTTCTTCCAACG	ORFeom
At1g07420	for	GCAGGCTCAGGAATGGCTTCCTTCGTGGAATCT	ORFeom
At1g07420	rev	GAAAGCTGGGTCTCACGTTTGTTTCATGTCACCG	ORFeom
AT1G07745	RAD51D for	GCAGGCTCAGGAATGGCGCCTCTCAAACATCT	ORFeom
AT1G07745	RAD51D rev	GAAAGCTGGGTCTTATGGACATTGTTGATTCTCCTTGC	ORFeom
AT1G08260	TIL1 for	GCAGGCTCAGGAATGAGCGGAGATAATCGAAGACG	ORFeom
AT1G08260	TIL1 rev	GAAAGCTGGGTCTTAATAGCTAGGGCCATATATGATCCA	ORFeom
AT1G08420	BSL2 for	GCAGGCTCAGGAATGGATGAAGATTCGTCTATGGTGG	ORFeom
AT1G08420	BSL2 rev	GAAAGCTGGGTCTCACATCCAAGCCAGAGAACC	ORFeom
AT1G09400	for	GCAGGCTCAGGAATGAAAAACTTCAATCTTACTCACAGA	ORFeom
AT1G09400	rev	GAAAGCTGGGTCTTACTTATTCAGCGGAGCATTGA	ORFeom
At1g09540	MYB61 for	GCAGGCTCAGGAATGGGGAGACATTCTTGCTGT	ORFeom
At1g09540	MYB61 rev	GAAAGCTGGGTCTTAGTTAGAAATAAGAAAGAAAGA	ORFeom
AT1G09570	PHYA for	GCAGGCTCAGGAATGTCAGGCTCTAGGCCGA	ORFeom
AT1G09570	PHYA rev	GAAAGCTGGGTCCTACTTGTTTGCTGCAGCGA	ORFeom
AT1G11310	MLO2 for	GCAGGCTCAGGAATGGCAGATCAAGTAAAAGAGCG	ORFeom
AT1G11310	MLO2 rev	GAAAGCTGGGTCTCATTTCTTAAAAGAAAAATCTCT	ORFeom
AT1G12890	for	GCAGGCTCAGGAATGTTGAAATCAAGTAACAAGAGA	ORFeom
AT1G12890	rev	GAAAGCTGGGTCTCACATAAGAAACTGTGGAGCA	ORFeom
AT1G13980	GN for	GCAGGCTCAGGAATGGGTCGCCTAAAGTTGCA	ORFeom
AT1G13980	GN rev	GAAAGCTGGGTCTCACGAACCAGTTGTGTTTTCA	ORFeom
AT1G15050	IAA34 for	GCAGGCTCAGGAATGTATTGCAGCGATCCT	ORFeom
AT1G15050	IAA34 for	GCAGGCTCAGGAATGTATTGCAGCGATCCT	ORFeom
AT1G15050	IAA34 rev	GAAAGCTGGGTCTTAAAAGGGAAGTACAGC	ORFeom
AT1G15050	IAA34 rev	GAAAGCTGGGTCTTAAAAGGGAAGTACAGC	ORFeom
AT1G15580	IAA5 for	GCAGGCTCAGGAATGGCGAATGAGAGT	ORFeom
AT1G15580	IAA5 for	GCAGGCTCAGGAATGGCGAATGAGAGT	ORFeom
AT1G15580	IAA5 rev	GAAAGCTGGGTCTCATCCTCTGTTACATGA	ORFeom
AT1G15580	IAA5 rev	GAAAGCTGGGTCTCATCCTCTGTTACATGA	ORFeom
AT1G15750	TPL for	GCAGGCTCAGGAATGTCTTCTCTTAGTAGA	ORFeom
AT1G15750	TPL for	GCAGGCTCAGGAATGTCTTCTCTTAGTAGA	ORFeom
AT1G15750	TPL rev	GAAAGCTGGGTCTCATCTCTGAGGCTGATC	ORFeom
AT1G15750	TPL rev	GAAAGCTGGGTCTCATCTCTGAGGCTGATC	ORFeom
At1g16390	OCT3 for	GCAGGCTCAGGAATGGCCGACTCGACTCGG	ORFeom
At1g16390	OCT3 rev	GAAAGCTGGGTCTCATCCAATAAATTGTCTTTTTGCCA	ORFeom
AT1G16490	MYB58 for	GCAGGCTCAGGAATGGGCAAAGGAAGAGCACC	ORFeom
AT1G16490	MYB58 rev	GAAAGCTGGGTCTTAATGTATGAGGAGCTCGT	ORFeom
AT1G16540	ABA3 for	GCAGGCTCAGGAATGGAAGCATTTCTTAAGGAATTCGG	ORFeom
AT1G16540	ABA3 rev	GAAAGCTGGGTCTTATTCAATATCTGGATTAACTTCT	ORFeom
AT1G17060	CYP72C1 for	GCAGGCTCAGGAATGTTAGAGATCATTACGGT	ORFeom
AT1G17060	CYP72C1 rev	GAAAGCTGGGTCCTACAGTTTTCGGATGATCA	ORFeom
At1g17730	VPS46.1 for	GCAGGCTCAGGAATGCTGCAGAAACAGGTCTC	ORFeom
At1g17730	VPS46.1 rev	GAAAGCTGGGTCTCAAACAGAACAAGGGCTTTGC	ORFeom
AT1G18350	MKK7 for	GCAGGCTCAGGAATGGCTCTTGTTCGTAAA	ORFeom
AT1G18350	MKK7 rev	GAAAGCTGGGTCTCAAAGACTTTCACGGAGAAA	ORFeom
At1g18970	GLP4 for	GCAGGCTCAGGAATGTTTTGTCTCTTTGTAATCCCA	ORFeom
At1g18970	GLP4 rev	GAAAGCTGGGTCTCAAACAGCAAACTTGGACTTGA	ORFeom
At1g19190	for	GCAGGCTCAGGAATGGATTCCGAAATCGCATTCG	ORFeom
At1g19190	rev	GAAAGCTGGGTCTTAAAATGTTTCTTCTTTAAGAAACTC	ORFeom
AT1G19220	ARF19 for	GCAGGCTCAGGAATGAAAGCTCCATCAAATGGA	ORFeom
AT1G19220	ARF19 rev	GAAAGCTGGGTCCTATCTGTTGAAAGAAGCTGCAGC	ORFeom
AT1G19640	JMT for	GCAGGCTCAGGAATGGAGGTAATGCGAGTTCTTCA	ORFeom
AT1G19640	JMT rev	GAAAGCTGGGTCTCAACCGGCTCTAACGAGC	ORFeom
AT1G19850	MP for	GCAGGCTCAGGAATGATGGCTTCATTGTCT	ORFeom
AT1G19850	ARF5 for	GCAGGCTCAGGAATGATGGCTTCATTGTCT	ORFeom
AT1G19850	MP rev	GAAAGCTGGGTCTTATGAAACAGAAGTCTT	ORFeom
AT1G19850	ARF5 rev	GAAAGCTGGGTCTTATGAAACAGAAGTCTT	ORFeom
At1g22985	CRF7 for	GCAGGCTCAGGAATGAAACGAATTGTTCGAATTTCA	ORFeom
At1g22985	CRF7 rev	GAAAGCTGGGTCTTAAAAGCAAAGAGCAAGATGATCA	ORFeom
AT1G23080	PIN7 for	GCAGGCTCAGGAATGATCACATGGCACGACCT	ORFeom
AT1G23080	PIN7 rev	GAAAGCTGGGTCTTATAGCCCGAGTAAAATGTAGT	ORFeom
AT1G23540	PERK12 for	GCAGGCTCAGGAATGTCAGACTTAGGCGAGTCG	ORFeom
AT1G23540	PERK12 rev	GAAAGCTGGGTCTCAGAACCGTCGGTTGTTGA	ORFeom
At1g24260	37865 for	GCAGGCTCAGGAATGGGAAGAGGGAGAGTAGA	ORFeom
At1g24260	37865 rev	GAAAGCTGGGTCTCAAATAGAGTTGGTGTCATAAGGT	ORFeom
AT1G26700	MLO14 for	GCAGGCTCAGGAATGAGAGAAGAAACAGAACCAAGC	ORFeom
AT1G26700	MLO14 rev	GAAAGCTGGGTCTTAACATTCTCTTCTCATTGGCA	ORFeom
AT1G26830	CUL3 for	GCAGGCTCAGGAATGAGTAATCAGAAGAAGAGGA	ORFeom
AT1G26830	CUL3 rev	GAAAGCTGGGTCTTAGGCTAGATAGCGGTAAAGT	ORFeom
AT1G28300	LEC2 for	GCAGGCTCAGGAATGGATAACTTCTTACCCTTTCCCT	ORFeom
AT1G28300	LEC2 rev	GAAAGCTGGGTCTCACCACCACTCAAAGTCGT	ORFeom

Table 4.4 continued from previous page

Locus ID	Name	Sequence	Use
AT1G29230	CIPK18 for	GCAGGCTCAGGAATGGCTCAAGCCTTGGCTC	ORFeom
AT1G29230	CIPK18 rev	GAAAGCTGGGTCCTATTCAGTATCAGATGGCA	ORFeom
AT1G29440	SAUR63 for	GCAGGCTCAGGAATGATAAACGCAAAGAAGCT	ORFeom
AT1G29440	SAUR63 rev	GAAAGCTGGGTCCTAAAATACAAGCAACTGTTGCGT	ORFeom
At1g29460	for	GCAGGCTCAGGAATGATCAACACTAAGAAACTACTCA	ORFeom
At1g29460	rev	GAAAGCTGGGTCCTAAAATACAAGTAATTGTTGGGT	ORFeom
AT1G29860	WRKY71 for	GCAGGCTCAGGAATGGATGATCATGTTGAGCACA	ORFeom
AT1G29860	WRKY71 rev	GAAAGCTGGGTCTCAAGACTCGTTCTTGGAGAACA	ORFeom
AT1G30330	ARF6 for	GCAGGCTCAGGAATGAGATTATCTTCAGCT	ORFeom
AT1G30330	ARF6 for	GCAGGCTCAGGAATGAGATTATCTTCAGCT	ORFeom
AT1G30330	ARF6 rev	GAAAGCTGGGTCCTAGTAGTTGAATGAACC	ORFeom
AT1G30330	ARF6 rev	GAAAGCTGGGTCCTAGTAGTTGAATGAACC	ORFeom
AT1G32130	IWS1 for	GCAGGCTCAGGAATGGGTTTCGAGGATGATCCG	ORFeom
AT1G32130	IWS1 rev	GAAAGCTGGGTCCTAGAGGTACTTGATCATACCCCG	ORFeom
AT1G34170	ARF13 for	GCAGGCTCAGGAATGGAAAATAATGGAGAAATGAATGCA	ORFeom
AT1G34170	ARF13 for	GCAGGCTCAGGAATGGAAAATAATGGAGAA	ORFeom
AT1G34170	ARF13 for	GCAGGCTCAGGAATGGAAAATAATGGAGAA	ORFeom
AT1G34170	ARF13 rev	GAAAGCTGGGTCTTAGTTATCTGTGACGTTTGGTGG	ORFeom
AT1G34170	ARF13 rev	GAAAGCTGGGTCTTAGTTATCTGTGACGTT	ORFeom
AT1G34170	ARF13 rev	GAAAGCTGGGTCTTAGTTATCTGTGACGTT	ORFeom
AT1G34310	ARF12 for	GCAGGCTCAGGAATGGAAAGTGGCAACGTTGTG	ORFeom
AT1G34310	ARF12 for	GCAGGCTCAGGAATGGAAAGTGGCAACGTT	ORFeom
AT1G34310	ARF12 for	GCAGGCTCAGGAATGGAAAGTGGCAACGTT	ORFeom
AT1G34310	ARF12 rev	GAAAGCTGGGTCTTACCTCCTCTTTTGAATGAA	ORFeom
AT1G34310	ARF12 rev	GAAAGCTGGGTCTTACCTCCTCTTTTGAAT	ORFeom
AT1G34310	ARF12 rev	GAAAGCTGGGTCTTACCTCCTCTTTTGAAT	ORFeom
AT1G34390	ARF22 for	GCAGGCTCAGGAATGGAAAGTGGCAACATTGTGA	ORFeom
AT1G34390	ARF22 for	GCAGGCTCAGGAATGGAAAGTGGCAACATT	ORFeom
AT1G34390	ARF22 for	GCAGGCTCAGGAATGGAAAGTGGCAACATT	ORFeom
AT1G34390	ARF22 rev	GAAAGCTGGGTCTTACTGGACTTCAAGTTTTTGACCT	ORFeom
AT1G34390	ARF22 rev	GAAAGCTGGGTCTTACTGGACTTCAAGTTT	ORFeom
AT1G34390	ARF22 rev	GAAAGCTGGGTCTTACTGGACTTCAAGTTT	ORFeom
AT1G34410	ARF21 for	GCAGGCTCAGGAATGGAAAGTGGCAACATTGTGA	ORFeom
AT1G34410	ARF21 for	GCAGGCTCAGGAATGGAAAGTGGCAACATT	ORFeom
AT1G34410	ARF21 rev	GAAAGCTGGGTCTCAACTTGAGAGACTCTTACTGGAC	ORFeom
AT1G34410	ARF21 rev	GAAAGCTGGGTCTCATCAACTTGAGAGACTCTT	ORFeom
AT1G35140	PHI-1 for	GCAGGCTCAGGAATGGCTTCTTTTGTGATGGGA	ORFeom
AT1G35140	PHI-1 rev	GAAAGCTGGGTCTCAAAACAGAGTCGAGCAAGA	ORFeom
AT1G35240	ARF20 for	GCAGGCTCAGGAATGGAAACTGGCAACGTTGTG	ORFeom
AT1G35240	ARF20 for	GCAGGCTCAGGAATGGAAACTGGCAACGTT	ORFeom
AT1G35240	ARF20 for	GCAGGCTCAGGAATGGAAACTGGCAACGTT	ORFeom
AT1G35240	ARF20 rev	GAAAGCTGGGTCTCAACTTGAGAGACTCTTACTGGAC	ORFeom
AT1G35240	ARF20 rev	GAAAGCTGGGTCTCAACTTGAGAGACTCTT	ORFeom
AT1G35240	ARF20 rev	GAAAGCTGGGTCTCAACTTGAGAGACTCTT	ORFeom
AT1G35520	ARF15 for	GCAGGCTCAGGAATGGAAACTGGCAACGTTGTG	ORFeom
AT1G35520	ARF15 for	GCAGGCTCAGGAATGGAAACTGGCAACGTT	ORFeom
AT1G35520	ARF15 rev	GAAAGCTGGGTCTTACCTCCTCTTTTGAATAT	ORFeom
AT1G35520	ARF15 rev	GAAAGCTGGGTCTCATTACCTCCTCTTTTGAAT	ORFeom
AT1G35540	ARF14 for	GCAGGCTCAGGAATGGAAAGTGGCAACGTTGTG	ORFeom
AT1G35540	ARF14 for	GCAGGCTCAGGAATGGAAAGTGGCAACGTT	ORFeom
AT1G35540	ARF14 for	GCAGGCTCAGGAATGGAAAGTGGCAACGTT	ORFeom
AT1G35540	ARF14 rev	GAAAGCTGGGTCTCAACTTGAGAGACTCTTCCTGG	ORFeom
AT1G35540	ARF14 rev	GAAAGCTGGGTCTCAACTTGAGAGACTGTT	ORFeom
AT1G35540	ARF14 rev	GAAAGCTGGGTCTCAACTTGAGAGACTGTT	ORFeom
AT1G42560	MLO9 for	GCAGGCTCAGGAATGGCTGGAGGTGGTGGT	ORFeom
AT1G42560	MLO9 rev	GAAAGCTGGGTCTCACTTTTCATTCTTTTTCCTCGCC	ORFeom
AT1G43950	ARF23 for	GCAGGCTCAGGAATGGAAAGTGGCAATGTT	ORFeom
AT1G43950	ARF23 rev	GAAAGCTGGGTCTCATCATCTGATACCAACTCG	ORFeom
AT1G44090	GA20OX5 for	GCAGGCTCAGGAATGTGCATATATGCATCTAGACAGAC	ORFeom
AT1G44090	GA20OX5 rev	GAAAGCTGGGTCTCAAGTTGATTTCTTGTCGGAGT	ORFeom
At1g44830	for	GCAGGCTCAGGAATGGTGAAAACACTTCAAAAGACAC	ORFeom
At1g44830	rev	GAAAGCTGGGTCTCAGCAGAAGTTCCATAATCTGA	ORFeom
AT1G48500	JAZ4 for	GCAGGCTCAGGAATGGAGAGAGATTTTCTCGGGC	ORFeom
AT1G48500	JAZ4 rev	GAAAGCTGGGTCTTAGTGCAGATGATGAGCTGGA	ORFeom
AT1G49040	SCD1 for	GCAGGCTCAGGAATGGGACGGATCTTCGAGTAC	ORFeom
AT1G49040	SCD1 rev	GAAAGCTGGGTCTCAGATGTTGATGGTGGCATC	ORFeom
AT1G49190	RR19 for	GCAGGCTCAGGAATGTTGGTGGGAAAGATAAGTGGA	ORFeom
AT1G49190	RR19 rev	GAAAGCTGGGTCCTAATTATAATTGTAGCCATTGA	ORFeom
AT1G49640	for	GCAGGCTCAGGAATGGAATCTGATCTAACCACAGAGC	ORFeom
AT1G49640	rev	GAAAGCTGGGTCTCAACTTATGATAAACTCCAAAAAACT	ORFeom
AT1G49660	CXE5 for	GCAGGCTCAGGAATGGAATCTGAAATCGCCTCCG	ORFeom
AT1G49660	CXE5 rev	GAAAGCTGGGTCTCAACCAATAATAAACTCGACAAACT	ORFeom
AT1G50960	GA2OX7 for	GCAGGCTCAGGAATGGCTTCTCAACCTCCCTT	ORFeom
AT1G50960	GA2OX7 rev	GAAAGCTGGGTCTCAAATGAGAAACCTGGACAAGC	ORFeom
AT1G51950	IAA18 for	GCAGGCTCAGGAATGGAGGGTTATTCAAGA	ORFeom
AT1G51950	IAA18 for	GCAGGCTCAGGAATGGAGGGTTATTCAAGA	ORFeom
AT1G51950	IAA18 rev	GAAAGCTGGGTCTCATCTTCTCATTTTCTC	ORFeom
AT1G51950	IAA18 rev	GAAAGCTGGGTCTCATCTTCTCATTTTCTC	ORFeom
AT1G51965	ABO5 for	GCAGGCTCAGGAATGAAGCTTCTCCGCCGC	ORFeom
AT1G51965	ABO5 rev	GAAAGCTGGGTCCTACAAAGGGCTGACAACCCA	ORFeom
AT1G52570	PLDALPHA2 for	GCAGGCTCAGGAATGGAAGAGTGTTTGTTACATGGA	ORFeom
AT1G52570	PLDALPHA2 rev	GAAAGCTGGGTCTTAGGTTGTAAGAATTGGAGGCA	ORFeom
AT1G52830	IAA6 for	GCAGGCTCAGGAATGGCAAAGGAAGGTCTA	ORFeom
AT1G52830	IAA6 rev	GAAAGCTGGGTCTCATTAATCTTGCTGGAGACC	ORFeom
AT1G52920	GPCR for	GCAGGCTCAGGAATGGGAGAACGGTTTTTCCGA	ORFeom
AT1G52920	GPCR rev	GAAAGCTGGGTCTTAGAGTTCATAACCTGGAAACAGA	ORFeom
AT1G53940	GLIP2 for	GCAGGCTCAGGAATGGAAAACTCTCGATCAACTTTGA	ORFeom
AT1G53940	GLIP2 rev	GAAAGCTGGGTCTTATAAGGTCCGGTAACATTGGC	ORFeom
AT1G55010	PDF1.5 for	GCAGGCTCAGGAATGGCTAAGTTTTGTACCACCA	ORFeom
AT1G55010	PDF1.5 rev	GAAAGCTGGGTCTTAGCAAGAGAAGAAACAGAAACA	ORFeom

Table 4.4 continued from previous page

Locus ID	Name	Sequence	Use
AT1G56160	MYB72 for	GCAGGCTCAGGAATGGGGAAAGGAAGAGCACC	ORFeom
AT1G56160	MYB72 rev	GAAAGCTGGGTCTCATAGACATACTTCTCCGACGA	ORFeom
AT1G59750	ARF1 for	GCAGGCTCAGGAATGGCAGCTTCCAATCATTCA	ORFeom
AT1G59750	ARF1 for	GCAGGCTCAGGAATGGCAGCTTCCAATCAT	ORFeom
AT1G59750	ARF1 rev	GAAAGCTGGGTCTCATCTTGATCCCGCCATAGA	ORFeom
AT1G59750	ARF1 rev	GAAAGCTGGGTCTCATCATCTTGATCCCGCCAT	ORFeom
AT1G59870	PEN3 for	GCAGGCTCAGGAATGGATTACAATCCAAATCTTCCTCC	ORFeom
AT1G59870	PEN3 rev	GAAAGCTGGGTCTTATCTGGTCTGGAAGTTGAGAGT	ORFeom
AT1G60980	GA20OX4 for	GCAGGCTCAGGAATGGAATGCATCATAAAGCTCCC	ORFeom
AT1G60980	GA20OX4 rev	GAAAGCTGGGTCTCAGAAACTTCCTTTGTTCTTGAGC	ORFeom
AT1G61630	ENT7 for	GCAGGCTCAGGAATGACTAATCCAGAGGATATCCCT	ORFeom
AT1G61630	ENT7 rev	GAAAGCTGGGTCCTAAAACGAATCGTTGCCAATGA	ORFeom
AT1G62430	CDS1 for	GCAGGCTCAGGAATGGAGGAAGAGAATGTTACT	ORFeom
AT1G62430	CDS1 rev	GAAAGCTGGGTCCTATGAGAGCTTGTCCTTCAGCA	ORFeom
At1g63030	ddf2 for	GCAGGCTCAGGAATGGAAAACGACGATATCACCG	ORFeom
At1g63030	ddf2 rev	GAAAGCTGGGTCTTAGTAACTCCAAAGTGACAAATCT	ORFeom
AT1G63440	HMA5 for	GCAGGCTCAGGAATGGCGACGAAGCTTTTGTC	ORFeom
AT1G63440	HMA5 rev	GAAAGCTGGGTCTTAAACTCGCTCCACCTGAA	ORFeom
AT1G63650	EGL3 for	GCAGGCTCAGGAATGGCAACCGGAGAAAACAGA	ORFeom
AT1G63650	EGL3 rev	GAAAGCTGGGTCTTAACATATCCATGCAACCCTTTGA	ORFeom
At1g64000	WRKY56 for	GCAGGCTCAGGAATGGAAGGGGTTGACAACACA	ORFeom
At1g64000	WRKY56 rev	GAAAGCTGGGTCTTACAGATCAGAAACTCTTGAGAGGA	ORFeom
AT1G66560	WRKY64 for	GCAGGCTCAGGAATGTTCTCCAACATCGATCAAACA	ORFeom
AT1G66560	WRKY64 rev	GAAAGCTGGGTCCTAATCAAGATTAGCAATATTGTCA	ORFeom
AT1G66600	ABO3 for	GCAGGCTCAGGAATGTTTTCAAACATCGATCACAAGG	ORFeom
AT1G66600	ABO3 rev	GAAAGCTGGGTCTCAAAACAACATCAGGTCTTCCG	ORFeom
AT1G67820	for	GCAGGCTCAGGAATGACTAATAAACTTCGCTCAGA	ORFeom
AT1G67820	rev	GAAAGCTGGGTCTCAGCCTTTGTAATGGTTGAGA	ORFeom
AT1G68210	APRR6 for	GCAGGCTCAGGAATGGCTGGATGCTTAGTTCCT	ORFeom
AT1G68210	APRR6 rev	GAAAGCTGGGTCTCATACATCTTTATTCATCTCTTCGT	ORFeom
At1g69310	WRKY57 for	GCAGGCTCAGGAATGAACGATCCTGATAATCCCGA	ORFeom
At1g69310	WRKY57 rev	GAAAGCTGGGTCTCAAGGGTTGCGCATAGTTTG	ORFeom
AT1G69560	MYB105 for	GCAGGCTCAGGAATGGAGATGGTGCATGCTGA	ORFeom
AT1G69560	MYB105 rev	GAAAGCTGGGTCTCACACCGTCCCCAACCC	ORFeom
AT1G69670	CUL3B for	GCAGGCTCAGGAATGAGTAATCAGAAGAAGAGA	ORFeom
AT1G69670	CUL3B rev	GAAAGCTGGGTCTTACGCTAGATAGCGGTAAAGT	ORFeom
AT1G69935	SHW1 for	GCAGGCTCAGGAATGGCCGCAGCTACAACAA	ORFeom
AT1G69935	SHW1 rev	GAAAGCTGGGTCTTAATTTACCGGGTTTGGTCCA	ORFeom
At1g70330	ENT1 for	GCAGGCTCAGGAATGACTCCCATTAGTCAACGA	ORFeom
At1g70330	ENT1 rev	GAAAGCTGGGTCTTAAACAAATACAGATAACAAAGCT	ORFeom
At1g71450	for	GCAGGCTCAGGAATGGCTGGTCTTAGGAATTCCG	ORFeom
At1g71450	rev	GAAAGCTGGGTCTTAAGGGTCCCAAAGAAAGTCACT	ORFeom
AT1G72570	for	GCAGGCTCAGGAATGAAGAAATGGTTGGGATTTTCA	ORFeom
AT1G72570	rev	GAAAGCTGGGTCTTAGTGGCCGGCGCCAGAG	ORFeom
AT1G73000	PYL3 for	GCAGGCTCAGGAATGAATCTTGCTCCAATC	ORFeom
AT1G73000	PYL3 rev	GAAAGCTGGGTCTCATCAGGTCGGAGAAGCCGT	ORFeom
At1g73220	OCT1 for	GCAGGCTCAGGAATGGAACCTTCAAAACAAGAAGT	ORFeom
At1g73220	OCT1 rev	GAAAGCTGGGTCTCAAGTAATCATGATTGTTTCGT	ORFeom
At1g73410	MYB54 for	GCAGGCTCAGGAATGATCATGTGCAGCCGAGG	ORFeom
At1g73410	MYB54 rev	GAAAGCTGGGTCCTAGGAGGCAGAGTTTCCAACG	ORFeom
At1g74080	MYB122 for	GCAGGCTCAGGAATGGTACGGACGCCGTGTT	ORFeom
At1g74080	MYB122 rev	GAAAGCTGGGTCTCATCCAAAATAATTGTCAATCCCT	ORFeom
At1g74650	MYB31 for	GCAGGCTCAGGAATGGGTAGACCACCTTGTTGC	ORFeom
At1g74650	MYB31 rev	GAAAGCTGGGTCTTATTTTAACTCCTCTAAAGACACGT	ORFeom
At1g74950	TIFY10B for	GCAGGCTCAGGAATGTCGAGTTTTTCTGCCGAG	ORFeom
At1g74950	TIFY10B rev	GAAAGCTGGGTCTTACCGTGAACTGAGCCAAGC	ORFeom
At1g75830	LCR67 for	GCAGGCTCAGGAATGGCTAAGTCTGCTACCATCG	ORFeom
At1g75830	LCR67 rev	GAAAGCTGGGTCTTAACATGGGAAGTAGCAGA	ORFeom
AT1G77110	PIN6 for	GCAGGCTCAGGAATGATAACGGGAAACGAATTCT	ORFeom
AT1G77110	PIN6 rev	GAAAGCTGGGTCTCATAGGCCCAAGAGGACGT	ORFeom
AT1G77850	ARF17 for	GCAGGCTCAGGAATGTCACCGCCGTCGGCAAC	ORFeom
AT1G77850	ARF17 for	GCAGGCTCAGGAATGTCACCGCCGTCGGCA	ORFeom
AT1G77850	ARF17 for	GCAGGCTCAGGAATGTCACCGCCGTCGGCA	ORFeom
AT1G77850	ARF17 rev	GAAAGCTGGGTCTTAACCTTGGGAGCTAGAACCTG	ORFeom
AT1G77850	ARF17 rev	GAAAGCTGGGTCTTAACCTTGGGAGCTAGA	ORFeom
AT1G77850	ARF17 rev	GAAAGCTGGGTCTTAACCTTGGGAGCTAGA	ORFeom
At1g78590	NADK3 for	GCAGGCTCAGGAATGGCGATTAGGAAGCTTTTGC	ORFeom
At1g78590	NADK3 rev	GAAAGCTGGGTCCTAGTACCTTGATCTGATCTGAGA	ORFeom
At1g79180	MYB63 for	GCAGGCTCAGGAATGGGGAAGGGAAGAGCACC	ORFeom
At1g79180	MYB63 rev	GAAAGCTGGGTCTCAATGTATCATGAGCTCGT	ORFeom
AT1G79360	OCT2 for	GCAGGCTCAGGAATGGCAGAACCAACTCAGCC	ORFeom
AT1G79360	OCT2 rev	GAAAGCTGGGTCTCATGCAATGACATTATTAACGGC	ORFeom
AT1G79460	GA2 for	GCAGGCTCAGGAATGTCTATCAACCTTCGCTCCT	ORFeom
AT1G79460	GA2 rev	GAAAGCTGGGTCTCAAGTTAAAGATTCTTCCTGTAAGCT	ORFeom
AT1G80330	GA3OX4 for	GCAGGCTCAGGAATGCCTTCACTAGCAGAAGAGA	ORFeom
AT1G80330	GA3OX4 rev	GAAAGCTGGGTCTTAATTGGTGGGATTAACGACCCT	ORFeom
AT1G80390	IAA15 for	GCAGGCTCAGGAATGTCACCGGAGGAATAC	ORFeom
AT1G80390	IAA15 for	GCAGGCTCAGGAATGTCACCGGAGGAATAC	ORFeom
AT1G80390	IAA15 rev	GAAAGCTGGGTCCTATAATCCAATAGCATC	ORFeom
AT1G80390	IAA15 rev	GAAAGCTGGGTCCTATAATCCAATAGCATC	ORFeom
At1g80580	for	GCAGGCTCAGGAATGGAAAACAGCTACACCGTTG	ORFeom
At1g80580	rev	GAAAGCTGGGTCTCACTTCCTAGACAACAACCCT	ORFeom
AT1G80590	WRKY66 for	GCAGGCTCAGGAATGTCTCTTGAGATTGATGCGA	ORFeom
AT1G80590	WRKY66 rev	GAAAGCTGGGTCTTAAGATTTATTAATGTTCAATCCTGG	ORFeom
AT2G01200	IAA32 for	GCAGGCTCAGGAATGGACCCAAACACACCT	ORFeom
AT2G01200	IAA32 for	GCAGGCTCAGGAATGGACCCAAACACACCT	ORFeom
AT2G01200	IAA32 rev	GAAAGCTGGGTCTTAAAAGGGAAGAAGAGC	ORFeom
AT2G01200	IAA32 rev	GAAAGCTGGGTCTTAAAAGGGAAGAAGAGC	ORFeom
At2g02820	MYB88 for	GCAGGCTCAGGAATGGAAGAGACAACTAAGCAGA	ORFeom
At2g02820	MYB88 rev	GAAAGCTGGGTCTCACCTCATTTTCTTAGTAAGAGGAGA	ORFeom

Table 4.4 continued from previous page

Locus ID	Name	Sequence	Use
At2g03760	SOT12 for	GCAGGCTCAGGAATGTCATCATCATCATCAGTTCCTG	ORFeom
At2g03760	SOT12 rev	GAAAGCTGGGTCTCAAGAAGAAAATTTAAGACCAGAACC	ORFeom
AT2G04450	NUDT6 for	GCAGGCTCAGGAATGGACAATGAAGATCAGGAGTCC	ORFeom
AT2G04450	NUDT6 rev	GAAAGCTGGGTCTCAACCAGAGGTGGAGGCTA	ORFeom
AT2G14920	ST4A for	GCAGGCTCAGGAATGGATGAAAAAGATAGACCAAAGA	ORFeom
AT2G14920	ST4A rev	GAAAGCTGGGTCTTAGAATTTCAAACCGGAACCT	ORFeom
AT2G16910	AMS for	GCAGGCTCAGGAATGGAGAGTAATATGCAAAACTTGT	ORFeom
AT2G16910	AMS rev	GAAAGCTGGGTCTTATTGGTTGTGGTAATGGTTGATGT	ORFeom
AT2G17430	MLO7 for	GCAGGCTCAGGAATGATCACAAGAAGCAGGTGTC	ORFeom
AT2G17430	MLO7 rev	GAAAGCTGGGTCCTAAGAGTTGTGGAATTGCATCTCC	ORFeom
AT2G17820	HK1 for	GCAGGCTCAGGAATGCGAGGAGATAGCTTCTCA	ORFeom
AT2G17820	HK1 rev	GAAAGCTGGGTCTCAAGCGGACAATGAAGTTTGG	ORFeom
At2g18550	HB21 for	GCAGGCTCAGGAATGAATAACCAGAATGTAGATGATCA	ORFeom
At2g18550	HB21 rev	GAAAGCTGGGTCTTACATAAATTGGCTCATCCAGTCT	ORFeom
AT2G18790	PHYB for	GCAGGCTCAGGAATGGTTTCCGGAGTCGGGG	ORFeom
AT2G18790	PHYB rev	GAAAGCTGGGTCCTAATATGGCATCATCAGCATCATGT	ORFeom
At2g20180	PIL5 for	GCAGGCTCAGGAATGGATCCTCAGCAGCAACC	ORFeom
At2g20180	PIL5 rev	GAAAGCTGGGTCTTAACCTGTTGTGTGGTTTCCG	ORFeom
AT2G21770	CESA9 for	GCAGGCTCAGGAATGAACACTGGAGGGAGACTC	ORFeom
AT2G21770	CESA9 rev	GAAAGCTGGGTCTCACTTTAAACAGTCAAGACCACA	ORFeom
At2g21900	WRKY59 for	GCAGGCTCAGGAATGAACTATCCTTCAAACCCTAACC	ORFeom
At2g21900	WRKY59 rev	GAAAGCTGGGTCTCAATATGGAGCAGAATGAGAGA	ORFeom
AT2G22330	CYP79B3 for	GCAGGCTCAGGAATGGATACTTTAGCTTCAAACTCTTCG	ORFeom
AT2G22330	CYP79B3 rev	GAAAGCTGGGTCTCACTTCACCATTGGGTAAAGGT	ORFeom
AT2G22670	IAA8 for	GCAGGCTCAGGAATGAGTTCTGGGAACGAT	ORFeom
AT2G22670	IAA8 for	GCAGGCTCAGGAATGAGTTCTGGGAACGAT	ORFeom
AT2G22670	IAA8 rev	GAAAGCTGGGTCTCAAACCCGCTCTTTGTT	ORFeom
AT2G22670	IAA8 rev	GAAAGCTGGGTCTCAAACCCGCTCTTTGTT	ORFeom
AT2G24765	ARF3 for	GCAGGCTCAGGAATGGGAATCTTATTCACG	ORFeom
AT2G24765	ARF3 for	GCAGGCTCAGGAATGGGAATCTTATTCACG	ORFeom
AT2G24765	ARF3 rev	GAAAGCTGGGTCTTAGCCACTTCCCGACTT	ORFeom
AT2G24765	ARF3 rev	GAAAGCTGGGTCTTAGCCACTTCCCGACTT	ORFeom
AT2G25230	MYB100 for	GCAGGCTCAGGAATGAAAAAAAATTATCAAAAGAAGA	ORFeom
AT2G25230	MYB100 rev	GAAAGCTGGGTCTTATTCCCACCAACGCAGCA	ORFeom
AT2G25540	CESA10 for	GCAGGCTCAGGAATGGTTGCGGGATCTTACCG	ORFeom
AT2G25540	CESA10 rev	GAAAGCTGGGTCTCACTCACCCATGAAACTGTTG	ORFeom
AT2G25820	ESE2 for	GCAGGCTCAGGAATGGTGGATTCTCATGGCTCC	ORFeom
AT2G25820	ESE2 rev	GAAAGCTGGGTCTTACTCATAATTCCACAAAAAGCT	ORFeom
AT2G26010	PDF1.3 for	GCAGGCTCAGGAATGGCTAAGTCTGCTGCCAT	ORFeom
AT2G26010	PDF1.3 rev	GAAAGCTGGGTCTTAACATGGGAAGTAACAGATACACT	ORFeom
AT2G26020	PDF1.2b for	GCAGGCTCAGGAATGGCTAAGTTTGCTTCCATCA	ORFeom
AT2G26020	PDF1.2b rev	GAAAGCTGGGTCTTAACATGGGACGTAACAGA	ORFeom
AT2G26040	PYL2 for	GCAGGCTCAGGAATGAGCTCATCCCCGGCC	ORFeom
AT2G26040	PYL2 rev	GAAAGCTGGGTCTCATTATTCATCATCATGCAT	ORFeom
At2g26710	BAS1 for	GCAGGCTCAGGAATGGAGGAAGAAAGTAGCAGCT	ORFeom
At2g26710	BAS1 rev	GAAAGCTGGGTCTCAATCCTCATGATTGGTCA	ORFeom
AT2G26870	NPC2 for	GCAGGCTCAGGAATGTCTATTAAAGCATTTGCTTTGA	ORFeom
AT2G26870	NPC2 rev	GAAAGCTGGGTCTTAAGGTCTTCTTCCGGTGAGG	ORFeom
AT2G27070	RR13 for	GCAGGCTCAGGAATGGCTTTTGCTCAATCTGTCT	ORFeom
AT2G27070	RR13 rev	GAAAGCTGGGTCCTAAACTTCTAAACCCGAAAACTTGA	ORFeom
AT2G27120	TIL2 for	GCAGGCTCAGGAATGAGCGGAAGGAGATGTGA	ORFeom
AT2G27120	TIL2 rev	GAAAGCTGGGTCTCAACAGCTGGTGGCAAATA	ORFeom
AT2G27150	AAO3 for	GCAGGCTCAGGAATGGATTTGGAGTTTGCAGT	ORFeom
AT2G27150	rev	GAAAGCTGGGTCTTATTGTCCTTTGATCTTTCCTTGT	ORFeom
AT2G27210	BSL3 for	GCAGGCTCAGGAATGGATTTGGATTCTTCAATGGTACC	ORFeom
AT2G27210	BSL3 rev	GAAAGCTGGGTCTTATATCCAAGCAAGAGAGCCGC	ORFeom
AT2G28350	ARF10 for	GCAGGCTCAGGAATGGAGCAAGAGAAAAGC	ORFeom
AT2G28350	ARF10 for	GCAGGCTCAGGAATGGAGCAAGAGAAAAGC	ORFeom
AT2G28350	ARF10 rev	GAAAGCTGGGTCTCAAGCGAAGATGCTGAG	ORFeom
AT2G28350	ARF10 rev	GAAAGCTGGGTCTCAAGCGAAGATGCTGAG	ORFeom
AT2G29060	for	GCAGGCTCAGGAATGGGTTCTTACTCAGCTGGC	ORFeom
AT2G29060	rev	GAAAGCTGGGTCCTACAAAGGAACCCAAATAGATGAACC	ORFeom
AT2G30470	HSI2 for	GCAGGCTCAGGAATGTTTGAAGTCAAAATGGGGTCA	ORFeom
AT2G30470	HSI2 rev	GAAAGCTGGGTCTCAGCTTGAAACTCTCGGCT	ORFeom
At2g31190	RUS2 for	GCAGGCTCAGGAATGCAGTTTCTTCAGGAGAAGGT	ORFeom
At2g31190	RUS2 rev	GAAAGCTGGGTCCTACCAAGCAAATCTTGTCCCC	ORFeom
AT2G31470	DOR for	GCAGGCTCAGGAATGAAATCACGGCGACAGAA	ORFeom
AT2G31470	DOR rev	GAAAGCTGGGTCTTATATAAGCTTCACATCCTCTACA	ORFeom
AT2G31660	SAD2 for	GCAGGCTCAGGAATGGATCTGCATAGCCTCGC	ORFeom
AT2G31660	SAD2 rev	GAAAGCTGGGTCTCATAGAGCAGTAACAGGAGT	ORFeom
AT2G32410	AXL for	GCAGGCTCAGGAATGGCGGAACCCAAAACCAA	ORFeom
AT2G32410	AXL rev	GAAAGCTGGGTCCTATAATGTCAAAGACTGAGACTTGTG	ORFeom
AT2G33310	IAA13 for	GCAGGCTCAGGAATGATTACTGAACTTGAG	ORFeom
AT2G33310	IAA13 for	GCAGGCTCAGGAATGATTACTGAACTTGAG	ORFeom
AT2G33310	IAA13 rev	GAAAGCTGGGTCCTAAACCGGCTGCTTTCG	ORFeom
AT2G33310	IAA13 rev	GAAAGCTGGGTCCTAAACCGGCTGCTTTCG	ORFeom
AT2G33670	MLO5 for	GCAGGCTCAGGAATGGCTGGAGGAGGAGGTG	ORFeom
AT2G33670	MLO5 rev	GAAAGCTGGGTCTTAGGGACCGCTTAAGAGGTC	ORFeom
AT2G34180	CIPK13 for	GCAGGCTCAGGAATGGCTCAAGTACTATCTACACCG	ORFeom
AT2G34180	CIPK13 rev	GAAAGCTGGGTCTCACTGTTCAATTTCAGGTGGC	ORFeom
At2g35320	EYA for	GCAGGCTCAGGAATGAATAATGATACATCAAAAAAGCTG	ORFeom
At2g35320	EYA for	GCAGGCTCAGGAATGAATAATGATACATCAAAAAAGCTG	ORFeom
At2g35320	EYA rev	GAAAGCTGGGTCTTAGGGTTTACTTGCATATTTTACA	ORFeom
At2g35320	EYA rev	GAAAGCTGGGTCTTACTCTTTGCTGGAATCAGCA	ORFeom
At2g35700	ERF38 for	GCAGGCTCAGGAATGGAACGTGACGACTGCC	ORFeom
At2g35700	ERF38 rev	GAAAGCTGGGTCCTAGTAACTTTGAGAGAGGAAGGGT	ORFeom
AT2G37650	for	GCAGGCTCAGGAATGATTACTGAACCAAGTCTAACCG	ORFeom
AT2G37650	rev	GAAAGCTGGGTCTCAAGCCTTGGACTCTGGTT	ORFeom
AT2G37700	for	GCAGGCTCAGGAATGGCGTCTAGACCAGGTTT	ORFeom
AT2G37700	rev	GAAAGCTGGGTCTTAGGTCTCTAAAGATGGCAGAAGT	ORFeom

Table 4.4 continued from previous page

Locus ID	Name	Sequence	Use
At2g38470	WRKY33 for	GCAGGCTCAGGAATGGCTGCTTCTTTTCTTACA	ORFeom
At2g38470	WRKY33 rev	GAAAGCTGGGTCTCAGGGCATAAACGAATCGA	ORFeom
AT2G39200	MLO12 for	GCAGGCTCAGGAATGGCAATAAAAGAGCGATCACT	ORFeom
AT2G39200	MLO12 rev	GAAAGCTGGGTCTCACTTCTTGAACGTAAACTCAGAC	ORFeom
AT2G39880	MYB25 for	GCAGGCTCAGGAATGAACGGAGAAATCTCTCGTCC	ORFeom
AT2G39880	MYB25 rev	GAAAGCTGGGTCTTAGCTCAAAGCCCTTAAATCTTGT	ORFeom
At2g40670	RR16 for	GCAGGCTCAGGAATGAACAGTTCAGGAGGTTCTTGT	ORFeom
At2g40670	RR16 rev	GAAAGCTGGGTCTTAGCTTCTGCAGTTCATGAGA	ORFeom
AT2G40750	WRKY54 for	GCAGGCTCAGGAATGGATTCGAATAGTAACAACACGA	ORFeom
AT2G40750	WRKY54 rev	GAAAGCTGGGTCTCACATAGCACTTGTTCTTTCA	ORFeom
AT2G41310	RR3 for	GCAGGCTCAGGAATGGTAATGGAAACAGAGTCAAAGT	ORFeom
AT2G41310	RR3 rev	GAAAGCTGGGTCTCAGACCGAGGTTGTGATATCA	ORFeom
AT2G41510	CKX1 for	GCAGGCTCAGGAATGGGATTGACCTCATCCTTACG	ORFeom
AT2G41510	CKX1 rev	GAAAGCTGGGTCTTATACAGTTCTAGGTTTCGGCAGT	ORFeom
AT2G42010	PLDBETA1 for	GCAGGCTCAGGAATGGATAATCACGGTCCTCGT	ORFeom
AT2G42010	PLDBETA1 rev	GAAAGCTGGGTCTCAAATGGTTAGATTCTCTTGTATGGC	ORFeom
At2g42430	LBD16 for	GCAGGCTCAGGAATGGCATCTTCCGGTAACGG	ORFeom
At2g42430	LBD16 rev	GAAAGCTGGGTCTTAGTTCTTCATCATTCTAAGAGCCA	ORFeom
AT2G43840	UGT74F1 for	GCAGGCTCAGGAATGGAGAAGATGAGAGGACATGT	ORFeom
AT2G43840	UGT74F1 rev	GAAAGCTGGGTCTTATTTGATTTGAATTTTTGATACA	ORFeom
AT2G44110	MLO15 for	GCAGGCTCAGGAATGGCGGGAGGAGGAACG	ORFeom
AT2G44110	MLO15 rev	GAAAGCTGGGTCTTAATCATGGTGAGCAATCTCTGA	ORFeom
AT2G44810	DAD1 for	GCAGGCTCAGGAATGGAGTATCAGGGGCTTCA	ORFeom
AT2G44810	DAD1 rev	GAAAGCTGGGTCTCATCTATGGAGAACTCTCCGAG	ORFeom
At2g44840	ERF13 for	GCAGGCTCAGGAATGAGCTCATCTGATTCCGT	ORFeom
At2g44840	ERF13 rev	GAAAGCTGGGTCTTAATACAGCAAAACTCGTTGGACA	ORFeom
AT2G44910	HB4 for	GCAGGCTCAGGAATGGGGGAAAGAGATGATGGG	ORFeom
AT2G44910	HB4 rev	GAAAGCTGGGTCCTAGCGACCTGATTTTTGCTGG	ORFeom
At2g45150	CDS4 for	GCAGGCTCAGGAATGGCGACTTTTGCTGAACT	ORFeom
At2g45150	CDS4 rev	GAAAGCTGGGTCTCAAACTCCGTAAAGTTTTAGGGA	ORFeom
At2g45160	HAM1 for	GCAGGCTCAGGAATGCCCTTATCCTTTGAAAGGT	ORFeom
At2g45160	HAM1 rev	GAAAGCTGGGTCCTAACATTTCCAAGCAGAGACAGT	ORFeom
At2g46070	MPK12 for	GCAGGCTCAGGAATGTCTGGAGAATCAAGCTCTGG	ORFeom
At2g46070	MPK12 rev	GAAAGCTGGGTCTCAGTGGTCAGGATTGAATTTGAC	ORFeom
AT2G46530	ARF11 for	GCAGGCTCAGGAATGAGCCAAACAAGCTTAGAGC	ORFeom
AT2G46530	ARF11 rev	GAAAGCTGGGTCTTAAACGTGAACTGTCCTCTGA	ORFeom
At2g46790	PRR9 for	GCAGGCTCAGGAATGGATCAGTTGCGTGATGA	ORFeom
At2g46790	PRR9 rev	GAAAGCTGGGTCTTAGCTGAGAAGAAGAAGCCA	ORFeom
AT2G46990	IAA20 for	GCAGGCTCAGGAATGGGAAGAGGGAGAAGT	ORFeom
AT2G46990	IAA20 for	GCAGGCTCAGGAATGGGAAGAGGGAGAAGT	ORFeom
AT2G46990	IAA20 rev	GAAAGCTGGGTCTCAGTAGTGGTAATTAGC	ORFeom
AT2G46990	IAA20 rev	GAAAGCTGGGTCTCAGTAGTGGTAATTAGC	ORFeom
AT2G47000	ABCB4 for	GCAGGCTCAGGAATGGCTTCAGAGAGCGGCTT	ORFeom
AT2G47000	ABCB4 rev	GAAAGCTGGGTCTCAAGAAGCCGCGGTTAGAT	ORFeom
At2g47190	MYB2 for	GCAGGCTCAGGAATGGAAGATTACGAGCGAAT	ORFeom
At2g47190	MYB2 rev	GAAAGCTGGGTCTTAATTATACGAATACGATGTCGT	ORFeom
At2g47240	LACS1 for	GCAGGCTCAGGAATGAAGTCTTTTGCGGCTAAGG	ORFeom
At2g47240	LACS1 rev	GAAAGCTGGGTCTCAGATTTTCTTTGAGGCCA	ORFeom
AT2G47430	CKI1 for	GCAGGCTCAGGAATGATGGTGAAAGTTACAAAGCTTGT	ORFeom
AT2G47430	CKI1 rev	GAAAGCTGGGTCCTAGTGACGTTTGCTTTCGA	ORFeom
At3g01040	GAUT13 for	GCAGGCTCAGGAATGCAGCTTCACATATCGCCT	ORFeom
At3g01040	GAUT13 rev	GAAAGCTGGGTCCTATTCCAAGATATGACAATTCT	ORFeom
AT3G01080	WRKY58 for	GCAGGCTCAGGAATGGCGGTTGAAGACGATGT	ORFeom
AT3G01080	WRKY58 rev	GAAAGCTGGGTCTCAAATTGTGATTTTCTCTTCTTTCA	ORFeom
AT3G01510	LSF1 for	GCAGGCTCAGGAATGGCGTTTCTTCAACAAATCTCC	ORFeom
AT3G01510	LSF1 rev	GAAAGCTGGGTCCTACGACTTTGGGCATAGTCT	ORFeom
AT3G02410	ICME-LIKE2 for	GCAGGCTCAGGAATGCAGTTGTCTCCGGAACG	ORFeom
AT3G02410	ICME-LIKE2 rev	GAAAGCTGGGTCTCAAAAAGGGCTGACCCTGC	ORFeom
At3g02610	for	GCAGGCTCAGGAATGGCTCTTCTCTTGAACTCGA	ORFeom
At3g02610	rev	GAAAGCTGGGTCTTATAGTTCAACTTCTCTCCCA	ORFeom
AT3G02620	for	GCAGGCTCAGGAATGGCTCTGCTCTTGAACTCG	ORFeom
AT3G02620	rev	GAAAGCTGGGTCTTAGAGTTCAACTTCTCTCCCGT	ORFeom
AT3G03540	NPC5 for	GCAGGCTCAGGAATGGCCGAGACGAAAAAAGG	ORFeom
AT3G03540	NPC5 rev	GAAAGCTGGGTCTTAATTTGACCAAGGAGTAGCATGTG	ORFeom
AT3g03740	BPM4 for	GCAGGCTCAGGAATGAAATCTGTCATTTTCACAGAGGA	ORFeom
AT3g03740	BPM4 rev	GAAAGCTGGGTCTCAATCTTCTAGTTCTGCCATTGG	ORFeom
AT3G04280	RR22 for	GCAGGCTCAGGAATGGCAACAAAATCCACCGG	ORFeom
AT3G04280	RR22 rev	GAAAGCTGGGTCTCAAGCATCGAAGAGGTGGC	ORFeom
AT3G04580	EIN4 for	GCAGGCTCAGGAATGTTAAGATCTTTAGGTCTTGGA	ORFeom
AT3G04580	EIN4 rev	GAAAGCTGGGTCTCACTCGCTCGCGGTCTG	ORFeom
AT3G04730	IAA16 for	GCAGGCTCAGGAATGATTAATTTTGAGGCC	ORFeom
AT3G04730	IAA16 for	GCAGGCTCAGGAATGATTAATTTTGAGGCC	ORFeom
AT3G04730	IAA16 for	GCAGGCTCAGGAATGATTAATTTTGAGGCC	ORFeom
AT3G04730	IAA16 rev	GAAAGCTGGGTCTCAACTTCTGTTCTTGCA	ORFeom
AT3G04730	IAA16 rev	GAAAGCTGGGTCTCAACTTCTGTTCTTGCA	ORFeom
AT3G04730	IAA16 rev	GAAAGCTGGGTCTCAACTTCTGTTCTTGCA	ORFeom
AT3G06860	MFP2 for	GCAGGCTCAGGAATGGATTCACGAACCAAGGGG	ORFeom
AT3G06860	MFP2 rev	GAAAGCTGGGTCTTACAACCGTGAGCTGGCTT	ORFeom
AT3G09100	for	GCAGGCTCAGGAATGGTTGCTACGATGGACTT	ORFeom
AT3G09100	rev	GAAAGCTGGGTCTCATCTGCGGCGCGCAGCTT	ORFeom
AT3G09990	for	GCAGGCTCAGGAATGGATACTAGCATTCTAGCTGTGA	ORFeom
AT3G09990	rev	GAAAGCTGGGTCTTACCAATCTTTACCAACTAACCA	ORFeom
AT3G10550	MTM1 for	GCAGGCTCAGGAATGACGCCGCCGAGACCA	ORFeom
AT3G10550	MTM1 rev	GAAAGCTGGGTCTCATTTAGGTTGGAAATAGCTATCGT	ORFeom
At3g10940	LSF2 for	GCAGGCTCAGGAATGAGTGTGATTGGAAGCAAGAG	ORFeom
At3g10940	LSF2 rev	GAAAGCTGGGTCTCAGGTTCCACGGAGGGC	ORFeom
AT3G11480	BSMT1 for	GCAGGCTCAGGAATGGATCCAAGATTCATCAACACC	ORFeom
AT3G11480	BSMT1 rev	GAAAGCTGGGTCTTACTTCTTAGTCAAGGAAACGACA	ORFeom
At3g11580	for	GCAGGCTCAGGAATGTCAGTCAACCATTACCACA	ORFeom
At3g11580	rev	GAAAGCTGGGTCTCATCTATTTTTATGAAAAAGACA	ORFeom

Table 4.4 continued from previous page

Locus ID	Name	Sequence	Use
AT3G11980	MS2 for	GCAGGCTCAGGAATGGAGGCTCTCTTCTTGAGT	ORFeom
AT3G11980	MS2 rev	GAAAGCTGGGTCTTAAGCTCTTCCTTTCAAGACATGC	ORFeom
At3g12250	TGA6 for	GCAGGCTCAGGAATGGCTGATACCAGTTCAAGGA	ORFeom
At3g12250	TGA6 rev	GAAAGCTGGGTCTCACTCTCTTGGCCGGGC	ORFeom
AT3G13380	BRL3 for	GCAGGCTCAGGAATGAAACAACAATGGCAGTTCT	ORFeom
AT3G13380	BRL3 rev	GAAAGCTGGGTCTTAAGGCTCCTTATCTCGTGA	ORFeom
At3g13540	MYB5 for	GCAGGCTCAGGAATGGAGTCAATGAAGATGAAGCT	ORFeom
At3g13540	MYB5 rev	GAAAGCTGGGTCTTAACAAAAAGCTCATGCCA	ORFeom
AT3g13920	EIF4A1 for	GCAGGCTCAGGAATGGCAGGATCTGCACCAG	ORFeom
AT3g13920	EIF4A1 rev	GAAAGCTGGGTCTCACAGCAGATCGGCCAC	ORFeom
AT3G14440	NCED3 for	GCAGGCTCAGGAATGGCTTCTTTCACGGCAAC	ORFeom
AT3G14440	NCED3 rev	GAAAGCTGGGTCTCACACGACCTGCTTCGC	ORFeom
AT3G15356	for	GCAGGCTCAGGAATGCAGATTCACAAACTCTGT	ORFeom
AT3G15356	rev	GAAAGCTGGGTCTTAGTTTTCAAACGACCAGCTCC	ORFeom
AT3G15540	IAA19 for	GCAGGCTCAGGAATGGAGAAGGAAGGACTC	ORFeom
AT3G15540	IAA19 rev	GAAAGCTGGGTCTCATCACTCGTCTACTCCTCT	ORFeom
AT3G16500	PAP1 for	GCAGGCTCAGGAATGGAAGGTTGTCCAAGA	ORFeom
AT3G16500	IAA26 for	GCAGGCTCAGGAATGGAAGGTTGTCCAAGA	ORFeom
AT3G16500	PAP1 rev	GAAAGCTGGGTCTCAGTGCATCATCTTCTC	ORFeom
AT3G16500	IAA26 rev	GAAAGCTGGGTCTCAGTGCATCATCTTCTC	ORFeom
AT3G17010	REM22 for	GCAGGCTCAGGAATGGGTAAGAGTAGTAACATAGT	ORFeom
AT3G17010	REM22 rev	GAAAGCTGGGTCTCAATCGATCATGCACTGATCCA	ORFeom
AT3G17600	IAA31 for	GCAGGCTCAGGAATGGAGGTCTCTAACTCT	ORFeom
AT3G17600	IAA31 for	GCAGGCTCAGGAATGGAGGTCTCTAACTCT	ORFeom
AT3G17600	IAA31 rev	GAAAGCTGGGTCTTAATACCTCTCCGGTCT	ORFeom
AT3G17600	IAA31 rev	GAAAGCTGGGTCTTAATACCTCTCCGGTCT	ORFeom
At3g18990	VRN1 for	GCAGGCTCAGGAATGCCACGCCCTTTCTTCC	ORFeom
At3g18990	VRN1 rev	GAAAGCTGGGTCTCAGACGTACTCGTTGACTCG	ORFeom
AT3G19160	IPT8 for	GCAGGCTCAGGAATGCAAAATCTTACGTCCACA	ORFeom
AT3G19160	IPT8 rev	GAAAGCTGGGTCTCACACTTTGTCTTTCACCAAGA	ORFeom
AT3G19270	CYP707A4 for	GCAGGCTCAGGAATGGCTGAAATTTGGTTCTTGGT	ORFeom
AT3G19270	CYP707A4 rev	GAAAGCTGGGTCCTAAAGAGAATGTCGACGAAATGT	ORFeom
At3g19770	VPS9A for	GCAGGCTCAGGAATGGAGAATACGGACGTCTTCT	ORFeom
At3g19770	VPS9A rev	GAAAGCTGGGTCTTAAGACTCTCATCACCAAGATGGG	ORFeom
AT3G22980	for	GCAGGCTCAGGAATGGATGAATCTGAAGGTAGGA	ORFeom
AT3G22980	rev	GAAAGCTGGGTCTCAAACTTTACGAGCCAAGGT	ORFeom
At3g23000	CIPK7 for	GCAGGCTCAGGAATGGAATCACTTCCCCAGCC	ORFeom
At3g23000	CIPK7 rev	GAAAGCTGGGTCTTACATGATGTCATTGTGCCATGA	ORFeom
AT3G23030	IAA2 for	GCAGGCTCAGGAATGGCGTACGAGAAAGTC	ORFeom
AT3G23030	IAA2 for	GCAGGCTCAGGAATGGCGTACGAGAAAGTC	ORFeom
AT3G23030	IAA2 rev	GAAAGCTGGGTCTCATAAGGAAGAGTCTAG	ORFeom
AT3G23030	IAA2 rev	GAAAGCTGGGTCTCATAAGGAAGAGTCTAG	ORFeom
At3g23140	URO for	GCAGGCTCAGGAATGAACCACCGGGACAAACA	ORFeom
At3g23140	URO rev	GAAAGCTGGGTCTTAATGATGACGATGACCGCC	ORFeom
AT3G23610	DSPTP1 for	GCAGGCTCAGGAATGAGTTCTAGAGACAGAGGATCAC	ORFeom
AT3G23610	DSPTP1 rev	GAAAGCTGGGTCTCAATGATCTTCACGCCTGACA	ORFeom
AT3G23770	for	GCAGGCTCAGGAATGACTCCTTTTGCTCTGTTCCT	ORFeom
AT3G23770	rev	GAAAGCTGGGTCTCACAATGTAACGCTAGGAAACT	ORFeom
AT3G24650	ABI3 for	GCAGGCTCAGGAATGAAAAGCTTGCATGTGGCG	ORFeom
AT3G24650	ABI3 rev	GAAAGCTGGGTCTCATTTAACAGTTTGAGAAGTTGGTGA	ORFeom
At3g25890	CRF11 for	GCAGGCTCAGGAATGGCTGAACGAAAGAAACGC	ORFeom
At3g25890	CRF11 rev	GAAAGCTGGGTCTTATGGGCACGCGATATTAAGAG	ORFeom
AT3G27140	for	GCAGGCTCAGGAATGGAGGATCGGTTCTCCAC	ORFeom
AT3G27140	rev	GAAAGCTGGGTCTCATCGCTTGTCTTCTTCAA	ORFeom
At3g27310	PUX1 for	GCAGGCTCAGGAATGTTTGTTGATGACCCTTCTCT	ORFeom
At3g27310	PUX1 rev	GAAAGCTGGGTCTCACATTTTAAACCACTTAGGCT	ORFeom
At3g27670	RST1 for	GCAGGCTCAGGAATGGCGAATGTGGATCGTGA	ORFeom
At3g27670	RST1 rev	GAAAGCTGGGTCCTACATTTATCGCGTTTCCAACTGA	ORFeom
AT3G29020	MYB110 for	GCAGGCTCAGGAATGAAGATGGATTTTTCATGTTTCCA	ORFeom
AT3G29020	MYB110 rev	GAAAGCTGGGTCTTAGTGACCAACTCCTAGAA	ORFeom
AT3G29030	EXPA5 for	GCAGGCTCAGGAATGGGAGTTTTAGTAATCTCGCT	ORFeom
AT3G29030	EXPA5 rev	GAAAGCTGGGTCTTAATACCGAAACTGCCCTCCG	ORFeom
AT3G43300	ATMIN7 for	GCAGGCTCAGGAATGGCGGCTGGTGGATTTTT	ORFeom
AT3G43300	ATMIN7 rev	GAAAGCTGGGTCTTACTGTTGCAAAAGTGGCTTCA	ORFeom
At3g43700	BPM6 for	GCAGGCTCAGGAATGTCAAAGCTAATGACCAGAACC	ORFeom
At3g43700	BPM6 rev	GAAAGCTGGGTCCTAAGTGGTTCGCTGCCTGA	ORFeom
At3g44540	FAR4 for	GCAGGCTCAGGAATGGACTCCAATTGCATTCAGT	ORFeom
At3g44540	FAR4 rev	GAAAGCTGGGTCTCAACCGCAGTTTCTCAGTA	ORFeom
AT3G44550	FAR5 for	GCAGGCTCAGGAATGGAACTCAATTGTGTTCA	ORFeom
AT3G44550	FAR5 rev	GAAAGCTGGGTCTCACTTCTTAAGCACGTGTGTG	ORFeom
AT3G44560	FAR8 for	GCAGGCTCAGGAATGGAATTCAGTTGTGTTCA	ORFeom
AT3G44560	FAR8 rev	GAAAGCTGGGTCTTACTTCTTAAGCACGTGAGTGA	ORFeom
AT3G44730	KP1 for	GCAGGCTCAGGAATGGACCAAGGCGCGATG	ORFeom
AT3G44730	KP1 rev	GAAAGCTGGGTCCTATGGTACCATGAACCTTGCA	ORFeom
AT3G45140	LOX2 for	GCAGGCTCAGGAATGTATTGTAGAGAGTCCTTGTCGA	ORFeom
AT3G45140	LOX2 rev	GAAAGCTGGGTCTCAAATAGAAATACTATAAGGAACACC	ORFeom
AT3G45290	MLO3 for	GCAGGCTCAGGAATGACGGATAAAGAAGAAAGCAACC	ORFeom
AT3G45290	MLO3 rev	GAAAGCTGGGTCTCACCTTTCAGTTTTCTCTTGT	ORFeom
AT3G46600	for	GCAGGCTCAGGAATGGATGCTATTTTGCCAGTACC	ORFeom
AT3G46600	rev	GAAAGCTGGGTCTTACTTCTTAGCAGGTTTCCAGCA	ORFeom
At3g48100	RR5 for	GCAGGCTCAGGAATGGCTGAGGTTTTGCGTCC	ORFeom
At3g48100	RR5 rev	GAAAGCTGGGTCTTAAAGCCGAAAGAATCAGGACA	ORFeom
AT3G48430	REF6 for	GCAGGCTCAGGAATGGCGGTTTCAGAGCAGAG	ORFeom
AT3G48430	REF6 rev	GAAAGCTGGGTCTCACCTTTTGTTGGTCTTCT	ORFeom
AT3G49700	ACS9 for	GCAGGCTCAGGAATGAAACAACTGTCGAGAAAAGTGA	ORFeom
AT3G49700	ACS9 rev	GAAAGCTGGGTCTCATCGTTCATCAGGTACACGG	ORFeom
AT3G50280	for	GCAGGCTCAGGAATGGCCGACGTAACTTTTATTTCC	ORFeom
AT3G50280	rev	GAAAGCTGGGTCCTAGCCACACTTCTCCAGAA	ORFeom
At3g51060	STY1 for	GCAGGCTCAGGAATGGCGGGGTTTTTCTCGC	ORFeom
At3g51060	STY1 rev	GAAAGCTGGGTCTCACACGCACGCACCTAAC	ORFeom

Table 4.4 continued from previous page

Locus ID	Name	Sequence	Use
AT3G51770	ETO1 for	GCAGGCTCAGGAATGCAGCATAATCTCTTCACAACA	ORFeom
AT3G51770	ETO1 rev	GAAAGCTGGGTCCTACTTTTGGTCGTTTGGTTCAC	ORFeom
AT3G52430	PAD4 for	GCAGGCTCAGGAATGGACGATTGTCGATTCGAGA	ORFeom
AT3G52430	PAD4 rev	GAAAGCTGGGTCCTAAGTCTCCATTGCGTCACTCT	ORFeom
AT3G53250	for	GCAGGCTCAGGAATGAAGAGCAAATCCATAGTTCTACC	ORFeom
AT3G53250	rev	GAAAGCTGGGTCTTACATGCCAATGCAGTTTCTCT	ORFeom
At3g54720	AMP1 for	GCAGGCTCAGGAATGTCACAACCTCTCACCACC	ORFeom
At3g54720	AMP1 rev	GAAAGCTGGGTCTCATGTGAAACCTCCTTTAAGAGC	ORFeom
AT3G55270	MKP1 for	GCAGGCTCAGGAATGGTGGGAAGAGAGGATGC	ORFeom
AT3G55270	MKP1 rev	GAAAGCTGGGTCTTATAGCGCGCTCAGCAGTG	ORFeom
AT3G56380	RR17 for	GCAGGCTCAGGAATGAATAAGGGCTGTGGAAGTG	ORFeom
AT3G56380	RR17 rev	GAAAGCTGGGTCTCAGCTTCTGCAATTTAAAAGATGG	ORFeom
AT3G56700	FAR6 for	GCAGGCTCAGGAATGGCTACCACAAATGTCCTCG	ORFeom
AT3G56700	FAR6 rev	GAAAGCTGGGTCTTACTCAGTCTTCTTCTTAGAAAGA	ORFeom
At3g57600	for	GCAGGCTCAGGAATGGAGAAATCATCCTCAATGAAACA	ORFeom
At3g57600	rev	GAAAGCTGGGTCTCAATCTAAGCTTCCGTAGTAGTCC	ORFeom
AT3G60460	DUO1 for	GCAGGCTCAGGAATGGAAGCGAAGAAGGAAGAGA	ORFeom
AT3G60460	DUO1 rev	GAAAGCTGGGTCCTAAGGACTTGGGATTGGATCA	ORFeom
At3g60490	for	GCAGGCTCAGGAATGGGAAAACAAATCAACATAGAGAGT	ORFeom
At3g60490	rev	GAAAGCTGGGTCTTAGTCATTTTGCCAATTAAACGGC	ORFeom
At3g61250	MYB17 for	GCAGGCTCAGGAATGGGAAGAACACCTTGTTGTG	ORFeom
At3g61250	MYB17 rev	GAAAGCTGGGTCCTAGAATTTGGAAACCATGGAAACA	ORFeom
At3g61850	DAG1 for	GCAGGCTCAGGAATGGATGCTACGAAGTGGACTC	ORFeom
At3g61850	DAG1 rev	GAAAGCTGGGTCTCACCATGAAGATCCTCCTGT	ORFeom
AT3G62100	IAA30 for	GCAGGCTCAGGAATGGGAAGAGGGAGAAGC	ORFeom
AT3G62100	IAA30 for	GCAGGCTCAGGAATGGGAAGAGGGAGAAGC	ORFeom
AT3G62100	IAA30 rev	GAAAGCTGGGTCTCAGTAGTGATAAGCTCT	ORFeom
AT3G62100	IAA30 rev	GAAAGCTGGGTCTCAGTAGTGATAAGCTCT	ORFeom
AT3G62340	WRKY68 for	GCAGGCTCAGGAATGGAAAATGTTGGTGTTGGGA	ORFeom
AT3G62340	WRKY68 rev	GAAAGCTGGGTCCTAATACTCTTCCTTAATGATATGAGA	ORFeom
AT3G63010	GID1B for	GCAGGCTCAGGAATGGCTGGTGGTAACGAAGT	ORFeom
AT3G63010	GID1B rev	GAAAGCTGGGTCCTAAGGAGTAAGAAGCACAGGACT	ORFeom
AT4G00240	PLDBETA2 for	GCAGGCTCAGGAATGGAGAATTATGGTTGGAATTACCC	ORFeom
AT4G00240	PLDBETA2 rev	GAAAGCTGGGTCTTAGATAGTGAGATTCTCCTGTATGGC	ORFeom
AT4G00540	MYB3R2 for	GCAGGCTCAGGAATGACAGAGTCTATTGATTTAAATCGA	ORFeom
AT4G00540	MYB3R2 rev	GAAAGCTGGGTCCTAACGTAACCAAAACGGACGC	ORFeom
AT4G00760	APRR8 for	GCAGGCTCAGGAATGATACGCAAATGCGGATA	ORFeom
AT4G00760	APRR8 rev	GAAAGCTGGGTCTTAAGGTTTAAGCTCTTTGGCGA	ORFeom
At4g02600	MLO1 for	GCAGGCTCAGGAATGGGTCACGGAGGAGAAGG	ORFeom
At4g02600	MLO1 rev	GAAAGCTGGGTCTTAATCCTCTAAATGGAAAAGA	ORFeom
AT4G02780	GA1 for	GCAGGCTCAGGAATGTCTCTTCAGTATCATGTTCT	ORFeom
AT4G02780	GA1 rev	GAAAGCTGGGTCCTAGACTTTTTGAAACAAGACTTTGGA	ORFeom
AT4G03080	BSL1 for	GCAGGCTCAGGAATGGGCTCGAAGCCTTGG	ORFeom
AT4G03080	BSL1 rev	GAAAGCTGGGTCTCAGATGTATGCAAGCGAGCT	ORFeom
AT4G05120	FUR1 for	GCAGGCTCAGGAATGGCGGATAGATATGAGAACCA	ORFeom
AT4G05120	FUR1 rev	GAAAGCTGGGTCTCAAAAGGCATTCTTCTTACCA	ORFeom
AT4G05130	ENT4 for	GCAGGCTCAGGAATGGCGGATGGATACGAGAAC	ORFeom
AT4G05130	ENT4 rev	GAAAGCTGGGTCTCAGAAAGCATATTTCTTGCCA	ORFeom
AT4G05140	for	GCAGGCTCAGGAATGGTGGCTAGGTTCGAGAA	ORFeom
AT4G05140	rev	GAAAGCTGGGTCTCAGAAGGCATTTTTCTTACCA	ORFeom
AT4G09570	CPK4 for	GCAGGCTCAGGAATGGAGAAACCAAACCCTAGAAGA	ORFeom
AT4G09570	CPK4 rev	GAAAGCTGGGTCTTACTTTGGTGAATCATCAGA	ORFeom
At4g11030	for	GCAGGCTCAGGAATGACGTCGCAGAAAAGATTCA	ORFeom
At4g11030	rev	GAAAGCTGGGTCTTACTGTCCGGAAGCTAGACT	ORFeom
AT4G11830	PLDGAMMA2 for	GCAGGCTCAGGAATGTCAATGGGAGGAGGGTC	ORFeom
AT4G11830	PLDGAMMA2 rev	GAAAGCTGGGTCTCAGATGGTGAGGTTTTCTTGT	ORFeom
At4g11850	PLDGAMMA1 for	GCAGGCTCAGGAATGGCGTATCATCCGGCTTA	ORFeom
At4g11850	PLDGAMMA1 rev	GAAAGCTGGGTCTTACCCTAAAGGCACACTTTCA	ORFeom
AT4G12020	WRKY19 for	GCAGGCTCAGGAATGTCGGAGAAGGAAGAACTTCC	ORFeom
AT4G12020	WRKY19 rev	GAAAGCTGGGTCTCATCCACGGAGGAGCGAAG	ORFeom
AT4G12400	Hop3 for	GCAGGCTCAGGAATGGCGGAAGAAGCAAAATCC	ORFeom
AT4G12400	Hop3 rev	GAAAGCTGGGTCTTACCGGACCTGAACAATTCCG	ORFeom
AT4G14560	IAA1 for	GCAGGCTCAGGAATGGAAGTCACCAATGGG	ORFeom
AT4G14560	IAA1 rev	GAAAGCTGGGTCTCATAAGGCAGTAGGAGC	ORFeom
AT4G14580	CIPK4 for	GCAGGCTCAGGAATGGAATCTCCATATCCAAAATCACC	ORFeom
AT4G14580	CIPK4 rev	GAAAGCTGGGTCTCAATTGTGCCATGAGAGCAC	ORFeom
AT4G154560	IAA1 for	GCAGGCTCAGGAATGGAAGTCACCAATGGG	ORFeom
AT4G154560	IAA1 rev	GAAAGCTGGGTCTCATAAGGCAGTAGGAGC	ORFeom
AT4G15530	PPDK for	GCAGGCTCAGGAATGCTTTATATAAGAAAGAAAATGACA	ORFeom
AT4G15530	PPDK rev	GAAAGCTGGGTCTCATGCAACAACTACTTGAGCA	ORFeom
AT4G15900	PRL1 for	GCAGGCTCAGGAATGCCGGCTCCGACGACG	ORFeom
AT4G15900	PRL1 rev	GAAAGCTGGGTCTTAGAAGCGCCTAATCTCCT	ORFeom
AT4G16280	FCA for	GCAGGCTCAGGAATGAATGGTCCCCCAGATAGAG	ORFeom
AT4G16280	FCA rev	GAAAGCTGGGTCTCAAGCTTTATTCTTCCACATGAGT	ORFeom
AT4G16350	CBL6 for	GCAGGCTCAGGAATGATGATGCAATGTTTA	ORFeom
AT4G16350	CBL6 rev	GAAAGCTGGGTCTCATCCATCCAGCTCACTAGG	ORFeom
AT4G18010	IP5PII for	GCAGGCTCAGGAATGAAAACAAGACGTGGGAAACG	ORFeom
AT4G18010	IP5PII rev	GAAAGCTGGGTCTCAAAAAGAAGGTTCAGGATGAACA	ORFeom
AT4G18130	PHYE for	GCAGGCTCAGGAATGGGATTCGAGAGTTCAAGCT	ORFeom
AT4G18130	PHYE rev	GAAAGCTGGGTCCTACTTTATGCTTGAACTACCCTCTG	ORFeom
AT4G18470	SNI1 for	GCAGGCTCAGGAATGTCGAAAGAGACGAAGGGT	ORFeom
AT4G18470	SNI1 rev	GAAAGCTGGGTCTTAAGCTTTTGCCTTGAGTACCA	ORFeom
AT4G18620	PYL13 for	GCAGGCTCAGGAATGGAAAGTTCTAAGCAA	ORFeom
AT4G18620	PYL13 rev	GAAAGCTGGGTCTCATTACTTCATCATTTTCTT	ORFeom
AT4G18710	BIN2 for	GCAGGCTCAGGAATGGCTGATGATAAGGAG	ORFeom
At4g18710	BIN2 for	GCAGGCTCAGGAATGGCTGATGATAAGGAGATGCC	ORFeom
AT4G18710	BIN2 rev	GAAAGCTGGGTCTCAAGTTCCAGATTGATTCAA	ORFeom
At4g18710	BIN2 rev	GAAAGCTGGGTCTTAAGTTCCAGATTGATTCAAGAAGCT	ORFeom
AT4G19850	PP2-A2 for	GCAGGCTCAGGAATGGGAATAATATGGTCTATCTTCTCA	ORFeom
AT4G19850	PP2-A2 rev	GAAAGCTGGGTCTCATGCCTCGTGTACATAAATCA	ORFeom

Table 4.4 continued from previous page

Locus ID	Name	Sequence	Use
AT4G21200	GA2OX8 for	GCAGGCTCAGGAATGGATCCACCATTCAACGA	ORFeom
AT4G21200	GA2OX8 rev	GAAAGCTGGGTCTTAGTAGACGTGATTAAGGAACCT	ORFeom
AT4G21550	VAL3 for	GCAGGCTCAGGAATGCTTTCCTCTTCATCCATGTC	ORFeom
AT4G21550	VAL3 rev	GAAAGCTGGGTCCTACATGGAGCTTGTGGTGGT	ORFeom
AT4G21690	GA3OX3 for	GCAGGCTCAGGAATGAGCTCTGTCACACAGCT	ORFeom
AT4G21690	GA3OX3 rev	GAAAGCTGGGTCTCAGCAACGGAACAAAGTCA	ORFeom
AT4G22070	WRKY31 for	GCAGGCTCAGGAATGTTCCGGTTTCCAGTGAGT	ORFeom
AT4G22070	WRKY31 rev	GAAAGCTGGGTCTTATTGCCTACTGTCATTGTTGCT	ORFeom
At4g23750	CRF2 for	GCAGGCTCAGGAATGGAAGCGGAGAAGAAAATGG	ORFeom
At4g23750	CRF2 rev	GAAAGCTGGGTCTTAAACAGCTAAAAGAGGATCCGAC	ORFeom
AT4G23850	LACS4 for	GCAGGCTCAGGAATGTCGCAGCAGAAGAAATACA	ORFeom
AT4G23850	LACS4 rev	GAAAGCTGGGTCCTACCCTCTGGAAGCAAATTTTGC	ORFeom
AT4G23980	ARF9 for	GCAGGCTCAGGAATGGCAAATCGCGGAGGT	ORFeom
AT4G23980	ARF9 for	GCAGGCTCAGGAATGGCAAATCGCGGAGGT	ORFeom
AT4G23980	ARF9 rev	GAAAGCTGGGTCTTAGTTGGAATGATTATC	ORFeom
AT4G23980	ARF9 rev	GAAAGCTGGGTCTTAGTTGGAATGATTATC	ORFeom
AT4G24470	ZIM for	GCAGGCTCAGGAATGTTTGGTCGCCATTCGAT	ORFeom
AT4G24470	ZIM rev	GAAAGCTGGGTCTTAGTGATCACCTAACAGATT	ORFeom
AT4G24650	IPT4 for	GCAGGCTCAGGAATGAAGTGTAATGACAAAATGGTTGTG	ORFeom
AT4G24650	IPT4 rev	GAAAGCTGGGTCCTAGTTAAGACTTAAAAATCTTT	ORFeom
AT4G25500	RS40 for	GCAGGCTCAGGAATGAAGCCAGTCTTCTGTGGG	ORFeom
AT4G25500	RS40 rev	GAAAGCTGGGTCTCACTCGTCAGCTGGTGG	ORFeom
AT4G26420	GAMT1 for	GCAGGCTCAGGAATGGAGTCGTCACGGAGCC	ORFeom
AT4G26420	GAMT1 rev	GAAAGCTGGGTCTTAAACCCTAACCGCTGAAACAG	ORFeom
AT4G26770	for	GCAGGCTCAGGAATGGCAATGGAGAAAGATCTCAGT	ORFeom
AT4G26770	rev	GAAAGCTGGGTCTTAAAACCTCCCTTGCAACT	ORFeom
AT4G26930	MYB97 for	GCAGGCTCAGGAATGATCGTGTACGGTGGGGG	ORFeom
AT4G26930	MYB97 rev	GAAAGCTGGGTCCTAGCAGATCCCTGGCAAGT	ORFeom
At4g27950	CRF4 for	GCAGGCTCAGGAATGATGATGGATGAGTTTATGGA	ORFeom
At4g27950	CRF4 rev	GAAAGCTGGGTCTCACACAAGTAAGAGATCGGA	ORFeom
AT4G28395	A7 for	GCAGGCTCAGGAATGCATAATAAACTCCACCT	ORFeom
AT4G28395	A7 rev	GAAAGCTGGGTCTTAATTTAATTTCTCAACGTCGGGA	ORFeom
AT4G28640	IAA11 for	GCAGGCTCAGGAATGGAAGGCGGTTCCGCT	ORFeom
AT4G28640	IAA11 for	GCAGGCTCAGGAATGGAAGGCGGTTCCGCT	ORFeom
AT4G28640	IAA11 for	GCAGGCTCAGGAATGGAAGGCGGTTCCGCT	ORFeom
AT4G28640	IAA11 rev	GAAAGCTGGGTCTTACAAAGAGAACATATA	ORFeom
AT4G28640	IAA11 rev	GAAAGCTGGGTCTTACAAAGAGAACATATA	ORFeom
AT4G28640	IAA11 rev	GAAAGCTGGGTCTTACAAAGAGAACATATA	ORFeom
AT4G29080	PAP2 for	GCAGGCTCAGGAATGTCTGTATCTGTAGCA	ORFeom
AT4G29080	PAP2 for	GCAGGCTCAGGAATGTCTGTATCTGTAGCA	ORFeom
AT4G29080	IAA27 for	GCAGGCTCAGGAATGTCTGTATCTGTAGCA	ORFeom
AT4G29080	PAP2 rev	GAAAGCTGGGTCCTAGTTCCTGCTTCTGCA	ORFeom
AT4G29080	PAP2 rev	GAAAGCTGGGTCCTAGTTCCTGCTTCTGCA	ORFeom
AT4G29080	IAA27 rev	GAAAGCTGGGTCCTAGTTCCTGCTTCTGCA	ORFeom
AT4G30080	ARF16 for	GCAGGCTCAGGAATGATAAATGTGATGAAT	ORFeom
AT4G30080	ARF16 for	GCAGGCTCAGGAATGATAAATGTGATGAAT	ORFeom
AT4G30080	ARF16 rev	GAAAGCTGGGTCTTATACTACAACGCTCTC	ORFeom
AT4G30080	ARF16 rev	GAAAGCTGGGTCTTATACTACAACGCTCTC	ORFeom
AT4G32010	HSL1 for	GCAGGCTCAGGAATGGAGTCAATAAAGGTTTGCATGA	ORFeom
AT4G32010	HSL1 rev	GAAAGCTGGGTCTTAGTTCACAGGATCATGAGCTCC	ORFeom
AT4G32180	PANK2 for	GCAGGCTCAGGAATGGCGGGTCAAGAGGATGA	ORFeom
AT4G32180	PANK2 rev	GAAAGCTGGGTCTTAAAGCGAGGGAGGCTCGT	ORFeom
AT4G32285	for	GCAGGCTCAGGAATGGCGCTAAGCATGCGAAA	ORFeom
AT4G32285	rev	GAAAGCTGGGTCTCAGTAAGGGTTGTTGTAGT	ORFeom
AT4G33790	CER4 for	GCAGGCTCAGGAATGTCGACAGAAATGGAGGTCG	ORFeom
AT4G33790	CER4 rev	GAAAGCTGGGTCTTAGAAGACATACTTAAGCAGCCCA	ORFeom
At4g34990	MYB32 for	GCAGGCTCAGGAATGGGAAGGTCTCCTTGCTG	ORFeom
At4g34990	MYB32 rev	GAAAGCTGGGTCTCATTTCATTTCCAAAGTGCT	ORFeom
At4g35230	BSK1 for	GCAGGCTCAGGAATGGGTTGTTGTCAATCCTTGT	ORFeom
At4g35230	BSK1 rev	GAAAGCTGGGTCTCAAGATCCTCTGCCGCCTC	ORFeom
AT4G36380	ROT3 for	GCAGGCTCAGGAATGCAACCTCCGGCAAGC	ORFeom
AT4G36380	ROT3 rev	GAAAGCTGGGTCTTAATGATCTTCAAGTGAGATCGGAGA	ORFeom
At4g36450	MPK14 for	GCAGGCTCAGGAATGGCGATGCTAGTTGATCCT	ORFeom
At4g36450	MPK14 rev	GAAAGCTGGGTCTTAAGCTCGGGGGAGGTAATG	ORFeom
At4g36900	RAP2.10 for	GCAGGCTCAGGAATGGAGACGGCGACTGAAGT	ORFeom
At4g36900	RAP2.10 rev	GAAAGCTGGGTCCTAATCGTCATCTGAAGTTTCCGG	ORFeom

4.2 Methods

4.2.1 PhyhormORFeome selection and cloning strategy

For the PhyHormORFeome collection all ORFs were collected, which have genetic evidence to be involved in phytohormone signaling. Additionally, complete gene families were included, if they were found to be enriched. In total 1216 ORFs were selected, of those 688 ORFs were picked from the AtORFeome collection [419], 276 ORFs were obtained from ABRC, 11 ORFs were derived from experts and 277 ORFs (253 ORFs from the 1. set, 24 ORFs from the 2. set) were amplified from Col-0 cDNA-mix prepared from tissue specific cDNAs. All ORFs include a stop codon and were cloned by using the Gateway system (*https : //www.thermofisher.com/de/de/home/life − science/cloning/gateway − cloning/protocols.html*) in a Gateway entry plasmid followed by subsequent Sanger sequencing to verify ORF sequences. Correct clones were cloned into destination plasmids via LR- Gateway cloning and yeast transformed according to Altmann et al., 2018 [293].

4.2.2 Tissue separation for total RNA extraction

All RNA samples are collected from *Arabidopsis thaliana* ecotype Col-0. RNA extraction were done using the Macherey & Nagel NucleoSpin RNA kit. For flower RNA all developmental stages of flowers were selected, whereby ORFs expressed only in pollen or inflorescence were amplified from the resulting flower cDNA. For seed RNA, dry seeds were imbibed for 3-5 days in the dark dark 4°C before harvest. For seedling RNA, seedlings were grown on full MS media, stratified for 3 days in 4°C in the dark and grown in LD light conditions (16/8h) in 21°C for 6-10 days. The complete seedlings were used for RNA extraction. For leaf RNA, cauline leaves and rosette leaves (including petiole) were separately collected from all developmental stages. The resulting two cDNAs were combined in one mixture of ration 1:1 and used as leaf cDNA. For node RNA, node sections from 3-8 weeks old plants were selected. For internode RNA, internode sections from 3-8 weeks old plants were used. For root RNA, seeds were stratified for 3 days in 4°C in the dark and grown on full MS media in LD light conditions (16/8h) in 21°C for 15 days on plates containing 0.8 % agarose in vertical orientation. For silique RNA, siliques from all developmental stages were collected. All plan samples were quick frozen in liquid nitrogen and stored at −80°C.

4.2.3 RNA extraction

For the RNA extraction, several methods like phenol-chloroform, trizol-chloroform and commercially available kit for RNA extraction were tested. The phenol-chloroform or trizol-chloroform RNA extraction yielded in larger amounts of RNA, but the quality of the resulting cDNA was less useful to amplify the ORFs of interest. Therefore, commercially available RNA extraction kits were used following the manufacturers recommendations. Total mRNA was used to generate tissue specific cDNA.

4.2.4 cDNA synthesis for ORF amplification

For cDNA synthesis, 1 μg total RNA was used per cDNA synthesis. 1 μg RNA (in an maximum volume of 5 μl) was mixed with 1,25 μl (0.2 μg/ μl) random primer (LIFE Technologies cat. number SO142) and 0.5 μl (50 μM) oligo d(T)16 primer. Then a heating

step in the thermal cycler with 5 minutes at 70°C followed by 10 minutes at 21°C was performed. In a separate tube 6.625 µl RNAse free water, 5 µl SuperScript III (SS III) buffer (250 mM Tris-HCl (pH 8.3 at room temperature), 375 mM KCl, 15 mM MgCl2), 2.5 µl 2 µM dNTPs, 2.5 µl 0.1 M DTT , 10 U RNase OUT Recombinant Ribonuclease Inhibitor (40 U/ µl) and 250 U SuperScript III (SS III) (200 U/ µl) (Thermo Fisher Cat. no. 18080) were mixed and transferred into the RNA containing tube. The following thermal cycler program runs again 10 minutes at 21°C followed by 120 minutes at 42°C. After the 42°C step, the PCR program was stopped and an additional volume of 250 U SSIII was added and then placed back into the cycler. The last cycler step consists of 30 minutes at 55°C followed by heating step for 15 minutes at 70°C before cooling down. The cDNAs were stored at −20°C.

4.2.5 cDNA synthesis for quantitative real time PCR

After RNA extraction the concentration were measured for the different RNAs and 1 µg were used per cDNA synthesis. For each sample 1 µg of total RNA were mixed with 1 µl (0.5 µg/ µl) oligo dT18 (LIFE Technologies cat. number SO123) and 1 µl (0.2 µg/ µl) random primer (LIFE Technologies cat. number SO142) in a PCR tube and add with DEPC water to 11.75 µl total volume. After mixing the tubes are transferred into the thermal cycler for a heating step for 5 minutes at 65°C, thereafter directly back on ice. In a separate tube 4 µl 5x M-MuLV RT-buffer (50 mM Tris-HCl, 75 mM KCl, 3 mM MgCl2, 10 mM DTT), 10 U RNase OUT Recombinant Ribonuclease Inhibitor (40 U/ µl (Life technology cat. no. 10777-019), 2 µl dNTPs and 400 U M-MuLV Reverse Transcriptase (200U/ µl) (Biozym cat. number 350400201) were mixed and add to each sample. This mixture is prepared as master mix for several samples. Then the tube is placed back into the thermal cycler with 10 minutes at 25°C, followed by 60 minutes at 37°C and enzyme inactivation for 10 minutes at 70°C.

4.2.6 Quantitative real time PCR protocol

Quantitative real time PCR (qRT-PCR) was performed in 384 well-plates with 4 biological and for each 4 technical replicates. For qRT-PCR the cDNAs were diluted 1:5 for final cDNA concentration of about 10 ng/ µl. For the 4 technical replicates of one biological replicate one mix is prepared, consisting of 18 µl SYBR green (Bio-Rad cat. number 1708880), 7.2 µl of a 2 µM primer mix and 8 µl DEPC water. For each biological replicate once 2.8 µl cDNA were added to the mix before pipetting 8 µl per well into a 384 well plate. qRT-PCR were performed using CFX384 Real-Time System Cycler from BioRad. The relative quantification was calculated according to Pfaffl et al., 2001 [622] using *ACTIN8* as reference gene. Significance was calculated using a two-sided t-test.

4.2.7 Genomic DNA extraction

For genotyping of the different T-DNA lines, genomic DNA were extracted using an extraction protocol from Edwards [623]. 150 ng of genomic DNA were used for each PCR reaction. The primers were designed specifically for each T-DNA line and were used in combination with the respective LB primer from SALK, SAIL, WiscDsLox or GabiKat lines.

4.2.8 Gene-amplification with Nested-PCR

For the gene amplification 150 ng of cDNA (specific or later on mixed one) were used for each PCR. As polymerase the KOD Hot Start DNA Polymerase (Merck cat. number 71086) with 0.5 U/ μl per reaction was used. The specific primer had a concentration of 2 μM, which were used for the first PCR, the second primers contains the complete attB site and were used with of 0.66 μM concentration. A dilution (1:10) of the first PCR is used as template for the second PCR (3 μl per reaction). The thermal-cycler program is based on the KOD manual and differs between the first and the second PCR just on the annealing temperature, which was about 56°C for the specific first PCR and at 58°C for the nested PCR. The elongation time depends on average ORF size per plate, whereby the KOD polymerase amplifies 1 kb in 20 seconds. Large fragments >4 kb, 1 minutes elongation time per 1 kb sequence was used. All PCR samples were analyzed by gel electrophoresis for correct ORF size.

4.2.8.1 Gateway cloning

The cloning was performed using the established Gateway System from Thermo Fisher. The first cloning step, the BP reaction, was performed using 2 μl of the nested PCR product with 2 μl pDONR223 (50ng/ μl), 0.5 μl TE buffer(10 mM Tris ph8.0, 1mM EDTA) and 0.5 μl BP II clonase mix (Thermo Fisher cat. no. 11789100). This cloning steps were almost exclusively performed in a 96 micro-titer plate. The sealed plate incubate at room temperature ($21 - 25$°C) for 4 hours or overnight at. 1.5 μl of the BP reaction mix was subsequently transformed into high competent $Dh5\alpha$ cells ($> 5 * 10^8$ cfu/μg). For the LR reaction, 2 μl (50ng/ μl) ORF containing entry, 2 μl (40-100 ng/ μl) of destination vector (pDEST AD, pDEST-DB), 0.5 μl TE buffer (10 mM Tris ph8.0, 1mM EDTA) and 0.5 μl LR II clonase mix were mixed and the sealed plate was incubated for 4 hours or overnight at room temperature ($21 - 25$°C). 1.5 μl of the BP reaction mix was subsequently transformed into high competent $Dh5\alpha$ cells ($> 5 * 10^8$ cfu/μg).

In addition to the reaction mixes, different controls were performed. The master mix without PCR amplicon or entry plasmid were always tested as a negative control in the BP or LR cloning step. For this purpose, 2 μl water is added to the BP or LR mixture instead of the PCR template or entry plasmid, respectively. This control was transformed together with all other samples, but should not show any bacterial growth. For specific individual cloning in single tubes, Gateway cloning events recipe were prepared as describes before.

4.2.9 Bacterial transformation and plasmid purification

The protocol for the transformation is adjusted for a 96-well micro-titer plate. 2 ml of competent DH5α cells ($> 5 * 10^8$ cfu/μg) were thawed on ice and 20 μl were pipetted into each well of 96-well micro-titer plate. For transformation of BP reaction mix or LR reaction mix 1.5 μl were added to the competent cells in each well. The plate was sealed and incubated on ice for minimal 30 minutes (max. 45 minutes) followed by heat shock with 1 minute at 42°C, chilling 2-min on ice. For recovery, 100 μl of pre-warmed SOC medium (0.5 % yeast extract, 2 % tryptone, 10 mM NaCl, 2.5 mM KCl, 10 mM MgCl2, 10 mM MgSO4, 20 mM glucose) was added to each well using an 8-channel pipette, followed by incubated at 37°C for 1 hr without shaking. Thereafter the transformation mix was transferred into the prepared deep-well plate (LB media

with antibiotics) and incubated on a plate shaker at 37°C for 16 to 18 hr. On the next day, 80 µl/well of overnight culture was transferred into a skirted 96-well u-bottom plate containing 80 µl/well of 40 % glycerol, mix gently, seal with adhesive aluminum foil, and store at −80°C. The remaining overnight cultures were centrifuged 10 min at 1000 * g, room temperature and the supernatants were removed with an 8-channel pipette or a liquid handling robot and stored at −20°C or were directly used for plasmid purification .For plasmid purification, a commercially available 96-well-compatible as well as single tube plasmid purification kit from Macherey-Nagel were used according to manufacturer's recommendations. Controls: To test for background from the BP or LR reaction mix, 1.5 µl of negative control BP or LR reaction mix was additionally transformed into competent DH5α cells. To test for contamination of the competent DH5α cells and transformation reagents, 20 µl of competent DH5α cells with empty destination vector without cloning enzyme or TE buffer was transformed. For specific individual transformations in single tubes, transformation protocol were prepared as described before, except from the amount of LB liquid medium used for recovery, here I used 1 ml instead of 100 µl.

4.2.10 Yeast transformation

The Y2H protocol outlined here is based on separate transformation of AD-ORF (AD-Y) and DB-ORF (DB-X) plasmids into yeast strains of opposite mating types. This enables the use of yeast mating to obtain pairwise AD-Y * DB-X combinations, which reduces the workload compared to co-transformation protocols. Our system is based on the yeast strains Y8800 (MATa mating-type for AD plasmids) and Y8930 (MATα mating-type for DB plasmids). Both strains are derived from PJ69-4 [620] and harbor the following genotype: leu2-3, 112 trp1-901 his3Δ200 ura3-52 gal4 gal80 GAL2::ADE2 GAL1::HIS@LYS2 GAL7::lacZ@met2 cyh2R. The complete yeast transformations were performed according to Altmann et al., 2018 [293]. AD-Y plasmid constructs were transformed in Y8800 (MATa) strain and DB-X plasmid constructs in Y8930 (MATα) strain, respectively. Y8800 and/or Y8930 yeast strains were streaked out on separate 145 mm YEPD plates and incubated at 30°C for 72 hr to obtain isolated colonies. For each strain, 10 colonies were used to inoculate 20 ml of YEPD liquid medium (2 % bacto peptone, 1 % yeast extract, 2 % glucose). The pre-cultures incubate at 30°C on a shaker (180 rpm) for 16 to 18 hr to an OD600 4.0 to 6.0. The pre-cultures were diluted to final OD600 of 0.1. (For each 96-well plate, 150 ml of yeast culture is needed.), thereafter cultures were incubated at 30°C on a shaker (180 rpm) for 4 to 6 hr until OD600 has reached 0.6 to 0.8. The yeast cultures were centrifuged 5 min at 800 * g, room temperature, the supernatant were discarded and the cell pellets were gently resuspended in 10 ml distilled H2O for each 150 ml culture. The mixtures were centrifuged again for 5 min at 800 * g, room temperature, and supernatants were discarded. The pellets were resuspended with 10 ml TE/LiAc solution (10mM TRIS pH 8.0, 0.5 mM EDTA, 100 mM LiAc), followed by an additional centrifugation step for 5 min at 800 * g, room temperature. The supernatants were discarded again and the pellets were resuspended 2 ml TE/LiAc (10mM TRIS pH 8.0, 0.5 mM EDTA, 100 mM LiAc) solution. 200 mg of single stranded carrier DNA (Sigma Cat.no. D1626) was boiled for 5 minutes and chilled on ice and thereafter mixed with 10 ml of TE/LiAc/PEG solution (10mM TRIS pH 8.0, 0.5 mM EDTA, 100 mM LiAc, 80 % of 44 % PEG stock solution). This mixture was added to the yeast mix and 120 µl cell suspension were dispensed into each well of a 96-well PCR plate using

an 8-channel pipette. 10 to 15 μl of 100 ng/ μl plasmid DNA per well were added to the competent yeast cells and mixed by slowly pipetting up and down several times using a liquid-handling robot or an 8-channel pipette. The PCR plates were sealed with adhesive aluminum foil and incubated at 30°C for 30 min without shaking. To heat shock, the PCR plates were carefully placed in a 42°C water bath for 15 min, followed by centrifugation for 5 min at 800 * g, room temperature. The supernatants were carefully removed using a liquid-handling robot or an 8-channel pipette. 10 μl of distilled H2O were added to each well and cell pellets were resuspended by carefully pipetting up and down. 5 μl/well of the resuspended cells were spotted onto the respective selective plate (Sc-Trp for AD-Y, Sc-Leu for DB-X) using a liquid-handling robot, or 8-channel pipette. The plates were incubated at 30°C for 72 hr. For each transformation plate, a half deep-well plate was prepared with 160 μl of the respective selective medium (Sc-Trp for AD-Y, Sc-Leu for DB-X). The yeast colonies were inoculated using an 8-channel pipette and incubated on a shaker at 30°C for 72 hr. For each transformed plate two glycerol stocks were prepared, one for immediate processing and the other as an archival stock. Therefore 80 μl of yeast culture was transferred into a skirted 96-well u-bottom plate containing 80 μl of 40 % glycerol, mixed gently, sealed, and stored at -80°C.

4.2.11 Y2H pipeline

Y2H mapping pipeline consists of four steps (2.4) primary screening, secondary phenotyping, candidate interaction partner identification, and 4-fold independent verification, which together ensure identification of highly reliable interactions. In the primary screen, all DB-X yeast clones are mated with the prepared AD-Y yeast pools (test plate) on full media plates YEPD and incubated at 30°C for 24 hours. Additionally DB-x yeast clones are mated with AD-empty containing yeast to identify spontaneous autoactivators. Then the yeast spots are replicated onto selective plates (Sc-W-L-H) and incubated again at 30°C for 24 hours , before the selective plates were cleaned, by using a velvet, to remove most yeast colonies. This step removes those cells which have stored histidine from the full media plates and showed growth without interactions that take place. After cleaning the plate incubate at 30°C for 72 hours. In the phenotyping step, two colonies from each yeast spot are separately inoculated in liquid Sc-W-L media and incubate at 30°C for 48h on an orbital shaker. If growth appears on the AD-empty control plate, the respective yeast spot on the test plate is excluded from further experiments. The yeast culture is spotted on selective plates (Sc-W-L) (5 μl) and incubated for additional 24 hours at 30°C. The yeast spots are replicated on selective media (Sc-W-L-H) and Sc-L-H + CHX (1 μg/l), as control plate to detect spontaneous autoactivators, and are cleaned directly, before incubation at 30°C for additional 72 hours. For the yeast lysis 45 U of Zymolyase 20T from amsbio (Cat. no: 120493-1) was dissolved in 1 ml 0.1M potassium phosphate buffer pH7.4 (80.2 % 1 M K2HPO4, 19.8 % 1M Kh2PO4) (sterile filtered before use). In each well of a 96-well micro-titer plate 15 μl were aliquoted and kept on ice. Using a 8-channel pipette, small amounts of the positive secondary yeast spots were dissolved in the lysis buffer. The plate was sealed and placed into the thermal cycler. The program contains only one cycle with 15 minutes at 37°C, followed by 5 minutes at 95°C. Then 100 μl of distilled water is added to each well and centrifuged 10 min at 800 * g, room temperature. For the PCR 2 μl were used as template. The PCR a master mix protocol was used for one 96-well plate. 300 μl of 10x DNA polymerase buffer (200 mM Tris-HCL pH8.4, 500 mM KCl, 25 mM $MgCl_2$), 300 μl of 2.5 mM dNTPs, 300 μl of 2 μM AD or DB

specific for primer, 300 µl of 2 µM term reverse primer, 20 µl of home made DNA polymerase and 1580 µl of distilled water were mixed in a 15 ml tube and mixed by vortexing. The 2 µl template (yeast lysis mixture) were aliquoted per well and 28 µl PCR mix was added. PCR was conducted as described in [293]. To identify the candidate interactors the PCR was sequenced either by Sanger sequencing, or by Next Generation Sequencing. In the last verification step, all identified candidate pairs are retested as individual pairs. All pairs that could be detected in three out of four independent verification steps are counted as confirmed Y2H interactions. The complete protocol for this Y2H mapping pipeline and all recipes are published in Altmann et al, 2018 [293].

4.2.12 Preparation of the artificial micro RNA for MKK7

The artificial micro RNA (amiR) was prepared according to the online protocol from Rebecca Schwab available on the weigelworld.org webpage[1]. The sequence of the MKK7 oligo to prepare the amiR construct was designed using weigelworld.org online tool[2] and the resulting sequence amiR MKK7-TGAATTGCAGTAATCTAGCGA- was used to prepare the amiR MKK7 construct. This sequence was also used for a blast search on TAIR to identify possible unspecific binding to other mRNAs. From this blast search six genes showed similarities in the sequence (see A.4.1). For those genes specific qRT-primer were designed to check gene expression of those genes in the amiR MKK7 plant lines. For transformation into plants the construct was cloned into pALLIGATOR3, which contains a C-terminal At2S3::GFP construct, that results in a fluorescent seed coat after successful transformation. This allows immediate selection of the transformed seeds in the F1 generation (kindly provided by Dr. Francois Parcy [433]). The pALLIGATOR3-amiR MKK7 construct was transformed into *Agrobacterium tumefaciens* GV3101, which could then be used for floral dipping.

4.2.13 Transformation in *Agrobacterium tumefaciens*

For transformation, 200 µl of competent GV3101 *Agrobacterium* cells thawed on ice. Thereafter, 500 ng plasmid DNA (with maximal volume of 10 µl) was added and mixed gently, before incubating 5 to 10 minutes on ice. The mixture was transferred to liquid nitrogen for 5 minutes and subsequently incubate 5 minutes at 37°C. Then 1 ml LB media was added followed by 2 hours incubation at 28°C on a shaker. The transformation mixture was centrifuged for 2 minutes at 2000 g, the cell pellet was resuspended in 100 µl LB media and spread on LB plates containing Rifampicin (10 mg/l) and Gentamycin (30 mg/l) for GV3101 selection and the respective antibiotic for the transformed plasmid. The plate was incubated at 28°C for 48-72 hours to obtain transformed cells.

4.2.14 Handling of transgenic plants

4.2.14.1 Seed sterilization

Seed sterilization with ethanol: Seeds were aliquoted into a clean spin column with collection tube (reused and cleaned with 80 % ethanol from plasmid purification kits) with a maximum volume of 50 mg per tube. 700 µ 75 % ethanol were added and mixed by inverting the tube for 4 minutes, followed by a centrifugation step of 1 minute at

[1] http://wmd3.weigelworld.org/downloads/Cloning_of_artificial_microRNAs.pdf
[2] http://wmd3.weigelworld.org/cgi-bin/webapp.cgi?page=Designer;project=stdwmd

11,000 g. The flow through were discarded and 700 μl 100 % ethanol were added and mixed by inverting the tube for 4 minutes followed by centrifugation. The flow through were removed and an additional centrifugation step with 5 minutes at 11,000 g were performed to dry the seeds. Seed sterilization with chloric gas: Seeds were aliquoted into 1.5 ml tubes. A small glass beaker with 100 ml hypochlorite and carefully added 3 ml HCL (37 %) was placed in the lower part of the desiccator and the open tubes were placed in a paper grid on top of the ceramic plate. The desiccator was closed and the seeds were sterilized for maximal 3 hours.

4.2.14.2 Plant growth

Sterile Arabidopsis seeds were sown on sterile MS plates and stratified in 4°C (dark) for three days, followed by 8-10 days LD (16 hours light/ 8 hours darkness) at 21°C. Thereafter the seedlings were transferred into soil pots as single plants. When the first inflorescence emerge the plant was covered by so called ARACON-bases and later on covered with ARACON tubes (BETATECH bvba http://www.arasystem.com/index.php) to collect seeds and prevent cross-pollination.

4.2.14.3 Floral dipping

Arabidopsis seed were sterilized, sowed on MS plates and stratified in 4°C (dark) for three days, followed by 8-10 days LD (16/8 h) at 21° C. Thereafter the seedlings are transferred into soil 10 to 12 plants per pot and grown at 21°C LD condition for additional 10- 14 days. The first inflorescence was cut after emergence to increase the number of inflorescences. Plants were ready for transformation, when the secondary inflorescences were about 8-10 cm tall and the majority of the flowers are open. *Agrobacterium tumefaciens* strain GV3101 were transformed with the respective plasmid including the gene of interest and stored as glycerol stock at −80°C. The glycerol stock was streaked out on LB plates containing the respective antibiotics and were incubated for 3 days at 28°C. From this plate, single colonies were used to inoculate a pre-culture of 2 ml volume (LB with respective antibiotics) which was incubated at 28°C on a shaker for additional 2 days. Thereafter a main-culture of 200 ml volume was inoculated with 1 ml pre-culture and incubated again at 28°C for 24 hours on the shaker. Cells were harvested by centrifugation for 20 minutes at 5500 g at room temperature and resuspended in dipping buffer (Murashige & Skoog 2.2 g/l, 2.5 mM Monohydrate 2-(N-morpholino) ethanesufonic acid (MES), 5 % sucrose, 0.44 mM 6-benzyladenine (BA), 0.3 % silwet L-77) to OD600 0.80 (minimal volume should be 400 ml). The bacteria culture was transferred into a glass beaker of 500 ml, the single pots were inverted, and the inflorescence dipped into the bacterial suspension. Plant were left in the suspension for about 30 seconds, then the pots were removed from the suspension and put aside into a covered tray for the next 24 hours. Thereafter the cover was removed, plants were rinsed with water, and returned to normal growing conditions. To enhance the transformation efficiency the floral dipping was repeated after three days.

4.2.14.4 *Nicotiana benthamiana* infiltration

For infiltration, 4-6 week old *N. benthamiana* plants are used. *Agrobacterium tumefaciens* strain GV3101 were transformed with the respective plasmid including the gene of interest and stored as glycerol stock at −80°C. The glycerol stock were streaked out on LB

plates containing the respective antibiotics and were incubated for 3 days at 28°C. Single colonies were used to inoculate a 2-4 ml culture (LB with respective antibiotics) which incubated at 28°C on a shaker overnight. 1 ml from the overnight culture was aliquoted into a 1.5 ml tube and centrifuged for 5 minutes at 5000 g at room temperature. The supernatant was removed and the pellet was gently resuspended in 1 ml infiltration buffer (for 10 ml infiltration buffer: 1 ml 0.5 M MES, 1 ml 0.02 M $Na3PO_4$ * 12 H_2O, 1 μl 1 M acetosyringone, 0.05 g glucose, add to final volume with water). This step was repeated to wash the sample twice. In the last step the OD600 is measured and the suspension was diluted to OD600 $0.1 - 0.4$ (depending on the construct). The suspension rested on the bench for $2 - 3$ hours prior to use. In the meantime, the plants were sprayed with water and stored under a transparent hood in the growth chamber (light), to enhance stomata opening. To inoculate suspension 1 ml syringes without needle was pressed against the underside of the leaf by exert a counter-pressure with finger on the other side. The plants were incubated in the dark over night and then moved back to LD light conditions (16/8 h) for additional two days. Leaf sample was analyzed under the fluorescent microscope.

4.2.15 Hormone treated seedling assays

All transgenic lines were propagated twice, in order to gain enough seeds. The plants were sterilized with ethanol and stratified on agar plates for three days and then placed in the growth chamber for additional 10 days. The seedlings were separated in soil pots and moved to the green house after additional 10 days. The seeds were harvested after 6-8 weeks. (LD light conditions: 16 h light, 8 dark, 23°C, light intensity about 75-85 $\mu M/m^2/s$). For BR pathways assays 1 μM brassinolide (BL) with 1% sucrose was tested. For the CK pathway assay 1 μM, and 10 μM 6-benzylamino purine (BA) with 1% or 3% sucrose were tested. For the ET pathway assay 10 μM 1-aminocyclopropane-1-carboxylic acid (ACC) with 1% sucrose was used. For GA pathway assays 0.1 μM, 1 μM, 10 μM GA3, or additionally 0.5 μM and 1.0 μM paclobutrazol (PAC) with 1% sucrose were used. For the JA pathway assays 25 μM methyl jasmonate (MeJa) with 1% sucrose was tested. For IAA pathway assays 1 μM and 10 μM indole-3-acetic acid (IAA) with 1% sucrose were tested. For the ABA pathway assay 30 μM abscisic acid (ABA) with 1% sucrose was used. For significance calculations a two sided t-test was performed.

4.2.15.1 Measuring hypocotyl length

Seeds were directly plated on MS plates or MS plates containing the respective hormone and stratified in the dark at 4°C for three days. The plates were transferred to the light growth chamber under LD light conditions (16/8 h). After six days the plates were photographed and the pictures were analyzed using Image J and the plugin Simple Neurite Tracer.

4.2.15.2 Measuring root elongation

The seedlings grow on MS plates up to 5 DAG, then they were transferred to MS mock and MS with the appropriate hormone. Then the tips of the root are marked and the plates are placed back into the growth chamber with LD light conditions, in vertical position for further 4 days. The plates with the seedlings were photographed and analyzed with ImageJ and the plugin Simple Neurite Tracer.

4.2.15.3 Measuring anthocyanin content

For cytokinin response the accumulation of anthocyanin was tested using the protocol from Nakat et al., 2014 [624]. Therefore, the sterilized seeds were plated on MS plates containing 1 % or 3 % sucrose, 0.8 % agar with and without 1 μM or 10 μM 6-benzylamino purine (BA) and stratified for 3 days. Then the plates were transferred into long day light conditions (16 hours light/ 8 hours dark) (75-85 μM/m2/s) , at 23°C for additional 10 days. For harvesting the fresh weight was measured of 15 seedlings per line, treatment and repeat and frozen with liquid nitrogen. The samples were ground in the tubes with a pestle and 5 volumes (based on fresh weight) of extraction buffer (45 % methanol, 5 % acetic acid, 50 % water) was added. Followed by mixing and centrifugation at 12,000 g for 5 minutes. The supernatant was transferred into a new 1.5 ml tube and centrifuged again at 12,000 g for 5 minutes. The resulting supernatant was transferred into a flat bottom micro titer plate and absorbance was measured at 530 nm and 657 nm using the plate reader. The blank was done with pure extraction buffer. The anthocyanin content was calculated by ($Absorbance\ 530\,nm/\,gfreshweight$) by [$Absorbance530\,nm - (0.25 * Absorbance657\,nm)$] $*5$. To correct the chlorophyll content in the absorptions at 530 nm, the formula Abs530 - (0.25 x Abs657) was used.

4.2.15.4 Measuring triple response

The sterile seeds were placed directly on the final plates containing 0 μM or 10 μM 1-aminocyclopropane-carboxylic acid (ACC), stratified in the dark for three days, then transferred into the light chamber for 1 hour. Thereafter the plates were moved into a vertical orientation and wrapped with in aluminum foil to block the light. The plates were analyzed after 3 days in 23°C.

4.2.15.5 Measuring germination rate

The seeds were sterilized and spread on MS plates and on MS plates containing the respective hormone. For stratification the plates were stored in the dark at 4°C for three days. Thereafter the plates were placed in the light growth chambers under LD light conditions (16/8 h) at 23°C for additional 48 hours. The same protocol were used for all germination assays with different hormone treatment amounts for GA3, Pac and ABA. For analysis the plates were photographed using a super macro objective and testa rupture was counted. 100 seeds per line per repeat was tested.

4.2.16 Enrichment analysis

4.2.16.1 GO enrichment analysis

The locus IDs from PhI_{out} nodes were separated according to their origin (AtORFeome or PhO). The locus IDs from group AtORFeome were uploaded to [3] [438] and all locus IDs from the AtORFeome collection [419] were additionally uploaded as reference. Both sets were then tested in a statistical over-representation test. The same was done for the PhO derived nodes from PhI_{out}, but as reference all locus IDs from PhO were used. The GO enrichment calculations were once performed without multiple hypothesis correction (MHC), twice with MHC using false discovery rate (FDR) and Bonferroni correction. The resulting GO terms with enrichment values were downloaded, modified and uploaded to the online tool of Revigo [4] [441] to visualize the data in a tree map. Additionally the visualizing data were downloaded and imported into Cytoscape. These file were modified for better visualization and used for preparing the GO enrichment figure 2.11.

4.2.16.2 Enrichment calculation of TCP interactions among all screens

TCP enrichment calculation: number of TCP proteins observed in network (a) were divided through the number of proteins in the network (b); the number of TCP proteins in the ORF collection (c) used for this screen were divided through the complete number of ORFs in the tested collection. The resulting value from (a dividing through b) is then divided through the value from (c divided through d). The resulting value indicates a fold enrichment of TCP proteins in the network, compared to the number of TCP proteins in the whole tested collection. Values ≤ 1 indicated no enrichment, values ≥ 1 indicates enriched numbers of TCP proteins in a tested network map.

4.2.17 Technical equipment

Far the Y2H experiment I used a Tecan liquid handling robot of series Freedom EVO. For all plant pictures the camera EOS M50 system camera with super-macro objective (Canon 1362C005AA EF-M 28-mm F/3.5 IS STM EU11 IS/Macro) were used.

[3] http://pantherdb.org/
[4] http://revigo.irb.hr/

Bibliography

[1] M. van de Wouw, C. Kik, T. van Hintum, R. van Treuren, and B. Visser. Genetic erosion in crops: concept, research results and challenges. *Plant Genetic Resources*, 8(01):1–15, April 2010. URL: http://www.journals.cambridge.org/abstract_S1479262109990062, doi:10.1017/S1479262109990062.

[2] Y. Wang, S. Mopper, and K. H. Hasenstein. Effects of salinity on endogenous ABA, IAA, JA, AND SA in Iris hexagona. *Journal of Chemical Ecology*, 27(2):327–342, February 2001.

[3] N. Tuteja. Mechanisms of High Salinity Tolerance in Plants. In *Methods in Enzymology*, volume 428, pages 419–438. Elsevier, 2007. URL: https://linkinghub.elsevier.com/retrieve/pii/S0076687907280243, doi:10.1016/S0076-6879(07)28024-3.

[4] S. Saud, X. Li, Y. Chen, L. Zhang, S. Fahad, S. Hussain, A. Sadiq, and Y. Chen. Silicon Application Increases Drought Tolerance of Kentucky Bluegrass by Improving Plant Water Relations and Morphophysiological Functions. *The Scientific World Journal*, 2014:1–10, 2014. URL: http://www.hindawi.com/journals/tswj/2014/368694/, doi:10.1155/2014/368694.

[5] Z. Su, X. Ma, H. Guo, N. L. Sukiran, B. Guo, S. M. Assmann, and H. Ma. Flower Development under Drought Stress: Morphological and Transcriptomic Analyses Reveal Acute Responses and Long-Term Acclimation in Arabidopsis. *The Plant Cell*, 25(10):3785–3807, October 2013. URL: http://www.plantcell.org/cgi/doi/10.1105/tpc.113.115428, doi:10.1105/tpc.113.115428.

[6] I. Schmalenbach, L. Zhang, M. Reymond, and J. M. Jimenez-Gomez. The relationship between flowering time and growth responses to drought in the Arabidopsis Landsberg erecta x Antwerp-1 population. *Frontiers in Plant Science*, 5, November 2014. URL: http://journal.frontiersin.org/article/10.3389/fpls.2014.00609/abstract, doi:10.3389/fpls.2014.00609.

[7] K. Kazan and J. M. Manners. The interplay between light and jasmonate signalling during defence and development. *Journal of Experimental Botany*, 62(12):4087–4100, August 2011. URL: https://academic.oup.com/jxb/article-lookup/doi/10.1093/jxb/err142, doi:10.1093/jxb/err142.

[8] R. Lyons, A. Rusu, J. Stiller, J. Powell, J. M. Manners, and K. Kazan. Investigating the Association between Flowering Time and Defense in the Arabidopsis thaliana-Fusarium oxysporum Interaction. *PLOS ONE*, 10(6):e0127699, June 2015. URL: https://dx.plos.org/10.1371/journal.pone.0127699, doi:10.1371/journal.pone.0127699.

[9] E. M. Kramer and E. M. Ackelsberg. Auxin metabolism rates and implications for plant development. *Frontiers in Plant Science*, 6, March 2015. URL: http://www.frontiersin.org/Plant_Biophysics_and_Modeling/10.3389/fpls.2015.00150/abstract, doi:10.3389/fpls.2015.00150.

[10] S. Eriksson. GA4 Is the Active Gibberellin in the Regulation of LEAFY Transcription and Arabidopsis Floral Initiation. *THE PLANT CELL ONLINE*, 18(9):2172–2181, September 2006. URL: http://www.plantcell.org/cgi/doi/10.1105/tpc.106.042317, doi:10.1105/tpc.106.042317.

[11] M. Kojima, T. Kamada-Nobusada, H. Komatsu, K. Takei, T. Kuroha, M. Mizutani, M. Ashikari, M. Ueguchi-Tanaka, M. Matsuoka, K. Suzuki, and H. Sakakibara. Highly Sensitive and High-Throughput Analysis of Plant Hormones Using MS-Probe Modification and Liquid Chromatography–Tandem Mass Spectrometry: An Application for Hormone Profiling in Oryza sativa. *Plant and Cell Physiology*, 50(7):1201–1214, July 2009. URL: https://academic.oup.com/pcp/article-lookup/doi/10.1093/pcp/pcp057, doi:10.1093/pcp/pcp057.

[12] K. V. Thimann and J. B. Koepfli. Identity of the Growth-Promoting and Root-Forming Substances of Plants. *Nature*, 135(3403):101–102, January 1935. URL: http://www.nature.com/articles/135101a0, doi:10.1038/135101a0.

[13] T. J. Cooke. The Role of Auxin in Plant Embryogenesis. *THE PLANT CELL ONLINE*, 5(11):1494–1495, November 1993. URL: http://www.plantcell.org/cgi/doi/10.1105/tpc.5.11.1494, doi:10.1105/tpc.5.11.1494.

[14] B. Moller and D. Weijers. Auxin Control of Embryo Patterning. *Cold Spring Harbor Perspectives in Biology*, 1(5):a001545–a001545, November 2009. URL: http://cshperspectives.cshlp.org/lookup/doi/10.1101/cshperspect.a001545, doi:10.1101/cshperspect.a001545.

[15] R. J. Pitts, A. Cernac, and M. Estelle. Auxin and ethylene promote root hair elongation in Arabidopsis. *The Plant Journal: For Cell and Molecular Biology*, 16(5):553–560, December 1998.

[16] A. Rahman. Auxin and Ethylene Response Interactions during Arabidopsis Root Hair Development Dissected by Auxin Influx Modulators. *PLANT PHYSIOLOGY*, 130(4):1908–1917, December 2002. URL: http://www.plantphysiol.org/cgi/doi/10.1104/pp.010546, doi:10.1104/pp.010546.

[17] B. Péret, B. De Rybel, I. Casimiro, E. Benková, R. Swarup, L. Laplaze, T. Beeckman, and M. J. Bennett. Arabidopsis lateral root development: an emerging story. *Trends in Plant Science*, 14(7):399–408, July 2009. URL: https://linkinghub.elsevier.com/retrieve/pii/S1360138509001460, doi:10.1016/j.tplants.2009.05.002.

[18] S. Saini, I. Sharma, N. Kaur, and P. K. Pati. Auxin: a master regulator in plant root development. *Plant Cell Reports*, 32(6):741–757, June 2013. URL: http://link.springer.com/10.1007/s00299-013-1430-5, doi:10.1007/s00299-013-1430-5.

[19] J. Petrásek and J. Friml. Auxin transport routes in plant development. *Development (Cambridge, England)*, 136(16):2675–2688, August 2009. doi:10.1242/dev.030353.

[20] T. Vernoux, F. Besnard, and J. Traas. Auxin at the Shoot Apical Meristem. *Cold Spring Harbor Perspectives in Biology*, 2(4):a001487–a001487, April 2010. URL: http://cshperspectives.cshlp.org/lookup/doi/10.1101/cshperspect.a001487, doi:10.1101/cshperspect.a001487.

[21] S. M. Velasquez, E. Barbez, J. Kleine-Vehn, and J. Estevez. Auxin and cellular elongation. *Plant Physiology*, page pp.01863.2015, January 2016. URL: http://www.plantphysiol.org/lookup/doi/10.1104/pp.15.01863, doi:10.1104/pp.15.01863.

[22] D. L. Rayle and R. E. Cleland. The Acid Growth Theory of auxin-induced cell elongation is alive and well. *PLANT PHYSIOLOGY*, 99(4):1271–1274, August 1992. URL: http://www.plantphysiol.org/cgi/doi/10.1104/pp.99.4.1271, doi:10.1104/pp.99.4.1271.

[23] R. Di Mambro, M. De Ruvo, E. Pacifici, E. Salvi, R. Sozzani, P. N. Benfey, W. Busch, O. Novak, K. Ljung, L. Di Paola, A. F. M. Marée, P. Costantino, V. A. Grieneisen, and S. Sabatini. Auxin minimum triggers the developmental switch from cell division to cell differentiation in the *Arabidopsis* root. *Proceedings of the National Academy of Sciences*, 114(36):E7641–E7649, September 2017. URL: http://www.pnas.org/lookup/doi/10.1073/pnas.1705833114, doi:10.1073/pnas.1705833114.

[24] C. Perrot-Rechenmann. Cellular Responses to Auxin: Division versus Expansion. *Cold Spring Harbor Perspectives in Biology*, 2(5):a001446–a001446, May 2010. URL: http://cshperspectives.cshlp.org/lookup/doi/10.1101/cshperspect.a001446, doi:10.1101/cshperspect.a001446.

[25] Z. Ding and J. Friml. Auxin regulates distal stem cell differentiation in Arabidopsis roots. *Proceedings of the National Academy of Sciences*, 107(26):12046–12051, June 2010. URL: http://www.pnas.org/cgi/doi/10.1073/pnas.1000672107, doi:10.1073/pnas.1000672107.

[26] M. E. J. Habets and R. Offringa. PIN-driven polar auxin transport in plant developmental plasticity: a key target for environmental and endogenous signals. *New Phytologist*, 203(2):362–377, July 2014. URL: http://doi.wiley.com/10.1111/nph.12831, doi:10.1111/nph.12831.

[27] M. Zourelidou, B. Absmanner, B. Weller, I. C. Barbosa, B. C. Willige, A. Fastner, V. Streit, S. A. Port, J. Colcombet, S. de la Fuente van Bentem, H. Hirt, B. Kuster, W. X. Schulze, U. Z. Hammes, and C. Schwechheimer. Auxin efflux by PIN-FORMED proteins is activated by two different protein kinases, D6 PROTEIN KINASE and PINOID. *eLife*, 3, June 2014. URL: https://elifesciences.org/articles/02860, doi:10.7554/eLife.02860.

[28] I. Barbosa, M. Zourelidou, B. Willige, B. Weller, and C. Schwechheimer. D6 PROTEIN KINASE Activates Auxin Transport-Dependent Growth and PIN-FORMED Phosphorylation at the Plasma Membrane. *Developmental Cell*, 29(6):674–685, June 2014. URL: https://linkinghub.elsevier.com/retrieve/pii/S1534580714003086, doi:10.1016/j.devcel.2014.05.006.

[29] J. Friml. A PINOID-Dependent Binary Switch in Apical-Basal PIN Polar Targeting Directs Auxin Efflux. *Science*, 306(5697):862–865, October 2004. URL: http://www.sciencemag.org/cgi/doi/10.1126/science.1100618, doi:10.1126/science.1100618.

[30] C. S. Galván-Ampudia and R. Offringa. Plant evolution: AGC kinases tell the auxin tale. *Trends in Plant Science*, 12(12):541–547, December 2007. URL: https://linkinghub.elsevier.com/retrieve/pii/S1360138507002750, doi:10.1016/j.tplants.2007.10.004.

[31] S. K. Christensen, N. Dagenais, J. Chory, and D. Weigel. Regulation of auxin response by the protein kinase PINOID. *Cell*, 100(4):469–478, February 2000.

[32] S. Henrichs, B. Wang, Y. Fukao, J. Zhu, L. Charrier, A. Bailly, S. C. Oehring, M. Linnert, M. Weiwad, A. Endler, P. Nanni, S. Pollmann, S. Mancuso, A. Schulz, and M. Geisler. Regulation of ABCB1/PGP1-catalysed auxin transport by linker phosphorylation: Regulation of ABCB1 by linker phosphorylation. *The EMBO Journal*, 31(13):2965–2980, June 2012. URL: http://emboj.embopress.org/cgi/doi/10.1038/emboj.2012.120, doi:10.1038/emboj.2012.120.

[33] M. Michniewicz, M. K. Zago, L. Abas, D. Weijers, A. Schweighofer, I. Meskiene, M. G. Heisler, C. Ohno, J. Zhang, F. Huang, R. Schwab, D. Weigel, E. M. Meyerowitz, C. Luschnig, R. Offringa, and J. Friml. Antagonistic Regulation of PIN Phosphorylation by PP2a and PINOID Directs Auxin Flux. *Cell*, 130(6):1044–1056, September 2007. URL: https://linkinghub.elsevier.com/retrieve/pii/S0092867407009713, doi:10.1016/j.cell.2007.07.033.

[34] B. Weller, M. Zourelidou, L. Frank, I. C. R. Barbosa, A. Fastner, S. Richter, G. Jürgens, U. Z. Hammes, and C. Schwechheimer. Dynamic PIN-FORMED auxin efflux carrier phosphorylation at the plasma membrane controls auxin efflux-dependent growth. *Proceedings of the National Academy of Sciences*, 114(5):E887–E896, January 2017. URL: http://www.pnas.org/lookup/doi/10.1073/pnas.1614380114, doi:10.1073/pnas.1614380114.

[35] T. S. Lewis, P. S. Shapiro, and N. G. Ahn. Signal transduction through MAP kinase cascades. *Advances in Cancer Research*, 74:49–139, 1998.

[36] H. D. Madhani and G. R. Fink. The riddle of MAP kinase signaling specificity. *Trends in genetics: TIG*, 14(4):151–155, April 1998.

[37] H. J. Schaeffer and M. J. Weber. Mitogen-activated protein kinases: specific messages from ubiquitous messengers. *Molecular and Cellular Biology*, 19(4):2435–2444, April 1999.

[38] G. Tena, T. Asai, W.-L. Chiu, and J. Sheen. Plant mitogen-activated protein kinase signaling cascades. *Current Opinion in Plant Biology*, 4(5):392–400, October 2001. URL: http://linkinghub.elsevier.com/retrieve/pii/S1369526600001916, doi:10.1016/S1369-5266(00)00191-6.

[39] K. F. Pedley and G. B. Martin. Role of mitogen-activated protein kinases in plant immunity. *Current Opinion in Plant Biology*, 8(5):541–547, October 2005. URL: http://linkinghub.elsevier.com/retrieve/pii/S1369526605000968, doi:10.1016/j.pbi.2005.07.006.

[40] T. Romeis. Protein kinases in the plant defence response. *Current Opinion in Plant Biology*, 4(5):407–414, October 2001.

[41] X. Meng and S. Zhang. MAPK Cascades in Plant Disease Resistance Signaling. *Annual Review of Phytopathology*, 51(1):245–266, August 2013. URL: http://www.annualreviews.org/doi/10.1146/annurev-phyto-082712-102314, doi:10.1146/annurev-phyto-082712-102314.

[42] J. Xu and S. Zhang. Mitogen-activated protein kinase cascades in signaling plant growth and development. *Trends in Plant Science*, 20(1):56–64, January 2015. URL: https://linkinghub.elsevier.com/retrieve/pii/S1360138514002490, doi:10.1016/j.tplants.2014.10.001.

[43] P. Jagodzik, M. Tajdel-Zielinska, A. Ciesla, M. Marczak, and A. Ludwikow. Mitogen-Activated Protein Kinase Cascades in Plant Hormone Signaling. *Frontiers in Plant Science*, 9, October 2018. URL: https://www.frontiersin.org/article/10.3389/fpls.2018.01387/full, doi:10.3389/fpls.2018.01387.

[44] Y. Dai. Increased Expression of MAP KINASE KINASE7 Causes Deficiency in Polar Auxin Transport and Leads to Plant Architectural Abnormality in Arabidopsis. *THE PLANT CELL ONLINE*, 18(2):308–320, February 2006. URL: http://www.plantcell.org/cgi/doi/10.1105/tpc.105.037846, doi:10.1105/tpc.105.037846.

[45] W. Jia, B. Li, S. Li, Y. Liang, X. Wu, M. Ma, J. Wang, J. Gao, Y. Cai, Y. Zhang, Y. Wang, J. Li, and Y. Wang. Mitogen-Activated Protein Kinase Cascade MKK7-MPK6 Plays Important Roles in Plant Development and Regulates Shoot Branching by Phosphorylating PIN1 in Arabidopsis. *PLOS Biology*, 14(9):e1002550, September 2016. URL: https://dx.plos.org/10.1371/journal.pbio.1002550, doi:10.1371/journal.pbio.1002550.

[46] J. Friml. Auxin transport — shaping the plant. *Current Opinion in Plant Biology*, 6(1):7–12, February 2003. URL: https://linkinghub.elsevier.com/retrieve/pii/S1369526602000031, doi:10.1016/S1369526602000031.

[47] S. Vanneste and J. Friml. Auxin: A Trigger for Change in Plant Development. *Cell*, 136(6):1005–1016, March 2009. URL: https://linkinghub.elsevier.com/retrieve/pii/S009286740900258X, doi:10.1016/j.cell.2009.03.001.

[48] T. Vernoux, G. Brunoud, E. Farcot, V. Morin, H. Van den Daele, J. Legrand, M. Oliva, P. Das, A. Larrieu, D. Wells, Y. Guedon, L. Armitage, F. Picard, S. Guyomarc'h, C. Cellier, G. Parry, R. Koumproglou, J. H. Doonan, M. Estelle, C. Godin, S. Kepinski, M. Bennett, L. De Veylder, and J. Traas. The auxin signalling network translates dynamic input into robust patterning at the shoot apex. *Molecular Systems Biology*, 7(1):508–508, April 2014. URL: http://msb.embopress.org/cgi/doi/10.1038/msb.2011.39, doi:10.1038/msb.2011.39.

[49] T. J. Guilfoyle and G. Hagen. Auxin response factors. *Current Opinion in Plant Biology*, 10(5):453–460, October 2007. URL: https://linkinghub.elsevier.com/retrieve/pii/S1369526607001239, doi:10.1016/j.pbi.2007.08.014.

[50] T. Ulmasov. Aux/IAA Proteins Repress Expression of Reporter Genes Containing Natural and Highly Active Synthetic Auxin Response Elements. *THE PLANT CELL ONLINE*, 9(11):1963–1971, November 1997. URL: http://www.plantcell.org/cgi/doi/10.1105/tpc.9.11.1963, doi:10.1105/tpc.9.11.1963.

[51] I. A. Paponov, M. Paponov, W. Teale, M. Menges, S. Chakrabortee, J. A. Murray, and K. Palme. Comprehensive Transcriptome Analysis of Auxin Responses in Arabidopsis. *Molecular Plant*, 1(2):321–337, March 2008. URL: https://linkinghub.elsevier.com/retrieve/pii/S1674205214604391, doi:10.1093/mp/ssm021.

[52] J. Kim, K. Harter, and A. Theologis. Protein-protein interactions among the Aux/IAA proteins. *Proceedings of the National Academy of Sciences of the United States of America*, 94(22):11786–11791, October 1997.

[53] K. Ljung. Sites and Regulation of Auxin Biosynthesis in Arabidopsis Roots. *THE PLANT CELL ONLINE*, 17(4):1090–1104, April 2005. URL: http://www.plantcell.org/cgi/doi/10.1105/tpc.104.029272, doi:10.1105/tpc.104.029272.

[54] T. Werner, V. Motyka, M. Strnad, and T. Schmulling. Regulation of plant growth by cytokinin. *Proceedings of the National Academy of Sciences*, 98(18):10487–10492, August 2001. URL: http://www.pnas.org/cgi/doi/10.1073/pnas.171304098, doi:10.1073/pnas.171304098.

[55] A. Nordstrom, P. Tarkowski, D. Tarkowska, R. Norbaek, C. Astot, K. Dolezal, and G. Sandberg. Auxin regulation of cytokinin biosynthesis in Arabidopsis thaliana: A factor of potential importance for auxin-cytokinin-regulated development. *Proceedings of the National Academy of Sciences*, 101(21):8039–8044, May 2004. URL: http://www.pnas.org/cgi/doi/10.1073/pnas.0402504101, doi:10.1073/pnas.0402504101.

[56] S. Negi, M. G. Ivanchenko, and G. K. Muday. Ethylene regulates lateral root formation and auxin transport in *Arabidopsis thaliana*. *The Plant Journal*, 55(2):175–187, July 2008. URL: http://doi.wiley.com/10.1111/j.1365-313X.2008.03495.x, doi:10.1111/j.1365-313X.2008.03495.x.

[57] A. N. Stepanova, J. Yun, A. V. Likhacheva, and J. M. Alonso. Multilevel Interactions between Ethylene and Auxin in Arabidopsis Roots. *THE PLANT CELL ONLINE*, 19(7):2169–2185, July 2007. URL: http://www.plantcell.org/cgi/doi/10.1105/tpc.107.052068, doi:10.1105/tpc.107.052068.

[58] D. Wang, K. Pajerowska-Mukhtar, A. H. Culler, and X. Dong. Salicylic Acid Inhibits Pathogen Growth in Plants through Repression of the Auxin Signaling Pathway. *Current Biology*, 17(20):1784–1790, October 2007. URL: https://linkinghub.elsevier.com/retrieve/pii/S0960982207019847, doi:10.1016/j.cub.2007.09.025.

[59] P. Nagpal. Auxin response factors ARF6 and ARF8 promote jasmonic acid production and flower maturation. *Development*, 132(18):4107–4118, August 2005. URL: http://dev.biologists.org/cgi/doi/10.1242/dev.01955, doi:10.1242/dev.01955.

[60] S. Khan and J. Stone. Arabidopsis thaliana GH3.9 in Auxin and Jasmonate Cross Talk. *Plant Signaling & Behavior*, 2(6):483–485, November 2007. URL: http://www.tandfonline.com/doi/abs/10.4161/psb.2.6.4498, doi:10.4161/psb.2.6.4498.

[61] L. E. Cracker and F. B. Abeles. Abscission: role of abscisic Acid. *Plant Physiology*, 44(8):1144–1149, August 1969.

[62] X. Luo, Z. Chen, J. Gao, and Z. Gong. Abscisic acid inhibits root growth in Arabidopsis through ethylene biosynthesis. *The Plant Journal*, 79(1):44–55, July 2014. URL: http://doi.wiley.com/10.1111/tpj.12534, doi:10.1111/tpj.12534.

[63] J. Leung and J. Giraudat. ABSCISIC ACID SIGNAL TRANSDUCTION. *Annual Review of Plant Physiology and Plant Molecular Biology*, 49:199–222, June 1998. doi:10.1146/annurev.arplant.49.1.199.

[64] R. R. Finkelstein and S. I. Gibson. ABA and sugar interactions regulating development: cross-talk or voices in a crowd? *Current Opinion in Plant Biology*, 5(1):26–32, February 2002.

[65] R. Finkelstein. Abscisic Acid Synthesis and Response. *The Arabidopsis Book*, 11:e0166, January 2013. URL: http://www.bioone.org/doi/abs/10.1199/tab.0166, doi:10.1199/tab.0166.

[66] C. M. Karssen, D. L. C. Brinkhorst-van der Swan, A. E. Breekland, and M. Koornneef. Induction of dormancy during seed development by endogenous abscisic acid: studies on abscisic acid deficient genotypes of Arabidopsis thaliana (L.) Heynh. *Planta*, 157(2):158–165, March 1983. URL: http://link.springer.com/10.1007/BF00393650, doi:10.1007/BF00393650.

[67] M. Koornneef, C. J. Hanhart, H. W. Hilhorst, and C. M. Karssen. In Vivo Inhibition of Seed Development and Reserve Protein Accumulation in Recombinants of Abscisic Acid Biosynthesis and Responsiveness Mutants in Arabidopsis thaliana. *Plant Physiology*, 90(2):463–469, June 1989.

[68] V. Raz, J. H. Bergervoet, and M. Koornneef. Sequential steps for developmental arrest in Arabidopsis seeds. *Development (Cambridge, England)*, 128(2):243–252, January 2001.

[69] L. Lopez-Molina, S. Mongrand, and N.-H. Chua. A postgermination developmental arrest checkpoint is mediated by abscisic acid and requires the ABI5 transcription factor in Arabidopsis. *Proceedings of the National Academy of Sciences*, 98(8):4782–4787, April 2001. URL: http://www.pnas.org/cgi/doi/10.1073/pnas.081594298, doi:10.1073/pnas.081594298.

[70] R. Finkelstein, W. Reeves, T. Ariizumi, and C. Steber. Molecular Aspects of Seed Dormancy. *Annual Review of Plant Biology*, 59(1):387–415, June 2008. URL: http://www.annualreviews.org/doi/10.1146/annurev.arplant.59.032607.092740, doi:10.1146/annurev.arplant.59.032607.092740.

[71] M. J. Holdsworth, L. Bentsink, and W. J. J. Soppe. Molecular networks regulating Arabidopsis seed maturation, after-ripening, dormancy and germination. *New Phytologist*, 179(1):33–54, July 2008. URL: http://doi.wiley.com/10.1111/j.1469-8137.2008.02437.x, doi:10.1111/j.1469-8137.2008.02437.x.

[72] A. A. Millar, J. V. Jacobsen, J. J. Ross, C. A. Helliwell, A. T. Poole, G. Scofield, J. B. Reid, and F. Gubler. Seed dormancy and ABA metabolism in Arabidopsis and barley: the role of ABA 8-hydroxylase. *The Plant Journal*, 45(6):942–954, March 2006. URL: http://doi.wiley.com/10.1111/j.1365-313X.2006.02659.x, doi:10.1111/j.1365-313X.2006.02659.x.

[73] Y. Ma, I. Szostkiewicz, A. Korte, D. Moes, Y. Yang, A. Christmann, and E. Grill. Regulators of PP2c Phosphatase Activity Function as Abscisic Acid Sensors. *Science*, April 2009. URL: http://www.sciencemag.org/cgi/doi/10.1126/science.1172408, doi:10.1126/science.1172408.

[74] S.-Y. Park, P. Fung, N. Nishimura, D. R. Jensen, H. Fujii, Y. Zhao, S. Lumba, J. Santiago, A. Rodrigues, T.-f. F. Chow, S. E. Alfred, D. Bonetta, R. Finkelstein, N. J. Provart, D. Desveaux, P. L. Rodriguez, P. McCourt, J.-K. Zhu, J. I. Schroeder, B. F. Volkman, and S. R. Cutler. Abscisic Acid Inhibits Type 2c Protein Phosphatases via the PYR/PYL Family of START Proteins. *Science*, April 2009. URL: http://www.sciencemag.org/cgi/doi/10.1126/science.1173041, doi:10.1126/science.1173041.

[75] N. Nishimura, K. Hitomi, A. S. Arvai, R. P. Rambo, C. Hitomi, S. R. Cutler, J. I. Schroeder, and E. D. Getzoff. Structural Mechanism of Abscisic Acid Binding and Signaling by Dimeric PYR1. *Science*, 326(5958):1373–1379, December 2009. URL: http://www.sciencemag.org/cgi/doi/10.1126/science.1181829, doi:10.1126/science.1181829.

[76] S. Fuchs, E. Grill, I. Meskiene, and A. Schweighofer. Type 2c protein phosphatases in plants: PP2cs. *FEBS Journal*, 280(2):681–693, January 2013. URL: http://doi.wiley.com/10.1111/j.1742-4658.2012.08670.x, doi:10.1111/j.1742-4658.2012.08670.x.

[77] T. Yoshida. ABA-Hypersensitive Germination3 Encodes a Protein Phosphatase 2c (AtPP2ca) That Strongly Regulates Abscisic Acid Signaling during Germination among Arabidopsis Protein Phosphatase 2cs. *PLANT PHYSIOLOGY*, 140(1):115–126, December 2005. URL: http://www.plantphysiol.org/cgi/doi/10.1104/pp.105.070128, doi:10.1104/pp.105.070128.

[78] T. Umezawa, N. Sugiyama, M. Mizoguchi, S. Hayashi, F. Myouga, K. Yamaguchi-Shinozaki, Y. Ishihama, T. Hirayama, and K. Shinozaki. Type 2c protein phosphatases directly regulate abscisic acid-activated protein kinases in Arabidopsis. *Proceedings of the National Academy of Sciences*, 106(41):17588–17593, October 2009. URL: http://www.pnas.org/cgi/doi/10.1073/pnas.0907095106, doi:10.1073/pnas.0907095106.

[79] E. M. Hrabak. The Arabidopsis CDPK-SnRK Superfamily of Protein Kinases. *PLANT PHYSIOLOGY*, 132(2):666–680, May 2003. URL: http://www.plantphysiol.org/cgi/doi/10.1104/pp.102.011999, doi:10.1104/pp.102.011999.

[80] K. Hedbacker and M. Carlson. SNF1/AMPK pathways in yeast. *Frontiers in Bioscience: A Journal and Virtual Library*, 13:2408–2420, January 2008.

[81] A. Kulik, I. Wawer, E. Krzywińska, M. Bucholc, and G. Dobrowolska. SnRK2 Protein Kinases—Key Regulators of Plant Response to Abiotic Stresses. *OMICS: A Journal of Integrative Biology*, 15(12):859–872, December 2011. URL: http://www.liebertpub.com/doi/10.1089/omi.2011.0091, doi:10.1089/omi.2011.0091.

[82] B. Sánchez-Romera, J. M. Ruiz-Lozano, G. Li, D.-T. Luu, M. D. C. Martínez-Ballesta, M. Carvajal, A. M. Zamarreño, J. M. García-Mina, C. Maurel, and R. Aroca. Enhancement of root hydraulic conductivity by methyl jasmonate and the role of calcium and abscisic acid in this process: MeJA enhances root hydraulic conductivity. *Plant, Cell & Environment*, 37(4):995–1008, April 2014. URL: http://doi.wiley.com/10.1111/pce.12214, doi:10.1111/pce.12214.

[83] C. de Ollas, V. Arbona, and A. GóMez-Cadenas. Jasmonoyl isoleucine accumulation is needed for abscisic acid build-up in roots of Arabidopsis under water stress conditions: JA-ABA interaction in roots. *Plant, Cell & Environment*, 38(10):2157–2170, October 2015. URL: http://doi.wiley.com/10.1111/pce.12536, doi:10.1111/pce.12536.

[84] A. Chini, J. J. Grant, M. Seki, K. Shinozaki, and G. J. Loake. Drought tolerance established by enhanced expression of the *CC-NBS-LRR* gene, *ADR1* , requires salicylic acid, EDS1 and ABI1. *The Plant Journal*, 38(5):810–822, June 2004. URL: http://doi.wiley.com/10.1111/j.1365-313X.2004.02086.x, doi:10.1111/j.1365-313X.2004.02086.x.

[85] K. Miura, H. Okamoto, E. Okuma, H. Shiba, H. Kamada, P. M. Hasegawa, and Y. Murata. SIZ1 deficiency causes reduced stomatal aperture and enhanced drought tolerance via controlling salicylic acid-induced accumulation of reactive oxygen species in Arabidopsis. *The Plant Journal*, 73(1):91–104, January 2013. URL: http://doi.wiley.com/10.1111/tpj.12014, doi:10.1111/tpj.12014.

[86] P. J. Seo, F. Xiang, M. Qiao, J.-Y. Park, Y. N. Lee, S.-G. Kim, Y.-H. Lee, W. J. Park, and C.-M. Park. The MYB96 Transcription Factor Mediates Abscisic Acid Signaling during Drought Stress Response in Arabidopsis. *PLANT PHYSIOLOGY*, 151(1):275–289, September 2009. URL: http://www.plantphysiol.org/cgi/doi/10.1104/pp.109.144220, doi:10.1104/pp.109.144220.

[87] I. Nir, M. Moshelion, and D. Weiss. The *Arabidopsis GIBBERELLIN METHYL TRANSFERASE 1* suppresses gibberellin activity, reduces whole-plant transpiration and promotes drought tolerance in transgenic tomato: *GAMT1* promotes drought tolerance. *Plant, Cell & Environment*, 37(1):113–123, January 2014. URL: http://doi.wiley.com/10.1111/pce.12135, doi:10.1111/pce.12135.

[88] S.-F. Lo, T.-H. D. Ho, Y.-L. Liu, M.-J. Jiang, K.-T. Hsieh, K.-T. Chen, L.-C. Yu, M.-H. Lee, C.-y. Chen, T.-P. Huang, M. Kojima, H. Sakakibara, L.-J. Chen, and S.-M. Yu. Ectopic expression of specific GA2 oxidase mutants promotes yield and stress tolerance in rice. *Plant Biotechnology Journal*, 15(7):850–864, July 2017. URL: http://doi.wiley.com/10.1111/pbi.12681, doi:10.1111/pbi.12681.

[89] S. Kagale, U. K. Divi, J. E. Krochko, W. A. Keller, and P. Krishna. Brassinosteroid confers tolerance in Arabidopsis thaliana and Brassica napus to a range of abiotic stresses. *Planta*, 225(2):353–364, December 2006. URL: http://link.springer.com/10.1007/s00425-006-0361-6, doi:10.1007/s00425-006-0361-6.

[90] R. K. Sairam. Effects of homobrassinolide application on plant metabolism and grain yield under irrigated and moisture-stress conditions of two wheat varieties. *Plant Growth Regulation*, 14(2):173–181, 1994. URL: https://doi.org/10.1007/BF00025220, doi:10.1007/BF00025220.

[91] S. Sahni, B. D. Prasad, Q. Liu, V. Grbic, A. Sharpe, S. P. Singh, and P. Krishna. Overexpression of the brassinosteroid biosynthetic gene DWF4 in Brassica napus simultaneously increases seed yield and stress tolerance. *Scientific Reports*, 6(1), September 2016. URL: http://www.nature.com/articles/srep28298, doi:10.1038/srep28298.

[92] W. Li, L. Herrera-Estrella, and L.-S. P. Tran. The Yin–Yang of Cytokinin Homeostasis and Drought Acclimation/Adaptation. *Trends in Plant Science*, 21(7):548–550, July 2016. URL: https://linkinghub.elsevier.com/retrieve/pii/S1360138516300450, doi:10.1016/j.tplants.2016.05.006.

[93] J. I. Kim, D. Baek, H. C. Park, H. J. Chun, D.-H. Oh, M. K. Lee, J.-Y. Cha, W.-Y. Kim, M. C. Kim, W. S. Chung, H. J. Bohnert, S. Y. Lee, R. A. Bressan, S.-W. Lee, and D.-J. Yun. Overexpression of Arabidopsis YUCCA6 in Potato Results in High-Auxin Developmental Phenotypes and Enhanced Resistance to Water Deficit. *Molecular Plant*, 6(2):337–349, March 2013. URL: https://linkinghub.elsevier.com/retrieve/pii/S1674205214600952, doi:10.1093/mp/sss100.

[94] R. Stracke, M. Werber, and B. Weisshaar. The R2r3-MYB gene family in Arabidopsis thaliana. *Current Opinion in Plant Biology*, 4(5):447–456, October 2001.

[95] S. Ambawat, P. Sharma, N. R. Yadav, and R. C. Yadav. MYB transcription factor genes as regulators for plant responses: an overview. *Physiology and Molecular Biology of Plants*, 19(3):307–321, July 2013. URL: http://link.springer.com/10.1007/s12298-013-0179-1, doi:10.1007/s12298-013-0179-1.

[96] M. Bakshi and R. Oelmüller. WRKY transcription factors: Jack of many trades in plants. *Plant Signaling & Behavior*, 9(2):e27700, February 2014. URL: http://www.tandfonline.com/doi/abs/10.4161/psb.27700, doi:10.4161/psb.27700.

[97] J. W. Mitchell, N. Mandava, J. F. Worley, J. R. Plimmer, and M. V. Smith. Brassins—a New Family of Plant Hormones from Rape Pollen. *Nature*, 225(5237):1065–1066, March 1970. URL: http://www.nature.com/articles/2251065a0, doi:10.1038/2251065a0.

[98] J. W. Mitchell and L. E. Gregory. Enhancement of Overall Plant Growth, a New Response to Brassins. *Nature New Biology*, 239(95):253–254, October 1972. URL: http://link.springer.com/10.1038/newbio239253a0, doi:10.1038/newbio239253a0.

[99] S. D. Clouse, M. Langford, and T. C. McMorris. A brassinosteroid-insensitive mutant in Arabidopsis thaliana exhibits multiple defects in growth and development. *Plant Physiology*, 111(3):671–678, July 1996.

[100] M. Szekeres, K. Németh, Z. Koncz-Kálmán, J. Mathur, A. Kauschmann, T. Altmann, G. P. Rédei, F. Nagy, J. Schell, and C. Koncz. Brassinosteroids rescue the deficiency of CYP90, a cytochrome P450, controlling cell elongation and de-etiolation in Arabidopsis. *Cell*, 85(2):171–182, April 1996.

[101] S. D. Clouse and J. M. Sasse. BRASSINOSTEROIDS: Essential Regulators of Plant Growth and Development. *Annual Review of Plant Physiology and Plant Molecular Biology*, 49(1):427–451, June 1998. URL: http://www.annualreviews.org/doi/10.1146/annurev.arplant.49.1.427, doi:10.1146/annurev.arplant.49.1.427.

[102] J. Li and J. Chory. Brassinosteroid actions in plants. *Journal of Experimental Botany*, 50(332):275–282, March 1999. URL: https://academic.oup.com/jxb/article-lookup/doi/10.1093/jxb/50.332.275, doi:10.1093/jxb/50.332.275.

[103] J. Li, P. Nagpal, V. Vitart, T. C. McMorris, and J. Chory. A Role for Brassinosteroids in Light-Dependent Development of Arabidopsis. *Science*, 272(5260):398–401, April 1996. URL: http://www.sciencemag.org/cgi/doi/10.1126/science.272.5260.398, doi:10.1126/science.272.5260.398.

[104] S. D. Clouse. Brassinosteroid Signal Transduction: From Receptor Kinase Activation to Transcriptional Networks Regulating Plant Development. *The Plant Cell*, 23(4):1219–1230, April 2011. URL: http://www.plantcell.org/lookup/doi/10.1105/tpc.111.084475, doi:10.1105/tpc.111.084475.

[105] C.-J. Yang, C. Zhang, Y.-N. Lu, J.-Q. Jin, and X.-L. Wang. The Mechanisms of Brassinosteroids' Action: From Signal Transduction to Plant Development. *Molecular Plant*, 4(4):588–600, July 2011. URL: https://linkinghub.elsevier.com/retrieve/pii/S1674205214606845, doi:10.1093/mp/ssr020.

[106] J. Li and J. Chory. A putative leucine-rich repeat receptor kinase involved in brassinosteroid signal transduction. *Cell*, 90(5):929–938, September 1997.

[107] Z. He, Z. Y. Wang, J. Li, Q. Zhu, C. Lamb, P. Ronald, and J. Chory. Perception of brassinosteroids by the extracellular domain of the receptor kinase BRI1. *Science (New York, N.Y.)*, 288(5475):2360–2363, June 2000.

[108] X. Wang. Brassinosteroids Regulate Dissociation of BKI1, a Negative Regulator of BRI1 Signaling, from the Plasma Membrane. *Science*, 313(5790):1118–1122, August 2006. URL: http://www.sciencemag.org/cgi/doi/10.1126/science.1127593, doi:10.1126/science.1127593.

[109] J. Li, J. Wen, K. A. Lease, J. T. Doke, F. E. Tax, and J. C. Walker. BAK1, an Arabidopsis LRR receptor-like protein kinase, interacts with BRI1 and modulates brassinosteroid signaling. *Cell*, 110(2):213–222, July 2002.

[110] K. H. Nam and J. Li. BRI1/BAK1, a receptor kinase pair mediating brassinosteroid signaling. *Cell*, 110(2):203–212, July 2002.

[111] M.-Y. Bai, L.-Y. Zhang, S. S. Gampala, S.-W. Zhu, W.-Y. Song, K. Chong, and Z.-Y. Wang. Functions of OsBZR1 and 14-3-3 proteins in brassinosteroid signaling in rice. *Proceedings of the National Academy of Sciences*, 104(34):13839–13844, August 2007. URL: http://www.pnas.org/cgi/doi/10.1073/pnas.0706386104, doi:10.1073/pnas.0706386104.

[112] S. S. Gampala, T.-W. Kim, J.-X. He, W. Tang, Z. Deng, M.-Y. Bai, S. Guan, S. Lalonde, Y. Sun, J. M. Gendron, H. Chen, N. Shibagaki, R. J. Ferl, D. Ehrhardt, K. Chong, A. L. Burlingame, and Z.-Y. Wang. An Essential Role for 14-3-3 Proteins in Brassinosteroid Signal Transduction in Arabidopsis. *Developmental Cell*, 13(2):177–189, August 2007. URL: https://linkinghub.elsevier.com/retrieve/pii/S1534580707002584, doi:10.1016/j.devcel.2007.06.009.

[113] G. Vert and J. Chory. Downstream nuclear events in brassinosteroid signalling. *Nature*, 441(7089):96–100, May 2006. URL: http://www.nature.com/articles/nature04681, doi:10.1038/nature04681.

[114] T.-W. Kim, S. Guan, A. Burlingame, and Z.-Y. Wang. The CDG1 Kinase Mediates Brassinosteroid Signal Transduction from BRI1 Receptor Kinase to BSU1 Phosphatase and GSK3-like Kinase BIN2. *Molecular Cell*, 43(4):561–571, August 2011. URL: https://linkinghub.elsevier.com/retrieve/pii/S1097276511005284, doi:10.1016/j.molcel.2011.05.037.

[115] W. Tang, T.-W. Kim, J. A. Oses-Prieto, Y. Sun, Z. Deng, S. Zhu, R. Wang, A. L. Burlingame, and Z.-Y. Wang. BSKs Mediate Signal Transduction from the Receptor Kinase BRI1 in Arabidopsis. *Science*, 321(5888):557–560, July 2008. URL: http://www.sciencemag.org/cgi/doi/10.1126/science.1156973, doi:10.1126/science.1156973.

[116] T.-W. Kim, S. Guan, Y. Sun, Z. Deng, W. Tang, J.-X. Shang, Y. Sun, A. L. Burlingame, and Z.-Y. Wang. Brassinosteroid signal transduction from cell-surface receptor kinases to nuclear transcription factors. *Nature Cell Biology*, 11(10):1254–1260, October 2009. URL: http://www.nature.com/articles/ncb1970, doi:10.1038/ncb1970.

[117] S. Mora-Garcia. Nuclear protein phosphatases with Kelch-repeat domains modulate the response to brassinosteroids in Arabidopsis. *Genes & Development*, 18(4):448–460, February 2004. URL: http://www.genesdev.org/cgi/doi/10.1101/gad.1174204, doi:10.1101/gad.1174204.

[118] P. Peng, Z. Yan, Y. Zhu, and J. Li. Regulation of the Arabidopsis GSK3-like Kinase BRASSINOSTEROID-INSENSITIVE 2 through Proteasome-Mediated Protein Degradation. *Molecular Plant*, 1(2):338–346, March 2008. URL: https://linkinghub.elsevier.com/retrieve/pii/S1674205214604408, doi:10.1093/mp/ssn001.

[119] W. Tang, M. Yuan, R. Wang, Y. Yang, C. Wang, J. A. Oses-Prieto, T.-W. Kim, H.-W. Zhou, Z. Deng, S. S. Gampala, J. M. Gendron, E. M. Jonassen, C. Lillo, A. DeLong, A. L. Burlingame, Y. Sun, and Z.-Y. Wang. PP2a activates brassinosteroid-responsive gene expression and plant growth by dephosphorylating BZR1. *Nature Cell Biology*, 13(2):124–131, February 2011. URL: http://www.nature.com/articles/ncb2151, doi:10.1038/ncb2151.

[120] J.-X. He. BZR1 Is a Transcriptional Repressor with Dual Roles in Brassinosteroid Homeostasis and Growth Responses. *Science*, 307(5715):1634–1638, March 2005. URL: http://www.sciencemag.org/cgi/doi/10.1126/science.1107580, doi:10.1126/science.1107580.

[121] Y. Sun, X.-Y. Fan, D.-M. Cao, W. Tang, K. He, J.-Y. Zhu, J.-X. He, M.-Y. Bai, S. Zhu, E. Oh, S. Patil, T.-W. Kim, H. Ji, W. H. Wong, S. Y. Rhee, and Z.-Y. Wang. Integration of Brassinosteroid Signal Transduction with the Transcription Network for Plant Growth Regulation in Arabidopsis. *Developmental Cell*, 19(5):765–777, November 2010. URL: https://linkinghub.elsevier.com/retrieve/pii/S1534580710004636, doi:10.1016/j.devcel.2010.10.010.

[122] Y. Yin, D. Vafeados, Y. Tao, S. Yoshida, T. Asami, and J. Chory. A New Class of Transcription Factors Mediates Brassinosteroid-Regulated Gene Expression in Arabidopsis. *Cell*, 120(2):249–259, January 2005. URL: http://linkinghub.elsevier.com/retrieve/pii/S0092867404011481, doi:10.1016/j.cell.2004.11.044.

[123] X. Yu, L. Li, L. Li, M. Guo, J. Chory, and Y. Yin. Modulation of brassinosteroid-regulated gene expression by jumonji domain-containing proteins ELF6 and REF6 in Arabidopsis. *Proceedings of the National Academy of Sciences*, 105(21):7618–7623, May 2008. URL: http://www.pnas.org/cgi/doi/10.1073/pnas.0802254105, doi:10.1073/pnas.0802254105.

[124] C. M. Steber. A Role for Brassinosteroids in Germination in Arabidopsis. *PLANT PHYSIOLOGY*, 125(2):763–769, February 2001. URL: http://www.plantphysiol.org/cgi/doi/10.1104/pp.125.2.763, doi:10.1104/pp.125.2.763.

[125] G. Leubner-Metzger. Brassinosteroids and gibberellins promote tobacco seed germination by distinct pathways. *Planta*, 213(5):758–763, September 2001.

[126] C. S. Hardtke. Transcriptional auxin–brassinosteroid crosstalk: Who's talking? *BioEssays*, 29(11):1115–1123, November 2007. URL: http://doi.wiley.com/10.1002/bies.20653, doi:10.1002/bies.20653.

[127] K. J. Halliday. Plant Hormones: The Interplay of Brassinosteroids and Auxin. *Current Biology*, 14(23):R1008–R1010, December 2004. URL: http://linkinghub.elsevier.com/retrieve/pii/S0960982204008930, doi:10.1016/j.cub.2004.11.025.

[128] S. Shahnejat-Bushehri, D. Tarkowska, Y. Sakuraba, and S. Balazadeh. Arabidopsis NAC transcription factor JUB1 regulates GA/BR metabolism and signalling. *Nature Plants*, 2(3):16013, February 2016. URL: http://www.nature.com/articles/nplants201613, doi:10.1038/nplants.2016.13.

[129] H. Tong, Y. Xiao, D. Liu, S. Gao, L. Liu, Y. Yin, Y. Jin, Q. Qian, and C. Chu. Brassinosteroid regulates cell elongation by modulating gibberellin metabolism in rice. *The Plant Cell*, 26(11):4376–4393, November 2014. doi:10.1105/tpc.114.132092.

[130] C. O. Miller, F. Skoog, F. S. Okumura, M. H. Von Saltza, and F. M. Strong. Isolation, Structure and Synthesis of Kinetin, a Substance Promoting Cell Division [1,2]. *Journal of the American Chemical Society*, 78(7):1375–1380, April 1956. URL: http://pubs.acs.org/doi/abs/10.1021/ja01588a032, doi:10.1021/ja01588a032.

[131] C. O. Miller. Kinetin and Related Compounds in Plant Growth. *Annual Review of Plant Physiology*, 12(1):395–408, June 1961. URL: http://www.annualreviews.org/doi/10.1146/annurev.pp.12.060161.002143, doi:10.1146/annurev.pp.12.060161.002143.

[132] T. Werner. Cytokinin-Deficient Transgenic Arabidopsis Plants Show Multiple Developmental Alterations Indicating Opposite Functions of Cytokinins in the Regulation of Shoot and Root Meristem Activity. *THE PLANT CELL ONLINE*, 15(11):2532–2550, October 2003. URL: http://www.plantcell.org/cgi/doi/10.1105/tpc.014928, doi:10.1105/tpc.014928.

[133] F. J. Ferreira and J. J. Kieber. Cytokinin signaling. *Current Opinion in Plant Biology*, 8(5):518–525, October 2005. URL: http://linkinghub.elsevier.com/retrieve/pii/S1369526605001032, doi:10.1016/j.pbi.2005.07.013.

[134] T. Kakimoto. CKI1, a Histidine Kinase Homolog Implicated in Cytokinin Signal Transduction. *Science*, 274(5289):982–985, November 1996. URL: http://www.sciencemag.org/lookup/doi/10.1126/science.274.5289.982, doi:10.1126/science.274.5289.982.

[135] I. Hwang. Two-Component Signal Transduction Pathways in Arabidopsis. *PLANT PHYSIOLOGY*, 129(2):500–515, June 2002. URL: http://www.plantphysiol.org/cgi/doi/10.1104/pp.005504, doi:10.1104/pp.005504.

[136] P. M. Wolanin, P. A. Thomason, and J. B. Stock. Histidine protein kinases: key signal transducers outside the animal kingdom. *Genome Biology*, 3(10):REVIEWS3013, September 2002.

[137] J.-R. Kim and K.-H. Cho. The multi-step phosphorelay mechanism of unorthodox two-component systems in E. coli realizes ultrasensitivity to stimuli while maintaining robustness to noises. *Computational Biology and Chemistry*, 30(6):438–444, December 2006. doi:10.1016/j.compbiolchem.2006.09.004.

[138] T. Urao, K. Yamaguchi-Shinozaki, and K. Shinozaki. Plant Histidine Kinases: An Emerging Picture of Two-Component Signal Transduction in Hormone and Environmental Responses. *Science Signaling*, 2001(109):re18–re18, November 2001. URL: http://stke.sciencemag.org/cgi/doi/10.1126/stke.2001.109.re18, doi:10.1126/stke.2001.109.re18.

[139] M. Higuchi, M. S. Pischke, A. P. Mahonen, K. Miyawaki, Y. Hashimoto, M. Seki, M. Kobayashi, K. Shinozaki, T. Kato, S. Tabata, Y. Helariutta, M. R. Sussman, and T. Kakimoto. In planta functions of the Arabidopsis cytokinin receptor family. *Proceedings of the National Academy of Sciences*, 101(23):8821–8826, June 2004. URL: http://www.pnas.org/cgi/doi/10.1073/pnas.0402887101, doi:10.1073/pnas.0402887101.

[140] C. Nishimura. Histidine Kinase Homologs That Act as Cytokinin Receptors Possess Overlapping Functions in the Regulation of Shoot and Root Growth in Arabidopsis. *THE PLANT CELL ONLINE*, 16(6):1365–1377, June 2004. URL: http://www.plantcell.org/cgi/doi/10.1105/tpc.021477, doi:10.1105/tpc.021477.

[141] T. Suzuki, K. Sakurai, A. Imamura, A. Nakamura, C. Ueguchi, and T. Mizuno. Compilation and Characterization of Histidine-Containing Phosphotransmitters Implicated in His-to-Asp Phosphorelay in Plants: AHP Signal Transducers of *Arabidopsis thaliana*. *Bioscience, Biotechnology, and Biochemistry*, 64(11):2486–2489, January 2000. URL: http://www.tandfonline.com/doi/full/10.1271/bbb.64.2486, doi:10.1271/bbb.64.2486.

[142] S. Miyata, T. Urao, K. Yamaguchi-Shinozaki, and K. Shinozaki. Characterization of genes for two-component phosphorelay mediators with a single HPt domain in Arabidopsis thaliana. *FEBS letters*, 437(1-2):11–14, October 1998.

[143] T. Suzuki, A. Imamura, C. Ueguchi, and T. Mizuno. Histidine-containing phosphotransfer (HPt) signal transducers implicated in His-to-Asp phosphorelay in Arabidopsis. *Plant & Cell Physiology*, 39(12):1258–1268, December 1998.

[144] M. Xie, H. Chen, L. Huang, R. C. O'Neil, M. N. Shokhirev, and J. R. Ecker. A B-ARR-mediated cytokinin transcriptional network directs hormone cross-regulation and shoot development. *Nature Communications*, 9(1), December 2018. URL: http://www.nature.com/articles/s41467-018-03921-6, doi:10.1038/s41467-018-03921-6.

[145] K. Hosoda. Molecular Structure of the GARP Family of Plant Myb-Related DNA Binding Motifs of the Arabidopsis Response Regulators. *THE PLANT CELL ONLINE*, 14(9):2015–2029, September 2002. URL: http://www.plantcell.org/cgi/doi/10.1105/tpc.002733, doi:10.1105/tpc.002733.

[146] I. B. D'Agostino, J. Deruère, and J. J. Kieber. Characterization of the Response of the Arabidopsis Response Regulator Gene Family to Cytokinin. *Plant Physiology*, 124(4):1706–1717, December 2000. URL: http://www.plantphysiol.org/lookup/doi/10.1104/pp.124.4.1706, doi:10.1104/pp.124.4.1706.

[147] V. Anantharaman and L. Aravind. The CHASE domain: a predicted ligand-binding module in plant cytokinin receptors and other eukaryotic and bacterial receptors. *Trends in Biochemical Sciences*, 26(10):579–582, October 2001. URL: http://linkinghub.elsevier.com/retrieve/pii/S0968000401019685, doi:10.1016/S0968-0004(01)01968-5.

[148] R. Nishiyama, Y. Watanabe, Y. Fujita, D. T. Le, M. Kojima, T. Werner, R. Vankova, K. Yamaguchi-Shinozaki, K. Shinozaki, T. Kakimoto, H. Sakakibara, T. Schmülling, and L.-S. P. Tran. Analysis of Cytokinin Mutants and Regulation of Cytokinin Metabolic Genes Reveals Important Regulatory Roles of Cytokinins in Drought, Salt and Abscisic Acid Responses, and Abscisic Acid Biosynthesis. *The Plant Cell*, 23(6):2169–2183, June 2011. URL: http://www.plantcell.org/lookup/doi/10.1105/tpc.111.087395, doi:10.1105/tpc.111.087395.

[149] K. H. Nguyen, C. V. Ha, R. Nishiyama, Y. Watanabe, M. A. Leyva-González, Y. Fujita, U. T. Tran, W. Li, M. Tanaka, M. Seki, G. E. Schaller, L. Herrera-Estrella, and L.-S. P. Tran. *Arabidopsis* type B cytokinin response regulators ARR1, ARR10, and ARR12 negatively regulate plant responses to drought. *Proceedings of the National Academy of Sciences*, 113(11):3090–3095, March 2016. URL: http://www.pnas.org/lookup/doi/10.1073/pnas.1600399113, doi:10.1073/pnas.1600399113.

[150] N. Iqbal, N. A. Khan, A. Ferrante, A. Trivellini, A. Francini, and M. I. R. Khan. Ethylene Role in Plant Growth, Development and Senescence: Interaction with Other Phytohormones. *Frontiers in Plant Science*, 08, April 2017. URL: http://journal.frontiersin.org/article/10.3389/fpls.2017.00475/full, doi:10.3389/fpls.2017.00475.

[151] M. Dubois, A. Skirycz, H. Claeys, K. Maleux, S. Dhondt, S. De Bodt, R. Vanden Bossche, L. De Milde, T. Yoshizumi, M. Matsui, and D. Inze. ETHYLENE RESPONSE FACTOR6 Acts as a Central Regulator of Leaf Growth under Water-Limiting Conditions in Arabidopsis. *PLANT PHYSIOLOGY*, 162(1):319–332, May 2013. URL: http://www.plantphysiol.org/cgi/doi/10.1104/pp.113.216341, doi:10.1104/pp.113.216341.

[152] R. F. Lacey and B. M. Binder. How plants sense ethylene gas — The ethylene receptors. *Journal of Inorganic Biochemistry*, 133:58–62, April 2014. URL: https://linkinghub.elsevier.com/retrieve/pii/S0162013414000105, doi:10.1016/j.jinorgbio.2014.01.006.

[153] A. B. Bleecker, M. A. Estelle, C. Somerville, and H. Kende. Insensitivity to Ethylene Conferred by a Dominant Mutation in Arabidopsis thaliana. *Science*, 241(4869):1086–1089, August 1988. URL: http://www.sciencemag.org/cgi/doi/10.1126/science.241.4869.1086, doi:10.1126/science.241.4869.1086.

[154] C. Chang, S. F. Kwok, A. B. Bleecker, and E. M. Meyerowitz. Arabidopsis ethylene-response gene ETR1: similarity of product to two-component regulators. *Science (New York, N.Y.)*, 262(5133):539–544, October 1993.

[155] P. Guzman. Exploiting the Triple Response of Arabidopsis To Identify Ethylene-Related Mutants. *THE PLANT CELL ONLINE*, 2(6):513–523, June 1990. URL: http://www.plantcell.org/cgi/doi/10.1105/tpc.2.6.513, doi:10.1105/tpc.2.6.513.

[156] J. Hua, C. Chang, Q. Sun, and E. M. Meyerowitz. Ethylene insensitivity conferred by Arabidopsis ERS gene. *Science (New York, N.Y.)*, 269(5231):1712–1714, September 1995.

[157] J. Hua and E. M. Meyerowitz. Ethylene Responses Are Negatively Regulated by a Receptor Gene Family in Arabidopsis thaliana. *Cell*, 94(2):261–271, July 1998. URL: http://linkinghub.elsevier.com/retrieve/pii/S0092867400814257, doi:10.1016/S0092-8674(00)81425-7.

[158] H. Sakai, J. Hua, Q. G. Chen, C. Chang, L. J. Medrano, A. B. Bleecker, and E. M. Meyerowitz. ETR2 is an ETR1-like gene involved in ethylene signaling in Arabidopsis. *Proceedings of the National Academy of Sciences of the United States of America*, 95(10):5812–5817, May 1998.

[159] Y.-F. Chen, M. D. Randlett, J. L. Findell, and G. E. Schaller. Localization of the Ethylene Receptor ETR1 to the Endoplasmic Reticulum of *Arabidopsis*. *Journal of Biological Chemistry*, 277(22):19861–19866, May 2002. URL: http://www.jbc.org/lookup/doi/10.1074/jbc.M201286200, doi:10.1074/jbc.M201286200.

[160] Z. Gao, Y.-F. Chen, M. D. Randlett, X.-C. Zhao, J. L. Findell, J. J. Kieber, and G. E. Schaller. Localization of the Raf-like Kinase CTR1 to the Endoplasmic Reticulum of *Arabidopsis* through Participation in Ethylene Receptor Signaling Complexes. *Journal of Biological Chemistry*, 278(36):34725–34732, September 2003. URL: http://www.jbc.org/lookup/doi/10.1074/jbc.M305548200, doi:10.1074/jbc.M305548200.

[161] Y.-S. J. Ho. Structure of the GAF domain, a ubiquitous signaling motif and a new class of cyclic GMP receptor. *The EMBO Journal*, 19(20):5288–5299, October 2000. URL: http://emboj.embopress.org/cgi/doi/10.1093/emboj/19.20.5288, doi:10.1093/emboj/19.20.5288.

[162] H. Kim, E. E. Helmbrecht, M. B. Stalans, C. Schmitt, N. Patel, C.-K. Wen, W. Wang, and B. M. Binder. Ethylene Receptor ETHYLENE RECEPTOR1 Domain Requirements for Ethylene Responses in Arabidopsis Seedlings. *PLANT PHYSIOLOGY*, 156(1):417–429, May 2011. URL: http://www.plantphysiol.org/cgi/doi/10.1104/pp.110.170621, doi:10.1104/pp.110.170621.

[163] C. Xie, J.-S. Zhang, H.-L. Zhou, J. Li, Z.-G. Zhang, D.-W. Wang, and S.-Y. Chen. Serine/threonine kinase activity in the putative histidine kinase-like ethylene receptor NTHK1 from tobacco. *The Plant Journal*, 33(2):385–393, January 2003. URL: http://doi.wiley.com/10.1046/j.1365-313X.2003.01631.x, doi:10.1046/j.1365-313X.2003.01631.x.

[164] P. Moussatche and H. J. Klee. Autophosphorylation Activity of the Arabidopsis Ethylene Receptor Multigene Family. *Journal of Biological Chemistry*, 279(47):48734–48741, November 2004. URL: http://www.jbc.org/lookup/doi/10.1074/jbc.M403100200, doi:10.1074/jbc.M403100200.

[165] R. L. Gamble, X. Qu, and G. E. Schaller. Mutational Analysis of the Ethylene Receptor ETR1. Role of the Histidine Kinase Domain in Dominant Ethylene Insensitivity. *PLANT PHYSIOLOGY*, 128(4):1428–1438, April 2002. URL: http://www.plantphysiol.org/cgi/doi/10.1104/pp.010777, doi:10.1104/pp.010777.

[166] X. Qu. Requirement of the Histidine Kinase Domain for Signal Transduction by the Ethylene Receptor ETR1. *PLANT PHYSIOLOGY*, 136(2):2961–2970, October 2004. URL: http://www.plantphysiol.org/cgi/doi/10.1104/pp.104.047126, doi:10.1104/pp.104.047126.

[167] C. Ju, G. M. Yoon, J. M. Shemansky, D. Y. Lin, Z. I. Ying, J. Chang, W. M. Garrett, M. Kessenbrock, G. Groth, M. L. Tucker, B. Cooper, J. J. Kieber, and C. Chang. CTR1 phosphorylates the central regulator EIN2 to control ethylene hormone signaling from the ER membrane to the nucleus in Arabidopsis. *Proceedings of the National Academy of Sciences*, 109(47):19486–19491, November 2012. URL: http://www.pnas.org/cgi/doi/10.1073/pnas.1214848109, doi:10.1073/pnas.1214848109.

[168] H. Guo and J. R. Ecker. Plant responses to ethylene gas are mediated by SCF(EBF1/EBF2)-dependent proteolysis of EIN3 transcription factor. *Cell*, 115(6):667–677, December 2003.

[169] K.-J. Dietz, M. O. Vogel, and A. Viehhauser. AP2/EREBP transcription factors are part of gene regulatory networks and integrate metabolic, hormonal and environmental signals in stress acclimation and retrograde signalling. *Protoplasma*, 245(1-4):3–14, September 2010. URL: http://link.springer.com/10.1007/s00709-010-0142-8, doi:10.1007/s00709-010-0142-8.

[170] J. L. Riechmann and E. M. Meyerowitz. The AP2/EREBP family of plant transcription factors. *Biological Chemistry*, 379(6):633–646, June 1998.

[171] C. J. Brady. Fruit Ripening. *Annual Review of Plant Physiology*, 38(1):155–178, June 1987. URL: http://www.annualreviews.org/doi/10.1146/annurev.pp.38.060187.001103, doi:10.1146/annurev.pp.38.060187.001103.

[172] X. Di, J. Gomila, and F. L. W. Takken. Involvement of salicylic acid, ethylene and jasmonic acid signalling pathways in the susceptibility of tomato to *Fusarium oxysporum*: Phytohormones and susceptibility to *Fol*. *Molecular Plant Pathology*, 18(7):1024–1035, September 2017. URL: http://doi.wiley.com/10.1111/mpp.12559, doi:10.1111/mpp.12559.

[173] N. Li, X. Han, D. Feng, D. Yuan, and L.-J. Huang. Signaling Crosstalk between Salicylic Acid and Ethylene/Jasmonate in Plant Defense: Do We Understand What They Are Whispering? *International Journal of Molecular Sciences*, 20(3):671, February 2019. URL: http://www.mdpi.com/1422-0067/20/3/671, doi:10.3390/ijms20030671.

[174] N. Beaudoin. Interactions between Abscisic Acid and Ethylene Signaling Cascades. *THE PLANT CELL ONLINE*, 12(7):1103–1116, July 2000. URL: http://www.plantcell.org/cgi/doi/10.1105/tpc.12.7.1103, doi:10.1105/tpc.12.7.1103.

[175] K. Sawada. Contributions on Formosan fungi. *Transactions of the Natural History Society of Formosa*, 4(7):131–133, 1917.

[176] N. Takahashi, H. Kitamura, A. Kawarada, Y. Seta, M. Takai, S. Tamura, and Y. Sumiki. Biochemical Studies on "Bakanae" Fungus. *Bulletin of the Agricultural Chemical Society of Japan*, 19(4):267–277, 1955. URL: http://joi.jlc.jst.go.jp/JST.Journalarchive/bbb1924/19.267?from=CrossRef, doi:10.1271/bbb1924.19.267.

[177] J. MacMillan. Occurrence of Gibberellins in Vascular Plants, Fungi, and Bacteria. *Journal of Plant Growth Regulation*, 20(4):387–442, December 2001. URL: http://link.springer.com/10.1007/s003440010038, doi:10.1007/s003440010038.

[178] J. Peng. The role of GA-mediated signalling in the control of seed germination. *Current Opinion in Plant Biology*, 5(5):376–381, October 2002. URL: http://linkinghub.elsevier.com/retrieve/pii/S1369526602002790, doi:10.1016/S1369-5266(02)00279-0.

[179] R. J. Cowling and N. P. Harberd. Gibberellins control Arabidopsis hypocotyl growth via regulation of cellular elongation. *Journal of Experimental Botany*, 50(337):1351–1357, August 1999. URL: https://academic.oup.com/jxb/article-lookup/doi/10.1093/jxb/50.337.1351, doi:10.1093/jxb/50.337.1351.

[180] M. Ueguchi-Tanaka, M. Ashikari, M. Nakajima, H. Itoh, E. Katoh, M. Kobayashi, T.-y. Chow, Y.-i. C. Hsing, H. Kitano, I. Yamaguchi, and M. Matsuoka. GIBBERELLIN INSENSITIVE DWARF1 encodes a soluble receptor for gibberellin. *Nature*, 437(7059):693–698, September 2005. URL: http://www.nature.com/articles/nature04028, doi:10.1038/nature04028.

[181] M. Nakajima, A. Shimada, Y. Takashi, Y.-C. Kim, S.-H. Park, M. Ueguchi-Tanaka, H. Suzuki, E. Katoh, S. Iuchi, M. Kobayashi, T. Maeda, M. Matsuoka, and I. Yamaguchi. Identification and characterization of Arabidopsis gibberellin receptors. *The Plant Journal*, 46(5):880–889, June 2006. URL: http://doi.wiley.com/10.1111/j.1365-313X.2006.02748.x, doi:10.1111/j.1365-313X.2006.02748.x.

[182] A. L. Silverstone, P. Y. Mak, E. C. Martínez, and T. P. Sun. The new RGA locus encodes a negative regulator of gibberellin response in Arabidopsis thaliana. *Genetics*, 146(3):1087–1099, July 1997.

[183] A. L. Silverstone, C. N. Ciampaglio, and T. Sun. The Arabidopsis RGA gene encodes a transcriptional regulator repressing the gibberellin signal transduction pathway. *The Plant Cell*, 10(2):155–169, February 1998.

[184] J. Peng, P. Carol, D. E. Richards, K. E. King, R. J. Cowling, G. P. Murphy, and N. P. Harberd. The Arabidopsis GAI gene defines a signaling pathway that negatively regulates gibberellin responses. *Genes & Development*, 11(23):3194–3205, December 1997.

[185] C.-K. Wen. Arabidopsis RGL1 Encodes a Negative Regulator of Gibberellin Responses. *THE PLANT CELL ONLINE*, 14(1):87–100, January 2002. URL: http://www.plantcell.org/cgi/doi/10.1105/tpc.010325, doi:10.1105/tpc.010325.

[186] S. Lee. Gibberellin regulates Arabidopsis seed germination via RGL2, a GAI/RGA-like gene whose expression is up-regulated following imbibition. *Genes & Development*, 16(5):646–658, March 2002. URL: http://www.genesdev.org/cgi/doi/10.1101/gad.969002, doi:10.1101/gad.969002.

[187] K. M. McGinnis, S. G. Thomas, J. D. Soule, L. C. Strader, J. M. Zale, T.-p. Sun, and C. M. Steber. The Arabidopsis SLEEPY1 gene encodes a putative F-box subunit of an SCF E3 ubiquitin ligase. *The Plant Cell*, 15(5):1120–1130, May 2003.

[188] A. Dill. The Arabidopsis F-Box Protein SLEEPY1 Targets Gibberellin Signaling Repressors for Gibberellin-Induced Degradation. *THE PLANT CELL ONLINE*, 16(6):1392–1405, June 2004. URL: http://www.plantcell.org/cgi/doi/10.1105/tpc.020958, doi:10.1105/tpc.020958.

[189] H. Yoshida, K. Hirano, T. Sato, N. Mitsuda, M. Nomoto, K. Maeo, E. Koketsu, R. Mitani, M. Kawamura, S. Ishiguro, Y. Tada, M. Ohme-Takagi, M. Matsuoka, and M. Ueguchi-Tanaka. DELLA protein functions as a transcriptional activator through the DNA binding of the INDETERMINATE DOMAIN family proteins. *Proceedings of the National Academy of Sciences*, 111(21):7861–7866, May 2014. URL: http://www.pnas.org/cgi/doi/10.1073/pnas.1321669111, doi:10.1073/pnas.1321669111.

[190] F. A. Razem, K. Baron, and R. D. Hill. Turning on gibberellin and abscisic acid signaling. *Current Opinion in Plant Biology*, 9(5):454–459, October 2006. URL: https://linkinghub.elsevier.com/retrieve/pii/S1369526606001130, doi:10.1016/j.pbi.2006.07.007.

[191] S. Lim, J. Park, N. Lee, J. Jeong, S. Toh, A. Watanabe, J. Kim, H. Kang, D. H. Kim, N. Kawakami, and G. Choi. ABA-INSENSITIVE3, ABA-INSENSITIVE5, and DELLAs Interact to Activate the Expression of SOMNUS and Other High-Temperature-Inducible Genes in Imbibed Seeds in Arabidopsis. *The Plant Cell*, 25(12):4863–4878, December 2013. URL: http://www.plantcell.org/cgi/doi/10.1105/tpc.113.118604, doi:10.1105/tpc.113.118604.

[192] E. Oh, J.-Y. Zhu, M.-Y. Bai, R. A. Arenhart, Y. Sun, and Z.-Y. Wang. Cell elongation is regulated through a central circuit of interacting transcription factors in the Arabidopsis hypocotyl. *eLife*, 3, May 2014. URL: https://elifesciences.org/articles/03031, doi:10.7554/eLife.03031.

[193] M.-Y. Bai, J.-X. Shang, E. Oh, M. Fan, Y. Bai, R. Zentella, T.-p. Sun, and Z.-Y. Wang. Brassinosteroid, gibberellin and phytochrome impinge on a common transcription module in Arabidopsis. *Nature Cell Biology*, 14(8):810–817, August 2012. URL: http://www.nature.com/articles/ncb2546, doi:10.1038/ncb2546.

[194] M.-Y. Bai, M. Fan, E. Oh, and Z.-Y. Wang. A Triple Helix-Loop-Helix/Basic Helix-Loop-Helix Cascade Controls Cell Elongation Downstream of Multiple Hormonal and Environmental Signaling Pathways in Arabidopsis. *The Plant Cell*, 24(12):4917–4929, December 2012. URL: http://www.plantcell.org/cgi/doi/10.1105/tpc.112.105163, doi:10.1105/tpc.112.105163.

[195] Q.-F. Li, C. Wang, L. Jiang, S. Li, S. S. M. Sun, and J.-X. He. An Interaction Between BZR1 and DELLAs Mediates Direct Signaling Crosstalk Between Brassinosteroids and Gibberellins in Arabidopsis. *Science Signaling*, 5(244):ra72–ra72, October 2012. URL: http://stke.sciencemag.org/cgi/doi/10.1126/scisignal.2002908, doi:10.1126/scisignal.2002908.

[196] L. Navarro, R. Bari, P. Achard, P. Lisón, A. Nemri, N. P. Harberd, and J. D. Jones. DELLAs Control Plant Immune Responses by Modulating the Balance of Jasmonic Acid and Salicylic Acid Signaling. *Current Biology*, 18(9):650–655, May 2008. URL: http://linkinghub.elsevier.com/retrieve/pii/S096098220800465X, doi:10.1016/j.cub.2008.03.060.

[197] X. Hou, L. Y. C. Lee, K. Xia, Y. Yan, and H. Yu. DELLAs modulate jasmonate signaling via competitive binding to JAZs. *Developmental Cell*, 19(6):884–894, December 2010. doi:10.1016/j.devcel.2010.10.024.

[198] Z. Q. Fu and X. Dong. Systemic Acquired Resistance: Turning Local Infection into Global Defense. *Annual Review of Plant Biology*, 64(1):839–863, April 2013. URL: http://www.annualreviews.org/doi/10.1146/annurev-arplant-042811-105606, doi:10.1146/annurev-arplant-042811-105606.

[199] C. Zipfel. Early molecular events in PAMP-triggered immunity. *Current Opinion in Plant Biology*, 12(4):414–420, August 2009. URL: https://linkinghub.elsevier.com/retrieve/pii/S1369526609000648, doi:10.1016/j.pbi.2009.06.003.

[200] U. Conrath, C. M. J. Pieterse, and B. Mauch-Mani. Priming in plant-pathogen interactions. *Trends in Plant Science*, 7(5):210–216, May 2002.

[201] U. Conrath, G. J. M. Beckers, V. Flors, P. García-Agustín, G. Jakab, F. Mauch, M.-A. Newman, C. M. J. Pieterse, B. Poinssot, M. J. Pozo, A. Pugin, U. Schaffrath, J. Ton, D. Wendehenne, L. Zimmerli, and B. Mauch-Mani. Priming: Getting Ready for Battle. *Molecular Plant-Microbe Interactions*, 19(10):1062–1071, October 2006. URL: http://apsjournals.apsnet.org/doi/10.1094/MPMI-19-1062, doi:10.1094/MPMI-19-1062.

[202] J. J. Furniss and S. H. Spoel. Cullin-RING ubiquitin ligases in salicylic acid-mediated plant immune signaling. *Frontiers in Plant Science*, 6, March 2015. URL: http://www.frontiersin.org/Plant-Microbe_Interaction/10.3389/fpls.2015.00154/abstract, doi:10.3389/fpls.2015.00154.

[203] Z. Q. Fu, S. Yan, A. Saleh, W. Wang, J. Ruble, N. Oka, R. Mohan, S. H. Spoel, Y. Tada, N. Zheng, and X. Dong. NPR3 and NPR4 are receptors for the immune signal salicylic acid in plants. *Nature*, 486(7402):228–232, June 2012. URL: http://www.nature.com/articles/nature11162, doi:10.1038/nature11162.

[204] H. Cao. Characterization of an Arabidopsis Mutant That Is Nonresponsive to Inducers of Systemic Acquired Resistance. *THE PLANT CELL ONLINE*, 6(11):1583–1592, November 1994. URL: http://www.plantcell.org/cgi/doi/10.1105/tpc.6.11.1583, doi:10.1105/tpc.6.11.1583.

[205] T. P. Delaney, L. Friedrich, and J. A. Ryals. Arabidopsis signal transduction mutant defective in chemically and biologically induced disease resistance. *Proceedings of the National Academy of Sciences of the United States of America*, 92(14):6602–6606, July 1995.

[206] Y. Wu, D. Zhang, J. Y. Chu, P. Boyle, Y. Wang, I. D. Brindle, V. De Luca, and C. Després. The Arabidopsis NPR1 protein is a receptor for the plant defense hormone salicylic acid. *Cell Reports*, 1(6):639–647, June 2012. doi:10.1016/j.celrep.2012.05.008.

[207] M. Kinkema, W. Fan, and X. Dong. Nuclear localization of NPR1 is required for activation of PR gene expression. *The Plant Cell*, 12(12):2339–2350, December 2000.

[208] Z. Mou, W. Fan, and X. Dong. Inducers of Plant Systemic Acquired Resistance Regulate NPR1 Function through Redox Changes. *Cell*, 113(7):935–944, June 2003. URL: http://linkinghub.elsevier.com/retrieve/pii/S009286740300429X, doi:10.1016/S0092-8674(03)00429-X.

[209] Y. Zhang, W. Fan, M. Kinkema, X. Li, and X. Dong. Interaction of NPR1 with basic leucine zipper protein transcription factors that bind sequences required for salicylic acid induction of the PR-1 gene. *Proceedings of the National Academy of Sciences of the United States of America*, 96(11):6523–6528, May 1999.

[210] C. Després, C. DeLong, S. Glaze, E. Liu, and P. R. Fobert. The Arabidopsis NPR1/NIM1 protein enhances the DNA binding activity of a subgroup of the TGA family of bZIP transcription factors. *The Plant Cell*, 12(2):279–290, February 2000.

[211] J.-M. Zhou, Y. Trifa, H. Silva, D. Pontier, E. Lam, J. Shah, and D. F. Klessig. NPR1 Differentially Interacts with Members of the TGA/OBF Family of Transcription Factors That Bind an Element of the PR-1 Gene Required for Induction by Salicylic Acid. *Molecular Plant-Microbe Interactions*, 13(2):191–202, February 2000. URL: http://apsjournals.apsnet.org/doi/10.1094/MPMI.2000.13.2.191, doi:10.1094/MPMI.2000.13.2.191.

[212] C. Després, C. Chubak, A. Rochon, R. Clark, T. Bethune, D. Desveaux, and P. R. Fobert. The Arabidopsis NPR1 disease resistance protein is a novel cofactor that confers redox regulation of DNA binding activity to the basic domain/leucine zipper transcription factor TGA1. *The Plant Cell*, 15(9):2181–2191, September 2003.

[213] R. R. Weigel, C. Bäuscher, A. J. Pfitzner, and U. M. Pfitzner. NIMIN-1, NIMIN-2 and NIMIN-3, members of a novel family of proteins from Arabidopsis that interact with NPR1/NIM1, a key regulator of systemic acquired resistance in plants. *Plant Molecular Biology*, 46(2):143–160, May 2001.

[214] I. Glocova, K. Thor, B. Roth, M. Babbick, A. J. P. Pfitzner, and U. M. Pfitzner. Salicylic acid (SA)-dependent gene activation can be uncoupled from cell death-mediated gene activation: the SA-inducible NIMIN-1 and NIMIN-2 promoters, unlike the PR-1a promoter, do not respond to cell death signals in tobacco. *Molecular Plant Pathology*, 6(3):299–314, May 2005. URL: http://doi.wiley.com/10.1111/j.1364-3703.2005.00288.x, doi:10.1111/j.1364-3703.2005.00288.x.

[215] M. Hermann, F. Maier, A. Masroor, S. Hirth, A. J. P. Pfitzner, and U. M. Pfitzner. The Arabidopsis NIMIN proteins affect NPR1 differentially. *Frontiers in Plant Science*, 4, 2013. URL: http://journal.frontiersin.org/article/10.3389/fpls.2013.00088/abstract, doi:10.3389/fpls.2013.00088.

[216] D. Van der Does, A. Leon-Reyes, A. Koornneef, M. C. Van Verk, N. Rodenburg, L. Pauwels, A. Goossens, A. P. Korbes, J. Memelink, T. Ritsema, S. C. M. Van Wees, and C. M. J. Pieterse. Salicylic Acid Suppresses Jasmonic Acid Signaling Downstream of SCFCOI1-JAZ by Targeting GCC Promoter Motifs via Transcription Factor ORA59. *The Plant Cell*, 25(2):744–761, February 2013. URL: http://www.plantcell.org/cgi/doi/10.1105/tpc.112.108548, doi:10.1105/tpc.112.108548.

[217] A. Koornneef and C. M. Pieterse. Cross Talk in Defense Signaling. *PLANT PHYSIOLOGY*, 146(3):839–844, March 2008. URL: http://www.plantphysiol.org/cgi/doi/10.1104/pp.107.112029, doi:10.1104/pp.107.112029.

[218] P. Zhao, G.-H. Lu, and Y.-H. Yang. Salicylic Acid Signaling and its Role in Responses to Stresses in Plants. In G. K. Pandey, editor, *Mechanism of Plant Hormone Signaling under Stress*, pages 413–441. John Wiley & Sons, Inc., Hoboken, NJ, USA, March 2017. URL: http://doi.wiley.com/10.1002/9781118889022.ch17, doi:10.1002/9781118889022.ch17.

[219] S. Gimenez-Ibanez, M. Boter, and R. Solano. Novel players fine-tune plant trade-offs. *Essays In Biochemistry*, 58(0):83–100, September 2015. URL: http://essays.biochemistry.org/cgi/doi/10.1042/bse0580083, doi:10.1042/bse0580083.

[220] D. X. Xie, B. F. Feys, S. James, M. Nieto-Rostro, and J. G. Turner. COI1: an Arabidopsis gene required for jasmonate-regulated defense and fertility. *Science (New York, N.Y.)*, 280(5366):1091–1094, May 1998.

[221] P. E. Staswick, W. Su, and S. H. Howell. Methyl jasmonate inhibition of root growth and induction of a leaf protein are decreased in an Arabidopsis thaliana mutant. *Proceedings of the National Academy of Sciences*, 89(15):6837–6840, August 1992. URL: http://www.pnas.org/cgi/doi/10.1073/pnas.89.15.6837, doi:10.1073/pnas.89.15.6837.

[222] E. Demole, E. Lederer, and D. Mercier. Isolement et détermination de la structure du jasmonate de méthyle, constituant odorant caractéristique de l'essence de jasmin. *Helvetica Chimica Acta*, 45(2):675–685, 1962. URL: http://doi.wiley.com/10.1002/hlca.19620450233, doi:10.1002/hlca.19620450233.

[223] S. Fonseca, A. Chini, M. Hamberg, B. Adie, A. Porzel, R. Kramell, O. Miersch, C. Wasternack, and R. Solano. (+)-7-iso-Jasmonoyl-L-isoleucine is the endogenous bioactive jasmonate. *Nature Chemical Biology*, 5(5):344–350, May 2009. URL: http://www.nature.com/articles/nchembio.161, doi:10.1038/nchembio.161.

[224] J. Ueda and J. Kato. Isolation and Identification of a Senescence-promoting Substance from Wormwood (Artemisia absinthium L.). *Plant Physiology*, 66(2):246–249, August 1980.

[225] W. Dathe, H. Roensch, A. Preiss, W. Schade, G. Sembdner, and K. Schreiber. Endogenous plant hormones of the broad bean, Vicia faba L. jasmonic acid, a plant growth inhibitor in pericarp. *Planta*, 153(6):530–535, December 1981. URL: http://link.springer.com/10.1007/BF00385537, doi:10.1007/BF00385537.

[226] B. Feys. Arabidopsis Mutants Selected for Resistance to the Phytotoxin Coronatine Are Male Sterile, Insensitive to Methyl Jasmonate, and Resistant to a Bacterial Pathogen. *THE PLANT CELL ONLINE*, 6(5):751–759, May 1994. URL: http://www.plantcell.org/cgi/doi/10.1105/tpc.6.5.751, doi:10.1105/tpc.6.5.751.

[227] L. Xu, F. Liu, E. Lechner, P. Genschik, W. L. Crosby, H. Ma, W. Peng, D. Huang, and D. Xie. The SCF(COI1) ubiquitin-ligase complexes are required for jasmonate response in Arabidopsis. *The Plant Cell*, 14(8):1919–1935, August 2002.

[228] S. Kepinski and O. Leyser. The Arabidopsis F-box protein TIR1 is an auxin receptor. *Nature*, 435:446, 2005. URL: https://doi.org/10.1038/nature03542.

[229] N. Dharmasiri, S. Dharmasiri, and M. Estelle. The F-box protein TIR1 is an auxin receptor. *Nature*, 435:441, 2005. URL: https://doi.org/10.1038/nature03543.

[230] L. Katsir, A. L. Schilmiller, P. E. Staswick, S. Y. He, and G. A. Howe. COI1 is a critical component of a receptor for jasmonate and the bacterial virulence factor coronatine. *Proceedings of the National Academy of Sciences*, 105(19):7100–7105, May 2008. URL: http://www.pnas.org/cgi/doi/10.1073/pnas.0802332105, doi:10.1073/pnas.0802332105.

[231] J. Yan, C. Zhang, M. Gu, Z. Bai, W. Zhang, T. Qi, Z. Cheng, W. Peng, H. Luo, F. Nan, Z. Wang, and D. Xie. The Arabidopsis CORONATINE INSENSITIVE1 Protein Is a Jasmonate Receptor. *THE PLANT CELL ONLINE*, 21(8):2220–2236, August 2009. URL: http://www.plantcell.org/cgi/doi/10.1105/tpc.109.065730, doi:10.1105/tpc.109.065730.

[232] A. Chini, S. Fonseca, G. Fernández, B. Adie, J. M. Chico, O. Lorenzo, G. García-Casado, I. López-Vidriero, F. M. Lozano, M. R. Ponce, J. L. Micol, and R. Solano. The JAZ family of repressors is the missing link in jasmonate signalling. *Nature*, 448(7154):666–671, August 2007. URL: http://www.nature.com/articles/nature06006, doi:10.1038/nature06006.

[233] B. Thines, L. Katsir, M. Melotto, Y. Niu, A. Mandaokar, G. Liu, K. Nomura, S. Y. He, G. A. Howe, and J. Browse. JAZ repressor proteins are targets of the SCFCOI1 complex during jasmonate signalling. *Nature*, 448:661, July 2007. URL: https://doi.org/10.1038/nature05960.

[234] Y. Yan, S. Stolz, A. Chetelat, P. Reymond, M. Pagni, L. Dubugnon, and E. E. Farmer. A Downstream Mediator in the Growth Repression Limb of the Jasmonate Pathway. *THE PLANT CELL ONLINE*, 19(8):2470–2483, August 2007. URL: http://www.plantcell.org/cgi/doi/10.1105/tpc.107.050708, doi:10.1105/tpc.107.050708.

[235] L. Pauwels, G. F. Barbero, J. Geerinck, S. Tilleman, W. Grunewald, A. C. Pérez, J. M. Chico, R. V. Bossche, J. Sewell, E. Gil, G. García-Casado, E. Witters, D. Inzé, J. A. Long, G. De Jaeger, R. Solano, and A. Goossens. NINJA connects the co-repressor TOPLESS to jasmonate signalling. *Nature*, 464(7289):788–791, April 2010. URL: http://www.nature.com/articles/nature08854, doi:10.1038/nature08854.

[236] L. Pauwels and A. Goossens. The JAZ Proteins: A Crucial Interface in the Jasmonate Signaling Cascade. *The Plant Cell*, 23(9):3089–3100, September 2011. URL: http://www.plantcell.org/lookup/doi/10.1105/tpc.111.089300, doi:10.1105/tpc.111.089300.

[237] H. S. Chung and G. A. Howe. A Critical Role for the TIFY Motif in Repression of Jasmonate Signaling by a Stabilized Splice Variant of the JASMONATE ZIM-Domain Protein JAZ10 in Arabidopsis. *THE PLANT CELL ONLINE*, 21(1):131–145, January 2009. URL: http://www.plantcell.org/cgi/doi/10.1105/tpc.108.064097, doi:10.1105/tpc.108.064097.

[238] B. Vanholme, W. Grunewald, A. Bateman, T. Kohchi, and G. Gheysen. The tify family previously known as ZIM. *Trends in Plant Science*, 12(6):239–244, June 2007. URL: https://linkinghub.elsevier.com/retrieve/pii/S1360138507000994, doi:10.1016/j.tplants.2007.04.004.

[239] S. Kagale, M. G. Links, and K. Rozwadowski. Genome-wide analysis of ethylene-responsive element binding factor-associated amphiphilic repression motif-containing transcriptional regulators in Arabidopsis. *Plant Physiology*, 152(3):1109–1134, March 2010. doi:10.1104/pp.109.151704.

[240] S. Kagale and K. Rozwadowski. EAR motif-mediated transcriptional repression in plants: An underlying mechanism for epigenetic regulation of gene expression. *Epigenetics*, 6(2):141–146, February 2011. URL: http://www.tandfonline.com/doi/abs/10.4161/epi.6.2.13627, doi:10.4161/epi.6.2.13627.

[241] A. Chini, S. Fonseca, J. M. Chico, P. Fernández-Calvo, and R. Solano. The ZIM domain mediates homo- and heteromeric interactions between Arabidopsis JAZ proteins. *The Plant Journal*, 59(1):77–87, July 2009. URL: http://doi.wiley.com/10.1111/j.1365-313X.2009.03852.x, doi:10.1111/j.1365-313X.2009.03852.x.

[242] H. S. Chung, T. F. Cooke, C. L. DePew, L. C. Patel, N. Ogawa, Y. Kobayashi, and G. A. Howe. Alternative splicing expands the repertoire of dominant JAZ repressors of jasmonate signaling: Alternative splicing of Arabidopsis JAZ genes. *The Plant Journal*, 63(4):613–622, August 2010. URL: http://doi.wiley.com/10.1111/j.1365-313X.2010.04265.x, doi:10.1111/j.1365-313X.2010.04265.x.

[243] X. Ma, S. Lv, C. Zhang, and C. Yang. Histone deacetylases and their functions in plants. *Plant Cell Reports*, 32(4):465–478, April 2013. URL: http://link.springer.com/10.1007/s00299-013-1393-6, doi:10.1007/s00299-013-1393-6.

[244] C. Wang, X. Du, and Z. Mou. The Mediator Complex Subunits MED14, MED15, and MED16 Are Involved in Defense Signaling Crosstalk in Arabidopsis. *Frontiers in Plant Science*, 7, December 2016. URL: http://journal.frontiersin.org/article/10.3389/fpls.2016.01947/full, doi:10.3389/fpls.2016.01947.

[245] C. An and Z. Mou. The function of the Mediator complex in plant immunity. *Plant Signaling & Behavior*, 8(3):e23182, March 2013. URL: http://www.tandfonline.com/doi/abs/10.4161/psb.23182, doi:10.4161/psb.23182.

[246] C. An, L. Li, Q. Zhai, Y. You, L. Deng, F. Wu, R. Chen, H. Jiang, H. Wang, Q. Chen, and C. Li. Mediator subunit MED25 links the jasmonate receptor to transcriptionally active chromatin. *Proceedings of the National Academy of Sciences*, 114(42):E8930–E8939, October 2017. URL: http://www.pnas.org/lookup/doi/10.1073/pnas.1710885114, doi:10.1073/pnas.1710885114.

[247] C. M. Pieterse, D. Van der Does, C. Zamioudis, A. Leon-Reyes, and S. C. Van Wees. Hormonal Modulation of Plant Immunity. *Annual Review of Cell and Developmental Biology*, 28(1):489–521, November 2012. URL: http://www.annualreviews.org/doi/10.1146/annurev-cellbio-092910-154055, doi:10.1146/annurev-cellbio-092910-154055.

[248] H. Cheng, S. Song, L. Xiao, H. M. Soo, Z. Cheng, D. Xie, and J. Peng. Gibberellin Acts through Jasmonate to Control the Expression of MYB21, MYB24, and MYB57 to Promote Stamen Filament Growth in Arabidopsis. *PLoS Genetics*, 5(3):e1000440, March 2009. URL: https://dx.plos.org/10.1371/journal.pgen.1000440, doi:10.1371/journal.pgen.1000440.

[249] H. Koltai, E. Dor, J. Hershenhorn, D. M. Joel, S. Weininger, S. Lekalla, H. Shealtiel, C. Bhattacharya, E. Eliahu, N. Resnick, R. Barg, and Y. Kapulnik. Strigolactones' Effect on Root Growth and Root-Hair Elongation May Be Mediated by Auxin-Efflux Carriers. *Journal of Plant Growth Regulation*, 29(2):129–136, June 2010. URL: https://doi.org/10.1007/s00344-009-9122-7, doi:10.1007/s00344-009-9122-7.

[250] C. Ruyter-Spira, W. Kohlen, T. Charnikhova, A. van Zeijl, L. van Bezouwen, N. de Ruijter, C. Cardoso, J. A. Lopez-Raez, R. Matusova, R. Bours, F. Verstappen, and H. Bouwmeester. Physiological Effects of the Synthetic Strigolactone Analog GR24 on Root System Architecture in Arabidopsis: Another Belowground Role for Strigolactones? *PLANT PHYSIOLOGY*, 155(2):721–734, February 2011. URL: http://www.plantphysiol.org/cgi/doi/10.1104/pp.110.166645, doi:10.1104/pp.110.166645.

[251] D. Koren, N. Resnick, E. M. Gati, E. Belausov, S. Weininger, Y. Kapulnik, and H. Koltai. Strigolactone signaling in the endodermis is sufficient to restore root responses and involves SHORT HYPOCOTYL 2 (SHY2) activity. *New Phytologist*, 198(3):866–874, May 2013. URL: http://doi.wiley.com/10.1111/nph.12189, doi:10.1111/nph.12189.

[252] C. E. Cook, L. P. Whichard, M. Wall, G. H. Egley, P. Coggon, P. A. Luhan, and A. T. McPhail. Germination stimulants. II. Structure of strigol, a potent seed germination stimulant for witchweed (Striga lutea). *Journal of the American Chemical Society*, 94(17):6198–6199, August 1972. URL: http://pubs.acs.org/doi/abs/10.1021/ja00772a048, doi:10.1021/ja00772a048.

[253] E. M. Mangnus, F. J. Dommerholt, R. L. P. De Jong, and B. Zwanenburg. Improved synthesis of strigol analog GR24 and evaluation of the biological activity of its diastereomers. *Journal of Agricultural and Food Chemistry*, 40(7):1230–1235, July 1992. URL: http://pubs.acs.org/doi/abs/10.1021/jf00019a031, doi:10.1021/jf00019a031.

[254] B. Zwanenburg, A. S. Mwakaboko, A. Reizelman, G. Anilkumar, and D. Sethumadhavan. Structure and function of natural and synthetic signalling molecules in parasitic weed germination. *Pest Management Science*, 65(5):478–491, May 2009. URL: http://doi.wiley.com/10.1002/ps.1706, doi:10.1002/ps.1706.

[255] B. Zwanenburg, S. K. Nayak, T. V. Charnikhova, and H. J. Bouwmeester. New strigolactone mimics: Structure–activity relationship and mode of action as germinating stimulants for parasitic weeds. *Bioorganic & Medicinal Chemistry Letters*, 23(18):5182–5186, September 2013. URL: https://linkinghub.elsevier.com/retrieve/pii/S0960894X1300838X, doi:10.1016/j.bmcl.2013.07.004.

[256] C. E. Cook, L. P. Whichard, B. Turner, M. E. Wall, and G. H. Egley. Germination of Witchweed (Striga lutea Lour.): Isolation and Properties of a Potent Stimulant. *Science*, 154(3753):1189–1190, December 1966. URL: http://www.sciencemag.org/cgi/doi/10.1126/science.154.3753.1189, doi:10.1126/science.154.3753.1189.

[257] X. Xie, K. Yoneyama, and K. Yoneyama. The Strigolactone Story. *Annual Review of Phytopathology*, 48(1):93–117, July 2010. URL: http://www.annualreviews.org/doi/10.1146/annurev-phyto-073009-114453, doi:10.1146/annurev-phyto-073009-114453.

[258] K. Akiyama, K.-i. Matsuzaki, and H. Hayashi. Plant sesquiterpenes induce hyphal branching in arbuscular mycorrhizal fungi. *Nature*, 435(7043):824–827, June 2005. URL: http://www.nature.com/articles/nature03608, doi:10.1038/nature03608.

[259] M. J. Soto, M. Fernández-Aparicio, V. Castellanos-Morales, J. M. García-Garrido, J. A. Ocampo, M. J. Delgado, and H. Vierheilig. First indications for the involvement of strigolactones on nodule formation in alfalfa (Medicago sativa). *Soil Biology and Biochemistry*, 42(2):383–385, February 2010. URL: https://linkinghub.elsevier.com/retrieve/pii/S0038071709004210, doi:10.1016/j.soilbio.2009.11.007.

[260] E. Foo and N. W. Davies. Strigolactones promote nodulation in pea. *Planta*, 234(5):1073–1081, November 2011. URL: http://link.springer.com/10.1007/s00425-011-1516-7, doi:10.1007/s00425-011-1516-7.

[261] M. Parniske. Arbuscular mycorrhiza: the mother of plant root endosymbioses. *Nature Reviews Microbiology*, 6(10):763–775, October 2008. URL: http://www.nature.com/articles/nrmicro1987, doi:10.1038/nrmicro1987.

[262] Y. Kapulnik, P.-M. Delaux, N. Resnick, E. Mayzlish-Gati, S. Wininger, C. Bhattacharya, N. Séjalon-Delmas, J.-P. Combier, G. Bécard, E. Belausov, T. Beeckman, E. Dor, J. Hershenhorn, and H. Koltai. Strigolactones affect lateral root formation and root-hair elongation in Arabidopsis. *Planta*, 233(1):209–216, January 2011. URL: http://link.springer.com/10.1007/s00425-010-1310-y, doi:10.1007/s00425-010-1310-y.

[263] P. Stirnberg, K. van De Sande, and H. M. O. Leyser. MAX1 and MAX2 control shoot lateral branching in Arabidopsis. *Development (Cambridge, England)*, 129(5):1131–1141, March 2002.

[264] P. Stirnberg, I. J. Furner, and H. M. Ottoline Leyser. MAX2 participates in an SCF complex which acts locally at the node to suppress shoot branching: An SCFMAX2 acts at the node to suppress branching. *The Plant Journal*, 50(1):80–94, March 2007. URL: http://doi.wiley.com/10.1111/j.1365-313X.2007.03032.x, doi:10.1111/j.1365-313X.2007.03032.x.

[265] V. Gomez-Roldan, S. Fermas, P. B. Brewer, V. Puech-Pagès, E. A. Dun, J.-P. Pillot, F. Letisse, R. Matusova, S. Danoun, J.-C. Portais, H. Bouwmeester, G. Bécard, C. A. Beveridge, C. Rameau, and S. F. Rochange. Strigolactone inhibition of shoot branching. *Nature*, 455(7210):189–194, September 2008. URL: http://www.nature.com/doifinder/10.1038/nature07271, doi:10.1038/nature07271.

[266] M. Umehara, A. Hanada, S. Yoshida, K. Akiyama, T. Arite, N. Takeda-Kamiya, H. Magome, Y. Kamiya, K. Shirasu, K. Yoneyama, J. Kyozuka, and S. Yamaguchi. Inhibition of shoot branching by new terpenoid plant hormones. *Nature*, 455(7210):195–200, September 2008. URL: http://www.nature.com/doifinder/10.1038/nature07272, doi:10.1038/nature07272.

[267] J. Agusti, S. Herold, M. Schwarz, P. Sanchez, K. Ljung, E. A. Dun, P. B. Brewer, C. A. Beveridge, T. Sieberer, E. M. Sehr, and T. Greb. Strigolactone signaling is required for auxin-dependent stimulation of secondary growth in plants. *Proceedings of the National Academy of Sciences*, 108(50):20242–20247, December 2011. URL: http://www.pnas.org/cgi/doi/10.1073/pnas.1111902108, doi:10.1073/pnas.1111902108.

[268] C. V. Ha, M. A. Leyva-Gonzalez, Y. Osakabe, U. T. Tran, R. Nishiyama, Y. Watanabe, M. Tanaka, M. Seki, S. Yamaguchi, N. V. Dong, K. Yamaguchi-Shinozaki, K. Shinozaki, L. Herrera-Estrella, and L.-S. P. Tran. Positive regulatory role of strigolactone in plant responses to drought and salt stress. *Proceedings of the National Academy of Sciences*, 111(2):851–856, January 2014. URL: http://www.pnas.org/cgi/doi/10.1073/pnas.1322135111, doi:10.1073/pnas.1322135111.

[269] E. Foo, C. G. Turnbull, and C. A. Beveridge. Long-distance signaling and the control of branching in the rms1 mutant of pea. *Plant Physiology*, 126(1):203–209, May 2001.

[270] W. Kohlen, T. Charnikhova, Q. Liu, R. Bours, M. A. Domagalska, S. Beguerie, F. Verstappen, O. Leyser, H. Bouwmeester, and C. Ruyter-Spira. Strigolactones Are Transported through the Xylem and Play a Key Role in Shoot Architectural Response to Phosphate Deficiency in Nonarbuscular Mycorrhizal Host Arabidopsis. *PLANT PHYSIOLOGY*, 155(2):974–987, February 2011. URL: http://www.plantphysiol.org/cgi/doi/10.1104/pp.110.164640, doi:10.1104/pp.110.164640.

[271] X. Xie, K. Yoneyama, T. Kisugi, T. Nomura, K. Akiyama, T. Asami, and K. Yoneyama. Strigolactones are transported from roots to shoots, although not through the xylem. *Journal of Pesticide Science*, 40(4):214–216, 2015. URL: https://www.jstage.jst.go.jp/article/jpestics/40/4/40_D15-045/_article, doi:10.1584/jpestics.D15-045.

[272] N. Shinohara, C. Taylor, and O. Leyser. Strigolactone Can Promote or Inhibit Shoot Branching by Triggering Rapid Depletion of the Auxin Efflux Protein PIN1 from the Plasma Membrane. *PLoS Biology*, 11(1):e1001474, January 2013. URL: http://dx.plos.org/10.1371/journal.pbio.1001474, doi:10.1371/journal.pbio.1001474.

[273] N. Pandya-Kumar, R. Shema, M. Kumar, E. Mayzlish-Gati, D. Levy, H. Zemach, E. Belausov, S. Wininger, M. Abu-Abied, Y. Kapulnik, and H. Koltai. Strigolactone analog GR24 triggers changes in PIN2 polarity, vesicle trafficking and actin filament architecture. *New Phytologist*, 202(4):1184–1196, June 2014. URL: http://doi.wiley.com/10.1111/nph.12744, doi:10.1111/nph.12744.

[274] J. E. Keeley, B. A. Morton, A. Pedrosa, and P. Trotter. Role of Allelopathy, Heat and Charred Wood in the Germination of Chaparral Herbs and Suffrutescents. *The Journal of Ecology*, 73(2):445, July 1985. URL: https://www.jstor.org/stable/2260486?origin=crossref, doi:10.2307/2260486.

[275] N. Brown and J. van Staden. Smoke as a germination cue: a review. *Plant Growth Regulation*, 22(2):115–124, July 1997. URL: https://doi.org/10.1023/A:1005852018644, doi:10.1023/A:1005852018644.

[276] G. R. Flematti. A Compound from Smoke That Promotes Seed Germination. *Science*, 305(5686):977–977, August 2004. URL: http://www.sciencemag.org/cgi/doi/10.1126/science.1099944, doi:10.1126/science.1099944.

[277] S. D. Chiwocha, K. W. Dixon, G. R. Flematti, E. L. Ghisalberti, D. J. Merritt, D. C. Nelson, J.-A. M. Riseborough, S. M. Smith, and J. C. Stevens. Karrikins: A new family of plant growth regulators in smoke. *Plant Science*, 177(4):252–256, October 2009. URL: https://linkinghub.elsevier.com/retrieve/pii/S0168945209001824, doi:10.1016/j.plantsci.2009.06.007.

[278] G. R. Flematti, E. L. Ghisalberti, K. W. Dixon, and R. D. Trengove. Identification of Alkyl Substituted 2 *H* -Furo[2,3- *c*]pyran-2-ones as Germination Stimulants Present in Smoke. *Journal of Agricultural and Food Chemistry*, 57(20):9475–9480, October 2009. URL: http://pubs.acs.org/doi/abs/10.1021/jf9028128, doi:10.1021/jf9028128.

[279] G. R. Flematti, M. T. Waters, A. Scaffidi, D. J. Merritt, E. L. Ghisalberti, K. W. Dixon, and S. M. Smith. Karrikin and Cyanohydrin Smoke Signals Provide Clues to New Endogenous Plant Signaling Compounds. *Molecular Plant*, 6(1):29–37, January 2013. URL: https://linkinghub.elsevier.com/retrieve/pii/S1674205214608789, doi:10.1093/mp/sss132.

[280] M. Daws, H. Pritchard, and J. Van Staden. Butenolide from plant-derived smoke functions as a strigolactone analogue: Evidence from parasitic weed seed germination. *South African Journal of Botany*, 74(1):116–120, January 2008. URL: https://linkinghub.elsevier.com/retrieve/pii/S0254629907003705, doi:10.1016/j.sajb.2007.09.005.

[281] D. C. Nelson, J.-A. Riseborough, G. R. Flematti, J. Stevens, E. L. Ghisalberti, K. W. Dixon, and S. M. Smith. Karrikins Discovered in Smoke Trigger Arabidopsis Seed Germination by a Mechanism Requiring Gibberellic Acid Synthesis and Light. *PLANT PHYSIOLOGY*, 149(2):863–873, December 2008. URL: http://www.plantphysiol.org/cgi/doi/10.1104/pp.108.131516, doi:10.1104/pp.108.131516.

[282] H. Nakamura, Y.-L. Xue, T. Miyakawa, F. Hou, H.-M. Qin, K. Fukui, X. Shi, E. Ito, S. Ito, S.-H. Park, Y. Miyauchi, A. Asano, N. Totsuka, T. Ueda, M. Tanokura, and T. Asami. Molecular mechanism of strigolactone perception by DWARF14. *Nature Communications*, 4(1), December 2013. URL: http://www.nature.com/articles/ncomms3613, doi:10.1038/ncomms3613.

[283] F. Zhou, Q. Lin, L. Zhu, Y. Ren, K. Zhou, N. Shabek, F. Wu, H. Mao, W. Dong, L. Gan, W. Ma, H. Gao, J. Chen, C. Yang, D. Wang, J. Tan, X. Zhang, X. Guo, J. Wang, L. Jiang, X. Liu, W. Chen, J. Chu, C. Yan, K. Ueno, S. Ito, T. Asami, Z. Cheng, J. Wang, C. Lei, H. Zhai, C. Wu, H. Wang, N. Zheng, and J. Wan. D14–SCFD3-dependent degradation of D53 regulates strigolactone signalling. *Nature*, 504(7480):406–410, December 2013. URL: http://www.nature.com/articles/nature12878, doi:10.1038/nature12878.

[284] Y. Wang, S. Sun, W. Zhu, K. Jia, H. Yang, and X. Wang. Strigolactone/MAX2-Induced Degradation of Brassinosteroid Transcriptional Effector BES1 Regulates Shoot Branching. *Developmental Cell*, 27(6):681–688, December 2013. URL: https://linkinghub.elsevier.com/retrieve/pii/S1534580713006734, doi:10.1016/j.devcel.2013.11.010.

[285] I. Soundappan, T. Bennett, N. Morffy, Y. Liang, J. P. Stanga, A. Abbas, O. Leyser, and D. C. Nelson. SMAX1-LIKE/D53 Family Members Enable Distinct MAX2-Dependent Responses to Strigolactones and Karrikins in Arabidopsis. *The Plant Cell*, 27(11):3143–3159, November 2015. URL: http://www.plantcell.org/lookup/doi/10.1105/tpc.15.00562, doi:10.1105/tpc.15.00562.

[286] J. P. Stanga, S. M. Smith, W. R. Briggs, and D. C. Nelson. SUPPRESSOR OF MORE AXILLARY GROWTH2 1 Controls Seed Germination and Seedling Development in Arabidopsis. *PLANT PHYSIOLOGY*, 163(1):318–330, September 2013. URL: http://www.plantphysiol.org/cgi/doi/10.1104/pp.113.221259, doi:10.1104/pp.113.221259.

[287] J. L. Nemhauser, F. Hong, and J. Chory. Different Plant Hormones Regulate Similar Processes through Largely Nonoverlapping Transcriptional Responses. *Cell*, 126(3):467–475, 2006. URL: http://dx.doi.org/10.1016/j.cell.2006.05.050, doi:10.1016/j.cell.2006.05.050.

[288] D. Ristova, C. Carré, M. Pervent, A. Medici, G. J. Kim, D. Scalia, S. Ruffel, K. D. Birnbaum, B. Lacombe, W. Busch, G. M. Coruzzi, and G. Krouk. Combinatorial interaction network of transcriptomic and phenotypic responses to nitrogen and hormones in the Arabidopsis thaliana root. *Science Signaling*, 9(451):rs13, 2016. URL: http://stke.sciencemag.org/content/9/451/rs13.abstract, doi:10.1126/scisignal.aaf2768.

[289] T.-p. Sun. The Molecular Mechanism and Evolution of the GA–GID1–DELLA Signaling Module in Plants. *Current Biology*, 21(9):R338–R345, May 2011. URL: https://linkinghub.elsevier.com/retrieve/pii/S0960982211002272, doi:10.1016/j.cub.2011.02.036.

[290] J. Gallego-Bartolomé, E. G. Minguet, F. Grau-Enguix, M. Abbas, A. Locascio, S. G. Thomas, D. Alabadí, and M. A. Blázquez. Molecular mechanism for the interaction between gibberellin and brassinosteroid signaling pathways in Arabidopsis. *Proceedings of the National Academy of Sciences of the United States of America*, 109(33):13446–13451, August 2012. doi:10.1073/pnas.1119992109.

[291] G.-J. Hong, X.-Y. Xue, Y.-B. Mao, L.-J. Wang, and X.-Y. Chen. *Arabidopsis* MYC2 Interacts with DELLA Proteins in Regulating Sesquiterpene Synthase Gene Expression. *The Plant Cell*, 24(6):2635–2648, June 2012. URL: http://www.plantcell.org/lookup/doi/10.1105/tpc.112.098749, doi:10.1105/tpc.112.098749.

[292] S. Fields and O.-k. Song. A novel genetic system to detect protein–protein interactions. *Nature*, 340(6230):245–246, July 1989. URL: https://doi.org/10.1038/340245a0, doi:10.1038/340245a0.

[293] M. Altmann, S. Altmann, C. Falter, and P. Falter-Braun. High-Quality Yeast-2-Hybrid Interaction Network Mapping. *Current Protocols in Plant Biology*, 3(3):e20067, September 2018. doi:10.1002/cppb.20067.

[294] N. F. Käufer, H. M. Fried, W. F. Schwindinger, M. Jasin, and J. R. Warner. Cycloheximide resistance in yeast: the gene and its protein. *Nucleic Acids Research*, 11(10):3123–3135, May 1983.

[295] W. Criekinge and R. Beyaert. Yeast two-hybrid: State of the art. *Biological Procedures Online*, 2(1):1–38, October 1999. URL: http://www.springerlink.com/index/10.1251/bpo16, doi:10.1251/bpo16.

[296] Arabidopsis Interactome Mapping Consortium. Evidence for network evolution in an Arabidopsis interactome map. *Science (New York, N.Y.)*, 333(6042):601–607, July 2011. doi:10.1126/science.1203877.

[297] J. L. Nemhauser, P. C. Zambryski, and J. L. Roe. Auxin signaling in Arabidopsis flower development? *Current Opinion in Plant Biology*, 1(6):531–535, December 1998. URL: http://linkinghub.elsevier.com/retrieve/pii/S1369526698800472, doi:10.1016/S1369-5266(98)80047-2.

[298] R. Aloni, E. Aloni, M. Langhans, and C. I. Ullrich. Role of Cytokinin and Auxin in Shaping Root Architecture: Regulating Vascular Differentiation, Lateral Root Initiation, Root Apical Dominance and Root Gravitropism. *Annals of Botany*, 97(5):883–893, May 2006. URL: http://academic.oup.com/aob/article/97/5/883/220115/Role-of-Cytokinin-and-Auxin-in-Shaping-Root, doi:10.1093/aob/mcl027.

[299] M. Etemadi, C. Gutjahr, J.-M. Couzigou, M. Zouine, D. Lauressergues, A. Timmers, C. Audran, M. Bouzayen, G. Bécard, and J.-P. Combier. Auxin Perception Is Required for Arbuscule Development in Arbuscular Mycorrhizal Symbiosis. *Plant Physiology*, 166(1):281–292, September 2014. URL: http://www.plantphysiol.org/lookup/doi/10.1104/pp.114.246595, doi:10.1104/pp.114.246595.

[300] J. Ludwig-Müller and M. Güther. Auxins as signals in arbuscular mycorrhiza formation. *Plant Signaling & Behavior*, 2(3):194–196, May 2007.

[301] K. Jentschel, D. Thiel, F. Rehn, and J. Ludwig-Müller. Arbuscular mycorrhiza enhances auxin levels and alters auxin biosynthesis in Tropaeolum majus during early stages of colonization. *Physiologia Plantarum*, 129(2):320–333, December 2006. URL: http://doi.wiley.com/10.1111/j.1399-3054.2006.00812.x, doi:10.1111/j.1399-3054.2006.00812.x.

[302] U. Mathesius. The Role of Auxin in Root-Symbiont and Root-Pathogen Interactions: From Development to Defense. In U. E. Lüttge, W. Beyschlag, B. Büdel, and D. Francis, editors, *Progress in Botany, Vol. 71*, volume 71, pages 185–210. Springer Berlin Heidelberg, Berlin, Heidelberg, 2010. URL: http://link.springer.com/10.1007/978-3-642-02167-1_8, doi:10.1007/978-3-642-02167-1_8.

[303] D. D. Figueiredo and C. Köhler. Auxin: a molecular trigger of seed development. *Genes & Development*, 32(7-8):479–490, April 2018. URL: http://genesdev.cshlp.org/lookup/doi/10.1101/gad.312546.118, doi:10.1101/gad.312546.118.

[304] H.-w. Shuai, Y.-j. Meng, X.-f. Luo, F. Chen, Y. Qi, W.-y. Yang, and K. Shu. The roles of auxin in seed dormancy and germination. *Yi Chuan = Hereditas*, 38(4):314–322, 2016. doi:10.16288/j.yczz.15-464.

[305] E. Sharma, R. Sharma, P. Borah, M. Jain, and J. P. Khurana. Emerging Roles of Auxin in Abiotic Stress Responses. In G. K. Pandey, editor, *Elucidation of Abiotic Stress Signaling in Plants*, pages 299–328. Springer New York, New York, NY, 2015. URL: http://link.springer.com/10.1007/978-1-4939-2211-6_11, doi:10.1007/978-1-4939-2211-6_11.

[306] B. Salopek-Sondi, I. Pavlović, A. Smolko, and D. Šamec. Auxin as a Mediator of Abiotic Stress Responses. In G. K. Pandey, editor, *Mechanism of Plant Hormone Signaling under Stress*, pages 1–36. John Wiley & Sons, Inc., Hoboken, NJ, USA, March 2017. URL: http://doi.wiley.com/10.1002/9781118889022.ch1, doi:10.1002/9781118889022.ch1.

[307] K. Kazan and J. M. Manners. Linking development to defense: auxin in plant–pathogen interactions. *Trends in Plant Science*, 14(7):373–382, July 2009. URL: https://linkinghub.elsevier.com/retrieve/pii/S1360138509001447, doi:10.1016/j.tplants.2009.04.005.

[308] J. Fu and S. Wang. Insights into Auxin Signaling in Plant?Pathogen Interactions. *Frontiers in Plant Science*, 2, 2011. URL: http://journal.frontiersin.org/article/10.3389/fpls.2011.00074/abstract, doi:10.3389/fpls.2011.00074.

[309] J. H. Rowe, J. F. Topping, J. Liu, and K. Lindsey. Abscisic acid regulates root growth under osmotic stress conditions via an interacting hormonal network with cytokinin, ethylene and auxin. *New Phytologist*, 211(1):225–239, July 2016. URL: http://doi.wiley.com/10.1111/nph.13882, doi:10.1111/nph.13882.

[310] J. M. Thole, E. R. Beisner, J. Liu, S. V. Venkova, and L. C. Strader. Abscisic Acid Regulates Root Elongation Through the Activities of Auxin and Ethylene in *Arabidopsis thaliana*. *G3: Genes|Genomes|Genetics*, 4(7):1259–1274, July 2014. URL: http://g3journal.org/lookup/doi/10.1534/g3.114.011080, doi:10.1534/g3.114.011080.

[311] M. E. LeNoble. Maintenance of shoot growth by endogenous ABA: genetic assessment of the involvement of ethylene suppression. *Journal of Experimental Botany*, 55(395):237–245, November 2003. URL: https://academic.oup.com/jxb/article-lookup/doi/10.1093/jxb/erh031, doi:10.1093/jxb/erh031.

[312] Y. Hayashi, K. Takahashi, S.-i. Inoue, and T. Kinoshita. Abscisic Acid Suppresses Hypocotyl Elongation by Dephosphorylating Plasma Membrane H+-ATPase in Arabidopsis thaliana. *Plant and Cell Physiology*, 55(4):845–853, April 2014. URL: https://academic.oup.com/pcp/article-lookup/doi/10.1093/pcp/pcu028, doi:10.1093/pcp/pcu028.

[313] A. H. Fitzpatrick, N. Shrestha, J. Bhandari, and D. N. Crowell. Roles for farnesol and ABA in Arabidopsis flower development. *Plant Signaling & Behavior*, 6(8):1189–1191, August 2011. URL: http://www.tandfonline.com/doi/abs/10.4161/psb.6.8.15772, doi:10.4161/psb.6.8.15772.

[314] Y. Wang, L. Li, T. Ye, Y. Lu, X. Chen, and Y. Wu. The inhibitory effect of ABA on floral transition is mediated by ABI5 in Arabidopsis. *Journal of Experimental Botany*, 64(2):675–684, January 2013. URL: https://academic.oup.com/jxb/article-lookup/doi/10.1093/jxb/ers361, doi:10.1093/jxb/ers361.

[315] K. Chandra Sekhar and V. Sawhney. Role of ABA in stamen and pistil development in the normal and solanifolia mutant of tomato (Lycopersicon esculentum). *Sexual Plant Reproduction*, 4(4), October 1991. URL: http://link.springer.com/10.1007/BF00200548, doi:10.1007/BF00200548.

[316] F. Tardieu, B. Parent, and T. Simonneau. Control of leaf growth by abscisic acid: hydraulic or non-hydraulic processes? *Plant, Cell & Environment*, 33(4):636–647, April 2010. URL: http://doi.wiley.com/10.1111/j.1365-3040.2009.02091.x, doi:10.1111/j.1365-3040.2009.02091.x.

[317] M. Charpentier, J. Sun, J. Wen, K. S. Mysore, and G. E. D. Oldroyd. Abscisic Acid Promotion of Arbuscular Mycorrhizal Colonization Requires a Component of the PROTEIN PHOSPHATASE 2a Complex. *PLANT PHYSIOLOGY*, 166(4):2077–2090, December 2014. URL: http://www.plantphysiol.org/cgi/doi/10.1104/pp.114.246371, doi:10.1104/pp.114.246371.

[318] F. Y. Cao, K. Yoshioka, and D. Desveaux. The roles of ABA in plant-pathogen interactions. *Journal of Plant Research*, 124(4):489–499, July 2011. doi:10.1007/s10265-011-0409-y.

[319] C. Lim, W. Baek, J. Jung, J.-H. Kim, and S. Lee. Function of ABA in Stomatal Defense against Biotic and Drought Stresses. *International Journal of Molecular Sciences*, 16(12):15251–15270, July 2015. URL: http://www.mdpi.com/1422-0067/16/7/15251, doi:10.3390/ijms160715251.

[320] B. A. Adie, J. Perez-Perez, M. M. Perez-Perez, M. Godoy, J.-J. Sanchez-Serrano, E. A. Schmelz, and R. Solano. ABA Is an Essential Signal for Plant Resistance to Pathogens Affecting JA Biosynthesis and the Activation of Defenses in Arabidopsis. *THE PLANT CELL ONLINE*, 19(5):1665–1681, May 2007. URL: http://www.plantcell.org/cgi/doi/10.1105/tpc.106.048041, doi:10.1105/tpc.106.048041.

[321] B. Asselbergh, D. De Vleesschauwer, and M. Höfte. Global Switches and Fine-Tuning—ABA Modulates Plant Pathogen Defense. *Molecular Plant-Microbe Interactions*, 21(6):709–719, June 2008. URL: http://apsjournals.apsnet.org/doi/10.1094/MPMI-21-6-0709, doi:10.1094/MPMI-21-6-0709.

[322] W.-B. Jiang and W.-H. Lin. Brassinosteroid functions in *Arabidopsis* seed development. *Plant Signaling & Behavior*, 8(10):e25928, October 2013. URL: http://www.tandfonline.com/doi/abs/10.4161/psb.25928, doi:10.4161/psb.25928.

[323] S. D. Clouse. Plant development: A role for sterols in embryogenesis. *Current Biology*, 10(16):R601–R604, August 2000. URL: http://linkinghub.elsevier.com/retrieve/pii/S0960982200006394, doi:10.1016/S0960-9822(00)00639-4.

[324] A. Ferrie, J. Dirpaul, J. Krishna, J. Krochko, and W. Keller. Effects of Brassinosteroids on Microspore Embryogenesis in Brassica Species. *In Vitro Cellular & Developmental Biology - Plant*, 6(41):742–745, 2005.

[325] Z. Wei and J. Li. Brassinosteroids Regulate Root Growth, Development, and Symbiosis. *Molecular Plant*, 9(1):86–100, January 2016. URL: https://linkinghub.elsevier.com/retrieve/pii/S1674205215004566, doi:10.1016/j.molp.2015.12.003.

[326] F. Bao. Brassinosteroids Interact with Auxin to Promote Lateral Root Development in Arabidopsis. *PLANT PHYSIOLOGY*, 134(4):1624–1631, April 2004. URL: http://www.plantphysiol.org/cgi/doi/10.1104/pp.103.036897, doi:10.1104/pp.103.036897.

[327] F. Vandenbussche, D. Suslov, L. De Grauwe, O. Leroux, K. Vissenberg, and D. Van Der Straeten. The Role of Brassinosteroids in Shoot Gravitropism. *PLANT PHYSIOLOGY*, 156(3):1331–1336, July 2011. URL: http://www.plantphysiol.org/cgi/doi/10.1104/pp.111.177873, doi:10.1104/pp.111.177873.

[328] J. Li, Y. Li, S. Chen, and L. An. Involvement of brassinosteroid signals in the floral-induction network of Arabidopsis. *Journal of Experimental Botany*, 61(15):4221–4230, October 2010. URL: https://academic.oup.com/jxb/article-lookup/doi/10.1093/jxb/erq241, doi:10.1093/jxb/erq241.

[329] M. Nakaya, H. Tsukaya, N. Murakami, and M. Kato. Brassinosteroids control the proliferation of leaf cells of Arabidopsis thaliana. *Plant & Cell Physiology*, 43(2):239–244, February 2002.

[330] P. Krishna, B. D. Prasad, and T. Rahman. Brassinosteroid Action in Plant Abiotic Stress Tolerance. In E. Russinova and A. I. Caño-Delgado, editors, *Brassinosteroids*, volume 1564, pages 193–202. Springer New York, New York, NY, 2017. URL: http://link.springer.com/10.1007/978-1-4939-6813-8_16, doi:10.1007/978-1-4939-6813-8_16.

[331] G. J. Ahammed, X.-J. Xia, X. Li, K. Shi, J.-Q. Yu, and Y.-H. Zhou. Role of brassinosteroid in plant adaptation to abiotic stresses and its interplay with other hormones. *Current Protein & Peptide Science*, 16(5):462–473, 2015.

[332] B. V. Vardhini and N. A. Anjum. Brassinosteroids make plant life easier under abiotic stresses mainly by modulating major components of antioxidant defense system. *Frontiers in Environmental Science*, 2, January 2015. URL: http://journal.frontiersin.org/article/10.3389/fenvs.2014.00067/abstract, doi:10.3389/fenvs.2014.00067.

[333] C. Albrecht, F. Boutrot, C. Segonzac, B. Schwessinger, S. Gimenez-Ibanez, D. Chinchilla, J. P. Rathjen, S. C. de Vries, and C. Zipfel. Brassinosteroids inhibit pathogen-associated molecular pattern-triggered immune signaling independent of the receptor kinase BAK1. *Proceedings of the National Academy of Sciences*, 109(1):303–308, January 2012. URL: http://www.pnas.org/cgi/doi/10.1073/pnas.1109921108, doi:10.1073/pnas.1109921108.

[334] Z.-Y. Wang. Brassinosteroids modulate plant immunity at multiple levels. *Proceedings of the National Academy of Sciences*, 109(1):7–8, January 2012. URL: http://www.pnas.org/cgi/doi/10.1073/pnas.1118600109, doi:10.1073/pnas.1118600109.

[335] L. De Bruyne, M. Höfte, and D. De Vleesschauwer. Connecting Growth and Defense: The Emerging Roles of Brassinosteroids and Gibberellins in Plant Innate Immunity. *Molecular Plant*, 7(6):943–959, June 2014. URL: https://linkinghub.elsevier.com/retrieve/pii/S1674205214607991, doi:10.1093/mp/ssu050.

[336] H. Nakashita, M. Yasuda, T. Nitta, T. Asami, S. Fujioka, Y. Arai, K. Sekimata, S. Takatsuto, I. Yamaguchi, and S. Yoshida. Brassinosteroid functions in a broad range of disease resistance in tobacco and rice. *The Plant Journal: For Cell and Molecular Biology*, 33(5):887–898, March 2003.

[337] D. Ernst, D. Oesterhelt, and W. Schäfer. Endogenous cytokinins during embryogenesis in an anise cell culture (Pimpinella anisum L.). *Planta*, 161(3):240–245, 1984. doi:10.2307/23377470.

[338] R. Aloni, E. Aloni, M. Langhans, and C. I. Ullrich. Role of auxin in regulating Arabidopsis flower development. *Planta*, 223(2):315–328, January 2006. URL: http://link.springer.com/10.1007/s00425-005-0088-9, doi:10.1007/s00425-005-0088-9.

[339] S. Howell. Cytokinins and shoot development. *Trends in Plant Science*, 8(9):453–459, September 2003. URL: http://linkinghub.elsevier.com/retrieve/pii/S1360138503001912, doi:10.1016/S1360-1385(03)00191-2.

[340] I. Bartrina, E. Otto, M. Strnad, T. Werner, and T. Schmülling. Cytokinin Regulates the Activity of Reproductive Meristems, Flower Organ Size, Ovule Formation, and Thus Seed Yield in *Arabidopsis thaliana*. *The Plant Cell*, 23(1):69–80, January 2011. URL: http://www.plantcell.org/lookup/doi/10.1105/tpc.110.079079, doi:10.1105/tpc.110.079079.

[341] X. G. Li, Y. H. Su, X. Y. Zhao, W. Li, X. Q. Gao, and X. S. Zhang. Cytokinin overproduction-caused alteration of flower development is partially mediated by CUC2 and CUC3 in Arabidopsis. *Gene*, 450(1-2):109–120, January 2010. URL: https://linkinghub.elsevier.com/retrieve/pii/S0378111909005721, doi:10.1016/j.gene.2009.11.003.

[342] V. M. Zuñiga-Mayo, C. R. Baños-Bayardo, D. Díaz-Ramírez, N. Marsch-Martínez, and S. de Folter. Conserved and novel responses to cytokinin treatments during flower and fruit development in Brassica napus and Arabidopsis thaliana. *Scientific Reports*, 8(1):6836, 2018. URL: https://doi.org/10.1038/s41598-018-25017-3, doi:10.1038/s41598-018-25017-3.

[343] G. Bertoni. Cytokinin and Compound Leaf Development. *The Plant Cell*, 22(10):3191–3191, October 2010. URL: http://www.plantcell.org/lookup/doi/10.1105/tpc.110.221010, doi:10.1105/tpc.110.221010.

[344] E. Shani, H. Ben-Gera, S. Shleizer-Burko, Y. Burko, D. Weiss, and N. Ori. Cytokinin Regulates Compound Leaf Development in Tomato. *The Plant Cell*, 22(10):3206–3217, October 2010. URL: http://www.plantcell.org/lookup/doi/10.1105/tpc.110.078253, doi:10.1105/tpc.110.078253.

[345] M. Cosme, E. Ramireddy, P. Franken, T. Schmülling, and S. Wurst. Shoot- and root-borne cytokinin influences arbuscular mycorrhizal symbiosis. *Mycorrhiza*, 26(7):709–720, October 2016. URL: http://link.springer.com/10.1007/s00572-016-0706-3, doi:10.1007/s00572-016-0706-3.

[346] P. J. Zwack and A. M. Rashotte. Interactions between cytokinin signalling and abiotic stress responses. *Journal of Experimental Botany*, 66(16):4863–4871, August 2015. URL: https://academic.oup.com/jxb/article-lookup/doi/10.1093/jxb/erv172, doi:10.1093/jxb/erv172.

[347] J. Pavlů, J. Novák, V. Koukalová, M. Luklová, B. Brzobohatý, and M. Černý. Cytokinin at the Crossroads of Abiotic Stress Signalling Pathways. *International Journal of Molecular Sciences*, 19(8):2450, August 2018. URL: http://www.mdpi.com/1422-0067/19/8/2450, doi:10.3390/ijms19082450.

[348] J. Choi, D. Choi, S. Lee, C.-M. Ryu, and I. Hwang. Cytokinins and plant immunity: old foes or new friends? *Trends in Plant Science*, 16(7):388–394, July 2011. URL: https://linkinghub.elsevier.com/retrieve/pii/S1360138511000513, doi:10.1016/j.tplants.2011.03.003.

[349] T. Albrecht and C. T. Argueso. Should I fight or should I grow now? The role of cytokinins in plant growth and immunity and in the growth–defence trade-off. *Annals of Botany*, page mcw211, November 2016. URL: https://academic.oup.com/aob/article-lookup/doi/10.1093/aob/mcw211, doi:10.1093/aob/mcw211.

[350] M. Naseem, M. Kunz, and T. Dandekar. Probing the Unknowns in Cytokinin-Mediated Immune Defense in *Arabidopsis* with Systems Biology Approaches. *Bioinformatics and Biology Insights*, 8:BBI.S13462, January 2014. URL: http://journals.sagepub.com/doi/10.4137/BBI.S13462, doi:10.4137/BBI.S13462.

[351] D. B. Hays, D. M. Reid, E. C. Yeung, and R. P. Pharis. Role of ethylene in cotyledon development of microspore-derived embryos of Brassica napus. *Journal of Experimental Botany*, 51(352):1851–1859, November 2000.

[352] K. Ruzicka, K. Ljung, S. Vanneste, R. Podhorska, T. Beeckman, J. Friml, and E. Benkova. Ethylene Regulates Root Growth through Effects on Auxin Biosynthesis and Transport-Dependent Auxin Distribution. *THE PLANT CELL ONLINE*, 19(7):2197–2212, July 2007. URL: http://www.plantcell.org/cgi/doi/10.1105/tpc.107.052126, doi:10.1105/tpc.107.052126.

[353] H. Qin and R. Huang. Auxin Controlled by Ethylene Steers Root Development. *International Journal of Molecular Sciences*, 19(11):3656, November 2018. URL: http://www.mdpi.com/1422-0067/19/11/3656, doi:10.3390/ijms19113656.

[354] M. V. Alarcón, P. G. Lloret, and J. Salguero. Synergistic action of auxin and ethylene on root elongation inhibition is caused by a reduction of epidermal cell length. *Plant Signaling & Behavior*, 9(3):e28361, March 2014. URL: http://www.tandfonline.com/doi/abs/10.4161/psb.28361, doi:10.4161/psb.28361.

[355] D. R. Lewis, S. Negi, P. Sukumar, and G. K. Muday. Ethylene inhibits lateral root development, increases IAA transport and expression of PIN3 and PIN7 auxin efflux carriers. *Development*, 138(16):3485–3495, August 2011. URL: http://dev.biologists.org/lookup/doi/10.1242/dev.065102, doi:10.1242/dev.065102.

[356] S. P. Chatfield and M. N. Raizada. Ethylene and shoot regeneration: hookless1 modulates de novo shoot organogenesis in Arabidopsis thaliana. *Plant Cell Reports*, 27(4):655–666, April 2008. URL: http://link.springer.com/10.1007/s00299-007-0496-3, doi:10.1007/s00299-007-0496-3.

[357] J. Smalle, M. Haegman, J. Kurepa, n. Van Montagu M, and D. V. Straeten. Ethylene can stimulate Arabidopsis hypocotyl elongation in the light. *Proceedings of the National Academy of Sciences of the United States of America*, 94(6):2756–2761, March 1997.

[358] P. Achard, M. Baghour, A. Chapple, P. Hedden, D. Van Der Straeten, P. Genschik, T. Moritz, and N. P. Harberd. The plant stress hormone ethylene controls floral transition via DELLA-dependent regulation of floral meristem-identity genes. *Proceedings of the National Academy of Sciences*, 104(15):6484–6489, April 2007. URL: http://www.pnas.org/cgi/doi/10.1073/pnas.0610717104, doi:10.1073/pnas.0610717104.

[359] F. Corbineau, Q. Xia, C. Bailly, and H. El-Maarouf-Bouteau. Ethylene, a key factor in the regulation of seed dormancy. *Frontiers in Plant Science*, 5, October 2014. URL: http://journal.frontiersin.org/article/10.3389/fpls.2014.00539/abstract, doi:10.3389/fpls.2014.00539.

[360] J. KeCpczynski and E. KeCpczynska. Ethylene in seed dormancy and germination. *Physiologia Plantarum*, 101(4):720–726, December 1997. URL: http://doi.wiley.com/10.1111/j.1399-3054.1997.tb01056.x, doi:10.1111/j.1399-3054.1997.tb01056.x.

[361] K. Kazan. Diverse roles of jasmonates and ethylene in abiotic stress tolerance. *Trends in Plant Science*, 20(4):219–229, April 2015. URL: https://linkinghub.elsevier.com/retrieve/pii/S136013851500031X, doi:10.1016/j.tplants.2015.02.001.

[362] H. Pei, H. Wang, L. Wang, F. Zheng, and C.-H. Dong. Regulatory Function of Ethylene in Plant Responses to Drought, Cold, and Salt Stresses. In G. K. Pandey, editor, *Mechanism of Plant Hormone Signaling under Stress*, pages 327–344. John Wiley & Sons, Inc., Hoboken, NJ, USA, March 2017. URL: http://doi.wiley.com/10.1002/9781118889022.ch13, doi:10.1002/9781118889022.ch13.

[363] O. Bouchez, C. Huard, S. Lorrain, D. Roby, and C. Balague. Ethylene Is One of the Key Elements for Cell Death and Defense Response Control in the Arabidopsis Lesion Mimic Mutant vad1. *PLANT PHYSIOLOGY*, 145(2):465–477, August 2007. URL: http://www.plantphysiol.org/cgi/doi/10.1104/pp.107.106302, doi:10.1104/pp.107.106302.

[364] S. T. Lund, R. E. Stall, and H. J. Klee. Ethylene regulates the susceptible response to pathogen infection in tomato. *The Plant Cell*, 10(3):371–382, March 1998.

[365] J. R. Ecker and R. W. Davis. Plant defense genes are regulated by ethylene. *Proceedings of the National Academy of Sciences of the United States of America*, 84(15):5202–5206, August 1987.

[366] W. F. Broekaert, S. L. Delauré, M. F. De Bolle, and B. P. Cammue. The Role of Ethylene in Host-Pathogen Interactions. *Annual Review of Phytopathology*, 44(1):393–416, September 2006. URL: http://www.annualreviews.org/doi/10.1146/annurev.phyto.44.070505.143440, doi:10.1146/annurev.phyto.44.070505.143440.

[367] Y. Hu, L. Zhou, M. Huang, X. He, Y. Yang, X. Liu, Y. Li, and X. Hou. Gibberellins play an essential role in late embryogenesis of Arabidopsis. *Nature Plants*, 4(5):289–298, May 2018. URL: http://www.nature.com/articles/s41477-018-0143-8, doi:10.1038/s41477-018-0143-8.

[368] B. T. Ayele, J. A. Ozga, L. V. Kurepin, and D. M. Reinecke. Developmental and Embryo Axis Regulation of Gibberellin Biosynthesis during Germination and Young Seedling Growth of Pea. *PLANT PHYSIOLOGY*, 142(3):1267–1281, September 2006. URL: http://www.plantphysiol.org/cgi/doi/10.1104/pp.106.086199, doi:10.1104/pp.106.086199.

[369] D. B. Hays, E. C. Yeung, and R. P. Pharis. The role of gibberellins in embryo axis development. *Journal of Experimental Botany*, 53(375):1747–1751, August 2002.

[370] S. Inada and T. Shimmen. Regulation of Elongation Growth by Gibberellin in Root Segments of Lemna minor. *Plant and Cell Physiology*, 41(8):932–939, August 2000. URL: http://academic.oup.com/pcp/article/41/8/932/2756566/Regulation-of-Elongation-Growth-by-Gibberellin-in, doi:10.1093/pcp/pcd018.

[371] E. Tanimoto. Gibberellin Requirement for the Normal Growth of Roots. In N. Takahashi, B. O. Phinney, and J. MacMillan, editors, *Gibberellins*, pages 229–240. Springer New York, New York, NY, 1991. URL: http://link.springer.com/10.1007/978-1-4612-3002-1_22, doi:10.1007/978-1-4612-3002-1_22.

[372] A. Serrano-Mislata, S. Bencivenga, M. Bush, K. Schiessl, S. Boden, and R. Sablowski. DELLA genes restrict inflorescence meristem function independently of plant height. *Nature Plants*, 3(9):749–754, September 2017. URL: http://www.nature.com/articles/s41477-017-0003-y, doi:10.1038/s41477-017-0003-y.

[373] V. C. Galvao, D. Horrer, F. Kuttner, and M. Schmid. Spatial control of flowering by DELLA proteins in Arabidopsis thaliana. *Development*, 139(21):4072–4082, November 2012. URL: http://dev.biologists.org/cgi/doi/10.1242/dev.080879, doi:10.1242/dev.080879.

[374] H. Yu, T. Ito, Y. Zhao, J. Peng, P. Kumar, and E. M. Meyerowitz. Floral homeotic genes are targets of gibberellin signaling in flower development. *Proceedings of the National Academy of Sciences*, 101(20):7827–7832, May 2004. URL: http://www.pnas.org/cgi/doi/10.1073/pnas.0402377101, doi:10.1073/pnas.0402377101.

[375] Q. Xu, S. Krishnan, E. Merewitz, J. Xu, and B. Huang. Gibberellin-Regulation and Genetic Variations in Leaf Elongation for Tall Fescue in Association with Differential Gene Expression Controlling Cell Expansion. *Scientific Reports*, 6(1), September 2016. URL: http://www.nature.com/articles/srep30258, doi:10.1038/srep30258.

[376] H. Nelissen, B. Rymen, Y. Jikumaru, K. Demuynck, M. Van Lijsebettens, Y. Kamiya, D. Inzé, and G. Beemster. A Local Maximum in Gibberellin Levels Regulates Maize Leaf Growth by Spatial Control of Cell Division. *Current Biology*, 22(13):1183–1187, July 2012. URL: https://linkinghub.elsevier.com/retrieve/pii/S0960982212005210, doi:10.1016/j.cub.2012.04.065.

[377] N. Takeda, Y. Handa, S. Tsuzuki, M. Kojima, H. Sakakibara, and M. Kawaguchi. Gibberellin regulates infection and colonization of host roots by arbuscular mycorrhizal fungi. *Plant Signaling & Behavior*, 10(6):e1028706, June 2015. URL: http://www.tandfonline.com/doi/full/10.1080/15592324.2015.1028706, doi:10.1080/15592324.2015.1028706.

[378] T. Ariizumi and C. M. Steber. Seed Germination of GA-Insensitive sleepy1 Mutants Does Not Require RGL2 Protein Disappearance in Arabidopsis. *THE PLANT CELL ONLINE*, 19(3):791–804, March 2007. URL: http://www.plantcell.org/cgi/doi/10.1105/tpc.106.048009, doi:10.1105/tpc.106.048009.

[379] E. H. Colebrook, S. G. Thomas, A. L. Phillips, and P. Hedden. The role of gibberellin signalling in plant responses to abiotic stress. *Journal of Experimental Biology*, 217(1):67–75, January 2014. URL: http://jeb.biologists.org/cgi/doi/10.1242/jeb.089938, doi:10.1242/jeb.089938.

[380] B. Vishal and P. P. Kumar. Regulation of Seed Germination and Abiotic Stresses by Gibberellins and Abscisic Acid. *Frontiers in Plant Science*, 9, June 2018. URL: https://www.frontiersin.org/article/10.3389/fpls.2018.00838/full, doi:10.3389/fpls.2018.00838.

[381] R. W. Wilen, G. J. van Rooijen, D. W. Pearce, R. P. Pharis, L. A. Holbrook, and M. M. Moloney. Effects of jasmonic Acid on embryo-specific processes in brassica and linum oilseeds. *Plant Physiology*, 95(2):399–405, February 1991.

[382] M. M. Mira, O. S. D. Wally, M. Elhiti, A. El-Shanshory, D. S. Reddy, R. D. Hill, and C. Stasolla. Jasmonic acid is a downstream component in the modulation of somatic embryogenesis by Arabidopsis Class 2 phytoglobin. *Journal of Experimental Botany*, 67(8):2231–2246, April 2016. URL: https://academic.oup.com/jxb/article-lookup/doi/10.1093/jxb/erw022, doi:10.1093/jxb/erw022.

[383] Z.-B. Yang, C. He, Y. Ma, M. Herde, and Z. Ding. Jasmonic Acid Enhances Al-Induced Root Growth Inhibition. *Plant Physiology*, 173(2):1420–1433, February 2017. URL: http://www.plantphysiol.org/lookup/doi/10.1104/pp.16.01756, doi:10.1104/pp.16.01756.

[384] H. Liu, L. C. Carvalhais, K. Kazan, and P. M. Schenk. Development of marker genes for jasmonic acid signaling in shoots and roots of wheat. *Plant Signaling & Behavior*, 11(5):e1176654, May 2016. URL: http://www.tandfonline.com/doi/full/10.1080/15592324.2016.1176654, doi:10.1080/15592324.2016.1176654.

[385] Z. Yuan and D. Zhang. Roles of jasmonate signalling in plant inflorescence and flower development. *Current Opinion in Plant Biology*, 27:44–51, October 2015. URL: https://linkinghub.elsevier.com/retrieve/pii/S1369526615000758, doi:10.1016/j.pbi.2015.05.024.

[386] E. Widemann, E. Smirnova, Y. Aubert, L. Miesch, and T. Heitz. Dynamics of Jasmonate Metabolism upon Flowering and across Leaf Stress Responses in Arabidopsis thaliana. *Plants*, 5(1):4, January 2016. URL: http://www.mdpi.com/2223-7747/5/1/4, doi:10.3390/plants5010004.

[387] S. Noir, M. Bomer, N. Takahashi, T. Ishida, T.-L. Tsui, V. Balbi, H. Shanahan, K. Sugimoto, and A. Devoto. Jasmonate Controls Leaf Growth by Repressing Cell Proliferation and the Onset of Endoreduplication while Maintaining a Potential Stand-By Mode. *PLANT PHYSIOLOGY*, 161(4):1930–1951, April 2013. URL: http://www.plantphysiol.org/cgi/doi/10.1104/pp.113.214908, doi:10.1104/pp.113.214908.

[388] Y. He, H. Fukushige, D. F. Hildebrand, and S. Gan. Evidence Supporting a Role of Jasmonic Acid in Arabidopsis Leaf Senescence. *PLANT PHYSIOLOGY*, 128(3):876–884, March 2002. URL: http://www.plantphysiol.org/cgi/doi/10.1104/pp.010843, doi:10.1104/pp.010843.

[389] L. Shi, L. Gong, X. Zhang, A. Ren, T. Gao, and M. Zhao. The regulation of methyl jasmonate on hyphal branching and GA biosynthesis in Ganoderma lucidum partly via ROS generated by NADPH oxidase. *Fungal Genetics and Biology*, 81:201–211, August 2015. URL: https://linkinghub.elsevier.com/retrieve/pii/S1087184514002175, doi:10.1016/j.fgb.2014.12.002.

[390] P. Singh, A. Dave, F. E. Vaistij, D. Worrall, G. H. Holroyd, J. G. Wells, F. Kaminski, I. A. Graham, and M. R. Roberts. Jasmonic acid-dependent regulation of seed dormancy following maternal herbivory in Arabidopsis. *New Phytologist*, 214(4):1702–1711, June 2017. URL: http://doi.wiley.com/10.1111/nph.14525, doi:10.1111/nph.14525.

[391] P. Ahmad, S. Rasool, A. Gul, S. A. Sheikh, N. A. Akram, M. Ashraf, A. M. Kazi, and S. Gucel. Jasmonates: Multifunctional Roles in Stress Tolerance. *Frontiers in Plant Science*, 7, June 2016. URL: http://journal.frontiersin.org/Article/10.3389/fpls.2016.00813/abstract, doi:10.3389/fpls.2016.00813.

[392] V. A. Halim, A. Vess, D. Scheel, and S. Rosahl. The Role of Salicylic Acid and Jasmonic Acid in Pathogen Defence. *Plant Biology*, 8(3):307–313, May 2006. URL: http://doi.wiley.com/10.1055/s-2006-924025, doi:10.1055/s-2006-924025.

[393] P. Vijayan, J. Shockey, C. A. Levesque, R. J. Cook, and J. Browse. A role for jasmonate in pathogen defense of Arabidopsis. *Proceedings of the National Academy of Sciences*, 95(12):7209–7214, June 1998. URL: http://www.pnas.org/cgi/doi/10.1073/pnas.95.12.7209, doi:10.1073/pnas.95.12.7209.

[394] S. M. Swarbreck, Y. Guerringue, E. Matthus, F. J. C. Jamieson, and J. M. Davies. Karrikin-sensing protein KAI2 is a new player in regulating root growth patterns. *bioRxiv*, September 2017. URL: http://biorxiv.org/lookup/doi/10.1101/195891, doi:10.1101/195891.

[395] S. M. Swarbreck, Y. Guerringue, E. Matthus, F. J. C. Jamieson, and J. M. Davies. Impairment in karrikin but not strigolactone sensing enhances root skewing in *Arabidopsis thaliana*. *The Plant Journal*, January 2019. URL: http://doi.wiley.com/10.1111/tpj.14233, doi:10.1111/tpj.14233.

[396] D. C. Nelson, G. R. Flematti, J.-A. Riseborough, E. L. Ghisalberti, K. W. Dixon, and S. M. Smith. Karrikins enhance light responses during germination and seedling development in Arabidopsis thaliana. *Proceedings of the National Academy of Sciences*, 107(15):7095–7100, April 2010. URL: http://www.pnas.org/cgi/doi/10.1073/pnas.0911635107, doi:10.1073/pnas.0911635107.

[397] L. Wang, M. T. Waters, and S. M. Smith. Karrikin-KAI2 signalling provides Arabidopsis seeds with tolerance to abiotic stress and inhibits germination under conditions unfavourable to seedling establishment. *New Phytologist*, 219(2):605–618, July 2018. URL: http://doi.wiley.com/10.1111/nph.15192, doi:10.1111/nph.15192.

[398] W. Li, K. H. Nguyen, H. D. Chu, C. V. Ha, Y. Watanabe, Y. Osakabe, M. A. Leyva-González, M. Sato, K. Toyooka, L. Voges, M. Tanaka, M. G. Mostofa, M. Seki, M. Seo, S. Yamaguchi, D. C. Nelson, C. Tian, L. Herrera-Estrella, and L.-S. P. Tran. The karrikin receptor KAI2 promotes drought resistance in Arabidopsis thaliana. *PLOS Genetics*, 13(11):e1007076, November 2017. URL: https://dx.plos.org/10.1371/journal.pgen.1007076, doi:10.1371/journal.pgen.1007076.

[399] W. Li and L.-S. P. Tran. Are karrikins involved in plant abiotic stress responses? *Trends in Plant Science*, 20(9):535–538, September 2015. URL: https://linkinghub.elsevier.com/retrieve/pii/S1360138515001971, doi:10.1016/j.tplants.2015.07.006.

[400] C. Martínez, E. Pons, G. Prats, and J. León. Salicylic acid regulates flowering time and links defence responses and reproductive development. *The Plant Journal: For Cell and Molecular Biology*, 37(2):209–217, January 2004.

[401] S. Lee, S.-G. Kim, and C.-M. Park. Salicylic acid promotes seed germination under high salinity by modulating antioxidant activity in Arabidopsis. *New Phytologist*, 188(2):626–637, October 2010. URL: http://doi.wiley.com/10.1111/j.1469-8137.2010.03378.x, doi:10.1111/j.1469-8137.2010.03378.x.

[402] M. I. R. Khan, M. Fatma, T. S. Per, N. A. Anjum, and N. A. Khan. Salicylic acid-induced abiotic stress tolerance and underlying mechanisms in plants. *Frontiers in Plant Science*, 6, June 2015. URL: http://journal.frontiersin.org/Article/10.3389/fpls.2015.00462/abstract, doi:10.3389/fpls.2015.00462.

[403] A. Bernal-Vicente, C. Petri, J. A. Hernandez, and P. Diaz-Vivancos. The effect of abiotic and biotic stress on the salicylic acid biosynthetic pathway from mandelonitrile in peach. *bioRxiv*, 2017. URL: http://biorxiv.org/lookup/doi/10.1101/204636, doi:10.1101/204636.

[404] Y. Wu, E. Dor, and J. Hershenhorn. Strigolactones affect tomato hormone profile and somatic embryogenesis. *Planta*, 245(3):583–594, March 2017. URL: http://link.springer.com/10.1007/s00425-016-2625-0, doi:10.1007/s00425-016-2625-0.

[405] L. Jiang, C. Matthys, B. Marquez-Garcia, C. De Cuyper, L. Smet, A. De Keyser, F.-D. Boyer, T. Beeckman, S. Depuydt, and S. Goormachtig. Strigolactones spatially influence lateral root development through the cytokinin signaling network. *Journal of Experimental Botany*, 67(1):379–389, January 2016. URL: https://academic.oup.com/jxb/article-lookup/doi/10.1093/jxb/erv478, doi:10.1093/jxb/erv478.

[406] T. Bennett, Y. Liang, M. Seale, S. Ward, D. Müller, and O. Leyser. Strigolactone regulates shoot development through a core signalling pathway. *Biology Open*, 5(12):1806–1820, December 2016. URL: http://bio.biologists.org/lookup/doi/10.1242/bio.021402, doi:10.1242/bio.021402.

[407] H. Ueda and M. Kusaba. Strigolactone Regulates Leaf Senescence in Concert with Ethylene in Arabidopsis. *Plant Physiology*, 169(1):138–147, September 2015. URL: http://www.plantphysiol.org/lookup/doi/10.1104/pp.15.00325, doi:10.1104/pp.15.00325.

[408] A. Besserer, V. Puech-Pagès, P. Kiefer, V. Gomez-Roldan, A. Jauneau, S. Roy, J.-C. Portais, C. Roux, G. Bécard, and N. Séjalon-Delmas. Strigolactones Stimulate Arbuscular Mycorrhizal Fungi by Activating Mitochondria. *PLoS Biology*, 4(7):e226, June 2006. URL: https://dx.plos.org/10.1371/journal.pbio.0040226, doi:10.1371/journal.pbio.0040226.

[409] L. Lanfranco, V. Fiorilli, F. Venice, and P. Bonfante. Strigolactones cross the kingdoms: plants, fungi, and bacteria in the arbuscular mycorrhizal symbiosis. *Journal of Experimental Botany*, 69(9):2175–2188, April 2018. URL: https://academic.oup.com/jxb/article/69/9/2175/4773819, doi:10.1093/jxb/erx432.

[410] R. Aroca, J. M. Ruiz-Lozano, n. M. Zamarreño, J. A. Paz, J. M. García-Mina, M. J. Pozo, and J. A. López-Ráez. Arbuscular mycorrhizal symbiosis influences strigolactone production under salinity and alleviates salt stress in lettuce plants. *Journal of Plant Physiology*, 170(1):47–55, January 2013. URL: https://linkinghub.elsevier.com/retrieve/pii/S0176161712004014, doi:10.1016/j.jplph.2012.08.020.

[411] J. M. Ruiz-Lozano, R. Aroca, n. M. Zamarreño, S. Molina, B. Andreo-Jiménez, R. Porcel, J. M. García-Mina, C. Ruyter-Spira, and J. A. López-Ráez. Arbuscular mycorrhizal symbiosis induces strigolactone biosynthesis under drought and improves drought tolerance in lettuce and tomato: Drought and AM symbiosis induce strigolactones. *Plant, Cell & Environment*, 39(2):441–452, February 2016. URL: http://doi.wiley.com/10.1111/pce.12631, doi:10.1111/pce.12631.

[412] S. Toh, P. McCourt, and Y. Tsuchiya. HY5 is involved in strigolactone-dependent seed germination in Arabidopsis. *Plant Signaling & Behavior*, 7(5):556–558, May 2012. doi:10.4161/psb.19839.

[413] W. Saeed, S. Naseem, and Z. Ali. Strigolactones Biosynthesis and Their Role in Abiotic Stress Resilience in Plants: A Critical Review. *Frontiers in Plant Science*, 8, August 2017. URL: http://journal.frontiersin.org/article/10.3389/fpls.2017.01487/full, doi:10.3389/fpls.2017.01487.

[414] M. G. Mostofa, W. Li, K. H. Nguyen, M. Fujita, and L.-S. P. Tran. Strigolactones in plant adaptation to abiotic stresses: An emerging avenue of plant research: Strigolactones in abiotic stress adaptation. *Plant, Cell & Environment*, 41(10):2227–2243, October 2018. URL: http://doi.wiley.com/10.1111/pce.13364, doi:10.1111/pce.13364.

[415] Y. Kapulnik and H. Koltai. Strigolactone Involvement in Root Development, Response to Abiotic Stress, and Interactions with the Biotic Soil Environment. *PLANT PHYSIOLOGY*, 166(2):560–569, October 2014. URL: http://www.plantphysiol.org/cgi/doi/10.1104/pp.114.244939, doi:10.1104/pp.114.244939.

[416] E. Stes, S. Depuydt, A. De Keyser, C. Matthys, K. Audenaert, K. Yoneyama, S. Werbrouck, S. Goormachtig, and D. Vereecke. Strigolactones as an auxiliary hormonal defence mechanism against leafy gall syndrome in *Arabidopsis thaliana*. *Journal of Experimental Botany*, 66(16):5123–5134, August 2015. URL: https://academic.oup.com/jxb/article-lookup/doi/10.1093/jxb/erv309, doi:10.1093/jxb/erv309.

[417] Z. Jiang, X. Liu, Z. Peng, Y. Wan, Y. Ji, W. He, W. Wan, J. Luo, and H. Guo. AHD2.0: an update version of Arabidopsis Hormone Database for plant systematic studies. *Nucleic Acids Research*, 39(Database issue):D1123–1129, January 2011. doi:10.1093/nar/gkq1066.

[418] M. S. Mukhtar, A.-R. Carvunis, M. Dreze, P. Epple, J. Steinbrenner, J. Moore, M. Tasan, M. Galli, T. Hao, M. T. Nishimura, S. J. Pevzner, S. E. Donovan, L. Ghamsari, B. Santhanam, V. Romero, M. M. Poulin, F. Gebreab, B. J. Gutierrez, S. Tam, D. Monachello, M. Boxem, C. J. Harbort, N. McDonald, L. Gai, H. Chen, Y. He, European Union Effectoromics Consortium, J. Vandenhaute, F. P. Roth, D. E. Hill, J. R. Ecker, M. Vidal, J. Beynon, P. Braun, and J. L. Dangl. Independently evolved virulence effectors converge onto hubs in a plant immune system network. *Science (New York, N.Y.)*, 333(6042):596–601, July 2011. doi:10.1126/science.1203659.

[419] R. Weßling, P. Epple, S. Altmann, Y. He, L. Yang, S. R. Henz, N. McDonald, K. Wiley, K. C. Bader, C. Gläßer, M. S. Mukhtar, S. Haigis, L. Ghamsari, A. E. Stephens, J. R. Ecker, M. Vidal, J. D. G. Jones, K. F. X. Mayer, E. Ver Loren van Themaat, D. Weigel, P. Schulze-Lefert, J. L. Dangl, R. Panstruga, and P. Braun. Convergent targeting of a common host protein-network by pathogen effectors from three kingdoms of life. *Cell Host & Microbe*, 16(3):364–375, September 2014. doi:10.1016/j.chom.2014.08.004.

[420] P. Shannon. Cytoscape: A Software Environment for Integrated Models of Biomolecular Interaction Networks. *Genome Research*, 13(11):2498–2504, November 2003. URL: http://www.genome.org/cgi/doi/10.1101/gr.1239303, doi:10.1101/gr.1239303.

[421] T. Rolland, M. Taşan, B. Charloteaux, S. J. Pevzner, Q. Zhong, N. Sahni, S. Yi, I. Lemmens, C. Fontanillo, R. Mosca, A. Kamburov, S. D. Ghiassian, X. Yang, L. Ghamsari, D. Balcha, B. E. Begg, P. Braun, M. Brehme, M. P. Broly, A.-R. Carvunis, D. Convery-Zupan, R. Corominas, J. Coulombe-Huntington, E. Dann, M. Dreze, A. Dricot, C. Fan, E. Franzosa, F. Gebreab, B. J. Gutierrez, M. F. Hardy, M. Jin, S. Kang, R. Kiros, G. N. Lin, K. Luck, A. MacWilliams, J. Menche, R. R. Murray, A. Palagi, M. M. Poulin, X. Rambout, J. Rasla, P. Reichert, V. Romero, E. Ruyssinck, J. M. Sahalie, A. Scholz, A. A. Shah, A. Sharma, Y. Shen, K. Spirohn, S. Tam, A. O. Tejeda, S. A. Trigg, J.-C. Twizere, K. Vega, J. Walsh, M. E. Cusick, Y. Xia, A.-L. Barabási, L. M. Iakoucheva, P. Aloy, J. De Las Rivas, J. Tavernier, M. A. Calderwood, D. E. Hill, T. Hao, F. P. Roth, and M. Vidal. A proteome-scale map of the human interactome network. *Cell*, 159(5):1212–1226, November 2014. doi:10.1016/j.cell.2014.10.050.

[422] H. Yu, P. Braun, M. A. Yildirim, I. Lemmens, K. Venkatesan, J. Sahalie, T. Hirozane-Kishikawa, F. Gebreab, N. Li, N. Simonis, T. Hao, J.-F. Rual, A. Dricot, A. Vazquez, R. R. Murray, C. Simon, L. Tardivo, S. Tam, N. Svrzikapa, C. Fan, A.-S. de Smet, A. Motyl, M. E. Hudson, J. Park, X. Xin, M. E. Cusick, T. Moore, C. Boone, M. Snyder, F. P. Roth, A.-L. Barabasi, J. Tavernier, D. E. Hill, and M. Vidal. High-Quality Binary Protein Interaction Map of the Yeast Interactome Network. *Science*, 322(5898):104–110, October 2008. URL: http://www.sciencemag.org/cgi/doi/10.1126/science.1158684, doi:10.1126/science.1158684.

[423] P. Braun. Interactome mapping for analysis of complex phenotypes: Insights from benchmarking binary interaction assays. *PROTEOMICS*, 12(10):1499–1518, May 2012. URL: http://doi.wiley.com/10.1002/pmic.201100598, doi:10.1002/pmic.201100598.

[424] C. Stark. BioGRID: a general repository for interaction datasets. *Nucleic Acids Research*, 34(90001):D535–D539, January 2006. URL: https://academic.oup.com/nar/article-lookup/doi/10.1093/nar/gkj109, doi:10.1093/nar/gkj109.

[425] S. Orchard, M. Ammari, B. Aranda, L. Breuza, L. Briganti, F. Broackes-Carter, N. H. Campbell, G. Chavali, C. Chen, N. del Toro, M. Duesbury, M. Dumousseau, E. Galeota, U. Hinz, M. Iannuccelli, S. Jagannathan, R. Jimenez, J. Khadake, A. Lagreid, L. Licata, R. C. Lovering, B. Meldal, A. N. Melidoni, M. Milagros, D. Peluso, L. Perfetto, P. Porras, A. Raghunath, S. Ricard-Blum, B. Roechert, A. Stutz, M. Tognolli, K. van Roey, G. Cesareni, and H. Hermjakob. The MIntAct project–IntAct as a common curation platform for 11 molecular interaction databases. *Nucleic Acids Research*, 42(Database issue):D358–363, January 2014. doi:10.1093/nar/gkt1115.

[426] H. Cui, Y. Wang, L. Xue, J. Chu, C. Yan, J. Fu, M. Chen, R. W. Innes, and J.-M. Zhou. Pseudomonas syringae Effector Protein AvrB Perturbs Arabidopsis Hormone Signaling by Activating MAP Kinase 4. *Cell Host & Microbe*, 7(2):164–175, February 2010. URL: https://linkinghub.elsevier.com/retrieve/pii/S1931312810000351, doi:10.1016/j.chom.2010.01.009.

[427] M. A. R. Khokon, M. A. Salam, F. Jammes, W. Ye, M. A. Hossain, M. Uraji, Y. Nakamura, I. C. Mori, J. M. Kwak, and Y. Murata. Two guard cell mitogen-activated protein kinases, MPK9 and MPK12, function in methyl jasmonate-induced stomatal closure in *Arabidopsis thaliana*. *Plant Biology*, 17(5):946–952, September 2015. URL: http://doi.wiley.com/10.1111/plb.12321, doi:10.1111/plb.12321.

[428] B. G. Forde, S. R. Cutler, N. Zaman, and P. J. Krysan. Glutamate signalling via a MEKK1 kinase-dependent pathway induces changes in Arabidopsis root architecture. *The Plant Journal*, 75(1):1–10, July 2013. URL: http://doi.wiley.com/10.1111/tpj.12201, doi:10.1111/tpj.12201.

[429] T. T. Pham, S. P. Angus, and G. L. Johnson. MAP3k1: Genomic Alterations in Cancer and Function in Promoting Cell Survival or Apoptosis. *Genes & Cancer*, 4(11-12):419–426, November 2013. URL: http://gan.sagepub.com/lookup/doi/10.1177/1947601913513950, doi:10.1177/1947601913513950.

[430] Y. Zhao, L. Xing, X. Wang, Y.-J. Hou, J. Gao, P. Wang, C.-G. Duan, X. Zhu, and J.-K. Zhu. The ABA Receptor PYL8 Promotes Lateral Root Growth by Enhancing MYB77-Dependent Transcription of Auxin-Responsive Genes. *Science Signaling*, 7(328):ra53–ra53, June 2014. URL: http://stke.sciencemag.org/cgi/doi/10.1126/scisignal.2005051, doi:10.1126/scisignal.2005051.

[431] J. H. Kim, N. H. Nguyen, C. Y. Jeong, N. T. Nguyen, S.-W. Hong, and H. Lee. Loss of the R2r3 MYB, AtMyb73, causes hyper-induction of the SOS1 and SOS3 genes in response to high salinity in Arabidopsis. *Journal of Plant Physiology*, 170(16):1461–1465, November 2013. URL: https://linkinghub.elsevier.com/retrieve/pii/S0176161713002241, doi:10.1016/j.jplph.2013.05.011.

[432] X. Zhang, Y. Dai, Y. Xiong, C. DeFraia, J. Li, X. Dong, and Z. Mou. Overexpression of Arabidopsis MAP kinase kinase 7 leads to activation of plant basal and systemic acquired resistance. *The Plant Journal*, 52(6):1066–1079, December 2007. URL: http://doi.wiley.com/10.1111/j.1365-313X.2007.03294.x, doi:10.1111/j.1365-313X.2007.03294.x.

[433] T. Kroj. Regulation of storage protein gene expression in Arabidopsis. *Development*, 130(24):6065–6073, October 2003. URL: http://dev.biologists.org/cgi/doi/10.1242/dev.00814, doi:10.1242/dev.00814.

[434] S. R. Bennett, J. Alvarez, G. Bossinger, and D. R. Smyth. Morphogenesis in pinoid mutants of Arabidopsis thaliana. *The Plant Journal*, 8(4):505–520, October 1995. URL: http://doi.wiley.com/10.1046/j.1365-313X.1995.8040505.x, doi:10.1046/j.1365-313X.1995.8040505.x.

[435] R. Benjamins, A. Quint, D. Weijers, P. Hooykaas, and R. Offringa. The PINOID protein kinase regulates organ development in Arabidopsis by enhancing polar auxin transport. *Development (Cambridge, England)*, 128(20):4057–4067, October 2001.

[436] C. Gehl, R. Waadt, J. Kudla, R.-R. Mendel, and R. Hänsch. New GATEWAY vectors for High Throughput Analyses of Protein–Protein Interactions by Bimolecular Fluorescence Complementation. *Molecular Plant*, 2(5):1051–1058, September 2009. URL: https://linkinghub.elsevier.com/retrieve/pii/S1674205214607188, doi:10.1093/mp/ssp040.

[437] P. Dhonukshe, F. Huang, C. S. Galvan-Ampudia, A. P. Mahonen, J. Kleine-Vehn, J. Xu, A. Quint, K. Prasad, J. Friml, B. Scheres, and R. Offringa. Plasma membrane-bound AGC3 kinases phosphorylate PIN auxin carriers at TPRXS(N/S) motifs to direct apical PIN recycling. *Development*, 137(19):3245–3255, October 2010. URL: http://dev.biologists.org/cgi/doi/10.1242/dev.052456, doi:10.1242/dev.052456.

[438] H. Mi, X. Huang, A. Muruganujan, H. Tang, C. Mills, D. Kang, and P. D. Thomas. PANTHER version 11: expanded annotation data from Gene Ontology and Reactome pathways, and data analysis tool enhancements. *Nucleic Acids Research*, 45(D1):D183–D189, January 2017. URL: https://academic.oup.com/nar/article-lookup/doi/10.1093/nar/gkw1138, doi:10.1093/nar/gkw1138.

[439] S. Carbon, A. Ireland, C. J. Mungall, S. Shu, B. Marshall, S. Lewis, the AmiGO Hub, and the Web Presence Working Group. AmiGO: online access to ontology and annotation data. *Bioinformatics*, 25(2):288–289, January 2009. URL: https://academic.oup.com/bioinformatics/article/25/2/288/220714, doi:10.1093/bioinformatics/btn615.

[440] J. Day-Richter, M. A. Harris, M. Haendel, The Gene Ontology OBO-Edit Working Group, and S. Lewis. OBO-Edit an ontology editor for biologists. *Bioinformatics*, 23(16):2198–2200, August 2007. URL: https://academic.oup.com/bioinformatics/article-lookup/doi/10.1093/bioinformatics/btm112, doi:10.1093/bioinformatics/btm112.

[441] F. Supek, M. Bošnjak, N. Škunca, and T. Šmuc. REVIGO Summarizes and Visualizes Long Lists of Gene Ontology Terms. *PLoS ONE*, 6(7):e21800, July 2011. URL: https://dx.plos.org/10.1371/journal.pone.0021800, doi:10.1371/journal.pone.0021800.

[442] J. Pruneda-Paz, G. Breton, D. Nagel, S. Kang, K. Bonaldi, C. Doherty, S. Ravelo, M. Galli, J. Ecker, and S. Kay. A Genome-Scale Resource for the Functional Characterization of Arabidopsis Transcription Factors. *Cell Reports*, 8(2):622–632, July 2014. URL: https://linkinghub.elsevier.com/retrieve/pii/S2211124714005178, doi:10.1016/j.celrep.2014.06.033.

[443] Y. Wang, L. Li, T. Ye, S. Zhao, Z. Liu, Y.-Q. Feng, and Y. Wu. Cytokinin antagonizes ABA suppression to seed germination of Arabidopsis by downregulating ABI5 expression: *The interplay of ABA and cytokinin in Arabidopsis*. *The Plant Journal*, 68(2):249–261, October 2011. URL: http://doi.wiley.com/10.1111/j.1365-313X.2011.04683.x, doi:10.1111/j.1365-313X.2011.04683.x.

[444] E. Oh, J.-Y. Zhu, and Z.-Y. Wang. Interaction between BZR1 and PIF4 integrates brassinosteroid and environmental responses. *Nature Cell Biology*, 14(8):802–809, August 2012. URL: http://www.nature.com/articles/ncb2545, doi:10.1038/ncb2545.

[445] W. Hanna-Rose and U. Hansen. Active repression mechanisms of eukaryotic transcription repressors. *Trends in genetics: TIG*, 12(6):229–234, June 1996.

[446] K. B. Singh. Transcriptional regulation in plants: the importance of combinatorial control. *Plant Physiology*, 118(4):1111–1120, December 1998.

[447] T. J. Guilfoyle. Auxin-regulated genes and promoters. In *New Comprehensive Biochemistry*, volume 33, pages 423–459. Elsevier, 1999. URL: https://linkinghub.elsevier.com/retrieve/pii/S0167730608604998, doi:10.1016/S0167-7306(08)60499-8.

[448] N. Ballas, L.-M. Wong, and A. Theologis. Identification of the Auxin-responsive Element, AuxRE, in the Primary indoleacetic Acid-inducible Gene, PS-IAA4/5, of Pea (Pisum sativum). *Journal of Molecular Biology*, 233(4):580–596, October 1993. URL: http://linkinghub.elsevier.com/retrieve/pii/S0022283683715378, doi:10.1006/jmbi.1993.1537.

[449] S. Abel, P. W. Oeller, and A. Theologis. Early auxin-induced genes encode short-lived nuclear proteins. *Proceedings of the National Academy of Sciences of the United States of America*, 91(1):326–330, January 1994.

[450] K. A. Dreher. The Arabidopsis Aux/IAA Protein Family Has Diversified in Degradation and Auxin Responsiveness. *THE PLANT CELL ONLINE*, 18(3):699–714, March 2006. URL: http://www.plantcell.org/cgi/doi/10.1105/tpc.105.039172, doi:10.1105/tpc.105.039172.

[451] D. Weijers, E. Benkova, K. E. Jäger, A. Schlereth, T. Hamann, M. Kientz, J. C. Wilmoth, J. W. Reed, and G. Jürgens. Developmental specificity of auxin response by pairs of ARF and Aux/IAA transcriptional regulators. *The EMBO Journal*, 24(10):1874–1885, May 2005. URL: http://emboj.embopress.org/cgi/doi/10.1038/sj.emboj.7600659, doi:10.1038/sj.emboj.7600659.

[452] Q. Guo, Y. Yoshida, I. T. Major, K. Wang, K. Sugimoto, G. Kapali, N. E. Havko, C. Benning, and G. A. Howe. JAZ repressors of metabolic defense promote growth and reproductive fitness in *Arabidopsis*. *Proceedings of the National Academy of Sciences*, 115(45):E10768–E10777, November 2018. URL: http://www.pnas.org/lookup/doi/10.1073/pnas.1811828115, doi:10.1073/pnas.1811828115.

[453] J. Li and K. H. Nam. Regulation of brassinosteroid signaling by a GSK3/SHAGGY-like kinase. *Science (New York, N.Y.)*, 295(5558):1299–1301, February 2002. doi:10.1126/science.1065769.

[454] M. Müller and S. Munné-Bosch. Ethylene Response Factors: A Key Regulatory Hub in Hormone and Stress Signaling. *Plant Physiology*, 169(1):32–41, September 2015. URL: http://www.plantphysiol.org/lookup/doi/10.1104/pp.15.00677, doi:10.1104/pp.15.00677.

[455] K. C. McGrath. Repressor- and Activator-Type Ethylene Response Factors Functioning in Jasmonate Signaling and Disease Resistance Identified via a Genome-Wide Screen of Arabidopsis Transcription Factor Gene Expression. *PLANT PHYSIOLOGY*, 139(2):949–959, September 2005. URL: http://www.plantphysiol.org/cgi/doi/10.1104/pp.105.068544, doi:10.1104/pp.105.068544.

[456] B. Ren, Y. Liang, Y. Deng, Q. Chen, J. Zhang, X. Yang, and J. Zuo. Genome-wide comparative analysis of type-A Arabidopsis response regulator genes by overexpression studies reveals their diverse roles and regulatory mechanisms in cytokinin signaling. *Cell Research*, 19(10):1178–1190, October 2009. URL: http://www.nature.com/articles/cr200988, doi:10.1038/cr.2009.88.

[457] J. Kim. Phosphorylation of A-Type ARR to function as negative regulator of cytokinin signal transduction. *Plant Signaling & Behavior*, 3(5):348–350, May 2008.

[458] J. P. To. Type-A Arabidopsis Response Regulators Are Partially Redundant Negative Regulators of Cytokinin Signaling. *THE PLANT CELL ONLINE*, 16(3):658–671, March 2004. URL: http://www.plantcell.org/cgi/doi/10.1105/tpc.018978, doi:10.1105/tpc.018978.

[459] T. Kiba, H. Yamada, and T. Mizuno. Characterization of the ARR15 and ARR16 response regulators with special reference to the cytokinin signaling pathway mediated by the AHK4 histidine kinase in roots of Arabidopsis thaliana. *Plant & Cell Physiology*, 43(9):1059–1066, September 2002.

[460] T. Kiba, H. Yamada, S. Sato, T. Kato, S. Tabata, T. Yamashino, and T. Mizuno. The type-A response regulator, ARR15, acts as a negative regulator in the cytokinin-mediated signal transduction in Arabidopsis thaliana. *Plant & Cell Physiology*, 44(8):868–874, August 2003.

[461] P. A. Salome. Arabidopsis Response Regulators ARR3 and ARR4 Play Cytokinin-Independent Roles in the Control of Circadian Period. *THE PLANT CELL ONLINE*, 18(1):55–69, January 2006. URL: http://www.plantcell.org/cgi/doi/10.1105/tpc.105.037994, doi:10.1105/tpc.105.037994.

[462] K. Ishida, T. Yamashino, and T. Mizuno. Expression of the cytokinin-induced type-A response regulator gene ARR9 is regulated by the circadian clock in Arabidopsis thaliana. *Bioscience, Biotechnology, and Biochemistry*, 72(11):3025–3029, November 2008.

[463] M. Chern, P. E. Canlas, and P. C. Ronald. Strong Suppression of Systemic Acquired Resistance in Arabidopsis by NRR is Dependent on its Ability to Interact with NPR1and its Putative Repression Domain. *Molecular Plant*, 1(3):552–559, May 2008. URL: https://linkinghub.elsevier.com/retrieve/pii/S1674205214603488, doi:10.1093/mp/ssn017.

[464] S. Zwicker, S. Mast, V. Stos, A. J. P. Pfitzner, and U. M. Pfitzner. Tobacco NIMIN2 proteins control PR gene induction through transient repression early in systemic acquired resistance. *Molecular Plant Pathology*, 8(4):385–400, July 2007. URL: http://doi.wiley.com/10.1111/j.1364-3703.2007.00399.x, doi:10.1111/j.1364-3703.2007.00399.x.

[465] B. Shuai. The Lateral Organ Boundaries Gene Defines a Novel, Plant-Specific Gene Family. *PLANT PHYSIOLOGY*, 129(2):747–761, June 2002. URL: http://www.plantphysiol.org/cgi/doi/10.1104/pp.010926, doi:10.1104/pp.010926.

[466] H. Iwakawa, Y. Ueno, E. Semiarti, H. Onouchi, S. Kojima, H. Tsukaya, M. Hasebe, T. Soma, M. Ikezaki, C. Machida, and Y. Machida. The ASYMMETRIC LEAVES2 gene of Arabidopsis thaliana, required for formation of a symmetric flat leaf lamina, encodes a member of a novel family of proteins characterized by cysteine repeats and a leucine zipper. *Plant & Cell Physiology*, 43(5):467–478, May 2002.

[467] C. Majer and F. Hochholdinger. Defining the boundaries: structure and function of LOB domain proteins. *Trends in Plant Science*, 16(1):47–52, January 2011. URL: https://linkinghub.elsevier.com/retrieve/pii/S1360138510002050, doi:10.1016/j.tplants.2010.09.009.

[468] A. Husbands, E. M. Bell, B. Shuai, H. M. Smith, and P. S. Springer. LATERAL ORGAN BOUNDARIES defines a new family of DNA-binding transcription factors and can interact with specific bHLH proteins. *Nucleic Acids Research*, 35(19):6663–6671, October 2007. URL: https://academic.oup.com/nar/article-lookup/doi/10.1093/nar/gkm775, doi:10.1093/nar/gkm775.

[469] C. Xu, F. Luo, and F. Hochholdinger. LOB Domain Proteins: Beyond Lateral Organ Boundaries. *Trends in Plant Science*, 21(2):159–167, February 2016. URL: https://linkinghub.elsevier.com/retrieve/pii/S1360138515002587, doi:10.1016/j.tplants.2015.10.010.

[470] B. W. Jeon and J. Kim. Role of *LBD14* during ABA-mediated control of root system architecture in Arabidopsis. *Plant Signaling & Behavior*, pages 1–3, August 2018. URL: https://www.tandfonline.com/doi/full/10.1080/15592324.2018.1507405, doi:10.1080/15592324.2018.1507405.

[471] E. Jeon, N. Young Kang, C. Cho, P. Joon Seo, M. Chung Suh, and J. Kim. LBD14/ASL17 Positively Regulates Lateral Root Formation and is Involved in ABA Response for Root Architecture in Arabidopsis. *Plant and Cell Physiology*, 58(12):2190–2201, December 2017. URL: http://academic.oup.com/pcp/article/58/12/2190/4457919, doi:10.1093/pcp/pcx153.

[472] L. An, Z. Zhou, A. Yan, and Y. Gan. Progress on trichome development regulated by phytohormone signaling. *Plant Signaling & Behavior*, 6(12):1959–1962, December 2011. URL: http://www.tandfonline.com/doi/abs/10.4161/psb.6.12.18120, doi:10.4161/psb.6.12.18120.

[473] T. Qi, S. Song, Q. Ren, D. Wu, H. Huang, Y. Chen, M. Fan, W. Peng, C. Ren, and D. Xie. The Jasmonate-ZIM-Domain Proteins Interact with the WD-Repeat/bHLH/MYB Complexes to Regulate Jasmonate-Mediated Anthocyanin Accumulation and Trichome Initiation in *Arabidopsis thaliana*. *The Plant Cell*, 23(5):1795–1814, May 2011. URL: http://www.plantcell.org/lookup/doi/10.1105/tpc.111.083261, doi:10.1105/tpc.111.083261.

[474] C. T. Payne, F. Zhang, and A. M. Lloyd. GL3 encodes a bHLH protein that regulates trichome development in arabidopsis through interaction with GL1 and TTG1. *Genetics*, 156(3):1349–1362, November 2000.

[475] Y. Yoshida, R. Sano, T. Wada, J. Takabayashi, and K. Okada. Jasmonic acid control of GLABRA3 links inducible defense and trichome patterning in Arabidopsis. *Development*, 136(6):1039–1048, March 2009. URL: http://dev.biologists.org/cgi/doi/10.1242/dev.030585, doi:10.1242/dev.030585.

[476] A. Mandaokar, B. Thines, B. Shin, B. Markus Lange, G. Choi, Y. J. Koo, Y. J. Yoo, Y. D. Choi, G. Choi, and J. Browse. Transcriptional regulators of stamen development in Arabidopsis identified by transcriptional profiling. *The Plant Journal*, 46(6):984–1008, June 2006. URL: http://doi.wiley.com/10.1111/j.1365-313X.2006.02756.x, doi:10.1111/j.1365-313x.2006.02756.x.

[477] S. Song, T. Qi, H. Huang, Q. Ren, D. Wu, C. Chang, W. Peng, Y. Liu, J. Peng, and D. Xie. The Jasmonate-ZIM Domain Proteins Interact with the R2r3-MYB Transcription Factors MYB21 and MYB24 to Affect Jasmonate-Regulated Stamen Development in Arabidopsis. *The Plant Cell*, 23(3):1000–1013, March 2011. URL: http://www.plantcell.org/cgi/doi/10.1105/tpc.111.083089, doi:10.1105/tpc.111.083089.

[478] C. Yanhui, Y. Xiaoyuan, H. Kun, L. Meihua, L. Jigang, G. Zhaofeng, L. Zhiqiang, Z. Yunfei, W. Xiaoxiao, Q. Xiaoming, S. Yunping, Z. Li, D. Xiaohui, L. Jingchu, D. Xing-Wang, C. Zhangliang, G. Hongya, and Q. Li-Jia. The MYB Transcription Factor Superfamily of Arabidopsis: Expression Analysis and Phylogenetic Comparison with the Rice MYB Family. *Plant Molecular Biology*, 60(1):107–124, January 2006. URL: http://link.springer.com/10.1007/s11103-005-2910-y, doi:10.1007/s11103-005-2910-y.

[479] M. Libault, J. Wan, T. Czechowski, M. Udvardi, and G. Stacey. Identification of 118 *Arabidopsis* Transcription Factor and 30 Ubiquitin-Ligase Genes Responding to Chitin, a Plant-Defense Elicitor. *Molecular Plant-Microbe Interactions*, 20(8):900–911, August 2007. URL: http://apsjournals.apsnet.org/doi/10.1094/MPMI-20-8-0900, doi:10.1094/MPMI-20-8-0900.

[480] K. Sarvepalli and U. Nath. Interaction of TCP4-mediated growth module with phytohormones. *Plant Signaling & Behavior*, 6(10):1440–1443, October 2011. URL: http://www.tandfonline.com/doi/abs/10.4161/psb.6.10.17097, doi:10.4161/psb.6.10.17097.

[481] S. Li and S. Zachgo. TCP3 interacts with R2r3-MYB proteins, promotes flavonoid biosynthesis and negatively regulates the auxin response in *Arabidopsis thaliana*. *The Plant Journal*, 76(6):901–913, December 2013. URL: http://doi.wiley.com/10.1111/tpj.12348, doi:10.1111/tpj.12348.

[482] K. Tatematsu, K. Nakabayashi, Y. Kamiya, and E. Nambara. Transcription factor AtTCP14 regulates embryonic growth potential during seed germination in *Arabidopsis thaliana*. *The Plant Journal*, 53(1):42–52, January 2008. URL: http://doi.wiley.com/10.1111/j.1365-313X.2007.03308.x, doi:10.1111/j.1365-313X.2007.03308.x.

[483] F. Resentini, A. Felipo-Benavent, L. Colombo, M. Blázquez, D. Alabadí, and S. Masiero. TCP14 and TCP15 Mediate the Promotion of Seed Germination by Gibberellins in Arabidopsis thaliana. *Molecular Plant*, 8(3):482–485, March 2015. URL: https://linkinghub.elsevier.com/retrieve/pii/S1674205214000392, doi:10.1016/j.molp.2014.11.018.

[484] L. E. Lucero, N. G. Uberti-Manassero, A. L. Arce, F. Colombatti, S. G. Alemano, and D. H. Gonzalez. TCP15 modulates cytokinin and auxin responses during gynoecium development in Arabidopsis. *The Plant Journal*, 84(2):267–282, October 2015. URL: http://doi.wiley.com/10.1111/tpj.12992, doi:10.1111/tpj.12992.

[485] J. Griffiths, K. Murase, I. Rieu, R. Zentella, Z.-L. Zhang, S. J. Powers, F. Gong, A. L. Phillips, P. Hedden, T.-p. Sun, and S. G. Thomas. Genetic Characterization and Functional Analysis of the GID1 Gibberellin Receptors in Arabidopsis. *THE PLANT CELL ONLINE*, 18(12):3399–3414, December 2006. URL: http://www.plantcell.org/cgi/doi/10.1105/tpc.106.047415, doi:10.1105/tpc.106.047415.

[486] M. Papacek, A. Christmann, and E. Grill. Interaction network of ABA receptors in grey poplar. *The Plant Journal*, 92(2):199–210, October 2017. URL: http://doi.wiley.com/10.1111/tpj.13646, doi:10.1111/tpj.13646.

[487] Y. Zhao, Z. Chan, J. Gao, L. Xing, M. Cao, C. Yu, Y. Hu, J. You, H. Shi, Y. Zhu, Y. Gong, Z. Mu, H. Wang, X. Deng, P. Wang, R. A. Bressan, and J.-K. Zhu. ABA receptor PYL9 promotes drought resistance and leaf senescence. *Proceedings of the National Academy of Sciences*, 113(7):1949–1954, February 2016. URL: http://www.pnas.org/lookup/doi/10.1073/pnas.1522840113, doi:10.1073/pnas.1522840113.

[488] A. Sirko, A. Wawrzynska, M. C. Rodriguez, and P. Sektas. The family of LSU-like proteins. *Frontiers in Plant Science*, 5, January 2015. URL: http://journal.frontiersin.org/article/10.3389/fpls.2014.00774/abstract, doi:10.3389/fpls.2014.00774.

[489] J.-X. Zhang, C. Wang, C.-Y. Yang, J.-Y. Wang, L. Chen, X.-M. Bao, Y.-X. Zhao, H. Zhang, and J. Liu. The role of arabidopsis AtFes1a in cytosolic Hsp70 stability and abiotic stress tolerance: The role of AtFes1a in thermotolerance. *The Plant Journal*, 62(4):539–548, February 2010. URL: http://doi.wiley.com/10.1111/j.1365-313X.2010.04173.x, doi:10.1111/j.1365-313X.2010.04173.x.

[490] H. Tsukagoshi, A. Morikami, and K. Nakamura. Two B3 domain transcriptional repressors prevent sugar-inducible expression of seed maturation genes in Arabidopsis seedlings. *Proceedings of the National Academy of Sciences*, 104(7):2543–2547, February 2007. URL: http://www.pnas.org/cgi/doi/10.1073/pnas.0607940104, doi:10.1073/pnas.0607940104.

[491] R. Antoni, M. Gonzalez-Guzman, L. Rodriguez, M. Peirats-Llobet, G. A. Pizzio, M. A. Fernandez, N. De Winne, G. De Jaeger, D. Dietrich, M. J. Bennett, and P. L. Rodriguez. PYRABACTIN RESISTANCE1-LIKE8 Plays an Important Role for the Regulation of Abscisic Acid Signaling in Root. *PLANT PHYSIOLOGY*, 161(2):931–941, February 2013. URL: http://www.plantphysiol.org/cgi/doi/10.1104/pp.112.208678, doi:10.1104/pp.112.208678.

[492] C. W. Lim, W. Baek, S.-W. Han, and S. C. Lee. Arabidopsis PYL8 Plays an Important Role for ABA Signaling and Drought Stress Responses. *The Plant Pathology Journal*, 29(4):471–476, December 2013. URL: http://koreascience.or.kr/journal/view.jsp?kj=E1PPBG&py=2013&vnc=v29n4&sp=471, doi:10.5423/PPJ.NT.07.2013.0071.

[493] F. Aleman, J. Yazaki, M. Lee, Y. Takahashi, A. Y. Kim, Z. Li, T. Kinoshita, J. R. Ecker, and J. I. Schroeder. An ABA-increased interaction of the PYL6 ABA receptor with MYC2 Transcription Factor: A putative link of ABA and JA signaling. *Scientific Reports*, 6(1), September 2016. URL: http://www.nature.com/articles/srep28941, doi:10.1038/srep28941.

[494] A. S. Raghavendra, V. K. Gonugunta, A. Christmann, and E. Grill. ABA perception and signalling. *Trends in Plant Science*, 15(7):395–401, July 2010. doi:10.1016/j.tplants.2010.04.006.

[495] T. Koyama, N. Mitsuda, M. Seki, K. Shinozaki, and M. Ohme-Takagi. TCP Transcription Factors Regulate the Activities of ASYMMETRIC LEAVES1 and miR164, as Well as the Auxin Response, during Differentiation of Leaves in Arabidopsis. *THE PLANT CELL ONLINE*, 22(11):3574–3588, November 2010. URL: http://www.plantcell.org/cgi/doi/10.1105/tpc.110.075598, doi:10.1105/tpc.110.075598.

[496] S. Danisman, F. van der Wal, S. Dhondt, R. Waites, S. de Folter, A. Bimbo, A. D. van Dijk, J. M. Muino, L. Cutri, M. C. Dornelas, G. C. Angenent, and R. G. H. Immink. Arabidopsis Class I and Class II TCP Transcription Factors Regulate Jasmonic Acid Metabolism and Leaf Development Antagonistically. *PLANT PHYSIOLOGY*, 159(4):1511–1523, August 2012. URL: http://www.plantphysiol.org/cgi/doi/10.1104/pp.112.200303, doi:10.1104/pp.112.200303.

[497] N. Gonzalez, L. Pauwels, A. Baekelandt, L. De Milde, J. Van Leene, N. Besbrugge, K. S. Heyndrickx, A. C. Pérez, A. N. Durand, R. De Clercq, E. Van De Slijke, R. Vanden Bossche, D. Eeckhout, K. Gevaert, K. Vandepoele, G. De Jaeger, A. Goossens, and D. Inzé. A Repressor Protein Complex Regulates Leaf Growth in Arabidopsis. *The Plant Cell*, 27(8):2273–2287, August 2015. URL: http://www.plantcell.org/lookup/doi/10.1105/tpc.15.00006, doi:10.1105/tpc.15.00006.

[498] J. T. Ascencio-Ibanez, R. Sozzani, T.-J. Lee, T.-M. Chu, R. D. Wolfinger, R. Cella, and L. Hanley-Bowdoin. Global Analysis of Arabidopsis Gene Expression Uncovers a Complex Array of Changes Impacting Pathogen Response and Cell Cycle during Geminivirus Infection. *PLANT PHYSIOLOGY*, 148(1):436–454, July 2008. URL: http://www.plantphysiol.org/cgi/doi/10.1104/pp.108.121038, doi:10.1104/pp.108.121038.

[499] C. W. Lim, S. Luan, and S. C. Lee. A Prominent Role for RCAR3-Mediated ABA Signaling in Response to Pseudomonas syringae pv. tomato DC3000 Infection in Arabidopsis. *Plant and Cell Physiology*, 55(10):1691–1703, October 2014. URL: https://academic.oup.com/pcp/article-lookup/doi/10.1093/pcp/pcu100, doi:10.1093/pcp/pcu100.

[500] K. Shu, Q. Chen, Y. Wu, R. Liu, H. Zhang, S. Wang, S. Tang, W. Yang, and Q. Xie. ABSCISIC ACID-INSENSITIVE 4 negatively regulates flowering through directly promoting Arabidopsis *FLOWERING LOCUS C* transcription. *Journal of Experimental Botany*, 67(1):195–205, January 2016. URL: https://academic.oup.com/jxb/article-lookup/doi/10.1093/jxb/erv459, doi:10.1093/jxb/erv459.

[501] M. Riboni, A. Robustelli Test, M. Galbiati, C. Tonelli, and L. Conti. ABA-dependent control of *GIGANTEA* signalling enables drought escape via up-regulation of *FLOWERING LOCUS T* in *Arabidopsis thaliana*. *Journal of Experimental Botany*, 67(22):6309–6322, December 2016. URL: https://academic.oup.com/jxb/article-lookup/doi/10.1093/jxb/erw384, doi:10.1093/jxb/erw384.

[502] J. Li, J. Zhang, X. Wang, and J. Chen. A membrane-tethered transcription factor ANAC089 negatively regulates floral initiation in Arabidopsis thaliana. *Science China Life Sciences*, 53(11):1299–1306, November 2010. URL: http://link.springer.com/10.1007/s11427-010-4085-2, doi:10.1007/s11427-010-4085-2.

[503] J. W. Chandler, B. Jacobs, M. Cole, P. Comelli, and W. Werr. DORNRÖSCHEN-LIKE expression marks Arabidopsis floral organ founder cells and precedes auxin response maxima. *Plant Molecular Biology*, 76(1-2):171–185, May 2011. URL: http://link.springer.com/10.1007/s11103-011-9779-8, doi:10.1007/s11103-011-9779-8.

[504] S. Sun, W. Fan, and Z. Mu. The spatio-temporal specificity of PYR1/PYL/RCAR ABA receptors in response to developmental and environmental cues. *Plant Signaling & Behavior*, 12(11):e1214793, November 2017. URL: https://www.tandfonline.com/doi/full/10.1080/15592324.2016.1214793, doi:10.1080/15592324.2016.1214793.

[505] M. Dai, C. Zhang, U. Kania, F. Chen, Q. Xue, T. Mccray, G. Li, G. Qin, M. Wakeley, W. Terzaghi, J. Wan, Y. Zhao, J. Xu, J. Friml, X. W. Deng, and H. Wang. A PP6-Type Phosphatase Holoenzyme Directly Regulates PIN Phosphorylation and Auxin Efflux in *Arabidopsis*. *The Plant Cell*, 24(6):2497–2514, June 2012. URL: http://www.plantcell.org/lookup/doi/10.1105/tpc.112.098905, doi:10.1105/tpc.112.098905.

[506] M. Singh, A. Gupta, and A. Laxmi. Glucose control of root growth direction in Arabidopsis thaliana. *Journal of Experimental Botany*, 65(12):2981–2993, July 2014. URL: https://academic.oup.com/jxb/article-lookup/doi/10.1093/jxb/eru146, doi:10.1093/jxb/eru146.

[507] T. Xue, D. Wang, S. Zhang, J. Ehlting, F. Ni, S. Jakab, C. Zheng, and Y. Zhong. Genome-wide and expression analysis of protein phosphatase 2c in rice and Arabidopsis. *BMC Genomics*, 9(1):550, 2008. URL: http://bmcgenomics.biomedcentral.com/articles/10.1186/1471-2164-9-550, doi:10.1186/1471-2164-9-550.

[508] L. Lopez-Molina. AFP is a novel negative regulator of ABA signaling that promotes ABI5 protein degradation. *Genes & Development*, 17(3):410–418, February 2003. URL: http://www.genesdev.org/cgi/doi/10.1101/gad.1055803, doi:10.1101/gad.1055803.

[509] M. E. Garcia, T. Lynch, J. Peeters, C. Snowden, and R. Finkelstein. A small plant-specific protein family of ABI five binding proteins (AFPs) regulates stress response in germinating Arabidopsis seeds and seedlings. *Plant Molecular Biology*, 67(6):643–658, August 2008. URL: http://link.springer.com/10.1007/s11103-008-9344-2, doi:10.1007/s11103-008-9344-2.

[510] M.-D. Huang and W.-L. Wu. Overexpression of TMAC2, a novel negative regulator of abscisic acid and salinity responses, has pleiotropic effects in Arabidopsis thaliana. *Plant Molecular Biology*, 63(4):557–569, February 2007. URL: http://link.springer.com/10.1007/s11103-006-9109-8, doi:10.1007/s11103-006-9109-8.

[511] S. Lumba, S. Toh, L.-F. Handfield, M. Swan, R. Liu, J.-Y. Youn, S. R. Cutler, R. Subramaniam, N. Provart, A. Moses, D. Desveaux, and P. McCourt. A mesoscale abscisic acid hormone interactome reveals a dynamic signaling landscape in Arabidopsis. *Developmental Cell*, 29(3):360–372, May 2014. doi:10.1016/j.devcel.2014.04.004.

[512] M. Ruegger, E. Dewey, W. M. Gray, L. Hobbie, J. Turner, and M. Estelle. The TIR1 protein of Arabidopsis functions in auxin response and is related to human SKP2 and yeast grr1p. *Genes & Development*, 12(2):198–207, January 1998.

[513] N. Dharmasiri, S. Dharmasiri, D. Weijers, E. Lechner, M. Yamada, L. Hobbie, J. S. Ehrismann, G. Jürgens, and M. Estelle. Plant Development Is Regulated by a Family of Auxin Receptor F Box Proteins. *Developmental Cell*, 9(1):109–119, July 2005. URL: http://linkinghub.elsevier.com/retrieve/pii/S153458070500184X, doi:10.1016/j.devcel.2005.05.014.

[514] G. Parry, L. I. Calderon-Villalobos, M. Prigge, B. Peret, S. Dharmasiri, H. Itoh, E. Lechner, W. M. Gray, M. Bennett, and M. Estelle. Complex regulation of the TIR1/AFB family of auxin receptors. *Proceedings of the National Academy of Sciences of the United States of America*, 106(52):22540–22545, December 2009. doi:10.1073/pnas.0911967106.

[515] L. I. A. C. Villalobos, S. Lee, C. De Oliveira, A. Ivetac, W. Brandt, L. Armitage, L. B. Sheard, X. Tan, G. Parry, H. Mao, N. Zheng, R. Napier, S. Kepinski, and M. Estelle. A combinatorial TIR1/AFB-Aux/IAA co-receptor system for differential sensing of auxin. *Nature chemical biology*, 8(5):477–485, 2012. URL: http://www.ncbi.nlm.nih.gov/pmc/articles/PMC3331960/, doi:10.1038/nchembio.926.

[516] W. Nan, X. Wang, L. Yang, Y. Hu, Y. Wei, X. Liang, L. Mao, and Y. Bi. Cyclic GMP is involved in auxin signalling during Arabidopsis root growth and development. *Journal of Experimental Botany*, 65(6):1571–1583, April 2014. URL: https://academic.oup.com/jxb/article-lookup/doi/10.1093/jxb/eru019, doi:10.1093/jxb/eru019.

[517] H. Kuroda, Y. Yanagawa, N. Takahashi, Y. Horii, and M. Matsui. A comprehensive analysis of interaction and localization of Arabidopsis SKP1-like (ASK) and F-box (FBX) proteins. *PloS One*, 7(11):e50009, 2012. doi:10.1371/journal.pone.0050009.

[518] C. Zubieta, J. R. Ross, P. Koscheski, Y. Yang, E. Pichersky, and J. P. Noel. Structural basis for substrate recognition in the salicylic acid carboxyl methyltransferase family. *The Plant Cell*, 15(8):1704–1716, August 2003.

[519] G. Qin. An Indole-3-Acetic Acid Carboxyl Methyltransferase Regulates Arabidopsis Leaf Development. *THE PLANT CELL ONLINE*, 17(10):2693–2704, October 2005. URL: http://www.plantcell.org/cgi/doi/10.1105/tpc.105.034959, doi:10.1105/tpc.105.034959.

[520] N. Zhao, J.-L. Ferrer, J. Ross, J. Guan, Y. Yang, E. Pichersky, J. P. Noel, and F. Chen. Structural, Biochemical, and Phylogenetic Analyses Suggest That Indole-3-Acetic Acid Methyltransferase Is an Evolutionarily Ancient Member of the SABATH Family. *PLANT PHYSIOLOGY*, 146(2):455–467, December 2007. URL: http://www.plantphysiol.org/cgi/doi/10.1104/pp.107.110049, doi:10.1104/pp.107.110049.

[521] Y. Yang, R. Xu, C.-j. Ma, A. C. Vlot, D. F. Klessig, and E. Pichersky. Inactive Methyl Indole-3-Acetic Acid Ester Can Be Hydrolyzed and Activated by Several Esterases Belonging to the AtMES Esterase Family of Arabidopsis. *PLANT PHYSIOLOGY*, 147(3):1034–1045, May 2008. URL: http://www.plantphysiol.org/cgi/doi/10.1104/pp.108.118224, doi:10.1104/pp.108.118224.

[522] G. Asher, J. Lotem, L. Sachs, C. Kahana, and Y. Shaul. Mdm-2 and ubiquitin-independent p53 proteasomal degradation regulated by NQO1. *Proceedings of the National Academy of Sciences*, 99(20):13125–13130, October 2002. URL: http://www.pnas.org/cgi/doi/10.1073/pnas.202480499, doi:10.1073/pnas.202480499.

[523] S. Sollner, M. Schober, A. Wagner, A. Prem, L. Lorkova, B. A. Palfey, M. Groll, and P. Macheroux. Quinone reductase acts as a redox switch of the 20s yeast proteasome. *EMBO reports*, 10(1):65–70, January 2009. URL: http://embor.embopress.org/cgi/doi/10.1038/embor.2008.218, doi:10.1038/embor.2008.218.

[524] E. Heyno, N. Alkan, and R. Fluhr. A dual role for plant quinone reductases in host-fungus interaction. *Physiologia Plantarum*, pages n/a–n/a, March 2013. URL: http://doi.wiley.com/10.1111/ppl.12042, doi:10.1111/ppl.12042.

[525] B. Causier, M. Ashworth, W. Guo, and B. Davies. The TOPLESS interactome: a framework for gene repression in Arabidopsis. *Plant Physiology*, 158(1):423–438, January 2012. doi:10.1104/pp.111.186999.

[526] C. Hamiaux, R. Drummond, B. Janssen, S. Ledger, J. Cooney, R. Newcomb, and K. Snowden. DAD2 Is an alpha beta Hydrolase Likely to Be Involved in the Perception of the Plant Branching Hormone, Strigolactone. *Current Biology*, 22(21):2032–2036, November 2012. URL: https://linkinghub.elsevier.com/retrieve/pii/S0960982212009359, doi:10.1016/j.cub.2012.08.007.

[527] A. Cuéllar Pérez, A. Nagels Durand, R. Vanden Bossche, R. De Clercq, G. Persiau, S. C. M. Van Wees, C. M. J. Pieterse, K. Gevaert, G. De Jaeger, A. Goossens, and L. Pauwels. The Non-JAZ TIFY Protein TIFY8 from Arabidopsis thaliana Is a Transcriptional Repressor. *PLoS ONE*, 9(1):e84891, January 2014. URL: http://dx.plos.org/10.1371/journal.pone.0084891, doi:10.1371/journal.pone.0084891.

[528] G.-L. Li, B. Li, H.-T. Liu, and R.-G. Zhou. The responses of AtJ2 and AtJ3 gene expression to environmental stresses in Arabidopsis]. *Zhi Wu Sheng Li Yu Fen Zi Sheng Wu Xue Xue Bao = Journal of Plant Physiology and Molecular Biology*, 31(1):47–52, February 2005.

[529] L. Shen, Y. G. G. Kang, L. Liu, and H. Yu. The J-domain protein J3 mediates the integration of flowering signals in Arabidopsis. *The Plant Cell*, 23(2):499–514, February 2011. doi:10.1105/tpc.111.083048.

[530] L. Shen and H. Yu. J3 regulation of flowering time is mainly contributed by its activity in leaves. *Plant Signaling & Behavior*, 6(4):601–603, April 2011.

[531] C. J. Lim, K. A. Yang, J. K. Hong, J. S. Choi, D.-J. Yun, J. C. Hong, W. S. Chung, S. Y. Lee, M. J. Cho, and C. O. Lim. Gene expression profiles during heat acclimation in Arabidopsis thaliana suspension-culture cells. *Journal of Plant Research*, 119(4):373–383, July 2006. URL: http://link.springer.com/10.1007/s10265-006-0285-z, doi:10.1007/s10265-006-0285-z.

[532] A. Scaffidi, M. T. Waters, Y. K. Sun, B. W. Skelton, K. W. Dixon, E. L. Ghisalberti, G. R. Flematti, and S. M. Smith. Strigolactone Hormones and Their Stereoisomers Signal through Two Related Receptor Proteins to Induce Different Physiological Responses in Arabidopsis. *PLANT PHYSIOLOGY*, 165(3):1221–1232, July 2014. URL: http://www.plantphysiol.org/cgi/doi/10.1104/pp.114.240036, doi:10.1104/pp.114.240036.

[533] A. V. Klepikova, A. S. Kasianov, E. S. Gerasimov, M. D. Logacheva, and A. A. Penin. A high resolution map of the Arabidopsis thaliana developmental transcriptome based on RNA-seq profiling. *The Plant Journal*, 88(6):1058–1070, December 2016. URL: http://doi.wiley.com/10.1111/tpj.13312, doi:10.1111/tpj.13312.

[534] E.-Y. Jeong, P. J. Seo, J. C. Woo, and C.-M. Park. AKIN10 delays flowering by inactivating IDD8 transcription factor through protein phosphorylation in Arabidopsis. *BMC Plant Biology*, 15(1), December 2015. URL: http://www.biomedcentral.com/1471-2229/15/110, doi:10.1186/s12870-015-0503-8.

[535] J. H. Im, Y.-H. Cho, G.-D. Kim, G.-H. Kang, J.-W. Hong, and S.-D. Yoo. Inverse modulation of the energy sensor Snf1-related protein kinase 1 on hypoxia adaptation and salt stress tolerance in *A rabidopsis thaliana*: Salt stress and hypoxia signalling in *Arabidopsis*. *Plant, Cell & Environment*, pages n/a–n/a, July 2014. URL: http://doi.wiley.com/10.1111/pce.12375, doi:10.1111/pce.12375.

[536] W. Shen, M. B. Dallas, M. B. Goshe, and L. Hanley-Bowdoin. SnRK1 Phosphorylation of AL2 Delays Cabbage Leaf Curl Virus Infection in Arabidopsis. *Journal of Virology*, 88(18):10598–10612, September 2014. URL: http://jvi.asm.org/cgi/doi/10.1128/JVI.00761-14, doi:10.1128/JVI.00761-14.

[537] S. Bhattacharjee, L.-Y. Lee, H. Oltmanns, H. Cao, Veena, J. Cuperus, and S. B. Gelvin. IMPa-4, an Arabidopsis Importin Isoform, Is Preferentially Involved in Agrobacterium-Mediated Plant Transformation. *THE PLANT CELL ONLINE*, 20(10):2661–2680, October 2008. URL: http://www.plantcell.org/cgi/doi/10.1105/tpc.108.060467, doi:10.1105/tpc.108.060467.

[538] J. J. Blakeslee, H.-W. Zhou, J. T. Heath, K. R. Skottke, J. A. R. Barrios, S.-Y. Liu, and A. DeLong. Specificity of RCN1-Mediated Protein Phosphatase 2a Regulation in Meristem Organization and Stress Response in Roots. *PLANT PHYSIOLOGY*, 146(2):539–553, December 2007. URL: http://www.plantphysiol.org/cgi/doi/10.1104/pp.107.112995, doi:10.1104/pp.107.112995.

[539] H.-W. Zhou. Disparate Roles for the Regulatory A Subunit Isoforms in Arabidopsis Protein Phosphatase 2a. *THE PLANT CELL ONLINE*, 16(3):709–722, March 2004. URL: http://www.plantcell.org/cgi/doi/10.1105/tpc.018994, doi:10.1105/tpc.018994.

[540] S. D. Clouse, A. F. Hall, M. Langford, T. C. McMorris, and M. E. Baker. Physiological and molecular effects of brassinosteroids on Arabidopsis thaliana. *Journal of Plant Growth Regulation*, 12(2):61–66, April 1993. URL: http://link.springer.com/10.1007/BF00193234, doi:10.1007/BF00193234.

[541] D. M. Friedrichsen, J. Nemhauser, T. Muramitsu, J. N. Maloof, J. Alonso, J. R. Ecker, M. Furuya, and J. Chory. Three redundant brassinosteroid early response genes encode putative bHLH transcription factors required for normal growth. *Genetics*, 162(3):1445–1456, November 2002.

[542] K. H. Nam. The Arabidopsis Transthyretin-Like Protein Is a Potential Substrate of BRASSINOSTEROID-INSENSITIVE 1. *THE PLANT CELL ONLINE*, 16(9):2406–2417, September 2004. URL: http://www.plantcell.org/cgi/doi/10.1105/tpc.104.023903, doi:10.1105/tpc.104.023903.

[543] B. S. Mishra, M. Singh, P. Aggrawal, and A. Laxmi. Glucose and Auxin Signaling Interaction in Controlling Arabidopsis thaliana Seedlings Root Growth and Development. *PLoS ONE*, 4(2):e4502, February 2009. URL: https://dx.plos.org/10.1371/journal.pone.0004502, doi:10.1371/journal.pone.0004502.

[544] S. Kushwah and A. Laxmi. The interaction between glucose and cytokinin signaling in controlling *Arabidopsis thaliana* seedling root growth and development. *Plant Signaling & Behavior*, 12(5):e1312241, May 2017. URL: https://www.tandfonline.com/doi/full/10.1080/15592324.2017.1312241, doi:10.1080/15592324.2017.1312241.

[545] J. Deikman and P. E. Hammer. Induction of Anthocyanin Accumulation by Cytokinins in Arabidopsis thaliana. *Plant Physiology*, 108(1):47–57, May 1995.

[546] Y. Greenboim-Wainberg. Cross Talk between Gibberellin and Cytokinin: The Arabidopsis GA Response Inhibitor SPINDLY Plays a Positive Role in Cytokinin Signaling. *THE PLANT CELL ONLINE*, 17(1):92–102, January 2005. URL: http://www.plantcell.org/cgi/doi/10.1105/tpc.104.028472, doi:10.1105/tpc.104.028472.

[547] O. Lorenzo. JASMONATE-INSENSITIVE1 Encodes a MYC Transcription Factor Essential to Discriminate between Different Jasmonate-Regulated Defense Responses in Arabidopsis. *THE PLANT CELL ONLINE*, 16(7):1938–1950, July 2004. URL: http://www.plantcell.org/cgi/doi/10.1105/tpc.022319, doi:10.1105/tpc.022319.

[548] B. Dombrecht, G. P. Xue, S. J. Sprague, J. A. Kirkegaard, J. J. Ross, J. B. Reid, G. P. Fitt, N. Sewelam, P. M. Schenk, J. M. Manners, and K. Kazan. MYC2 Differentially Modulates Diverse Jasmonate-Dependent Functions in Arabidopsis. *THE PLANT CELL ONLINE*, 19(7):2225–2245, July 2007. URL: http://www.plantcell.org/cgi/doi/10.1105/tpc.106.048017, doi:10.1105/tpc.106.048017.

[549] H. Abe. Role of Arabidopsis MYC and MYB Homologs in Drought-and Abscisic Acid-Regulated Gene Expression. *THE PLANT CELL ONLINE*, 9(10):1859–1868, October 1997. URL: http://www.plantcell.org/cgi/doi/10.1105/tpc.9.10.1859, doi:10.1105/tpc.9.10.1859.

[550] H. Abe, T. Urao, T. Ito, M. Seki, K. Shinozaki, and K. Yamaguchi-Shinozaki. Arabidopsis AtMYC2 (bHLH) and AtMYB2 (MYB) function as transcriptional activators in abscisic acid signaling. *The Plant Cell*, 15(1):63–78, January 2003.

[551] W. Grunewald, B. Vanholme, L. Pauwels, E. Plovie, D. Inzé, G. Gheysen, and A. Goossens. Expression of the Arabidopsis jasmonate signalling repressor JAZ1/TIFY10a is stimulated by auxin. *EMBO reports*, 10(8):923–928, August 2009. URL: http://embor.embopress.org/cgi/doi/10.1038/embor.2009.103, doi:10.1038/embor.2009.103.

[552] Q. Chao, M. Rothenberg, R. Solano, G. Roman, W. Terzaghi, and J. R. Ecker. Activation of the ethylene gas response pathway in Arabidopsis by the nuclear protein ETHYLENE-INSENSITIVE3 and related proteins. *Cell*, 89(7):1133–1144, June 1997.

[553] L. Knight, R. Rose, and W. Crocker. Effects of various gases and vapors upon etiolated seedlings of the sweet pea. *Science*, 31:635–636, 1910.

[554] F. An, Q. Zhao, Y. Ji, W. Li, Z. Jiang, X. Yu, C. Zhang, Y. Han, W. He, Y. Liu, S. Zhang, J. R. Ecker, and H. Guo. Ethylene-Induced Stabilization of ETHYLENE INSENSITIVE3 and EIN3-LIKE1 Is Mediated by Proteasomal Degradation of EIN3 Binding F-Box 1 and 2 That Requires EIN2 in Arabidopsis. *THE PLANT CELL ONLINE*, 22(7):2384–2401, July 2010. URL: http://www.plantcell.org/cgi/doi/10.1105/tpc.110.076588, doi:10.1105/tpc.110.076588.

[555] G.-H. Kang, S. Son, Y.-H. Cho, and S.-D. Yoo. Regulatory role of BOTRYTIS INDUCED KINASE1 in ETHYLENE INSENSITIVE3-dependent gene expression in Arabidopsis. *Plant Cell Reports*, 34(9):1605–1614, September 2015. URL: http://link.springer.com/10.1007/s00299-015-1812-y, doi:10.1007/s00299-015-1812-y.

[556] R. Dhawan, H. Luo, A. M. Foerster, S. AbuQamar, H.-N. Du, S. D. Briggs, O. M. Scheid, and T. Mengiste. HISTONE MONOUBIQUITINATION1 Interacts with a Subunit of the Mediator Complex and Regulates Defense against Necrotrophic Fungal Pathogens in Arabidopsis. *THE PLANT CELL ONLINE*, 21(3):1000–1019, March 2009. URL: http://www.plantcell.org/cgi/doi/10.1105/tpc.108.062364, doi:10.1105/tpc.108.062364.

[557] P. B. Larsen and C. Chang. The Arabidopsis eer1 mutant has enhanced ethylene responses in the hypocotyl and stem. *Plant Physiology*, 125(2):1061–1073, February 2001.

[558] X. Lu, Y. Li, Y. Su, Q. Liang, H. Meng, S. Li, S. Shen, Y. Fan, and C. Zhang. An Arabidopsis gene encoding a C2h2-domain protein with alternatively spliced transcripts is essential for endosperm development. *Journal of Experimental Botany*, 63(16):5935–5944, October 2012. URL: https://academic.oup.com/jxb/article-lookup/doi/10.1093/jxb/ers243, doi:10.1093/jxb/ers243.

[559] G. K. Pandey. The Calcium Sensor Calcineurin B-Like 9 Modulates Abscisic Acid Sensitivity and Biosynthesis in Arabidopsis. *THE PLANT CELL ONLINE*, 16(7):1912–1924, July 2004. URL: http://www.plantcell.org/cgi/doi/10.1105/tpc.021311, doi:10.1105/tpc.021311.

[560] H. Li, W. S. Wong, L. Zhu, H. W. Guo, J. Ecker, and N. Li. Phosphoproteomic analysis of ethylene-regulated protein phosphorylation in etiolated seedlings of Arabidopsis mutant ein2 using two-dimensional separations coupled with a hybrid quadrupole time-of-flight mass spectrometer. *PROTEOMICS*, 9(6):1646–1661, March 2009. URL: http://doi.wiley.com/10.1002/pmic.200800420, doi:10.1002/pmic.200800420.

[561] T. M. Quist, I. Sokolchik, H. Shi, R. J. Joly, R. A. Bressan, A. Maggio, M. Narsimhan, and X. Li. HOS3, an ELO-Like Gene, Inhibits Effects of ABA and Implicates a S-1-P/Ceramide Control System for Abiotic Stress Responses in Arabidopsis thaliana. *Molecular Plant*, 2(1):138–151, January 2009. URL: http://linkinghub.elsevier.com/retrieve/pii/S1674205214603889, doi:10.1093/mp/ssn085.

[562] M. Ikezaki, M. Kojima, H. Sakakibara, S. Kojima, Y. Ueno, C. Machida, and Y. Machida. Genetic networks regulated by *ASYMMETRIC LEAVES1* (*AS1*) and *AS2* in leaf development in *Arabidopsis thaliana* : *KNOX* genes control five morphological events. *The Plant Journal*, 61(1):70–82, January 2010. URL: http://doi.wiley.com/10.1111/j.1365-313X.2009.04033.x, doi:10.1111/j.1365-313X.2009.04033.x.

[563] C. M. Karssen, S. Zagorski, J. Kepczynski, and S. P. C. Groot. Key Role for Endogenous Gibberellins in the Control of Seed Germination. *Annals of Botany*, 63(1):71–80, January 1989. URL: https://academic.oup.com/aob/article/175770/Key, doi:10.1093/oxfordjournals.aob.a087730.

[564] H. W. M. Hilhorst and C. M. Karssen. Seed dormancy and germination: the role of abscisic acid and gibberellins and the importance of hormone mutants. *Plant Growth Regulation*, 11(3):225–238, August 1992. URL: http://link.springer.com/10.1007/BF00024561, doi:10.1007/BF00024561.

[565] S. Ubeda-Tomás, F. Federici, I. Casimiro, G. T. Beemster, R. Bhalerao, R. Swarup, P. Doerner, J. Haseloff, and M. J. Bennett. Gibberellin Signaling in the Endodermis Controls Arabidopsis Root Meristem Size. *Current Biology*, 19(14):1194–1199, July 2009. URL: http://linkinghub.elsevier.com/retrieve/pii/S0960982209012962, doi:10.1016/j.cub.2009.06.023.

[566] A. Lang. THE EFFECT OF GIBBERELLIN UPON FLOWER FORMATION. *Proceedings of the National Academy of Sciences of the United States of America*, 43(8):709–717, August 1957.

[567] E. Mutasa-Gottgens and P. Hedden. Gibberellin as a factor in floral regulatory networks. *Journal of Experimental Botany*, 60(7):1979–1989, May 2009. URL: https://academic.oup.com/jxb/article-lookup/doi/10.1093/jxb/erp040, doi:10.1093/jxb/erp040.

[568] A. Dill and T.-p. Sun. Synergistic Derepression of Gibberellin Signaling by Removing RGA and GAI Function in Arabidopsis thaliana. *Genetics*, 159(2):777, 2001. URL: http://www.genetics.org/content/159/2/777.abstract.

[569] R. Nishiyama, Y. Watanabe, M. A. Leyva-Gonzalez, C. Van Ha, Y. Fujita, M. Tanaka, M. Seki, K. Yamaguchi-Shinozaki, K. Shinozaki, L. Herrera-Estrella, and L.-S. P. Tran. Arabidopsis AHP2, AHP3, and AHP5 histidine phosphotransfer proteins function as redundant negative regulators of drought stress response. *Proceedings of the National Academy of Sciences*, 110(12):4840–4845, March 2013. URL: http://www.pnas.org/cgi/doi/10.1073/pnas.1302265110, doi:10.1073/pnas.1302265110.

[570] H. Wang, J. Tang, J. Liu, J. Hu, J. Liu, Y. Chen, Z. Cai, and X. Wang. Abscisic Acid Signaling Inhibits Brassinosteroid Signaling through Dampening the Dephosphorylation of BIN2 by ABI1 and ABI2. *Molecular Plant*, 11(2):315–325, February 2018. URL: https://linkinghub.elsevier.com/retrieve/pii/S1674205217303830, doi:10.1016/j.molp.2017.12.013.

[571] J. Li, S. Besseau, P. Törönen, N. Sipari, H. Kollist, L. Holm, and E. T. Palva. Defense-related transcription factors WRKY70 and WRKY54 modulate osmotic stress tolerance by regulating stomatal aperture in *Arabidopsis*. *New Phytologist*, 200(2):457–472, October 2013. URL: http://doi.wiley.com/10.1111/nph.12378, doi:10.1111/nph.12378.

[572] J. Li, R. Zhong, and E. T. Palva. WRKY70 and its homolog WRKY54 negatively modulate the cell wall-associated defenses to necrotrophic pathogens in Arabidopsis. *PLOS ONE*, 12(8):e0183731, August 2017. URL: https://dx.plos.org/10.1371/journal.pone.0183731, doi:10.1371/journal.pone.0183731.

[573] Z.-Q. Liu, J. Gao, A.-W. Dong, and W.-H. Shen. A Truncated Arabidopsis NUCLEOSOME ASSEMBLY PROTEIN 1, AtNAP1;3t, Alters Plant Growth Responses to Abscisic Acid and Salt in the Atnap1;3-2 Mutant. *Molecular Plant*, 2(4):688–699, July 2009. URL: https://linkinghub.elsevier.com/retrieve/pii/S1674205214607528, doi:10.1093/mp/ssp026.

[574] P. Braun, M. Tasan, M. Dreze, M. Barrios-Rodiles, I. Lemmens, H. Yu, J. M. Sahalie, R. R. Murray, L. Roncari, A.-S. de Smet, K. Venkatesan, J.-F. Rual, J. Vandenhaute, M. E. Cusick, T. Pawson, D. E. Hill, J. Tavernier, J. L. Wrana, F. P. Roth, and M. Vidal. An experimentally derived confidence score for binary protein-protein interactions. *Nature Methods*, 6(1):91–97, January 2009. URL: http://www.nature.com/doifinder/10.1038/nmeth.1281, doi:10.1038/nmeth.1281.

[575] M. R. Thorpe, A. P. Ferrieri, M. M. Herth, and R. A. Ferrieri. 11c-imaging: methyl jasmonate moves in both phloem and xylem, promotes transport of jasmonate, and of photoassimilate even after proton transport is decoupled. *Planta*, 226(2):541–551, June 2007. URL: http://link.springer.com/10.1007/s00425-007-0503-5, doi:10.1007/s00425-007-0503-5.

[576] K. Okada, H. Abe, and G.-i. Arimura. Jasmonates Induce Both Defense Responses and Communication in Monocotyledonous and Dicotyledonous Plants. *Plant and Cell Physiology*, 56(1):16–27, January 2015. URL: https://academic.oup.com/pcp/article-lookup/doi/10.1093/pcp/pcu158, doi:10.1093/pcp/pcu158.

[577] C. Wasternack and M. Strnad. Jasmonate signaling in plant stress responses and development – active and inactive compounds. *New Biotechnology*, 33(5):604–613, September 2016. URL: https://linkinghub.elsevier.com/retrieve/pii/S1871678415002526, doi:10.1016/j.nbt.2015.11.001.

[578] I. Apostol, P. F. Heinstein, and P. S. Low. Rapid Stimulation of an Oxidative Burst during Elicitation of Cultured Plant Cells : Role in Defense and Signal Transduction. *Plant Physiology*, 90(1):109–116, May 1989.

[579] M. A. Horn. Receptor-Mediated Endocytosis in Plant Cells. *THE PLANT CELL ONLINE*, 1(10):1003–1009, October 1989. URL: http://www.plantcell.org/cgi/doi/10.1105/tpc.1.10.1003, doi:10.1105/tpc.1.10.1003.

[580] C. Lamb and R. A. Dixon. THE OXIDATIVE BURST IN PLANT DISEASE RESISTANCE. *Annual Review of Plant Physiology and Plant Molecular Biology*, 48(1):251–275, June 1997. URL: http://www.annualreviews.org/doi/10.1146/annurev.arplant.48.1.251, doi:10.1146/annurev.arplant.48.1.251.

[581] A. Levine, R. Tenhaken, R. Dixon, and C. Lamb. H2o2 from the oxidative burst orchestrates the plant hypersensitive disease resistance response. *Cell*, 79(4):583–593, November 1994. URL: https://linkinghub.elsevier.com/retrieve/pii/0092867494905444, doi:10.1016/0092-8674(94)90544-4.

[582] J. L. Heazlewood, P. Durek, J. Hummel, J. Selbig, W. Weckwerth, D. Walther, and W. X. Schulze. PhosPhAt: a database of phosphorylation sites in Arabidopsis thaliana and a plant-specific phosphorylation site predictor. *Nucleic Acids Research*, 36(Database):D1015–D1021, December 2007. URL: https://academic.oup.com/nar/article-lookup/doi/10.1093/nar/gkm812, doi:10.1093/nar/gkm812.

[583] P. Durek, R. Schmidt, J. L. Heazlewood, A. Jones, D. MacLean, A. Nagel, B. Kersten, and W. X. Schulze. PhosPhAt: the Arabidopsis thaliana phosphorylation site database. An update. *Nucleic Acids Research*, 38(suppl_1):D828–D834, January 2010. URL: https://academic.oup.com/nar/article-lookup/doi/10.1093/nar/gkp810, doi:10.1093/nar/gkp810.

[584] M. Zulawski, R. Braginets, and W. X. Schulze. PhosPhAt goes kinases—searchable protein kinase target information in the plant phosphorylation site database PhosPhAt. *Nucleic Acids Research*, 41(D1):D1176–D1184, November 2012. URL: http://academic.oup.com/nar/article/41/D1/D1176/1056196/PhosPhAt-goes-kinasessearchable-protein-kinase, doi:10.1093/nar/gks1081.

[585] H. Zegzouti, R. G. Anthony, N. Jahchan, L. Bogre, and S. K. Christensen. Phosphorylation and activation of PINOID by the phospholipid signaling kinase 3-phosphoinositide-dependent protein kinase 1 (PDK1) in Arabidopsis. *Proceedings of the National Academy of Sciences*, 103(16):6404–6409, April 2006. URL: http://www.pnas.org/cgi/doi/10.1073/pnas.0510283103, doi:10.1073/pnas.0510283103.

[586] M. Schmid, T. S. Davison, S. R. Henz, U. J. Pape, M. Demar, M. Vingron, B. Schölkopf, D. Weigel, and J. U. Lohmann. A gene expression map of Arabidopsis thaliana development. *Nature Genetics*, 37(5):501–506, May 2005. doi:10.1038/ng1543.

[587] S. A. Trigg, R. M. Garza, A. MacWilliams, J. R. Nery, A. Bartlett, R. Castanon, A. Goubil, J. Feeney, R. O'Malley, S.-S. C. Huang, Z. Z. Zhang, M. Galli, and J. R. Ecker. CrY2h-seq: a massively multiplexed assay for deep-coverage interactome mapping. *Nature Methods*, 14(8):819–825, August 2017. doi:10.1038/nmeth.4343.

[588] H. Cho, H. Ryu, S. Rho, K. Hill, S. Smith, D. Audenaert, J. Park, S. Han, T. Beeckman, M. J. Bennett, D. Hwang, I. De Smet, and I. Hwang. A secreted peptide acts on BIN2-mediated phosphorylation of ARFs to potentiate auxin response during lateral root development. *Nature Cell Biology*, 16(1):66–76, January 2014. URL: http://www.nature.com/articles/ncb2893, doi:10.1038/ncb2893.

[589] G. B. Bhaskara, T. T. Nguyen, and P. E. Verslues. Unique Drought Resistance Functions of the Highly ABA-Induced Clade A Protein Phosphatase 2cs. *PLANT PHYSIOLOGY*, 160(1):379–395, September 2012. URL: http://www.plantphysiol.org/cgi/doi/10.1104/pp.112.202408, doi:10.1104/pp.112.202408.

[590] C. Mussig. Brassinosteroids Promote Root Growth in Arabidopsis. *PLANT PHYSIOLOGY*, 133(3):1261–1271, October 2003. URL: http://www.plantphysiol.org/cgi/doi/10.1104/pp.103.028662, doi:10.1104/pp.103.028662.

[591] M. Riemann, R. Dhakarey, M. Hazman, B. Miro, A. Kohli, and P. Nick. Exploring Jasmonates in the Hormonal Network of Drought and Salinity Responses. *Frontiers in Plant Science*, 6, December 2015. URL: http://journal.frontiersin.org/article/10.3389/fpls.2015.01077, doi:10.3389/fpls.2015.01077.

[592] J. Fu, H. Wu, S. Ma, D. Xiang, R. Liu, and L. Xiong. OsJAZ1 Attenuates Drought Resistance by Regulating JA and ABA Signaling in Rice. *Frontiers in Plant Science*, 8, December 2017. URL: http://journal.frontiersin.org/article/10.3389/fpls.2017.02108/full, doi:10.3389/fpls.2017.02108.

[593] J. Menz, Z. Li, W. X. Schulze, and U. Ludewig. Early nitrogen-deprivation responses in Arabidopsis roots reveal distinct differences on transcriptome and (phospho-) proteome levels between nitrate and ammonium nutrition. *The Plant Journal*, 88(5):717–734, December 2016. URL: http://doi.wiley.com/10.1111/tpj.13272, doi:10.1111/tpj.13272.

[594] V. K. Nagarajan, V. Satheesh, M. D. Poling, K. G. Raghothama, and A. Jain. Arabidopsis MYB-Related HHO2 Exerts a Regulatory Influence on a Subset of Root Traits and Genes Governing Phosphate Homeostasis. *Plant and Cell Physiology*, 57(6):1142–1152, June 2016. URL: https://academic.oup.com/pcp/article-lookup/doi/10.1093/pcp/pcw063, doi:10.1093/pcp/pcw063.

[595] M. A. Leyva-González, E. Ibarra-Laclette, A. Cruz-Ramírez, and L. Herrera-Estrella. Functional and Transcriptome Analysis Reveals an Acclimatization Strategy for Abiotic Stress Tolerance Mediated by Arabidopsis NF-YA Family Members. *PLoS ONE*, 7(10):e48138, October 2012. URL: https://dx.plos.org/10.1371/journal.pone.0048138, doi:10.1371/journal.pone.0048138.

[596] H. Cui, Y. Hao, and D. Kong. SCARECROW Has a SHORT-ROOT-Independent Role in Modulating the Sugar Response1. *PLANT PHYSIOLOGY*, 158(4):1769–1778, April 2012. URL: http://www.plantphysiol.org/cgi/doi/10.1104/pp.111.191502, doi:10.1104/pp.111.191502.

[597] G. J. M. Beckers and S. H. Spoel. Fine-Tuning Plant Defence Signalling: Salicylate versus Jasmonate. *Plant Biology*, 8(1):1–10, January 2006. URL: http://doi.wiley.com/10.1055/s-2005-872705, doi:10.1055/s-2005-872705.

[598] R. Schweiger, A.-M. Heise, M. Persicke, and C. Müller. Interactions between the jasmonic and salicylic acid pathway modulate the plant metabolome and affect herbivores of different feeding types: Phytohormone interactions affect metabolome and herbivores. *Plant, Cell & Environment*, 37(7):1574–1585, July 2014. URL: http://doi.wiley.com/10.1111/pce.12257, doi:10.1111/pce.12257.

[599] P. Cubas, N. Lauter, J. Doebley, and E. Coen. The TCP domain: a motif found in proteins regulating plant growth and development. *The Plant Journal: For Cell and Molecular Biology*, 18(2):215–222, April 1999.

[600] J. A. Aguilar-Martinez, C. Poza-Carrion, and P. Cubas. Arabidopsis BRANCHED1 Acts as an Integrator of Branching Signals within Axillary Buds. *THE PLANT CELL ONLINE*, 19(2):458–472, February 2007. URL: http://www.plantcell.org/cgi/doi/10.1105/tpc.106.048934, doi:10.1105/tpc.106.048934.

[601] D. Luo, R. Carpenter, C. Vincent, L. Copsey, and E. Coen. Origin of floral asymmetry in Antirrhinum. *Nature*, 383(6603):794–799, October 1996. URL: http://www.nature.com/articles/383794a0, doi:10.1038/383794a0.

[602] I. Efroni, E. Blum, A. Goldshmidt, and Y. Eshed. A Protracted and Dynamic Maturation Schedule Underlies Arabidopsis Leaf Development. *THE PLANT CELL ONLINE*, 20(9):2293–2306, September 2008. URL: http://www.plantcell.org/cgi/doi/10.1105/tpc.107.057521, doi:10.1105/tpc.107.057521.

[603] C. Li, T. Potuschak, A. Colon-Carmona, R. A. Gutierrez, and P. Doerner. Arabidopsis TCP20 links regulation of growth and cell division control pathways. *Proceedings of the National Academy of Sciences*, 102(36):12978–12983, September 2005. URL: http://www.pnas.org/cgi/doi/10.1073/pnas.0504039102, doi:10.1073/pnas.0504039102.

[604] M. Kieffer, V. Master, R. Waites, and B. Davies. TCP14 and TCP15 affect internode length and leaf shape in Arabidopsis: *TCP14/15 affect internode length and leaf shape*. *The Plant Journal*, 68(1):147–158, October 2011. URL: http://doi.wiley.com/10.1111/j.1365-313X.2011.04674.x, doi:10.1111/j.1365-313X.2011.04674.x.

[605] S. Li. The Arabidopsis thaliana TCP Transcription Factors: A Broadening Horizon Beyond Development. *Plant Signaling & Behavior*, pages 00–00, June 2015. URL: http://www.tandfonline.com/doi/full/10.1080/15592324.2015.1044192, doi:10.1080/15592324.2015.1044192.

[606] A. Kauschmann, A. Jessop, C. Koncz, M. Szekeres, L. Willmitzer, and T. Altmann. Genetic evidence for an essential role of brassinosteroids in plant development. *The Plant Journal*, 9(5):701–713, May 1996. URL: http://doi.wiley.com/10.1046/j.1365-313X.1996.9050701.x, doi:10.1046/j.1365-313X.1996.9050701.x.

[607] X. Yu, L. Li, J. Zola, M. Aluru, H. Ye, A. Foudree, H. Guo, S. Anderson, S. Aluru, P. Liu, S. Rodermel, and Y. Yin. A brassinosteroid transcriptional network revealed by genome-wide identification of BESI target genes in Arabidopsis thaliana: Brassinosteroid transcriptional network. *The Plant Journal*, 65(4):634–646, February 2011. URL: http://doi.wiley.com/10.1111/j.1365-313X.2010.04449.x, doi:10.1111/j.1365-313X.2010.04449.x.

[608] E. Steiner, I. Efroni, M. Gopalraj, K. Saathoff, T.-S. Tseng, M. Kieffer, Y. Eshed, N. Olszewski, and D. Weiss. The Arabidopsis O-Linked N-Acetylglucosamine Transferase SPINDLY Interacts with Class I TCPs to Facilitate Cytokinin Responses in Leaves and Flowers. *The Plant Cell*, 24(1):96–108, January 2012. URL: http://www.plantcell.org/cgi/doi/10.1105/tpc.111.093518, doi:10.1105/tpc.111.093518.

[609] M. Hu, B.-L. Pei, L.-F. Zhang, and Y.-Z. Li. Histone H2b Monoubiquitination Is Involved in Regulating the Dynamics of Microtubules during the Defense Response to Verticillium dahliae Toxins in Arabidopsis. *PLANT PHYSIOLOGY*, 164(4):1857–1865, April 2014. URL: http://www.plantphysiol.org/cgi/doi/10.1104/pp.113.234567, doi:10.1104/pp.113.234567.

[610] S. Zhou, Q. Chen, Y. Sun, and Y. Li. Histone H2b monoubiquitination regulates salt stress-induced microtubule depolymerization in *Arabidopsis*: H2bub1 regulates salt stress-induced MT depolymerization. *Plant, Cell & Environment*, 40(8):1512–1530, August 2017. URL: http://doi.wiley.com/10.1111/pce.12950, doi:10.1111/pce.12950.

[611] C. Bourbousse, I. Ahmed, F. Roudier, G. Zabulon, E. Blondet, S. Balzergue, V. Colot, C. Bowler, and F. Barneche. Histone H2b Monoubiquitination Facilitates the Rapid Modulation of Gene Expression during Arabidopsis Photomorphogenesis. *PLoS Genetics*, 8(7):e1002825, July 2012. URL: http://dx.plos.org/10.1371/journal.pgen.1002825, doi:10.1371/journal.pgen.1002825.

[612] K. Himanen, M. Woloszynska, T. M. Boccardi, S. De Groeve, H. Nelissen, L. Bruno, M. Vuylsteke, and M. Van Lijsebettens. Histone H2b monoubiquitination is required to reach maximal transcript levels of circadian clock genes in Arabidopsis: HUB1 regulates transcript levels. *The Plant Journal*, 72(2):249–260, October 2012. URL: http://doi.wiley.com/10.1111/j.1365-313X.2012.05071.x, doi:10.1111/j.1365-313X.2012.05071.x.

[613] P. A. Salome, Q. Xie, and C. R. McClung. Circadian Timekeeping during Early Arabidopsis Development. *PLANT PHYSIOLOGY*, 147(3):1110–1125, May 2008. URL: http://www.plantphysiol.org/cgi/doi/10.1104/pp.108.117622, doi:10.1104/pp.108.117622.

[614] N. Nakamichi, M. Kita, K. Niinuma, S. Ito, T. Yamashino, T. Mizoguchi, and T. Mizuno. Arabidopsis Clock-Associated Pseudo-Response Regulators PRR9, PRR7 and PRR5 Coordinately and Positively Regulate Flowering Time Through the Canonical CONSTANS-Dependent Photoperiodic Pathway. *Plant and Cell Physiology*, 48(6):822–832, June 2007. URL: https://academic.oup.com/pcp/article-lookup/doi/10.1093/pcp/pcm056, doi:10.1093/pcp/pcm056.

[615] Y. Sakuraba, S. Bülbül, W. Piao, G. Choi, and N.-C. Paek. Arabidopsis EARLY FLOWERING3 increases salt tolerance by suppressing salt stress response pathways. *The Plant Journal*, 92(6):1106–1120, December 2017. URL: http://doi.wiley.com/10.1111/tpj.13747, doi:10.1111/tpj.13747.

[616] J. A. Kim, H.-e. Jung, J. K. Hong, V. Hermand, C. Robertson McClung, Y.-H. Lee, J. Y. Kim, S. I. Lee, M.-J. Jeong, J. Kim, D. Yun, and W. Kim. Reduction of GIGANTEA expression in transgenic Brassica rapa enhances salt tolerance. *Plant Cell Reports*, 35(9):1943–1954, September 2016. URL: http://link.springer.com/10.1007/s00299-016-2008-9, doi:10.1007/s00299-016-2008-9.

[617] S. Cao, M. Ye, and S. Jiang. Involvement of GIGANTEA gene in the regulation of the cold stress response in Arabidopsis. *Plant Cell Reports*, 24(11):683–690, December 2005. URL: http://link.springer.com/10.1007/s00299-005-0061-x, doi:10.1007/s00299-005-0061-x.

[618] T. Mizoguchi. Distinct Roles of GIGANTEA in Promoting Flowering and Regulating Circadian Rhythms in Arabidopsis. *THE PLANT CELL ONLINE*, 17(8):2255–2270, August 2005. URL: http://www.plantcell.org/cgi/doi/10.1105/tpc.105.033464, doi:10.1105/tpc.105.033464.

[619] M. Sawa and S. A. Kay. GIGANTEA directly activates Flowering Locus T in Arabidopsis thaliana. *Proceedings of the National Academy of Sciences*, 108(28):11698–11703, July 2011. URL: http://www.pnas.org/cgi/doi/10.1073/pnas.1106771108, doi:10.1073/pnas.1106771108.

[620] P. James, J. Halladay, and E. A. Craig. Genomic libraries and a host strain designed for highly efficient two-hybrid selection in yeast. *Genetics*, 144(4):1425–1436, December 1996.

[621] T. E. Gookin and S. M. Assmann. Significant reduction of BiFC non-specific assembly facilitates *in planta* assessment of heterotrimeric G-protein interactors. *The Plant Journal*, 80(3):553–567, November 2014. URL: http://doi.wiley.com/10.1111/tpj.12639, doi:10.1111/tpj.12639.

[622] M. W. Pfaffl. A new mathematical model for relative quantification in real-time RT-PCR. *Nucleic Acids Research*, 29(9):45e–45, May 2001. URL: https://academic.oup.com/nar/article-lookup/doi/10.1093/nar/29.9.e45, doi:10.1093/nar/29.9.e45.

[623] K. Edwards, C. Johnstone, and C. Thompson. A simple and rapid method for the preparation of plant genomic DNA for PCR analysis. *Nucleic Acids Research*, 19(6):1349, March 1991.

[624] M. Nakata and M. Ohme-Takagi. Quantification of Anthocyanin Content. *BIO-PROTOCOL*, 4(7), 2014. URL: https://bio-protocol.org/e1098, doi:10.21769/BioProtoc.1098.

A Appendix

A.1 Phytohormones overview

A.1.1 Auxin

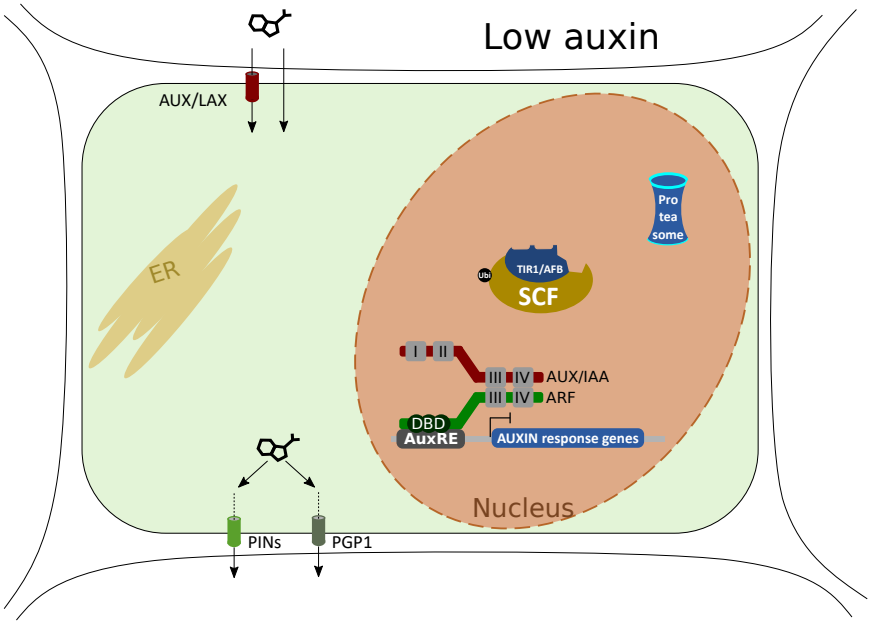

Figure A.1: IAA signaling pathway: low auxin. (A) Exemplary representation of the three core components of the IAA signaling pathway, the SKP1-CULLIN-F-Box (SCF) TIR/AFB complex, the AUXIN RESPONSE FACTORS (ARF) and the AUX/IAA. (B) In the presence of low auxin concentration. IAA import by AUX1 influx carrier and PIN1 as well as PGP1 auxin efflux transporter. At a low auxin concentration, the AUX/IAA form homo- or hetero
dimers and bind to the different ARF. An ARF is bound to the AuxRE in the promoter of the target gene, induction of the gene also requires homo- or hetero dimers of the AFR. This is prevented by the binding of the AUX/IAA. Thus there is no expression of the target gene.

A.2 PhI

Table A.1: PhyHormORFeome collection. All ORFs are cloned in full length using the Gateway cloning system. For some ORFs different splicing variants were included.

Locus ID	Symbol	Locus ID	Symbol	Locus ID	Symbol
AT1G01030	NGA3	AT2G29380	HAI3	AT4G22070	WRKY31
AT1G01060	LHY	AT2G29390	SMO2-2	AT4G22340	CDS2
AT1G01090	PDH-E1 ALPHA	AT2G29980	FAD3	AT4G22680	MYB85
AT1G01140	CIPK9	AT2G30020		AT4G22750	
AT1G01250		AT2G30250	WRKY25	AT4G23550	WRKY29
AT1G01360	RCAR1	AT2G30360	SIP4	AT4G23650	CDPK6
AT1G01560	MPK11	AT2G30470	HSI2	AT4G23750	CRF2
AT1G02120	VAD1	AT2G30590	WRKY21	AT4G23810	WRKY53
AT1G02190		AT2G30860	GSTF9	AT4G23850	LACS4
AT1G02205	CER1	AT2G30980	SKdZeta	AT4G24210	SLY1
AT1G02400	GA2OX6	AT2G31180	MYB14	AT4G24230	ACBP3
AT1G02630		AT2G31190	RUS2	AT4G24240	WRKY7
AT1G03445	BSU1	AT2G31230	ERF15	AT4G24250	MLO13
AT1G03800	ERF10	AT2G31470	DOR	AT4G24400	CIPK8
AT1G04120	ABCC5	AT2G31660	SAD2	AT4G24470	ZIM
AT1G04240	SHY2	AT2G32410	AXL	AT4G24650	IPT4
AT1G04250	AXR3	AT2G32460	MYB101	AT4G25420	GA20OX1
AT1G04310	ERS2	AT2G32960	PFA-DSP2	AT4G25470	CBF2
AT1G04370	ERF14	AT2G33150	PKT3	AT4G25480	DREB1A
AT1G04550	IAA12	AT2G33670	MLO5	AT4G25490	CBF1
AT1G04710	PKT4	AT2G33710		AT4G25500	RS40
AT1G05000	PFA-DSP1	AT2G33790	AGP30	AT4G25560	LAF1
AT1G05180	AXR1	AT2G33830		AT4G26070	MEK1
AT1G06160	ORA59	AT2G33860	ETT	AT4G26080	ABI1
AT1G06180	MYB13	AT2G34180	CIPK13	AT4G26110	NAP1;1
AT1G06390	GSK1	AT2G34600	JAZ7	AT4G26150	CGA1
AT1G06400	ARA-2	AT2G34650	PID	AT4G26420	GAMT1
AT1G07230	NPC1	AT2G34830	WRKY35	AT4G26440	WRKY34
AT1G07340	STP2	AT2G34900	IMB1	AT4G26640	WRKY20
AT1G07420	SMO2-1	AT2G35320	EYA	AT4G26770	
AT1G07430	HAI2	AT2G35635	UBQ7	AT4G26840	SUMO1
AT1G07520		AT2G35680		AT4G26930	MYB97
AT1G07530	SCL14	AT2G35700	ERF38	AT4G27260	WES1
AT1G07745	RAD51D	AT2G36080	ABS2	AT4G27330	SPL
AT1G07880	ATMPK13	AT2G36270	ABI5	AT4G27440	PORB
AT1G08260	TIL1	AT2G36450	HRD	AT4G27450	
AT1G08420	BSL2	AT2G36800	DOGT1	AT4G27630	GTG2
AT1G08810	MYB60	AT2G36890	RAX2	AT4G27780	ACBP2
AT1G08920	ESL1	AT2G37260	TTG2	AT4G27920	PYL10
AT1G09400		AT2G37340	RS2Z33	AT4G27950	CRF4
AT1G09540	MYB61	AT2G37550	AGD7	AT4G28110	MYB41
AT1G09570	PHYA	AT2G37630	AS1	AT4G28140	
AT1G09700	HYL1	AT2G37650		AT4G28395	A7
AT1G09950	RAS1	AT2G37700		AT4G28910	NINJA
AT1G10210	MPK1	AT2G37940	AtIPCS2	AT4G29010	AIM1
AT1G10470	ARR4	AT2G38050	DET2	AT4G29740	CKX4
AT1G10940	SNRK2.4	AT2G38120	AUX1	AT4G29800	PLP8
AT1G11000	MLO4	AT2G38310	PYL4	AT4G29810	MKK2
AT1G11310	MLO2	AT2G38340	DREB19	AT4G30080	ARF16
AT1G11680	CYP51G1	AT2G38470	WRKY33	AT4G30160	VLN4
AT1G12270	Hop1	AT2G38490	CIPK22	AT4G30480	TPR1
AT1G12610	DDF1	AT2G39200	MLO12	AT4G30610	BRS1
AT1G12630		AT2G39220	PLP6	AT4G30935	WRKY32
AT1G12820	AFB3	AT2G39250	SNZ	AT4G30960	SIP3
AT1G12890		AT2G39550	PGGT-I	AT4G31060	
AT1G12980	ESR1	AT2G39760	BPM3	AT4G31500	CYP83B1
AT1G13260	RAV1	AT2G39880	MYB25	AT4G31550	WRKY11
AT1G13960	WRKY4	AT2G39940	COI1	AT4G31780	MGD1
AT1G13980	GN	AT2G40180	PP2C5	AT4G31800	WRKY18
AT1G14280	PKS2	AT2G40220	ABI4	AT4G31920	RR10
AT1G14350	FLP	AT2G40330	PYL6	AT4G32010	HSL1
AT1G14410	WHY1	AT2G40340	DREB2C	AT4G32180	PANK2
AT1G14920	GAI	AT2G40350		AT4G32280	IAA29
AT1G15100	RHA2A	AT2G40670	RR16	AT4G32285	
AT1G15360	SHN1	AT2G40740	WRKY55	AT4G32410	CESA1
AT1G15550	GA3OX1	AT2G40750	WRKY54	AT4G32540	YUC1
AT1G16060	ADAP	AT2G40940	ERS1	AT4G32570	TIFY8
AT1G16370	OCT6	AT2G41310	RR3	AT4G32730	PC-MYB1
AT1G16390	OCT3	AT2G41510	CKX1	AT4G32800	
AT1G16490	MYB58	AT2G41710		AT4G33430	BAK1
AT1G16540	ABA3	AT2G42010	PLDBETA1	AT4G33450	MYB69
AT1G17060	CYP72C1	AT2G42430	LBD16	AT4G33520	PAA1
AT1G17380	JAZ5	AT2G42680	MBF1A	AT4G33790	CER4
AT1G17420	LOX3	AT2G42880	MPK20	AT4G33950	OST1
AT1G17440	EER4	AT2G43710	SSI2	AT4G34410	RRTF1
AT1G17550	HAB2	AT2G43790	MPK6	AT4G34990	MYB32
AT1G17730	VPS46.1	AT2G43820	UGT74F2	AT4G35230	BSK1
AT1G17950	MYB52	AT2G43840	UGT74F1	AT4G35790	PLDDELTA
AT1G17990		AT2G44050	COS1	AT4G36380	ROT3
AT1G18080	ATARCA	AT2G44110	MLO15	AT4G36450	MPK14
AT1G18150	ATMPK8	AT2G44745	WRKY12	AT4G36540	BEE2
AT1G18350	MKK7	AT2G44810	DAD1	AT4G36710	HAM4

Table A.1 continued from previous page

Locus ID	Symbol	Locus ID	Symbol	Locus ID	Symbol
AT1G18400	BEE1	AT2G44840	ERF13	AT4G36780	BEH2
AT1G18570	MYB51	AT2G44910	HB4	AT4G36830	HOS3-1
AT1G18710	MYB47	AT2G44940		AT4G36900	RAP2.10
AT1G18860	WRKY61	AT2G44950	HUB1	AT4G36920	AP2
AT1G18970	GLP4	AT2G45150	CDS4	AT4G37050	PLP4
AT1G19050	ARR7	AT2G45160	HAM1	AT4G37060	PLP5
AT1G19180	JAZ1	AT2G45420	LBD18	AT4G37070	PLP1
AT1G19190		AT2G45820		AT4G37260	MYB73
AT1G19210		AT2G46070	MPK12	AT4G37390	BRU6
AT1G19220	ARF19	AT2G46130	WRKY43	AT4G37580	HLS1
AT1G19350	BES1	AT2G46310	CRF5	AT4G37650	SHR
AT1G19610	PDF1.4	AT2G46370	JAR1	AT4G37750	ANT
AT1G19640	JMT	AT2G46400	WRKY46	AT4G37780	MYB87
AT1G19850	MP	AT2G46530	ARF11	AT4G37870	PCK1
AT1G20330	SMT2	AT2G46790	PRR9	AT4G38130	HD1
AT1G20780	SAUL1	AT2G46830	CCA1	AT4G38620	MYB4
AT1G21450	SCL1	AT2G46870	NGA1	AT4G38630	RPN10
AT1G21690	EMB1968	AT2G47000	ABCB4	AT4G38830	CRK26
AT1G21910	DREB26	AT2G47190	MYB2	AT4G38850	SAUR15
AT1G21970	LEC1	AT2G47240	LACS1	AT4G39030	EDS5
AT1G22070	TGA3	AT2G47260	WRKY23	AT4G39350	CESA2
AT1G22190		AT2G47430	CKI1	AT4G39400	BRI1
AT1G22640	MYB3	AT2G47460	MYB12	AT4G39410	WRKY13
AT1G22770	GI	AT2G47520	ERF71	AT4G39780	
AT1G22810		AT2G47770	TSPO	AT4G39850	ABCD1
AT1G22985	CRF7	AT3G01040	GAUT13	AT4G39950	CYP79B2
AT1G23080	PIN7	AT3G01080	WRKY58	AT5G01240	LAX1
AT1G23540	PERK12	AT3G01140	MYB106	AT5G01290	
AT1G23860	RSZ21	AT3G01510	LSF1	AT5G01540	LECRKA4.1
AT1G24180	IAR4	AT3G01530	MYB57	AT5G01550	LECRKA4.2
AT1G24260	37865	AT3G01970	WRKY45	AT5G01600	FER1
AT1G24590	DRNL	AT3G02410	ICME-LIKE2	AT5G01810	CIPK15
AT1G25220	ASB1	AT3G02610		AT5G01820	SR1
AT1G25340	MYB116	AT3G02620		AT5G01900	WRKY62
AT1G25470	CRF12	AT3G02630		AT5G01990	
AT1G25490	RCN1	AT3G02800	PFA-DSP3	AT5G02310	PRT6
AT1G25560	TEM1	AT3G02940	MYB107	AT5G02320	MYB3R-5
AT1G26120	ICME-LIKE1	AT3G03450	RGL2	AT5G02810	PRR7
AT1G26700	MLO14	AT3G03520	NPC3	AT5G03280	EIN2
AT1G26780	MYB117	AT3G03530	NPC4	AT5G03310	
AT1G26830	CUL3	AT3G03540	NPC5	AT5G03455	CDC25
AT1G27320	HK3	AT3G03740	BPM4	AT5G03690	FBA4
AT1G28160		AT3G03850	SAUR26	AT5G03730	CTR1
AT1G28300	LEC2	AT3G04240	SEC	AT5G04040	SDP1
AT1G28330	DYL1	AT3G04280	RR22	AT5G04190	PKS4
AT1G28360	ERF12	AT3G04580	EIN4	AT5G04240	ELF6
AT1G28370	ERF11	AT3G04670	WRKY39	AT5G04430	BTR1L
AT1G29230	CIPK18	AT3G05120	GID1A	AT5G04540	MTM2
AT1G29280	WRKY65	AT3G05420	ACBP4	AT5G04870	CPK1
AT1G29440	SAUR63	AT3G06110	MKP2	AT5G05170	CEV1
AT1G29450		AT3G06230	MKK8	AT5G05410	DREB2A
AT1G29460		AT3G06460		AT5G05440	PYL5
AT1G29500		AT3G06470		AT5G05580	FAD8
AT1G29510	SAUR68	AT3G06490	MYB108	AT5G05690	CPD
AT1G29860	WRKY71	AT3G06860	MFP2	AT5G05700	ATE1
AT1G30135	JAZ8	AT3G07390	AIR12	AT5G05730	ASA1
AT1G30270	CIPK23	AT3G08500	MYB83	AT5G06100	MYB33
AT1G30330	ARF6	AT3G08550	KOB1	AT5G06250	DPA4
AT1G30650	WRKY14	AT3G09100		AT5G06950	AHBP-1B
AT1G31340	RUB1	AT3G09230	MYB1	AT5G06960	OBF5
AT1G31812	ACBP6	AT3G09370	MYB3R-3	AT5G07070	CIPK2
AT1G31880	BRX	AT3G09990		AT5G07100	WRKY26
AT1G32130	IWS1	AT3G10550	MTM1	AT5G07210	RR21
AT1G32320	MKK10	AT3G10940	LSF2	AT5G07310	
AT1G32640	MYC2	AT3G11020	DREB2B	AT5G07340	
AT1G33270		AT3G11170	FAD7	AT5G07580	
AT1G33760		AT3G11240	ATE2	AT5G07690	MYB29
AT1G34120	IP5PI	AT3G11410	PP2CA	AT5G07700	MYB76
AT1G34170	ARF13	AT3G11440	MYB65	AT5G08130	BIM1
AT1G34310	ARF12	AT3G11480	BSMT1	AT5G09870	CESA5
AT1G34390	ARF22	AT3G11540	SPY	AT5G10030	TGA4
AT1G34410	ARF21	AT3G11580		AT5G10280	MYB92
AT1G34670	MYB93	AT3G11980	MS2	AT5G10510	AIL6
AT1G35140	PHI-1	AT3G12120	FAD2	AT5G10560	
AT1G35240	ARF20	AT3G12250	TGA6	AT5G10720	HK5
AT1G35515	HOS10	AT3G12390		AT5G10930	CIPK5
AT1G35520	ARF15	AT3G12490	CYSB	AT5G11050	MYB64
AT1G35540	ARF14	AT3G12720	MYB67	AT5G11190	SHN2
AT1G35670	CDPK2	AT3G12820	MYB10	AT5G11270	OCP3
AT1G36060		AT3G13224		AT5G11320	YUC4
AT1G37130	NIA2	AT3G13380	BRL3	AT5G11510	MYB3R-4
AT1G42560	MLO9	AT3G13540	MYB5	AT5G11590	TINY2
AT1G43160	RAP2.6	AT3G13730	CYP90D1	AT5G12210	RGTB1
AT1G43800	FTM1	AT3G13840		AT5G12870	MYB46
AT1G43950	ARF23	AT3G13890	MYB26	AT5G13080	WRKY75
AT1G44090	GA20OX5	AT3G13920	EIF4A1	AT5G13170	SAG29
AT1G44830		AT3G14230	RAP2.2	AT5G13220	JAZ10
AT1G46768	RAP2.1	AT3G14440	NCED3	AT5G13320	PBS3
AT1G48000	MYB112	AT3G14720	MPK19	AT5G13330	Rap2.6L
AT1G48260	CIPK17	AT3G15150	HPY2	AT5G13630	GUN5

Table A.1 continued from previous page

Locus ID	Symbol	Locus ID	Symbol	Locus ID	Symbol
AT1G48500	JAZ4	AT3G15210	ERF4	AT5G13680	ABO1
AT1G48630	RACK1B_AT	AT3G15356		AT5G13910	LEP
AT1G49040	SCD1	AT3G15540	IAA19	AT5G13930	TT4
AT1G49120	CRF9	AT3G15730	PLDALPHA1	AT5G14310	CXE16
AT1G49190	RR19	AT3G16280		AT5G14340	MYB40
AT1G49430	LACS2	AT3G16420	PBP1	AT5G14750	MYB66
AT1G49640		AT3G16570	RALF23	AT5G14930	SAG101
AT1G49660	CXE5	AT3G16770	EBP	AT5G15100	PIN8
AT1G50200	ALATS	AT3G16857	RR1	AT5G15130	WRKY72
AT1G50420	SCL3	AT3G17010	REM22	AT5G15310	MYB16
AT1G50600	SCL5	AT3G17510	CIPK1	AT5G15860	PCME
AT1G50640	ERF3	AT3G17860	JAZ3	AT5G15970	KIN2
AT1G50680		AT3G18040	MPK9	AT5G16080	CXE17
AT1G50960	GA2OX7	AT3G18130	RACK1C_AT	AT5G16230	
AT1G51120		AT3G18240		AT5G16240	
AT1G51190	PLT2	AT3G18910	ETP2	AT5G16260	ELF9
AT1G51500	ABCG12	AT3G18980	ETP1	AT5G16480	PFA-DSP5
AT1G51600	ZML2	AT3G18990	VRN1	AT5G16530	PIN5
AT1G51660	MKK4	AT3G19160	IPT8	AT5G16600	MYB43
AT1G51965	ABO5	AT3G19270	CYP707A4	AT5G16770	MYB9
AT1G52340	ABA2	AT3G19420	PEN2	AT5G16780	DOT2
AT1G52570	PLDALPHA2	AT3G19770	VPS9A	AT5G17420	IRX3
AT1G52920	GPCR	AT3G19820	DWF1	AT5G17430	BBM
AT1G53170	ERF8	AT3G20310	ERF7	AT5G17490	RGL3
AT1G53510	MPK18	AT3G20550	DDL	AT5G17690	TFL2
AT1G53910	RAP2.12	AT3G20660	OCT4	AT5G17800	MYB56
AT1G53940	GLIP2	AT3G20770	EIN3	AT5G18010	SAUR19
AT1G54270	EIF4A-2	AT3G20840	PLT1	AT5G18020	SAUR20
AT1G54350	ABCD2	AT3G21175	ZML1	AT5G18030	
AT1G54490	XRN4	AT3G21220	MKK5	AT5G18050	SAUR22
AT1G54990	AXR4	AT3G22850		AT5G18060	SAUR23
AT1G55010	PDF1.5	AT3G22980		AT5G18080	SAUR24
AT1G55180	PLDEPSILON	AT3G23000	CIPK7	AT5G18450	
AT1G55580	LAS	AT3G23050	IAA7	AT5G18560	PUCHI
AT1G55600	WRKY10	AT3G23140	URO	AT5G18930	BUD2
AT1G55610	BRL1	AT3G23150	ETR2	AT5G19000	BPM1
AT1G56070	LOS1	AT3G23220	ESE1	AT5G19010	MPK16
AT1G56160	MYB72	AT3G23230	TDR1	AT5G19140	AILP1
AT1G56650	PAP1	AT3G23240	ERF1	AT5G19180	ECR1
AT1G57560	MYB50	AT3G23250	MYB15	AT5G19330	ARIA
AT1G59580	MPK2	AT3G23610	DSPTP1	AT5G19770	TUA3
AT1G59750	ARF1	AT3G23770		AT5G19780	TUA5
AT1G59870	PEN3	AT3G24280	SMAP2	AT5G19790	RAP2.11
AT1G59900	E1 ALPHA	AT3G24310	MYB305	AT5G20270	HHP1
AT1G59940	ARR3	AT3G24500	MBF1C	AT5G20410	MGD2
AT1G60980	GA20OX4	AT3G24520	HSFC1	AT5G20570	RBX1
AT1G61110	NAC025	AT3G24650	ABI3	AT5G20730	NPH4
AT1G61560	MLO6	AT3G25730	EDF3	AT5G20900	JAZ12
AT1G61630	ENT7	AT3G25890	CRF11	AT5G20910	AIP2
AT1G62300	WRKY6	AT3G26090	RGS1	AT5G21010	BPM5
AT1G62430	CDS1	AT3G26790	FUS3	AT5G22010	RFC1
AT1G62740	Hop2	AT3G26810	AFB2	AT5G22110	DPB2
AT1G62830	LDL1	AT3G27140		AT5G22260	MS1
AT1G63030	ddf2	AT3G27310	PUX1	AT5G22420	FAR7
AT1G63100		AT3G27320		AT5G22500	FAR1
AT1G63160	RFC2	AT3G27670	RST1	AT5G22570	WRKY38
AT1G63440	HMA5	AT3G27810	MYB21	AT5G23000	MYB37
AT1G63650	EGL3	AT3G27920	MYB0	AT5G23720	PHS1
AT1G63910	AtMYB103	AT3G28470	TDF1	AT5G24110	WRKY30
AT1G64000	WRKY56	AT3G28860	ABCB19	AT5G24470	PRR5
AT1G64280	NPR1	AT3G28910	MYB30	AT5G24520	TTG1
AT1G64380		AT3G29020	MYB110	AT5G25110	CIPK25
AT1G64400	LACS3	AT3G29030	EXPA5	AT5G25190	ESE3
AT1G64520	RPN12a	AT3G29350	AHP2	AT5G25350	EBF2
AT1G64990	GTG1	AT3G30180	BR6OX2	AT5G25370	PLDALPHA3
AT1G65620	AS2	AT3G30210	MYB121	AT5G25390	SHN3
AT1G66230	MYB20	AT3G42960	ATA1	AT5G25620	YUC6
AT1G66340	ETR1	AT3G43300	ATMIN7	AT5G25810	tny
AT1G66350	RGL1	AT3G43440	JAZ11	AT5G25890	IAA28
AT1G66370	MYB113	AT3G43700	BPM6	AT5G25900	GA3
AT1G66380	MYB114	AT3G44540	FAR4	AT5G26140	LOG9
AT1G66390	MYB90	AT3G44550	FAR5	AT5G26170	WRKY50
AT1G66550	WRKY67	AT3G44560	FAR8	AT5G26660	MYB86
AT1G66560	WRKY64	AT3G44620		AT5G26780	SHM2
AT1G66600	ABO3	AT3G44730	KP1	AT5G26920	CBP60G
AT1G67080	ABA4	AT3G45140	LOX2	AT5G27320	GID1C
AT1G67260	TCP1	AT3G45290	MLO3	AT5G27740	EMB2775
AT1G67560	LOX6	AT3G45640	MPK3	AT5G28210	
AT1G67710	ARR11	AT3G45780	PHOT1	AT5G28650	WRKY74
AT1G67820		AT3G46130	MYB48	AT5G35410	SOS2
AT1G68150	WRKY9	AT3G46600		AT5G35550	TT2
AT1G68210	APRR6	AT3G46930		AT5G35750	HK2
AT1G68320	MYB62	AT3G47600	MYB94	AT5G35840	PHYC
AT1G68550	CRF10	AT3G48040	ROP10	AT5G36210	
AT1G68620		AT3G48090	EDS1	AT5G37020	ARF8
AT1G68840	RAV2	AT3G48100	RR5	AT5G38860	BIM3
AT1G69010	BIM2	AT3G48360	BT2	AT5G38970	BR6OX1
AT1G69270	RPK1	AT3G48430	REF6	AT5G39400	PTEN1
AT1G69310	WRKY57	AT3G48610	NPC6	AT5G39700	MYB89
AT1G69560	MYB105	AT3G48690	CXE12	AT5G40280	ERA1

Table A.1 continued from previous page

Locus ID	Symbol	Locus ID	Symbol	Locus ID	Symbol
AT1G69670	CUL3B	AT3G48700	CXE13	AT5G40330	MYB23
AT1G69810	WRKY36	AT3G48920	MYB45	AT5G40350	MYB24
AT1G69935	SHW1	AT3G49530	NAC062	AT5G40360	MYB115
AT1G70330	ENT1	AT3G49690	MYB84	AT5G40430	MYB22
AT1G70560	TAA1	AT3G49700	ACS9	AT5G40440	MKK3
AT1G70700	TIFY7	AT3G49950		AT5G40990	GLIP1
AT1G70940	PIN3	AT3G50060	MYB77	AT5G41570	WRKY24
AT1G71130	CRF8	AT3G50070	CYCD3;3	AT5G41920	
AT1G71260	ATWHY2	AT3G50110	PEN3	AT5G42650	AOS
AT1G71450		AT3G50260	CEJ1	AT5G42750	BKI1
AT1G71520		AT3G50280		AT5G43290	WRKY49
AT1G71830	SERK1	AT3G50650		AT5G43410	
AT1G71860	PTP1	AT3G50660	DWF4	AT5G43590	
AT1G71960	ABCG25	AT3G50750	BEH1	AT5G43830	
AT1G72360	ERF73	AT3G51060	STY1	AT5G43940	HOT5
AT1G72450	JAZ6	AT3G51590	LTP12	AT5G44030	CESA4
AT1G72520	LOX4	AT3G51770	ETO1	AT5G44200	CBP20
AT1G72570		AT3G52180	SEX4	AT5G44210	ERF9
AT1G72770	HAB1	AT3G52430	PAD4	AT5G44420	PDF1.2
AT1G73030	VPS46.2	AT3G52930	FBA8	AT5G44430	PDF1.2c
AT1G73220	OCT1	AT3G53200	MYB27	AT5G44790	RAN1
AT1G73410	MYB54	AT3G53250		AT5G45050	TTR1
AT1G73500	MKK9	AT3G53480	ABCG37	AT5G45340	CYP707A3
AT1G73590	PIN1	AT3G53710	AGD6	AT5G45510	
AT1G73670	MPK15	AT3G54220	SCR	AT5G45550	MOB1-like
AT1G73740		AT3G54320	WRI1	AT5G45710	RHA1
AT1G73830	BEE3	AT3G54720	AMP1	AT5G45810	CIPK19
AT1G74080	MYB122	AT3G54950	pPLAIIIbeta	AT5G45820	CIPK20
AT1G74430	MYB95	AT3G54990	SMZ	AT5G46350	WRKY8
AT1G74650	MYB31	AT3G55270	MKP1	AT5G46570	BSK2
AT1G74710	EDS16	AT3G55530	SDIR1	AT5G46790	PYL1
AT1G74890	ARR15	AT3G55730	MYB109	AT5G47100	CBL9
AT1G74910		AT3G56380	RR17	AT5G47220	ERF2
AT1G74930	ORA47	AT3G56400	WRKY70	AT5G47230	ERF5
AT1G74950	TIFY10B	AT3G56700	FAR6	AT5G48150	PAT1
AT1G75000		AT3G57040	ARR9	AT5G48170	SLY2
AT1G75080	BZR1	AT3G57140	SDP1-LIKE	AT5G48870	SAD1
AT1G75490		AT3G57600		AT5G48880	KAT5
AT1G75830	LCR67	AT3G58680	MBF1B	AT5G49240	APRR4
AT1G76090	SMT3	AT3G58710	WRKY69	AT5G49330	MYB111
AT1G76420	CUC3	AT3G59790	MPK10	AT5G49520	WRKY48
AT1G76680	OPR1	AT3G60460	DUO1	AT5G49620	MYB78
AT1G76690	OPR2	AT3G60490		AT5G49720	GH9A1
AT1G77110	PIN6	AT3G60620	CDS5	AT5G49980	AFB5
AT1G77120	ADH1	AT3G60630	HAM2	AT5G50080	ERF110
AT1G77200		AT3G61250	MYB17	AT5G51190	
AT1G77470	RFC3	AT3G61630	CRF6	AT5G51550	EXL3
AT1G77640		AT3G61830	ARF18	AT5G51760	AHG1
AT1G77690	LAX3	AT3G61850	DAG1	AT5G51810	GA20OX2
AT1G77760	NIA1	AT3G61860	RS31	AT5G51990	CBF4
AT1G77850	ARF17	AT3G61970	NGA2	AT5G52020	
AT1G77920	TGA7	AT3G62340	WRKY68	AT5G52040	RS41
AT1G78080	RAP2.4	AT3G62610	MYB11	AT5G52240	MSBP1
AT1G78440	ATGA2OX1	AT3G62670	RR20	AT5G52260	MYB19
AT1G78590	NADK3	AT3G62980	TIR1	AT5G52300	LTI65
AT1G78700	BEH4	AT3G63010	GID1B	AT5G52310	LTI78
AT1G79040	PSBR	AT3G63200	PLP9	AT5G52510	SCL8
AT1G79180	MYB63	AT3G63210		AT5G52600	MYB82
AT1G79360	OCT2	AT4G00120	IND	AT5G52830	WRKY27
AT1G79410	OCT5	AT4G00150	HAM3	AT5G53160	RCAR3
AT1G79460	GA2	AT4G00240	PLDBETA2	AT5G53280	PDV1
AT1G79530	GAPCP-1	AT4G00540	MYB3R2	AT5G53290	CRF3
AT1G79700	WRI4	AT4G00710	BSK3	AT5G53470	ACBP1
AT1G80330	GA3OX4	AT4G00760	APRR8	AT5G53760	MLO11
AT1G80340	GA3OX2	AT4G01026	PYL7	AT5G53950	CUC2
AT1G80580		AT4G01250	WRKY22	AT5G54190	PORA
AT1G80590	WRKY66	AT4G01370	MPK4	AT5G54230	MYB49
AT1G80840	WRKY40	AT4G01500	NGA4	AT5G54510	DFL1
AT2G01420	PIN4	AT4G01680	MYB55	AT5G55020	MYB120
AT2G01450	MPK17	AT4G01720	WRKY47	AT5G55160	SUMO2
AT2G01570	RGA1	AT4G02570	CUL1	AT5G55170	SUMO3
AT2G01650	PUX2	AT4G02600	MLO1	AT5G55250	IAMT1
AT2G01760	RR14	AT4G02780	GA1	AT5G56010	HSP81-3
AT2G01830	WOL	AT4G03080	BSL1	AT5G56110	MYB80
AT2G02560	CAND1	AT4G03190	GRH1	AT5G56270	WRKY2
AT2G02740	WHY3	AT4G03560	TPC1	AT5G56300	GAMT2
AT2G02820	MYB88	AT4G03960	PFA-DSP4	AT5G56330	ACA8
AT2G02950	PKS1	AT4G04450	WRKY42	AT5G56580	MKK6
AT2G03340	WRKY3	AT4G04500	CRK37	AT5G56610	
AT2G03760	SOT12	AT4G05100	MYB74	AT5G56860	GNC
AT2G04240	XERICO	AT4G05110	ENT6	AT5G56970	CKX3
AT2G04350	LACS8	AT4G05120	FUR1	AT5G57050	ABI2
AT2G04450	NUDT6	AT4G05130	ENT4	AT5G57090	EIR1
AT2G04550	IBR5	AT4G05140		AT5G57390	AIL5
AT2G04880	ZAP1	AT4G08150	KNAT1	AT5G57620	MYB36
AT2G04890	SCL21	AT4G08250		AT5G57630	CIPK21
AT2G06050	OPR3	AT4G08260		AT5G57685	GDU3
AT2G11810	MGDC	AT4G08920	CRY1	AT5G57740	XBAT32
AT2G13540	ABH1	AT4G08950	EXO	AT5G57800	CER3
AT2G14920	ST4A	AT4G09460	MYB6	AT5G58080	RR18

Table A.1 continued from previous page

Locus ID	Symbol	Locus ID	Symbol	Locus ID	Symbol
AT2G16070	PDV2	AT4G09570	CPK4	AT5G58140	PHOT2
AT2G16720	MYB7	AT4G11030		AT5G58160	
AT2G16910	AMS	AT4G11070	WRKY41	AT5G58220	TTL
AT2G16940		AT4G11140	CRF1	AT5G58230	MSI1
AT2G17230	EXL5	AT4G11260	SGT1B	AT5G58350	WNK4
AT2G17290	CPK6	AT4G11330	MPK5	AT5G58380	SIP1
AT2G17430	MLO7	AT4G11830	PLDGAMMA2	AT5G58850	MYB119
AT2G17480	MLO8	AT4G11840	PLDGAMMA3	AT5G58950	
AT2G17820	HK1	AT4G11850	PLDGAMMA1	AT5G59220	HAI1
AT2G18170	MPK7	AT4G12020	WRKY19	AT5G59450	
AT2G18470	PERK4	AT4G12110	SMO1-1	AT5G59780	MYB59
AT2G18550	HB21	AT4G12350	MYB42	AT5G60100	PRR3
AT2G18790	PHYB	AT4G12400	Hop3	AT5G60120	TOE2
AT2G19500	CKX2	AT4G12470	AZI1	AT5G60410	SIZ1
AT2G20180	PIL5	AT4G13260	YUC2	AT5G60450	ARF4
AT2G20350		AT4G13480	MYB79	AT5G60890	MYB34
AT2G20610	SUR1	AT4G13520	SMAP1	AT5G61380	TOC1
AT2G20880	ERF53	AT4G13620		AT5G61420	MYB28
AT2G20950		AT4G14400	ACD6	AT5G61430	NAC100
AT2G21050	LAX2	AT4G14550	IAA14	AT5G61590	
AT2G21770	CESA9	AT4G14560	IAA1	AT5G61600	ERF104
AT2G21900	WRKY59	AT4G14580	CIPK4	AT5G61790	CNX1
AT2G22090	UBA1A	AT4G14713	PPD1	AT5G61890	
AT2G22200		AT4G14720		AT5G62000	ARF2
AT2G22330	CYP79B3	AT4G15530	PPDK	AT5G62470	MYB96
AT2G23290	MYB70	AT4G15560	CLA1	AT5G62920	ARR6
AT2G23320	WRKY15	AT4G15900	PRL1	AT5G63980	SAL1
AT2G23340	DEAR3	AT4G16110	RR2	AT5G64740	CESA6
AT2G23430	ICK1	AT4G16250	PHYD	AT5G64750	ABR1
AT2G24570	WRKY17	AT4G16280	FCA	AT5G64810	WRKY51
AT2G25000	WRKY60	AT4G16420	ADA2B	AT5G64813	LIP1
AT2G25090	CIPK16	AT4G16750		AT5G65130	
AT2G25180	RR12	AT4G17230	SCL13	AT5G65210	TGA1
AT2G25230	MYB100	AT4G17490	ERF6	AT5G65230	MYB53
AT2G25490	EBF1	AT4G17500	ERF-1	AT5G65510	AIL7
AT2G25540	CESA10	AT4G17720		AT5G65790	MYB68
AT2G25820	ESE2	AT4G17780		AT5G65800	ACS5
AT2G26010	PDF1.3	AT4G17870	PYR1	AT5G65970	MLO10
AT2G26020	PDF1.2b	AT4G18010	IP5PII	AT5G66400	RAB18
AT2G26070	RTE1	AT4G18020	APRR2	AT5G66770	
AT2G26290	ARSK1	AT4G18130	PHYE	AT5G67000	
AT2G26560	PLA2A	AT4G18170	WRKY28	AT5G67030	ABA1
AT2G26710	BAS1	AT4G18450		AT5G67190	DEAR2
AT2G26870	NPC2	AT4G18470	SNI1	AT5G67300	MYBR1
AT2G26950	MYB104	AT4G18700	CIPK12	AT5G67500	VDAC2
AT2G26960	MYB81	AT4G18710	BIN2	ATMG01090	ORF262
AT2G26980	CIPK3	AT4G18770	MYB98	AT5G62320	MYB99
AT2G27050	EIL1	AT4G18780	IRX1	AT1G03790	SOM
AT2G27070	RR13	AT4G18880	HSF A4A	AT3G50500	SNRK2.2
AT2G27120	TIL2	AT4G18890	BEH3	AT4G36930	SPT
AT2G27150	AAO3	AT4G19230	CYP707A1	AT5G45830	DOG1
AT2G27210	BSL3	AT4G19850	PP2-A2	AT1G35560	
AT2G28305	LOG1	AT4G21200	GA2OX8	AT5G66880	SNRK2.3
AT2G28350	ARF10	AT4G21440	MYB102	AT1G04400	CRY2
AT2G28550	RAP2.7	AT4G21550	VAL3	AT5G55910	D6PK
AT2G29060		AT4G21670	CPL1	AT3G32130	
AT2G29090	CYP707A2	AT4G21690	GA3OX3	AT2G42620	MAX2

Table A.2: List of PhI interactions. All interactions are based on Y2H experiments and were confirmed in at least three independent experiments.

Int A	Symbol A	Int B	Symbol B	Int A	Symbol A	Int B	Symbol B
AT1G22640	MYB3	AT1G31880	BRX	AT5G05410	DREB2A	AT5G45830	DOG1
AT2G42880	MPK20	AT4G37260	MYB73	AT2G04550	IBR5	AT3G23610	DSPTP1
AT1G69810	WRKY36	AT2G25000	WRKY60	AT2G04550	IBR5	AT5G47100	CBL9
AT2G42880	MPK20	AT3G03450	RGL2	AT2G04550	IBR5	AT3G11410	PP2CA
AT3G14720	MPK19	AT4G37260	MYB73	AT2G22090	UBA1A	AT2G22090	UBA1A
AT2G01760	RR14	AT2G23290	MYB70	AT2G22090	UBA1A	AT5G61380	TOC1
AT2G01760	RR14	AT2G46990	IAA20	AT4G29810	MKK2	AT5G58950	
AT1G80840	WRKY40	AT5G22570	WRKY38	AT1G21690	EMB1968	AT3G23610	DSPTP1
AT2G01760	RR14	AT3G16500	PAP1	AT1G21690	EMB1968	AT1G35560	
AT2G01760	RR14	AT3G17600	IAA31	AT1G21690	EMB1968	AT1G77470	RFC3
AT2G01760	RR14	AT3G62100	IAA30	AT4G33520	PAA1	AT5G17490	RGL3
AT2G01760	RR14	AT4G00120	IND	AT1G21690	EMB1968	AT1G25490	RCN1
AT2G01760	RR14	AT4G37260	MYB73	AT3G29350	AHP2	AT4G37260	MYB73
AT4G18880	HSF A4A	AT5G64813	LIP1	AT3G29350	AHP2	AT4G16110	RR2
AT2G01760	RR14	AT2G44050	COS1	AT5G07310		AT5G48150	PAT1
AT3G16500	PAP1	AT3G23050	IAA7	AT3G29350	AHP2	AT4G31920	RR10
AT2G01760	RR14	AT2G25000	WRKY60	AT3G29350	AHP2	AT4G32570	TIFY8
AT3G16500	PAP1	AT3G61830	ARF18	AT1G35540	ARF14	AT3G61830	ARF18
AT3G20550	DDL	AT5G58220	TTL	AT2G38310	PYL4	AT3G11410	PP2CA
AT2G01760	RR14	AT4G32570	TIFY8	AT4G24400	CIPK8	AT5G47100	CBL9
AT3G16500	PAP1	AT4G14560	IAA1	AT1G19220	ARF19	AT3G23050	IAA7
AT2G01760	RR14	AT2G22090	UBA1A	AT4G28910	NINJA	AT4G32570	TIFY8
AT3G16500	PAP1	AT5G17690	TFL2	AT4G28910	NINJA	AT5G13220	JAZ10
AT2G01760	RR14	AT4G36930	SPT	AT4G28910	NINJA	AT5G20900	JAZ12
AT4G14720		AT4G28910	NINJA	AT2G33830		AT3G03530	NPC4
AT4G14720		AT4G32570	TIFY8	AT1G18400	BEE1	AT5G41920	
AT1G63160	RFC2	AT1G77470	RFC3	AT1G18400	BEE1	AT1G35560	
AT1G06400	ARA-2	AT4G17720		AT2G18170	MPK7	AT4G29810	MKK2
AT1G23860	RSZ21	AT3G61860	RS31	AT1G18400	BEE1	AT1G25490	RCN1
AT3G23030	IAA2	AT3G23050	IAA7	AT1G19050	ARR7	AT3G29350	AHP2
AT1G23860	RSZ21	AT2G01760	RR14	AT1G51600	ZML2	AT4G24470	ZIM
AT1G23860	RSZ21	AT1G23860	RSZ21	AT1G51600	ZML2	AT3G21175	ZML1
AT1G23860	RSZ21	AT4G08150	KNAT1	AT1G22770	GI	AT1G51950	IAA18
AT4G14560	IAA1	AT4G14560	IAA1	AT1G22770	GI	AT2G23290	MYB70
AT4G14560	IAA1	AT5G25890	IAA28	AT1G22770	GI	AT2G37630	AS1
AT1G69010	BIM2	AT5G38860	BIM3	AT1G22770	GI	AT2G44950	HUB1
AT1G69010	BIM2	AT1G69010	BIM2	AT1G22770	GI	AT3G16500	PAP1
AT1G69010	BIM2	AT5G08130	BIM1	AT1G22770	GI	AT4G08150	KNAT1
AT1G04240	SHY2	AT1G04250	AXR3	AT1G22770	GI	AT4G32570	TIFY8
AT4G39780		AT5G21010	BPM5	AT1G22770	GI	AT4G37260	MYB73
AT1G04240	SHY2	AT4G14560	IAA1	AT1G22770	GI	AT5G60120	TOE2
AT4G39780		AT5G19000	BPM1	AT3G21175	ZML1	AT4G24470	ZIM
AT1G04240	SHY2	AT3G15540	IAA19	AT3G21175	ZML1	AT5G11270	OCP3
AT2G43790	MPK6	AT4G29810	MKK2	AT3G21175	ZML1	AT3G21175	ZML1
AT1G04240	SHY2	AT5G25890	IAA28	AT1G51950	IAA18	AT3G24520	HSFC1
AT2G43790	MPK6	AT5G56580	MKK6	AT1G51950	IAA18	AT3G45640	MPK3
AT1G04240	SHY2	AT1G04550	IAA12	AT1G51950	IAA18	AT3G61830	ARF18
AT3G62100	IAA30	AT4G11070	WRKY41	AT1G14280	PKS2	AT1G35560	
AT3G62100	IAA30	AT4G24240	WRKY7	AT1G14280	PKS2	AT1G31880	BRX
AT3G62100	IAA30	AT5G61380	TOC1	AT1G28360	ERF12	AT1G35560	
AT2G40750	WRKY54	AT4G26110	NAP1;1	AT2G37630	AS1	AT5G51760	AHG1
AT4G26110	NAP1;1	AT4G26110	NAP1;1	AT2G37630	AS1	AT2G37630	AS1
AT4G00120	IND	AT4G36930	SPT	AT2G37630	AS1	AT2G42880	MPK20
AT4G00120	IND	AT5G55170	SUMO3	AT2G37630	AS1	AT3G24520	HSFC1
AT1G25490	RCN1	AT5G51760	AHG1	AT3G01970	WRKY45	AT3G21175	ZML1
AT1G25490	RCN1	AT5G45810	CIPK19	AT1G10210	MPK1	AT4G37260	MYB73
AT1G25490	RCN1	AT3G48090	EDS1	AT1G10210	MPK1	AT1G35560	
AT1G25490	RCN1	AT4G29800	PLP8	AT1G10210	MPK1	AT5G40440	MKK3
AT2G02560	CAND1	AT4G08150	KNAT1	AT1G10210	MPK1	AT3G63210	
AT1G25490	RCN1	AT5G64813	LIP1	AT2G44950	HUB1	AT2G44950	HUB1
AT2G02560	CAND1	AT3G21175	ZML1	AT1G18350	MKK7	AT4G32010	HSL1
AT1G25490	RCN1	AT1G53170	ERF8	AT2G44950	HUB1	AT3G24520	HSFC1
AT1G25490	RCN1	AT4G36540	BEE2	AT1G18350	MKK7	AT1G35560	
AT1G25490	RCN1	AT2G25090	CIPK16	AT2G44950	HUB1	AT3G48090	EDS1
AT1G25490	RCN1	AT2G37630	AS1	AT1G18350	MKK7	AT2G34650	PID
AT1G25490	RCN1	AT5G08130	BIM1	AT2G44950	HUB1	AT4G08150	KNAT1
AT1G25490	RCN1	AT2G26980	CIPK3	AT1G18350	MKK7	AT4G32570	TIFY8
AT2G25090	CIPK16	AT4G37260	MYB73	AT2G44950	HUB1	AT5G51760	AHG1
AT2G25090	CIPK16	AT5G47100	CBL9	AT1G18350	MKK7	AT1G24590	DRNL
AT5G53160	RCAR3	AT5G67300	MYBR1	AT1G07340	STP2	AT1G10210	MPK1
AT5G53160	RCAR3	AT5G57050	ABI2	AT1G07340	STP2	AT1G18350	MKK7
AT5G53160	RCAR3	AT5G59220	HAI1	AT3G15150	HPY2	AT3G23610	DSPTP1
AT1G04250	AXR3	AT3G15540	IAA19	AT2G30020		AT4G01370	MPK4
AT1G04250	AXR3	AT1G04250	AXR3	AT2G30020		AT2G43790	MPK6
AT5G67300	MYBR1	AT5G67300	MYBR1	AT4G08150	KNAT1	AT4G08150	KNAT1
AT1G04250	AXR3	AT4G14560	IAA1	AT4G08150	KNAT1	AT5G60120	TOE2
AT2G25490	EBF1	AT2G44950	HUB1	AT4G01370	MPK4	AT4G29810	MKK2
AT1G04250	AXR3	AT3G61830	ARF18	AT4G08150	KNAT1	AT5G64810	WRKY51
AT2G25490	EBF1	AT4G37260	MYB73	AT4G01370	MPK4	AT4G26070	MEK1
AT1G04250	AXR3	AT1G04550	IAA12	AT4G08150	KNAT1	AT4G32570	TIFY8
AT2G25490	EBF1	AT4G36930	SPT	AT4G01370	MPK4	AT5G56580	MKK6
AT2G25490	EBF1	AT4G02570	CUL1	AT4G08150	KNAT1	AT4G32010	HSL1
AT2G25490	EBF1	AT4G08150	KNAT1	AT4G08150	KNAT1	AT5G17490	RGL3
AT2G25490	EBF1	AT4G32570	TIFY8	AT2G44050	COS1	AT5G01810	CIPK15
AT2G26980	CIPK3	AT5G47100	CBL9	AT2G44050	COS1	AT2G44050	COS1
AT2G26980	CIPK3	AT5G25190	ESE3	AT2G44050	COS1	AT5G13930	TT4

Table A.2 continued from previous page

Int A	Symbol A	Int B	Symbol B	Int A	Symbol A	Int B	Symbol B
AT2G28350	ARF10	AT3G17600	IAA31	AT5G01810	CIPK15	AT5G47100	CBL9
AT2G29380	HAI3	AT4G01026	PYL7	AT1G74950	TIFY10B	AT4G28910	NINJA
AT2G29380	HAI3	AT5G45860	PYL11	AT4G32570	TIFY8	AT5G51760	AHG1
AT2G29380	HAI3	AT4G37260	MYB73	AT4G32570	TIFY8	AT5G41920	
AT2G29380	HAI3	AT5G45830	DOG1	AT1G50960	GA2OX7	AT3G54220	SCR
AT2G29380	HAI3	AT5G53160	RCAR3	AT1G31880	BRX	AT2G44745	WRKY12
AT3G52930	FBA8	AT5G03690	FBA4	AT1G31880	BRX	AT5G51760	AHG1
AT2G29380	HAI3	AT4G27920	PYL10	AT1G31880	BRX	AT5G55910	D6PK
AT2G39760	BPM3	AT3G24520	HSFC1	AT1G31880	BRX	AT1G69560	MYB105
AT2G39760	BPM3	AT4G39780		AT1G31880	BRX	AT1G51660	MKK4
AT2G39760	BPM3	AT2G39760	BPM3	AT1G31880	BRX	AT1G54490	XRN4
AT3G15540	IAA19	AT3G17600	IAA31	AT1G31880	BRX	AT5G16080	CXE17
AT3G15540	IAA19	AT3G23030	IAA2	AT1G31880	BRX	AT1G37130	NIA2
AT3G15540	IAA19	AT4G14560	IAA1	AT4G37260	MYB73	AT5G67300	MYBR1
AT3G15540	IAA19	AT3G23050	IAA7	AT1G31880	BRX	AT2G02950	PKS1
AT3G15540	IAA19	AT3G61830	ARF18	AT4G37260	MYB73	AT5G53160	RCAR3
AT2G39220	PLP6	AT2G44950	HUB1	AT1G31880	BRX	AT5G61380	TOC1
AT2G40330	PYL6	AT4G26080	ABI1	AT4G37260	MYB73	AT5G58950	
AT2G40330	PYL6	AT5G57050	ABI2	AT1G31880	BRX	AT2G32960	PFA-DSP2
AT2G40330	PYL6	AT3G11410	PP2CA	AT4G37260	MYB73	AT5G17690	TFL2
AT1G04550	IAA12	AT1G04550	IAA12	AT1G31880	BRX	AT2G24570	WRKY17
AT1G04550	IAA12	AT2G33310	IAA13	AT1G31880	BRX	AT1G53510	MPK18
AT1G04550	IAA12	AT3G04730	IAA16	AT1G31880	BRX	AT5G60120	TOE2
AT1G04550	IAA12	AT3G15540	IAA19	AT1G31880	BRX	AT1G53170	ERF8
AT1G04550	IAA12	AT5G25890	IAA28	AT1G31880	BRX	AT2G46870	NGA1
AT1G04550	IAA12	AT3G23050	IAA7	AT1G31880	BRX	AT1G69810	WRKY36
AT1G04550	IAA12	AT4G14560	IAA1	AT1G31880	BRX	AT2G01760	RR14
AT3G04240	SEC	AT3G28910	MYB30	AT1G31880	BRX	AT5G04190	PKS4
AT1G04550	IAA12	AT2G01760	RR14	AT1G31880	BRX	AT2G25090	CIPK16
AT3G04240	SEC	AT5G60120	TOE2	AT1G31880	BRX	AT5G08130	BIM1
AT1G04550	IAA12	AT3G61830	ARF18	AT1G31880	BRX	AT2G42880	MPK20
AT3G42960	ATA1	AT3G42960	ATA1	AT1G25470	CRF12	AT5G08130	BIM1
AT5G58220	TTL	AT5G58220	TTL	AT5G08130	BIM1	AT5G38860	BIM3
AT2G26560	PLA2A	AT2G26560	PLA2A	AT5G08130	BIM1	AT5G08130	BIM1
AT5G17690	TFL2	AT5G17690	TFL2	AT5G08130	BIM1	AT5G60120	TOE2
AT2G26560	PLA2A	AT5G41920		AT1G30270	CIPK23	AT5G47100	CBL9
AT1G54990	AXR4	AT2G38120	AUX1	AT5G47100	CBL9	AT5G58380	SIP1
AT4G11070	WRKY41	AT5G60120	TOE2	AT1G32640	MYC2	AT3G29350	AHP2
AT4G11070	WRKY41	AT5G22570	WRKY38	AT1G32640	MYC2	AT1G70700	TIFY7
AT4G14713	PPD1	AT5G17690	TFL2	AT1G32640	MYC2	AT3G20550	DDL
AT4G14713	PPD1	AT4G32570	TIFY8	AT1G69560	MYB105	AT5G48870	SAD1
AT4G14713	PPD1	AT4G14720		AT1G66560	WRKY64	AT5G22570	WRKY38
AT4G14713	PPD1	AT4G28910	NINJA	AT5G22570	WRKY38	AT5G62000	ARF2
AT4G15560	CLA1	AT4G15560	CLA1	AT1G74910		AT3G03540	NPC5
AT1G07430	HAI2	AT4G01026	PYL7	AT1G14920	GAI	AT4G36930	SPT
AT4G16420	ADA2B	AT5G51760	AHG1	AT1G37130	NIA2	AT1G37130	NIA2
AT1G07430	HAI2	AT4G18620	PYL13	AT1G14920	GAI	AT4G24210	SLY1
AT1G07430	HAI2	AT5G45830	DOG1	AT1G37130	NIA2	AT5G18930	BUD2
AT1G07430	HAI2	AT5G53160	RCAR3	AT1G14920	GAI	AT2G44950	HUB1
AT1G07430	HAI2	AT2G25000	WRKY60	AT1G37130	NIA2	AT5G60120	TOE2
AT1G07430	HAI2	AT4G27920	PYL10	AT1G14920	GAI	AT1G53510	MPK18
AT1G07430	HAI2	AT4G14720		AT1G37130	NIA2	AT4G32570	TIFY8
AT4G27920	PYL10	AT5G57050	ABI2	AT1G14920	GAI	AT1G70700	TIFY7
AT4G27920	PYL10	AT5G59220	HAI1	AT1G37130	NIA2	AT2G37630	AS1
AT2G04890	SCL21	AT5G67000		AT1G14920	GAI	AT2G42880	MPK20
AT2G04890	SCL21	AT5G07310		AT1G50600	SCL5	AT2G20350	
AT5G05440	PYL5	AT5G57050	ABI2	AT1G50600	SCL5	AT5G67000	
AT2G04890	SCL21	AT4G14720		AT1G51660	MKK4	AT4G08150	KNAT1
AT5G04870	CPK1	AT5G17690	TFL2	AT1G51660	MKK4	AT4G37260	MYB73
AT3G17510	CIPK1	AT5G47100	CBL9	AT1G51660	MKK4	AT3G45640	MPK3
AT2G30980	SKdZeta	AT4G18890	BEH3	AT1G51660	MKK4	AT4G32570	TIFY8
AT5G10930	CIPK5	AT5G47100	CBL9	AT1G51660	MKK4	AT2G43790	MPK6
AT5G35410	SOS2	AT5G47100	CBL9	AT3G45640	MPK3	AT3G63210	
AT5G45820	CIPK20	AT5G47100	CBL9	AT3G61830	ARF18	AT4G32010	HSL1
AT1G78590	NADK3	AT1G78590	NADK3	AT3G61830	ARF18	AT5G25890	IAA28
AT1G24590	DRNL	AT1G73410	MYB54	AT1G01030	NGA3	AT3G17600	IAA31
AT4G32010	HSL1	AT5G51760	AHG1	AT3G61830	ARF18	AT3G61830	ARF18
AT1G24590	DRNL	AT4G36930	SPT	AT3G17600	IAA31	AT4G30080	ARF16
AT4G32010	HSL1	AT5G55170	SUMO3	AT1G52340	ABA2	AT1G52340	ABA2
AT1G24590	DRNL	AT4G11070	WRKY41	AT1G53170	ERF8	AT5G19000	BPM1
AT4G32010	HSL1	AT5G41920		AT1G53170	ERF8	AT4G37260	MYB73
AT1G24590	DRNL	AT5G60120	TOE2	AT1G53170	ERF8	AT2G39760	BPM3
AT4G32010	HSL1	AT5G17490	RGL3	AT1G01140	CIPK9	AT2G23290	MYB70
AT1G10940	SNRK2.4	AT2G36270	ABI5	AT1G01140	CIPK9	AT4G37260	MYB73
AT4G24470	ZIM	AT4G24470	ZIM	AT1G01140	CIPK9	AT1G31880	BRX
AT3G23610	DSPTP1	AT5G45810	CIPK19	AT1G01140	CIPK9	AT5G47100	CBL9
AT1G22070	TGA3	AT3G12250	TGA6	AT2G23290	MYB70	AT2G25090	CIPK16
AT3G23610	DSPTP1	AT4G29810	MKK2	AT2G23290	MYB70	AT5G53160	RCAR3
AT1G22070	TGA3	AT1G64280	NPR1	AT2G23290	MYB70	AT5G58950	
AT3G23610	DSPTP1	AT3G29350	AHP2	AT2G23290	MYB70	AT5G67300	MYBR1
AT1G22070	TGA3	AT5G06950	AHBP-1B	AT1G53510	MPK18	AT2G01570	RGA1
AT3G23610	DSPTP1	AT3G45640	MPK3	AT1G53510	MPK18	AT3G03450	RGL2
AT4G36930	SPT	AT4G36930	SPT	AT2G01570	RGA1	AT2G30590	WRKY21
AT5G45830	DOG1	AT5G51760	AHG1	AT2G01570	RGA1	AT2G42880	MPK20
AT5G45830	DOG1	AT5G45830	DOG1	AT2G01570	RGA1	AT3G14720	MPK19
AT1G35560		AT5G51760	AHG1	AT2G01570	RGA1	AT4G16110	RR2
AT1G35560		AT1G73410	MYB54	AT2G01570	RGA1	AT5G41920	
AT1G35560		AT4G00240	PLDBETA2	AT1G01360	RCAR1	AT4G26080	ABI1
AT1G35560		AT5G45810	CIPK19	AT1G01360	RCAR1	AT1G17550	HAB2
AT1G35560		AT4G36930	SPT	AT1G01360	RCAR1	AT1G07430	HAI2

Table A.2 continued from previous page

Int A	Symbol A	Int B	Symbol B	Int A	Symbol A	Int B	Symbol B
AT1G75000		AT5G08130	BIM1	AT1G01360	RCAR1	AT5G57050	ABI2
AT1G35560		AT1G35560		AT1G01360	RCAR1	AT2G29380	HAI3
AT5G05730	ASA1	AT5G08130	BIM1	AT1G01360	RCAR1	AT3G11410	PP2CA
AT1G35560		AT2G25490	EBF1	AT3G03450	RGL2	AT5G54190	PORA
AT5G05730	ASA1	AT5G20900	JAZ12	AT3G03450	RGL2	AT5G64813	LIP1
AT1G35560		AT4G08150	KNAT1	AT4G26080	ABI1	AT4G27920	PYL10
AT1G35560		AT2G04550	IBR5	AT4G26080	ABI1	AT5G05440	PYL5
AT4G33790	CER4	AT5G08130	BIM1	AT4G26080	ABI1	AT5G53160	RCAR3
AT1G35560		AT4G29810	MKK2	AT5G01600	FER1	AT5G01600	FER1
AT1G13980	GN	AT3G11410	PP2CA	AT1G72450	JAZ6	AT4G28910	NINJA
AT1G35560		AT3G24520	HSFC1	AT1G04100	IAA10	AT1G15050	IAA34
AT1G35560		AT3G29350	AHP2	AT1G04100	IAA10	AT2G33310	IAA13
AT1G35560		AT1G64520	RPN12a	AT1G04100	IAA10	AT3G04730	IAA16
AT1G35560		AT3G57040	ARR9	AT1G04100	IAA10	AT3G16500	PAP1
AT3G11410	PP2CA	AT5G45830	DOG1	AT1G04100	IAA10	AT3G23030	IAA2
AT1G35560		AT5G62000	ARF2	AT1G04100	IAA10	AT4G14560	IAA1
AT3G11410	PP2CA	AT4G27920	PYL10	AT1G53910	RAP2.12	AT2G38490	CIPK22
AT1G35560		AT2G46130	WRKY43	AT2G24570	WRKY17	AT2G44050	COS1
AT3G11410	PP2CA	AT5G05440	PYL5	AT2G38490	CIPK22	AT3G17600	IAA31
AT1G35560		AT4G11070	WRKY41	AT2G38490	CIPK22	AT4G28640	IAA11
AT3G11410	PP2CA	AT5G53160	RCAR3	AT2G38490	CIPK22	AT2G44050	COS1
AT1G35560		AT4G29800	PLP8	AT2G38490	CIPK22	AT3G25890	CRF11
AT1G35560		AT1G50600	SCL5	AT1G68550	CRF10	AT2G38490	CIPK22
AT1G35560		AT1G53170	ERF8	AT1G54490	XRN4	AT5G60120	TOE2
AT1G35560		AT5G13080	WRKY75	AT1G64280	NPR1	AT5G06950	AHBP-1B
AT1G35560		AT5G43290	WRKY49	AT1G64280	NPR1	AT3G12250	TGA6
AT1G35560		AT2G39250	SNZ	AT1G64280	NPR1	AT5G06960	OBF5
AT1G35560		AT2G01760	RR14	AT1G64280	NPR1	AT5G65210	TGA1
AT1G35560		AT2G30590	WRKY21	AT2G02950	PKS1	AT2G39760	BPM3
AT1G35560		AT3G45640	MPK3	AT5G06950	AHBP-1B	AT5G06960	OBF5
AT3G23050	IAA7	AT5G25890	IAA28	AT1G64520	RPN12a	AT4G08150	KNAT1
AT1G35560		AT4G36540	BEE2	AT1G15050	IAA34	AT3G23050	IAA7
AT3G23050	IAA7	AT3G61830	ARF18	AT2G25000	WRKY60	AT3G24520	HSFC1
AT1G35560		AT5G55170	SUMO3	AT2G25000	WRKY60	AT3G29350	AHP2
AT1G35560		AT3G01970	WRKY45	AT2G25000	WRKY60	AT2G25000	WRKY60
AT1G35560		AT3G15150	HPY2	AT1G65620	AS2	AT2G37630	AS1
AT1G35560		AT2G26980	CIPK3	AT1G73410	MYB54	AT2G20350	
AT1G35560		AT2G42880	MPK20	AT1G73410	MYB54	AT4G08150	KNAT1
AT1G35560		AT4G14713	PPD1	AT1G73410	MYB54	AT4G37260	MYB73
AT1G35560		AT1G80340	GA3OX2	AT1G73410	MYB54	AT4G30080	ARF16
AT1G35560		AT3G14720	MPK19	AT2G45820		AT3G44620	
AT1G35560		AT5G05440	PYL5	AT1G73410	MYB54	AT5G25190	ESE3
AT1G15550	GA3OX1	AT5G60120	TOE2	AT1G73410	MYB54	AT5G41920	
AT1G15550	GA3OX1	AT4G36930	SPT	AT1G75080	BZR1	AT2G01570	RGA1
AT1G15550	GA3OX1	AT1G35560		AT1G75080	BZR1	AT5G17490	RGL3
AT1G15550	GA3OX1	AT1G31880	BRX	AT4G27450		AT5G43830	
AT1G15550	GA3OX1	AT4G32570	TIFY8	AT5G43830		AT5G43830	
AT1G15550	GA3OX1	AT5G25890	IAA28	AT1G19180	JAZ1	AT4G28910	NINJA
AT1G15550	GA3OX1	AT1G24590	DRNL	AT1G19180	JAZ1	AT3G29350	AHP2
AT1G15550	GA3OX1	AT4G32010	HSL1	AT1G19180	JAZ1	AT1G30135	JAZ8
AT5G17490	RGL3	AT5G54190	PORA	AT1G19180	JAZ1	AT1G19180	JAZ1
AT1G15550	GA3OX1	AT2G37630	AS1	AT1G19180	JAZ1	AT5G41920	
AT5G60120	TOE2	AT5G60120	TOE2	AT2G33310	IAA13	AT3G15540	IAA19
AT1G17380	JAZ5	AT3G29350	AHP2	AT2G33310	IAA13	AT3G23050	IAA7
AT1G77200		AT4G08150	KNAT1	AT1G70700	TIFY7	AT4G28910	NINJA
AT1G17380	JAZ5	AT4G28910	NINJA	AT2G30590	WRKY21	AT2G46990	IAA20
AT1G17550	HAB2	AT2G40330	PYL6	AT2G30590	WRKY21	AT3G62100	IAA30
AT1G17380	JAZ5	AT1G32640	MYC2	AT3G04730	IAA16	AT3G15540	IAA19
AT1G17550	HAB2	AT5G05440	PYL5	AT2G30590	WRKY21	AT4G37260	MYB73
AT1G17550	HAB2	AT5G53160	RCAR3	AT2G30590	WRKY21	AT2G44050	COS1
AT1G17550	HAB2	AT4G27920	PYL10	AT2G04550	IBR5	AT3G62340	WRKY68
AT2G04550	IBR5	AT3G62340	WRKY68				

A.2.1 PhI communities

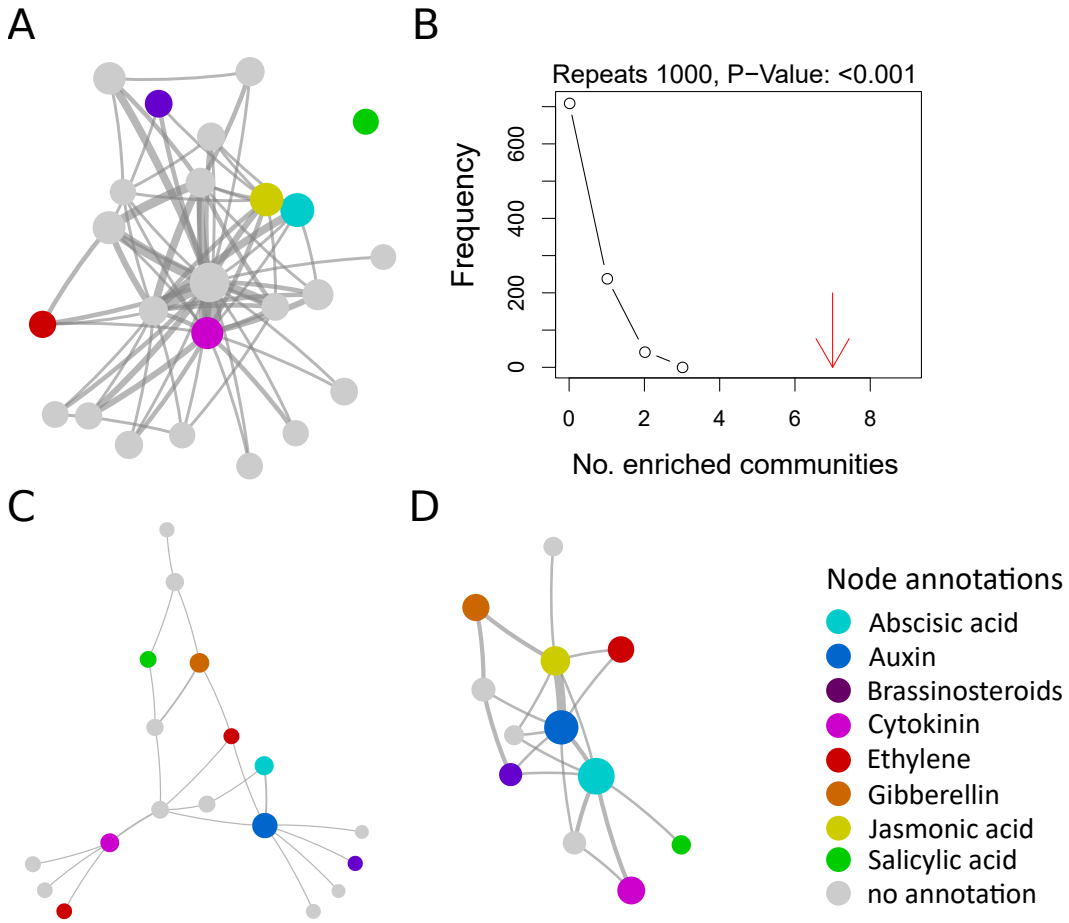

Figure A.2: Community analysis PhI vs IntAct and BioGRID databases. (A) shows a community enrichment analysis for PhI. (B) shows degree preserved random rewiring of the community enrichment analysis. (C+D) the community enrichment analysis for literature interactions from IntAct (C) and BioGRID (D) are shown. The thickness of the edges show the amount of interactions between the communities. The size of the nodes indicate the amount of proteins per community.

A.3 Quality assessment

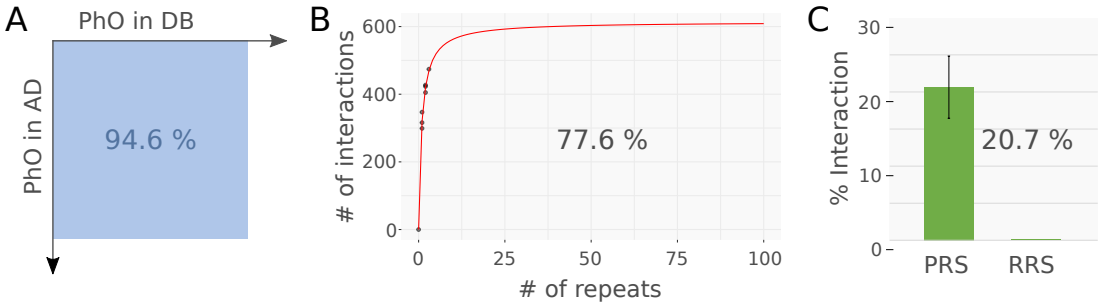

Figure A.3: Quality assessment. Three parameters of the quality assessment are presented. (A) Completeness of the PhI is about 94.6 %. (B) Sampling sensitivity (degree of saturation of the PhI screen) is about 77.6 % ±4.7 %. (C) Assay sensitivity (PRS and RRS sets were tested in the Y2H system) is about 20.7 % ±4.2 %. Error bars indicate the standard error of the proportion.

A.4 MAP-kinase interactions

A.4.1 Analysis of the amiR MKK7 construct for unspecific binding

```
Query= user-submitted sequence
         (21 letters)

Database: Araport11 transcripts (DNA)
           55,854 sequences; 87,813,715 total letters

Searching.....................................................done
```

Sequences producing significant alignments:	Score (bits)	E Value
AT1G18350.1 | Symbols: BUD1, MKK7, ATMKK7 | BUSHY AND DWARF...	32	0.11
AT3G18362.1 | Symbols: no symbol available | no full name a...	28	1.6
AT1G54510.5 | Symbols: ATNEK1, NEK1 | NIMA-related serine/t...	28	1.6
AT5G67420.2 | Symbols: ASL39, LBD37 | ASYMMETRIC LEAVES2-LI...	26	6.5
AT5G67420.1 | Symbols: ASL39, LBD37 | ASYMMETRIC LEAVES2-LI...	26	6.5
AT4G21440.1 | Symbols: ATM4, ATMYB102, MYB102 | MYB-like 10...	26	6.5
AT4G20410.1 | Symbols: GAMMA-SNAP, GSNAP | gamma-soluble NS...	26	6.5
AT4G20410.2 | Symbols: GAMMA-SNAP, GSNAP | gamma-soluble NS...	26	6.5
AT3G22010.1 | Symbols: no symbol available | no full name a...	26	6.5

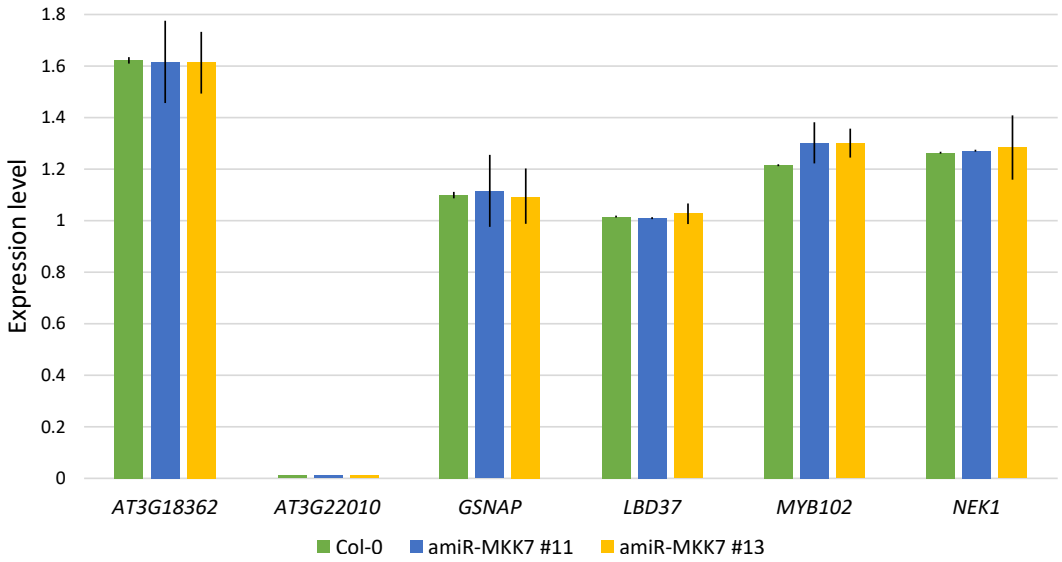

Figure A.4: Expression level of possible amiR MKK7 targets. The possible target genes *AT3G18362, AT3G22010, GSNAP, LBD37, MYB102* and *NEK1* were checked for altered expression levels in MKK7-Col-0 #11 and #13 plant lines, due to amiR MKK7 binding and *ACT8* was used for normalization. The expression levels were generated by qRT-PCR with four biological and four technical replicates each. The values indicate no unspecific binding by the amiR MKK7 construct. Error bars indicate standard deviation of four biological replicates.

A.5 PhI_{out}

Table A.3: List of PhI out interactions. All interactions are based on Y2H experiments and were confirmed in at least three independent experiments.

Int A	Symbol A	Int B	Symbol B	Int A	Symbol A	Int B	Symbol B
AT2G25880	AUR2	AT4G37260	MYB73	AT3G46060	RABE1c	AT4G17720	
AT1G72670	IQD8	AT4G37260	MYB73	AT1G51950	IAA18	AT5G25890	IAA28
AT2G42880	MPK20	AT4G37260	MYB73	AT1G19010		AT4G37260	MYB73
AT2G25010		AT4G13260	YUC2	AT1G55190	PRA7	AT4G17720	
AT4G09060		AT4G32010	HSL1	AT1G28360	ERF12	AT1G77770	
AT3G15450		AT5G43830		AT1G28360	ERF12	AT5G24660	LSU2
AT4G09060		AT4G32570	TIFY8	AT3G13672		AT4G37260	MYB73
AT4G14710	ATARD2	AT5G43830		AT1G28360	ERF12	AT2G44740	CYCP4;1
AT3G62550		AT4G32010	HSL1	AT1G66160	CMPG1	AT4G37260	MYB73
AT1G79650	RAD23B	AT4G32010	HSL1	AT1G66160	CMPG1	AT5G08130	BIM1
AT3G29370	P1R3	AT4G36540	BEE2	AT3G02140	TMAC2	AT4G37260	MYB73
AT4G22720		AT4G32010	HSL1	AT3G02140	TMAC2	AT4G32010	HSL1
AT4G14716	ARD1	AT5G43830		AT3G02140	TMAC2	AT4G14720	
AT4G22720		AT4G32570	TIFY8	AT4G17615	CBL1	AT4G24400	CIPK8
AT1G80840	WRKY40	AT5G22570	WRKY38	AT4G17615	CBL1	AT5G58380	SIP1
AT4G05450	MFDX1	AT4G32010	HSL1	AT4G17615	CBL1	AT5G10930	CIPK5
AT2G01760	RR14	AT4G37260	MYB73	AT2G37630	AS1	AT4G37260	MYB73
AT2G35940	BLH1	AT4G32010	HSL1	AT4G17615	CBL1	AT5G35410	SOS2
AT4G38850	SAUR15	AT5G02760		AT1G10210	MPK1	AT3G63210	
AT2G01760	RR14	AT4G32570	TIFY8	AT2G17670		AT4G37260	MYB73
AT5G02760		AT5G18020	SAUR20	AT1G18350	MKK7	AT4G32010	HSL1
AT2G01760	RR14	AT2G22090	UBA1A	AT2G44840	ERF13	AT3G05000	
AT2G24090	PRPL35	AT4G26110	NAP1;1	AT2G44840	ERF13	AT4G16143	IMPA-2
AT4G14720		AT4G28910	NINJA	AT4G16143	IMPA-2	AT4G37260	MYB73
AT1G77770		AT4G00120	IND	AT4G16143	IMPA-2	AT4G24470	ZIM
AT4G14720		AT4G32295		AT4G16143	IMPA-2	AT5G01600	FER1
AT2G38270	CXIP2	AT4G00120	IND	AT4G08150	KNAT1	AT4G08150	KNAT1
AT4G14720		AT4G16143	IMPA-2	AT4G01370	MPK4	AT4G29810	MKK2
AT2G38270	CXIP2	AT5G25890	IAA28	AT1G05710		AT1G31880	BRX
AT4G14720		AT5G63470	NF-YC4	AT4G01370	MPK4	AT4G26070	MEK1
AT4G17720		AT5G03520	RAB8C	AT4G08150	KNAT1	AT4G32010	HSL1
AT2G18730	DGK3	AT2G43790	MPK6	AT4G01370	MPK4	AT5G14600	
AT4G17720		AT5G47200	RAB1A	AT4G01370	MPK4	AT5G07260	
AT4G17720		AT4G18800	RABA1d	AT4G08150	KNAT1	AT5G59730	EXO70H7
AT4G00780		AT4G24470	ZIM	AT4G08150	KNAT1	AT5G50680	SAE1B
AT5G18580	FASS	AT5G25890	IAA28	AT4G08150	KNAT1	AT5G11980	
AT2G31955	CNX2	AT3G03450	RGL2	AT2G44050	COS1	AT2G44050	COS1
AT1G23860	RSZ21	AT3G61860	RS31	AT2G44050	COS1	AT3G13672	
AT1G12860	SCRM2	AT2G43790	MPK6	AT2G44050	COS1	AT5G01820	SR1
AT3G18240		AT5G18580	FASS	AT2G44050	COS1	AT4G18650	
AT3G23030	IAA2	AT4G14560	IAA1	AT2G44050	COS1	AT5G62520	SRO5
AT3G14080	LSM1B	AT3G53250		AT2G44050	COS1	AT3G50670	U1-70K
AT1G23860	RSZ21	AT5G54580		AT2G44050	COS1	AT3G05640	
AT1G23860	RSZ21	AT4G32660	AME3	AT2G44050	COS1	AT3G60360	EDA14
AT1G68590	PSRP3/1	AT5G01600	FER1	AT2G44050	COS1	AT5G22890	
AT1G23860	RSZ21	AT3G50670	U1-70K	AT4G02150	MOS6	AT4G37260	MYB73
AT5G12190		AT5G67300	MYBR1	AT4G02150	MOS6	AT5G01600	FER1
AT3G06790	MORF3	AT5G67300	MYBR1	AT1G01210		AT1G31880	BRX
AT3G06790	MORF3	AT4G16420	ADA2B	AT4G32570	TIFY8	AT5G41920	
AT3G06790	MORF3	AT5G17490	RGL3	AT4G32570	TIFY8	AT5G38410	RBCS3B
AT1G30880		AT4G26110	NAP1;1	AT4G32570	TIFY8	AT5G64960	CDKC2
AT3G29770	MES11	AT4G26110	NAP1;1	AT4G32570	TIFY8	AT5G59730	EXO70H7
AT1G09700	HYL1	AT5G41070	DRB5	AT4G32570	TIFY8	AT4G37470	KAI2
AT1G09700	HYL1	AT3G58380		AT4G32570	TIFY8	AT5G10710	
AT3G61860	RS31	AT4G32660	AME3	AT4G32570	TIFY8	AT5G43820	
AT1G09700	HYL1	AT1G50670		AT4G32570	TIFY8	AT5G50230	
AT1G09700	HYL1	AT3G22490		AT4G32570	TIFY8	AT5G48470	
AT1G09700	HYL1	AT4G19200		AT1G03330	LSM2	AT1G31880	BRX
AT1G61150		AT3G23610	DSPTP1	AT4G32570	TIFY8	AT5G05790	
AT5G57950		AT5G60890	MYB34	AT1G03900	ABCI18	AT1G31880	BRX
AT4G00180	YAB3	AT5G67300	MYBR1	AT4G32570	TIFY8	AT5G18110	NCBP
AT4G00180	YAB3	AT5G08130	BIM1	AT4G32570	TIFY8	AT5G47830	
AT1G69010	BIM2	AT1G69010	BIM2	AT4G32570	TIFY8	AT5G08290	YLS8
AT1G05510		AT4G18010	IP5PII	AT4G32570	TIFY8	AT5G64180	
AT1G69010	BIM2	AT5G08130	BIM1	AT4G32570	TIFY8	AT5G07260	
AT1G69010	BIM2	AT3G18960		AT4G32570	TIFY8	AT5G22480	
AT3G48680	GAMMA CAL2	AT4G24470	ZIM	AT4G31300	PBA1	AT4G37260	MYB73
AT3G48680	GAMMA CAL2	AT4G32570	TIFY8	AT4G32570	TIFY8	AT5G62600	MOS14
AT2G43790	MPK6	AT5G07260		AT1G23220		AT1G31880	BRX
AT1G04240	SHY2	AT4G02150	MOS6	AT4G32570	TIFY8	AT5G60690	REV
AT1G04240	SHY2	AT3G23030	IAA2	AT5G14070	ROXY2	AT5G65210	TGA1
AT4G20130	PTAC14	AT4G24470	ZIM	AT1G10760	SEX1	AT1G31880	BRX
AT1G04240	SHY2	AT3G04730	IAA16	AT5G14070	ROXY2	AT5G17490	RGL3
AT1G04240	SHY2	AT1G51950	IAA18	AT1G10760	SEX1	AT1G71260	ATWHY2
AT1G04240	SHY2	AT1G09500		AT4G25670		AT4G37260	MYB73
AT3G54130		AT5G05690	CPD	AT3G52120		AT4G37260	MYB73
AT1G04240	SHY2	AT5G52547		AT4G18040	EIF4E	AT4G37260	MYB73
AT3G08710	TH9	AT5G18930	BUD2	AT1G31880	BRX	AT1G51660	MKK4
AT1G18710	MYB47	AT3G54130		AT1G14685	BPC2	AT1G31880	BRX
AT1G64000	WRKY56	AT2G22880		AT3G50670	U1-70K	AT4G37260	MYB73

Table A.3 continued from previous page

Int A	Symbol A	Int B	Symbol B	Int A	Symbol A	Int B	Symbol B
AT3G50330	HEC2	AT4G00120	IND	AT3G50670	U1-70K	AT3G61860	RS31
AT1G64000	WRKY56	AT5G08480		AT1G31880	BRX	AT5G16080	CXE17
AT1G64000	WRKY56	AT4G37710		AT1G20140	SK4	AT2G04550	IBR5
AT2G22880		AT5G41570	WRKY24	AT4G37260	MYB73	AT5G67300	MYBR1
AT3G56910	PSRP5	AT4G26110	NAP1;1	AT4G37260	MYB73	AT5G53160	RCAR3
AT2G22880		AT3G01970	WRKY45	AT4G37260	MYB73	AT5G58950	
AT1G08580		AT4G26110	NAP1;1	AT1G31880	BRX	AT2G32960	PFA-DSP2
AT2G41680	NTRC	AT4G32010	HSL1	AT1G31880	BRX	AT2G24570	WRKY17
AT2G43060	IBH1	AT4G26110	NAP1;1	AT4G37260	MYB73	AT5G16400	TRXF2
AT3G06590		AT4G26110	NAP1;1	AT4G37260	MYB73	AT5G59730	EXO70H7
AT3G62870		AT4G26110	NAP1;1	AT1G09500		AT4G14560	IAA1
AT3G48150	APC8	AT4G32010	HSL1	AT4G37260	MYB73	AT5G39340	AHP3
AT4G00120	IND	AT5G27690		AT3G05640		AT4G37260	MYB73
AT3G48150	APC8	AT4G32570	TIFY8	AT4G37260	MYB73	AT5G42900	COR27
AT4G00120	IND	AT5G61230	ANK6	AT1G31880	BRX	AT2G46870	NGA1
AT4G00120	IND	AT5G52010		AT4G37260	MYB73	AT5G37055	SEF
AT3G22490		AT5G59220	HAI1	AT4G37260	MYB73	AT5G61010	EXO70E2
AT4G33950	OST1	AT5G39360	EDL2	AT4G37260	MYB73	AT5G62520	SRO5
AT1G25490	RCN1	AT3G62550		AT4G37260	MYB73	AT5G14070	ROXY2
AT1G25490	RCN1	AT5G17710	EMB1241	AT4G37260	MYB73	AT5G61230	ANK6
AT1G25490	RCN1	AT3G02140	TMAC2	AT2G33430	DAL1	AT4G37260	MYB73
AT2G25090	CIPK16	AT5G47100	CBL9	AT1G31880	BRX	AT5G08130	BIM1
AT1G25490	RCN1	AT2G35900		AT4G37260	MYB73	AT5G45680	FKBP13
AT1G25490	RCN1	AT1G51520		AT2G33430	DAL1	AT3G11410	PP2CA
AT1G25490	RCN1	AT3G14080	LSM1B	AT1G31880	BRX	AT2G42880	MPK20
AT1G25490	RCN1	AT3G56270		AT4G37260	MYB73	AT5G49210	
AT1G25490	RCN1	AT1G53000	CKS	AT1G31880	BRX	AT5G16400	TRXF2
AT1G25490	RCN1	AT5G57950		AT4G37260	MYB73	AT5G49690	
AT5G53160	RCAR3	AT5G59220	HAI1	AT1G31880	BRX	AT1G66160	CMPG1
AT5G67300	MYBR1	AT5G67300	MYBR1	AT4G37260	MYB73	AT5G14170	CHC1
AT1G04250	AXR3	AT1G51950	IAA18	AT1G31880	BRX	AT3G02140	TMAC2
AT4G14160		AT5G19000	BPM1	AT4G37260	MYB73	AT5G22890	
AT1G04250	AXR3	AT4G16143	IMPA-2	AT1G31880	BRX	AT4G26610	D6PKL1
AT1G29260	PEX7	AT4G32010	HSL1	AT4G37260	MYB73	AT5G48335	
AT1G04250	AXR3	AT4G02150	MOS6	AT1G31880	BRX	AT1G63480	
AT1G29260	PEX7	AT2G33150	PKT3	AT4G37260	MYB73	AT5G62770	
AT2G25490	EBF1	AT4G32570	TIFY8	AT1G31880	BRX	AT4G30860	SDG4
AT1G04250	AXR3	AT1G09500		AT4G37260	MYB73	AT5G05790	
AT2G35900		AT5G59220	HAI1	AT1G31880	BRX	AT4G02770	PSAD-1
AT1G29260	PEX7	AT4G32570	TIFY8	AT4G37260	MYB73	AT5G20920	EIF2 BETA
AT2G25490	EBF1	AT4G32010	HSL1	AT1G31880	BRX	AT5G23130	
AT2G25490	EBF1	AT2G46900		AT4G37260	MYB73	AT5G25510	
AT1G11430	MORF9	AT1G25490	RCN1	AT1G31880	BRX	AT5G22310	
AT2G25490	EBF1	AT2G29540	RPC14	AT4G37260	MYB73	AT5G25280	
AT1G11430	MORF9	AT5G17490	RGL3	AT1G31880	BRX	AT3G11400	EIF3G1
AT2G26980	CIPK3	AT5G47100	CBL9	AT4G37260	MYB73	AT5G27720	emb1644
AT1G01225		AT4G32010	HSL1	AT1G31880	BRX	AT5G03740	HD2C
AT1G01225		AT4G32570	TIFY8	AT1G31880	BRX	AT5G50180	
AT3G17090		AT3G53250		AT3G60360	EDA14	AT4G37260	MYB73
AT3G17090		AT4G38850	SAUR15	AT1G31880	BRX	AT1G49850	
AT3G17090		AT5G18020	SAUR20	AT1G31880	BRX	AT5G65683	WAVH2
AT5G08480		AT5G41570	WRKY24	AT1G31880	BRX	AT3G15660	GRX4
AT5G13180	NAC083	AT5G19000	BPM1	AT1G31880	BRX	AT5G59490	
AT1G76080	CDSP32	AT5G67300	MYBR1	AT1G31880	BRX	AT5G41070	DRB5
AT1G76080	CDSP32	AT5G19000	BPM1	AT1G31880	BRX	AT5G22890	
AT2G30540		AT5G65210	TGA1	AT1G31880	BRX	AT3G54170	FIP37
AT3G52930	FBA8	AT5G03690	FBA4	AT1G31880	BRX	AT2G27840	HDT4
AT1G60950	FED A	AT4G32010	HSL1	AT1G31880	BRX	AT5G05190	
AT2G29380	HAI3	AT3G02140	TMAC2	AT5G08130	BIM1	AT5G67220	
AT4G15670		AT5G65210	TGA1	AT1G31880	BRX	AT3G27580	ATPK7
AT3G44610		AT4G17490	ERF6	AT5G08130	BIM1	AT5G18260	
AT1G04710	PKT4	AT1G29260	PEX7	AT1G31880	BRX	AT5G19340	
AT3G04300		AT5G10930	CIPK5	AT1G30270	CIPK23	AT5G47100	CBL9
AT2G39760	BPM3	AT3G24520	HSFC1	AT1G31880	BRX	AT3G18295	
AT4G17500	ERF-1	AT5G41650		AT1G31880	BRX	AT1G51100	CRR41
AT1G80940		AT4G32010	HSL1	AT1G31880	BRX	AT4G22745	MBD1
AT1G80780		AT4G37580	HLS1	AT3G19120		AT4G37260	MYB73
AT3G18430		AT4G32010	HSL1	AT1G31880	BRX	AT3G49810	
AT2G39760	BPM3	AT4G22720		AT1G31880	BRX	AT5G18110	NCBP
AT3G56090	FER3	AT5G01600	FER1	AT1G31880	BRX	AT1G76080	CDSP32
AT2G39760	BPM3	AT4G14160		AT1G31880	BRX	AT4G31050	
AT4G11140	CRF1	AT5G04820	OFP13	AT1G31880	BRX	AT1G68130	IDD14
AT2G39760	BPM3	AT5G28770	BZO2H3	AT5G47100	CBL9	AT5G58380	SIP1
AT2G39760	BPM3	AT5G51100	FSD2	AT1G31880	BRX	AT5G11460	
AT3G03270		AT5G49620	MYB78	AT2G42260	UVI4	AT4G37260	MYB73
AT2G39760	BPM3	AT5G25340		AT1G31880	BRX	AT4G37710	
AT2G29540	RPC14	AT4G32010	HSL1	AT1G31880	BRX	AT4G03250	
AT1G68160		AT4G32010	HSL1	AT1G31880	BRX	AT1G54200	
AT1G68160		AT3G60630	HAM2	AT1G31880	BRX	AT2G35010	TO1
AT1G68160		AT4G32570	TIFY8	AT1G31880	BRX	AT3G48510	
AT2G40330	PYL6	AT3G11410	PP2CA	AT1G31880	BRX	AT4G14020	
AT3G59810	LSM6A	AT5G48870	SAD1	AT1G31880	BRX	AT4G39540	SK2
AT1G80370	CYCA2;4	AT4G32010	HSL1	AT1G31880	BRX	AT4G21660	
AT3G13720	PRA8	AT3G53710	AGD6	AT1G31880	BRX	AT3G16560	
AT5G25890	IAA28	AT5G59730	EXO70H7	AT1G31880	BRX	AT1G76070	
AT1G05730		AT4G32010	HSL1	AT1G31880	BRX	AT5G58960	GIL1
AT3G51030	TRX1	AT5G18930	BUD2	AT1G31880	BRX	AT4G18830	OFP5
AT3G22810		AT5G01810	CIPK15	AT1G31880	BRX	AT5G42050	
AT1G51090		AT2G44050	COS1	AT1G31880	BRX	AT1G56450	PBG1

Table A.3 continued from previous page

Int A	Symbol A	Int B	Symbol B	Int A	Symbol A	Int B	Symbol B
AT1G51090		AT4G00120	IND	AT3G18210		AT4G37260	MYB73
AT5G17300	RVE1	AT5G24520	TTG1	AT2G30360	SIP4	AT4G37260	MYB73
AT1G04550	IAA12	AT5G18580	FASS	AT3G12720	MYB67	AT5G57860	
AT5G24520	TTG1	AT5G43650	BHLH92	AT3G23240	ERF1	AT4G17680	
AT1G04550	IAA12	AT2G36145		AT4G17680		AT4G32570	TIFY8
AT1G04550	IAA12	AT1G51950	IAA18	AT1G74910		AT2G39770	CYT1
AT1G04550	IAA12	AT5G62520	SRO5	AT1G37130	NIA2	AT1G37130	NIA2
AT2G41710		AT2G45640	SAP18	AT1G15570	CYCA2;3	AT3G12720	MYB67
AT4G18650		AT5G17490	RGL3	AT3G06430	PPR2	AT4G37260	MYB73
AT1G04550	IAA12	AT3G17600	IAA31	AT3G06430	PPR2	AT4G32570	TIFY8
AT2G41710		AT3G56900		AT5G18930	BUD2	AT5G39950	TRX2
AT1G04550	IAA12	AT3G23030	IAA2	AT1G51660	MKK4	AT4G37260	MYB73
AT1G50170	SIRB	AT3G60630	HAM2	AT1G51660	MKK4	AT3G45640	MPK3
AT3G60630	HAM2	AT4G28880	ckl3	AT1G51660	MKK4	AT2G43790	MPK6
AT3G60630	HAM2	AT5G25280		AT3G01690		AT4G37260	MYB73
AT2G26560	PLA2A	AT5G41920		AT4G31800	WRKY18	AT5G42980	TRX3
AT1G72030		AT3G60630	HAM2	AT1G51580		AT4G37260	MYB73
AT2G26560	PLA2A	AT4G35620	CYCB2;2	AT1G51580		AT4G32570	TIFY8
AT1G54990	AXR4	AT2G38120	AUX1	AT3G61830	ARF18	AT3G61830	ARF18
AT4G11070	WRKY41	AT5G22570	WRKY38	AT2G32650		AT4G37260	MYB73
AT4G11070	WRKY41	AT4G37260	MYB73	AT3G61830	ARF18	AT5G13930	TT4
AT4G11070	WRKY41	AT5G11010		AT3G18140	LST8-1	AT4G37260	MYB73
AT2G33610	SWI3B	AT4G08150	KNAT1	AT3G18140	LST8-1	AT4G32570	TIFY8
AT4G14713	PPD1	AT5G63470	NF-YC4	AT3G18140	LST8-1	AT4G14560	IAA1
AT1G07430	HAI2	AT4G01026	PYL7	AT4G18372		AT4G37260	MYB73
AT1G17980	PAPS1	AT5G08130	BIM1	AT1G52340	ABA2	AT1G52340	ABA2
AT4G16420	ADA2B	AT5G49210		AT4G23910		AT4G37260	MYB73
AT1G07430	HAI2	AT5G53160	RCAR3	AT1G52340	ABA2	AT4G33460	ABCI10
AT1G06180	MYB13	AT2G04630	NRPB6B	AT3G55150	EXO70H1	AT4G37260	MYB73
AT1G06180	MYB13	AT5G51940	NRPB6A	AT3G55150	EXO70H1	AT4G32570	TIFY8
AT3G23060		AT5G08130	BIM1	AT4G09650	ATPD	AT4G37260	MYB73
AT2G04890	SCL21	AT5G07310		AT4G09650	ATPD	AT4G32570	TIFY8
AT5G23710		AT5G57685	GDU3	AT3G21150	BBX32	AT4G37260	MYB73
AT2G30120		AT5G08130	BIM1	AT1G01140	CIPK9	AT4G37260	MYB73
AT2G33860	ETT	AT5G41650		AT1G13690	ATE1	AT4G39410	WRKY13
AT5G10930	CIPK5	AT5G47100	CBL9	AT1G13690	ATE1	AT3G23610	DSPTP1
AT2G30980	SKdZeta	AT5G65300		AT4G15770		AT4G25470	CBF2
AT1G67340		AT2G32460	MYB101	AT4G15770		AT4G37260	MYB73
AT5G35410	SOS2	AT5G47100	CBL9	AT4G15770		AT4G32570	TIFY8
AT3G56270		AT4G08150	KNAT1	AT1G07210		AT4G37260	MYB73
AT1G62520		AT4G08150	KNAT1	AT1G07210		AT4G00120	IND
AT5G45820	CIPK20	AT5G47100	CBL9	AT3G12830		AT4G37260	MYB73
AT5G05360		AT5G41920		AT3G17668	ENA	AT4G37260	MYB73
AT1G76680	OPR1	AT3G63260	ATMRK1	AT1G07350	SR45a	AT3G61860	RS31
AT2G32840		AT4G08150	KNAT1	AT2G23290	MYB70	AT5G67300	MYBR1
AT2G32840		AT4G16420	ADA2B	AT5G04430	BTR1L	AT5G46190	
AT4G32010	HSL1	AT5G41920		AT1G51100	CRR41	AT4G37260	MYB73
AT2G32840		AT4G00120	IND	AT3G57290	EIF3E	AT4G32570	TIFY8
AT2G03710	38231	AT5G41920		AT3G57290	EIF3E	AT5G08130	BIM1
AT1G24590	DRNL	AT1G68590	PSRP3/1	AT1G05410		AT4G32570	TIFY8
AT4G32010	HSL1	AT5G59730	EXO70H7	AT1G05410		AT1G25490	RCN1
AT1G24590	DRNL	AT3G56270		AT3G50910		AT5G44420	PDF1.2
AT4G32010	HSL1	AT5G39340	AHP3	AT3G54850	PUB14	AT4G32570	TIFY8
AT1G24590	DRNL	AT4G18630		AT1G06460	ACD32.1	AT4G37260	MYB73
AT4G32010	HSL1	AT5G50230		AT1G06460	ACD32.1	AT1G31880	BRX
AT1G24590	DRNL	AT2G38300		AT1G06460	ACD32.1	AT4G11140	CRF1
AT4G32010	HSL1	AT5G42970	COP8	AT1G01360	RCAR1	AT4G26080	ABI1
AT1G24590	DRNL	AT5G14070	ROXY2	AT3G05420	ACBP4	AT4G28880	ckl3
AT4G32010	HSL1	AT5G55620		AT3G05420	ACBP4	AT5G27630	ACBP5
AT1G24590	DRNL	AT2G42750		AT3G05420	ACBP4	AT4G28860	ckl4
AT4G32010	HSL1	AT5G48470		AT3G49810		AT4G37260	MYB73
AT2G32600		AT4G11140	CRF1	AT1G01360	RCAR1	AT1G21600	PTAC6
AT1G24590	DRNL	AT2G24860		AT3G57720		AT4G37260	MYB73
AT4G32010	HSL1	AT5G05790		AT1G01360	RCAR1	AT1G54830	NF-YC3
AT1G24590	DRNL	AT5G49210		AT3G21215		AT5G04430	BTR1L
AT4G32010	HSL1	AT4G33925	SSN2	AT3G57720		AT4G32570	TIFY8
AT1G24590	DRNL	AT2G33430	DAL1	AT2G39100		AT4G37260	MYB73
AT4G32010	HSL1	AT5G51940	NRPB6A	AT1G72360	ERF73	AT2G38490	CIPK22
AT1G24590	DRNL	AT5G24660	LSU2	AT1G68450	PDE337	AT5G41570	WRKY24
AT4G32010	HSL1	AT4G36030	ARO3	AT5G41570	WRKY24	AT5G67520	APK4
AT5G07690	MYB29	AT5G62520	SRO5	AT4G21560	VPS28-1	AT4G32570	TIFY8
AT1G24590	DRNL	AT5G48335		AT3G13200	EMB2769	AT4G37260	MYB73
AT4G32010	HSL1	AT5G64150		AT4G02770	PSAD-1	AT4G37260	MYB73
AT1G24590	DRNL	AT5G05790		AT1G73060	LPA3	AT4G32570	TIFY8
AT1G35210		AT2G30980	SKdZeta	AT3G03450	RGL2	AT5G54190	PORA
AT4G24470	ZIM	AT5G18580	FASS	AT3G59910		AT4G32570	TIFY8
AT4G24470	ZIM	AT5G63470	NF-YC4	AT3G03450	RGL2	AT5G59450	
AT3G23610	DSPTP1	AT4G29810	MKK2	AT3G03450	RGL2	AT5G23130	
AT1G22070	TGA3	AT1G64280	NPR1	AT1G18660		AT4G32570	TIFY8
AT1G48450		AT2G22090	UBA1A	AT3G03450	RGL2	AT5G25580	
AT1G22070	TGA3	AT5G27560		AT1G67090	RBCS1A	AT4G37260	MYB73
AT3G23610	DSPTP1	AT5G04820	OFP13	AT3G03450	RGL2	AT5G28770	BZO2H3
AT1G22070	TGA3	AT3G27560	ATN1	AT1G67090	RBCS1A	AT4G32570	TIFY8
AT3G19820	DWF1	AT3G54130		AT3G03450	RGL2	AT5G65683	WAVH2
AT1G05860		AT4G08150	KNAT1	AT3G03450	RGL2	AT3G48680	GAMMA CAL2
AT1G22070	TGA3	AT5G06960	OBF5	AT3G03450	RGL2	AT3G13740	
AT1G22070	TGA3	AT2G30540		AT4G26080	ABI1	AT5G05440	PYL5
AT1G22070	TGA3	AT3G18210		AT2G04630	NRPB6B	AT4G32570	TIFY8
AT1G22070	TGA3	AT4G12100		AT1G02140	MAGO	AT4G37260	MYB73

Table A.3 continued from previous page

Int A	Symbol A	Int B	Symbol B	Int A	Symbol A	Int B	Symbol B
AT1G22070	TGA3	AT4G15670		AT5G01600	FER1	AT5G01600	FER1
AT1G22070	TGA3	AT1G28480	GRX480	AT4G12100		AT4G32570	TIFY8
AT2G01620	MEE11	AT4G08150	KNAT1	AT1G72450	JAZ6	AT4G28910	NINJA
AT1G22070	TGA3	AT3G02000	ROXY1	AT1G01630		AT4G32570	TIFY8
AT1G03457		AT2G22090	UBA1A	AT3G11850		AT3G30210	MYB121
AT1G22070	TGA3	AT5G11010		AT2G43370		AT4G37260	MYB73
AT3G07090		AT4G38630	RPN10	AT1G04100	IAA10	AT1G19220	ARF19
AT1G54080	UBP1A	AT2G22090	UBA1A	AT2G43370		AT3G61860	RS31
AT3G07090		AT3G11410	PP2CA	AT1G04100	IAA10	AT1G04240	SHY2
AT1G27650	ATU2AF35A	AT2G16940		AT1G04100	IAA10	AT3G61830	ARF18
AT2G17190		AT2G35635	UBQ7	AT3G49060		AT4G32570	TIFY8
AT1G50420	SCL3	AT4G22220	ISU1	AT1G53910	RAP2.12	AT2G16030	
AT1G50420	SCL3	AT3G52155		AT1G04100	IAA10	AT1G04550	IAA12
AT1G50420	SCL3	AT5G52210	GB1	AT1G77950	AGL67	AT4G32570	TIFY8
AT3G11410	PP2CA	AT5G05440	PYL5	AT2G24570	WRKY17	AT2G44050	COS1
AT3G11410	PP2CA	AT5G16080	CXE17	AT1G53910	RAP2.12	AT4G21450	
AT1G03860	PHB2	AT5G17490	RGL3	AT1G53910	RAP2.12	AT2G25880	AUR2
AT3G11410	PP2CA	AT3G56270		AT3G16980	NRPB9A	AT4G32570	TIFY8
AT3G11410	PP2CA	AT4G37240		AT2G38490	CIPK22	AT3G25890	CRF11
AT3G11410	PP2CA	AT4G25670		AT1G68550	CRF10	AT2G38490	CIPK22
AT3G07670		AT5G17490	RGL3	AT2G44740	CYCP4;1	AT4G32570	TIFY8
AT2G37560	ORC2	AT5G17490	RGL3	AT1G11810		AT4G32570	TIFY8
AT1G76420	CUC3	AT4G25740		AT1G11810		AT2G33860	ETT
AT1G76420	CUC3	AT5G52650		AT1G64280	NPR1	AT5G06960	OBF5
AT1G20780	SAUL1	AT5G03050		AT1G28480	GRX480	AT4G32570	TIFY8
AT5G15802		AT5G17490	RGL3	AT1G64280	NPR1	AT5G64150	
AT1G17650	GLYR2	AT1G50420	SCL3	AT1G77710	CCP2	AT4G37260	MYB73
AT3G46630		AT5G17490	RGL3	AT4G20300		AT4G37260	MYB73
AT1G31240		AT1G50420	SCL3	AT1G56590	ZIP4	AT4G32570	TIFY8
AT1G66370	MYB113	AT5G18580	FASS	AT3G02000	ROXY1	AT4G32570	TIFY8
AT1G66370	MYB113	AT2G01620	MEE11	AT3G02000	ROXY1	AT5G65210	TGA1
AT1G66370	MYB113	AT3G58650	TRM7	AT2G32960	PFA-DSP2	AT2G32960	PFA-DSP2
AT1G01560	MPK11	AT1G08780	AIP3	AT4G28860	ckl4	AT4G37260	MYB73
AT1G15550	GA3OX1	AT1G31880	BRX	AT1G80720		AT4G32570	TIFY8
AT1G15550	GA3OX1	AT5G25890	IAA28	AT4G28860	ckl4	AT5G67300	MYBR1
AT1G15550	GA3OX1	AT1G24590	DRNL	AT4G18700	CIPK12	AT4G37260	MYB73
AT3G49950		AT4G32570	TIFY8	AT3G07300		AT4G32570	TIFY8
AT3G24730		AT4G32570	TIFY8	AT4G02485		AT4G32570	TIFY8
AT1G12840	DET3	AT4G32570	TIFY8	AT4G02485		AT5G04190	PKS4
AT5G17490	RGL3	AT5G63670	SPT42	AT3G47910		AT4G32570	TIFY8
AT1G17380	JAZ5	AT4G28910	NINJA	AT2G34590		AT4G32570	TIFY8
AT1G17550	HAB2	AT2G40330	PYL6	AT1G56170	NF-YC2	AT2G46790	PRR9
AT1G17550	HAB2	AT5G05440	PYL5	AT1G56170	NF-YC2	AT4G24470	ZIM
AT1G17380	JAZ5	AT3G02090	MPPBETA	AT2G25000	WRKY60	AT5G52650	
AT1G17550	HAB2	AT5G53160	RCAR3	AT3G12210		AT4G16420	ADA2B
AT1G17550	HAB2	AT4G01026	PYL7	AT1G56170	NF-YC2	AT4G14713	PPD1
AT2G05170	VPS11	AT4G32570	TIFY8	AT3G50800		AT5G40440	MKK3
AT2G22090	UBA1A	AT2G22090	UBA1A	AT1G56170	NF-YC2	AT4G14720	
AT2G04550	IBR5	AT3G58680	MBF1B	AT1G56450	PBG1	AT4G32570	TIFY8
AT2G22090	UBA1A	AT5G06770		AT3G28710		AT4G32570	TIFY8
AT2G22090	UBA1A	AT2G38610		AT3G28710		AT5G14750	MYB66
AT2G22090	UBA1A	AT3G19130	RBP47B	AT3G51130		AT4G32570	TIFY8
AT4G29810	MKK2	AT5G58950		AT2G23760	BLH4	AT4G32570	TIFY8
AT1G21690	EMB1968	AT1G77470	RFC3	AT2G46790	PRR9	AT5G63470	NF-YC4
AT1G21690	EMB1968	AT3G29090	PME31	AT2G45820		AT4G02150	MOS6
AT3G29350	AHP2	AT4G14720		AT2G45820		AT5G23750	
AT2G46130	WRKY43	AT5G08480		AT2G45820		AT3G57870	SCE1
AT2G46130	WRKY43	AT4G37710		AT2G25250		AT4G37260	MYB73
AT2G38310	PYL4	AT3G11410	PP2CA	AT4G18060		AT4G32570	TIFY8
AT4G24400	CIPK8	AT5G47100	CBL9	AT1G09810	ECT11	AT4G37260	MYB73
AT1G19220	ARF19	AT1G51950	IAA18	AT1G09810	ECT11	AT1G31880	BRX
AT1G19220	ARF19	AT3G04730	IAA16	AT1G50710	38200	AT4G32570	TIFY8
AT4G28910	NINJA	AT4G32570	TIFY8	AT4G27450		AT5G43830	
AT4G28910	NINJA	AT5G13220	JAZ10	AT2G28000	CPN60A	AT4G32570	TIFY8
AT4G28910	NINJA	AT5G20900	JAZ12	AT1G54200		AT4G37260	MYB73
AT1G15200		AT4G37260	MYB73	AT3G02460		AT4G37260	MYB73
AT1G15200		AT4G08150	KNAT1	AT1G19180	JAZ1	AT4G28910	NINJA
AT1G02690	IMPA-6	AT1G04250	AXR3	AT3G02460		AT4G32570	TIFY8
AT1G02690	IMPA-6	AT5G01600	FER1	AT1G76890	GT2	AT4G37260	MYB73
AT1G02690	IMPA-6	AT4G00120	IND	AT1G19180	JAZ1	AT1G30135	JAZ8
AT1G02690	IMPA-6	AT1G04550	IAA12	AT3G48510		AT4G37260	MYB73
AT1G02690	IMPA-6	AT5G05410	DREB2A	AT2G21630		AT4G32570	TIFY8
AT1G16705		AT2G45820		AT3G48510		AT4G32010	HSL1
AT1G16705		AT4G32570	TIFY8	AT3G15650		AT4G32570	TIFY8
AT2G20610	SUR1	AT5G37478		AT1G01260		AT1G51600	ZML2
AT1G63090	PP2-A11	AT2G25490	EBF1	AT1G01260		AT3G43440	JAZ11
AT1G51600	ZML2	AT5G18580	FASS	AT4G18830	OFP5	AT4G37260	MYB73
AT1G51600	ZML2	AT5G04820	OFP13	AT1G10650		AT4G37260	MYB73
AT1G12120		AT1G31880	BRX	AT1G10650		AT2G44840	ERF13
AT1G51600	ZML2	AT3G01990	ACR6	AT1G10650		AT4G32570	TIFY8
AT1G12120		AT2G39760	BPM3	AT1G10650		AT1G31880	BRX
AT1G51600	ZML2	AT4G28880	ckl3	AT3G09370	MYB3R-3	AT3G18210	
AT1G51600	ZML2	AT4G03420		AT1G21600	PTAC6	AT4G37260	MYB73
AT1G51600	ZML2	AT2G47450	CAO	AT1G21600	PTAC6	AT4G32010	HSL1
AT1G51600	ZML2	AT3G58380		AT1G21600	PTAC6	AT4G32570	TIFY8
AT1G51600	ZML2	AT1G54380		AT3G57730		AT4G37260	MYB73
AT3G21175	ZML1	AT4G24470	ZIM	AT1G54380		AT5G48870	SAD1
AT3G21175	ZML1	AT4G09060		AT2G32180	PTAC18	AT4G37260	MYB73
AT3G21175	ZML1	AT4G37470	KAI2	AT1G70700	TIFY7	AT4G28910	NINJA
AT3G21175	ZML1	AT5G04820	OFP13	AT2G27020	PAG1	AT4G37260	MYB73

Table A.3 continued from previous page

Int A	Symbol A	Int B	Symbol B	Int A	Symbol A	Int B	Symbol B
AT3G21175	ZML1	AT5G24660	LSU2	AT1G03130	PSAD-2	AT4G37260	MYB73

A.5.1 PhIout GO enrichment analysis

Figure A.5: PhI_{out} GO enrichment TreeMap. The interactions in PhI_{out} were sorted by nodes originated from PhO and AtORFeome, analyzed by using the GO enrichment tool Panther [438] and visualized by using Revigo [441].

A.6 Repressor vs transcription factor-collection

Table A.4: Interactions of the Rep-TF screen. All interactions are based on Y2H experiments and were confirmed in at least three independent experiments.

Int A	Symbol A	Int B	Symbol B	Int A	Symbol A	Int B	Symbol B
AT1G02450	NIMIN1	AT1G24230		AT1G04240	SHY2	AT5G60142	
AT1G02450	NIMIN1	AT1G53230	TCP3	AT1G04250	AXR3	AT1G04100	IAA10
AT1G02450	NIMIN1	AT1G69690	TCP15	AT1G04250	AXR3	AT1G04240	SHY2
AT1G02450	NIMIN1	AT2G43220		AT1G04250	AXR3	AT1G04250	AXR3
AT1G02450	NIMIN1	AT5G41315	GL3	AT1G04250	AXR3	AT1G14687	HB32
AT1G03800	ERF10	AT1G69690	TCP15	AT1G04250	AXR3	AT1G25550	
AT1G04550	IAA12	AT1G04100	IAA10	AT1G04250	AXR3	AT1G53230	TCP3
AT1G04550	IAA12	AT1G04240	SHY2	AT1G04250	AXR3	AT1G68670	
AT1G04550	IAA12	AT1G04250	AXR3	AT1G04250	AXR3	AT1G69690	TCP15
AT1G04550	IAA12	AT1G52830	IAA6	AT1G04250	AXR3	AT2G01200	IAA32
AT1G04550	IAA12	AT1G80390	IAA15	AT1G04250	AXR3	AT2G22670	IAA8
AT1G04550	IAA12	AT2G22670	IAA8	AT1G04250	AXR3	AT2G23290	MYB70
AT1G04550	IAA12	AT2G23290	MYB70	AT1G04250	AXR3	AT2G31720	
AT1G04550	IAA12	AT2G33310	IAA13	AT1G04250	AXR3	AT3G02150	PTF1
AT1G04550	IAA12	AT2G46990	IAA20	AT1G04250	AXR3	AT3G12910	
AT1G04550	IAA12	AT3G04730	IAA16	AT1G04250	AXR3	AT3G23250	MYB15
AT1G04550	IAA12	AT3G15540	IAA19	AT1G04250	AXR3	AT3G45150	TCP16
AT1G04550	IAA12	AT3G16500	PAP1	AT1G04250	AXR3	AT3G61830	ARF18
AT1G04550	IAA12	AT3G17600	IAA31	AT1G04250	AXR3	AT4G13640	UNE16
AT1G04550	IAA12	AT3G23030	IAA2	AT1G04250	AXR3	AT4G22745	MBD1
AT1G04550	IAA12	AT4G14560	IAA1	AT1G04250	AXR3	AT5G08330	TCP11
AT1G04550	IAA12	AT4G29080	PAP2	AT1G04250	AXR3	AT5G18240	MYR1
AT1G04550	IAA12	AT5G25890	IAA28	AT1G04250	AXR3	AT5G39820	NAC094
AT1G04550	IAA12	AT5G43700	AUX2-11	AT1G04250	AXR3	AT5G62000	ARF2
AT1G09415	NIMIN-3	AT1G14687	HB32	AT1G15050	IAA34	AT1G04100	IAA10
AT1G09415	NIMIN-3	AT1G25550		AT1G15050	IAA34	AT1G04240	SHY2
AT1G09415	NIMIN-3	AT1G30500	NF-YA7	AT1G15050	IAA34	AT1G04250	AXR3
AT1G09415	NIMIN-3	AT1G53230	TCP3	AT1G15050	IAA34	AT1G21970	LEC1
AT1G09415	NIMIN-3	AT1G68670		AT1G15050	IAA34	AT1G24590	DRNL
AT1G09415	NIMIN-3	AT1G69690	TCP15	AT1G15050	IAA34	AT1G53230	TCP3
AT1G09415	NIMIN-3	AT2G31720		AT1G15050	IAA34	AT1G69690	TCP15
AT1G09415	NIMIN-3	AT3G02150	PTF1	AT1G15050	IAA34	AT2G02540	HB21
AT1G09415	NIMIN-3	AT3G12910		AT1G15050	IAA34	AT2G20880	ERF53
AT1G09415	NIMIN-3	AT3G25790		AT1G15050	IAA34	AT2G22670	IAA8
AT1G09415	NIMIN-3	AT3G45150	TCP16	AT1G15050	IAA34	AT2G23290	MYB70
AT1G09415	NIMIN-3	AT4G13640	UNE16	AT1G15050	IAA34	AT2G33310	IAA13
AT1G09415	NIMIN-3	AT5G08330	TCP11	AT1G15050	IAA34	AT2G47700	RFI2
AT1G09415	NIMIN-3	AT5G18240	MYR1	AT1G15050	IAA34	AT3G02150	PTF1
AT1G15580	IAA5	AT1G04100	IAA10	AT1G15050	IAA34	AT3G13960	GRF5
AT1G15580	IAA5	AT1G04240	SHY2	AT1G15050	IAA34	AT3G16500	PAP1
AT1G15580	IAA5	AT1G04250	AXR3	AT1G15050	IAA34	AT3G21330	
AT1G15580	IAA5	AT1G15050	IAA34	AT1G15050	IAA34	AT3G23030	IAA2
AT1G15580	IAA5	AT1G52830	IAA6	AT1G15050	IAA34	AT3G23050	IAA7
AT1G15580	IAA5	AT1G53230	TCP3	AT1G15050	IAA34	AT3G23250	MYB15
AT1G15580	IAA5	AT1G69690	TCP15	AT1G15050	IAA34	AT3G61830	ARF18
AT1G15580	IAA5	AT1G80390	IAA15	AT1G15050	IAA34	AT4G14560	IAA1
AT1G15580	IAA5	AT2G22670	IAA8	AT1G15050	IAA34	AT4G36930	SPT
AT1G15580	IAA5	AT2G23290	MYB70	AT1G15050	IAA34	AT4G37260	MYB73
AT1G15580	IAA5	AT2G33310	IAA13	AT1G15050	IAA34	AT5G09250	KIWI
AT1G15580	IAA5	AT2G46990	IAA20	AT1G15050	IAA34	AT5G18560	PUCHI
AT1G15580	IAA5	AT3G04730	IAA16	AT1G15050	IAA34	AT5G39820	NAC094
AT1G15580	IAA5	AT3G15540	IAA19	AT1G15050	IAA34	AT5G41410	BEL1
AT1G15580	IAA5	AT3G16500	PAP1	AT1G15050	IAA34	AT5G43700	AUX2-11
AT1G15580	IAA5	AT3G17600	IAA31	AT1G15050	IAA34	AT5G47790	
AT1G15580	IAA5	AT3G23030	IAA2	AT1G15050	IAA34	AT5G57420	IAA33
AT1G15580	IAA5	AT4G14560	IAA1	AT1G15050	IAA34	AT5G60120	TOE2
AT1G15580	IAA5	AT4G29080	PAP2	AT1G15050	IAA34	AT5G60142	
AT1G15580	IAA5	AT4G30080	ARF16	AT1G15050	IAA34	AT5G62000	ARF2
AT1G15580	IAA5	AT4G37260	MYB73	AT1G15050	IAA34	AT5G66350	SHI
AT1G15580	IAA5	AT5G25890	IAA28	AT1G52830	IAA6	AT1G04100	IAA10
AT1G15580	IAA5	AT5G43700	AUX2-11	AT1G52830	IAA6	AT1G04240	SHY2
AT1G15580	IAA5	AT5G47790		AT1G52830	IAA6	AT1G04250	AXR3
AT1G17380	JAZ5	AT1G01260		AT1G52830	IAA6	AT1G15050	IAA34
AT1G17380	JAZ5	AT1G69690	TCP15	AT1G52830	IAA6	AT1G52830	IAA6
AT1G17380	JAZ5	AT4G17880	MYC4	AT1G52830	IAA6	AT1G53230	TCP3
AT1G28360	ERF12	AT1G21970	LEC1	AT1G52830	IAA6	AT1G69690	TCP15
AT1G28360	ERF12	AT1G24590	DRNL	AT1G52830	IAA6	AT2G22670	IAA8
AT1G28360	ERF12	AT1G31320	LBD4	AT1G52830	IAA6	AT2G23290	MYB70
AT1G28360	ERF12	AT1G53230	TCP3	AT1G52830	IAA6	AT4G37260	MYB73
AT1G28360	ERF12	AT1G69690	TCP15	AT1G52830	IAA6	AT5G47790	
AT1G28360	ERF12	AT2G02540	HB21	AT1G80390	IAA15	AT1G04100	IAA10
AT1G28360	ERF12	AT2G20880	ERF53	AT1G80390	IAA15	AT1G04240	SHY2
AT1G28360	ERF12	AT2G30340	LBD13	AT1G80390	IAA15	AT1G04250	AXR3
AT1G28360	ERF12	AT2G47700	RFI2	AT1G80390	IAA15	AT1G14687	HB32
AT1G28360	ERF12	AT3G02150	PTF1	AT1G80390	IAA15	AT1G15050	IAA34
AT1G28360	ERF12	AT3G12910		AT1G80390	IAA15	AT1G52830	IAA6
AT1G28360	ERF12	AT3G13960	GRF5	AT1G80390	IAA15	AT1G53230	TCP3
AT1G28360	ERF12	AT3G27810	MYB21	AT1G80390	IAA15	AT1G69690	TCP15
AT1G28360	ERF12	AT5G39820	NAC094	AT1G80390	IAA15	AT1G80390	IAA15
AT1G28360	ERF12	AT5G41410	BEL1	AT1G80390	IAA15	AT2G01200	IAA32
AT1G28360	ERF12	AT5G60120	TOE2	AT1G80390	IAA15	AT2G22670	IAA8
AT1G28370	ERF11	AT1G53230	TCP3	AT1G80390	IAA15	AT3G02150	PTF1

Table A.4 continued from previous page

Int A	Symbol A	Int B	Symbol B	Int A	Symbol A	Int B	Symbol B
AT1G28370	ERF11	AT1G69690	TCP15	AT1G80390	IAA15	AT3G12910	
AT1G30135	JAZ8	AT1G01260		AT1G80390	IAA15	AT3G17600	IAA31
AT1G30135	JAZ8	AT1G69690	TCP15	AT1G80390	IAA15	AT3G23030	IAA2
AT1G30135	JAZ8	AT4G17880	MYC4	AT1G80390	IAA15	AT3G45150	TCP16
AT1G51950	IAA18	AT1G04100	IAA10	AT1G80390	IAA15	AT4G36930	SPT
AT1G51950	IAA18	AT1G04240	SHY2	AT1G80390	IAA15	AT4G37260	MYB73
AT1G51950	IAA18	AT1G04250	AXR3	AT1G80390	IAA15	AT5G08330	TCP11
AT1G51950	IAA18	AT1G52830	IAA6	AT2G22670	IAA8	AT1G53230	TCP3
AT1G51950	IAA18	AT1G80390	IAA15	AT2G22670	IAA8	AT1G69690	TCP15
AT1G51950	IAA18	AT2G22670	IAA8	AT2G33310	IAA13	AT1G04100	IAA10
AT1G51950	IAA18	AT2G33310	IAA13	AT2G33310	IAA13	AT1G04240	SHY2
AT1G51950	IAA18	AT2G46990	IAA20	AT2G33310	IAA13	AT1G04250	AXR3
AT1G51950	IAA18	AT3G04730	IAA16	AT2G33310	IAA13	AT1G52830	IAA6
AT1G51950	IAA18	AT3G15540	IAA19	AT2G33310	IAA13	AT1G80390	IAA15
AT1G51950	IAA18	AT3G16500	PAP1	AT2G33310	IAA13	AT2G22670	IAA8
AT1G51950	IAA18	AT3G17600	IAA31	AT2G33310	IAA13	AT2G33310	IAA13
AT1G51950	IAA18	AT3G23030	IAA2	AT2G46990	IAA20	AT1G04100	IAA10
AT1G51950	IAA18	AT3G61830	ARF18	AT2G46990	IAA20	AT1G04240	SHY2
AT1G51950	IAA18	AT4G14560	IAA1	AT2G46990	IAA20	AT1G04250	AXR3
AT1G51950	IAA18	AT4G29080	PAP2	AT2G46990	IAA20	AT1G14687	HB32
AT1G51950	IAA18	AT4G32570	TIFY8	AT2G46990	IAA20	AT1G15050	IAA34
AT1G51950	IAA18	AT5G25890	IAA28	AT2G46990	IAA20	AT1G30500	NF-YA7
AT1G51950	IAA18	AT5G43700	AUX2-11	AT2G46990	IAA20	AT1G52830	IAA6
AT1G51950	IAA18	AT5G62000	ARF2	AT2G46990	IAA20	AT1G53230	TCP3
AT1G53170	ERF8	AT1G14920	GAI	AT2G46990	IAA20	AT1G69690	TCP15
AT1G53170	ERF8	AT1G21970	LEC1	AT2G46990	IAA20	AT1G80390	IAA15
AT1G53170	ERF8	AT1G23420	INO	AT2G46990	IAA20	AT2G02160	
AT1G53170	ERF8	AT1G24590	DRNL	AT2G46990	IAA20	AT2G02540	HB21
AT1G53170	ERF8	AT1G53230	TCP3	AT2G46990	IAA20	AT2G22670	IAA8
AT1G53170	ERF8	AT1G68510	LBD42	AT2G46990	IAA20	AT2G33310	IAA13
AT1G53170	ERF8	AT1G68670		AT2G46990	IAA20	AT2G46990	IAA20
AT1G53170	ERF8	AT1G69690	TCP15	AT2G46990	IAA20	AT3G02150	PTF1
AT1G53170	ERF8	AT1G72210		AT2G46990	IAA20	AT3G12910	
AT1G53170	ERF8	AT2G02540	HB21	AT2G46990	IAA20	AT3G23050	IAA7
AT1G53170	ERF8	AT2G20880	ERF53	AT2G46990	IAA20	AT3G23250	MYB15
AT1G53170	ERF8	AT2G23290	MYB70	AT2G46990	IAA20	AT3G25790	
AT1G53170	ERF8	AT2G45190	AFO	AT2G46990	IAA20	AT3G28917	MIF2
AT1G53170	ERF8	AT2G47700	RFI2	AT2G46990	IAA20	AT3G45150	TCP16
AT1G53170	ERF8	AT3G02150	PTF1	AT2G46990	IAA20	AT3G50890	HB28
AT1G53170	ERF8	AT3G12910		AT2G46990	IAA20	AT4G29080	PAP2
AT1G53170	ERF8	AT3G25790		AT2G46990	IAA20	AT4G32570	TIFY8
AT1G53170	ERF8	AT3G27810	MYB21	AT2G46990	IAA20	AT5G39820	NAC094
AT1G53170	ERF8	AT3G45150	TCP16	AT2G46990	IAA20	AT5G57420	IAA33
AT1G53170	ERF8	AT3G51180		AT2G46990	IAA20	AT5G60120	TOE2
AT1G53170	ERF8	AT3G57600		AT3G04730	IAA16	AT1G04100	IAA10
AT1G53170	ERF8	AT4G13640	UNE16	AT3G04730	IAA16	AT1G04240	SHY2
AT1G53170	ERF8	AT4G30080	ARF16	AT3G04730	IAA16	AT1G04250	AXR3
AT1G53170	ERF8	AT4G37260	MYB73	AT3G04730	IAA16	AT1G15050	IAA34
AT1G53170	ERF8	AT5G08330	TCP11	AT3G04730	IAA16	AT1G52830	IAA6
AT1G53170	ERF8	AT5G18240	MYR1	AT3G04730	IAA16	AT1G53230	TCP3
AT1G53170	ERF8	AT5G18560	PUCHI	AT3G04730	IAA16	AT1G80390	IAA15
AT1G53170	ERF8	AT5G39820	NAC094	AT3G04730	IAA16	AT2G02160	
AT1G53170	ERF8	AT5G41410	BEL1	AT3G04730	IAA16	AT2G02540	HB21
AT1G53170	ERF8	AT5G60120	TOE2	AT3G04730	IAA16	AT2G22670	IAA8
AT1G59940	ARR3	AT1G69690	TCP15	AT3G04730	IAA16	AT2G33310	IAA13
AT1G59940	ARR3	AT1G76870		AT3G04730	IAA16	AT2G46990	IAA20
AT1G70700	TIFY7	AT1G01260		AT3G04730	IAA16	AT3G04730	IAA16
AT1G70700	TIFY7	AT1G14920	GAI	AT3G04730	IAA16	AT3G12910	
AT1G70700	TIFY7	AT1G53230	TCP3	AT3G04730	IAA16	AT3G17600	IAA31
AT1G70700	TIFY7	AT1G69690	TCP15	AT3G04730	IAA16	AT3G23050	IAA7
AT1G70700	TIFY7	AT4G17880	MYC4	AT3G04730	IAA16	AT3G23250	MYB15
AT1G70700	TIFY7	AT5G39820	NAC094	AT3G04730	IAA16	AT3G61830	ARF18
AT1G72450	JAZ6	AT1G01260		AT3G04730	IAA16	AT4G32570	TIFY8
AT1G72450	JAZ6	AT1G69690	TCP15	AT3G04730	IAA16	AT4G36930	SPT
AT1G72450	JAZ6	AT4G17880	MYC4	AT3G04730	IAA16	AT5G08330	TCP11
AT1G74890	ARR15	AT1G69690	TCP15	AT3G04730	IAA16	AT5G60120	TOE2
AT1G19180	JAZ1	AT1G01260		AT3G15540	IAA19	AT1G04100	IAA10
AT1G19180	JAZ1	AT1G14920	GAI	AT3G15540	IAA19	AT1G04240	SHY2
AT1G19180	JAZ1	AT1G19180	JAZ1	AT3G15540	IAA19	AT1G04250	AXR3
AT1G19180	JAZ1	AT1G30135	JAZ8	AT3G15540	IAA19	AT1G15050	IAA34
AT1G19180	JAZ1	AT1G53230	TCP3	AT3G15540	IAA19	AT1G52830	IAA6
AT1G19180	JAZ1	AT1G69690	TCP15	AT3G15540	IAA19	AT1G53230	TCP3
AT1G19180	JAZ1	AT2G27110	FRS3	AT3G15540	IAA19	AT1G80390	IAA15
AT1G19180	JAZ1	AT4G17880	MYC4	AT3G15540	IAA19	AT2G02540	HB21
AT1G19180	JAZ1	AT5G39820	NAC094	AT3G15540	IAA19	AT2G22670	IAA8
AT1G19180	JAZ1	AT5G41315	GL3	AT3G15540	IAA19	AT2G23290	MYB70
AT1G74950	TIFY10B	AT1G01260		AT3G15540	IAA19	AT2G33310	IAA13
AT1G74950	TIFY10B	AT1G19180	JAZ1	AT3G15540	IAA19	AT2G46990	IAA20
AT1G74950	TIFY10B	AT1G53230	TCP3	AT3G15540	IAA19	AT3G04730	IAA16
AT1G74950	TIFY10B	AT1G69690	TCP15	AT3G15540	IAA19	AT3G15540	IAA19
AT1G74950	TIFY10B	AT1G74950	TIFY10B	AT3G15540	IAA19	AT3G23050	IAA7
AT1G74950	TIFY10B	AT2G27110	FRS3	AT3G15540	IAA19	AT3G23250	MYB15
AT1G74950	TIFY10B	AT4G17880	MYC4	AT3G15540	IAA19	AT3G50890	HB28
AT1G75080	BZR1	AT1G14920	GAI	AT3G15540	IAA19	AT4G32570	TIFY8
AT1G75080	BZR1	AT1G25550		AT3G15540	IAA19	AT4G36930	SPT
AT1G75080	BZR1	AT1G53230	TCP3	AT3G15540	IAA19	AT5G47790	
AT1G75080	BZR1	AT1G69690	TCP15	AT3G16500	PAP1	AT1G04100	IAA10
AT1G75080	BZR1	AT3G02150	PTF1	AT3G16500	PAP1	AT1G04240	SHY2
AT1G75080	BZR1	AT3G12910		AT3G16500	PAP1	AT1G04250	AXR3
AT1G75080	BZR1	AT3G27810	MYB21	AT3G16500	PAP1	AT1G52830	IAA6

Table A.4 continued from previous page

Int A	Symbol A	Int B	Symbol B	Int A	Symbol A	Int B	Symbol B
AT1G75080	BZR1	AT3G45150	TCP16	AT3G16500	PAP1	AT1G80390	IAA15
AT1G75080	BZR1	AT3G51180		AT3G16500	PAP1	AT2G22670	IAA8
AT1G75080	BZR1	AT5G08330	TCP11	AT3G16500	PAP1	AT2G33310	IAA13
AT1G75080	BZR1	AT5G39820	NAC094	AT3G16500	PAP1	AT2G46990	IAA20
AT1G75080	BZR1	AT5G41410	BEL1	AT3G16500	PAP1	AT3G04730	IAA16
AT1G75080	BZR1	AT5G47790		AT3G16500	PAP1	AT3G15540	IAA19
AT2G34600	JAZ7	AT1G69690	TCP15	AT3G16500	PAP1	AT3G16500	PAP1
AT2G34600	JAZ7	AT4G17880	MYC4	AT3G16500	PAP1	AT3G23250	MYB15
AT2G40670	RR16	AT1G69690	TCP15	AT3G16500	PAP1	AT4G37260	MYB73
AT2G41310	RR3	AT1G69690	TCP15	AT3G16500	PAP1	AT5G47790	
AT3G15210	ERF4	AT1G23420	INO	AT3G16500	PAP1	AT5G62000	ARF2
AT3G15210	ERF4	AT1G25550		AT3G17600	IAA31	AT1G04100	IAA10
AT3G15210	ERF4	AT1G53230	TCP3	AT3G17600	IAA31	AT1G04240	SHY2
AT3G15210	ERF4	AT1G68670		AT3G17600	IAA31	AT1G04250	AXR3
AT3G15210	ERF4	AT1G69690	TCP15	AT3G17600	IAA31	AT1G15050	IAA34
AT3G15210	ERF4	AT3G02150	PTF1	AT3G17600	IAA31	AT1G52830	IAA6
AT3G15210	ERF4	AT3G12910		AT3G17600	IAA31	AT2G33310	IAA13
AT3G15210	ERF4	AT3G25790		AT3G17600	IAA31	AT2G46990	IAA20
AT3G15210	ERF4	AT3G45150	TCP16	AT3G17600	IAA31	AT3G15540	IAA19
AT3G15210	ERF4	AT5G08330	TCP11	AT3G17600	IAA31	AT3G16500	PAP1
AT3G15210	ERF4	AT5G39820	NAC094	AT3G17600	IAA31	AT3G17600	IAA31
AT3G15210	ERF4	AT5G60120	TOE2	AT3G17600	IAA31	AT4G30080	ARF16
AT3G17860	JAZ3	AT1G01260		AT3G17600	IAA31	AT4G37260	MYB73
AT3G17860	JAZ3	AT1G14920	GAI	AT3G17600	IAA31	AT5G43700	AUX2-11
AT3G17860	JAZ3	AT1G23420	INO	AT3G17600	IAA31	AT5G60142	
AT3G17860	JAZ3	AT1G34180	NAC016	AT3G23030	IAA2	AT1G04100	IAA10
AT3G17860	JAZ3	AT1G53230	TCP3	AT3G23030	IAA2	AT1G04240	SHY2
AT3G17860	JAZ3	AT1G69690	TCP15	AT3G23030	IAA2	AT1G04250	AXR3
AT3G17860	JAZ3	AT2G27110	FRS3	AT3G23030	IAA2	AT1G52830	IAA6
AT3G17860	JAZ3	AT2G45190	AFO	AT3G23030	IAA2	AT2G22670	IAA8
AT3G17860	JAZ3	AT4G01550	NAC069	AT3G23030	IAA2	AT2G33310	IAA13
AT3G17860	JAZ3	AT4G14720		AT3G23030	IAA2	AT2G46990	IAA20
AT3G17860	JAZ3	AT4G17880	MYC4	AT3G23030	IAA2	AT3G04730	IAA16
AT3G17860	JAZ3	AT4G32570	TIFY8	AT3G23030	IAA2	AT3G15540	IAA19
AT3G25882	NIMIN-2	AT1G01260		AT3G23030	IAA2	AT3G16500	PAP1
AT3G25882	NIMIN-2	AT1G14920	GAI	AT3G23030	IAA2	AT3G23030	IAA2
AT3G25882	NIMIN-2	AT1G53230	TCP3	AT3G23030	IAA2	AT4G22745	MBD1
AT3G25882	NIMIN-2	AT1G69690	TCP15	AT4G14560	IAA1	AT1G04100	IAA10
AT3G25882	NIMIN-2	AT3G02150	PTF1	AT4G14560	IAA1	AT1G04240	SHY2
AT3G25882	NIMIN-2	AT3G27810	MYB21	AT4G14560	IAA1	AT1G04250	AXR3
AT3G25882	NIMIN-2	AT3G45150	TCP16	AT4G14560	IAA1	AT1G52830	IAA6
AT3G25882	NIMIN-2	AT4G17880	MYC4	AT4G14560	IAA1	AT1G69690	TCP15
AT3G25882	NIMIN-2	AT5G08330	TCP11	AT4G14560	IAA1	AT1G80390	IAA15
AT3G57040	ARR9	AT1G53230	TCP3	AT4G14560	IAA1	AT2G22670	IAA8
AT3G57040	ARR9	AT1G69690	TCP15	AT4G14560	IAA1	AT2G23290	MYB70
AT4G14550	IAA14	AT1G69690	TCP15	AT4G14560	IAA1	AT2G33310	IAA13
AT4G18710	BIN2	AT1G69690	TCP15	AT4G14560	IAA1	AT2G46990	IAA20
AT4G18710	BIN2	AT2G02540	HB21	AT4G14560	IAA1	AT3G04730	IAA16
AT4G18710	BIN2	AT2G30340	LBD13	AT4G14560	IAA1	AT3G15540	IAA19
AT4G18710	BIN2	AT3G13960	GRF5	AT4G14560	IAA1	AT3G16500	PAP1
AT4G18710	BIN2	AT3G58630		AT4G14560	IAA1	AT3G23030	IAA2
AT4G18710	BIN2	AT5G08070	TCP17	AT4G14560	IAA1	AT4G14560	IAA1
AT4G18710	BIN2	AT5G62000	ARF2	AT4G29080	PAP2	AT1G04100	IAA10
AT4G28640	IAA11	AT1G04100	IAA10	AT4G29080	PAP2	AT1G04240	SHY2
AT4G28640	IAA11	AT1G04240	SHY2	AT4G29080	PAP2	AT1G04250	AXR3
AT4G28640	IAA11	AT1G04250	AXR3	AT4G29080	PAP2	AT1G15050	IAA34
AT4G28640	IAA11	AT1G52830	IAA6	AT4G29080	PAP2	AT1G52830	IAA6
AT4G28640	IAA11	AT1G80390	IAA15	AT4G29080	PAP2	AT1G53230	TCP3
AT4G28640	IAA11	AT2G22670	IAA8	AT4G29080	PAP2	AT1G69690	TCP15
AT4G28640	IAA11	AT2G23290	MYB70	AT4G29080	PAP2	AT1G80390	IAA15
AT4G28640	IAA11	AT2G33310	IAA13	AT4G29080	PAP2	AT2G22670	IAA8
AT4G28640	IAA11	AT2G46990	IAA20	AT4G29080	PAP2	AT2G33310	IAA13
AT4G28640	IAA11	AT3G04730	IAA16	AT4G29080	PAP2	AT2G36340	
AT4G28640	IAA11	AT3G15540	IAA19	AT4G29080	PAP2	AT3G04730	IAA16
AT4G28640	IAA11	AT3G16500	PAP1	AT4G29080	PAP2	AT3G15540	IAA19
AT4G28640	IAA11	AT3G17600	IAA31	AT4G29080	PAP2	AT3G16500	PAP1
AT4G28640	IAA11	AT3G23030	IAA2	AT4G29080	PAP2	AT3G17600	IAA31
AT4G28640	IAA11	AT4G14560	IAA1	AT4G29080	PAP2	AT3G23030	IAA2
AT4G28640	IAA11	AT4G29080	PAP2	AT4G29080	PAP2	AT3G61830	ARF18
AT4G28640	IAA11	AT5G25890	IAA28	AT4G29080	PAP2	AT4G14560	IAA1
AT4G28640	IAA11	AT5G43700	AUX2-11	AT4G29080	PAP2	AT4G29080	PAP2
AT4G32280	IAA29	AT1G14687	HB32	AT5G25890	IAA28	AT1G04100	IAA10
AT4G32280	IAA29	AT1G69690	TCP15	AT5G25890	IAA28	AT1G04240	SHY2
AT4G32280	IAA29	AT2G02540	HB21	AT5G25890	IAA28	AT1G04250	AXR3
AT4G32280	IAA29	AT5G25890	IAA28	AT5G25890	IAA28	AT1G15050	IAA34
AT4G32280	IAA29	AT5G62000	ARF2	AT5G25890	IAA28	AT1G52830	IAA6
AT5G13220	JAZ10	AT1G01260		AT5G25890	IAA28	AT1G53230	TCP3
AT5G13220	JAZ10	AT1G69690	TCP15	AT5G25890	IAA28	AT1G75340	
AT5G13220	JAZ10	AT4G17880	MYC4	AT5G25890	IAA28	AT1G80390	IAA15
AT5G20900	JAZ12	AT1G01260		AT5G25890	IAA28	AT2G22670	IAA8
AT5G20900	JAZ12	AT4G17880	MYC4	AT5G25890	IAA28	AT2G33310	IAA13
AT5G44210	ERF9	AT1G53230	TCP3	AT5G25890	IAA28	AT2G46990	IAA20
AT5G44210	ERF9	AT1G69690	TCP15	AT5G25890	IAA28	AT3G04730	IAA16
AT5G44210	ERF9	AT2G02540	HB21	AT5G25890	IAA28	AT3G15540	IAA19
AT5G44210	ERF9	AT2G20880	ERF53	AT5G25890	IAA28	AT3G16500	PAP1
AT5G44210	ERF9	AT3G02150	PTF1	AT5G25890	IAA28	AT3G17600	IAA31
AT5G44210	ERF9	AT3G45150	TCP16	AT5G25890	IAA28	AT3G23030	IAA2
AT5G44210	ERF9	AT5G39820	NAC094	AT5G25890	IAA28	AT3G23050	IAA7
AT5G44210	ERF9	AT5G60120	TOE2	AT5G25890	IAA28	AT3G61830	ARF18
AT2G01200	IAA32	AT1G04100	IAA10	AT5G25890	IAA28	AT4G14560	IAA1

Table A.4 continued from previous page

Int A	Symbol A	Int B	Symbol B	Int A	Symbol A	Int B	Symbol B
AT2G01200	IAA32	AT1G04240	SHY2	AT5G25890	IAA28	AT4G29080	PAP2
AT2G01200	IAA32	AT1G52830	IAA6	AT5G25890	IAA28	AT5G25890	IAA28
AT2G01200	IAA32	AT1G53230	TCP3	AT5G43700	AUX2-11	AT1G04100	IAA10
AT2G01200	IAA32	AT1G69690	TCP15	AT5G43700	AUX2-11	AT1G04240	SHY2
AT2G01200	IAA32	AT2G33310	IAA13	AT5G43700	AUX2-11	AT1G04250	AXR3
AT2G01200	IAA32	AT2G46990	IAA20	AT5G43700	AUX2-11	AT1G52830	IAA6
AT2G01200	IAA32	AT3G15540	IAA19	AT5G43700	AUX2-11	AT1G80390	IAA15
AT2G01200	IAA32	AT3G16500	PAP1	AT5G43700	AUX2-11	AT2G22670	IAA8
AT2G01200	IAA32	AT3G17600	IAA31	AT5G43700	AUX2-11	AT2G33310	IAA13
AT2G01200	IAA32	AT3G23030	IAA2	AT5G43700	AUX2-11	AT2G46990	IAA20
AT2G01200	IAA32	AT4G14560	IAA1	AT5G43700	AUX2-11	AT3G04730	IAA16
AT2G01200	IAA32	AT4G29080	PAP2	AT5G43700	AUX2-11	AT3G15540	IAA19
AT2G01200	IAA32	AT5G25890	IAA28	AT5G43700	AUX2-11	AT3G16500	PAP1
AT2G01200	IAA32	AT5G43700	AUX2-11	AT5G43700	AUX2-11	AT3G23030	IAA2
AT2G01200	IAA32	AT5G62000	ARF2	AT5G43700	AUX2-11	AT4G14560	IAA1
AT5G57420	IAA33	AT1G04100	IAA10	AT5G43700	AUX2-11	AT4G29080	PAP2
AT5G57420	IAA33	AT1G04240	SHY2	AT5G43700	AUX2-11	AT4G37260	MYB73
AT5G57420	IAA33	AT1G04250	AXR3	AT5G43700	AUX2-11	AT5G08330	TCP11
AT5G57420	IAA33	AT1G35240	ARF20	AT5G43700	AUX2-11	AT5G09250	KIWI
AT5G57420	IAA33	AT1G52830	IAA6	AT5G43700	AUX2-11	AT5G25890	IAA28
AT5G57420	IAA33	AT1G53230	TCP3	AT5G43700	AUX2-11	AT5G43700	AUX2-11
AT5G57420	IAA33	AT1G69690	TCP15	AT5G65670	IAA9	AT1G04100	IAA10
AT5G57420	IAA33	AT2G01200	IAA32	AT5G65670	IAA9	AT1G04240	SHY2
AT5G57420	IAA33	AT2G33310	IAA13	AT5G65670	IAA9	AT1G04250	AXR3
AT5G57420	IAA33	AT3G15540	IAA19	AT5G65670	IAA9	AT1G14687	HB32
AT5G57420	IAA33	AT3G16500	PAP1	AT5G65670	IAA9	AT1G15050	IAA34
AT5G57420	IAA33	AT3G17600	IAA31	AT5G65670	IAA9	AT1G30500	NF-YA7
AT5G57420	IAA33	AT3G25790		AT5G65670	IAA9	AT1G52830	IAA6
AT5G57420	IAA33	AT3G61830	ARF18	AT5G65670	IAA9	AT1G53230	TCP3
AT5G57420	IAA33	AT4G29080	PAP2	AT5G65670	IAA9	AT1G69690	TCP15
AT5G57420	IAA33	AT4G30080	ARF16	AT5G65670	IAA9	AT1G80390	IAA15
AT5G57420	IAA33	AT5G25890	IAA28	AT5G65670	IAA9	AT2G22670	IAA8
AT5G57420	IAA33	AT5G43700	AUX2-11	AT5G65670	IAA9	AT2G23290	MYB70
AT5G57420	IAA33	AT5G62000	ARF2	AT5G65670	IAA9	AT2G33310	IAA13
AT5G62920	ARR6	AT1G69690	TCP15	AT5G65670	IAA9	AT2G46990	IAA20
AT1G04100	IAA10	AT1G04100	IAA10	AT5G65670	IAA9	AT3G02150	PTF1
AT1G04100	IAA10	AT1G25550		AT5G65670	IAA9	AT3G04730	IAA16
AT1G04100	IAA10	AT1G53230	TCP3	AT5G65670	IAA9	AT3G12910	
AT1G04100	IAA10	AT1G69690	TCP15	AT5G65670	IAA9	AT3G15540	IAA19
AT1G04100	IAA10	AT2G22670	IAA8	AT5G65670	IAA9	AT3G16500	PAP1
AT1G04100	IAA10	AT3G61830	ARF18	AT5G65670	IAA9	AT3G17600	IAA31
AT1G04100	IAA10	AT4G37260	MYB73	AT5G65670	IAA9	AT3G23030	IAA2
AT1G04100	IAA10	AT5G08330	TCP11	AT5G65670	IAA9	AT3G45150	TCP16
AT1G04100	IAA10	AT5G60142		AT5G65670	IAA9	AT4G14560	IAA1
AT1G04100	IAA10	AT5G62000	ARF2	AT5G65670	IAA9	AT4G29080	PAP2
AT1G04240	SHY2	AT1G04100	IAA10	AT5G65670	IAA9	AT4G37260	MYB73
AT1G04240	SHY2	AT1G04240	SHY2	AT5G65670	IAA9	AT5G09250	KIWI
AT1G04240	SHY2	AT1G53230	TCP3	AT5G65670	IAA9	AT5G25890	IAA28
AT1G04240	SHY2	AT1G69690	TCP15	AT5G65670	IAA9	AT5G43700	AUX2-11
AT1G04240	SHY2	AT2G22670	IAA8	AT5G65670	IAA9	AT5G47790	
AT1G04240	SHY2	AT2G23290	MYB70	AT5G65670	IAA9	AT5G60142	
AT1G04240	SHY2	AT4G32570	TIFY8				
AT1G04240	SHY2	AT4G37260	MYB73				

Table A.5: ABA-related Rep-TF interactions

Interactor A	**Symbol A**	**Interactor B**	**Symbol B**
AT1G07430	HAI2	AT2G25000	WRKY60
AT1G07430	HAI2	AT4G14720	
AT1G07430	HAI2	AT1G20910	
AT1G07430	HAI2	AT5G23280	
AT1G07430	HAI2	AT2G22760	
AT1G07430	HAI2	AT3G54390	
AT1G07430	HAI2	AT3G44350	NAC061
AT2G29380	HAI3	AT4G37260	MYB73
AT5G51760	AHG1	AT1G35560	TCP23
AT5G51760	AHG1	AT4G32010	HSL1
AT5G51760	AHG1	AT1G69690	TCP15
AT5G51760	AHG1	AT2G31310	LBD14

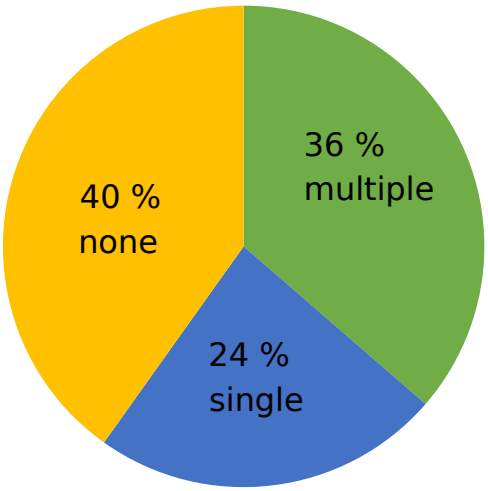

Figure A.6: MYB TF hormone annotation. MYB transcription factor family, base on Stracke et al., 2001[94], was used to identify multiple and single hormone annotated family members using AHD2.0 data for involvement in genetic evidences and TAIR 10 for GO annotations.

A.7 Hormone-dependent screens

A.7.1 ABA screen

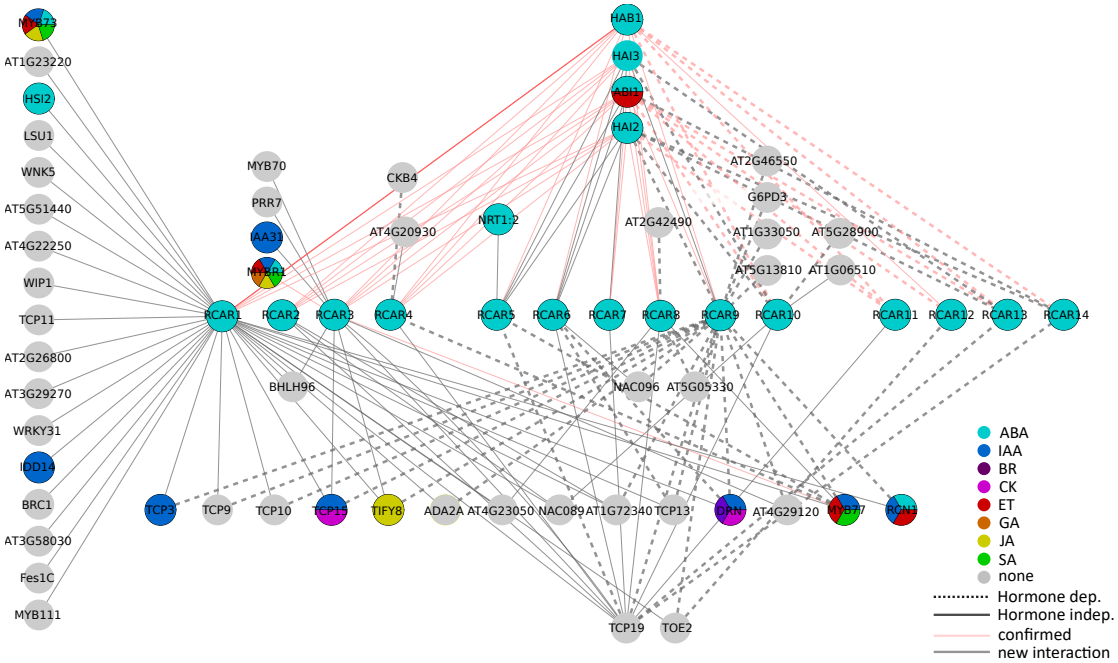

Figure A.7: ABA Y2H interactions including PP2Cs. The RCAR receptors are centered in the network and devided in the three subgroups (RCAR1-4, RCAR5-10, RCAR11-14). The nodes are colored according to their hormone annotations. Dashed lines represent ABA-dependent interactions. Solid lines represent ABA-independent interactions. Light red lines indicate confirmed interactions, gray lines indicate new interactions. These interactions are independently tested four times and could be confirmed at least 3 times. The verification was systematically performed with and without ABA (30 μM).

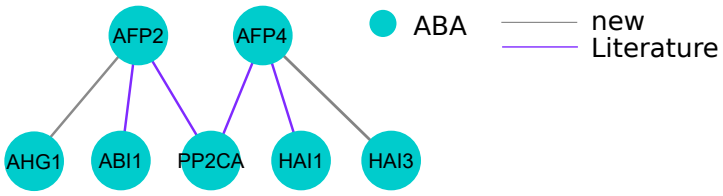

Figure A.8: AFP new and literature interactions. Edges in purple are exclusively literature interaction from [511], edges in gray are new detected interactions.

Table A.6: ABA hormone-dependent/independent interactions

AD-Interactor	Symbol	RCAR	Symbol	ABA dep.	new/confirmed
AT3G50060	MYB77	AT4G27920	RCAR4	yes	new
AT5G51910		AT5G45860	RCAR5	yes	new
AT3G50060	MYB77	AT5G45860	RCAR5	yes	new
AT3G02150	PTF1	AT5G45870	RCAR6	yes	new
AT1G12980	ESR1	AT5G45870	RCAR6	yes	new
AT2G42490		AT5G05440	RCAR8	yes	new
AT5G05330		AT5G05440	RCAR8	yes	new
AT4G29120		AT2G40330	RCAR9	yes	new
AT1G07430	HAI2	AT2G40330	RCAR9	yes	new
AT1G33050		AT2G40330	RCAR9	yes	new
AT5G13810		AT2G40330	RCAR9	yes	new
AT1G69690	TCP15	AT2G40330	RCAR9	yes	new
AT1G24280	G6PD3	AT2G40330	RCAR9	yes	new
AT4G32570	TIFY8	AT2G40330	RCAR9	yes	new
AT3G02150	PTF1	AT2G40330	RCAR9	yes	new
AT5G51910		AT2G40330	RCAR9	yes	new
AT5G46590	NAC096	AT2G40330	RCAR9	yes	new
AT1G25490	RCN1	AT2G40330	RCAR9	yes	new
AT1G72340		AT2G40330	RCAR9	yes	new
AT2G31070	TCP10	AT2G40330	RCAR9	yes	new
AT2G46550		AT2G40330	RCAR9	yes	new
AT2G45680	TCP9	AT2G40330	RCAR9	yes	new
AT3G50060	MYB77	AT2G40330	RCAR9	yes	new
AT3G07740	ADA2A	AT2G40330	RCAR9	yes	new
AT5G60120	TOE2	AT2G40330	RCAR9	yes	new
AT1G53230	TCP3	AT2G40330	RCAR9	yes	new
AT5G05330		AT2G40330	RCAR9	yes	new
AT1G12980	ESR1	AT2G40330	RCAR9	yes	new
AT1G07430	HAI2	AT2G38310	RCAR10	yes	new
AT5G28900		AT2G38310	RCAR10	yes	new
AT4G26080	ABI1	AT2G38310	RCAR10	yes	confirmed
AT1G72770	HAB1	AT2G38310	RCAR10	yes	confirmed
AT2G29380	HAI3	AT2G38310	RCAR10	yes	new
AT1G07430	HAI2	AT4G17870	RCAR11	yes	confirmed
AT4G26080	ABI1	AT4G17870	RCAR11	yes	confirmed
AT1G72770	HAB1	AT4G17870	RCAR11	yes	confirmed
AT4G26080	ABI1	AT5G46790	RCAR12	yes	confirmed
AT5G60120	TOE2	AT5G46790	RCAR12	yes	new
AT1G07430	HAI2	AT1G73000	RCAR13	yes	new
AT5G51910		AT1G73000	RCAR13	yes	new
AT4G26080	ABI1	AT1G73000	RCAR13	yes	confirmed
AT1G72770	HAB1	AT1G73000	RCAR13	yes	confirmed
AT2G29380	HAI3	AT1G73000	RCAR13	yes	new
AT1G07430	HAI2	AT2G26040	RCAR14	yes	new
AT5G51910		AT2G26040	RCAR14	yes	new
AT4G26080	ABI1	AT2G26040	RCAR14	yes	new
AT1G72770	HAB1	AT2G26040	RCAR14	yes	confirmed
AT2G26800		AT1G01360	RCAR1	no	new
AT1G07430	HAI2	AT1G01360	RCAR1	no	confirmed
AT3G29270		AT1G01360	RCAR1	no	new
AT3G49580	LSU1	AT1G01360	RCAR1	no	new
AT5G02150	Fes1C	AT1G01360	RCAR1	no	new
AT4G22250		AT1G01360	RCAR1	no	new
AT3G51630	WNK5	AT1G01360	RCAR1	no	new
AT5G22290	NAC089	AT1G01360	RCAR1	no	new
AT5G08330	TCP11	AT1G01360	RCAR1	no	new
AT1G69690	TCP15	AT1G01360	RCAR1	no	new
AT4G26455	WIP1	AT1G01360	RCAR1	no	new
AT4G32570	TIFY8	AT1G01360	RCAR1	no	new
AT3G02150	PTF1	AT1G01360	RCAR1	no	new
AT5G51910	TCP19	AT1G01360	RCAR1	no	new
AT4G26080	ABI1	AT1G01360	RCAR1	no	confirmed
AT5G51440		AT1G01360	RCAR1	no	new
AT1G72770	HAB1	AT1G01360	RCAR1	no	confirmed
AT2G29380	HAI3	AT1G01360	RCAR1	no	confirmed
AT4G23050		AT1G01360	RCAR1	no	new
AT1G25490	RCN1	AT1G01360	RCAR1	no	new
AT1G72340		AT1G01360	RCAR1	no	new
AT2G31070	TCP10	AT1G01360	RCAR1	no	new
AT1G72210		AT1G01360	RCAR1	no	new
AT1G68130	IDD14	AT1G01360	RCAR1	no	new
AT3G07740	ADA2A	AT1G01360	RCAR1	no	new
AT1G23220		AT1G01360	RCAR1	no	new
AT3G58030		AT1G01360	RCAR1	no	new
AT2G45680	TCP9	AT1G01360	RCAR1	no	new
AT3G50060	MYB77	AT1G01360	RCAR1	no	new
AT5G60120	TOE2	AT1G01360	RCAR1	no	new
AT5G49330	MYB111	AT1G01360	RCAR1	no	new
AT3G18550	BRC1	AT1G01360	RCAR1	no	new
AT1G53230	TCP3	AT1G01360	RCAR1	no	new
AT4G37260	MYB73	AT1G01360	RCAR1	no	new
AT4G22070	WRKY31	AT1G01360	RCAR1	no	new
AT1G12980	ESR1	AT1G01360	RCAR1	no	new
AT2G30470	HSI2	AT1G01360	RCAR1	no	new
AT1G07430	HAI2	AT4G01026	RCAR2	no	confirmed
AT5G51910		AT4G01026	RCAR2	no	new
AT4G26080	ABI1	AT4G01026	RCAR2	no	confirmed
AT1G72770	HAB1	AT4G01026	RCAR2	no	confirmed

Table A.6 continued from previous page

AD-Interactor	Symbol	RCAR	Symbol	ABA dep.	new/confirmed
AT2G29380	HAI3	AT4G01026	RCAR2	no	confirmed
AT1G72340		AT4G01026	RCAR2	no	new
AT5G22290	NAC089	AT4G01026	RCAR2	no	new
AT5G67300	MYBR1	AT5G53160	RCAR3	no	confirmed
AT4G29120		AT5G53160	RCAR3	no	new
AT1G07430	HAI2	AT5G53160	RCAR3	no	confirmed
AT5G02810	PRR7	AT5G53160	RCAR3	no	new
AT2G23290	MYB70	AT5G53160	RCAR3	no	new
AT5G51910		AT5G53160	RCAR3	no	new
AT4G26080	ABI1	AT5G53160	RCAR3	no	confirmed
AT1G72770	HAB1	AT5G53160	RCAR3	no	confirmed
AT2G29380	HAI3	AT5G53160	RCAR3	no	confirmed
AT1G72210		AT5G53160	RCAR3	no	new
AT1G69690	TCP15	AT5G53160	RCAR3	no	new
AT3G50060	MYB77	AT5G53160	RCAR3	no	confirmed
AT3G17600	IAA31	AT5G53160	RCAR3	no	new
AT4G32570	TIFY8	AT5G53160	RCAR3	no	new
AT1G07430	HAI2	AT4G27920	RCAR4	no	confirmed
AT5G51910		AT4G27920	RCAR4	no	new
AT4G26080	ABI1	AT4G27920	RCAR4	no	confirmed
AT1G72770	HAB1	AT4G27920	RCAR4	no	confirmed
AT2G29380	HAI3	AT4G27920	RCAR4	no	confirmed
AT4G20930		AT4G27920	RCAR4	no	new
AT2G44680	CKB4	AT4G27920	RCAR4	no	new
AT1G07430	HAI2	AT5G45860	RCAR5	no	new
AT4G26080	ABI1	AT5G45860	RCAR5	no	new
AT1G72770	HAB1	AT5G45860	RCAR5	no	confirmed
AT2G29380	HAI3	AT5G45860	RCAR5	no	new
AT1G69850	NRT1:2	AT5G45860	RCAR5	no	new
AT1G07430	HAI2	AT5G45870	RCAR6	no	new
AT5G51910		AT5G45870	RCAR6	no	new
AT4G26080	ABI1	AT5G45870	RCAR6	no	new
AT1G72770	HAB1	AT5G45870	RCAR6	no	confirmed
AT2G29380	HAI3	AT5G45870	RCAR6	no	new
AT5G46590	NAC096	AT5G45870	RCAR6	no	new
AT1G07430	HAI2	AT4G18620	RCAR7	no	confirmed
AT5G51910		AT4G18620	RCAR7	no	new
AT4G26080	ABI1	AT4G18620	RCAR7	no	confirmed
AT2G29380	HAI3	AT4G18620	RCAR7	no	new
AT1G07430	HAI2	AT5G05440	RCAR8	no	confirmed
AT5G51910		AT5G05440	RCAR8	no	new
AT4G26080	ABI1	AT5G05440	RCAR8	no	confirmed
AT1G72770	HAB1	AT5G05440	RCAR8	no	confirmed
AT2G29380	HAI3	AT5G05440	RCAR8	no	confirmed
AT4G23050		AT5G05440	RCAR8	no	new
AT3G50060	MYB77	AT5G05440	RCAR8	no	new
AT4G26080	ABI1	AT2G40330	RCAR9	no	confirmed
AT1G72770	HAB1	AT2G40330	RCAR9	no	confirmed
AT2G29380	HAI3	AT2G40330	RCAR9	no	new
AT1G06510		AT2G38310	RCAR10	no	new
AT5G22290	NAC089	AT2G38310	RCAR10	no	new
AT5G51910		AT2G38310	RCAR10	no	new
AT5G51910		AT4G17870	RCAR11	no	new
AT1G72770	HAB1	AT5G46790	RCAR12	no	confirmed

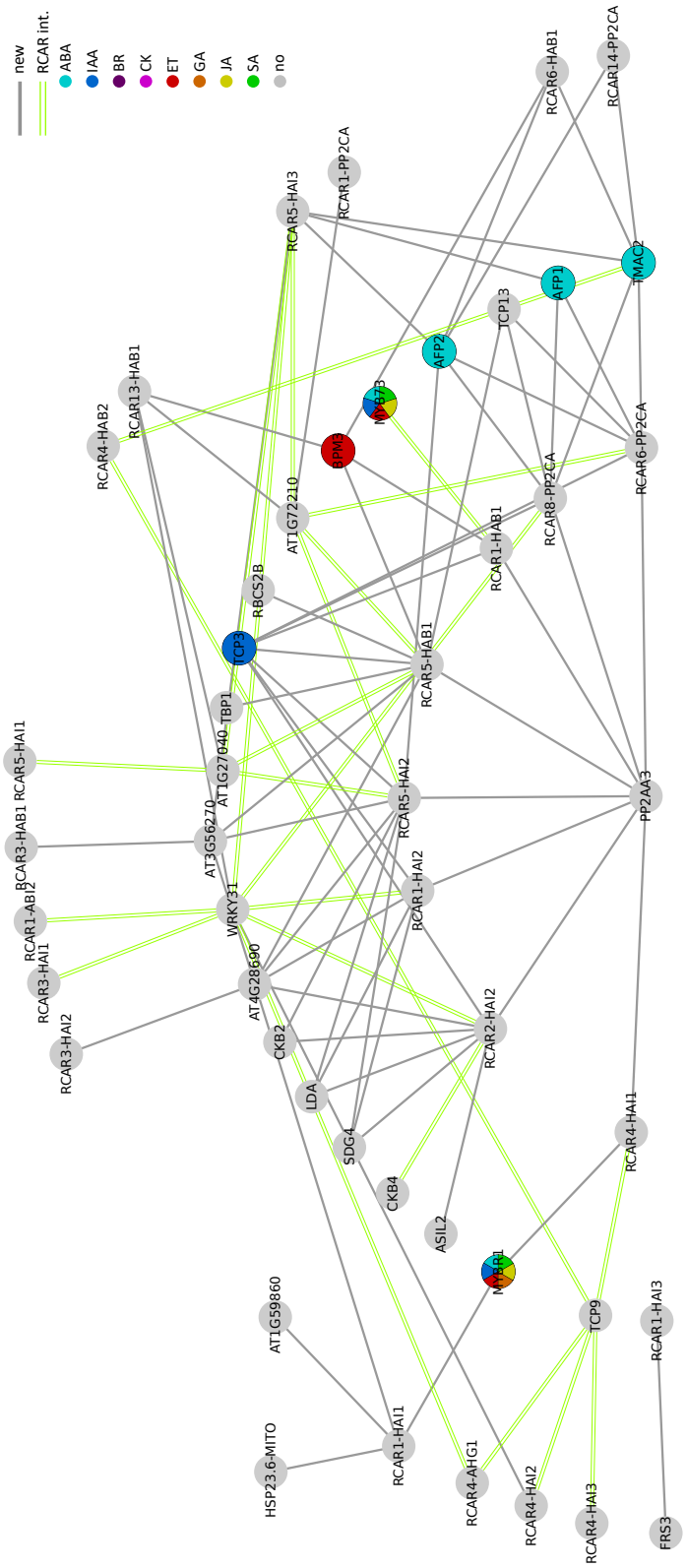

Figure A.9: Y3H ABA-dependent interaction map. 90 ABA-dependent interactions were identified in the Y3H screen. Solid lines are new Y3H interactions. double green lines indicate interaction that appear also between RCARs and interactors without PP2C. The nodes are colored according to their hormone annotations. These interactions are independently tested four times and could be confirmed at least 3 times. The verification was systematically performed with and without ABA (30 μM).

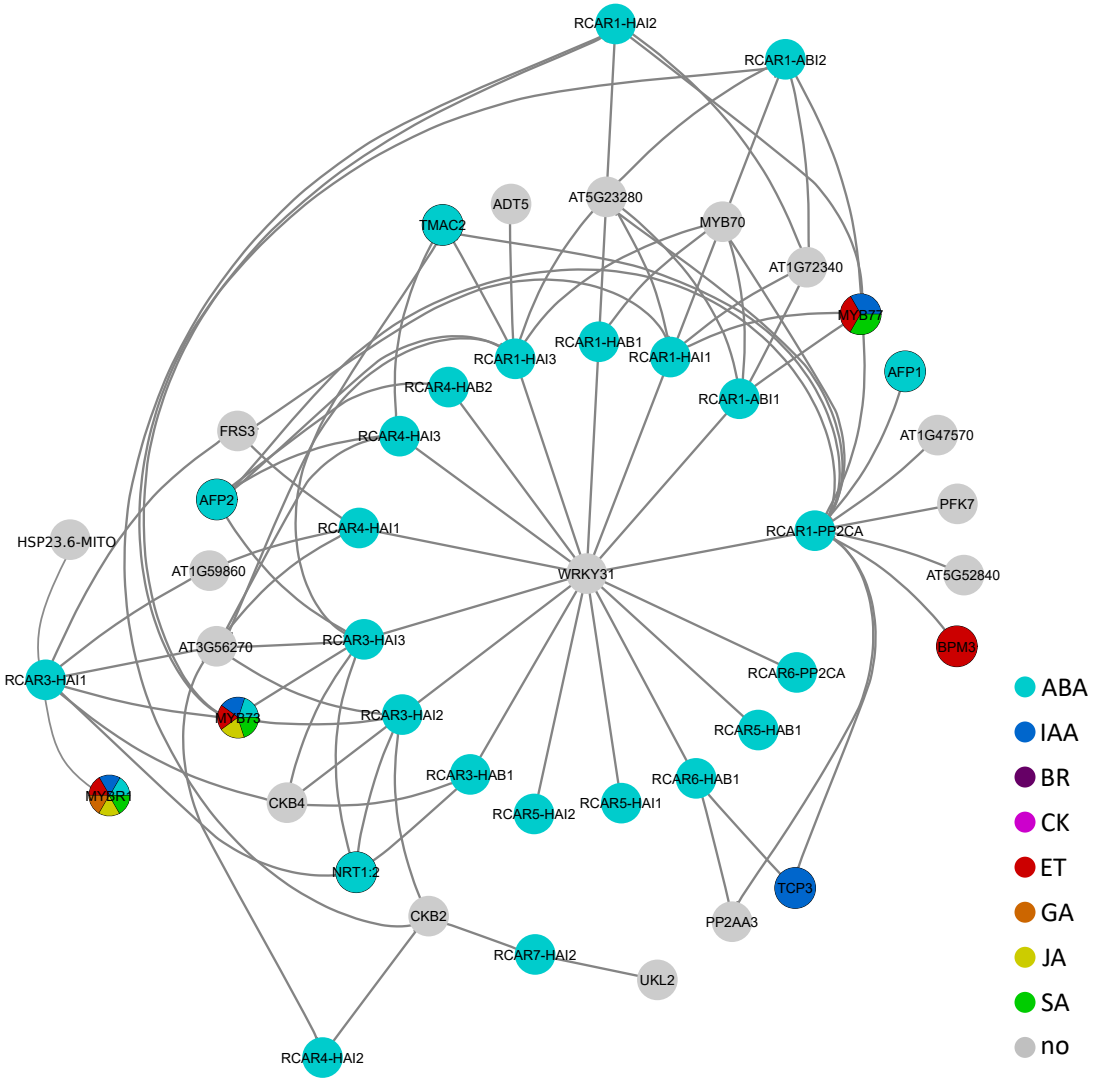

Figure A.10: Y3H ABA-independent interactions. 89 ABA-independent were identified in the Y3H screen. The nodes are colored according to their hormone annotations. These interactions are independently tested four times and could be confirmed at least 3 times. The verification was systematically performed with and without ABA (30 μM).

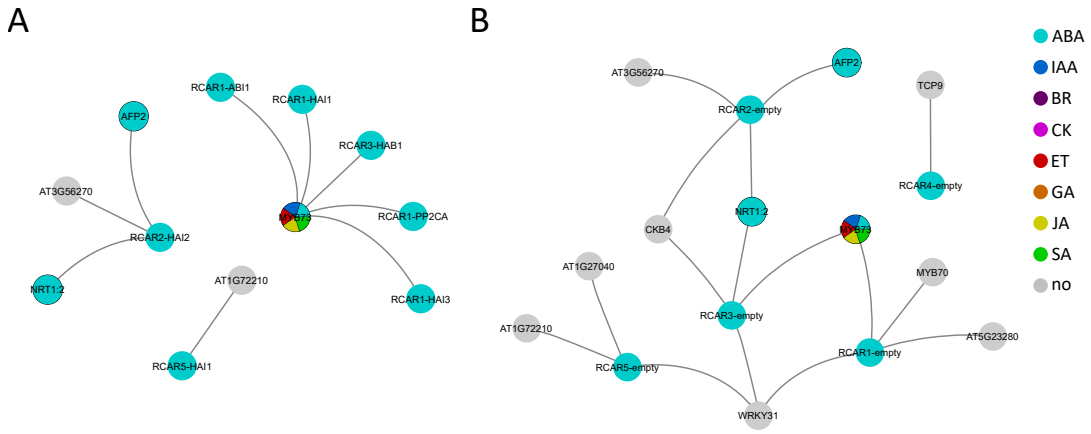

Figure A.11: Y3H ABA blocked and control interactions. (A) 9 blocked interactions through the PP2C in the adapter plasmid. In (B) 16 control interaction with RCAR-empty control combinations. The nodes are colored according to their hormone annotations. These interactions are independently tested four times and could be confirmed at least 3 times. The verification was systematically performed with and without ABA (30 μM).

Table A.7: ABA Y3H interactions

Locus ID AD	Symbol AD	Locus ID DB	Symbol DB	Locus ID pVTU-DEST	Symbol pVTU-DEST	ABA
AT1G72340		AT1G01360	RCAR1	AT4G26080	ABI1	no
AT2G23290	MYB70	AT1G01360	RCAR1	AT4G26080	ABI1	no
AT3G50060	MYB77	AT1G01360	RCAR1	AT4G26080	ABI1	no
AT5G23280		AT1G01360	RCAR1	AT4G26080	ABI1	no
AT1G72340		AT1G01360	RCAR1	AT4G26080	ABI1	+
AT2G23290	MYB70	AT1G01360	RCAR1	AT4G26080	ABI1	+
AT3G50060	MYB77	AT1G01360	RCAR1	AT4G26080	ABI1	+
AT5G23280		AT1G01360	RCAR1	AT4G26080	ABI1	+
AT1G72340		AT1G01360	RCAR1	AT5G57050	ABI2	no
AT2G23290	MYB70	AT1G01360	RCAR1	AT5G57050	ABI2	no
AT3G50060	MYB77	AT1G01360	RCAR1	AT5G57050	ABI2	no
AT4G37260	MYB73	AT1G01360	RCAR1	AT5G57050	ABI2	no
AT5G23280		AT1G01360	RCAR1	AT5G57050	ABI2	no
AT1G72340		AT1G01360	RCAR1	AT5G57050	ABI2	+
AT2G23290	MYB70	AT1G01360	RCAR1	AT5G57050	ABI2	+
AT3G50060	MYB77	AT1G01360	RCAR1	AT5G57050	ABI2	+
AT4G37260	MYB73	AT1G01360	RCAR1	AT5G57050	ABI2	+
AT5G23280		AT1G01360	RCAR1	AT5G57050	ABI2	+
AT2G23290	MYB70	AT1G01360	RCAR1		empty	no
AT4G37260	MYB73	AT1G01360	RCAR1		empty	no
AT5G23280		AT1G01360	RCAR1		empty	no
AT2G23290	MYB70	AT1G01360	RCAR1		empty	+
AT4G37260	MYB73	AT1G01360	RCAR1		empty	+
AT5G23280		AT1G01360	RCAR1		empty	+
AT2G23290	MYB70	AT1G01360	RCAR1	AT1G72770	HAB1	no
AT5G23280		AT1G01360	RCAR1	AT1G72770	HAB1	no
AT1G13320	PP2AA3	AT1G01360	RCAR1	AT1G72770	HAB1	+
AT2G39760	BPM3	AT1G01360	RCAR1	AT1G72770	HAB1	+
AT1G53230	TCP3	AT1G01360	RCAR1	AT1G72770	HAB1	+
AT2G23290	MYB70	AT1G01360	RCAR1	AT1G72770	HAB1	+
AT4G37260	MYB73	AT1G01360	RCAR1	AT1G72770	HAB1	+
AT5G23280		AT1G01360	RCAR1	AT1G72770	HAB1	+
AT2G27110	FRS3	AT1G01360	RCAR1	AT5G59220	HAI1	no
AT1G72340		AT1G01360	RCAR1	AT5G59220	HAI1	no
AT2G23290	MYB70	AT1G01360	RCAR1	AT5G59220	HAI1	no
AT3G50060	MYB77	AT1G01360	RCAR1	AT5G59220	HAI1	no
AT5G23280		AT1G01360	RCAR1	AT5G59220	HAI1	no
AT1G59860		AT1G01360	RCAR1	AT5G59220	HAI1	+
AT2G27110	FRS3	AT1G01360	RCAR1	AT5G59220	HAI1	+
AT3G56270		AT1G01360	RCAR1	AT5G59220	HAI1	+
AT4G25200	HSP23.6-MITO	AT1G01360	RCAR1	AT5G59220	HAI1	+
AT1G72340		AT1G01360	RCAR1	AT5G59220	HAI1	+
AT2G23290	MYB70	AT1G01360	RCAR1	AT5G59220	HAI1	+
AT3G50060	MYB77	AT1G01360	RCAR1	AT5G59220	HAI1	+
AT5G23280		AT1G01360	RCAR1	AT5G59220	HAI1	+
AT5G67300	MYBR1	AT1G01360	RCAR1	AT5G59220	HAI1	+
AT4G17640	CKB2	AT1G01360	RCAR1	AT1G07430	HAI2	no
AT1G72340		AT1G01360	RCAR1	AT1G07430	HAI2	no
AT2G23290	MYB70	AT1G01360	RCAR1	AT1G07430	HAI2	no
AT3G50060	MYB77	AT1G01360	RCAR1	AT1G07430	HAI2	no
AT4G37260	MYB73	AT1G01360	RCAR1	AT1G07430	HAI2	no
AT5G23280		AT1G01360	RCAR1	AT1G07430	HAI2	no
AT1G13320	PP2AA3	AT1G01360	RCAR1	AT1G07430	HAI2	+
AT4G17640	CKB2	AT1G01360	RCAR1	AT1G07430	HAI2	+
AT4G28690		AT1G01360	RCAR1	AT1G07430	HAI2	+
AT4G30860	SDG4	AT1G01360	RCAR1	AT1G07430	HAI2	+
AD-empty		AT1G01360	RCAR1	AT1G07430	HAI2	+
AT1G53230	TCP3	AT1G01360	RCAR1	AT1G07430	HAI2	+
AT2G23290	MYB70	AT1G01360	RCAR1	AT1G07430	HAI2	+
AT3G50060	MYB77	AT1G01360	RCAR1	AT1G07430	HAI2	+
AT4G37260	MYB73	AT1G01360	RCAR1	AT1G07430	HAI2	+
AT5G23280		AT1G01360	RCAR1	AT1G07430	HAI2	+
AT1G13740	AFP2	AT1G01360	RCAR1	AT2G29380	HAI3	no
AT3G02140	TMAC2	AT1G01360	RCAR1	AT2G29380	HAI3	no
AT3G56270		AT1G01360	RCAR1	AT2G29380	HAI3	no
AT5G22630	ADT5	AT1G01360	RCAR1	AT2G29380	HAI3	no
AT2G23290	MYB70	AT1G01360	RCAR1	AT2G29380	HAI3	no
AT2G44680	CKB4	AT1G01360	RCAR1	AT2G29380	HAI3	-
AT5G23280		AT1G01360	RCAR1	AT2G29380	HAI3	no
AT1G13740	AFP2	AT1G01360	RCAR1	AT2G29380	HAI3	+
AT2G27110	FRS3	AT1G01360	RCAR1	AT2G29380	HAI3	+
AT3G02140	TMAC2	AT1G01360	RCAR1	AT2G29380	HAI3	+
AT3G56270		AT1G01360	RCAR1	AT2G29380	HAI3	+
AT5G22630	ADT5	AT1G01360	RCAR1	AT2G29380	HAI3	+
AT2G23290	MYB70	AT1G01360	RCAR1	AT2G29380	HAI3	+
AT5G23280		AT1G01360	RCAR1	AT2G29380	HAI3	+
AT1G13320	PP2AA3	AT1G01360	RCAR1	AT3G11410	PP2CA	no
AT1G13740	AFP2	AT1G01360	RCAR1	AT3G11410	PP2CA	no
AT1G47570		AT1G01360	RCAR1	AT3G11410	PP2CA	no
AT1G69260	AFP1	AT1G01360	RCAR1	AT3G11410	PP2CA	no
AT2G39760	BPM3	AT1G01360	RCAR1	AT3G11410	PP2CA	no
AT3G02140	TMAC2	AT1G01360	RCAR1	AT3G11410	PP2CA	no
AT5G52840		AT1G01360	RCAR1	AT3G11410	PP2CA	no
AT5G56630	PFK7	AT1G01360	RCAR1	AT3G11410	PP2CA	no
AT1G53230	TCP3	AT1G01360	RCAR1	AT3G11410	PP2CA	no

Table A.7 continued from previous page

Locus ID AD	Symbol AD	Locus ID DB	Symbol DB	Locus ID pVTU-DEST	Symbol pVTU-DEST	ABA
AT1G72340		AT1G01360	RCAR1	AT3G11410	PP2CA	-
AT2G23290	MYB70	AT1G01360	RCAR1	AT3G11410	PP2CA	no
AT3G50060	MYB77	AT1G01360	RCAR1	AT3G11410	PP2CA	no
AT5G23280		AT1G01360	RCAR1	AT3G11410	PP2CA	no
AT1G13320	PP2AA3	AT1G01360	RCAR1	AT3G11410	PP2CA	+
AT1G13740	AFP2	AT1G01360	RCAR1	AT3G11410	PP2CA	+
AT1G47570		AT1G01360	RCAR1	AT3G11410	PP2CA	+
AT1G69260	AFP1	AT1G01360	RCAR1	AT3G11410	PP2CA	+
AT2G39760	BPM3	AT1G01360	RCAR1	AT3G11410	PP2CA	+
AT3G02140	TMAC2	AT1G01360	RCAR1	AT3G11410	PP2CA	+
AT5G52840		AT1G01360	RCAR1	AT3G11410	PP2CA	+
AT5G56630	PFK7	AT1G01360	RCAR1	AT3G11410	PP2CA	+
AT1G53230	TCP3	AT1G01360	RCAR1	AT3G11410	PP2CA	+
AT1G72210		AT1G01360	RCAR1	AT3G11410	PP2CA	+
AT2G23290	MYB70	AT1G01360	RCAR1	AT3G11410	PP2CA	+
AT3G50060	MYB77	AT1G01360	RCAR1	AT3G11410	PP2CA	+
AT5G23280		AT1G01360	RCAR1	AT3G11410	PP2CA	+
AT1G69850	NRT1:2	AT4G17870	RCAR11	AT1G72770	HAB1	no
AT2G44680	CKB4	AT4G17870	RCAR11	AT1G72770	HAB1	no
AT3G56270		AT4G17870	RCAR11	AT1G72770	HAB1	+
AT1G69850	NRT1:2	AT4G17870	RCAR11	AT1G72770	HAB1	+
AT2G44680	CKB4	AT4G17870	RCAR11	AT1G72770	HAB1	+
AT1G27040		AT1G73000	RCAR13	AT1G72770	HAB1	+
AT2G39760	BPM3	AT1G73000	RCAR13	AT1G72770	HAB1	+
AT1G72210		AT1G73000	RCAR13	AT1G72770	HAB1	+
AT1G13740	AFP2	AT2G26040	RCAR14	AT3G11410	PP2CA	+
AT3G02140	TMAC2	AT2G26040	RCAR14	AT3G11410	PP2CA	+
AT1G13740	AFP2	AT4G01026	RCAR2		empty	no
AT1G69850	NRT1:2	AT4G01026	RCAR2		empty	no
AT2G44680	CKB4	AT4G01026	RCAR2		empty	no
AT1G13740	AFP2	AT4G01026	RCAR2		empty	+
AT3G56270		AT4G01026	RCAR2		empty	+
AT1G69850	NRT1:2	AT4G01026	RCAR2		empty	+
AT1G13320	PP2AA3	AT4G01026	RCAR2	AT1G07430	HAI2	+
AT3G14180	ASIL2	AT4G01026	RCAR2	AT1G07430	HAI2	+
AT4G17640	CKB2	AT4G01026	RCAR2	AT1G07430	HAI2	+
AT4G28690		AT4G01026	RCAR2	AT1G07430	HAI2	+
AT4G30860	SDG4	AT4G01026	RCAR2	AT1G07430	HAI2	+
AD-empty		AT4G01026	RCAR2	AT1G07430	HAI2	+
AT1G53230	TCP3	AT4G01026	RCAR2	AT1G07430	HAI2	+
AT2G44680	CKB4	AT4G01026	RCAR2	AT1G07430	HAI2	+
AT1G69850	NRT1:2	AT5G53160	RCAR3		empty	no
AT2G44680	CKB4	AT5G53160	RCAR3		empty	no
AT4G37260	MYB73	AT5G53160	RCAR3		empty	no
AT1G69850	NRT1:2	AT5G53160	RCAR3		empty	+
AT2G44680	CKB4	AT5G53160	RCAR3		empty	+
AT4G37260	MYB73	AT5G53160	RCAR3		empty	+
AT1G13740	AFP2	AT5G53160	RCAR3	AT1G17550	HAB2	+
AT3G02140	TMAC2	AT5G53160	RCAR3	AT1G17550	HAB2	+
AT2G45680	TCP9	AT5G53160	RCAR3	AT1G17550	HAB2	+
AT1G59860		AT5G53160	RCAR3	AT5G59220	HAI1	no
AT2G27110	FRS3	AT5G53160	RCAR3	AT5G59220	HAI1	no
AT3G56270		AT5G53160	RCAR3	AT5G59220	HAI1	no
AT4G25200	HSP23.6-MITO	AT5G53160	RCAR3	AT5G59220	HAI1	no
AT1G69850	NRT1:2	AT5G53160	RCAR3	AT5G59220	HAI1	no
AT2G44680	CKB4	AT5G53160	RCAR3	AT5G59220	HAI1	no
AT4G37260	MYB73	AT5G53160	RCAR3	AT5G59220	HAI1	no
AT5G67300	MYBR1	AT5G53160	RCAR3	AT5G59220	HAI1	no
AT1G59860		AT5G53160	RCAR3	AT5G59220	HAI1	+
AT2G27110	FRS3	AT5G53160	RCAR3	AT5G59220	HAI1	+
AT3G56270		AT5G53160	RCAR3	AT5G59220	HAI1	+
AT4G25200	HSP23.6-MITO	AT5G53160	RCAR3	AT5G59220	HAI1	+
AT1G69850	NRT1:2	AT5G53160	RCAR3	AT5G59220	HAI1	+
AT2G44680	CKB4	AT5G53160	RCAR3	AT5G59220	HAI1	+
AT4G37260	MYB73	AT5G53160	RCAR3	AT5G59220	HAI1	+
AT5G67300	MYBR1	AT5G53160	RCAR3	AT5G59220	HAI1	+
AT3G56270		AT5G53160	RCAR3	AT1G07430	HAI2	no
AT4G17640	CKB2	AT5G53160	RCAR3	AT1G07430	HAI2	no
AT1G69850	NRT1:2	AT5G53160	RCAR3	AT1G07430	HAI2	no
AT2G44680	CKB4	AT5G53160	RCAR3	AT1G07430	HAI2	no
AT4G37260	MYB73	AT5G53160	RCAR3	AT1G07430	HAI2	no
AT3G56270		AT5G53160	RCAR3	AT1G07430	HAI2	+
AT4G17640	CKB2	AT5G53160	RCAR3	AT1G07430	HAI2	+
AT4G28690		AT5G53160	RCAR3	AT1G07430	HAI2	+
AT1G69850	NRT1:2	AT5G53160	RCAR3	AT1G07430	HAI2	+
AT2G44680	CKB4	AT5G53160	RCAR3	AT1G07430	HAI2	+
AT4G37260	MYB73	AT5G53160	RCAR3	AT1G07430	HAI2	+
AT1G13740	AFP2	AT5G53160	RCAR3	AT2G29380	HAI3	no
AT3G02140	TMAC2	AT5G53160	RCAR3	AT2G29380	HAI3	no
AT3G56270		AT5G53160	RCAR3	AT2G29380	HAI3	no
AT1G69850	NRT1:2	AT5G53160	RCAR3	AT2G29380	HAI3	no
AT2G44680	CKB4	AT5G53160	RCAR3	AT2G29380	HAI3	no
AT4G37260	MYB73	AT5G53160	RCAR3	AT2G29380	HAI3	no
AT1G13740	AFP2	AT5G53160	RCAR3	AT2G29380	HAI3	+
AT3G02140	TMAC2	AT5G53160	RCAR3	AT2G29380	HAI3	+
AT3G56270		AT5G53160	RCAR3	AT2G29380	HAI3	+

Table A.7 continued from previous page

Locus ID AD	Symbol AD	Locus ID DB	Symbol DB	Locus ID pVTU-DEST	Symbol pVTU-DEST	ABA
AT1G69850	NRT1:2	AT5G53160	RCAR3	AT2G29380	HAI3	+
AT2G44680	CKB4	AT5G53160	RCAR3	AT2G29380	HAI3	+
AT4G37260	MYB73	AT5G53160	RCAR3	AT2G29380	HAI3	+
AT2G45680	TCP9	AT4G27920	RCAR4	AT5G51760	AHG1	+
AT2G45680	TCP9	AT4G27920	RCAR4		empty	+
AT1G13740	AFP2	AT4G27920	RCAR4	AT1G17550	HAB2	no
AT1G59860		AT4G27920	RCAR4	AT5G59220	HAI1	no
AT2G27110	FRS3	AT4G27920	RCAR4	AT5G59220	HAI1	no
AT3G56270		AT4G27920	RCAR4	AT5G59220	HAI1	no
AT1G13320	PP2AA3	AT4G27920	RCAR4	AT5G59220	HAI1	+
AT1G59860		AT4G27920	RCAR4	AT5G59220	HAI1	+
AT2G27110	FRS3	AT4G27920	RCAR4	AT5G59220	HAI1	+
AT3G56270		AT4G27920	RCAR4	AT5G59220	HAI1	+
AT2G45680	TCP9	AT4G27920	RCAR4	AT5G59220	HAI1	+
AT5G67300	MYBR1	AT4G27920	RCAR4	AT5G59220	HAI1	+
AT3G56270		AT4G27920	RCAR4	AT1G07430	HAI2	no
AT4G17640	CKB2	AT4G27920	RCAR4	AT1G07430	HAI2	no
AT3G56270		AT4G27920	RCAR4	AT1G07430	HAI2	+
AT4G17640	CKB2	AT4G27920	RCAR4	AT1G07430	HAI2	+
AT2G45680	TCP9	AT4G27920	RCAR4	AT1G07430	HAI2	+
AT1G13740	AFP2	AT4G27920	RCAR4	AT2G29380	HAI3	no
AT3G02140	TMAC2	AT4G27920	RCAR4	AT2G29380	HAI3	no
AT3G56270		AT4G27920	RCAR4	AT2G29380	HAI3	no
AT1G13740	AFP2	AT4G27920	RCAR4	AT2G29380	HAI3	+
AT3G02140	TMAC2	AT4G27920	RCAR4	AT2G29380	HAI3	+
AT3G56270		AT4G27920	RCAR4	AT2G29380	HAI3	+
AT2G45680	TCP9	AT4G27920	RCAR4	AT2G29380	HAI3	+
AT1G27040		AT5G45860	RCAR5		empty	+
AT1G72210		AT5G45860	RCAR5		empty	+
AT1G13320	PP2AA3	AT5G45860	RCAR5	AT1G72770	HAB1	+
AT1G27040		AT5G45860	RCAR5	AT1G72770	HAB1	+
AT2G39760	BPM3	AT5G45860	RCAR5	AT1G72770	HAB1	+
AT3G13445	TBP1	AT5G45860	RCAR5	AT1G72770	HAB1	+
AT3G13445	TBP1	AT5G45860	RCAR5	AT1G72770	HAB1	+
AT3G56270		AT5G45860	RCAR5	AT1G72770	HAB1	+
AT4G28690		AT5G45860	RCAR5	AT1G72770	HAB1	+
AT5G38420	RBCS2B	AT5G45860	RCAR5	AT1G72770	HAB1	+
AT5G38420	RBCS2B	AT5G45860	RCAR5	AT1G72770	HAB1	+
AT5G38420	RBCS2B	AT5G45860	RCAR5	AT1G72770	HAB1	+
AT1G53230	TCP3	AT5G45860	RCAR5	AT1G72770	HAB1	+
AT1G72210		AT5G45860	RCAR5	AT1G72770	HAB1	+
AT3G02150	PTF1	AT5G45860	RCAR5	AT1G72770	HAB1	+
AT1G27040		AT5G45860	RCAR5	AT5G59220	HAI1	+
AT1G13320	PP2AA3	AT5G45860	RCAR5	AT1G07430	HAI2	+
AT1G13740	AFP2	AT5G45860	RCAR5	AT1G07430	HAI2	+
AT1G27040		AT5G45860	RCAR5	AT1G07430	HAI2	+
AT3G56270		AT5G45860	RCAR5	AT1G07430	HAI2	+
AT4G17640	CKB2	AT5G45860	RCAR5	AT1G07430	HAI2	+
AT4G28690		AT5G45860	RCAR5	AT1G07430	HAI2	+
AT4G30860	SDG4	AT5G45860	RCAR5	AT1G07430	HAI2	+
AD-empty		AT5G45860	RCAR5	AT1G07430	HAI2	+
AT1G53230	TCP3	AT5G45860	RCAR5	AT1G07430	HAI2	+
AT1G72210		AT5G45860	RCAR5	AT1G07430	HAI2	+
AT1G13740	AFP2	AT5G45860	RCAR5	AT2G29380	HAI3	+
AT1G27040		AT5G45860	RCAR5	AT2G29380	HAI3	+
AT1G69260	AFP1	AT5G45860	RCAR5	AT2G29380	HAI3	+
AT3G02140	TMAC2	AT5G45860	RCAR5	AT2G29380	HAI3	+
AT3G56270		AT5G45860	RCAR5	AT2G29380	HAI3	+
AT1G72210		AT5G45860	RCAR5	AT2G29380	HAI3	+
AT1G13320	PP2AA3	AT5G45870	RCAR6	AT1G72770	HAB1	no
AT1G53230	TCP3	AT5G45870	RCAR6	AT1G72770	HAB1	no
AT1G13320	PP2AA3	AT5G45870	RCAR6	AT1G72770	HAB1	+
AT1G13740	AFP2	AT5G45870	RCAR6	AT1G72770	HAB1	+
AT2G39760	BPM3	AT5G45870	RCAR6	AT1G72770	HAB1	+
AT3G02140	TMAC2	AT5G45870	RCAR6	AT1G72770	HAB1	+
AT1G53230	TCP3	AT5G45870	RCAR6	AT1G72770	HAB1	+
AT1G13320	PP2AA3	AT5G45870	RCAR6	AT3G11410	PP2CA	+
AT1G13740	AFP2	AT5G45870	RCAR6	AT3G11410	PP2CA	+
AT1G69260	AFP1	AT5G45870	RCAR6	AT3G11410	PP2CA	+
AT3G02140	TMAC2	AT5G45870	RCAR6	AT3G11410	PP2CA	+
AT1G53230	TCP3	AT5G45870	RCAR6	AT3G11410	PP2CA	+
AT1G72210		AT5G45870	RCAR6	AT3G11410	PP2CA	+
AT3G02150	PTF1	AT5G45870	RCAR6	AT3G11410	PP2CA	+
AT3G27190	UKL2	AT4G18620	RCAR7	AT1G07430	HAI2	no
AT4G17640	CKB2	AT4G18620	RCAR7	AT1G07430	HAI2	no
AT3G27190	UKL2	AT4G18620	RCAR7	AT1G07430	HAI2	+
AT4G17640	CKB2	AT4G18620	RCAR7	AT1G07430	HAI2	+
AT1G13320	PP2AA3	AT5G05440	RCAR8	AT3G11410	PP2CA	+
AT1G13740	AFP2	AT5G05440	RCAR8	AT3G11410	PP2CA	+
AT1G69260	AFP1	AT5G05440	RCAR8	AT3G11410	PP2CA	+
AT3G02140	TMAC2	AT5G05440	RCAR8	AT3G11410	PP2CA	+
AT1G53230	TCP3	AT5G05440	RCAR8	AT3G11410	PP2CA	+
AT3G02150	PTF1	AT5G05440	RCAR8	AT3G11410	PP2CA	+

A.7.2 PP2C clade A alignment

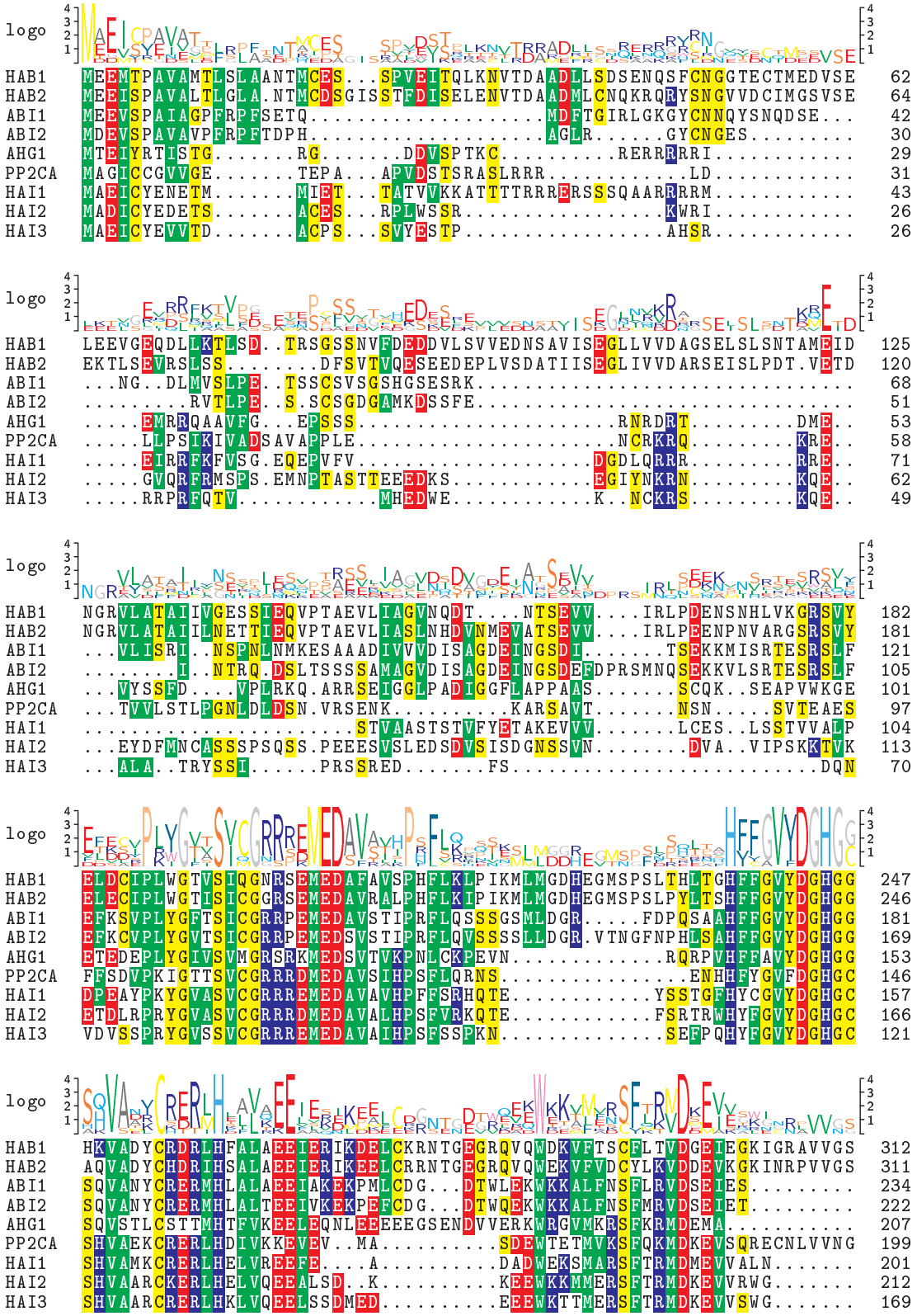

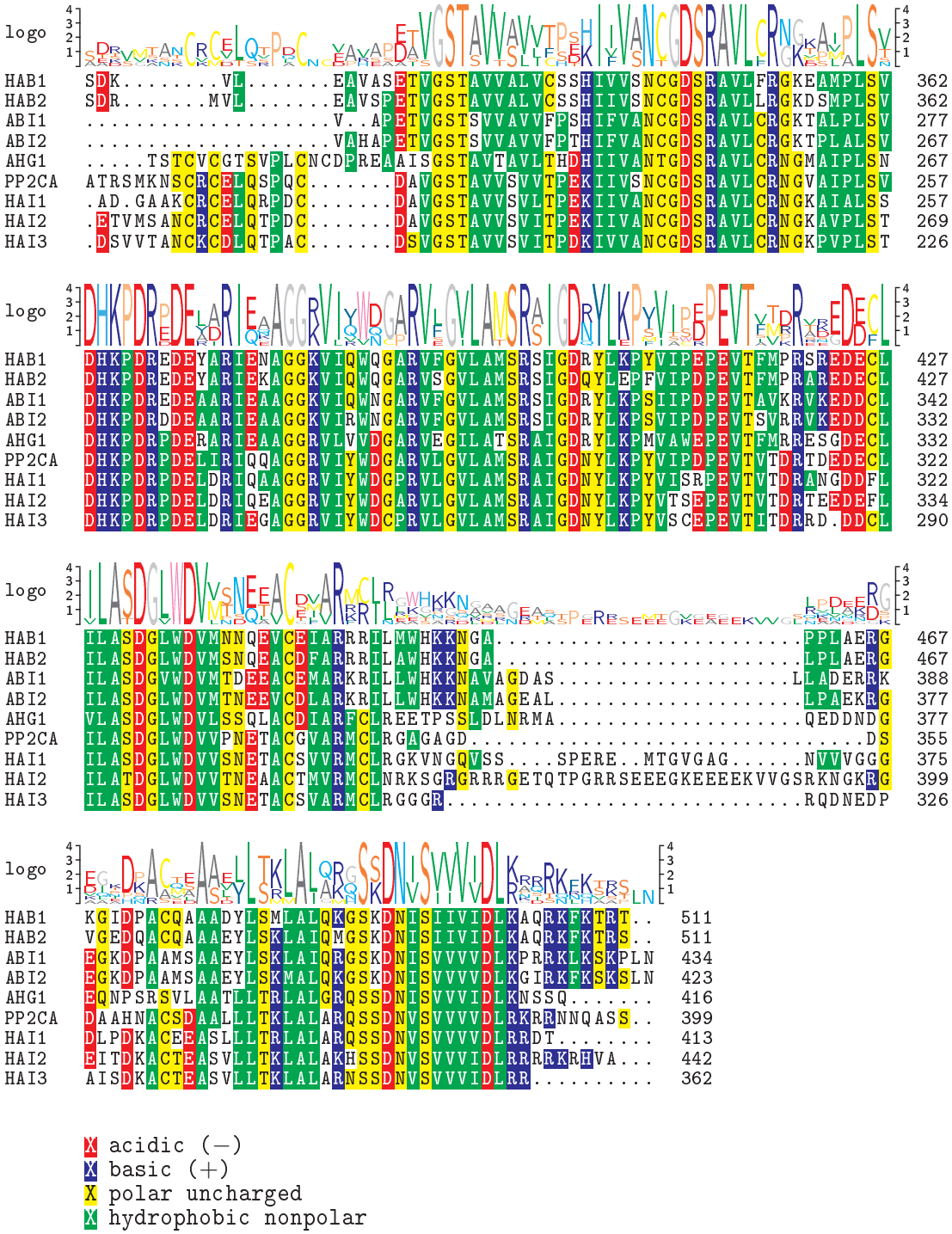

Figure A.12: PP2C clade A alignment based on amino acid sequence. Logo indicates the consensus sequence from all nine PP2Cs.

Table A.8: ABA Y3H blocked AD-DB interaction by PP2Cs

Locus ID AD	Symbol AD	Locus ID DB	Symbol DB	Locus ID pVTU-DEST	Symbol pVTU-DEST
AT4G37260	MYB73	AT1G01360	RCAR1	AT4G26080	ABI1
AT4G37260	MYB73	AT1G01360	RCAR1	AT5G59220	HAI1
AT4G37260	MYB73	AT1G01360	RCAR1	AT2G29380	HAI3
AT4G37260	MYB73	AT1G01360	RCAR1	AT3G11410	PP2CA
AT1G13740	AFP2	AT4G01026	RCAR2	AT1G07430	HAI2
AT3G56270	AT3G56270	AT4G01026	RCAR2	AT1G07430	HAI2
AT1G69850	NRT1:2	AT4G01026	RCAR2	AT1G07430	HAI2
AT4G37260	MYB73	AT5G53160	RCAR3	AT1G72770	HAB1
AT1G72210	AT1G72210	AT5G45860	RCAR5	AT5G59220	HAI1

A.8 Genetic validation *in planta*

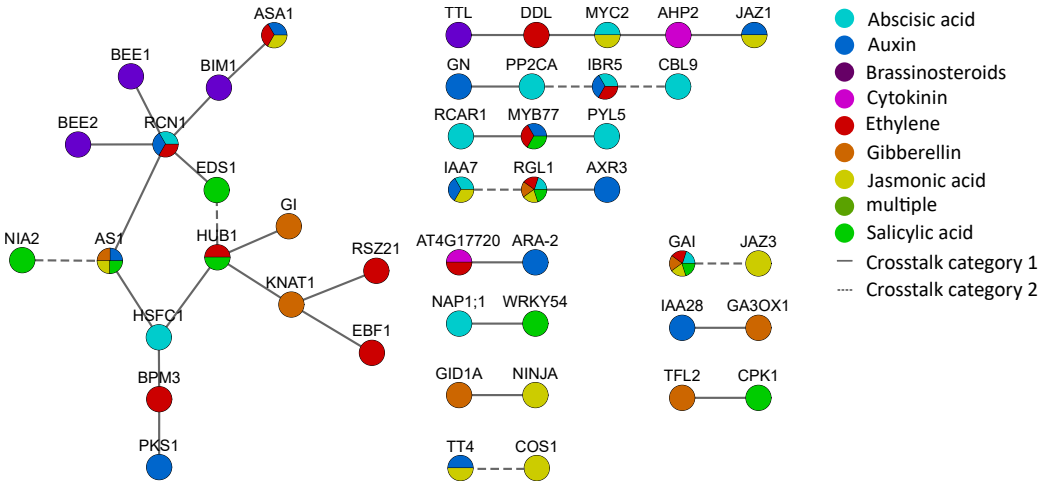

Figure A.13: Selection of interaction pairs expressed in seedlings. For validation in plants, the interaction pairs were selected according to whether both genes are expressed in seedlings. Only for these 34 of 54 interactions, it was possible to order T-DNA lines containing the T-DNA insertion at the beginning of the sequence. Of these 34 pairs, 19 could finally be tested. Interactions that take place between two differently annotated proteins were assigned to category 1. Interactions between proteins, one of which is annotated multiple times and among those carries the hormone annotation of the interaction partner, are assigned to category 2. These interaction pairs are the basis for the validation of the PhI and for the identification of new points of signal integration.

A.8.1 Gene expression level of candidate plant lines (qRT-PCR)

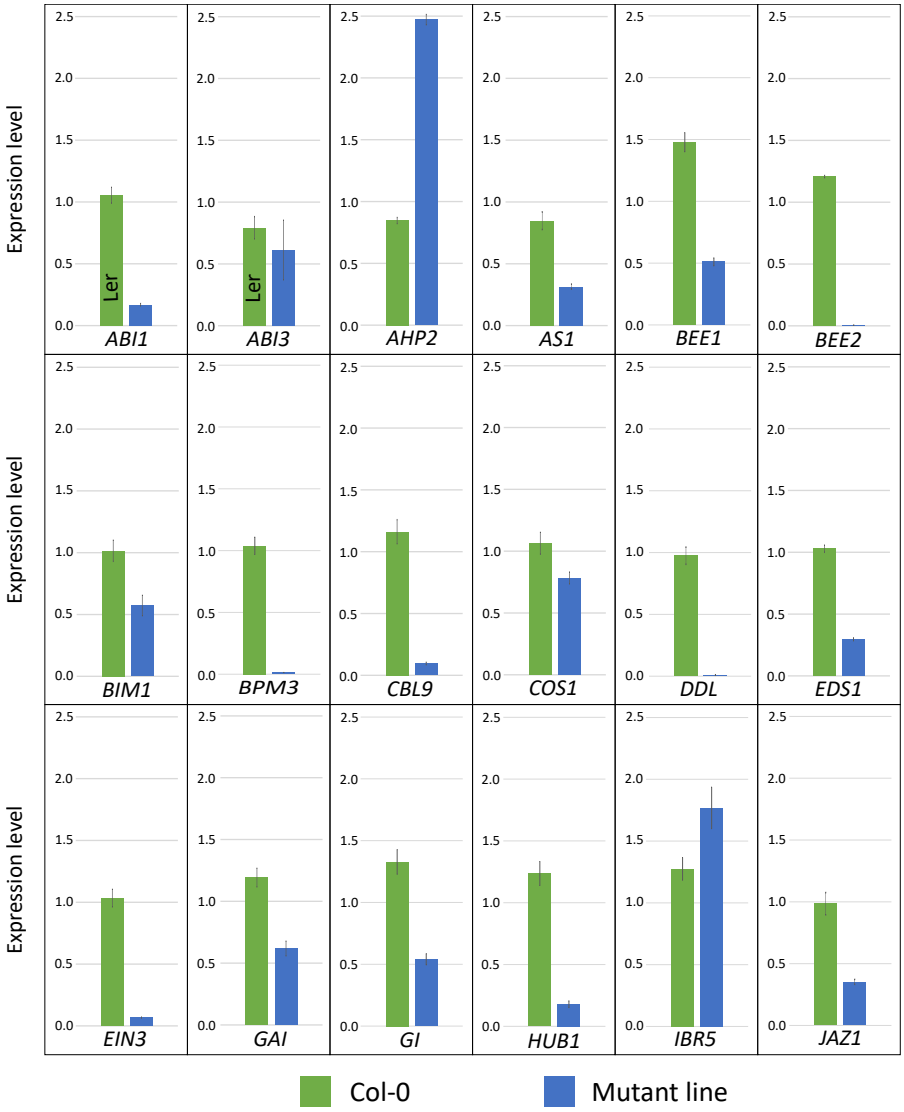

Figure A.14: Gene expression level of candidate plant lines part 1. Gene expression levels were tested for *abi1*, *abi3* (Ler background), *ahp2*, *as1*, *bee1*, *bee2*, *bim1*, *bpm3*, *cbl9*, *cos1*, *ddl*, *eds1*, *ein3*, *gai*, *gi*, *hub1*, *ibr5* and *jaz1*. The expression levels were generated by qRT-PCR with four biological and four technical replicas each. The target genes and the mutant lines are labeled below the bar graphs, respectively. The green bar shows the expression in Col-0, which in most cases is the background of the candidate lines. Ler background is indicated in the bar graphs. The blue bars show the expression level of the candidate line. For normalization the gene expression of *ACT8* was used. Error bars indicate standard deviation of four biological replicates.

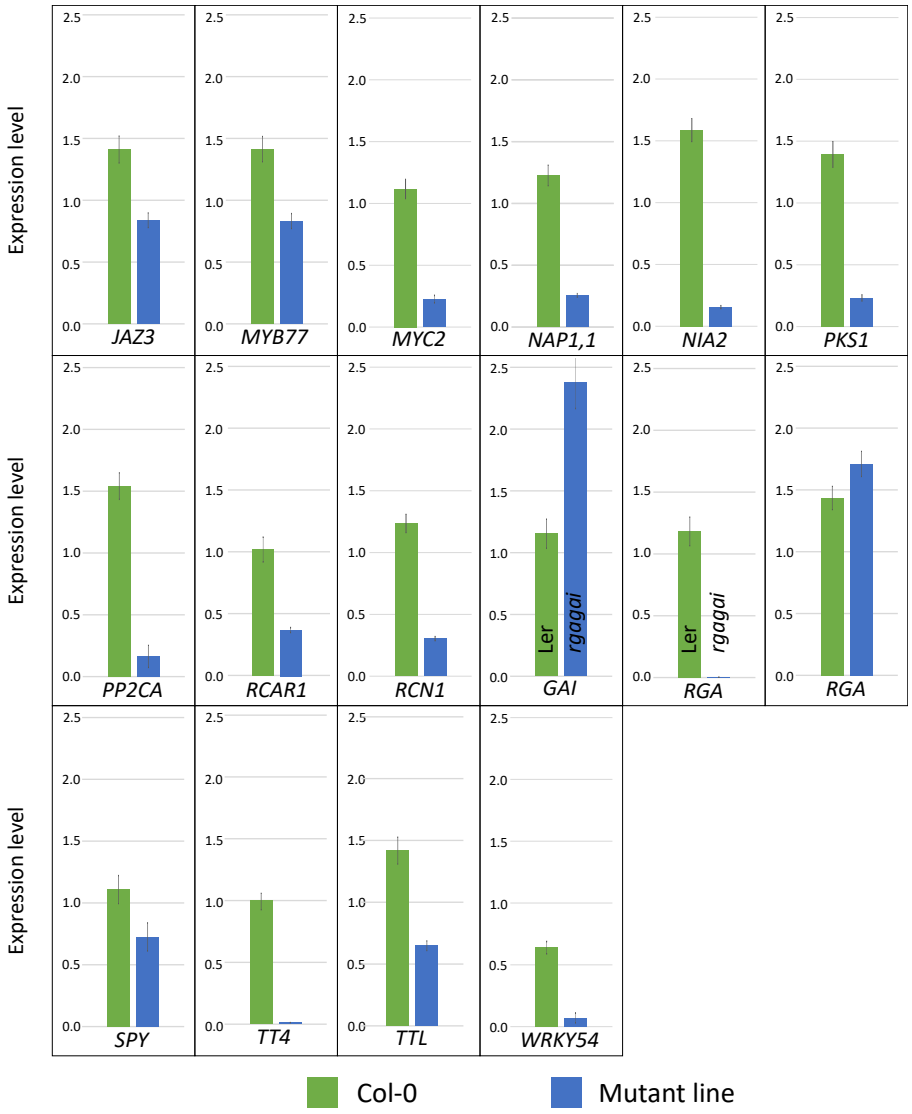

Figure A.15: Gene expression level of candidate plant lines part 2. Gene expression levels were tested for *jaz3, myb77, myc2, nap1;1, nia2, pks1, pp2ca, rcar1, rcn1, rga-gai* (Ler background), *rga, spy, tt4, ttl*, and *wrky54*. The expression levels were generated by qRT-PCR with four biological and four technical replicas each. The target genes and the mutant lines are labeled below the bar graphs, respectively. The green bar shows the expression in Col-0, which in most cases is the background of the candidate lines. Ler background is indicated in the bar graphs. The blue bars show the expression level of the candidate line. For normalization the gene expression of *ACT8* was used. Error bars indicate standard deviation of four biological replicates. In the case of the double mutant *rgagai*, it is marked separately in the blue bar.

A.8.2 BR hypocotyl elongation assay

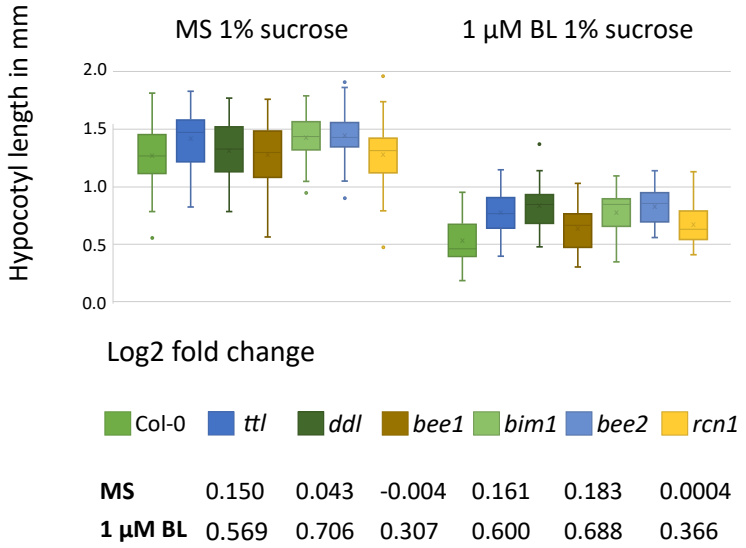

MS	0.150	0.043	-0.004	0.161	0.183	0.0004
1 µM BL	0.569	0.706	0.307	0.600	0.688	0.366

Figure A.16: Brassinosteroid hypocotyl measurement. Hypocotyl measurement was performed with 1 μM BL, once with 30-40 seedlings per line.

A.8.3 CK root elongation assay

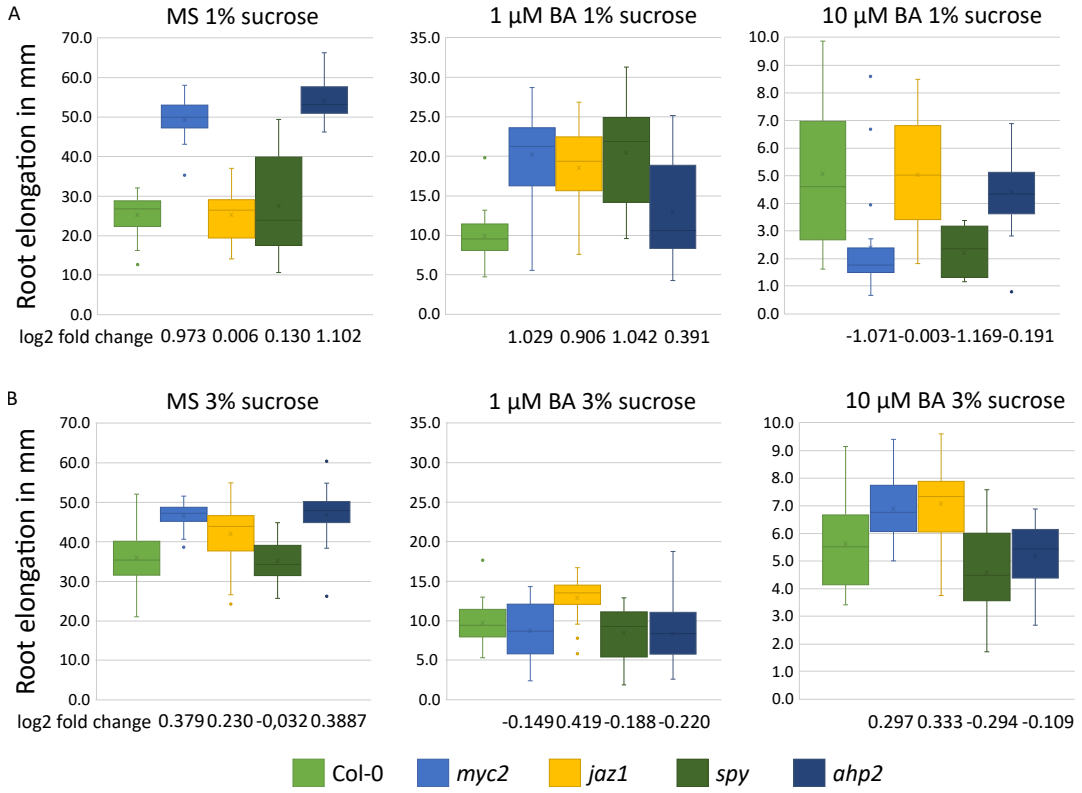

Figure A.17: Cytokinin: Root elongation measurement. Root elongation was performed with 1 and 10 μM BA and 1 % and 3 % sucrose. The log2 fold change was also calculated for all mutant lines. This assay was performed once with 30-40 seedlings per line.

A.8.4 GA seedling assay

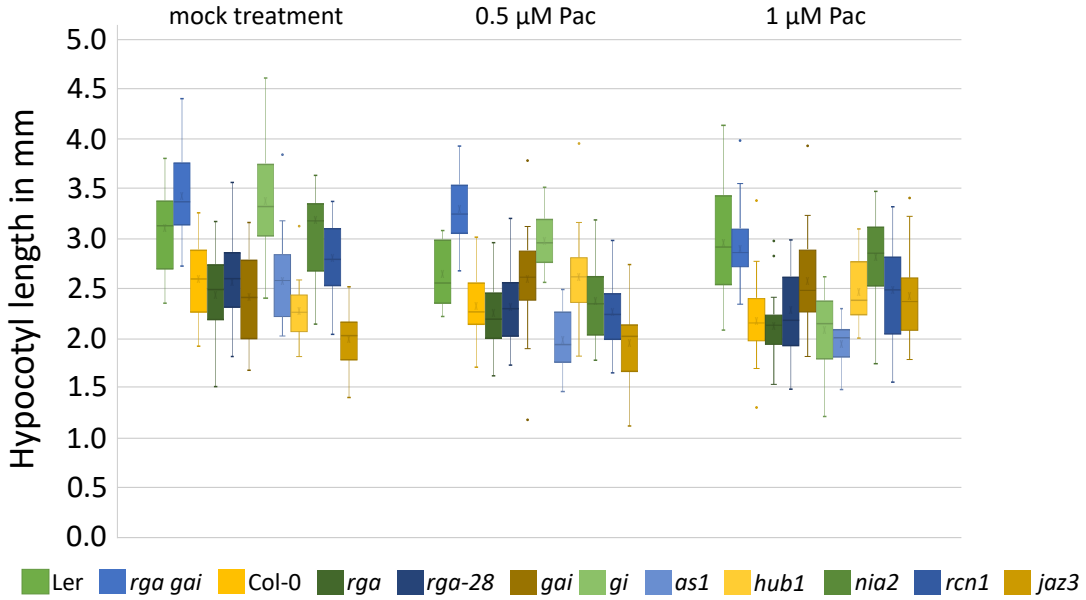

Figure A.18: Gibberellin hypocotyl measurement. Hypocotyl measurement was performed . Log2 fold change was calculated and is shown in table A.9. Hypocotyl measurement was performed on MS (mock treated) plates, 0.5 μM Pac and 1.0 μM Pac with 30-40 seedlings per line.

Table A.9: GA hypocotyl length log2 fold change values. *rgagai* has a Ler background, whereas all other mutant lines were in Col-0 background. Log2 fold change were calculated for one repeat.

Background	**Ler**	**Col-0**	**Col-0**	**Col-0**	**Col-0**
mutant line	***rgagai***	***rga***	***rga-28***	***gai***	***gi***
MS	0,1421	-0,0901	-0,0140	-0,1068	0,3789
0.5 μM Pac	0,3210	-0,0463	-0,0076	0,1593	0,3598
1.0 μM Pac	-0,0271	-0,0430	0,0629	0,2369	-0,0741

Background	**Col-0**	**Col-0**	**Col-0**	**Col-0**	**Col-0**
mutant line	***as1***	***hub1***	***nia2***	***rcn1***	***jaz3***
MS	-0,0123	-0,1913	0,2024	0,1179	-0,3786
0.5 μM Pac	-0,2386	0,1707	0,0267	-0,0423	-0,2546
1.0 μM Pac	-0,1748	0,1718	0,3650	0,1664	0,1471

A.8.5 JA seedling assay

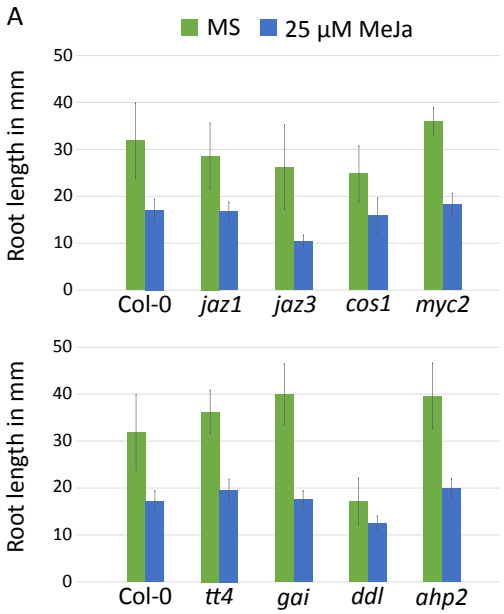

B

Fold change calculations:

Background	Col-0	Col-0	Col-0
mutant line	*jaz1*	*jaz3*	*cos1*
MS	-0,156	-0,285	-0,367
25 µM MeJa	-0,023	-0,730	-0,110

Background	Col-0	Col-0	Col-0
mutant line	*myc2*	*tt4*	*gai*
MS	0,174	0,187	0,324
25 µM MeJa	0,094	0,202	0,039

Background	Col-0	Col-0
mutant line	*ddl*	*ahp2*
MS	-0,895	0,313
25 µM MeJa	-0,454	0,227

Figure A.19: Jasmonic acid root elongation assay. Root elongation was performed with 25 μM MeJa. (A) Root elongation bar graphs (B)JA root length log2 fold values. 30-40 seedlings per line. Error bars indicate standard error of one biological replicates.

A.8.6 ABA seedling assay

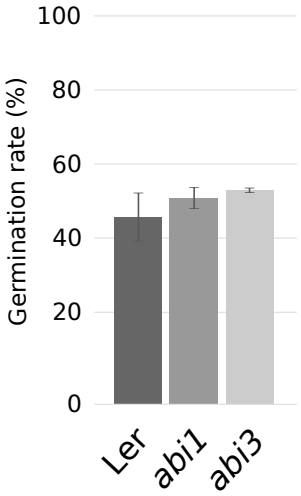

Figure A.20: ABA germination assay: positive controls in Ler background under 30 μM ABA treatment. Germination rate of Ler and the positive control lines *abi1* and *abi3* are shown. The assay was performed in three replicated with about 90-120 seeds per line. Error bars indicate standard deviation of three biological replicates.

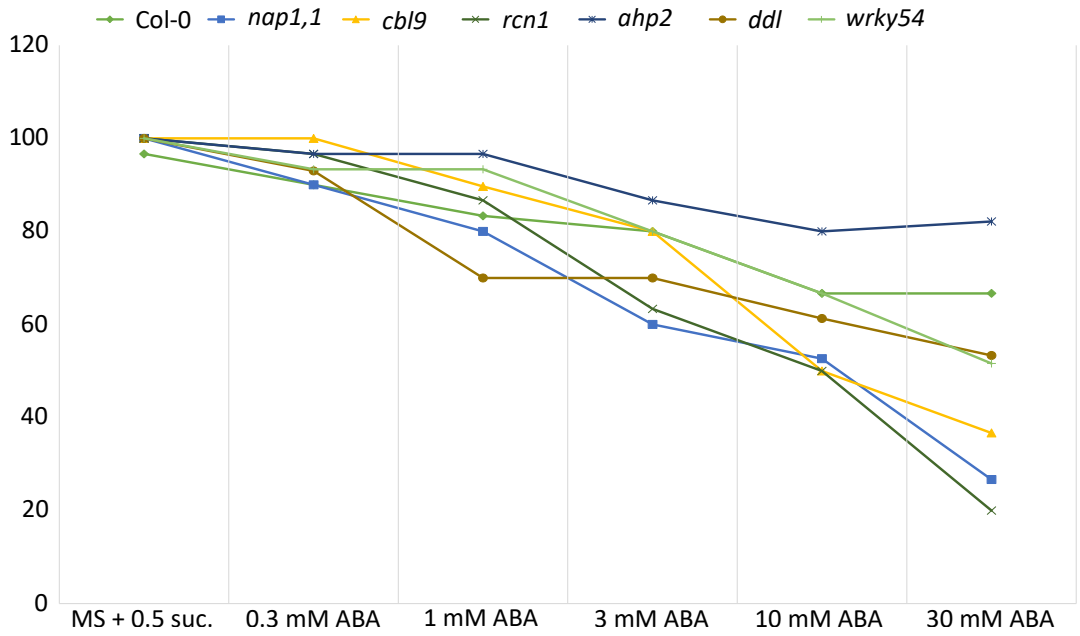

Figure A.21: Abscisic acid germination test titration. Col-0 and six mutant lines (*nap1;1, cbl9, rcn1, ahp2, ddl, wrky54*) were used for ABA titration using 0.3 mM, 1 mM, 3 mM, 10 mM and 30 mM ABA in MS plus 0.5 % sucrose. This titration assay was performed by a member of Prof. Grill group (Botany, TUM).

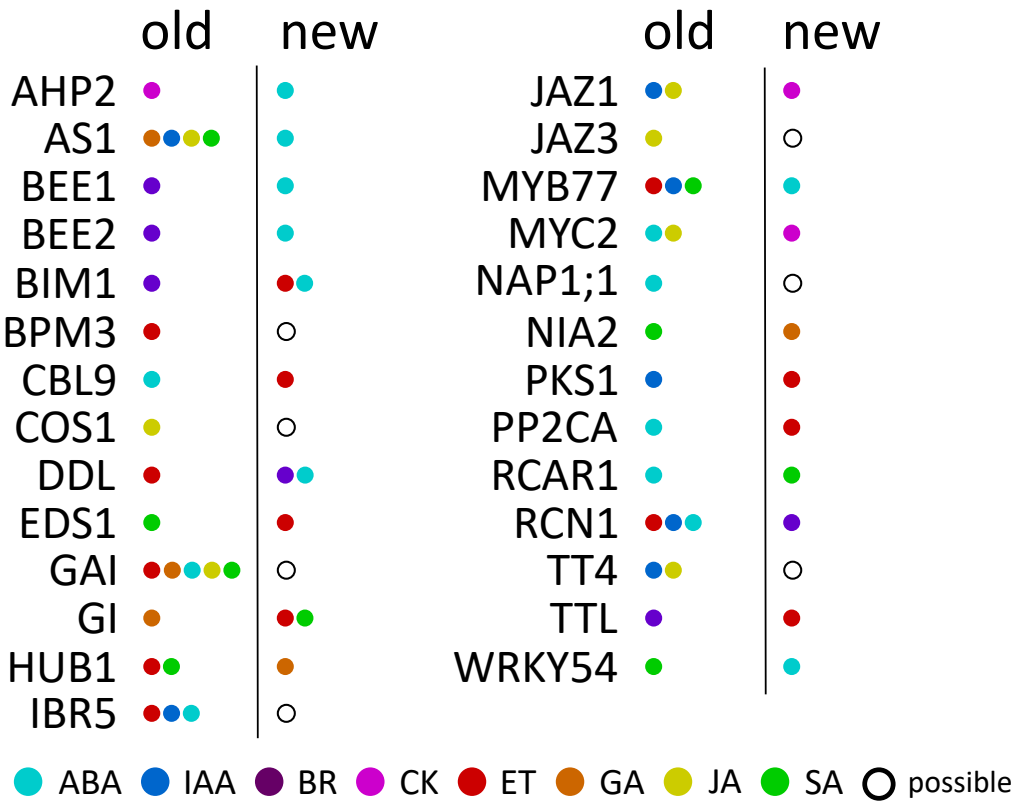

Figure A.22: Overview hormone annotation of all candidate plant lines. All proteins of the respective plant lines are alphabetically sorted and colored dots indicate hormone annotations of current literature knowledge (based on TAIR GO and AHD2.0 database) and new annotations based on my experiments. Black circles indicate that new annotations are possible but were not tested.

A.8.7 Salicylic acid assay

For salicylic acid an infection assay with *Pseudomonas syringae pathovar tomato* DC3000 (*Pst* DC3000) was performed by group members of Dr. Corina Vlot-Schuster's lab (BIOP; HMGU). Leaves were infected with *Pst* DC3000 and infection rate was counted by colony number (colony forming units). This assay was performed twice, additional repeats are ongoing (see figure A.23). The results showed a significant difference to Col-0 for the positive control *eds16* (in one repeat) and *eds21* (in both repeats). This two mutant lines of *eds* were provided by Dr. Corina Vlot-Schuster's lab, as *eds1* mutant, which I already used in the ethylene assay, showed no EDS-like phenotype.

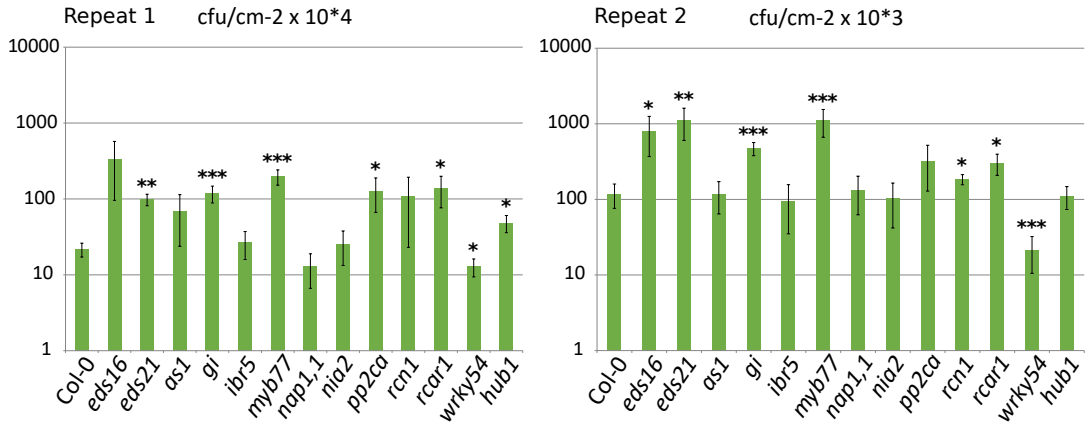

Figure A.23: Infection assay for salicylic acid. For the infection assay, the *Pst* DC3000 titer was measured 3 days after leaf infiltration from 4-5 week old plants. The repeats are evaluated individually and not combined, as the infection rate varies in different repetitions. Cfu (colony forming unit) were counted per line. Error bars indicate standard error of two biological replicates. * indicates a p-value of < 0.05, ** < 0.005, *** < 0.001.

The infection assay showed that *gi*, and *rcar1* candidate lines were more susceptible to *Pst* DC3000 compared to wild type. These differences were highly significant and could be observed in both repeats. The candidate lines *rcn1* and *pp2ca* were more susceptible to *Pst* DC3000 compared to wild type, in one repeat.

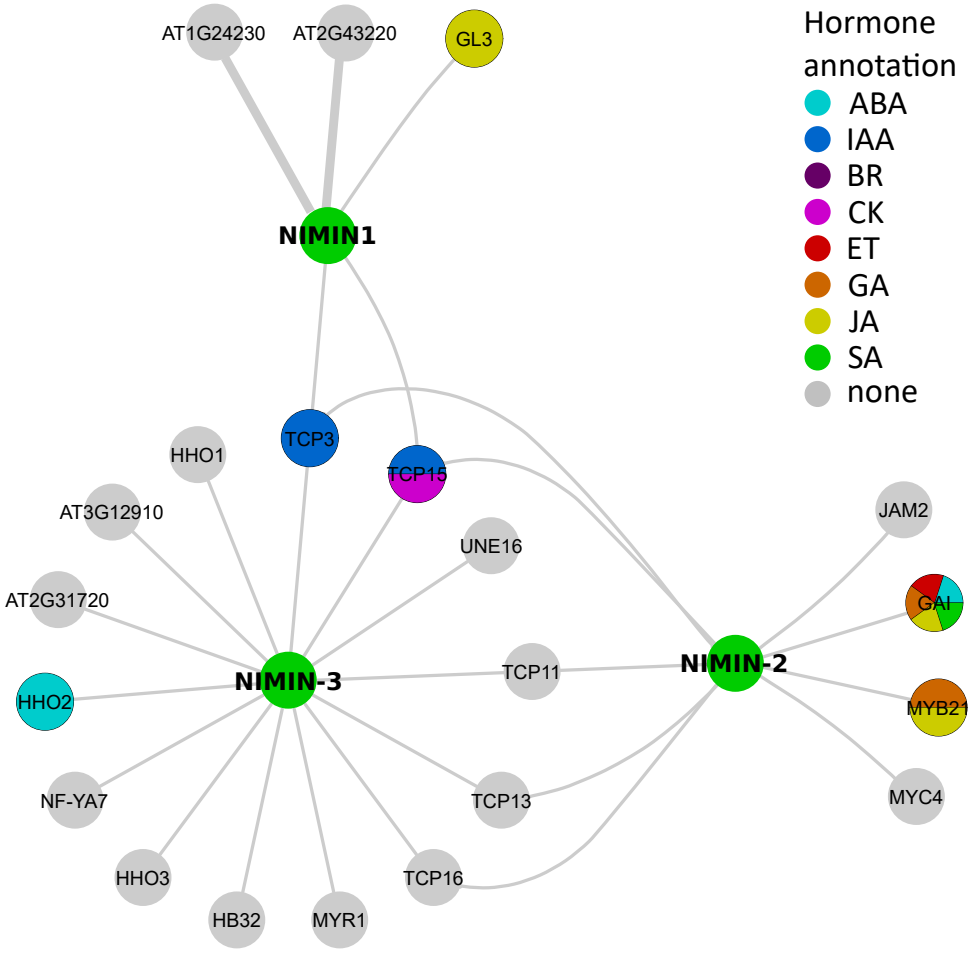

Figure A.24: NIMIN transcription factor interactions. These interactions are based on Rep-TF screen. Interactions represented here by edges were confirmed at least three times in single validation assays.

Table A.10: Published NIMIN interactions (BioGRID)

Interactor A	Symbol	Interactor B	Symbol
AT1G02450	NIMIN1	AT1G64280	NPR1
AT1G02450	NIMIN1	AT1G22920	CSN5A
AT1G02450	NIMIN1	AT5G45110	NPR3
AT3G25882	NIMIN2	AT1G64280	NPR1
AT3G25882	NIMIN2	AT1G22920	CSN5A
AT3G25882	NIMIN2	AT3G06720	IMPA-1
AT3G25882	NIMIN2	AT4G16143	IMPA-2
AT3G25882	NIMIN2	AT1G09270	IMPA-4
AT3G25882	NIMIN2	AT1G15750	TPL
AT1G09415	NIMIN3	AT1G64280	NPR1
AT1G09415	NIMIN3	AT1G15750	TPL
AT1G09415	NIMIN3	AT5G49890	CLC-C

Table A.11: TCP interactions with phytohormone related proteins

Interactor A	Symbol	Interactor B	Symbol	new/conf.	TCP clade
AT1G53230	TCP3	AT1G01360	RCAR1	new	TCP clade 1
AT1G53230	TCP3	AT1G02450	NIMIN1	new	TCP clade 1
AT1G53230	TCP3	AT1G04100	IAA10	new	TCP clade 1
AT1G53230	TCP3	AT1G04240	SHY2	new	TCP clade 1
AT1G53230	TCP3	AT1G04250	AXR3	new	TCP clade 1
AT1G53230	TCP3	AT1G09415	NIMIN-3	new	TCP clade 1
AT1G53230	TCP3	AT1G15050	IAA34	new	TCP clade 1
AT1G53230	TCP3	AT1G15580	IAA5	new	TCP clade 1
AT1G53230	TCP3	AT1G19180	JAZ1	new	TCP clade 1
AT1G53230	TCP3	AT1G28360	ERF12	new	TCP clade 1
AT1G53230	TCP3	AT1G28370	ERF11	new	TCP clade 1
AT1G53230	TCP3	AT1G52830	IAA6	new	TCP clade 1
AT1G53230	TCP3	AT1G53170	ERF8	new	TCP clade 1
AT1G53230	TCP3	AT4G24470	ZIM	new	TCP clade 1
AT1G53230	TCP3	AT5G05700	ATE1	new	TCP clade 1
AT1G53230	TCP3	AT3G57040	ARR9	new	TCP clade 1
AT1G53230	TCP3	AT3G15210	ERF4	new	TCP clade 1
AT1G53230	TCP3	AT5G44210	ERF9	new	TCP clade 1
AT1G53230	TCP3	AT1G75080	BZR1	new	TCP clade 1
AT1G53230	TCP3	AT1G74950	TIFY10B	new	TCP clade 1
AT1G53230	TCP3	AT3G17860	JAZ3	new	TCP clade 1
AT1G53230	TCP3	AT1G70700	TIFY7	new	TCP clade 1
AT1G53230	TCP3	AT3G25882	NIMIN-2	new	TCP clade 1
AT1G53230	TCP3	AT2G22670	IAA8	new	TCP clade 1
AT1G53230	TCP3	AT5G65670	IAA9	new	TCP clade 1
AT1G53230	TCP3	AT1G80390	IAA15	new	TCP clade 1
AT1G53230	TCP3	AT3G04730	IAA16	new	TCP clade 1
AT1G53230	TCP3	AT3G15540	IAA19	new	TCP clade 1
AT1G53230	TCP3	AT2G46990	IAA20	new	TCP clade 1
AT1G53230	TCP3	AT4G29080	PAP2	new	TCP clade 1
AT1G53230	TCP3	AT5G25890	IAA28	new	TCP clade 1
AT1G53230	TCP3	AT2G01200	IAA32	new	TCP clade 1
AT1G53230	TCP3	AT5G57420	IAA33	new	TCP clade 1
AT1G53230	TCP3	AT2G01570	RGA1	new	TCP clade 1
AT1G53230	TCP3	AT2G40330	PYL6	new	TCP clade 1
AT2G31070	TCP10	AT1G01360	RCAR1	new	TCP clade 1
AT2G31070	TCP10	AT2G40330	PYL6	new	TCP clade 1
AT3G02150	TCP13	AT1G01360	RCAR1	new	TCP clade 1
AT3G02150	TCP13	AT1G04250	AXR3	new	TCP clade 1
AT3G02150	TCP13	AT1G09415	NIMIN-3	new	TCP clade 1
AT3G02150	TCP13	AT1G14920	GAI	confirmed	TCP clade 1
AT3G02150	TCP13	AT1G15050	IAA34	new	TCP clade 1
AT3G02150	TCP13	AT1G28360	ERF12	new	TCP clade 1
AT3G02150	TCP13	AT1G53170	ERF8	new	TCP clade 1
AT3G02150	TCP13	AT1G75080	BZR1	new	TCP clade 1
AT3G02150	TCP13	AT1G80390	IAA15	new	TCP clade 1
AT3G02150	TCP13	AT2G01570	RGA1	new	TCP clade 1
AT3G02150	TCP13	AT2G40330	PYL6	new	TCP clade 1
AT3G02150	TCP13	AT2G46990	IAA20	new	TCP clade 1
AT3G02150	TCP13	AT3G48090	EDS1	new	TCP clade 1
AT3G02150	TCP13	AT3G15210	ERF4	new	TCP clade 1
AT3G02150	TCP13	AT5G44210	ERF9	new	TCP clade 1
AT3G02150	TCP13	AT3G25882	NIMIN-2	new	TCP clade 1
AT3G02150	TCP13	AT5G65670	IAA9	new	TCP clade 1
AT3G02150	TCP13	AT5G27320	GID1C	new	TCP clade 1
AT3G02150	TCP13	AT3G03450	RGL2	new	TCP clade 1
AT3G02150	TCP13	AT5G17490	RGL3	new	TCP clade 1
AT3G02150	TCP13	AT5G45870	PYL12	new	TCP clade 1
AT5G08070	TCP17	AT1G14920	GAI	new	TCP clade 1
AT5G08070	TCP17	AT3G03450	RGL2	new	TCP clade 1
AT5G08070	TCP17	AT4G08150	KNAT1	new	TCP clade 1
AT5G08070	TCP17	AT4G18710	BIN2	new	TCP clade 1
AT5G08070	TCP17	AT5G17490	RGL3	new	TCP clade 1
AT1G35560	TCP23	AT1G10210	MPK1	new	TCP clade 2
AT1G35560	TCP23	AT1G14280	PKS2	new	TCP clade 2
AT1G35560	TCP23	AT1G15550	GA3OX1	new	TCP clade 2
AT1G35560	TCP23	AT1G18350	MKK7	new	TCP clade 2
AT1G35560	TCP23	AT1G18400	BEE1	new	TCP clade 2
AT1G35560	TCP23	AT1G21690	EMB1968	new	TCP clade 2
AT1G35560	TCP23	AT1G28360	ERF12	new	TCP clade 2
AT1G35560	TCP23	AT5G51760	AHG1	new	TCP clade 2
AT1G35560	TCP23	AT1G73410	MYB54	new	TCP clade 2
AT1G35560	TCP23	AT4G00240	PLDBETA2	new	TCP clade 2
AT1G35560	TCP23	AT5G45810	CIPK19	new	TCP clade 2
AT1G35560	TCP23	AT4G36930	SPT	new	TCP clade 2
AT1G35560	TCP23	AT1G35560	TCP23	new	TCP clade 2
AT1G35560	TCP23	AT2G25490	EBF1	new	TCP clade 2
AT1G35560	TCP23	AT4G08150	KNAT1	new	TCP clade 2
AT1G35560	TCP23	AT2G04550	IBR5	new	TCP clade 2
AT1G35560	TCP23	AT4G29810	MKK2	new	TCP clade 2
AT1G35560	TCP23	AT3G24520	HSFC1	new	TCP clade 2
AT1G35560	TCP23	AT3G29350	AHP2	new	TCP clade 2
AT1G35560	TCP23	AT1G64520	RPN12a	new	TCP clade 2
AT1G35560	TCP23	AT3G57040	ARR9	new	TCP clade 2
AT1G35560	TCP23	AT5G62000	ARF2	new	TCP clade 2
AT1G35560	TCP23	AT2G46130	WRKY43	new	TCP clade 2
AT1G35560	TCP23	AT4G11070	WRKY41	new	TCP clade 2
AT1G35560	TCP23	AT4G29800	PLP8	new	TCP clade 2

Table A.11 continued from previous page

Interactor A	Symbol	Interactor B	Symbol	new/conf.	TCP clade
AT1G35560	TCP23	AT1G50600	SCL5	new	TCP clade 2
AT1G35560	TCP23	AT1G53170	ERF8	new	TCP clade 2
AT1G35560	TCP23	AT5G13080	WRKY75	new	TCP clade 2
AT1G35560	TCP23	AT5G43290	WRKY49	new	TCP clade 2
AT1G35560	TCP23	AT2G39250	SNZ	new	TCP clade 2
AT1G35560	TCP23	AT2G01760	RR14	new	TCP clade 2
AT1G35560	TCP23	AT2G30590	WRKY21	new	TCP clade 2
AT1G35560	TCP23	AT3G45640	MPK3	new	TCP clade 2
AT1G35560	TCP23	AT4G36540	BEE2	new	TCP clade 2
AT1G35560	TCP23	AT5G55170	SUMO3	new	TCP clade 2
AT1G35560	TCP23	AT3G01970	WRKY45	new	TCP clade 2
AT1G35560	TCP23	AT3G15150	HPY2	new	TCP clade 2
AT1G35560	TCP23	AT2G26980	CIPK3	new	TCP clade 2
AT1G35560	TCP23	AT2G42880	MPK20	new	TCP clade 2
AT1G35560	TCP23	AT4G14713	PPD1	new	TCP clade 2
AT1G35560	TCP23	AT1G80340	GA3OX2	new	TCP clade 2
AT1G35560	TCP23	AT3G14720	MPK19	new	TCP clade 2
AT1G35560	TCP23	AT5G05440	PYL5	new	TCP clade 2
AT1G69690	TCP15	AT1G01360	RCAR1	new	TCP clade 2
AT1G69690	TCP15	AT1G02450	NIMIN1	new	TCP clade 2
AT1G69690	TCP15	AT1G03800	ERF10	new	TCP clade 2
AT1G69690	TCP15	AT1G04100	IAA10	new	TCP clade 2
AT1G69690	TCP15	AT1G04240	SHY2	new	TCP clade 2
AT1G69690	TCP15	AT1G04250	AXR3	new	TCP clade 2
AT1G69690	TCP15	AT1G09415	NIMIN-3	new	TCP clade 2
AT1G69690	TCP15	AT1G15050	IAA34	new	TCP clade 2
AT1G69690	TCP15	AT1G15580	IAA5	new	TCP clade 2
AT1G69690	TCP15	AT1G17380	JAZ5	new	TCP clade 2
AT1G69690	TCP15	AT1G19180	JAZ1	new	TCP clade 2
AT1G69690	TCP15	AT1G28360	ERF12	confirmed	TCP clade 2
AT1G69690	TCP15	AT1G28370	ERF11	new	TCP clade 2
AT1G69690	TCP15	AT1G30135	JAZ8	new	TCP clade 2
AT1G69690	TCP15	AT1G52830	IAA6	new	TCP clade 2
AT1G69690	TCP15	AT1G53170	ERF8	new	TCP clade 2
AT1G69690	TCP15	AT1G59940	ARR3	new	TCP clade 2
AT1G69690	TCP15	AT5G16080	CXE17	new	TCP clade 2
AT1G69690	TCP15	AT3G48090	EDS1	new	TCP clade 2
AT1G69690	TCP15	AT5G05700	ATE1	new	TCP clade 2
AT1G69690	TCP15	AT4G00240	PLDBETA2	new	TCP clade 2
AT1G69690	TCP15	AT5G51760	AHG1	new	TCP clade 2
AT1G69690	TCP15	AT4G16110	RR2	new	TCP clade 2
AT1G69690	TCP15	AT5G62920	ARR6	new	TCP clade 2
AT1G69690	TCP15	AT2G41310	RR3	new	TCP clade 2
AT1G69690	TCP15	AT3G57040	ARR9	new	TCP clade 2
AT1G69690	TCP15	AT1G74890	ARR15	new	TCP clade 2
AT1G69690	TCP15	AT2G40670	RR16	new	TCP clade 2
AT1G69690	TCP15	AT3G15210	ERF4	new	TCP clade 2
AT1G69690	TCP15	AT5G44210	ERF9	new	TCP clade 2
AT1G69690	TCP15	AT1G75080	BZR1	new	TCP clade 2
AT1G69690	TCP15	AT4G18710	BIN2	new	TCP clade 2
AT1G69690	TCP15	AT1G74950	TIFY10B	new	TCP clade 2
AT1G69690	TCP15	AT3G17860	JAZ3	new	TCP clade 2
AT1G69690	TCP15	AT1G72450	JAZ6	new	TCP clade 2
AT1G69690	TCP15	AT2G34600	JAZ7	new	TCP clade 2
AT1G69690	TCP15	AT1G70700	TIFY7	new	TCP clade 2
AT1G69690	TCP15	AT5G13220	JAZ10	new	TCP clade 2
AT1G69690	TCP15	AT3G25882	NIMIN-2	new	TCP clade 2
AT1G69690	TCP15	AT4G14560	IAA1	new	TCP clade 2
AT1G69690	TCP15	AT2G22670	IAA8	new	TCP clade 2
AT1G69690	TCP15	AT5G65670	IAA9	new	TCP clade 2
AT1G69690	TCP15	AT4G14550	IAA14	new	TCP clade 2
AT1G69690	TCP15	AT1G80390	IAA15	new	TCP clade 2
AT1G69690	TCP15	AT2G46990	IAA20	new	TCP clade 2
AT1G69690	TCP15	AT4G29080	PAP2	new	TCP clade 2
AT1G69690	TCP15	AT4G32280	IAA29	new	TCP clade 2
AT1G69690	TCP15	AT2G01200	IAA32	new	TCP clade 2
AT1G69690	TCP15	AT5G57420	IAA33	new	TCP clade 2
AT1G69690	TCP15	AT3G05120	GID1A	new	TCP clade 2
AT1G69690	TCP15	AT5G53160	RCAR3	new	TCP clade 2
AT1G69690	TCP15	AT2G40330	PYL6	new	TCP clade 2
AT2G45680	TCP9	AT1G01360	RCAR1	new	TCP clade 2
AT2G45680	TCP9	AT1G59580	MPK2	new	TCP clade 2
AT2G45680	TCP9	AT2G22090	UBA1A	new	TCP clade 2
AT2G45680	TCP9	AT2G40330	PYL6	new	TCP clade 2
AT2G45680	TCP9	AT4G00240	PLDBETA2	new	TCP clade 2
AT2G45680	TCP9	AT4G37470	KAI2	new	TCP clade 2
AT3G45150	TCP16	AT1G04250	AXR3	new	TCP clade 2
AT3G45150	TCP16	AT1G09415	NIMIN-3	new	TCP clade 2
AT3G45150	TCP16	AT1G53170	ERF8	new	TCP clade 2
AT3G45150	TCP16	AT1G75080	BZR1	new	TCP clade 2
AT3G45150	TCP16	AT1G80390	IAA15	new	TCP clade 2
AT3G45150	TCP16	AT2G46990	IAA20	new	TCP clade 2
AT3G45150	TCP16	AT3G05120	GID1A	new	TCP clade 2
AT3G45150	TCP16	AT3G15210	ERF4	new	TCP clade 2
AT3G45150	TCP16	AT3G25882	NIMIN-2	new	TCP clade 2
AT3G45150	TCP16	AT5G44210	ERF9	new	TCP clade 2
AT3G45150	TCP16	AT5G65670	IAA9	new	TCP clade 2
AT3G47620	TCP14	AT1G14920	GAI	confirmed	TCP clade 2
AT3G47620	TCP14	AT2G01570	RGA1	confirmed	TCP clade 2
AT3G47620	TCP14	AT4G37470	KAI2	new	TCP clade 2

Table A.11 continued from previous page

Interactor A	Symbol	Interactor B	Symbol	new/conf.	TCP clade
AT3G47620	TCP14	AT3G63010	GID1B	new	TCP clade 2
AT5G08330	TCP11	AT1G01360	RCAR1	new	TCP clade 2
AT5G08330	TCP11	AT1G04100	IAA10	new	TCP clade 2
AT5G08330	TCP11	AT1G04250	AXR3	new	TCP clade 2
AT5G08330	TCP11	AT1G09415	NIMIN-3	new	TCP clade 2
AT5G08330	TCP11	AT1G53170	ERF8	new	TCP clade 2
AT5G08330	TCP11	AT1G75080	BZR1	new	TCP clade 2
AT5G08330	TCP11	AT1G80390	IAA15	new	TCP clade 2
AT5G08330	TCP11	AT3G04730	IAA16	new	TCP clade 2
AT5G08330	TCP11	AT3G15210	ERF4	new	TCP clade 2
AT5G08330	TCP11	AT3G25882	NIMIN-2	new	TCP clade 2
AT5G08330	TCP11	AT5G43700	AUX2-11	new	TCP clade 2
AT5G23280	TCP7	AT1G07430	HAI2	new	TCP clade 2
AT5G23280	TCP7	AT4G00240	PLDBETA2	new	TCP clade 2
AT5G51910	TCP19	AT1G01360	RCAR1	new	TCP clade 2
AT5G51910	TCP19	AT1G73000	PYL3	new	TCP clade 2
AT5G51910	TCP19	AT2G26040	PYL2	new	TCP clade 2
AT5G51910	TCP19	AT2G38310	PYL4	new	TCP clade 2
AT5G51910	TCP19	AT2G40330	PYL6	new	TCP clade 2
AT5G51910	TCP19	AT4G01026	PYL7	new	TCP clade 2
AT5G51910	TCP19	AT4G08150	KNAT1	new	TCP clade 2
AT5G51910	TCP19	AT4G17870	PYR1	new	TCP clade 2
AT5G51910	TCP19	AT4G18620	PYL13	new	TCP clade 2
AT5G51910	TCP19	AT4G27920	PYL10	new	TCP clade 2
AT5G51910	TCP19	AT5G05440	PYL5	new	TCP clade 2
AT5G51910	TCP19	AT5G45860	PYL11	new	TCP clade 2
AT5G51910	TCP19	AT5G45870	PYL12	new	TCP clade 2
AT5G51910	TCP19	AT5G53160	RCAR3	new	TCP clade 2

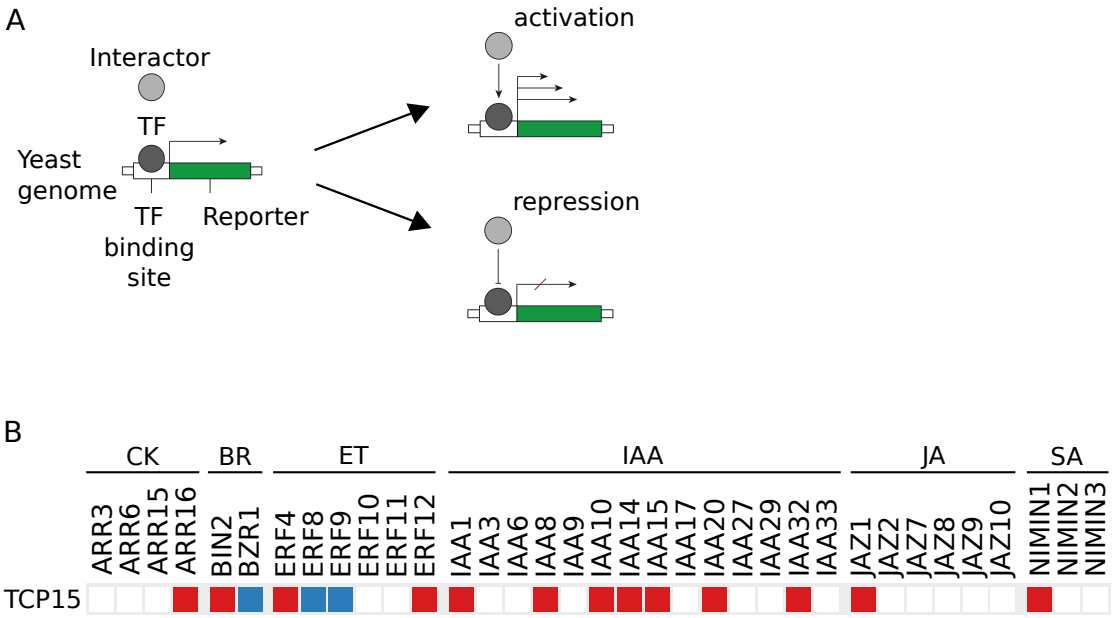

Figure A.25: TCP15 functional regulation by phytohormone associated regulators. (A) schematic description of the yeast-based functional assay to identify regulatory effects of interactors on activity of interacting TF. (B) modulation of TCP15 activity by interacting regulators.

A.9 Material and methods

A.9.1 Y2H vector maps

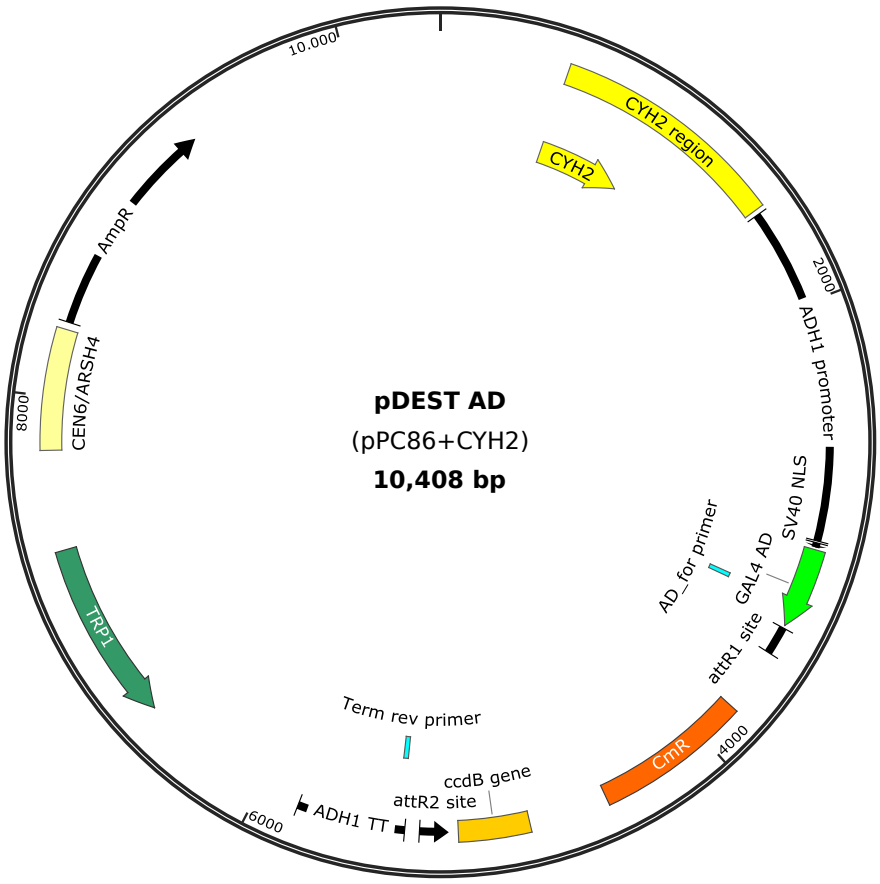

Figure A.26: pDEST-AD vector map. pDEST-AD vector map contains a specific CHY2 gene, which encodes for a yeast ribosomal subunit, which is sensitive to CHX treatment and results in growth inhibition of the yeast. The AD plasmid contains a TRY1 gene that induces the production of tryptophane in yeast. This enables the selection of positively transformed yeast cells. The plasmids contains also an antibiotic resistance for Ampicillin or Carbenicillin, which enables selection in *E. coli*.

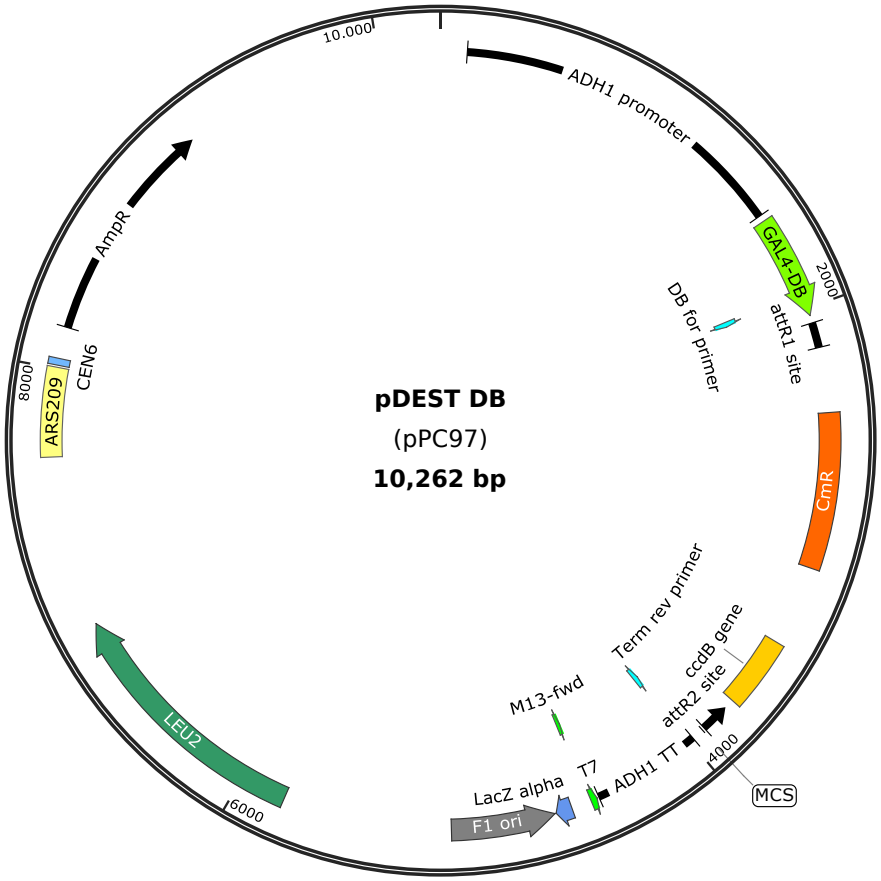

Figure A.27: pDEST-DB vector map. pDEST-DB vector contains a LEU2 gene that induces the production of leucine in yeast. This enables the selection of positively transformed yeast cells. The plasmids contains also an antibiotic resistance for Ampicillin or Carbenicillin, which enables selection in *E. coli*.

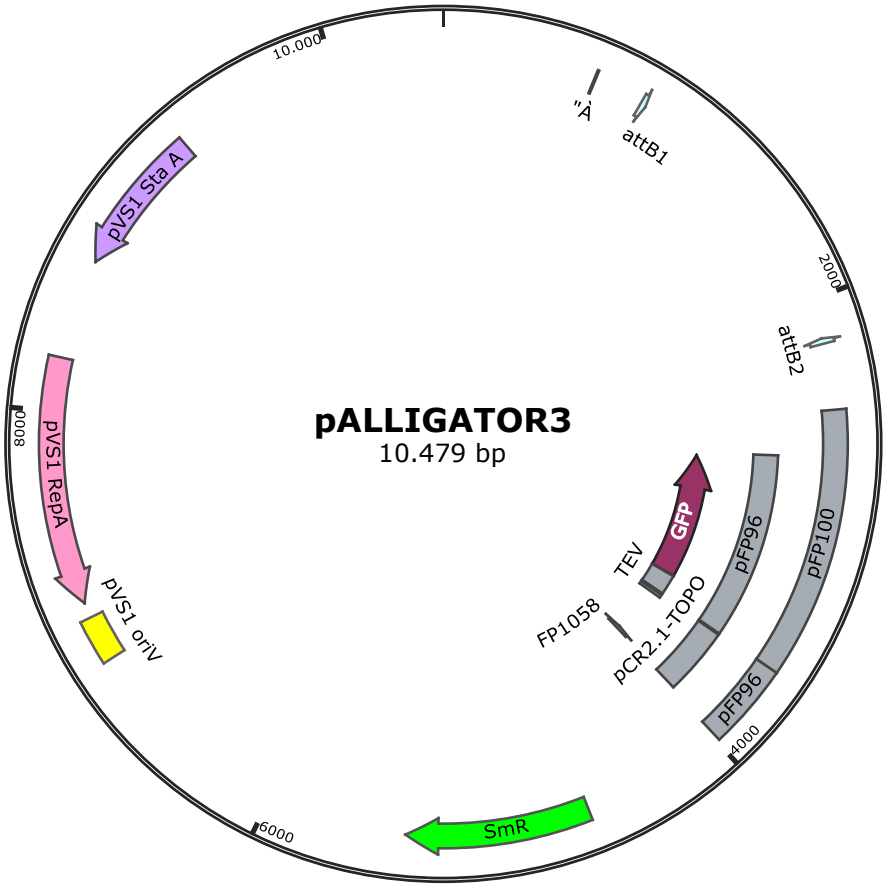

Figure A.28: pAlligator3 map. This plasmid fuse a C-terminal At2S3::GFP construct to the gene of interest, that results in a fluorescent seed coat after successful transformation. This plasmid was constructed by a member of Dr. Francois Parcy group [433].

B Acknowledgment

Mein Dank gilt zu allererst meinem Betreuer Prof. Dr. Pascal Falter-Braun für die Möglichkeit an diesem Thema zu arbeiten und die Betreuung bei diesem Projekt. Ich möchte mich für die vielen vielen Ratschläge bezüglich wissenschaftlicher Vorträge bedanken, die es mir ermöglicht haben, mein Projekt auch auf internationalen Konferenzen sehr gut präsentieren zu könnte. Danke für deine Unterstützung und Ideen in den letzten sechs Jahren und die fast familiäre Atmosphäre.

Bedanken möchte ich mich auch bei meinem Erstprüfer Prof. Dr. Claus Schwechheimer, der es mir ermöglicht hat, unter Leitung seines Lehrstuhls Systembiologie der Pflanzen zu promovieren und für die hilfreichen Tipps zu meiner Arbeit.

Ein herzliches Dankeschön möchte ich an Prof. Dr. Caroline Gutjahr richten, die sich bereiterklärt hat den Prüfungsvorsitz zu übernehmen und danke für sehr angenehme und erfolgreiche Kooperationen. Und ich bedanke mich bei Prof. Dr. Geert De Jaeger, der sich bereiterklärt hat meine Arbeit zu begutachten und ein Teil des Prüfungskomitees zu sein.

Ein Dankeschön möchte ich auch an die gesamte Arbeitsgruppe (INET) richten, für die gute Atmosphäre und dafür, dass man immer Hilfe und Unterstützung bekommt, wenn man sie braucht.

Bedanken möchte ich mich auch bei meinen Eltern für ihre Unterstützung in allen Lebenslagen und die Motivation niemals aufzugeben. Danke dass ihr immer für mich da seid.

Ein großer Dank geht an meinen Mann Stefan, der mit mir zusammen an diesem Thema gearbeitet hat. Danke für deine Unterstützung in wirklich jeder Lebenslage. Ohne dich hätte ich diese Promotion vermutlich nicht überstanden. Ich bin glücklich und dankbar dafür, dass ich dich kennengelernt habe und freue mich darauf das restliche Leben mit dir zu verbringen.